

ADVANCED OXIDATION TECHNIQUES FOR THE REMOVAL OF  
REFRACTORY ORGANICS FROM TEXTILE WASTEWATERS

A THESIS SUBMITTED TO  
THE GRADUATE SCHOOL OF NATURAL AND APPLIED SCIENCES  
OF  
MIDDLE EAST TECHNICAL UNIVERSITY

BY

FUNDA EROL

IN PARTIAL FULFILLMENT OF THE REQUIREMENTS  
FOR  
THE DEGREE OF DOCTOR OF PHILOSOPHY  
IN  
CHEMICAL ENGINEERING

SEPTEMBER 2008

Approval of the thesis:

**ADVANCED OXIDATION TECHNIQUES FOR THE REMOVAL OF  
REFRACTORY ORGANICS FROM TEXTILE WASTEWATERS**

submitted by **FUNDA EROL** in partial fulfillment of the requirements for the degree of Doctor of Philosophy in **Chemical Engineering Department, Middle East Technical University** by,

Prof. Dr. Canan Özgen  
Dean, Graduate School of **Natural and Applied Sciences**

\_\_\_\_\_

Prof. Dr. Gürkan Karakaş  
Head of Department, **Chemical Engineering**

\_\_\_\_\_

Prof. Dr. Tülay A. Özbelge  
Supervisor, **Chemical Engineering Dept., METU**

\_\_\_\_\_

**Examining Committee Members:**

Prof. Dr. Timur Doğu  
Chemical Engineering Dept., METU

\_\_\_\_\_

Prof.Dr. Tülay A. Özbelge  
Chemical Engineering Dept., METU

\_\_\_\_\_

Assoc. Prof. Dr. Nail Yaşyerli  
Chemical Engineering Dept., Gazi University

\_\_\_\_\_

Assist. Prof. Dr. Ayşegül Latifoğlu  
Environmental Engineering Dept., Hacettepe University

\_\_\_\_\_

Assoc.Prof. Dr Halil Kalıpçılar  
Chemical Engineering Dept., METU

\_\_\_\_\_

**Date: 05.09.2008**

**I hereby declare that all information in this document has been obtained and presented in accordance with academic rules and ethical conduct. I also declare that, as required by these rules and conduct, I have fully cited and referenced all material and results that are not original to this work.**

Name, Last Name: Funda Erol

Signature:

## ABSTRACT

### ADVANCED OXIDATION TECHNIQUES FOR THE REMOVAL OF REFRACTORY ORGANICS FROM TEXTILE WASTEWATERS

Erol, Funda

Ph.D., Department of Chemical Engineering

Supervisor: Prof. Dr. Tülay A. Özbelge

September 2008, 400 pages

Ozonation is an efficient method to degrade refractory organics in textile wastewaters. In recent years, catalytic ozonation is applied to reduce ozone consumption and to increase “chemical oxygen demand” and “total organic carbon” (TOC) removal efficiencies.

The ozonation of two industrial dyes, namely Acid Red-151 (*AR-151*) and Remazol Brilliant Blue R (*RBBR*) was examined separately both in a semi-batch reactor and also in a fluidized bed reactor (FBR) by conventional and catalytic ozonation with alumina and perfluorooctyl alumina (PFOA) catalysts. The conventional and catalytic ozonation reactions followed a pseudo-first order kinetics with respect to the dye concentration. The highest COD reductions were obtained in the presence of the catalysts at pH=13, with alumina for *AR-151* and with PFOA for *RBBR*. “Residence time distribution” experiments were performed to understand the degree of liquid mixing in the reactor. The behaviour of the FBR was almost equivalent to the behaviour of one or two completely stirred tank reactors in series in the presence of the solid catalyst particles.

The volumetric ozone-water mass transfer coefficients ( $k_La$ ) were found at various gas and liquid flow rates and catalyst dosages in the FBR. A model was developed to find

$k_{La}$  in the reactor by comparing the dissolved  $O_3$  concentrations in the experiments with the model results.  $k_{La}$  increased significantly by the increase of gas flow rate. Higher catalyst dosages at the fluidization conditions yielded higher  $k_{La}$  values indicating higher rates of mass transfer.

Dye ozonation experiments without catalyst and with alumina or PFOA catalyst were conducted at different conditions of the inlet dye concentration, gas and liquid flow rates, inlet ozone concentration in the gas, catalyst dosage, particle size and pH. The dye and TOC removal percentages were increased with the increase of gas flow rate and with the decrease of both the liquid flow rate and inlet dye concentration. The addition of the catalyst was beneficial to enhance the TOC degradation. The ozone consumed per liter of wastewater was much lower when the catalyst was present in the reactor. In terms of TOC removal and  $O_3$  consumption, the most efficient catalyst was PFOA. According to the organic analysis, the intermediate by-products were oxalic, acetic, formic and glyoxalic acids in *RBBR* and *AR-151* ozonation.

The dye and dissolved ozone concentration profiles were predicted from a developed model and the model results were compared with the experimental results to obtain the enhanced  $k_{La}$  values. The presence of the chemical reaction and the catalysts in the FBR, enhanced the  $k_{La}$  values significantly. The enhancement factor ( $E$ ) was found as between 0.97 and 1.93 for the non-catalytic ozonation and 0.96 and 1.53 for the catalytic ozonation at pH = 2.5. The dimensionless number of *Hatta* values were calculated between 0.04-0.103 for the sole ozonation of *RBBR* and *AR-151* solutions. According to the calculated *Ha* values, the reaction occurred in the bulk liquid and in the film being called as the “intermediate regime” in the literature.

Keywords: Ozonation, Catalytic Ozonation, Alumina, Perfluorooctyl Alumina (PFOA), Textile Wastewaters.

## ÖZ

### TEKSTİL ATIKSULARINDA BULUNAN KARARLI ORGANİKLERİN İLERİ OKSİDASYON TEKNİKLERİ İLE ARITIMI

Erol, Funda

Doktora, Kimya Mühendisliği Bölümü

Tez Yöneticisi: Prof. Dr. Tülay A. Özbelge

Eylül 2008, 400 sayfa

Ozonlama, tekstil atıksularında bulunan kararlı organiklerin arıtımında etkili bir yöntemdir. Son yıllarda katalitik ozonlama, ozon sarfiyatının düşürülmesi ve kimyasal oksijen ihtiyacı ve “toplam organik karbon” (TOK) giderim yüzdelerinin arttırılmasında uygulanmaktadır.

Asit Kırmızı-151 (*AR-151*) ve Remazol Mavisi (*RBBR*) olarak adlandırılan iki farklı endstriyel boyanın arıtımı ayrı ayrı konvensiyonel ozonlama ve alumina veya perflorooktil alumina ile katalitik ozonlama ile yarı-kesikli ve akışkan yataklı reaktörde (AYR’de) gerçekleştirilmiştir. Konvensiyonel ve katalitik ozonlama prosesi boya konsantrasyonuna göre sahte-birinci derece reaksiyon kinetiği izlemiştir. En yüksek KOİ giderimleri pH’nın 13 olduğu şartlarda, *AR-151* için alumina ve *RBBR* için de % 100 PFOA varlığında gerçekleşmiştir. “Alıkonma Zamanı Dağılımı” deneyleri reaktörde sıvı fazı karışma seviyesinin anlaşılması için yapılmıştır. AYR’nin reaktör olarak davranışı bir veya iki “sürekli karışan tank reaktör”ün davranışına eşit olarak bulunmuştur.

AYR’de, volumetrik ozon-su kütle transfer katsayısı ( $k_{La}$ ), farklı gaz debisi, sıvı debisi ve katalizör dozları için bulunmuştur. Deneysel bulunan çözünmüş ozon

konsantrasyonları model sonuçları ile karşılaştırılarak  $k_{La}$ 'nin bulunması için bir model geliştirilmiştir.  $k_{La}$ 'nin değeri gaz debisinin artması ile artmıştır. Akışkanlaştırma şartlarında, yüksek miktardaki katalizör dozları yüksek kütle transfer hızları ile  $k_{La}$ 'nin yüksek olmasını sağlamıştır.

Farklı giriş boya konsantrasyonu, gaz ve sıvı debileri, giriş ozon konsantrasyonu, katalizör dozu, katalizör parçacık boyutu ve pH şartlarında boya ozonlama deneyleri katalizörsüz ve alumina veya PFOA varlığında yapılmıştır. Boya ve TOK giderimleri gaz debisinin artması ve sıvı debisi ile giriş boya konsantrasyonunun azalması ile artmıştır. Reaktöre katalizör eklenmesi TOK gideriminin artmasında yararlı olmuştur; TOK giderimi katalizör dozunun artması ile artmıştır. Reaktörde katalizör bulunduğunda, çözeltilerin birim hacmi başına harcanan ozon çok daha düşük bulunmuştur. TOK giderimi ve  $O_3$  sarfiyatına bakıldığında en etkili katalizör PFOA olmuştur. Organik analizi sonuçlarına göre, *RBBR* ve *AR-151* ozonlanmasında yan ürünler oksalik, asetik, formik ve gliokzalik asitler olmuştur.

Sıvı içindeki boya ve çözülmüş ozon konsantrasyonları modelden tahmin edilmiş ve ve model sonuçları deneysel sonuçlarla kimyasal tepkime varlığında  $k_{La}$  değerlerinin bulunması için karşılaştırılmıştır. Kimyasal tepkimenin ve katalizörlerin AYR'de bulunması  $k_{La}$  değerlerini önemli derecede arttırmıştır. Artış faktörü ( $E$ ) pH=2.5'de katalizörsüz ozonlama için 0.97 ve 1.93, katalizörlü ozonlama için 0.96 ve 1.53 aralığında bulunmuştur. Birimsiz bir sayı olan Hatta değerleri *RBBR* ve *AR-151* çözeltilerinin konvensiyonel ozonlanmasında 0.04 ile 0.103 arasında hesaplanmıştır. Hesaplanan  $Ha$  değerlerine göre, tepkime literatürde "ara rejim" denilen rejimde gerçekleşmiştir.

Anahtar kelimeler: Ozonlama, Katalitik Ozonlama, Alümina, Perflorooktil Alümina (PFOA), Tekstil Atıksuları.

*To my family*

## ACKNOWLEDGEMENTS

I would like to express my deepest thanks to my supervisor Prof. Dr. Tülay A. Özbelge for her great knowledge, helpful guidance, major support and encouragement as a supervisor and as a person like a mother. During the study, her great advises for the development of the thesis, gave me an inspiration to finish the study.

I wish to declare my gratitude to Prof. Dr. H. Önder Özbelge for his suggestions about the study and support to complete the thesis. His valuable suggestions contributed substantially to bringing the original conception to this final stage.

I am also grateful to the members of my progress committee, Prof. Dr. Timur Doğu and Assoc. Dr. Ayşegül Latifoğlu for great help during the thesis. Their guidance and support with an enormous knowledge resulted in the development of the thesis.

I wish to express thanks to Assoc. Dr. Ahmet Eraslan for great help in solving the modeling equations with the Fortran computer programs. He gave a valuable contribution to my thesis and suggested very special techniques in solving the equations.

I would like to acknowledge that this study has been supported by the METU research fund and Scientific and Technical Research Council of Turkey (Tübitak) with the project numbers BAP-2006-03-04-07 and 106Y078, respectively.

I want to thank my old laboratory partners Gülden Camçı Ünal, Fulya Gökçen and Ebru Acar and also my new partner Saltuk Pirgalioglu for their friendship, valuable helps and guidance in solving the problems in the laboratory. I have enjoyed working with those people greatly. Saltuk also gave me a hand physically by carrying liters and liters of distilled water from the Unit Laboratory.

I gratefully acknowledge the friendship of Kerime Güney during the study. Her insistence on the continuation of this work brought the final stage. Also, it would be an error to forget my friends, Mümin Alaçam, Okan Sonuçar, Umut Yul, Sadık Yetkin, Necati Özkan for their support during the progress of the work.

Finally, I wish to thank Güneş Kadir Ünal for simply everything. I am sure that I could not continue to this work without him. Besides, physical and technical help, he tolerated this crazy, egoistic and most of the time stressed girl during the study.

## TABLE OF CONTENTS

ABSTRACT.....	iv
ÖZ.....	vi
ACKNOWLEDGEMENTS.....	ix
TABLE OF CONTENTS.....	xi
LIST OF TABLES .....	xvi
LIST OF FIGURES .....	xxii
LIST OF SYMBOLS .....	xxx
CHAPTER	
1 INTRODUCTION .....	1
1.1 Characteristics of textile wastewaters.....	1
1.2 Treatment technologies for textile wastewaters.....	4
1.3 Use of ozone in wastewater treatment processes.....	7
1.4 Aim and scope of the study.....	8
2 LITERATURE SURVEY.....	12
2.1 Ozonation process.....	12
2.1.1 Ozonation chemistry.....	12
2.1.2 Effects of pH on ozonation process .....	17
2.1.3 Effect of wastewater characteristics on ozonation process.....	19
2.1.4 Mass transfer effects in ozonation .....	20
2.2 Ozonation studies in wastewater treatment .....	25
2.3 Advanced oxidation processes (AOPs) for wastewater treatment.....	27
2.4 Evaluation of catalytic ozonation .....	30
2.4.1 Use of metal ions/complexes in ozonation .....	31
2.4.2 Non-polar catalytic ozonation for wastewater treatment.....	40
2.5 Ozonation by-products .....	43

3	MODELING OF SEMI-BATCH AND CONTINUOUS OZONATION PROCESSES .....	48
3.1	The determination of reaction rate constants in semi-batch process for catalytic and non-catalytic ozonations .....	48
3.2	Determination of axial dispersion coefficient ( $D_L$ ) and Péclet number ( $Pe$ ) from tracer experiments in continuous gas-liquid and gas-liquid-solid reactors .....	50
3.3	Modeling of ozone absorption into water in continuously operated bubble column.....	52
3.3.1	Model assumptions .....	52
3.3.2	Model equations.....	53
3.3.3	Estimation of $D_L$ and $k_{La}$ from modeling .....	54
3.4	Modeling of dye ozonation process .....	54
3.4.1	Sole ozonation.....	54
3.4.1.1	Model assumptions .....	55
3.4.1.2	Model equations.....	55
3.4.1.3	Estimation of $(k_{La})_E$ from modeling .....	56
3.4.2	Catalytic ozonation .....	56
3.4.2.1	Model equations in FBR.....	59
3.4.2.2	Estimation of $(k_{La})_E$ from modeling .....	61
4	MATERIALS AND METHODS .....	62
4.1	Materials .....	62
4.1.1	Specifications of <i>AR-151</i> and <i>RBBR</i> dyes .....	62
4.2	Apparatus .....	63
4.2.1	Semi-batch reactor .....	63
4.2.2	Fluidized bed reactor .....	64
4.3	Characterization of the catalysts .....	68
4.3.1	Specifications of alumina and perfluorooctyl alumina (PFOA) ..	68
4.3.2	Preparation of perfluorooctyl alumina (PFOA).....	72
4.4	Experiments in semi-batch reactor .....	73
4.4.1	Preparation of the dye solutions .....	73
4.4.2	Experimental procedure.....	73
4.5	Experiments in fluidized bed reactor (gas-liquid-solid) .....	75
4.5.1	Tracer experiments .....	75

4.5.2	Ozone absorption experiments.....	77
4.5.3	Hydrodynamic experiments in the reactor .....	78
4.5.4	Dye ozonation experiments .....	80
4.6	Analytical methods .....	81
4.6.1	Determination of dye concentration .....	81
4.6.2	Determination of dissolved O <sub>3</sub> concentration .....	82
4.6.3	Chemical Oxygen Demand (COD) analysis .....	83
4.6.4	Total Organic Carbon (TOC) analysis .....	84
4.6.5	Determination of O <sub>3</sub> concentration in the gas phase .....	84
4.6.6	High Performance Liquid Chromatography (HPLC) method for analysis of ozonation by-products .....	85
5	RESULTS AND DISCUSSION .....	86
5.1	Non-catalytic and catalytic ozonation experiments in semi-batch reactor .....	86
5.1.1	Dye and COD removals in <i>AR-151</i> and <i>RBBR</i> aqueous dye solution .....	86
5.1.1.1	Ozonation experiments .....	86
5.1.1.2	Catalytic ozonation experiments .....	88
5.1.2	Kinetics of non-catalytic and catalytic ozonation-determination of reaction rate constants .....	94
5.2	Residence time distribution studies in the fluidized bed reactor .....	99
5.2.1	Effects of gas and liquid flow rates on RTD distribution .....	99
5.2.2	Distribution behaviour in the presence of the catalyst .....	102
5.3	Reactor hydrodynamics .....	104
5.3.1	Minimum fluidization velocity in the column .....	105
5.3.2	Determination of hold-up values for gas, liquid and solid phases .....	107
5.4	Ozone absorption experiments in the fluidized bed reactor .....	110
5.4.1	Ozonation experiments without particles at different gas and liquid flow rates .....	111
5.3.2	Ozonation experiments with particles at different catalyst dosages .....	116
5.5	Dye ozonation experiments in the fluidized bed reactor .....	119
5.5.1	Ozonation experiments .....	120

5.5.1.1	Effect of gas and liquid flow rate and inlet dye concentration in ozonation of <i>AR-151</i> and <i>RBBR</i> dyes .....	120
5.5.1.2	Effect of inlet ozone concentration on ozonation of <i>AR-151</i> and <i>RBBR</i> dyes .....	131
5.5.1.3	Effect of $Q_G/Q_L$ ratio in ozonation of <i>AR-151</i> and <i>RBBR</i> dyes .....	132
5.5.1.4	By-products of dye ozonation .....	136
5.6	Dye ozonation in the presence of catalysts .....	144
5.6.1	The effect of catalyst dosage on dye ozonation .....	144
5.6.2	The effect of catalyst particle size on dye ozonation .....	157
5.6.3	Reproducibility of the experiments .....	162
5.6.4	Effect of $Q_L$ in catalytic ozonation .....	163
5.6.5	Effect of pH on catalytic ozonation .....	165
5.6.6	Catalyst properties .....	174
5.6.7	The effect of catalyst dosage on the concentrations of by-products .....	176
5.7	Modeling results of the dye ozonation experiments .....	181
5.7.1	Non-catalytic ozonation .....	181
5.7.2	Catalytic ozonation .....	186
6	CONCLUSIONS .....	192
7	RECOMMENDATIONS .....	197
	REFERENCES .....	198
	APPENDICES	
A	CALIBRATION CURVES OF <i>AR-151</i> AND <i>RBBR</i> DYES .....	217
B	SAMPLE CALCULATIONS .....	221
B.1	The calculation of ozone production .....	221
B.1.1	Sample calculation .....	223
B.2	The calculation of dissolved $O_3$ concentration in the liquid phase .....	224
B.2.1	Sample calculation .....	225
B.3	The calculation of concentrations of <i>AR-151</i> and <i>RBBR</i> dyes .....	226
B.3.1	Sample calculation .....	226
B.4	Calculation of dye, TOC removals, $O_3$ consumption rate and utilization ratios .....	227

B.4.1	Sample calculation .....	228
B.5	Calculation of Henry's Law constant at different pH values .....	229
B.5.1	Sample calculation .....	229
B.6	Calculation of by-product concentration from their calibration curves ..	230
B.7	The determination of main parameters in tracer experiments .....	231
C	SEMI-BATCH EXPERIMENTS DATA .....	234
D	TRACER EXPERIMENTS DATA .....	249
E	OZONE ABSORPTION EXPERIMENTS DATA .....	264
F	DYE OZONATION EXPERIMENTS DATA .....	278
G	COMPUTER PROGRAMS .....	363
G.1	Ozone absorption experiments .....	363
G.2	Dye ozonation experiments .....	369
G.3	Catalytic dye ozonation experiments .....	375
H	MODELING GRAPHS .....	381
H.1	Ozone absorption graphs .....	381
H.2	Dye ozonation graphs .....	386
I	BUBBLE AND CATALYST PROPERTIES .....	390
I.1	Bubble size graphs .....	390
I.2	Thermogravimetric Analysis (TGA) graphs .....	395
I.3	Order of magnitude analysis .....	397
	CURRICULUM VITAE .....	399

## LIST OF TABLES

### TABLES

Table 1.1	The characterization of the wastewaters taken from a textile plant in Bursa ..	2
Table 1.2	Treatment methods for textile wastewaters .....	6
Table 2.1	Rate constants of some organics with ozone or with $HO^{\bullet}$ .....	14
Table 2.2	The kinetic regime and enhancement factor as a function of $Ha$ for a second order reaction .....	24
Table 2.3	The ozonation studies that used alumina as the catalyst .....	34
Table 2.4	The $pH_{PZC}$ values of different alumina types .....	36
Table 4.1	The main properties of activated alumina .....	68
Table 4.2	Differential screen analysis of alumina particles .....	71
Table 4.3	The characterization of alumina and PFOA .....	71
Table 4.4	The variables in the semi-batch experiments .....	74
Table 4.5	Independent variables of the ozone absorption experiments in the FBR .....	78
Table 4.6	Variables for non-catalytic and catalytic ozonation experiments in FBR .....	82
Table 5.1	Dye removal percentages for <i>AR-151</i> and <i>RBBR</i> for different pH values and catalyst types. Conditions: $C_{D,i} = 200$ mg/L, $T = 25^{\circ}C$ , stirrer rate = 300 rpm, $Q_G = 150$ L/h, $D_{O_3} = 46.04$ mmol/h, reaction time = 30 min .....	90
Table 5.2	COD removal percentages of <i>AR-151</i> or <i>RBBR</i> by ozonation with 100% PFOA catalyst. Conditions: $T = 25^{\circ}C$ , stirrer rate = 300 rpm, $Q_G = 150$ L/h, reaction time = 30 min .....	93
Table 5.3	Pseudo-first order and overall kinetic constants for <i>AR-151</i> or <i>RBBR</i> , in cases of sole ozonation and catalytic ozonation. Conditions: $C_{D,i} = 200$ mg/L, $D_{O_3} = 46.04$ mmol/h, $m_{cat} = 5$ g, $Q_G = 150$ L/h, $T = 25^{\circ}C$ , stirrer rate = 300 rpm .....	98
Table 5.4	Effect of ozone dose and initial dye concentration on kinetic constant in catalytic ozonation of <i>AR-151</i> or <i>RBBR</i> . Conditions: $Q_G = 150$ L/h, $T = 25^{\circ}C$ , stirrer rate = 300 rpm .....	99

Table 5.5	Calculated results from the data. Conditions: Tracer = <i>RBBR</i> , tracer concentration = 4 mg/L, $T = 20.3^{\circ}\text{C}$ .....	101
Table 5.6	Calculated results from the residence time distribution data. Conditions: Tracer = <i>RBBR</i> , tracer concentration = 4 mg/L, $T = 20.3^{\circ}\text{C}$ .....	103
Table 5.7	Minimum fluidization velocities at the studied gas velocities. Catalyst = PFOA, $m_{cat} = 25$ g, $d_{cat} = 2.0$ mm .....	106
Table 5.8	The calculated gas and liquid hold-up values for the experiments. $A = 5.02 \times 10^{-3}$ m <sup>2</sup> , $\rho_{cat}$ : 1300 kg/m <sup>3</sup> for PFOA, $\rho_{cat}$ : 2580 kg/m <sup>3</sup> for alumina .....	108
Table 5.9	The calculated gas, liquid and solid phase hold-up values under different operating conditions.....	109
Table 5.10	Hydraulic retention time of liquid in the bed at different $Q_L$ . Effective reactor volume, $V_{R,eff} = 5.02$ L .....	112
Table 5.11	Experimental and theoretical outlet gas O <sub>3</sub> concentrations at different gas and liquid flow rates. Conditions: $T = (22.0 \pm 0.9)^{\circ}\text{C}$ , $C_{O_3,G,in} = (0.306 \pm 0.017)$ mmol O <sub>3</sub> /L gas, particles = none .....	114
Table 5.12	$D_L$ and $k_La$ values at different gas and liquid flow rates. Conditions: $T = (22.0 \pm 0.9)^{\circ}\text{C}$ , $C_{O_3,G,in} = (0.306 \pm 0.017)$ mmol O <sub>3</sub> /L gas, catalyst = none .	115
Table 5.13	$D_L$ and $k_La$ values for different catalyst loadings. Conditions: $Q_G = 150$ L/h, $Q_L = 30$ L/h, $T = (22.0 \pm 0.9)^{\circ}\text{C}$ , $C_{O_3,Gi} = (0.306 \pm 0.017)$ mmol O <sub>3</sub> /L gas, no dye in the medium, un-fluidized bed, $u_{L,min} = 130$ L/h for alumina, $u_{L,min} = 110$ L/h for PFOA. ....	117
Table 5.14	$D_L$ and $k_La$ values for different catalyst dosages. Conditions: $Q_G = 150$ L/h, $Q_L = 150$ L/h, pH = 2.5, $T = (22.0 \pm 0.9)^{\circ}\text{C}$ , $C_{O_3,Gi} = (43.2 \pm 1.4)$ mg O <sub>3</sub> /L gas, no dye in the medium, $d_{cat} = 2.0$ mm, fluidized bed, $u_{L,min} = 130$ L/h for alumina, $u_{L,min} = 110$ L/h for PFOA, $H_E = 13.4$ cm, $H_S = 7.5$ cm .	118
Table 5.15	Ozone doses applied in the experiments. $C_{O_3,G,in} = 0.306 \pm 0.017$ mmol O <sub>3</sub> /L gas .....	125
Table 5.16	Calculated $R_{cons,O_3}$ and $U_{O_3}$ for the dyes. $Q_G = 150$ L/h, $Q_L = 30$ L/h. $Appl_{O_3} = 1.531$ mmol/L liq .....	127
Table 5.17	Calculated $R_{cons,O_3}$ and $U_{O_3}$ for the dyes. $Q_G = 70$ L/h, $Q_L = 30$ L/h. $Appl_{O_3} = 0.715$ mmol/L liq .....	128

Table 5.18 Calculated $R_{cons,O_3}$ and $U_{O_3}$ for the dyes. $Q_G=30$ L/h, $Q_L=30$ L/h. $Appl_{O_3}$ = 0.314 mmol/L liq .....	128
Table 5.19 % TOC Removals and $O_3$ consumption values at different gas and liquid flow rates. Conditions: pH = 2.51, $T = 22.0^\circ\text{C}$ , $C_{O_3,G,in} = 0.306 \pm 0.017$ mmol $O_3$ /L gas, $z = 0.88$ m, particles= none .....	130
Table 5.20 Calculated $R_{cons,O_3}$ and $U_{O_3}$ for the dyes. $Q_G=70$ L/h, $Q_L=70$ L/h. $Appl_{O_3}$ = 0.306 mmol/L liq .....	131
Table 5.21 Calculated $R_{cons,O_3}$ and $U_{O_3}$ for the dyes. $Q_G=70$ L/h, $Q_L=250$ L/h. $Appl_{O_3}$ = 0.085 mmol/L liq .....	131
Table 5.22 The effect of inlet ozone concentration in the gas on dye, TOC removal And $Cons_{O_3}$ . $Q_G= 70$ L/h, $Q_L= 30$ L/h, $C_{D,in} = 19.2 \times 10^{-2}$ mmol/L for <i>RBBR</i> , $C_{D,in} = 26.4 \times 10^{-2}$ mmol/L for <i>AR-151</i> , pH=2.5 .....	132
Table 5.23 The effect of inlet ozone concentration in the gas on dye, TOC removal and $O_3$ consumption. $Q_G= 70$ L/h, $Q_L= 30$ L/h, $C_{D,in} = 4.8 \times 10^{-2}$ mmol/L for <i>RBBR</i> , $C_{D,in} = 6.6 \times 10^{-2}$ mmol/L for <i>AR-151</i> , pH=2.5 .....	132
Table 5.24 The effect of $Q_G$ and $Q_L$ on TOC removal and $O_3$ consumption. Conditions: $Q_G/Q_L = 1.0$ , pH = 2.51, $T = 22.0^\circ\text{C}$ , $C_{O_3,G,in} = 0.306 \pm 0.017$ mmol $O_3$ / L gas, $z = 0.88$ m, particles= none .....	135
Table 5.25 Calculated $R_{cons,O_3}$ and $U_{O_3}$ at different $Q_G$ and $Q_L$ . Conditions: $Q_G/Q_L =$ 1.0, Dye = <i>RBBR</i> , pH = 2.54, $T = 22.3^\circ\text{C}$ , $C_{O_3,G,in} = 0.306 \pm 0.017$ mmol $O_3$ /L gas, no catalyst, $C_{D,in} = 4.8 \times 10^{-2}$ mmol/L .....	135
Table 5.26 Calculated $R_{cons,O_3}$ and $U_{O_3}$ at different $Q_G$ and $Q_L$ . Conditions: $Q_G/Q_L = 1.0$ , Dye = <i>AR-151</i> , pH = 2.54, $T = 22.3^\circ\text{C}$ , $C_{O_3,G,in} = 0.306 \pm 0.017$ mmol $O_3$ / L gas, no catalyst, $C_{D,in} = 6.6 \times 10^{-2}$ mmol/L .....	135
Table 5.27 Dye and TOC removal percentages with inlet ozone consumptions at different catalyst dosages. $Q_G = 150$ L/h, $Q_L = 150$ L/h, pH= 2.5, $C_{O_3,G,in}$ $= 0.92 \pm 0.09$ mmol/L gas, $d_{cat} = 2.0$ mm, reactor =FBR, $H_S = 7.5$ cm, (a) for catalyst = Alumina, $u_{L,min} = 130$ L/h, $H_E = 12.6$ cm, (b) for catalyst =PFOA, $u_{L,min} = 110$ L/h, $H_E = 13.4$ cm. ....	154

Table 5.28 O <sub>3</sub> consumption rates and utilization ratios at different catalyst dosages. $Q_G = 150$ L/h, $Q_L = 150$ L/h, pH= 2.5, $C_{O_3,G,in} = 0.92\pm 0.09$ mmol/L gas, $d_{cat} = 2.0$ mm, reactor =FBR, $H_S = 7.5$ cm, (a) for catalyst = Alumina, $u_{L,min} = 130$ L/h, $H_E = 12.6$ cm, (b) for catalyst =PFOA, $u_{L,min} = 110$ L/h, $H_E = 13.4$ cm. ....	155
Table 5.29 Dye and TOC removal percentages with ozone consumption at different particle sizes. $Q_G = 150$ L/h, $Q_L = 150$ L/h, pH= 2.5, $C_{O_3,G,i} = 0.92\pm 0.09$ mmol/L gas, $m_{cat} = 125$ g .....	161
Table 5.30 Reproducibility of the experiments as dye removal, TOC removal and O <sub>3</sub> consumption. Dye = RBBR, pH=2.5, $Q_G = 150$ L/h, $Q_L = 150$ L/h, $C_{D,i} = 6.6 \times 10^{-2}$ mmol/L, $C_{O_3,G,i} = 0.92 \pm 0.02$ mmol O <sub>3</sub> /L gas, $z =$ 0.88 m, no catalyst .....	162
Table 5.31 Reproducibility of the experiments as dye removal,TOC removal and O <sub>3</sub> consumption. Dye = AR-151, pH = 2.5, $Q_G = 150$ L/h, $Q_L = 150$ L/h, $C_{D,i} = 26.4 \times 10^{-2}$ mmol/L, $C_{O_3,G,i} = 0.92\pm 0.02$ mmol O <sub>3</sub> /L gas, $z = 0.88$ m, no catalyst .....	162
Table 5.32 Reproducibility of the FBR experiments as dye removal, TOC removal and O <sub>3</sub> consumption. pH = 2.5, $Q_G = 150$ L/h, $Q_L = 150$ L/h, $C_{O_3,G,in} = 0.92$ $\pm 0.02$ mmol O <sub>3</sub> /L gas, $z = 0.88$ m, $m_{cat} = 125$ g, $d_{cat} = 2.0$ mm .....	163
Table 5.33 The effect of $Q_L$ on dye and TOC removal. Conditions: $Q_G = 150$ L/h, pH= 2.5, $C_{O_3,G,in} = 0.92\pm 0.09$ mmol/L gas, $C_{D,in} = 4.8 \times 10^{-2}$ mmol/L for RBBR, $C_{D,in} = 6.6 \times 10^{-2}$ mmol/L for AR-151, $m_{cat} = 125$ g, $d_{cat} = 2.0$ mm, reactor = FBR, $H_S = 7.5$ cm, at $Q_L = 230$ L/h, (a) for catalyst = Alumina, $u_{L,min} = 130$ L/h, $H_E = 15.9$ cm, (b) for catalyst =PFOA, $u_{L,min} = 110$ L/h, $H_E = 17.2$ cm. ..	164
Table 5.34 The effect of $Q_L$ on dye and TOC removal. Conditions: $Q_G = 150$ L/h, pH= 2.5, $C_{O_3,G,in} = 0.92\pm 0.09$ mmol/L gas, $C_{D,in} = 19.2 \times 10^{-2}$ mmol/L for RBBR, $C_{D,in} = 26.4 \times 10^{-2}$ mmol/L for AR-151, $m_{cat} = 125$ g, $d_{cat} = 2.0$ mm, reactor = FBR, $H_S = 7.5$ cm, at $Q_L = 230$ L/h, (a) for catalyst = Alumina, $u_{L,min} = 130$ L/h, $H_E = 15.9$ cm, (b) for catalyst =PFOA, $u_{L,min} = 110$ L/h, $H_E = 17.2$ cm....	165
Table 5.35 The effect of $Q_L$ on TOC removal increase. Conditions: $Q_G = 150$ L/h, pH= 2.5, $C_{O_3,G,in} = 0.92\pm 0.09$ mmol/L gas, $m_{cat} = 125$ g, $d_{cat} = 2.0$ mm, reactor = FBR, $H_S = 7.5$ cm, at $Q_L = 230$ L/h, (a) for catalyst = Alumina, $u_{L,min} = 130$ L/h, $H_E = 15.9$ cm, (b) for catalyst =PFOA, $u_{L,min} = 110$ L/h, $H_E = 17.2$ cm ...	165

Table 5.36 The effect of pH on the $R_{cons,O_3}$ and $U_{O_3}$ for the dyes. Conditions: $Q_G=150$ L/h, $Q_L=150$ L/h, $C_{O_3,G,in}=0.92\pm 0.09$ mmol/L gas, $C_{D,in}=19.2\times 10^{-2}$ mmol /L for <i>RBBR</i> , $C_{D,in}=26.4\times 10^{-2}$ mmol/L for <i>AR-151</i> , $m_{cat}=125$ g, $d_{cat}=2.0$ mm, reactor = FBR, $H_S=7.5$ cm, at $Q_L=230$ L/h, (a) for catalyst = alumina, $u_{L,min}=130$ L/h, $H_E=12.6$ cm, (b) for catalyst = <i>PFOA</i> , $u_{L,min}=110$ L/h, $H_E=13.4$ cm .....	167
Table 5.37 The effect of catalyst dosage on the TOC removal and $Cons_{O_3}$ . Conditions: $Q_G=150$ L/h, $Q_L=150$ L/h, pH=2.5, $C_{O_3,G,in}=1.42\pm 0.13$ mmol/L gas, $C_{D,in}$ $=22.4\times 10^{-2}$ mmol/L for <i>RBBR</i> , $C_{D,in}=26.4\times 10^{-2}$ mmol/L for <i>AR-151</i> , reactor = FBR, $H_S=7.5$ cm, for catalyst = Alumina, $u_{L,min}=130$ L/h, $H_E=$ 12.6 cm, for catalyst = <i>PFOA</i> , $u_{L,min}=110$ L/h, $H_E=13.4$ cm.....	171
Table 5.38 Calculated $R_{cons,O_3}$ and $U_{O_3}$ for the dyes. Conditions: $Q_G=150$ L/h, $Q_L=$ 150 L/h, pH=2.5, $C_{O_3,G,in}=1.42\pm 0.13$ mmol/L gas, $C_{D,in}=22.4\times 10^{-2}$ mmol /L for <i>RBBR</i> , $C_{D,in}=26.4\times 10^{-2}$ mmol/L for <i>AR-151</i> , reactor = FBR, $H_S=$ 7.5 cm, for catalyst = Alumina, $u_{L,min}=130$ L/h, $H_E=12.6$ cm, for catalyst = <i>PFOA</i> , $u_{L,min}=110$ L/h, $H_E=13.4$ cm.....	173
Table 5.39 The determined enhanced $k_{LA}$ and $E$ values at different conditions. No catalyst, $Q_G=150$ L/h, $Q_L=30$ L/h, $Q_G/Q_L=5.0$ .....	182
Table 5.40 The determined enhanced $k_{LA}$ and $E$ values at different conditions. No catalyst, $Q_G=70$ L/h, $Q_L=30$ L/h, $Q_G/Q_L=2.3$ .....	183
Table 5.41 The determined enhanced $k_{LA}$ and $E$ values at different conditions. No catalyst, $Q_G=70$ L/h, $Q_L=250$ L/h, $Q_G/Q_L=0.28$ .....	183
Table 5.42 The determined enhanced $k_{LA}$ and $E$ values at different conditions. Dye = <i>RBBR</i> , pH = 2.5, $Q_G=150$ L/h, $Q_L=150$ L/h, $Q_G/Q_L=1.0$ , $D_L=3.15\times$ $10^{-3}$ m <sup>2</sup> /s, $C_{O_3,G,in}=0.969$ mmol/L gas, $k_{LA}=7.6\times 10^{-2}$ s <sup>-1</sup> .....	186
Table 5.43 The determined enhanced $k_{LA}$ and $E$ values at different conditions. Dye = <i>AR-151</i> , pH = 2.5, $Q_G=150$ L/h, $Q_L=150$ L/h, $Q_G/Q_L=1.0$ , $D_L=3.15\times$ $10^{-3}$ m <sup>2</sup> /s, $C_{O_3,G,in}=0.969$ mmol/L gas, $k_{LA}=7.6\times 10^{-2}$ s <sup>-1</sup> .....	187
Table 5.44 The determined enhanced $k_{LA}$ and $E$ values at different conditions. $Q_G=$ 150 L/h, $Q_L=150$ L/h, $Q_G/Q_L=1.0$ , $D_L=3.15\times 10^{-3}$ m <sup>2</sup> /s, $C_{O_3,G,in}=$ 0.969 mmol/L gas, $m_{cat}=125$ g, $k_{LA}=7.6\times 10^{-2}$ s <sup>-1</sup> .....	190

Table 5.45 The values used in the modeling of catalytic ozonation reactions.

Conditions:  $Q_G = 150$  L/h,  $Q_L = 150$  L/h,  $T = (22.0 \pm 0.9)^\circ\text{C}$ ,  $C_{O_3,G,in} = 0.969$  mmol  $O_3$ /L gas, catalyst = Alumina,  $u_{L,min} = 130$  L/h,  $D_L = 3.15 \times 10^{-3}$  m<sup>2</sup>/s. .... 191

Table 5.46 The values used in the modeling of catalytic ozonation reactions.

Conditions:  $Q_G = 150$  L/h,  $Q_L = 150$  L/h,  $T = (22.0 \pm 0.9)^\circ\text{C}$ ,  $C_{O_3,G,in} = 0.969$  mmol  $O_3$ /L gas, catalyst = PFOA,  $u_{L,min} = 110$  L/h,  $D_L = 3.15 \times 10^{-3}$  m<sup>2</sup>/s. .... 191

## LIST OF FIGURES

### FIGURES

Figure 2.1 Kinetic regimes in a gas-liquid reaction .....	22
Figure 2.2 The surface charge of alumina changing with pH .....	35
Figure 2.3 The mechanism of ozonation with PFOA according to Kasprzyk-Hordern et al. ....	42
Figure 2.4 The stages of ozonation of organics .....	44
Figure 3.1 The resistances involved in the ozonation process in the three phase FBR ..	57
Figure 4.1 The chemical structures of the dyes used in the experiments .....	63
Figure 4.2 The semi-batch reactor .....	64
Figure 4.3 The configuration of the gas fritted discs .....	65
Figure 4.4 The configuration of the liquid distributor .....	66
Figure 4.5 The schematic diagram of the overall fluidized bed system (un-scaled) .....	67
Figure 4.6 Schematics of the fluidized bed column .....	69
Figure 4.7 The photograph of the fluidized bed column .....	70
Figure 5.1 Dye removal values with ozonation at different pH values. Conditions: $C_{D,i}=200$ mg/L; $T=25^{\circ}\text{C}$ ; stirrer rate=300 rpm; $Q_G=150$ L/h, $D_{O_3}=2.21$ g/h, reaction time=30 min. Bold shapes: <i>AR-151</i> ; apparent: <i>RBBR</i> .....	87
Figure 5.2 COD removal values obtained in ozonation for <i>AR-151</i> and <i>RBBR</i> at different pH values. Conditions: $C_{D,i}=200$ mg/L, $T=25^{\circ}\text{C}$ ; stirrer rate =300 rpm; $Q_G=150$ L/h, $D_{O_3}=2.21$ g/h, reaction time=30 min .....	89
Figure 5.3 The change of COD removal percentage for the dyes by catalytic ozonation. Conditions: $C_{D,i}=200$ mg/L, $T=25^{\circ}\text{C}$ ; stirrer rate=300 rpm; $Q_G=150$ L/h, $D_{O_3}=2.21$ g/h, reaction time=30 min. Bold shapes: <i>AR-151</i> ; apparent: <i>RBBR</i> .....	91
Figure 5.4 The effect of ozone dose on the dye removal. Conditions: catalyst=100% PFOA, $C_{D,i}=100$ mg/L, $T=25^{\circ}\text{C}$ ; stirrer rate=300 rpm; $Q_G=150$ L/h, reaction time=30 min. Bold shapes: <i>AR-151</i> , pH 2.5; apparent: <i>RBBR</i> , pH 7 .....	93

Figure 5.5 The effect of initial dye concentration on the dye removal. Conditions: Catalyst=100% PFOA, $D_{O_3} = 2.21$ g/h, $T=25^\circ\text{C}$ ; stirrer rate=300 rpm; $Q_G=150\text{L/h}$ , reaction time=30 min. Bold shapes: <i>AR-151</i> , pH 2.5; apparent : <i>RBBR</i> , pH 7 .....	94
Figure 5.6 The pseudo-first order kinetic constants of <i>AR-151</i> . Conditions: ozonation only; $C_{D,i} = 200$ mg/L, $D_{O_3} = 46.04$ mmol/h, $Q_G=150\text{L/h}$ , $T=25^\circ\text{C}$ , stirrer rate=300 rpm .....	96
Figure 5.7 The pseudo-first order kinetic constants of <i>RBBR</i> . Conditions: ozonation only; $C_{D,i} = 200$ mg/L, $D_{O_3} = 46.04$ mmol/h, $Q_G=150\text{L/h}$ , $T=25^\circ\text{C}$ , stirrer rate=300 rpm .....	96
Figure 5.8 The pseudo-first order kinetic constants of <i>AR-151</i> at different treatment methods. Conditions: $C_{D,i} = 200$ mg/L, $D_{O_3} = 46.04$ mmol/h, $m_{cat}=5$ g, $Q_G=150$ L/h, $T=25^\circ\text{C}$ , stirrer rate =300 rpm .....	97
Figure 5.9 The pseudo-first order kinetic constants of <i>RBBR</i> at different treatment methods. Conditions: $C_{D,i} = 200$ mg/L, $D_{O_3} = 2.21$ g/h, $m_{cat}=5$ g, $Q_G = 150$ L/h, $T=25^\circ\text{C}$ , stirrer rate =300 rpm .....	97
Figure 5.10 The effect of superficial liquid velocity on the residence time distribution without the catalyst particles ( $u_G=5.5\times 10^{-3}$ m/s) Conditions: Tracer = <i>RBBR</i> , tracer concentration = 4 mg/L, $T = 20.3^\circ\text{C}$ . .....	101
Figure 5.11 Effect of superficial liquid velocity on axial dispersion coefficient, $D_L$ in the gas-liquid system. Conditions: Tracer = <i>RBBR</i> , tracer concentration = 4 mg/L, $T = 20.3^\circ\text{C}$ .....	102
Figure 5.12 The effect of superficial liquid velocity on the residence time distribution with the catalyst particles ( $u_G=5.5\times 10^{-3}$ m/s). Conditions: Tracer = <i>RBBR</i> , tracer concentration = 4 mg/L, $T = 20.3^\circ\text{C}$ .....	103
Figure 5.13 Effect of superficial liquid velocity on axial dispersion coefficient, $D_L$ in the gas-liquid-solid system. Conditions: Tracer = <i>RBBR</i> , tracer concentration = 4 mg/L, $T = 20.3^\circ\text{C}$ .....	104
Figure 5.14 Pressure drop versus superficial liquid velocity for different superficial gas velocities. Catalyst = PFOA, $m_{cat} = 25$ g, $d_{cat} = 2.0$ mm .....	105
Figure 5.15 Pressure drop versus superficial liquid velocity for different superficial gas velocities. Catalyst = alumina, $m_{cat} = 25$ g, $d_{cat} = 2.0$ mm .....	106

Figure 5.16 Pressure drop versus superficial liquid velocity for different catalyst dosages. Catalyst = PFOA, $m_{cat} = 25$ g, $d_{cat} = 2.0$ mm .....	107
Figure 5.17 Pressure drop versus superficial liquid velocity for different catalyst dosages. $Q_G = 150$ L/h, catalyst = alumina, $d_{cat} = 2.0$ mm .....	108
Figure 5.18 Steady-state $C_{O_3,L}$ at different gas flow rates. Conditions: $Q_L = 30$ L/h, $T = (22.0 \pm 0.9)^\circ\text{C}$ , $C_{O_3,G,in} = (0.306 \pm 0.017)$ mmol $\text{O}_3/\text{L}$ gas, particles = none .....	112
Figure 5.19 $C_{O_3,L}$ at different liquid flow rates. Conditions: $Q_G = 100$ L/h, $T = (22.0 \pm 0.9)^\circ\text{C}$ , $C_{O_3,G,in} = (0.306 \pm 0.017)$ mmol $\text{O}_3/\text{L}$ gas, particles = none .....	113
Figure 5.20 The comparison of theoretical and experimental steady state liquid phase ozone concentrations for the best fit of $D_L$ and $k_L a$ values. Conditions: $Q_G = 150$ L/h, $Q_L = 30$ L/h, $T = 23^\circ\text{C}$ , $C_{O_3,G,in} = 0.298$ mmol $\text{O}_3/\text{L}$ gas, particles = none, $D_L = 1.2 \times 10^{-3}$ $\text{m}^2/\text{s}$ , $k_L a = 9.6 \times 10^{-2}$ $\text{s}^{-1}$ .....	114
Figure 5.21 The relationship between $k_L a$ and $u_G$ at $Q_L = 30$ L/h in the gas ( $\text{O}_3$ )-liquid (water) system .....	116
Figure 5.22 The comparison of theoretical and experimental steady state liquid phase ozone concentrations for the best fit of $D_L$ and $k_L a$ values. Conditions: $Q_G = 150$ L/h, $Q_L = 30$ L/h, $T = 23^\circ\text{C}$ , $C_{O_3,G,in} = 0.298$ mmol $\text{O}_3/\text{L}$ gas, Catalyst = alumina, $m_{cat} = 25$ g, $D_L = 0.98 \times 10^{-3}$ $\text{m}^2/\text{s}$ , $k_L a = 9.8 \times 10^{-2}$ $\text{s}^{-1}$ .....	117
Figure 5.23 Dissolved ozone concentration curves for different catalyst dosages in the column. $Q_G = 150$ L/h, $Q_L = 150$ L/h, catalyst = alumina, $\text{pH} = 2.5$ , $T = (22.0 \pm 0.9)^\circ\text{C}$ , $C_{O_3,G,in} = (43.2 \pm 1.4)$ mg $\text{O}_3/\text{L}$ gas, no dye in the medium, $d_{cat} = 2.0$ mm .....	118
Figure 5.24 Dissolved ozone concentration curves for different catalyst dosages in the column. $Q_G = 150$ L/h, $Q_L = 150$ L/h, catalyst = PFOA, $\text{pH} = 2.5$ , $T = (22.0 \pm 0.9)^\circ\text{C}$ , $C_{O_3,G,in} = (43.2 \pm 1.4)$ mg $\text{O}_3/\text{L}$ gas, no dye in the medium, $d_{cat} = 2.0$ mm .....	119
Figure 5.25 $C_D/C_{D,in}$ and $C_{O_3,L}$ at different $C_{D,in}$ . Conditions: $Q_G = 150$ L/h, $Q_L = 30$ L/h, $\text{pH} = 2.54$ , $T = 22.3^\circ\text{C}$ , $C_{O_3,G,in} = 0.306 \pm 0.017$ mmol $\text{O}_3/\text{L}$ gas, no catalyst. Solid lines: $C_D/C_{D,in}$ , dashed lines: $C_{O_3,L}$ , (a): <i>RBBR</i> , (b): <i>AR-151</i> .....	121

Figure 5.26 $C_D/C_{D,in}$ and $C_{O_3,L}$ at different $C_{D,in}$ . Conditions: $Q_G = 70$ L/h, $Q_L = 30$ L/h, pH = 2.54, $T = 22.3^\circ\text{C}$ , $C_{O_3,G,in} = 0.306 \pm 0.017$ mmol $\text{O}_3/\text{L}$ gas, no catalyst. Solid lines: $C_D/C_{D,in}$ , dashed lines: $C_{O_3,L}$ , (a): <i>RBBR</i> , (b): <i>AR-151</i> .....	122
Figure 5.27 The effect $Q_G$ on dye, TOC removal and $\text{O}_3$ consumption at different $C_{D,in}$ . Conditions: $Q_L = 30$ L/h, pH = 2.51, $T = 22.0^\circ\text{C}$ , $C_{O_3,G,in} = 0.306 \pm 0.017$ mmol $\text{O}_3/\text{L}$ gas, $z = 0.88$ m, particles= none, (a): <i>RBBR</i> , (b): <i>AR-151</i> .....	126
Figure 5.28 The effect of liquid flow rate on dye, TOC removal and $\text{O}_3$ consumption. Conditions: $Q_G = 70$ L/h, pH = 2.51, $T = 22.0^\circ\text{C}$ , $C_{O_3,G,in} = 0.306 \pm 0.017$ mmol $\text{O}_3/\text{L}$ gas, $z = 0.88$ m, particle= no, (a) <i>RBBR</i> , (b) <i>AR-151</i> .....	129
Figure 5.29 $C_D/C_{D,in}$ ratio for different $Q_G$ and $Q_L$ . Conditions: $Q_G/Q_L = 1.0$ , Dye = <i>RBBR</i> , pH = 2.54, $T = 22.3^\circ\text{C}$ , $C_{O_3,G,in} = 0.306 \pm 0.017$ mmol $\text{O}_3/\text{L}$ gas, no catalyst. Solid lines: for $C_{D,in} = 4.8 \times 10^{-2}$ mmol/L, dashed lines: for $C_{D,in} = 19.2 \times 10^{-2}$ mmol/L .....	134
Figure 5.30 $C_D/C_{D,in}$ ratio for different $Q_G$ and $Q_L$ . Conditions: $Q_G/Q_L = 1.0$ , Dye = <i>AR-151</i> , pH=2.54, $T=22.3^\circ\text{C}$ , $C_{O_3,G,in} = 0.306 \pm 0.017$ mmol $\text{O}_3/\text{L}$ gas, no catalyst. Solid lines: for $C_{D,in} = 6.6 \times 10^{-2}$ mmol/L, dashed lines: for $C_{D,in} = 26.4 \times 10^{-2}$ mmol/L .....	134
Figure 5.31 The by-products at different $C_{D,in}$ . Conditions: $Q_G = 150$ L/h, $Q_L = 30$ L/h, pH = 2.54, $T = 22.3^\circ\text{C}$ , $C_{O_3,G,in} = 0.306 \pm 0.017$ mmol $\text{O}_3/\text{L}$ gas, no catalyst. Solid lines: <i>RBBR</i> , dashed lines: <i>AR-151</i> , (a) OA, (b) AA, (c) GA .....	138
Figure 5.32 The by-products at different $Q_G$ . Conditions: $C_{D,in} = 4.8 \times 10^{-2}$ mmol/L for <i>RBBR</i> , $C_{D,in} = 6.6 \times 10^{-2}$ mmol/L for <i>AR-151</i> , $Q_L = 30$ L/h, pH = 2.54, $T = 22.3^\circ\text{C}$ , $C_{O_3,G,in} = 0.306 \pm 0.017$ mmol $\text{O}_3/\text{L}$ gas, no catalyst. Solid lines: <i>RBBR</i> , dashed lines: <i>AR-151</i> , (a) OA, (b) AA, (c) GA.....	139
Figure 5.33 The by-products at different $Q_L$ . Conditions: $C_{D,in} = 4.8 \times 10^{-2}$ mmol/L for <i>RBBR</i> , $C_{D,in} = 6.6 \times 10^{-2}$ mmol/L for <i>AR-151</i> , $Q_G = 70$ L/h, pH = 2.54, $T = 22.3^\circ\text{C}$ , $C_{O_3,G,in} = 0.306 \pm 0.017$ mmol $\text{O}_3/\text{L}$ gas, no catalyst. Solid lines: <i>RBBR</i> , dashed lines: <i>AR-151</i> , (a) OA, (b) AA .....	140
Figure 5.34 The by-products at different $C_{O_3,G,in}$ . Conditions: $C_{D,in} = 4.8 \times 10^{-2}$ mmol/L for <i>RBBR</i> , $C_{D,in} = 6.6 \times 10^{-2}$ mmol/L for <i>AR-151</i> , $Q_G = 70$ L/h, $Q_L = 30$ L/h, pH = 2.54, $T = 22.3^\circ\text{C}$ , no catalyst. Solid lines: <i>RBBR</i> , dashed lines: <i>AR-151</i> , (a) OA, (b) AA, (c) GA .....	142

Figure 5.35 The by-products at different $Q_G$ and $Q_L$ . Conditions: $C_{D,in}=4.8\times 10^{-2}$ mmol/L for <i>RBBR</i> , $C_{D,in}=6.6\times 10^{-2}$ mmol/L for <i>AR-151</i> , $C_{O_3,G,in} = 0.306 \pm 0.017$ mmol $O_3$ / L gas, pH = 2.54, T = 22.3°C, particles = none. Solid lines: <i>RBBR</i> , dashed lines: <i>AR-151</i> , (a) OA, (b) AA .....	143
Figure 5.36 The effect of catalyst dosage on the dye removal and dissolved $O_3$ concentration. Conditions: $Q_G = 150$ L/h, $Q_L = 150$ L/h, dye = <i>RBBR</i> , pH = 2.5, $C_{O_3,G,in} = 0.92\pm 0.09$ mmol/L gas, catalyst = alumina, $d_{cat} = 2.0$ mm, (a) for $C_{D,in} = 4.8\times 10^{-2}$ mmol/L, (b) for $C_{D,in} = 19.2\times 10^{-2}$ mmol/L, $u_{L,min} = 130$ L/h, $H_E=12.6$ cm, $H_S=7.5$ cm .....	145
Figure 5.37 The effect of catalyst dosage on the dye removal and dissolved $O_3$ concentration. Conditions: $Q_G = 150$ L/h, $Q_L = 150$ L/h, dye = <i>RBBR</i> , pH = 2.5, $C_{O_3,G,in} = 0.92\pm 0.09$ mmol/L gas, catalyst = PFOA, $d_{cat} = 2.0$ mm, (a) for $C_{D,in} = 4.8\times 10^{-2}$ mmol/L, (b) for $C_{D,in} = 19.2\times 10^{-2}$ mmol/L, $u_{L,min} = 110$ L/h, $H_E=13.4$ cm, $H_S=7.5$ cm. ....	146
Figure 5.38 The effect of catalyst dosage on the dye removal and dissolved $O_3$ concentration. Conditions: $Q_G = 150$ L/h, $Q_L = 150$ L/h, dye = <i>AR-151</i> , pH = 2.5, $C_{O_3,G,in} = 0.92\pm 0.09$ mmol/L gas, catalyst = alumina, $d_{cat} = 2.0$ mm, (a) for $C_{D,in} = 6.6\times 10^{-2}$ mmol/L, (b) for $C_{D,in} = 26.4\times 10^{-2}$ mmol/L, $u_{L,min} = 130$ L/h, $H_E=12.6$ cm, $H_S=7.5$ cm.....	147
Figure 5.39 The effect of catalyst dosage on the dye removal and dissolved $O_3$ concentration. Conditions: $Q_G = 150$ L/h, $Q_L = 150$ L/h, dye = <i>AR-151</i> , pH = 2.5, $C_{O_3,G,in} = 0.92\pm 0.09$ mmol/L gas, catalyst = PFOA, $d_{cat} = 2.0$ mm, (a) for $C_{D,in} = 6.6\times 10^{-2}$ mmol/L, (b) for $C_{D,in} = 26.4\times 10^{-2}$ mmol/L, $u_{L,min} = 110$ L/h, $H_E=13.4$ cm, $H_S=7.5$ cm .....	148
Figure 5.40 The comparison of dye and TOC removals in the presence or absence of a radical scavenger. Dye = <i>RBBR</i> , T = 25°C, Scavenger = Carbonate, $C_{D,i} = 0.16$ mmol/L, catalyst = Alumina, $m_{cat}= 10$ g, pH = 2.5, reactor= Semi-batch .....	149
Figure 5.41 The comparison of dye and TOC removals in the presence or absence of a radical scavenger. Dye = <i>AR-151</i> , T = 25°C, Scavenger = Carbonate, $C_{D,i} = 0.16$ mmol/L, catalyst = Alumina, $m_{cat}=10$ g,pH = 2.5, reactor= Semi-batch .....	150

- Figure 5.42 The effect of catalyst dosage on the dye removal, TOC removal and O<sub>3</sub> consumption. Conditions:  $Q_G = 150$  L/h,  $Q_L = 150$  L/h, Dye = *RBBR*,  $C_{D,in} = 4.8 \times 10^{-2}$  mmol/L, pH= 2.5,  $C_{O_3,G,in} = 0.92 \pm 0.09$  mmol/L gas,  $d_{cat} = 2.0$  mm, reactor = FBR,  $H_S = 7.5$  cm. (a) for catalyst = Alumina,  $u_{L,min} = 130$  L/h,  $H_E = 12.6$  cm, (b) for catalyst = *PFOA*,  $u_{L,min} = 110$  L/h,  $H_E = 13.4$  cm. .. 151
- Figure 5.43 The effect of catalyst dosage on the dye removal, TOC removal and O<sub>3</sub> consumption. Conditions:  $Q_G = 150$  L/h,  $Q_L = 150$  L/h, Dye = *AR-151*,  $C_{D,in} = 6.6 \times 10^{-2}$  mmol/L, pH= 2.5,  $C_{O_3,G,in} = 0.92 \pm 0.09$  mmol/L gas,  $d_{cat} = 2.0$  mm, reactor = FBR,  $H_S = 7.5$  cm, (a) for catalyst = Alumina,  $u_{L,min} = 130$  L/h,  $H_E = 12.6$  cm, (b) for catalyst = *PFOA*,  $u_{L,min} = 110$  L/h,  $H_E = 13.4$  cm.... 152
- Figure 5.44 The adsorption of *RBBR* and *AR-151* dyes on alumina or *PFOA*. pH= 3.6,  $C_{D,i} = 15$  mg/L, T=25°C,  $m_{cat} = 2$  g, reactor = Semi-batch ..... 157
- Figure 5.45 The effect of catalyst particle size on the dye removal. Conditions: Dye = *RBBR*,  $Q_G = 150$  L/h,  $Q_L = 150$  L/h, pH= 2.5,  $C_{O_3,G,in} = 0.92 \pm 0.09$  mmol/L gas, catalyst = alumina, (a)  $C_{D,in} = 4.8 \times 10^{-2}$  mmol/L, (b)  $C_{D,in} = 19.2 \times 10^{-2}$  mmol/L; solid lines with dark marks: for  $C_D/C_{D,in}$ ; dashed lines with light marks: for  $C_{O_3,L}$  ..... 158
- Figure 5.46 The effect of catalyst particle size on the dye removal. Conditions: Dye = *RBBR*,  $Q_G = 150$  L/h,  $Q_L = 150$  L/h, pH= 2.5,  $C_{O_3,G,in} = 0.92 \pm 0.09$  mmol/L gas, catalyst = *PFOA*, (a)  $C_{D,in} = 4.8 \times 10^{-2}$  mmol/L, (b)  $C_{D,in} = 19.2 \times 10^{-2}$  mmol/L; solid lines with dark marks: for  $C_D/C_{D,in}$ ; dashed lines with light marks: for  $C_{O_3,L}$  ..... 159
- Figure 5.47 The effect of catalyst particle size on the dye removal. Conditions: Dye = *AR-151*,  $Q_G = 150$  L/h,  $Q_L = 150$  L/h, pH= 2.5,  $C_{O_3,G,in} = 0.92 \pm 0.09$  mmol/L gas,  $C_{D,in} = 6.6 \times 10^{-2}$  mmol/L; (a) catalyst = alumina, (b) catalyst=*PFOA*, solid lines with dark marks: for  $C_D/C_{D,in}$ ; dashed lines with light marks: for  $C_{O_3,L}$  ..... 160
- Figure 5.48 The effect of pH on dye, TOC removals and O<sub>3</sub> consumption. Conditions: Dye=*RBBR*,  $Q_G = 150$  L/h,  $Q_L = 150$  L/h,  $C_{O_3,G,in} = 0.92 \pm 0.09$  mmol/L gas,  $C_{D,in} = 19.2 \times 10^{-2}$  mmol/L,  $m_{cat} = 125$  g,  $d_{cat} = 2.0$  mm, (a) no cat., (b) alumina, (c) *PFOA*, reactor = FBR,  $H_S = 7.5$  cm, for catalyst = Alumina,  $u_{L,min} = 130$  L/h,  $H_E = 12.6$  cm, for catalyst = *PFOA*,  $u_{L,min} = 110$  L/h,  $H_E = 13.4$  cm. .... 168

Figure 5.49 The effect of pH on dye, TOC removals and O <sub>3</sub> consumption. Conditions: Dye=AR-151, Q <sub>G</sub> = 150 L/h, Q <sub>L</sub> = 150 L/h, C <sub>O<sub>3,G,in</sub></sub> = 0.92±0.09 mmol/L gas, C <sub>D,in</sub> = 26.4× 10 <sup>-2</sup> mmol/L, m <sub>cat</sub> = 125 g, d <sub>cat</sub> = 2.0 mm, (a) no cat., (b) alumina, (c) PFOA, reactor =FBR, H <sub>S</sub> =7.5 cm, for catalyst = Alumina, u <sub>L,min</sub> =130 L/h, H <sub>E</sub> =12.6 cm, for catalyst =PFOA, u <sub>L,min</sub> =110 L/h, H <sub>E</sub> = 13.4 cm. ....	169
Figure 5.50 The effect of catalyst dose on the dye removal. Conditions: Q <sub>G</sub> =150 L/h, Q <sub>L</sub> =150 L/h, pH=2.5, C <sub>O<sub>3,G,in</sub></sub> =1.42±0.13 mmol/L gas, C <sub>D,in</sub> = 22.4×10 <sup>-2</sup> mmol/L for RBBR, C <sub>D,in</sub> = 26.4×10 <sup>-2</sup> mmol/L for AR-151, (a) alumina, (b) PFOA, reactor =FBR, H <sub>S</sub> =7.5 cm, for catalyst = Alumina, u <sub>L,min</sub> =130 L/h, H <sub>E</sub> =12.6 cm, for catalyst =PFOA, u <sub>L,min</sub> =110 L/h, H <sub>E</sub> =13.4 cm. ....	171
Figure 5.51 FT-IR spectra of fresh calcined alumina .....	175
Figure 5.52 FT-IR spectra of fresh PFOA .....	175
Figure 5.53 FT-IR spectra of PFOA used in RBBR ozonation in the FBR .....	177
Figure 5.54 FT-IR spectra of PFOA used in AR-151 ozonation in the FBR .....	177
Figure 5.55 The by-products at different catalyst dosages. Conditions: Q <sub>G</sub> = 150 L/h, Q <sub>L</sub> = 150 L/h, pH = 2.54, T = 22.3°C, dye = RBBR, C <sub>O<sub>3,G,in</sub></sub> = 0.902 ± 0.017 mmol O <sub>3</sub> / L gas, C <sub>D,in</sub> = 4.8 × 10 <sup>-2</sup> mmol/L, (a) OA, (b) AA, (c) FA, reactor =FBR, H <sub>S</sub> =7.5 cm, for catalyst = Alumina, u <sub>L,min</sub> =130 L/h, H <sub>E</sub> =12.6 cm, for catalyst =PFOA, u <sub>L,min</sub> =110 L/h, H <sub>E</sub> =13.4 cm. ....	178
Figure 5.56 The by-products at different catalyst dosages. Conditions: Q <sub>G</sub> = 150 L/h, Q <sub>L</sub> = 150 L/h, pH = 2.54, T = 22.3°C, dye = AR-151, C <sub>O<sub>3,G,in</sub></sub> = 0.902 ± 0.017 mmol O <sub>3</sub> / L gas, C <sub>D,in</sub> = 6.6 × 10 <sup>-2</sup> mmol/L, (a) OA, (b) AA, (c) FA, reactor =FBR, H <sub>S</sub> =7.5 cm, for catalyst = Alumina, u <sub>L,min</sub> =130 L/h, H <sub>E</sub> =12.6 cm, for catalyst =PFOA, u <sub>L,min</sub> =110 L/h, H <sub>E</sub> =13.4 cm. ....	180
Figure 5.57 The comparison of theoretical and experimental steady state liquid phase ozone and dye concentrations for the best fit of D <sub>L</sub> and k <sub>L</sub> a values. Conditions: Q <sub>G</sub> = 150 L/h, Q <sub>L</sub> = 30 L/h, Dye=RBBR, C <sub>D,in</sub> =17.8×10 <sup>-2</sup> mmol /L, T = 23°C, C <sub>O<sub>3,G,in</sub></sub> = 0.313 mmol O <sub>3</sub> /L gas, catalyst = no, D <sub>L</sub> = 0.9×10 <sup>-3</sup> m <sup>2</sup> /s, k <sub>L</sub> a = 12.6 × 10 <sup>-2</sup> s <sup>-1</sup> .....	184

- Figure 5.58 The comparison of theoretical and experimental steady state liquid phase ozone and dye concentrations for the best fit of  $D_L$  and  $k_L a$  values.  
 Conditions:  $Q_G = 70$  L/h,  $Q_L = 30$  L/h, Dye=AR-151,  $C_{D,in}=8.3 \times 10^{-2}$  mmol/L,  $T = 23^\circ\text{C}$ ,  $C_{O_3,G,in} = 0.334$  mmol O<sub>3</sub>/L gas, catalyst = no,  $D_L = 3.0 \times 10^{-3}$  m<sup>2</sup>/s,  $k_L a = 5.4 \times 10^{-2}$  s<sup>-1</sup> ..... 184
- Figure 5.59 The comparison of theoretical and experimental steady state liquid phase ozone and dye concentrations for the best fit of  $D_L$  and  $k_L a$  values.  
 Conditions:  $Q_G = 70$  L/h,  $Q_L = 250$  L/h, Dye=RBBR,  $C_{D,in}=9.4 \times 10^{-2}$  mmol/L,  $T = 23^\circ\text{C}$ ,  $C_{O_3,G,in} = 0.332$  mmol O<sub>3</sub>/L gas, catalyst = no,  $D_L = 6.2 \times 10^{-3}$  m<sup>2</sup>/s,  $k_L a = 1.7 \times 10^{-2}$  s<sup>-1</sup> ..... 185
- Figure 5.60 The comparison of theoretical and experimental steady state liquid phase ozone and dye concentrations for the best fit of  $D_L$  and  $k_L a$  values.  
 Conditions:  $Q_G = 70$  L/h,  $Q_L = 250$  L/h, Dye=AR-151,  $C_{D,in}=13.6 \times 10^{-2}$  mmol/L,  $T = 23^\circ\text{C}$ ,  $C_{O_3,G,in} = 0.298$  mmol O<sub>3</sub>/L gas, catalyst = no,  $D_L = 6.8 \times 10^{-3}$  m<sup>2</sup>/s,  $k_L a = 1.5 \times 10^{-2}$  s<sup>-1</sup> ..... 185
- Figure 5.61 The comparison of theoretical and experimental dye and O<sub>3</sub> concentration values in dye ozonation. Conditions: Dye = RBBR, pH = 2.5,  $Q_G = 150$  L/h,  $Q_L = 150$  L/h,  $Q_G/Q_L = 1.0$ ,  $D_L = 3.15 \times 10^{-3}$  m<sup>2</sup>/s,  $C_{O_3,G,in} = 0.969$  mmol/L gas,  $C_{D,in} = 5.0 \times 10^{-2}$  mmol/L, catalyst = PFOA,  $m_{cat} = 25$  g,  $(k_L a)_E = 10.6 \times 10^{-2}$  s<sup>-1</sup>. (a)  $C_D$ , (b)  $C_{O_3}$ ..... 188
- Figure 5.62 The comparison of theoretical and experimental dye and O<sub>3</sub> concentration values in dye ozonation. Conditions: Dye = AR-151, pH = 2.5,  $Q_G = 150$  L/h,  $Q_L = 150$  L/h,  $Q_G/Q_L = 1.0$ ,  $D_L = 3.15 \times 10^{-3}$  m<sup>2</sup>/s,  $C_{O_3,G,in} = 0.966$  mmol/L gas,  $C_{D,in} = 7.2 \times 10^{-2}$  mmol/L, catalyst = PFOA,  $m_{cat} = 25$  g,  $(k_L a)_E = 9.3 \times 10^{-2}$  s<sup>-1</sup>. (a)  $C_D$ , (b)  $C_{O_3}$ ..... 189

## LIST OF SYMBOLS

$a$	gas-liquid interfacial area for gas bubbles, $\text{m}^2/\text{m}^3$ reactor
$a_s$	external surface area of the particles, $\text{m}^2$ catalyst/g catalyst
$A$	cross-sectional area of the fluidized bed reactor, $\text{m}^2$
$A_{BET}$	surface area of the catalyst as BET, $\text{m}^2/\text{g}$
$Appl_{O_3}$	applied $O_3$ dose, $\text{mmol/L}$ liq
<i>AR-151</i>	Acid Red-151
BOD	biological oxygen demand, $\text{mg/L}$
COD	chemical oxygen demand, $\text{mg/L}$
$COD_i$	initial COD, $\text{mg/L}$
$C_{O_3,L}$	the concentration of $A$ in the liquid phase, $\text{mM}$
$C_D$	the concentration of dye in the liquid phase, $\text{mM}$
$C_{D,i}$	initial dye concentration, $\text{mg/L}$
$C_{D,in}$	inlet dye concentration, $\text{mmol/L}$
$C_{D,s}$	dye concentration at the catalyst surface, $\text{mmol/L}$
$C_{O_3,e}$	equilibrium $O_3$ concentration in the liquid phase, $\text{mg/L}$
$C_{O_3,G}$	gas phase ozone concentration, $\text{mmol/L}$ gas
$C_{O_3,G,in}$	inlet gas phase ozone concentration, $\text{mmol/L}$ gas
$C_{O_3,G,out}$	outlet gas phase ozone concentration, $\text{mmol/L}$ gas
$C_{O_3,L}^*$	equilibrium concentration of dissolved ozone, $\text{mmol/L}$ liq
$C_{OH^-}$	the concentration of hydroxyl ions, $\text{mmol/L}$
$C_{O_3,s}$	ozone concentration on the catalyst surface, $\text{mmol/L}$ liq
$Cons_{O_3}$	$O_3$ consumption in the fluidized bed reactor, $\text{mmol/L}$ liq
$C_T(t)$	tracer concentration, $\text{mg/L}$
$C_{T,i}$	injected tracer concentration, $\text{mg/L}$
$d_{cat}$	catalyst particle size, $\text{mm}$
$d_{cat,ave}$	average catalyst particle size, $\text{mm}$

$d_p$	catalyst pore diameter, °A
$D_L$	axial dispersion coefficient for liquid phase, m <sup>2</sup> /s
$Diff_D$	dye diffusivity, m <sup>2</sup> /s
$Diff_{O_2}$	oxygen diffusivity, m <sup>2</sup> /s
$Diff_{O_3}$	ozone diffusivity, m <sup>2</sup> /s
$D_{O_3}$	ozone dosage, mmol/h
$E$ :	enhancement factor
$E_i$	instantaneous enhancement factor
$E(t)$	residence time distribution function
$h$	height of the aerated liquid, m
$h_0$	original height of the liquid, m
$H$ :	total column height, m
$H_E$ :	expanded bed height, m
$H_T$ :	height of the column from tracer injection point to liquid discharge point, m
$Ha$	<i>Hatta</i> number
$H_{O_3}$	Henry's Law constant for ozone, atm
$k_d$ :	decomposition rate constant of ozone in water, s <sup>-1</sup>
$k_G a$ :	mass transfer coefficient in gas film, moles O <sub>3</sub> consumed/(Pa.m <sup>2</sup> .s)
$k_L$ :	mass transfer coefficient in liquid film, m.s <sup>-1</sup>
$k_L a$ :	volumetric mass transfer coefficient in liquid film, s <sup>-1</sup>
$(k_L a)_E$ :	enhanced volumetric mass transfer coefficient in liquid film, s <sup>-1</sup>
$(k_L a)_{O_2}$	volumetric mass transfer coefficient of oxygen in liquid film, s <sup>-1</sup>
$(k_L a)_{O_3}$	volumetric mass transfer coefficient of ozone in liquid film, s <sup>-1</sup>
$k_s$ :	film coefficient around the catalyst particle, m <sup>3</sup> reactor/(m <sup>2</sup> catalyst.s)
$k$	rate constant between dye and ozone in the bulk liquid, (mM) <sup>-1</sup> (s) <sup>-1</sup>
$k'$	pseudo first order rate constant between dye and ozone in the bulk liquid, s <sup>-1</sup>
$k_I$ :	the rate constant on the catalyst surface, m <sup>3</sup> catalyst/(m <sup>2</sup> catalyst.s)
$m_{cat}$	catalyst dosage, g
$m$	solid loading per unit volume of the reactor, g.catalyst/m <sup>3</sup> reactor
$n$	the order of hydroxyl radical concentration in ozone decomposition reaction
$N_{CSTRs}$	number of CSTRs in series
$P_{O_3}$	pressure of reactant O <sub>3</sub> in the gas bulk, Pa or kPa

$Pe_L$	Péclet number
PFOA	perfluorooctyl alumina
PZC	point of zero charge
$R_{cons,O_3}$	O <sub>3</sub> consumption rate, %
$Q_G$	volumetric flow rate of gas, L/h
$Q_L$	volumetric flow rate of liquid, L/h
RBBR	Remazol Brilliant Blue R
$r_D$	rate of the reaction between dye and ozone in the bulk, L. (mM) <sup>-1</sup> s <sup>-1</sup>
$Re$	Reynolds number, $u_L \cdot d_{cat} \cdot \rho_{cat} / \mu_L$
$r_s$	stoichiometric ratio between ozone and dye in the ozonation reaction
$Sc$	Schmidt number, $\nu / D_{O_3,D}$
$Sh$	Sherwood number, $k_s \cdot d_{cat} / D_{O_3,D}$
$t$	time, s or min
$T$	temperature, °C or K
$t_m$	mean residence time, s
TOC	total organic carbon, mg/L
TSS	total suspended solids, mg/L
$u_G$	superficial gas velocity, m/s
$u_L$	superficial liquid velocity, m/s
$U_{O_3}$ (dye)	utilization ratio for dye, mmol dye/mmol O <sub>3</sub>
$U_{O_3}$ (TOC)	utilization ratio for TOC, mmol TOC/mmol O <sub>3</sub>
$V_{inj}$	injected volume of the tracer, L
$V_{T,p}$	total pore volume of the catalyst, cc/g
$V_{R,eff}$	effective reactor volume, L
$z$	column or reactor height, m

### **Greek Letters**

$\varepsilon_G$	gas hold-up
$\varepsilon_L$	liquid hold-up
$\varepsilon_s$	solid hold-up
$\rho_{cat}$	catalyst density, g catalyst/m <sup>3</sup> catalyst
$\rho_L$	liquid density, kg/m <sup>3</sup>

$\mu_L$	liquid viscosity, kg/(m.s)
$\rho_w$	water density, kg/m <sup>3</sup>
$\tau_L$	hydraulic retention time of the liquid in the fluidized bed reactor, min
$\sigma^2$	variance, s <sup>2</sup>
$\mu_w$	water viscosity, kg/(m.s)
$\mu$	the rate of the reaction, L/(mmol.s)

# CHAPTER 1

## INTRODUCTION

### 1.1 Characteristics of textile wastewaters

Textile industry plays an important role for the economies of Fareast countries, USA and Turkey. In Turkey, 13 percent of the total industrial production has been realized by textile industry [1]. Due to the increasing investment on textile production, new textile plants in Kayseri, Manisa, Eskişehir and Çorum were constructed besides those in İstanbul, Bursa and Adana.

Textile industry is based on the conversion of polymers into fibers and yarns. The common fibers used in Turkey are cotton, wool and synthetic fibers such as nylon, polyester and acrylics [2]. Then, fabrics are produced from yarns with several operations. The production of textiles is constituted of several “Wet Processes” such as cleaning, bleaching, dyeing and finishing of fibers and yarns; in each step, high amount of water is used in addition to different types of organics and inorganics [3,4]. As a result, textile industry wastewater is accepted as one of the most pollutant sectors to the environment due to its discharge volume, organic/inorganic content and intensity of color. In addition, most of the textile effluents are intolerable for the environment with high “Chemical Oxygen Demand” (COD), “Biological Oxygen Demand” (BOD), “Total Organic Carbon” (TOC) and “Total Suspended Solids” (TSS).

The characteristics of textile wastewaters show great variety depending on the types of inorganic/organic compounds used in the processes. The wastewater mainly contains high level of color coming from the dyes in the dyeing process, high level of TOC and COD due to the used organics such as dyes, surfactants, dye auxiliaries, and some heavy metals being in the dye structure. In addition, some chemicals including salts, acids, bases and buffers can be used for the regulation of pH. Textile effluent is generally alkaline; it has a BOD value between 700-2000 mg/L, and a COD value between 1400-

10000 mg/L [5]. The BOD/COD ratio ( $< 0.1$ ) is considerably low showing the non-biodegradability of most organics [6]. BOD, suspended solids and oil values can be much higher in the wool processes. In contrast to wool wastewaters, cotton processes do not contain oil but excessive color may be found. The organic/inorganic content of the textile wastewaters need to be removed from the wastewaters in appropriate treatment plants to meet the environmental legislations. Table 1.1 summarizes the characterization of a wastewater taken from a textile plant in Bursa and the standards to meet for the environment.

Table 1.1. The characterization of the wastewater taken from a textile plant in Bursa [7].

Parameter	Unit	Measured Value	Standard	
pH	-	$7.4 \pm 0.3$	6.5-8.5	
COD	mg/L	$131.0 \pm 17.7$	-	
TSS		$75.0 \pm 13.2$	20	
$\text{SO}_4^{-3}$		$244.3 \pm 45.1$	192	
$\text{Cl}^-$		$1281.7 \pm 190.0$	142	
Conductivity	( $\mu\text{S/cm}$ )	$3590 \pm 311.9$	250	
DFZ	436 nm	$m^{-1}$	$9.6 \pm 3.3$	7
	525 nm	$m^{-1}$	$8.3 \pm 2.9$	5
	620 nm	$m^{-1}$	$4.2 \pm 1.3$	3

The amount of wastewater produced in textile plants increases from year to year due to the increase in capacity and number of textile plants. A research realized in an “Organized Industrial Region” of Turkey showed that the textile wastewater amount increased from  $7.5 \times 10^7 \text{ m}^3$  to  $10.8 \times 10^7 \text{ m}^3$  by the years 2000 to 2002, respectively [7]. Only 66% treatment efficiency of such wastewaters indicated that the treatment methods and/or treatment plants were insufficient in Turkey.

In textile industry, dyeing process is made to give color to the fiber. At the end of the process, most of the dyes applied remain in the wastewater without being used and those dyes result in the increase of color. The characterization of the wastewaters, in which reactive dyes were used, showed that 30% of the applied dyes remained in the water being unused [8]. The unused dyes were found to constitute 24 to 35% of the

COD and 90 to 95% of the color in the wastewaters. The suspended and colloidal colored compounds accounted for the remaining small fraction of the color [9].

In textile plants, used dyes show a wide variety; azo, anthraquinone, sulfur, and indigoid derivatives are mostly employed. The dyes are classified according to their chromophore groups, an aromatic group giving color, according to the types of groups on the chromophore such as acidic, basic, direct, disperse or reactive, and according to their application area. The most common of the chromophore groups are azo and anthraquinone groups. Azo type constitutes 60-70% of the textile dyestuff produced [10]. In acid dyes, an acidic functional group such as nitro, carboxyl or sulfonic group is bound to the chromophore and the dye becomes a water-soluble anionic dye. Similarly, basic dyes are cationic type with amino groups in the structure. Direct and reactive dyes are highly water-soluble salts of acidic azo dyes, reactive dyes can bind to textile fibers easily via covalent bonds [6]. According to the application area, acid, reactive, vat, disperse or sulfur dyes become varied.

Synthetic dyes are toxic to the environment. It was shown that azo dyes in the wastewater could produce carcinogenic aromatic amines [11, 12]. They show resistance to self purification in the environment since they are produced in chemical stability for a long term usage in the industries. Besides aesthetical problems, color resulted from the dyes has an influence on the filtration of sunlight in the rivers and on the decay of food chain.

The color in textile effluents, is represented by ADMI color unit, absorbance unit or DFZ (Durchsichtsfarbzahl) unit. ADMI (American Dye Manufacture Institute) color unit is a measurement method according to American Standard Method 2120 [13]. The absorbance unit determines the absorbance of the wastewater at the maximum wavelength of absorption [14,15]. DFZ is a color unit in Germany based on the color standart of ISO 7887. The DFZ of the dyed wastewater measures the absorbances of the dye at the wavelengths 436 nm, 525 nm and 620 nm, then, the sample absorbances at these wavelengths are compared with the standard values of 7, 5 and 3  $\text{m}^{-1}$ , respectively. Although, the color standards are changed from region to region or country to country, color removal generally more than 99% is required to meet the color standards of the wastewaters. In Turkey, the standards of TS 11825 and TS 11826 define the limit values

of cotton and wool textile industry wastewaters, respectively [16]. However, no standardization exists for the color parameter of the industrial wastewaters. The government is planning to develop a standard for the color level of the industrial wastewaters during European Community Progression.

In many studies, artificial (synthetic) wastewaters were used in the investigation of the efficiency of treatment technologies. In such cases, the content of the wastewater was completely known with a constant dye composition. Then, the color of the solution was represented by the dye concentration. However, in real wastewaters, the description of textile effluents by its ADMI unit or absorbance value is more useful since such real wastewaters include dye mixtures rather than one type of dye.

## **1.2 Treatment technologies for textile wastewaters**

Many methods have been applied for the treatment of the wastewaters containing synthetic dyes such as coagulation, membrane filtration, chemical oxidation or microbial decomposition [6]. The reduction in the color of the wastewater is the main target of the treatment technologies. The color of water is reduced by the cleavages of some bonds such as  $-C=C-$  or/and  $-N=N-$  in the dye molecules by oxidation or by the adsorption of the dyes onto a support, membrane or microorganism.

Carbon based supports were used as the adsorbent to get simple solution. By this method, both cationic and anionic dyes were removed from the solution. However, carbon support preparation was an energy consuming operation. In recent years, some other inorganic supports such as silica or clay or organic supports like microbial waste were proposed instead of carbon. However, in such cases, inorganic/organic supports need to be regenerated and during regeneration, the resulting dye solution creates environmental problems. Additionally, ultrafiltration of wash water may be needed. Also, according to the type of the support, the system may not be advisable in economical point of view.

In industry, activated sludge treatment is the most widely used method to treat textile wastewaters but the inefficiency of the method is observed. The method is limited to low degradation of color and surfactants because of the low BOD/COD ratio, which

means low biodegradability of such wastewaters. Only a few bacteria or fungi such as manganese peroxidases, manganese laccases, lignolytic fungi and white rot fungi were shown to decolorize dye aerobically [17]. Especially, the high solubility of reactive dyes in water makes their removal difficult with active sludge process [18]. Also, dye molecules hardly pass through biological cells of microorganisms due to high molecular weights. O'Neill et al. [19] showed that only 10% of the azo dye molecules were adsorbed into the biological cell. The anaerobic method is more successful in decolorization but the reduction rate of dyes is limited to sulfonation of them and dye permeation into the cells. As a result, anaerobic treatment methods are not generally used.

In full-scale and pilot scale operations, coagulation, precipitation, ozonation and chlorination methods are the chemically extended methods. The treatment efficiency can be increased easily by the change of chemical or its dose in the operation. With coagulation and precipitation, part of the COD and dye can be removed from the wastewater. Alum was practiced as a coagulant in the treatment and gained success as the first-stage treatment. Gahr et al. [8] reported coagulation as the most widely used treatment type in Germany. However, a large amount of harmful sludge containing heavy metals, is produced and it requires another application to be disposed such as combustion. Also, in some studies, toxic products were found after the lime coagulation of a textile wastewater [20]. In addition, some reactive or acid dyes were observed to resist to coagulation, giving a maximum 20% color removal. Therefore, coagulation is continued with another treatment process such as biological treatment or oxidation. With the two-stage operation, up to 95% BOD removal can be achieved [5].

Membrane technology is a new technology for the dye removal from wastewaters. Nanofiltration, reverse osmosis or ultrafiltration methods are available. Yet, the treatment capacity of the membranes is limited because of the excessive waste generation. Also, treatment with a high wastewater flow rate requires more money.

In electrochemical methods, electrical current is passed through the electrodes to result in some chemical reactions. At the same time, the dye molecules are oxidized by oxidation agents such as  $\text{Cl}_2$  and  $\text{O}_3$ . The method achieves high percent of dye removal but COD and TOC removals are limited. The dye degradation is accomplished by the

cleavage of azo link producing smaller molecules. But, the degradation of these small molecules by electric current is hard.

The biodegradability of the wastewater can be increased by chlorination. The efficiency of the process depends on the type of the dye, chlorine dosage and pH. Optimum operating conditions must be applied for a satisfactory treatment. In chlorination, chlorine or sodium hypochlorite molecule breaks up the azo group of the dye. Generally, high treatment results are achieved for acid and direct dyes but more application time is needed for the degradation of reactive dyes [21]. The main disadvantage of chlorination is the production of halogenated carcinogen organics such as chloroanilines and chloronitrobenzenes during treatment. Therefore, a second treatment stage such as incineration is needed before the disposal of the residue.

In addition to those methods, electrolysis is applied to the wastewaters containing acid dyes and by the sorption on to the precipitated iron electrode, reduction of the dye is achieved [22, 23]. The method is used in the laboratory scale; as a pilot scale operation, combined method with the coagulation and biological treatment is encouraged due to the high cost of electrolysis. Table 1.2 shows the treatment methods for the textile industry wastewaters.

Table 1.2. Treatment methods for textile wastewaters

Types	Processes	Examples
Physical	Membrane	Nanofiltration
	Flotation	Electroflotation
Electrochemical	Oxidation/reduction	Electro-coagulation, electro-oxidation
Chemical	Coagulation/precipitation	Iron/aluminium/lime
	Chlorination/ozonation	Cl <sub>2</sub> , NaOCl, O <sub>3</sub>
	Adsorption	Carbon or polymeric materials
	Wet air oxidation	High pressure and temperature
	Fenton reagent oxidation	H <sub>2</sub> O <sub>2</sub> /Fe(II)
	Ion exchange	Anion exchange resin
Photocatalytic	UV/H <sub>2</sub> O <sub>2</sub>	UV/H <sub>2</sub> O <sub>2</sub> , UV/TiO <sub>2</sub> , UV/O <sub>3</sub>
Biological	Anaerobic, aerobic, anoxic	Activated sludge, fungi

In the Fenton's reagent process, hydrogen peroxide is the main oxidant and used with iron salts [6, 21, 24]. The oxidation efficiency of hydrogen peroxide is activated with Fe(II) or Fe(III). The method is advantageous in COD, color and toxicity removals but the transformation of substances from wastewater to sludge creates a problem. In such a case, the mechanical separation of the Fenton sludge can be applied. For the dyes, reactive, direct, disperse and metal complex, the method was shown to be suitable [24].

### **1.3 Use of ozone in wastewater treatment processes**

Most dyes are decolorized by ozone successfully. It is known as a powerful oxidant with 2.07 V oxidation potential. The complex dye molecules are degraded by the oxidation with ozone producing smaller, more polar and hydrophilic molecules, and easily biodegradable organics. More than 90% color reduction is achieved with moderate COD and TOC reductions since the produced organics such as dicarboxylic acids and aldehydes show resistance to the further oxidation with ozone. The treatment plants built in Europe reduced successfully the color content and surfactants from the textile wastewaters but capital costs were high in addition to the unwanted by-products. Therefore, ozonation was applied as a final treatment method after coagulation and active sludge methods. In England, a full-scale ozone process was built and operated for color removal successfully. However, some newly-formed by-products such as oxalate remained in the solution [25].

The limited (insufficient) degradations of TOC and COD in the wastewater is the main disadvantage of ozonation. The introduction of some catalysts to the ozonation process may help to increase the TOC and COD removals, and thus the ozone utilization efficiency. In recent years, ozonation studies in the literature were concentrated on the usage of homogeneous or heterogeneous catalysts in the process. Besides, in some cases, ozonation was followed by the biological treatment for the removal of aldehydes and carboxylic acids [26,27].

Ozonation in textile wastewater treatment has the advantage of producing no hazardous chemical sludge. However, the treatment efficiency mainly depends on the ozone dose and the wastewater characteristics. The increase of ozone dose is advisable for especially higher COD and TOC reductions but this brings out an economical

deficiency. The ozonation reactions are realized in simple systems such as bubble columns. Yet, the half life of ozone in the solution is short decomposing to some radicals. Its half life is affected by the water characteristics such as pH and the presence of some salts and organics. At alkaline pH, the decomposition of ozone occurs decreasing the concentration of ozone in the liquid phase.

Advanced Oxidation Processes (AOPs) have been used in wastewater treatment recently. These techniques, including UV/H<sub>2</sub>O<sub>2</sub>, O<sub>3</sub>/catalyst, O<sub>3</sub>/H<sub>2</sub>O<sub>2</sub> methods, are based on the production of high oxidative radicals such as hydroxyl radicals. The decolorization achieved is often followed by a noticeable COD, TOC reductions and mineralization to carbon dioxide and water. Ozonation in the presence of an active catalyst can initiate the radical reactions in water realizing more organic degradation.

#### **1.4 Aim and scope of the study**

As being one of the advanced oxidation techniques, catalytic ozonation gives many advantages. By catalytic ozonation, not only dyes but also the ozonation by-products can be removed from wastewater. Additionally, the needed ozone consumption in the treatment can be decreased by the presence of the catalyst in the medium.

Aim of the present study is to investigate the degradation of two industrial dyes with ozonation in the presence and absence of the catalyst particles in a fluidized bed reactor (FBR). The selected dyes are an azo dye, namely Acid Red-151 (*AR-151*) and an anthraquinone dye, Remazol Brilliant Blue R (*RBBR*), which are commonly used dyes in the textile industry.

In recent studies, alumina has been applied as a support and a catalyst in ozonation of industrial wastewaters. High treatment efficiency in ozonation was observed by using alumina due to its high surface area, mechanical and thermal stabilities [28-30]. Alumina was used as a support material for many studies in which metal oxides such as titanium dioxide (TiO<sub>2</sub>) or iron oxide (Fe<sub>2</sub>O<sub>3</sub>) was impregnated on the alumina surface [30,31]. Therefore, alumina was selected as one of the catalysts used in this study.

Perfluorinated hydrocarbons, compounds in which all hydrogens are replaced by fluorines, have been used in environmental applications due to their high stability and low reactivity [32]. These chemicals have found a wide application area in ozonation as a means of enhancing molecular ozone reactions. Ozonation with perfluorinated chemicals is based on two methods: two phase ozonation and catalytic ozonation in the presence of perfluorinated alumina phase [32].

Organic pollutants are extracted from aqueous solution to organic perfluorinated phase in two phase ozonation. The perfluorinated phase is saturated with ozone so that organic pollutants are oxidized subsequently by ozone in the perfluorinated phase. Perfluorinated hydrocarbons enhance the solubilization of ozone due to the low polarity of ozone [32].

Catalytic ozonation in the presence of perfluorinated alumina phase is another method. In this method, perfluorinated hydrocarbon is impregnated onto the alumina surface by forming non-polar perfluorinated alkyl chains. Non-polar alkyl chains on the alumina surface are active towards ozone and organics [32]. Perfluorooctanoic and perfluorooctadecanoic acids are the mostly used hydrocarbons on alumina. In many studies, it was found that perfluorinated alumina catalysts might be very effective in the ozonation of organic pollutants [32-35]. Hence, perfluorooctyl alumina (PFOA) was selected as another catalyst in the ozonation process.

In the study, at first, the kinetics of ozonation and catalytic ozonation were investigated for the determination of reaction rate constants of *AR-151* and *RBBR* in a semi-batch reactor. In addition the efficiency of catalytic ozonation process was evaluated using alumina and PFOA for the treatment of the dyes.

The hydrodynamic characteristics of the continuous gas-liquid reactor in the absence and presence of the particles were important to be determined before the modeling of the reactor used. Then, the modeling of the reactor can be realized for non-catalytic and catalytic ozonation processes by understanding the dispersion in the reactor, the minimum fluidization velocities in the presence of the particles and the ratios of gas, liquid and solid hold-up values. To determine the residence time distributions and

mixing characteristics in the reactor, a tracer (stimulus-response) technique was used. Then, gas, liquid and solid phase hold-up values were determined in the column.

In ozonation process, the mass transfer of ozone from gas to liquid phase occurs and the organic pollutants are oxidized by ozone in the liquid bulk phase. A precise knowledge of volumetric gas-liquid mass transfer coefficient ( $k_{La}$ ) is essential to operate the ozonation reactor under the most beneficial conditions in the respect of dye degradation. A low rate of ozone mass transfer provides a decrease in oxidation of dye molecules. In the next step, ozone absorption experiments were conducted in the FBR to determine the  $k_{La}$  values under different operating conditions of gas and liquid flow rates and catalyst dosages. A mathematical model was devised to obtain  $k_{La}$  values by numerically solving two model equations written as mass balances of ozone in the gas and liquid phases at the steady state. The experimentally determined concentration profile of ozone in the liquid phase along the column-height was used to get the best fit to the theoretical values. The axial dispersion coefficient and mass transfer coefficient at each operating condition of different gas and liquid flow rates were estimated by this computational method.

Finally, the ozonation processes of *AR-151* and *RBBR* in the gas-liquid reactor, in the presence and absence of alumina or PFOA particles were examined. The main operating parameters were gas and liquid flow rates, inlet dye concentration, inlet ozone concentration in the gas phase, gas to liquid volume ratio, catalyst dosage and catalyst particle size. As a result, concentration profiles of the dyes, dissolved ozone, and TOC with respect to axial direction were determined for different conditions in the reactor. The applicability and effectiveness of catalytic ozonation with respect to the dye and TOC removals and  $O_3$  consumption were compared with conventional ozonation for the treatment of *AR-151* and *RBBR*. The ozonation by-products were determined and the ozonation mechanisms for both of the dyes were developed with a reaction sequence in ozonation and catalytic ozonation.

The mathematical representation of the dye ozonation process requires an evaluation of several parameters such as the reaction rate constants, the enhanced volumetric mass transfer coefficients, and the axial dispersion coefficients at the studied flow conditions. A mathematical model was developed to represent the gas-liquid and in the catalytic

case, the gas-liquid-solid phases dye and ozone mass balances. The enhanced mass transfer coefficients due to the chemical reaction were found in the dye ozonation experiments by solving the gas and liquid phase ozone and dye concentration equations. As a result, ozone concentration in the gas and liquid phases and dye concentration profiles along the column-height at the steady state were found. The theoretical and experimental concentration profiles were compared to predict the enhanced  $k_La$  values at the studied conditions.

## CHAPTER 2

### LITERATURE SURVEY

#### 2.1 Ozonation process

Ozone and ozonation process have been used for public and industrial wastewater treatments since early 1800's. The ozonation technology and the studies on its usage have been developed for the treatment requirements. Its technology was advanced by the foundation of ozone generating tubes in 1857 [36]. Then, ozonation has become one of the most successful methods for the decolorization of textile wastewaters besides for other industrial wastewaters containing organic compounds at high concentrations.

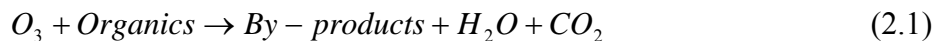
##### 2.1.1 Ozonation chemistry

Ozone ( $O_3$ ) is a strong oxidant with an electrical potential of  $E^0 = 2.07$  V and degrades most of the organic compounds effectively in aqueous solution [37]. Its structure is triatomic form of oxygen. The  $\pi$  electrons are equally shared by the three oxygen atoms making ozone molecule hybrid and this structure gives ozone an ability to react electrophilically [38].  $O_3$  is produced from oxygen in ozone generators by electrical discharge method. In the ozone generator, the oxygen molecules ( $O_2$ ) are separated to oxygen atoms (O) and one oxygen atom combines with one oxygen molecule producing  $O_3$ .

At normal temperature and pressure,  $O_3$  exists as a gas in the atmosphere. Then, the reactions of  $O_3$  in aqueous phase is realized first by the mass transfer of  $O_3$  molecules from the gas to the liquid phase. In the aqueous phase, the reaction of  $O_3$  with organics or inorganics occurs by either molecular ozone or through a radical mechanism initiated by the decomposition of ozone [39-44].

At acidic pH, the decomposition of ozone into the radicals is negligibly small in aqueous solution. Therefore, all ozone dissolved in water is used to oxidize

organics/inorganics. Molecular ozone reacts with the compounds present in water as expressed in Equation (2.1). Sometimes, the reaction between ozone and organic may yield hydroxyl radical  $HO^\bullet$  [45].



The reactions in Equations (2.1) and (2.2) are the direct reactions of ozone with the organics since it reacts directly with them without being decomposed to active radicals. If dye molecules are the target compounds to be degraded, ozone attacks the chromophore group of the dye breaking it up [46, 47]. Hoigne and Bader [48, 49] investigated the rate constants of reaction between many organics and molecular ozone. Those studies showed that the organics such as amines, phenols, aromatic compounds were reacted with ozone readily. On the other hand, many carboxylic acids, aldehydes and alcohols were observed to hardly undergo a reaction with molecular ozone. The resultant second order rate constants of organics with direct ozonation lied in the range between  $10^{-2}$  to  $10^9$  mmol/(L.s) [48, 49]. Then, the rate of molecular ozone reactions are said to be dependent on the chemical structure of the target compounds. The destruction of azo dyes was shown to be fast with a second order rate constant of  $10^5$ - $10^7$  L/(mol.s) [50].

The direct reaction of ozone with organics is selective. In these reactions,  $O_3$  attacks the target compounds as an electrophile or nucleophile [51]. When electron donor groups such as  $-OH$ ,  $-NH_2$  are in the structure, the compounds are oxidized by ozone electrophilically (electrophilic reactions). The electrophilic attack of ozone occurs with N, P, O atoms having a negative density [52]. In nucleophilic reactions, ozone attacks the nucleophilic centers (centers where electron density is high) such as  $-C=C-$ ,  $-N=N-$  groups. However, in these centers, the existed  $C=O$ ,  $COOH$ ,  $Cl$  and  $NO_2$  groups cause the decrease in activity of organic substances toward ozone [53]. The addition of ozone molecule to a double bond, called 1-3 cycloaddition, breaks up the double bond creating carbon-carbon double bonded unstable molecules [54]. Similarly, alkenes with electron-withdrawing substituents are ozonated via 1,3- dipolar cycloaddition [55].

Sulfonic group in the chemical structure of the target organic ensures the deactivation of aromatic ring to bacterial and electrophilic attack [56]. This is because electron density of aromatic ring decreases due to the electron-withdrawing sulfonic groups causing the deactivation of the ring [57]. On the other hand, the presence of amino groups equip the molecule with an ability to break up faster by ozone [47].

Decomposition of  $O_3$  is initiated by the reaction of hydroxyl ions ( $OH^-$ ) with  $O_3$ . The decomposition proceeds in the aqueous phase and some radicals with a high oxidation potential such as  $HO^\bullet$  are produced. Numerous studies showed major importance of  $HO^\bullet$  in the oxidation of organic compounds when pH exceeded 5 [58, 59]. Similarly, Oyama et al. [53] and Poznyak et al. [47] stated that at a low pH, below 7, organic compounds are reacted principally with molecular  $O_3$ . The oxidation potential of hydroxyl radicals (2.80 V) is higher than the oxidation potential of ozone (2.07 V) and that property results in greater reactivity of  $HO^\bullet$  [60]. The rate constant of reactions between some organics and hydroxyl radicals was shown to be higher than that of reactions between those organics with ozone in the literature [44, 48]. As a comparison, the rate constants of reactions between some organics with ozone and with  $HO^\bullet$  radicals are given in Table 2.1.

Table 2.1. Rate constants of some organics with ozone [44, 48] or with  $HO^\bullet$  [62].

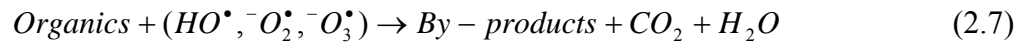
Organic	$k_{O_3}$ , mmol/(L.s)	$k_{HO^\bullet}$ , mmol/(L.s)
Benzene	$2 \pm 0.4^a$	$7.8 \times 10^9$
Nitrobenzene	$0.09 \pm 0.02^a$	$3.9 \times 10^9$
Formic acid	$5 \pm 5^a$	$1.3 \times 10^8$
Oxalic acid	$(< 4 \times 10^{-2})^a$	$1.4 \times 10^6$
Acetic acid	$(< 3 \times 10^{-5})^a$	$1.6 \times 10^7$
Succinic acid	$(< 3 \times 10^{-2})^a$	$3.1 \times 10^8$
Salicylic acid	$(< 500)^a$	$2.2 \times 10^{10}$

<sup>a</sup> Acidic pH, in the presence of a scavenger for  $HO^\bullet$

The mechanism of radical reactions in ozonation was proposed mainly by Staehelin and Hoigne [41]. According to the mechanism, at basic pH,  $O_3$  goes through the following reaction with  ${}^{-}OH$  :



The Equation (2.3), was shown to be the slowest one being most probably the rate determining step [61]. It is obvious that more radicals are produced at basic pH due to the higher concentration of  ${}^{-}OH$  . In other words, at high pH, the radical pathway will be dominant because of the self decomposition of ozone abundantly [52]. Then, the following reactions occur in aqueous solution enabling the production of the strong oxidant,  $HO^{\bullet}$  :



Free radicals such as  $HO^{\bullet}$  and  $HO_2^{\bullet}$  can act as chain carriers [41]. The radicals in ozonation were classified by Legube et al. [63] according to their activities toward organic compounds. It was found that  $HO_2^{\bullet}$  was inert to organics while  ${}^{-}O_2^{\bullet}$  and  ${}^{-}O_3^{\bullet}$  were active. The most active radical was  $HO^{\bullet}$  . According to Chen [64], the ozonation of methyl orange was realized by  $HO^{\bullet}$  significantly. However, increasing pH from 8 to 11 did not yield any remarkable increase in the decolorization rate. They emphasized that both  ${}^{-}OH$  and  $H^+$  ions promoted the production of  $HO^{\bullet}$  radicals. The optimum reaction pH at which more  $HO^{\bullet}$  radicals were produced, was to be determined to get the most efficient dye decolorization.

Several compounds in water are able to initiate, promote or inhibit the radical reactions. Hydrogen peroxide, formate ions, humic substances are well-known initiators whereas some alcohols, formate ions and humic substances can promote the reactions. While

some initiators such as  $\text{Fe}^{2+}$  may originally be present in the raw water, others such as formate ions can be produced during ozonation [41, 65]. Promoters are known to react with  $\text{HO}^\bullet$  to propagate the chain by producing active radicals such as  $\text{HO}_2^\bullet$  continuously [41, 45]. Tertiary alcohols and carbonates are the main inhibitors (scavengers) of radicals [42, 49, 59, 66, 67]. Also, the phosphate ions in the medium were demonstrated to act as scavengers for  $\text{HO}^\bullet$  [68]. The inhibitors or scavengers terminate the chain by consuming the important oxidative radicals [38]. The products from these reactions do not react further with ozone.

In the ozonation of organic molecules, both direct ozonation and radical oxidation can be important mechanisms for dye and TOC degradations [54, 69]. At high pH, there exists a competition between the molecular ozone and the radical components to oxidize the organics; the contribution and importance of each mechanism in the oxidation depend on the type of the organic. The azo groups of azo dyes are mainly bonded to benzene and naphthalene rings and most of the dyes include aromaticity in their structures [70]. It is known that the aromatic ring of dye molecules can easily be broken by ozone and even by hydroxyl radicals in the aqueous phase [71]. However, Beltran et al. [30, 72] proposed that direct oxidation by ozone was negligible in the ozonation of compounds without a double bond or nucleophile. Then, for those compounds, ozonation is realized by the contribution of radical mechanism at high pH mainly. As shown in Table 2.1, the degradations of many carboxylic acids are achieved by hydroxyl radicals [48, 49].

The degradability of a dye molecule with  $\text{O}_3$  depends mainly on the components in its structure. Dyes with more azo links were shown to be degraded more by ozone than mono-azo dyes [73]. The breakage of the dye molecule having more azo groups was easier than that of the molecule with one azo group. Similarly, Lopez-Lopez et al. [46] found that the reaction rate constants of mono-azo dyes were higher than those of di-azo dyes. Acid dyes possessing only naphthalene rings in their structures undergo faster decolorization than the dyes with the combination of benzene and naphthalene rings. The sulphonic acid group in the dye structure ensures its solubility in water. However, those groups make the molecule non-biodegradable and hardly destructible by ozonation [74-77].

### 2.1.2 Effect of pH on ozonation process

Since oxidation of organics by radical mechanism becomes important at alkaline conditions, the effect of pH in the ozonation of dyes and textile wastewaters have been investigated in many studies [13, 78, 79]. For the ozonation of dyes and textile wastewaters, the effect of pH showed some contradictory results in view of dye degradation efficiency. First of all, the stability of ozone was decreased by the increase of pH which was a main disadvantage for the dyes preferentially oxidized by molecular ozone according to direct mechanism [80]. Snider and Porter [78] could not find a certain rule showing the effect of pH on the treatment of textile wastewaters by ozone. Koyuncu and Afşar [80] however observed higher degradation rates of several dyes at pH = 9 than those at pH = 2. Similarly, the change of pH from 2 to 12 decreased the decolorization time of Isma Fast Red 8 B dye by 32% providing an advantage to the process [81]. In some cases, neutral pH was the optimum pH for the complete decolorization of the dyes [80]. At neutral pH, some dyes were oxidized by both molecular O<sub>3</sub> and also by radicals with a greater efficiency.

The fact that the increase of reaction pH affecting the dye degradation rate positively or not, depends mainly on the type of the dye to be ozonated. For some dyes, radical reactions occurring at alkaline pH, may oxidize the dye molecules less efficiently resulting in lower dye removals than those obtained by the direct mechanism at acidic pH. For example, azo dyes can be degraded by direct ozone at acidic pH voluntarily [50]. Chen [64] observed little influence of pH on the ozonation of methyl orange, an azo dye. In addition, the oxidation of dyes by HO• radicals may produce some radical scavengers such as Cl<sup>-</sup> or SO<sub>4</sub><sup>2-</sup> ions due to the cleavage of the chlorinated or sulfonated group in the dye molecule. Those scavengers inhibit the radical reactions by reacting with some oxidizing radicals such as HO• [82]. At acidic pH, the ozone decomposition is negligibly small so that more molecular ozone will be available to degrade the dye molecules. Neamtu et al. [83] pointed out that hydrogen peroxide (H<sub>2</sub>O<sub>2</sub>) was produced during the oxidation of some reactive azo dyes and excess H<sub>2</sub>O<sub>2</sub> in the medium caused to inhibit the radical reactions. As a result, in some studies, more efficient dye removals were observed at the lower pH values (pH=2) than those at the higher pH levels (pH=5 or 9) [82].

Chu and Ma [70] reported the positive effect of pH increase on the removal of azo dyes with ozonation. Interestingly, acidic pH was observed to provide higher dye removal rates than those of alkaline pH for anthraquinone dyes. Kornmüller et al. [79] found a critical pH value (pH=7.8) for the ozonation of cucurbituril (a reactive dye) so that the oxidation of the dye was influenced by the radical mechanism in addition to the oxidation by molecular ozone. At the lower pH values than that critical pH, there was no remarkable oxidation of the dye.

Solution pH is an important parameter for the degradation of COD and TOC contents of the wastewaters. Alaton et al. [59] emphasized that color could be removed by both direct and radical mechanisms of ozonation; but for a high TOC removal, the solution pH had to be at least 7 to increase the contribution of radical reactions. That was confirmed by the observation of 28% and 17% TOC removals at pH = 7 and 3, respectively.

Balcıoğlu and Arslan [84] observed 86% COD removal at pH =11, in the ozone treatment of textile dyestuff. At pH of 2, the COD removal was only 65%. The decolorization rate constant was shown to increase by a factor of two compared to the value at pH = 2. Sarayu et al. [85] observed an increase in COD removal ( $\Delta\text{COD}/\text{COD}_i$ ) from 0.2 to 0.8 by the increase of pH from 5 to 10 in the ozonation of commercial azo dyes. Moreover, 90% color removal was found at pH = 10. Garcia-Montano et al. [86] stated that at alkaline pH (pH=10), the produced  $HO^\bullet$  radicals oxidized both aromatic compounds and also the aliphatic by-products in the ozonation of Cibacron Red FN-R providing 83 % of mineralization. The faster mineralization results were obtained at the higher pH values in the ozonation of Mordant Black 11 azo dye [87, 88].

The amounts of ozone consumed in ozonation at alkaline pH values were found to be higher than those consumed at the lower pH values in many cases [59, 84, 89]. That was due to the increase in ozone decomposition producing oxidative radicals; the presence of those radicals resulted in higher mineralization levels in the solution.

### **2.1.3 Effect of wastewater characteristics on ozonation process**

The chemical content of a wastewater plays a significant role on ozonation process due to the presence of inorganic and organic compounds effective in the production of ozonation chain radicals [45]. Some inorganics present in water such as  $\text{Fe}^{2+}$  acts as an initiator for the radicals [41]. Some scavengers of the radicals such as carbonate and phosphate ions are used as buffers in the dyeing and finishing processes [90, 91]. The kinetic interpretation of ozone reactions in the presence of carbonate or phosphate ions showed some differences compared to that of ozonation reactions without buffers. For example, the order of ozone decomposition reaction was changed from 1 to 2 or 3/2 with respect to  $\text{O}_3$  concentration in the absence or presence of those ions, respectively [44, 92]. Yurteri and Gürol [93] developed a model for ozone decomposition kinetics showing the contributions of initiator, promoter and scavenger concentrations in clean and naturally occurring waters. The apparent value of decomposition rate constant was found to be a function of pH and the composition of the water matrix. According to that model, the presence of initiators or promoters yielded a first order kinetics of ozone decomposition with respect to  $\text{O}_3$  concentration [94].

Besides buffer ions, other chemicals may be introduced in textile preparation steps. Salts are extensively used in the application of dyes on textiles, as exhausting and retarding agents. Sodium chloride ( $\text{NaCl}$ ) and sodium sulfate ( $\text{Na}_2\text{SO}_4$ ) are the most applied salts in textile industry. The effect of salts on decolorization efficiency was investigated in many studies [8, 14]. The decolorization time changed as a result of the salt type and quantity of the salts [14]. The presence of  $\text{NaCl}$  and  $\text{Na}_2\text{SO}_4$  generally yielded longer decolorization time.  $\text{NaCl}$  salt in solution consumed ozone at both acidic and alkaline pH by reacting  $\text{O}_3$  and  $\text{HO}^\bullet$ .  $\text{Na}_2\text{SO}_4$  contrarily, did not affect the ozonation at acidic pH but at alkaline pH it consumed  $\text{HO}^\bullet$ . In another study, it was shown that the production of  $\text{Cl}^\bullet$  radicals during ozonation of the dye was attributed to the cease of dye oxidation [95].

Arslan and Balcıoğlu [96] investigated the effect of some dye auxiliaries such as  $\text{NaCl}$ , acetic acid and sodium carbonate ( $\text{Na}_2\text{CO}_3$ ).  $\text{NaCl}$  and acetic acid concentrations did not affect the dye ozonation rate; however, the presence of  $\text{Na}_2\text{CO}_3$  retarded the oxidation of the dye seriously. Some studies showed that at high alkalinity conditions (presence of  $\text{HCO}_3^-$  and  $\text{CO}_3^{2-}$  ions in water), the radicals produced from  $\text{HCO}_3^-$  or  $\text{CO}_3^{2-}$  degraded

the dye molecules by cleaving chromophoric or aromatic groups [58]. Also the pH increase, when  $HCO_3^-$  or  $CO_3^{2-}$  ions were present, promoted the decomposition of ozone and generated additional  $OH^\bullet$  radicals in the solution [94, 97].

The other compounds present in the textile wastewaters yielded diverse effects on dye ozonation. Low level of surfactants was demonstrated to enhance dye degradation by decreasing surface tension of the solution [97]. Because, the dissolved  $O_3$  concentration in the liquid was increased. Ethylenediaminetetraacetic acid (EDTA) and defoaming agents consumed more ozone and caused higher ozonation time for complete color removal as comparing ozonation with no agent [98]. Addition of chelating agents retarded color removal since they were preferentially oxidized by ozone, instead of dye [94].

#### **2.1.4 Mass transfer effects in ozonation**

Until the early 2000's, the main target of ozonation studies was to determine the kinetics of ozone decomposition and chemical reaction between the organic pollutant and ozone. Ozone self-decomposition reaction was found to be first order with respect to ozone concentration, with the decomposition rate constant ( $k_d$ ) being a function of pH [99-102].

The kinetics of reactions between organic pollutant and ozone were investigated by neglecting the mass transfer effect in the reactions [70, 103-105]. The reaction between an organic and ozone followed a second order reaction, being first order with respect to both  $O_3$  and organic pollutant (dye) concentrations [65, 104, 106, 107].

In an ozonation process, ozone gas diffuses toward the liquid phase through the gas-liquid interface as a first step. Therefore, the design and modeling of ozone reactors are mainly based on the accurate contribution of mass transfer for the process and the determination of gas-liquid mass transfer coefficient ( $k_La$ ) [108]. The transfer rate of ozone from gas to liquid phase is described according to the two-film theory [109]. This theory assumes a film at the surface of the gas bubble next to the liquid. The bulk liquid is kept uniform in composition by agitation. The concentration at the gas-liquid interface changes linearly in the film according to the following equation:

$$\mu = k_L a (C_{O_3}^* - C_{O_3,L}) \quad (2.8)$$

where  $\mu$  is the transfer rate,  $k_L a$  is the gas-liquid volumetric mass transfer coefficient,  $C_{O_3}^*$  is the equilibrium concentration of  $O_3$  at the gas-liquid interface and  $C_{O_3,L}$  is the concentration of  $O_3$  in the bulk liquid. The concentration of  $O_3$  at the gas-liquid interface is related to the ozone concentration in the gas phase according to the Henry's Law as follows:

$$C_{O_3}^* = \frac{C_{O_3,G}}{H_{O_3}} \quad (2.9)$$

here  $H_{O_3}$  is the Henry's Law constant and  $C_{O_3,G}$  is the gas phase  $O_3$  concentration. In literature, correlations to determine the Henry's Law constant at different pH and temperature can be found [110-112]. Mass transfer coefficient of  $O_3$ ,  $(k_L a)_{O_3}$ , in a given reactor is generally found from the determination of the mass transfer coefficient of  $O_2$ ,  $(k_L a)_{O_2}$ , at the unsteady-state condition (Eqn. 2.11) [111]:

$$\frac{dC_{O_2,L}}{dt} = (k_L a)_{O_2} (C_{O_2}^* - C_{O_2,L}) \quad (2.10)$$

where  $C_{O_2}^*$  and  $C_{O_2,L}$  are the concentrations of  $O_2$  in gas-liquid interface and in the bulk liquid, respectively.

Then,  $(k_L a)_{O_3}$  is found by using the diffusivities of  $O_3$  ( $Diff_{O_3}$ ) and of  $O_2$  ( $Diff_{O_2}$ ) according to the Dankwerts theory [109]:

$$(k_L a)_{O_3} = (k_L a)_{O_2} \sqrt{\frac{Diff_{O_3}}{Diff_{O_2}}} \quad (2.11)$$

In a gas absorption with a chemical reaction system, the reaction can occur in the liquid film, in the bulk of the liquid or in both zones at the same time according to the relative

rates of the chemical reaction and mass transfer. For slow and very slow reactions, the reaction develops in the bulk being the rate limiting step as seen in Figure 2.1 [113, 114]. Compounds undergo a reaction in the liquid film when fast or instantaneous reactions are considered; in that case, mass transfer phenomenon is the rate limiting step. In intermediate rate reactions, the reaction may develop both in the liquid film and in the bulk liquid [115].

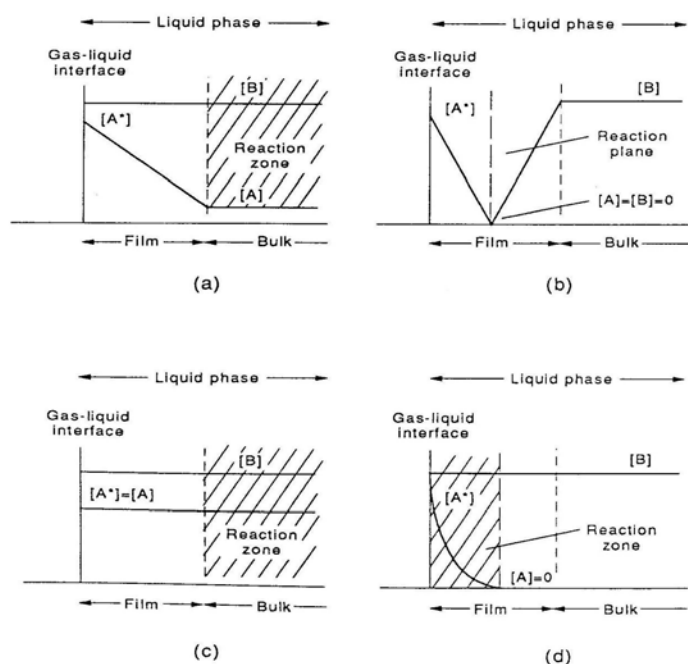


Figure 2.1. Kinetic regimes in a gas-liquid reaction [114].

As being a very strong oxidant, ozone reacts very fast with most of the organic pollutants, especially with dyes in the liquid phase. Also since ozone is known as a sparingly soluble gas in water, mass transfer of ozone into the liquid phase is the rate-limiting step in its reactions mostly [107; 116, 117].

Fast reactions of ozone in liquid leads to the enhancement of mass transfer significantly. The  $O_3$  concentration in bulk is approximately zero in most cases showing fast consumption of ozone in the liquid. The driving force for mass transfer increases due to the fast chemical reaction of  $O_3$  with the organics. The criterion showing the enhancement of mass transfer coefficient is shown by Hatta number ( $Ha$ ) and

Enhancement Factor ( $E$ ). Hatta number is a dimensionless parameter that compares the maximum possible reaction rate in the gas-liquid film to the maximum rate of physical absorption defined by Levenspiel [113] for a second order reaction (the reaction between dye and ozone):

$$Ha = \frac{\sqrt{k.C_D.Diff_{O_3}}}{k_L} \quad (2.12)$$

where  $k$  is the reaction rate constant between dye and ozone in  $M^{-1}s^{-1}$ ,  $C_D$  is the dye concentration in  $M$ ,  $Diff_{O_3}$  is the ozone diffusivity in  $m^2/s$  and  $k_L$  is the mass transfer coefficient in  $m/s$ .

The magnitude of *Hatta* number provides a general idea about the reaction zone in the system. When  $Ha$  is small, the chemical reaction is slow and occurs in the liquid bulk solution, whereas the reaction is in the film when  $Ha$  is sufficiently large (Table 2.2). Enhancement factor was defined by Dankwerts [109] for an irreversible chemical reaction as follows:

$$E = \frac{\text{amount of absorbed reactant in a given time in a reacting liquid}}{\text{amount of absorbed reactant if there were no reaction}} \quad (2.13)$$

$$E = \frac{Ha \sqrt{\frac{E_i - E}{E_i - 1}}}{\tanh \left[ Ha \sqrt{\frac{E_i - E}{E_i - 1}} \right]} \quad (2.14)$$

Here  $E_i$  is the enhancement factor for an infinitely fast reaction and is found from the following equation:

$$E_i = 1 + \frac{Diff_D.C_D}{r_s.Diff_{O_3}.C_{O_3}^*} \quad (2.15)$$

where  $Diff_D$  is the diffusivity of the dye in  $m^2/s$  and  $r_s$  is the stoichiometric mole ratio between dye and ozone, in mole dye/mole ozone. As noted, the enhancement of mass

transfer coefficient is highly affected by  $Ha$  and  $E_i$ . The kinetic regime and enhancement of mass transfer in the system change as a function of  $Ha$  as shown in Table 2.2.

Table 2.2. The kinetic regime and enhancement factor as a function of  $Ha$  for a second order reaction [113].

<b>Kinetic regime</b>	<b>Condition</b>	<b>Reaction zone</b>	<b><math>E</math></b>
Very slow	$Ha < 0.02$	Liquid bulk	1
Slow	$0.02 < Ha < 0.3$	Liquid bulk	1
Moderate	$0.3 < Ha < 3$	Both bulk and film	$E > 1$
Very fast	$3 < Ha$	Film	$E > 1$
Pseudo first order	$3 < Ha$ and $Ha < E_i \sqrt{2}$	$C_D$ is constant	$E = Ha$
Instantaneous	$3 < Ha$ and $Ha > 10E_i$	Mass transfer control	$E = E_i$

The mass transfer coefficients in ozonation systems were investigated widely and some correlations relating  $k_L a$  to gas and liquid flow rates were found for the studied reactors [46, 118]. Mitani et al. [118] reported the following correlation for overall liquid phase mass transfer coefficient ( $K_L a$ ) in a microporous diffuser contactor (continuous reactor in both gas and liquid phases) in the absence of chemical reaction changing with gas flow rate ( $Q_G$  in  $m^3/s$ ) and liquid flow rate ( $Q_L$  in  $m^3/s$ ):

$$K_L a = 3.96 \times 10^8 (Q_L)^{1.53} (Q_G)^{0.40} \quad (2.16)$$

Velasquez and Ramirez [119] studied the ozonation of landfill leachates in a bubble column. Volumetric mass transfer coefficient was found in the presence or absence of a chemical reaction. Remarkable enhancement of  $k_L a$  in the absence of the chemical reaction was observed with the increase of superficial gas velocity ( $u_G$ ) and superficial liquid velocity ( $u_L$ ) as shown in Eqns. (2.17). The superficial liquid velocity ( $u_L$ ) affected  $k_L a$  in the presence of the chemical reaction insignificantly while the effect of  $u_G$  was noteworthy [Eqn. (2.17)].

$$k_L a = 1.35 (u_G)^{0.35} (u_L)^{0.23} \quad (2.17)$$

$$Ek_La = 12.3(u_G)^{0.99}(u_L)^{-0.04} \quad (2.18)$$

Zhou and Smith [120] showed gas flow rate as the most important factor affecting the mass transfer of ozone into the liquid phase. Mass transfer coefficient ( $k_La$ ) increased with the increase of gas flow rate. The presence of catalyst particles in a gas-liquid reactor was shown to enhance the mass transfer from gas to liquid phase since the bulk concentration of gaseous reactant decreased due to the adsorption onto the catalyst surface. The adsorption process resulted in the increase of driving force between gas and liquid phases.

## 2.2 Ozonation studies in wastewater treatment

Generally, a successful ozonation process for organic pollutants requires the achievement of almost 100% conversion of organics by oxidation to carbon dioxide (CO<sub>2</sub>), nitrogen gas (N<sub>2</sub>) and water (H<sub>2</sub>O) (complete mineralization). Then, in addition to 100% dye degradation, high TOC and COD removals are achieved. Ozonation is very effective in the cleavage of unsaturated bonds of dye molecules, giving high efficiency in color removal and the reactions generally are completed in a short time [78, 121]. Over 90% color removal was obtained in many researchs studies of dye ozonation [64, 85, 122, 123]. Hsu et al. [123] observed a very fast reaction of textile effluent with ozone; half of the color was removed in the first minutes of the reaction. However, the complete color removal was achieved in 60 min. According to Sarayu et al. [85], percent color removal was a function of the dye type; for example almost 100% color removal was obtained for Remazol Blue, but 80% of the color was removed in Remazol Yellow by ozonation.

The reaction of O<sub>3</sub> with dyes and textile wastewaters has been extensively studied in the recent years [85]. The mechanism of ozonation reactions in addition to the main factors affecting the mechanism was investigated in detail. Percent color and COD (and/or TOC) removals and biodegradability grade shown by BOD/COD ratio, were the important parameters which show the success of ozonation in wastewater treatment.

The dependency of decolorization time on the initial dye concentration is evident. By the increase of initial dye concentration, the organic load of the wastewater to be treated

by ozone increases. Therefore, inlet dye concentration was investigated as an operating variable in many studies [37, 81, 85, 87, 88]. At lower concentrations of dyes, the color removal was very fast; but when the dye concentration increased to 200-500 mg/L, more ozonation times were needed [85]. The degradation rate of COD and TOC was also high at the low dye concentration. Hsu et al. [87] investigated the effect of initial dye concentration on the ozonation of Mordant Black 11. They observed that 10 min of ozonation was sufficient to get 90% decolorization at the initial concentration of 200 mg/L whereas 500 mg/L of dye required 22 min to yield the same decolorization efficiency. Konsowa [81] found a linear relationship between the decolorization time and the initial dye concentration.

Ozone consumption per liter of liquid was shown to increase by the increase of inlet dye concentration [37] since more ozone was required for the oxidation of dye molecules at higher concentrations and higher amounts of ozonation by-products were accumulated in the solution.

Applied ozone dosage was observed to be a very important factor affecting the reaction time for complete color removal. Koch et al. [124] decolorized Reactive Yellow 84 completely in 60 min at the high ozone dosage and in 90 min at the low dosage. Sevimli and Sarıkaya [89] observed the increase of color, COD and dissolved organic carbon (DOC) removal percentages by the increase of ozone dose.

By sole ozonation, TOC and COD removal percentages were quite low achieving only limited mineralization [83, 122]. Removal of COD in the ozonation of dye effluents was limited to 50 % [78]. Mostly, higher values of COD removal were achieved than TOC removals in the process. Wang et al. [69] obtained 65% COD removal with 25% TOC removal in the ozonation of Remazol Black 5.

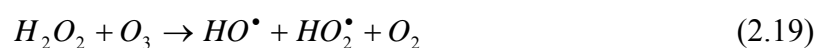
During ozonation and catalytic ozonation, intermediates and by-products are obtained as a result of the dye degradation. The types of by-products and intermediates mainly depend on ozone dose, reaction time, dye chemical structure and the presence of the catalyst. Chen [64] impressed the possible competition between the dye molecules and ozonation by-products for ozone in the solution. The yield of such products decreased the decolorization efficiency of the dyes, by accumulating in water.

COD and TOC removals were also affected by the applied O<sub>3</sub> dose and the reaction time. Gül et al. [125] found that COD reduction was increased by the applied O<sub>3</sub> dose. They stated that the complete conversion of organics to CO<sub>2</sub> and H<sub>2</sub>O was not feasible economically since it required a large amount of ozone. Soares et al. [37] obtained 5 to 19% TOC removals for several dyes for the O<sub>3</sub> concentrations of 6.25×10<sup>-4</sup> and 12.5×10<sup>-4</sup> mol/L gas (30 and 60 g/m<sup>3</sup> gas), respectively. But, contradictory results were also found. Singer [126] stated that even excess ozone in the medium did not result in complete mineralization. Similarly, Szpyrkowicz et al. [127] observed the increase of COD removal up to 1.04×10<sup>-5</sup> mol/L gas (0.5 g/m<sup>3</sup> gas) ozone concentrations but a further increase of O<sub>3</sub> concentration did not affect the COD removal.

### 2.3 Advanced oxidation processes for wastewater treatment

Ozone in principle should be able to oxidize organic compounds to carbon dioxide and water. However, in actual practice, it is quite selective in its oxidation reactions [39-41, 128]. Therefore, it may be favorable to utilize HO• which is non-selective and is produced as a result of the ozone decomposition reactions in aqueous phase at alkaline pH. In recent years, the processes generating HO• in aqueous phase called “Advanced Oxidation Processes” (AOPs) have been developed to accelerate the oxidation reactions [129]. AOPs have been achieved generally by adding some oxidizing agents such as H<sub>2</sub>O<sub>2</sub>, ultraviolet (UV) light, or some catalysts to ozonation process [130-132]. Those oxidation agents or metal oxides can initiate the production of HO• in the solution apart from the O<sub>3</sub> decomposition reactions [133].

By AOPs, the effectiveness of ozonation can be increased. H<sub>2</sub>O<sub>2</sub>/O<sub>3</sub> system was applied to many organics with high removal efficiency [133-138]. The initiation of O<sub>3</sub> decomposition in AOPs was indicated to be more rapid than that with HO<sup>-</sup> ions [134]. Volatile organic carbons (VOCs) for example, were oxidized to CO<sub>2</sub> and H<sub>2</sub>O completely by H<sub>2</sub>O<sub>2</sub>/O<sub>3</sub> process [133]. The production of HO• from H<sub>2</sub>O<sub>2</sub> and O<sub>3</sub> have been reported in several studies [39, 133, 135]:





The oxidation of organics with produced  $HO^\bullet$  is fast [133]. This suggests shorter contact time of organics with the oxidants in AOPs than that in sole ozonation. The ratio of the reactants may affect the process efficiency. Bellamy et al. [133] stated that  $H_2O_2/O_3$  ratio was an important parameter in the oxidation of organics and excess  $H_2O_2$  would act as a scavenger in the ozonation process.

Acar and Özbelge [137] studied the ozonation of Acid Red-151 in the presence of  $H_2O_2$ . The addition of  $H_2O_2$  into the system increased the decomposition of ozone at the studied pH range of 2.5-10. Besides, the ozonation was applied at different initial concentration ratio of  $H_2O_2$  to  $O_3$  ( $r = [H_2O_2]/[O_3]$ ). The highest dye and COD removal percentages were found to be at the  $r$  ratio of 0.5.

In some cases, the addition of  $H_2O_2$  to the system did not affect the rate of the process. Balcioğlu and Arslan [84] could not observe an increase of dye removal efficiency in peroxone ( $H_2O_2/O_3$ ) system. Conversely, ozonation at alkaline pH (pH=11) was more effective than  $H_2O_2/O_3$  peroxone process yielding 100% color, 75% COD and 15% TOC removals.

When the solution is irradiated with UV light (UV/ $O_3$  system),  $HO^\bullet$  radicals are produced in the solution via the following reactions [135]:



UV/ $O_3$  system also called photo-ozonation was applied to the treatment of such organics which were hardly degradable by ozone [139-142]. However, in some cases it was revealed that photo-ozonation produced toxic intermediates [139]. In addition, the TOC removal by photo-ozonation was low although the degradation of the target compound (chloroethylenes, chloroethanes and some ethers) was quick. In that case, longer photoozonation times were advised to reach total mineralization.

In the AOP reactions,  $HO^\bullet$  reacted through three different mechanisms [141, 143]:

- hydrogen abstraction



- electrophilic or radical addition



- electron transfer



Here *RH* and *RX* show the aliphatic compound to be treated whereas *PhX* is the aromatic compound. Hence, both aliphatic and aromatic compounds were degraded in an advanced oxidation process producing lower concentrations of by-products and achieving higher mineralization levels.

Fazzini and Young [140] compared the efficiency of O<sub>3</sub>, UV and UV/O<sub>3</sub> processes for the treatment of refractory organics in landfill leachate. UV/O<sub>3</sub> process indicated a small improvement in organic removal compared to O<sub>3</sub> alone. Appreciable amounts of TOC (34%) and COD (61%) were removed as opposed to the results in the study of Skorska and Davis [139]. Sauleda and Brillas [143] observed total mineralization of aniline and 4-chlorophenol by UV/O<sub>3</sub> system. In addition, the biodegradability of refractory organics was increased in UV/O<sub>3</sub> system showing that the UV/O<sub>3</sub> system combined with biological treatment could be efficient and economically feasible. Similarly, Ledakowicz et al. [145] found the increase of biodegradation level of textile wastewater by UV/H<sub>2</sub>O<sub>2</sub> treatment.

Advanced Oxidation Processes were used for the degradation of dyes and textile effluents [141, 146, 147]. The treatment of some azo and anthraquinone dyes was realized by UV/H<sub>2</sub>O<sub>2</sub> process (photolysis of H<sub>2</sub>O<sub>2</sub>) [141]. In almost 3 h, over than 90% mineralization was obtained. While without irradiation no change in TOC was observed, UV/H<sub>2</sub>O<sub>2</sub> achieved a remarkable TOC removal. Sadik and Nashed [145] applied UV/H<sub>2</sub>O<sub>2</sub> process for the treatment of Acid Alizarine Violet N dye. An increase in decolorization rate with the increase of H<sub>2</sub>O<sub>2</sub> concentration was noticed. As an AOP, Sadik and Nashed [145] also used UV/periodate (*IO<sub>4</sub><sup>-</sup>*) combination to oxidize the dye since periodate in the presence of UV produced highly reactive radicals including *HO<sup>•</sup>*

radicals. They stated that UV/ $IO_4^-$  process was better than UV/ $H_2O_2$  in the degradation of the dye.

Gomes de-Moraes et al. [143] treated textile effluent by  $O_3$ ,  $TiO_2/UV$  and  $O_3/TiO_2/UV$  methods. The most efficient method was  $O_3/TiO_2/UV$  method, giving 95% color removal. At the same conditions, the color removal was only 60% with  $O_3$ . 60% of TOC was removed by  $O_3/TiO_2/UV$  method in comparison with no significant TOC degradation by sole ozonation.

## 2.4 Evaluation of catalytic ozonation

The oxidative properties of  $O_3$  can be enhanced by the addition of a catalyst into the ozonation process. Recent studies on ozonation were concentrated on the use of homogeneous or heterogeneous catalysts for wastewater treatment. The enhancement of ozonation was realized by metals in solution, by metal complexes on supports or by non-polar organics creating a second phase in solution or on alumina support.

The effect of catalysts in ozonation of organics can be observed by producing free radicals or enhancing the reaction by adsorption. Some catalysts have been shown to have a promoting result in the generation of  $HO^\bullet$  radicals [52, 147, 148]. Gül et al. [149] investigated the effect of granular active carbon (GAC) on the treatment of Reactive Red 194 and Reactive Yellow 145 solutions by ozonation. The presence of the active carbon in ozonation catalyzed the decomposition of ozone to hydroxyl radicals. Hence, the consumption of ozone was increased when the active carbon was present in the solution. Additionally, the increase of the catalyst dose from 10 to 30 g in ozonation decreased the TOC removal efficiency of both dyes. This result supported the idea that the reaction between the dye and ozone occurred in the bulk phase rather than on the catalyst surface, and the GAC particles had an effect only on catalyzing ozone decomposition reactions. The solution pH was almost constant at neutral pH when the GAC was present in the process meaning that the adsorption of acidic by-products took place on the GAC surface.

Similarly, an enhancement of dissolved organic carbon (DOC) removal was explained by the production of  $HO^\bullet$  radicals on  $CuO/Al_2O_3$  catalyst surface in the ozonation of

oxalic acid [28]. Also, the formation of  $HO^\bullet$  was observed in the usage of Fenton's reagent ( $Fe^{2+}$  salt + hydrogen peroxide) or  $TiO_2$  [77].

#### 2.4.1 Use of metal ions/complexes in ozonation

Ozone may be activated by several metal ions such as Fe, Mn, Ni, Cu in solution. Some complex ions may be produced due to the reaction between the metal and ozone; as a result, highly oxidative radicals such as hydroxyl radicals may be observed. Wu et al. [151] ozonated Reactive Red 2 (RR2) and Acid Orange 6 (AO6) solutions in the presence of  $MnO_2$  in the solution. They observed the acceleration of dye removal rate by the addition of  $MnO_2$  in the ozonation process. The change of  $MnO_2$  dose affected the removal of oxalic acid, existed as a by-product in ozonation. The consumed amount of ozone was decreased by the presence of  $MnO_2$  markedly. However, the catalytic ozonation was effective at low ozone doses mainly; the increase of ozone dose had a minor effect on dye decolorization rate. It was stated that the catalytic activity of  $MnO_2$  could be realized by the formation of manganese-dye complex on the catalyst surface. Then, the ozonation of manganese-dye complex occurred.

Solution pH can be an important parameter even for catalytic ozonation reactions for both enabling the production of  $HO^\bullet$  and influencing the surface properties of the catalyst [152]. Sometimes the used catalysts can be efficient at both acidic and alkaline pH. Ferral, a combination of catalysts  $Fe_2O_3$  and  $Al_2O_3$ , was used a catalyst in the ozonation of several dyes including *RBBR* and it was demonstrated that the catalyst had the greatest activity for both color and COD removals at acidic pH [31]. Ferral increased the color removal efficiency for all dyes except chromium complex acid dye. Here, the negative effect of chromium ions in ferral-catalyzed ozonation was pointed out. The efficiencies of ferral-catalyzed ozonation and ozonation+ferral coagulation processes were compared with each other resulting that ferral catalyzed ozonation had a better efficiency in color and COD removals. Hereby, the activity of ferral as a catalyst was understood apparently. In the case of Congo Red ozonation with  $Cu(NO_3)_2$ , the enhanced activity of the catalyst was observed at neutral and alkaline pH [153]. However, the decolorization rate was not improved by the catalyst at the acidic pH. Leitner and Fu [152] achieved high TOC removal percentages at pH = 3.6 and 10.0 using Ru on  $CeO_2/TiO_2$  catalyst. The relationship between pH and ozone consumption

(mmol O<sub>3</sub> consumed/L liq) differed in ozonation and catalytic ozonation. While in catalytic ozonation, ozone consumption was minimum at pH = 5, it was increased by the increase of pH in conventional ozonation.

Andreozzi et al. [102] used MnSO<sub>4</sub> solution as the homogeneous catalyst in the ozonation of glyoxalic acid. The experiments at pH=2.0 pointed out that the presence of Mn<sup>2+</sup> ions in the medium increased the degradation of glyoxalic acid compared to ozonation alone. Difference in reaction by-products of catalytic and non-catalytic ozonations was observed indicating a change in the reaction mechanism with the catalyst. The interactions of Mn<sup>2+</sup> ions with glyoxalic acid molecules gave rise to an oxidation reaction which further achieved almost complete mineralization (oxidation to carbon dioxide and water).

In catalytic ozonation, ozone molecules can interact with the active sites of the catalyst creating oxidation centers/species. Delanoe et al. [154] proposed ruthenium as the active site in the catalyst Ru-CeO<sub>2</sub>/TiO<sub>2</sub>. The characteristics of the active site was mainly affected by the change of pH.

The adsorption of organics and/or ozone on the catalyst surface is an important mechanism in catalytic ozonation. Metal oxides like titania, alumina, zirconia carry Brönsted and Lewis acid sites on their surface. This is why the catalyst surface is affected by the change in pH. A property called “pH of point zero charge” (pH<sub>PZC</sub>) characterizes the surface charge of the catalyst at a certain pH; pH<sub>PZC</sub> shows the pH at which the surface net charge of the catalyst is zero [152, 155]. In acidic pH with a value much lower than the pH of “Point of Zero Charge” (pH<sub>PZC</sub>) of the catalyst, the catalyst surface became positively charged. Hence, the adsorption of negatively charged ions such as carboxylic acid anions occurred. For pH higher than pH<sub>PZC</sub>, the catalyst surface was negative, adsorbing positive ions [155].

Ozone molecule has an electron density on one of its oxygen atoms; as a result it may be absorbed on the Lewis acid site of the catalyst surface [156]. Leitner and Fu [152] claimed that there was a remarkable competition between HO• and active sites of the catalyst surface for the organics at basic pH. Hence, higher mineralization was achieved

with catalytic ozonation than sole ozonation because of the organic degradation both in aqueous phase and on the catalyst surface.

Another important factor is the  $pK_a$  value of the dissolved organic pollutant which is a sign of the ionic state of the organic affecting the charge of the organic. A pH higher than the  $pK_a$  of the organic results in the organic to be in ionic form in the solution. Uncharged organic molecules are present in the medium when pH is lower than the  $pK_a$  of the organic. As understood, both the charge of the organic and surface characteristic of the catalyst are important in the adsorption of organics to the catalyst surface. Leitner and Fu [152] showed that the adsorption process was the limiting step in catalytic ozonation in most cases.

Alumina can be used as a catalyst and catalyst support in wastewater treatment processes. As an adsorbent, several organics can be adsorbed on alumina and removed from the wastewater. The acid-base properties of alumina are the main reason of its wide usage. The synthesis of the types of alumina used in water treatment are obtained by the dehydration of gibbsite, bayerit or boehmite which are different forms of  $Al(OH)_3$ . Recently, alumina has been applied in ozonation as a catalyst alone or the support for metal oxides and non-polar organics [32-35, 157-160]. Bandara et al. [161] observed more adsorptive and catalytic activity of  $\gamma$ -alumina ( $Al_2O_3$ ) type than other types of alumina. In pilot-scale and laboratory usage  $\gamma$ -alumina has been widely applied to wastewater treatment.

In industry, mostly used two groups of alumina are [155]:

- low temperature alumina [ $Al_2O_3 \cdot nH_2O$  ( $0 < n < 6$ )]. This group belongs to  $\rho$ ,  $\chi$ ,  $\eta$  and  $\gamma$ - $Al_2O_3$  which are named according to their crystal structure. The dehydration of low temperature alumina is applied at temperatures not exceeding  $600^\circ C$ .
- high temperature alumina [ $\kappa$ ,  $\theta$  and  $\delta$ - $Al_2O_3$ ]. Nearly unhydrous alumina is obtained between  $900$ - $1000^\circ C$ .

The crystal structure of all alumina types is close-packed oxygen lattice with aluminium ions. Low temperature aluminas show cubic-close packing oxygen lattices, but high

temperature aluminas are hexagonal close-packed lattices [155]. High temperature alumina is less active than low temperature alumina. It has lower surface area and larger particle size, different population of surface active sites. Low temperature transition alumina is used as both catalyst and adsorbent in water treatment technology [155]. Some ozonation studies in the presence of alumina are given in Table 2.3.

Table 2.3. The ozonation studies that used alumina as the catalyst.

Reference	Reactor	Organic	Particle Size (mm)	Surface area (m <sup>2</sup> /g)	Pore volume (cm <sup>3</sup> /g)
Pi et al. [68]	Stirred glass	benzene	2-5	119	0.758
Bandara et al. [161]	-	chlorophenols	-	170 16	-
Ni and Chen [162]	Semi-batch stirred	2-chlorophenol	0.06-0.2	120-190	-
Einaga and Futamura [163]	-	Benzene	-	170	-
Volk et al. [164]	-	Fulvic acid	1.5-2.5	-	-
Kasprzyk Hordern et al. [34]	-	Humic acids	0.25	190.4	0.23
Kasprzyk Hordern et al. [35]	Stirred semi-batch, Semi-continuous	Several ethers	0.25 3×5 mesh	190 196	0.23 0.42
Beltran et al. [71]	Agitated tank	Oxalic acid	0.5-1.6 2.0-3.0	139	
Ernst et al. [29]	Batch, Semi-continuous	Oxalic acid	-	139.9 144	-

The groups on the alumina surface determine its acidity or basicity in different solutions. In aqueous solution, there exists a chemisorption process between Al<sup>3+</sup> ions and hydroxyl ions (<sup>-</sup>OH) of water creating hydroxyl (HO) groups on alumina [32, 155]. If dehydration is applied to alumina, the surface characteristics may change since HO groups react with each other to form oxygen bridges. The hydroxyl groups and oxygen bridges were shown to be responsible for the adsorption of organic molecules

on alumina surface. Kasprzyk-Hordern [155] highlighted that the some complex alumina surface groups were created in the presence of water molecules. Also, it was stated that the surface hydroxyl groups of alumina showed an amphoteric character with respect to acidity-basicity and, the surface of alumina was affected by its  $\text{pH}_{\text{PZC}}$  and reaction pH, similar to other metal oxides (Figure 2.2).

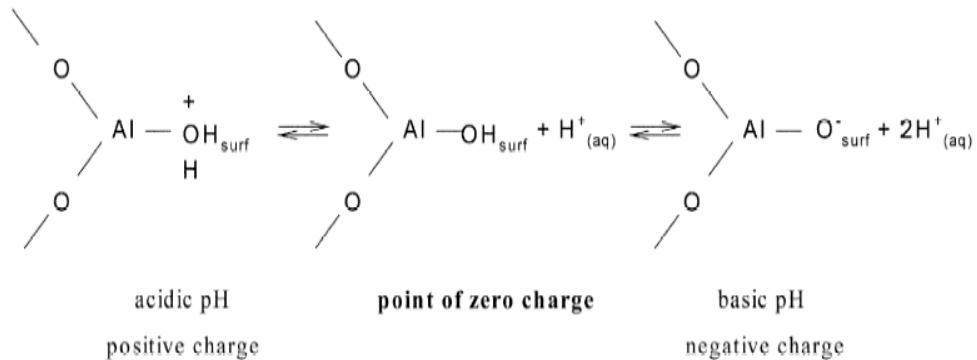


Figure 2.2. The surface charge of alumina changing with pH [155].

The typical activated alumina used in water treatment are 28×48 mesh (0.3 to 0.6-mm diameter) mixtures of amorphous and  $\gamma$ -alumina prepared by low temperature dehydration of  $\text{Al}(\text{OH})_3$ . They have surface areas of 50-300  $\text{m}^2/\text{g}$ . The  $\text{pH}_{\text{PZC}}$  values of different alumina types were investigated in the literature and Kasprzyk-Hordern [155] listed those values in Table 2.4 to give an idea about the surface charge of alumina at different pH.

The surface characteristics of alumina determine the type of organics that will be adsorbed on the surface. Kasprzyk-Hordern [155] stated that small molecular weighted organics were not adsorbed on oxide surfaces of alumina. Only, the substances containing functional groups such as carboxylic or amino groups were attached to the surface since those groups created complexes replacing the hydroxyl group of alumina on the surface. Also, the adsorption of non-ionic hydrophobic chemicals was hard on alumina due to the competition between water molecules and those chemicals for the

surface. Due to its ionic character, water molecules were preferentially attached to the surface.

Table 2.4. The  $\text{pH}_{\text{PZC}}$  values of different alumina types [155].

<b>Material</b>	<b><math>\text{pH}_{\text{PZC}}</math></b>
$\alpha\text{-Al}_2\text{O}_3$	8.4-9.2
$\gamma\text{-Al}_2\text{O}_3$	8.0-9.0
$\delta\text{-Al}_2\text{O}_3$	7.3
$\gamma\text{-AlOOH}$	7.7-9.4
$\text{Al}(\text{OH})_3$	7.7-9.4

The studies about catalytic ozonation of the dyes and dyehouse effluents are limited. The used catalysts were generally in metallic form such as  $\text{MnSO}_4$ ,  $\text{FeSO}_4$  and  $\text{TiCl}_3$ . Hassan and Hawkyard [165] studied the effect of several catalysts including carbon, ferral,  $\text{Fe}_2\text{O}_3\text{-SiO}_2$ , and hydrated alumina ( $\text{Al}(\text{OH})_3$ ) on the color removal of several dyes. 63% of COD was reduced in ozonation with ferral compared to 7.9% COD reduction in ozonation only. They concluded that the positive effect of ferral in ozonation was from its catalytic activity because ozonation with ferral showed higher dye and COD removal efficiencies than both adsorption with ferral and sole ozonation. Hydrated alumina-catalyzed ozonation was superior to remove color among all the other catalysts. Using hydrated alumina, the highest color removals were obtained at acidic pH ( $\text{pH}=4$ ) and at basic pH ( $\text{pH}=10$ ), showing the lowest efficiency at pH of 7. The increase of removal efficiency was explained by the formation of  $\text{HO}^\bullet$  radicals during catalysed ozonation. Additionally, hydrogen peroxide ( $\text{H}_2\text{O}_2$ ) was observed in the system and a complex oxidation system including  $\text{O}_3$ ,  $\text{H}_2\text{O}_2$  and  $\text{Al}(\text{OH})_3$  was considered to have importance in color removal.

Trapido et al. [166] studied several metal oxide catalysts such as  $\text{MnO}_2$ ,  $\text{Fe}_2\text{O}_3$  and  $\text{Al}_2\text{O}_3$  to understand the catalyst efficiency in the ozonation of *m*-dinitrobenzene (*m*-DNB). The presence of those transition metals in ozonation increased the degradation rate of *m*-DNB for all catalysts used except  $\text{V}_2\text{O}_5$ . The ozonation rate of *m*-DNB was decreased in the presence of  $\text{V}_2\text{O}_5$ . In those experiments, dissolved ozone concentrations in the liquid phase were found to be lower in catalytic ozonation

compared to those in ozonation only. Lower dissolved ozone concentrations indicated that more ozone was decomposed in catalytic ozonation enabling the production of reactive radicals according to Trapido et al. [166]. Hence, the removal of COD was increased with the addition of the catalysts. Comparing all catalysts, the most efficient catalysts were found as  $\text{Al}_2\text{O}_3$  and  $\text{Ni}_2\text{O}_3$  in view of COD removal efficiency. The higher efficiencies of those catalysts were explained by the enhanced degradation of ozonation intermediates with  $\text{Al}_2\text{O}_3$  and  $\text{Ni}_2\text{O}_3$ .

The superiority of catalytic ozonation for the TOC removal of several dissolved organic pollutants was observed in several studies [162, 167, 168]. Using catalyst in ozonation achieved higher TOC removal than those attained in sole ozonation. Al-Hayek et al. [169] observed 90% TOC reduction by applying  $\text{Fe}^{3+}/\text{Al}_2\text{O}_3$  catalyst in ozonation of phenol. With sole ozonation, the TOC removal was less than 40%.

Ni and Chen [162] used  $\gamma$ -alumina as the catalyst in the ozonation of 2-chlorophenol and they observed that the TOC removal was increased more than two times in the catalytic ozonation compared to that in ozonation alone. The level of TOC removal was a factor of catalyst dosage, it increased with the ozone dosage up to 2 g  $\text{O}_3/\text{L}$ , then remained unchanged. Ni and Chen [162] proposed that the reaction between the organic and ozone occurred both in the bulk liquid phase and solid phase simultaneously. On the alumina surface, ozone molecules were converted to  $\text{O}^\bullet$  radicals and the reaction on the surface was catalyzed by those radicals.

Ernst et al. [29] observed the remarkable efficiency of  $\gamma$ -alumina in the ozonation of refractory organics such as acetic, oxalic and salicylic acids. However, the usage of phosphate buffer caused a decrease in the removal rate since phosphate ions were adsorbed on the catalyst surface deactivating it.

Einaga and Futamura [163] investigated the ozonation of benzene in the presence of alumina supported manganese oxide. The evolution of  $\text{CO}_2$  and CO on the catalyst surface was an indication of surface reaction between ozonation intermediates and ozone. The oxidation of intermediates on the catalyst surface produced  $\text{CO}_2$  and CO. A

competition between benzene and intermediates for the catalyst surface was observed since the presence of benzene inhibited CO<sub>2</sub> formation.

Titanium dioxide (TiO<sub>2</sub>) was another catalyst in the ozonation processes [62]. Hernandez-Alonso et al. [62] used TiO<sub>2</sub> for the ozonation of cyanide, and their FT-IR analysis on used TiO<sub>2</sub> demonstrated that O<sub>3</sub> adsorption on the catalyst surface occurred generating  $^{-}O_3^{\bullet}$  and  $HO^{\bullet}$  radicals. Those radicals enhanced the degradation of cyanide in the bulk.

Beltran et al. [71] used powdered TiO<sub>2</sub> in the ozonation of oxalic acid, a hardly degradable compound by molecular ozone. The removal rate of the target compound was increased effectively with the catalyst. They suggested a mechanism including the adsorption of ozone and the production of free radicals on the catalyst surface. Also, oxalic acid adsorption was assumed in the mechanism.

In another study by Beltran et al. [30], the catalyst was the TiO<sub>2</sub> impregnated on  $\gamma$ -alumina spherical pellets for oxalic acid removal. Ozone dissolution kinetics was not affected by the presence of the catalyst showing that ozone adsorption on the catalyst surface did not occur. As a result, ozone was assumed to be in water phase only. Beltran et al. [30] found that gas flow rate higher than 24 L/h did not affect the removal efficiency of oxalic acid in catalytic ozonation. Therefore, the experiments were carried out at 24 L/h gas flow rate to obtain a chemically controlled regime. The effect of the particle size was investigated also. For the particle sizes equal or lower than 1.6-2 mm, the removal rate of oxalic acid remained unchanged therefore internal mass transfer resistance in the particles was neglected. The higher removal rates observed at the higher catalyst doses indicated that the reaction occurring on the catalyst was significant.

Even in catalytic ozonation, ozone dosage and contact time between the target solution and ozone are important parameters. In some studies, the catalytic effect was more clear with longer contact times [68]. Additional TOC reduction was obtained with sufficient ozone dosage in catalysed ozonation [170].

Generally, catalytic ozonation studies have shown that the efficiency of the catalyst in the ozonation process was dependent on the compound type to be ozonated and the treatment conditions such as pH, ozone to catalyst dose ratio and the surface characteristics of the catalyst [166]. The ozone utilization rate was increased by the presence of the catalyst in the process. Trapido et al. [166] supported the idea that the performance of the catalysts in ozonation was compound-selective. In most cases, the presence of the catalysts deteriorates or does not affect the removal efficiency of the target compound but it helps the degradation of intermediates and/or final products of ozonation enabling the decreases of TOC and COD.

Fontanier et al. [171] found a linear relationship between COD and TOC in ozonation in the presence of metal oxides as the catalysts. They pointed out no remarkable relation of COD with TOC in non-catalytic case. From this observation, it was highlighted that the organic matter in solution was oxidized to complete mineralization in one step.

Catalytic ozonation is supposed to give a lower ozone consumption than that in sole ozonation [32, 35, 158]. Balcıoğlu et al. [172] conducted the treatment of pulp and paper effluents with granular active carbon catalyzed ozonation. Lower O<sub>3</sub> consumption per mg of COD removal was declared in catalytic ozonation as a result of the remarkable contribution of the radical reactions. On the contrary, the consumed ozone was increased by the presence of CuO/Al<sub>2</sub>O<sub>3</sub> catalyst in phenol ozonation [173].

According to Fontanier et al. [171] whatever the target compound, ozone consumption remained almost constant at about 50% of the applied ozone in catalytic ozonation. Even when the mineralization kinetics changed, the consumption rate was constant showing that ozone interacted with the catalyst surface producing an oxide on the surface; then, afterwards the targeted compound was mineralized on the catalyst surface by the reaction with the produced oxide.

Besides catalytic ozonation, sole adsorption process of the dyes onto a catalytic surface has been utilized to remove color from the textile effluents. However, adsorption has been shown not to be very effective for the dye removal, the adsorbents are to be disposed or their regeneration is required. Problems associated with the regeneration become significant. During regeneration, some chemicals and energy are used.

Ni and Chen [162] studied the adsorption of 2-chlorophenol (2-CP) on alumina under different pH. The highest adsorption of 2-CP was observed at pH=2 with 2.2% in 60 min. This showed the insignificant removal of 2-CP by the adsorption on alumina. Similarly, Ma et al. [174] found only 5% nitrobenzene removal with the adsorption on granular activated carbon (GAC).

Beltran et al. [30] stated that although adsorption on  $\text{TiO}_2/\text{Al}_2\text{O}_3$  catalyst was an important mechanism in oxalic acid treatment, it was not sufficient to remove the required high levels of oxalic acid. In several studies, the adsorption capability of alumina towards organic compounds has been extensively investigated [25]. Most of the alumina types used were impractical for the treatment of textile industry effluents. Also, it was shown that the adsorbents were insufficient to remove disperse and vat dyes.

#### **2.4.2 Non-polar catalytic ozonation for wastewater treatment**

The application of perfluorinated compounds (compounds in which all hydrogens are replaced with fluorines) gained much attention in wastewater treatment. These compounds are widely used in the molecular ozonation to increase the reaction rate. Due to the presence of fluorine atom with an electronegativity of 4.0 V, the compound has a characteristics of having higher oxidized state carbons with a high chemical stability [175, 176]. Therefore, the perfluorinated compound shows a resistivity toward oxidation by ozone. The resistivity of compound was proven by the FT-IR studies of perfluorooctanoic acid bonded alumina. It was seen that C-F bonds adsorbed on the alumina surface were not oxidized by ozone [158]. The hydrophobic character of those compounds as a result of the low polarizability of fluorine atom, has been reported [158].

The treatment of organics from the wastewater with perfluorinated hydrocarbons is made by two methods: the application of two-phase ozonation with perfluorinated hydrocarbons and catalytic ozonation with perfluorinated alumina bonded phase [158]. Two-phase ozonation, is based on the diffusion of organic pollutant from the water phase to the organic phase (saturated with ozone, nonpolar perfluorinated hydrocarbon solvent) and then, the oxidation of the organic pollutant by molecular ozone in the hydrocarbon solvent. Because, in this case, ozone at low polarity also diffused to the

hydrocarbon phase. The diffusion of ozone to the organic phase increases its stability and solubility in the organic phase. It was proven that the solubility of ozone in the organic hydrocarbon solvent phase was 10 times higher than its solubility in water phase [30]. Also, the efficiency of perfluorinated hydrocarbons in the ozonation of organic pollutants was shown [33-35, 157-160].

Alumina is known to possess a high adsorption capacity especially toward perfluorinated surfactants. That is the reason why the usage of bare alumina in water treatment processes can be profitable [155]. Catalytic ozonation based on perfluorinated hydrocarbon fixed on alumina is the second method in treatment of wastewaters; here ozone or organic pollutant is adsorbed on the surface of the alumina impregnated with non-polar perfluorinated hydrocarbon. Perfluorinated hydrocarbon is fixed on the alumina surface producing a monolayer and this prevents its passage back to the water phase. The  $-\text{COOH}$  group of perfluoro acids makes a bond with the  $-\text{HO}$  group of the alumina [158]. Non-polar perfluorinated alkyl chains on the alumina surface are very active towards ozone and dissolved organic pollutants in wastewater. The low polarity of  $\text{O}_3$  with a dipole moment of 0.46 debye (D) provides its high affinity towards PFOA surface [34].

Perfluorooctanoic and perfluorooctadecanoic acids are mostly used hydrocarbons on alumina [32]. Kasprzyk-Hordern et al. [33, 34, 157-160] used perfluorooctyl alumina (PFOA) mostly in their studies and they applied PFOA/ $\text{O}_3$  method to the treatment of aromatics like benzene, toluene; ethers like methyl *tert*-butyl; humic acids (HA) and natural organic matter (NOM) [33-35, 157-160]. They proposed a mechanism showing PFOA catalyzed ozonation [Figure 2.3]. According to that mechanism, both  $\text{O}_3$  and the organic pollutant were adsorbed on the surface of PFOA; the oxidation reaction between them occurred on the surface and then, the hydrophilic by-products were desorbed from the catalyst into the liquid phase. The treatment efficiency of the aromatics was increased by 24-43% compared to ozonation alone [158]. In another study, the removal efficiency of methyl *tert*-butyl ether was 22.7% by ozonation with PFOA whereas by ozonation alone it was only 10.6% [35]. Also, the high affinity of Natural Organic Matter (NOM) towards PFOA enabled higher removal rates of NOM in PFOA catalyzed ozonation [34].

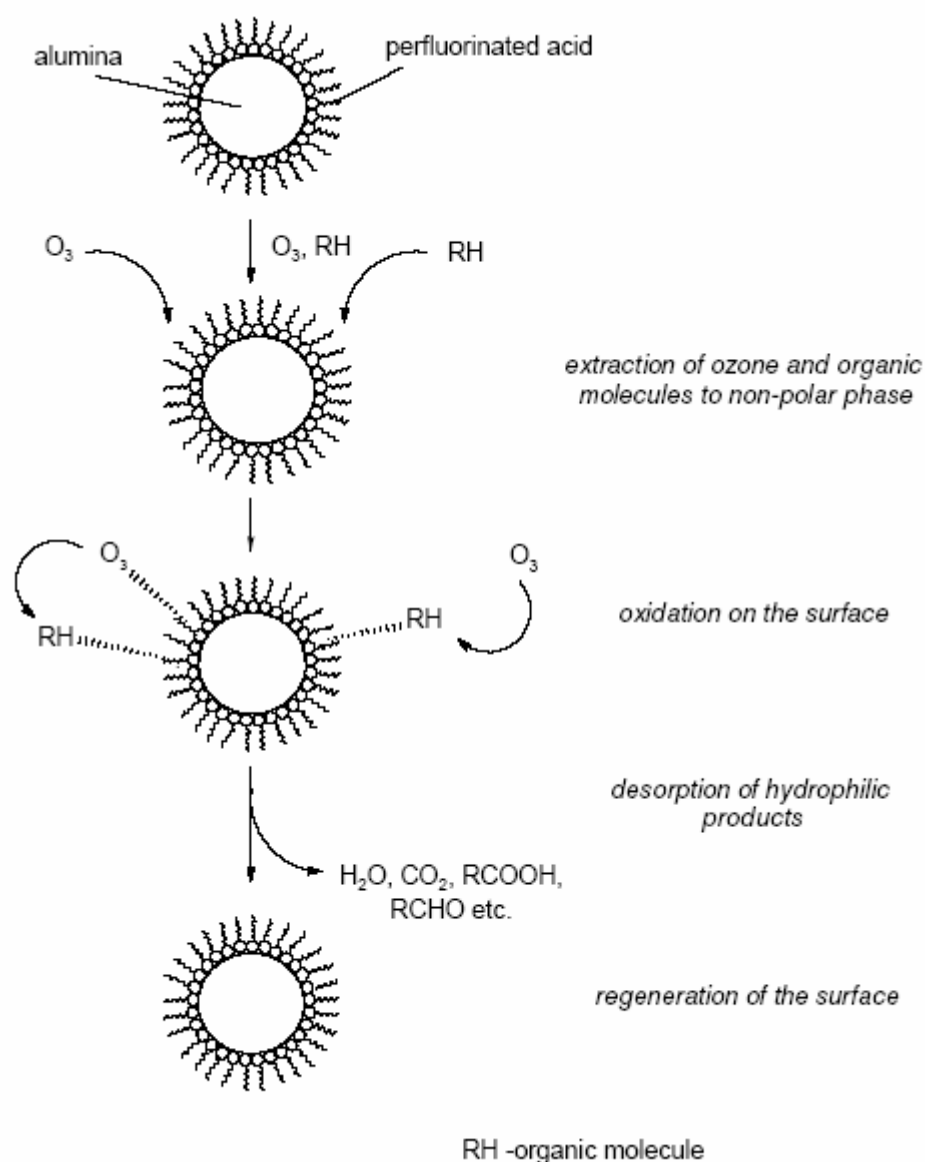


Figure 2.3. The mechanism of ozonation with PFOA according to Kasprzyk-Hordern et al. [155].

The application of perfluorooctanoic acid on alumina enhanced the stability of ozone in the system. Kasprzyk-Hordern et al. [158] showed that PFOA/ $O_3$  system was more effective at acidic pH and no decomposition of  $O_3$  occurred in the presence of PFOA. They concluded that direct ozonation mechanism was responsible for oxidation of the organic pollutants with PFOA/ $O_3$  system. The use of lower ozone dosages in PFOA/ $O_3$  system was observed with equal or greater removal efficiency of the organic compared to the non-catalyzed ozonation. Contrarily, the adverse effect of high  $O_3$  dosages was

seen due to the possible blockage of PFOA sites with ozonation by-products. High O<sub>3</sub> dosages provided the oxidation of the organic in the bulk of the liquid also producing some compounds such as carboxylic acids which were active towards PFOA surface.

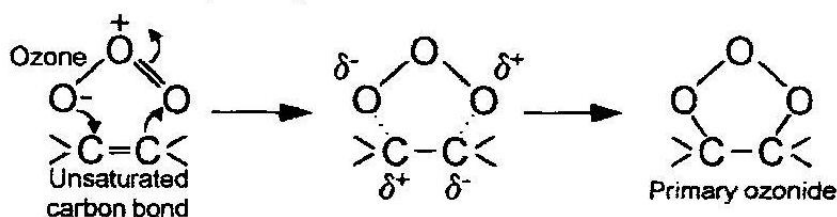
In literature, the use of perfluorinated alumina catalysts is limited. In addition, there is no study about the removal of industrial dyes by the ozonation in the presence of perfluorinated alkyl alumina. By this method, the treatment efficiency of the dyes which are resistant to ozonation may be increased. Especially, non-polar disperse dyes may be removed from the wastewater effectively. Also, since several by-products such as aldehydes and carboxylic acids are produced after the ozonation of dyes, these undesired by-products may be removed by catalytic ozonation.

## **2.5 Ozonation by-products**

According to the dye structure, the ozonation intermediates and by-products show a variety. Generally, it is known that ozonation of dyes yields two types of by-products, namely aldehydes and carboxylic acids. Since the dyes used in industry were mainly azo and anthraquinone dyes having aromatic structures (phenol and naphthalene rings), the ozonation of phenol and phenol-like substances was investigated to understand the basic reaction steps and the types of formed by-products [54, 177, 178].

In the degradation of aromatic structure of any molecule, aromatic ring is opened by oxidation with ozone and intermediates containing  $-C=C-$  bonds are formed (Figure 2.4). The ozonation products of phenol were classified in three groups according to Zhu et al. [177]: (i). primary products (catechol, resorcinol, hydroquinone), (ii). more oxidized products (maleic acid, oxalic acid), (iii). final products (CO<sub>2</sub> and H<sub>2</sub>O). The primary products contained mostly carbon-carbon double bonds and such compounds were quickly oxidized to oxalic acid due to the unsaturated bonds they had. In other words, oxalic acid was found to be the main by-product of phenol at the studied experimental conditions. They stated that oxalic acid had to be a certain product of ozonation since it was symmetrical and each carbon was stable with carboxyl groups. Then, a reaction mechanism was proposed for phenol ozonation throughout the oxalic acid and carbon dioxide. Zhang et al. [54] claimed that benzene and naphthalene rings were opened to produce formic and oxalic acids.

**STAGE 1: 1-3 dipolar cyclo addition of ozone on unsaturated bonds**



**STAGE 2: Decomposition of primary ozonide in water**

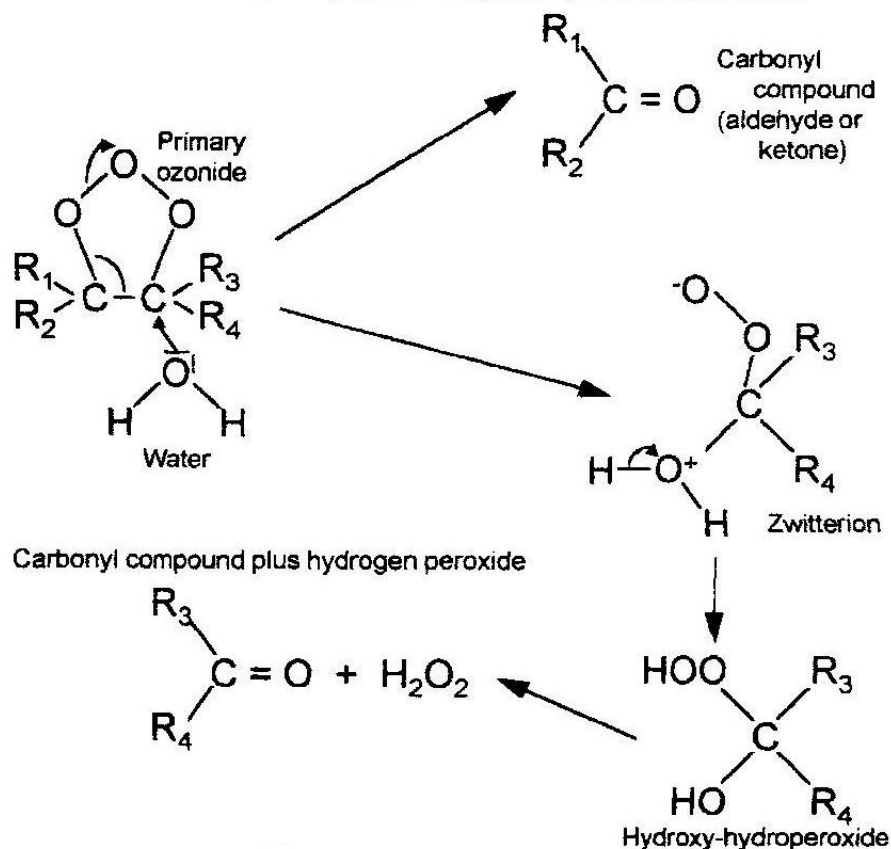


Figure 2.4. The stages of ozonation of organics

The breakage of a long-complicated dye molecule is achieved by the oxidation of other groups such as azo or sulfonate group besides the aromatic groups during ozonation. In the azo dye structure, due to the cleavage of  $-\text{N}=\text{N}-$ , nitrogen gas and/or nitrate ions ( $\text{NO}_3^-$ ) are produced [166]. The last studies on the ozonation of azo dyes proved that azo group in the structure was converted to mainly nitrogen gas instead of another compound containing nitrogen [8]. The source of nitrate ions was due to the oxidation of amino ( $\text{NH}_2$ ) groups in the structure. Also, ammonium ions were detected due to the oxidation of  $\text{NH}_2$  group. Trapido et al. [166] observed  $\text{NO}_3^-$  ions in the ozonation of

nitrobenzene throughout the reaction and they concluded that nitro groups were converted to  $\text{NO}_3^-$  ions. Zhang et al. [54] postulated that nitrogen was removed from the structure of the azo dye, Reactive Red 120, as nitrogen gas preferentially but small amounts of nitrate and ammonium ions were also observed in the medium. Similarly, the sulfonic groups in the dye structure were oxidized to sulfate ions.

Phenol and phenol-like intermediates can be found in the ozonation of dyes. Zhang et al. [54] observed phenol, 1,2-dihydroxysulfobenzene and 1-hydroxysulfobenzene as the reaction intermediates of Reactive Red 120. They considered that the reaction was initiated by the replacement of hydroxyl group with amino group in the dye structure. Azo linkages were hydrogenated, the azo bonds were broken giving benzene and naphthalene derivatives.

Aldehydes were primarily seen as the by-products of many dyes. Lopez et al. [179] specified the final products of the ozonation of azo dyes as formaldehyde, acetaldehyde, glyoxal, acetone, acetic acid, formic acid, oxalic acid and carbonic acid. Dabrowska et al. [180] demonstrated that formaldehyde and acetaldehyde were the main by-products in water comprising 80% of all aldehydes. The aldehyde concentration produced during ozonation was observed to increase by the increase of  $\text{O}_3$  dose [180]. Can and Gürol [181] noticed that the structure of ozonated organics could be a determining step for aldehyde formation. Formaldehyde production reached a peak level and then, its concentration began to decrease. They stated that aliphatic organics probably had a tendency to produce more formaldehyde than aromatic organics. Contrary to Dabrowska et al. [180], Can and Gürol [181] pointed out that at low  $\text{O}_3$  dose, formaldehyde was accumulated in the system but its concentration was decreased at high  $\text{O}_3$  dose.

Song et al. [182] listed the main by-products of Direct Red 23 as nitrate, sulfate, formic, acetic and oxalic acids. Interestingly, no aldehyde was found. Mascolo et al. [183] and Miltner et al. [184] confirmed this case by the fact that at the higher ozone doses, the oxidation of aldehydes to corresponding carboxylic acids occurred. As a result, instead of formaldehyde, acetaldehyde and glyoxal, formic, acetic and oxalic acids were detected. In the study of Liakou et al. [73], oxalate, formate and benzenesulfonate ions were the main products resulting from the ozonation of Orange II dye.

Demirev and Nenov [185], found oxalic acid and nitrate ions in the ozonation of Schwarz GRS azo dye, and only oxalic acid in the ozonation of Orange Acid 8 in 30 min. In Schwarz GRS dye, there was an amino group ( $\text{NH}_2$ ) withdrawing electrons. Instead, in Orange Acid 8, there was a methyl group ( $\text{CH}_3$ ) increasing the electronegativity of the molecule. Then, Orange Acid 8 was shown to degrade by ozone more due to its higher electronegativity.

The presence of a catalyst in ozonation was shown to affect the reaction mechanism. First of all, the mineralization ratio was increased with the catalyst in ozonation observed by the increase of TOC removal percentage. Therefore, the types and quantity of by-products are expected to alter in catalyzed ozonation. The studies on the by-products of catalytic ozonation of organics were limited. Qu et al. [186] observed more denitration (mineralization of nitrogen) and cleavage of the aromatic ring in the  $\text{Cu}/\text{Al}_2\text{O}_3$  catalyzed ozonation of alachlor compared to sole ozonation. Kasprzyk-Hordern et al. [33-35, 157-160] aimed to find main ozonation by-products in their several studies in the presence of PFOA. They ozonated several ethers in the aqueous medium and observed the by-products of formic, acetic and oxalic acids (main), formaldehyde and acetone [35]. The concentration of oxalic acid was increased in the catalytic ozonation case using PFOA compared to that in ozonation only. On the contrary, the amounts of formic acid and formaldehyde were decreased when the catalyst was added to the ozonation.

In another study [159], a wastewater containing Natural Organic Matter (NOM) was ozonated in the presence of PFOA and the most important products were found as formaldehyde and acetone. It was stated that acetone was produced only in the case of catalytic ozonation.

Faria et al. [187] ozonated sulfonated aromatic compounds in the presence or absence of activated carbon. The concentration of accumulated oxalic acid in the solution was found to be lower in the presence of activated carbon than that in sole ozonation. The enhancement of mineralization by the catalyst was obvious. Alvarez et al. [188] detected acetic acid as the main reaction product of pyruvic acid ozonation when  $\text{Co}/\text{Al}_2\text{O}_3$  catalyst was used in the process. Interestingly, a negligible amount of oxalic acid was found in contrast to the case in sole ozonation.

Both conventional and catalytic ozonations resulted in the degradation of high molecular weight compounds to low molecular weight compounds according to Fontanier et al. [171]. However, the metal oxide catalyst resulted in the degradation of produced low molecular weight compounds to CO<sub>2</sub> and H<sub>2</sub>O. Udrea and Bradu [173] observed malonic acid as a product in the CuO/Al<sub>2</sub>O<sub>3</sub> catalyzed ozonation of phenol in addition to propionic, glycolic and acetic acids. The last three compounds were also detected in conventional ozonation. Manganese-catalyzed ozonation of glyoxalic acid formed methanoic acid, a different product not observed in sole ozonation [102].

## CHAPTER 3

### MODELING OF SEMI-BATCH AND CONTINUOUS OZONATION PROCESSES

#### 3.1 The determination of reaction rate constants in semi batch process for catalytic and non-catalytic ozonations

Data taken from the semi-batch reactor were analyzed for both *AR-151* and *RBBR* dyes to determine the reaction rate constants in the presence and absence of the catalyst particles. The data available were the dye concentrations measured as a function of ozonation time and they were used in the rate analysis by Differential Method [189].

The reaction between ozone and dye molecule follows a second order kinetics with respect to both ozone and dye concentrations [103]. The rate law for the reactant dye is interpreted by the following equation [113,189]:

$$-r_D = k.C_{O_3,L}.C_D \quad (3.1)$$

where  $-r_D$  is the reaction rate for dye in mol/(L.s),  $k$  is the reaction rate constant in L/(mol.s),  $C_{O_3}$  is the  $O_3$  concentration in the liquid phase in mol/L and  $C_D$  is the dye concentration in mol/L. In a constant volume semi-batch reactor, the measure of reaction rate of dye is given by the rate of change of the dye concentration with time:

$$-r_D = \frac{dC_D}{dt} \quad (3.2)$$

Here,  $t$  is the time in s. The reaction in Equation (3.1) can be simplified for the semi-batch reactor by taking the  $O_3$  concentration in the liquid phase constant, now the rate law becomes pseudo-first order which is the order of a reaction when the concentration of one of the reactants being much larger than the concentration of the other which does

not change appreciably during the reaction. In the semi-batch experiments, the liquid phase  $O_3$  concentration was accepted as constant since the solution was ozonated to reach the equilibrium concentration of ozone so that  $O_3$  concentration in the aqueous phase was almost uniform during the ozonation of dye molecules. Therefore, at the uniform dissolved ozone concentration, the concentration of ozone in the aqueous phase at any time was assumed to be equal to the equilibrium concentration of ozone corresponding to the used operating conditions in the experiment.

$$C_{O_3,L}(t) = C_{O_3,e} \quad (3.3)$$

$$-r_D = \frac{dC_D}{dt} = k.C_{O_3,L}.C_D = k'.C_D \quad (3.4)$$

$$k' = k.C_{O_3,e} \quad (3.5)$$

where  $k'$  is the pseudo-first order rate constant in  $s^{-1}$  and  $C_{O_3,e}$  is the equilibrium concentration of  $O_3$  in mol/L.

The pseudo-first order rate constant ( $k'$ ) can be found by the integration of Equation (3.4) as follows:

$$\int_{C_{D,i}}^{C_D} \frac{dC_D}{C_D} = k' \int_0^t dt \quad (3.6)$$

$$\ln\left(\frac{C_D}{C_{D,i}}\right) = k't \quad (3.7)$$

Here,  $C_{D,i}$  is the initial dye concentration in mol/L. The slope of the line in “ $\ln\left(\frac{C_D}{C_{D,i}}\right)$  vs.  $t$ ” graph gives the pseudo-first order rate constant. Then, the overall rate constant ( $k$ ) can be determined by  $k = \frac{k'}{C_{O_3,e}}$ . The results of the semi-batch experiments were evaluated to find  $k'$  and  $k$  for the ozonation and catalytic ozonation of both *AR-151* and *RBBR*, separately.

### 3.2 Determination of axial dispersion coefficient ( $D_L$ ) and Péclet number ( $Pe$ ) from tracer experiments in continuous gas-liquid and gas-liquid-solid reactors

The residence time distribution ( $RTD$ ) of a chemical reactor is a probability distribution function that describes the amount of time a fluid element spends inside the reactor. Chemical engineers use the  $RTD$  data to characterize the mixing and flow within reactors and to compare the behavior of real reactors to their ideal models. To determine the residence time distribution in a reactor, tracer experiments are conducted by injecting a non-reactive tracer with a known initial concentration into the reactor and by measuring its output concentration with respect to time. Then, total tracer input injected and tracer output are found from the following equations:

$$\text{Total tracer input} = V_{inj} \times C_{T,i} \quad (3.8)$$

$$\text{Total tracer output} = Q_L \int_0^{\infty} C_T(t) dt \quad (3.9)$$

Here,  $V_{inj}$  is the tracer injection volume in L,  $C_T$  is the inlet tracer concentration in mg/L,  $C_T(t)$  is the concentration of the tracer at any time after its injection into the reactor in mg/L and  $Q_L$  is the liquid flow rate in L/h. In a pulse tracer experiment, the integral in Equation (3.9) is calculated numerically by evaluating the area under  $C_T(t)$  versus  $t$  graph according to the Simpson's Rule [189].

$$\int_0^{\infty} C_T(t) dt = \sum_i C_{T,i} \Delta t_i \quad (3.10)$$

Then, residence time distribution function,  $E(t)$ , can be found by the division of the tracer concentration at any time to the area under the concentration versus  $t$  curve.  $E(t)$  shows the exit age distribution with a unit of  $s^{-1}$ .

$$E(t) = \frac{C_T(t)}{\int_0^{\infty} C_T(t) dt} \quad (3.11)$$

The mean residence time of the reactor,  $t_m$ , can be described by distribution functions, the mean value of the variable is equal to the area under the “ $tE(t)$  vs.  $t$ ” curve. The mean residence time is the first moment of the residence time distribution function. The area under the “ $tE(t)$  vs.  $t$ ” curve is found from Simpson’s rule numerically [189].

$$t_m = \int_0^{\infty} tE(t)dt \quad (3.12)$$

$$t_m = \frac{\sum_i t_i \cdot C_{T,i} \cdot \Delta t_i}{\sum_i C_{T,i} \cdot \Delta t_i} \quad (3.13)$$

The second moment of the residence time distribution function is called variance ( $\sigma^2$ ), it is the square of the standard deviation and shows the degree of dispersion around the mean. Variance is calculated by the area under “ $(t-t_m)^2 E(t)$  vs.  $t$ ” curve in Equation (3.14).

$$\sigma^2 = \int_0^{\infty} (t-t_m)^2 E(t)dt \quad (3.14)$$

$$\sigma^2 = \frac{\sum_i (t_i - t_m)^2 \cdot C_{T,i} \cdot \Delta t_i}{\sum_i C_{T,i} \cdot \Delta t_i} \quad (3.15)$$

The calculation of mean residence time and variance enables the determination of *Péclet* number ( $Pe_L$ ), a dimensionless number relating the rate of convective mass transfer to the rate of mass diffusion.

$$\frac{\sigma^2}{t_m^2} = \frac{2}{Pe_L} - \frac{2}{Pe_L^2} (1 - e^{-Pe_L}) \quad (3.16)$$

$$Pe_L = \frac{u_L H_T}{D_L} \quad (3.17)$$

where  $u_L$  is the superficial liquid velocity in m/s,  $H_T$  is the column height from the injection point of the tracer to the point where tracer discharge is measured in m,  $D_L$  is

the liquid axial dispersion coefficient in  $\text{m}^2/\text{s}$ . After calculating  $Pe_L$ ,  $D_L$  can be found from Equation (3.17) for a given liquid velocity.  $N_{CSTR}$  represents the number of “Continuously Stirred Tank Reactors” (CSTRs) in series equivalent to model the non-ideal reactor. It is calculated from the ratio between the mean residence time and the variance.

$$N_{CSTR} = \frac{t_m^2}{\sigma^2} \quad (3.18)$$

### 3.3 Modeling of ozone absorption into water in continuously operated bubble column

Ozone absorption into water resulted from the gas-liquid mass transfer with the simultaneously occurring ozone decomposition reaction. Additionally, the non-ideal flow in the reactor was considered by adding a term showing the axial dispersion of ozone in the liquid phase. The equations were written for the concentrations of  $\text{O}_3$  in the gas and liquid phases at the steady state.

#### 3.3.1 Model assumptions

In the reactor, ozone absorption was modeled considering the following assumptions:

- The reactor behaves according to the Axial Dispersion Model.
- Absorption process is realized at the isothermal condition so that all temperature dependent properties such as liquid density, liquid viscosity, are constant.
- Superficial gas and liquid velocities are constant along the  $z$ -direction of the column.
- Ozone gas is an ideal gas.
- In gas phase, there is no reaction of  $\text{O}_3$ .
- Gas flows ideally in the gas phase.
- Henry’s Law is applied for the equilibrium concentration of ozone [190].
- Mass transfer resistance in the gas film is negligible [191,192].
- At acidic pH (pH=2.5), the decomposition of ozone is negligible [193,194].

The equilibrium concentration of dissolved ozone,  $(C_{O_3,L}^*)$ , was calculated according to Henry’s Law by the following equation [192]:

$$C_{O_3,L}^* = \frac{\rho_w}{MW_w} \frac{RT}{H_{O_3}} C_{O_3,G} \quad (3.19)$$

Here,  $\rho_w$  and  $MW_w$  are the water density in  $\text{kg/m}^3$  and molecular weight of water, in  $\text{kg/kmol}$ , respectively.  $C_{O_3,G}$  is the gas phase  $O_3$  concentration.  $H_{O_3}$  is the Henry's Law constant calculated from the correlation of Sullivan [190].

$$H_{O_3} = 3.84 \times 10^7 [OH^-]^{0.035} \exp\left(\frac{-2428}{T}\right) \quad (3.20)$$

where  $[OH^-]$  is the concentration of hydroxyl radicals in  $\text{mol/L}$  and  $T$  is the temperature in  $\text{K}$ .

### 3.3.2 Model equations

Model equations in Equations (3.21) and (3.22) were written in gas and liquid phases for ozone concentrations, respectively:

$$\frac{Q_G}{A} \frac{dC_{O_3,G}}{dz} = -k_L a (C_{O_3,L}^* - C_{O_3,L}) \quad (3.21)$$

$$\frac{Q_L}{A} \frac{dC_{O_3,L}}{dz} = -D_L \frac{d^2 C_{O_3,L}}{dz^2} + k_L a (C_{O_3,L}^* - C_{O_3,L}) \quad (3.22)$$

Here,  $C_{O_3,L}$  is the  $O_3$  concentration in the liquid phase and  $k_L a$  is the volumetric liquid phase mass transfer coefficient. The following boundary conditions were applied in solving these equations:

at  $z = 0$ ,

$$C_{O_3,G} = C_{O_3,G,in} \quad (3.23)$$

$$C_{O_3,L} = 0 \quad (3.24)$$

at  $z = H$ ,

$$\frac{dC_{O_3,L}}{dz} = 0 \quad (3.25)$$

where  $C_{O_3,G,in}$  is the inlet  $O_3$  concentration in the gas phase.

### 3.3.3 Estimation of $D_L$ and $k_La$ from modeling

The equations (3.21) and (3.22) included the unknowns  $D_L$  and  $k_La$ , which were to be found or estimated. The RTD experiments enabled the evaluation of  $D_L$  at different flow conditions. In the modeling, the  $D_L$  values calculated from the results of the RTD experiments were used as the initial guesses of the axial dispersion coefficients at the corresponding operating conditions. However, during the evaluation of the numerical solution, a small modification of the  $D_L$  value was needed to fit the experimental and theoretical results satisfactorily.

The liquid phase ozone concentrations along the column measured in the ozone absorption experiments were used to determine the “modified  $D_L$ ” and  $k_La$  values according to the model. The solution procedure in the model is given in Appendix G1. The most appropriate  $D_L$  and  $k_La$  values were selected in the numerical solution giving a good match between the experimentally and theoretically determined liquid phase ozone concentrations along the column. In the numerical solution, the gas phase ozone concentrations were found by making a simple iteration for a height increment of 0.1 m. The dissolved  $O_3$  concentrations in the liquid phase were determined by solving linear simultaneous equations with a tridiagonal coefficient matrix. The computer program and the algorithm for the model are given in Appendix G1.

## 3.4 Modeling of dye ozonation process

Dye ozonation was modeled considering the mass transfer of ozone from gas to liquid phase and the reaction in the liquid phase. In catalytic ozonation, also the transfer of both the dye and ozone from the liquid phase to the catalyst surface was considered.

### 3.4.1 Sole ozonation

In the modeling of dye ozonation process, three equations namely, for gas phase  $O_3$  concentration, liquid phase  $O_3$  concentration and liquid phase dye concentration were written. In the liquid phase equation, a term related with the chemical reaction between the dye and  $O_3$  was added. Also, the mass transfer coefficient ( $k_La$ ) was written in the enhanced form  $[(k_La)_E]$  due to the chemical reaction. The modeling equations were written at steady state condition.

### 3.4.1.1 Model assumptions

The same assumptions as in Section 3.1 were applied in the modeling of dye ozonation.

In addition, the following assumptions were used:

- The reaction occurs between dye molecules and ozone. The reaction between ozonation by-products and ozone is not included in the liquid phase equation.
- The dyes are not volatile so that an equation is written only for the liquid phase dye concentration.

### 3.4.1.2 Model equations

Model equations of (3.26) and (3.27) were written in gas and liquid phase ozone concentrations, respectively; besides, Equation (3.28) was for the liquid phase dye concentration:

$$\frac{Q_G}{A} \frac{dC_{O_3,G}}{dz} = -(k_L a)_E \cdot (C_{O_3}^* - C_{O_3,L}) \quad (3.26)$$

$$\frac{Q_L}{A} \frac{dC_{O_3,L}}{dz} = -D_L \frac{d^2 C_{O_3,L}}{dz^2} + (k_L a)_E \cdot (C_{O_3}^* - C_{O_3,L}) - k \cdot C_D \cdot C_{O_3,L} - k_D C_{O_3,L} C_{-OH}^n \quad (3.27)$$

$$\frac{Q_L}{A} \frac{dC_D}{dz} = -D_L \frac{d^2 C_D}{dz^2} - r_s \cdot k \cdot C_D \cdot C_{O_3,L} \quad (3.28)$$

Here,  $r_s$  is the stoichiometric mole ratio between ozone and dye in the unit of (mole of dye/mole of ozone).  $k_D$  is the decomposition rate constant of ozone in the liquid. The term related with the ozone decomposition was added for the experiments at pH = 7 and 10. The terms for the values of  $(k_D C_{-OH}^n)$  group in the ozone decomposition term at pH = 7 and 10 were determined by observing the dissolved  $O_3$  concentrations with respect to time in a batch reactor previously by the author [195]. Those values  $(k_D C_{-OH}^n)$  were found as  $3.5 \times 10^{-4} \text{ s}^{-1}$  at pH = 7 and  $15.3 \times 10^{-4} \text{ s}^{-1}$  at pH = 10. The following boundary conditions were applied in solving the Equations (3.26-3.28):

at  $z = 0$ ,

$$C_{O_3,G} = C_{O_3,G,in} \quad (3.29)$$

$$C_{O_3,L} = 0 \quad (3.30)$$

$$C_D = C_{D,in} \quad (3.31)$$

at  $z = H$ ,

$$\frac{dC_{O_3,L}}{dz} = 0 \quad (3.32)$$

$$\frac{dC_D}{dz} = 0 \quad (3.33)$$

where  $C_{D,in}$  is the inlet dye concentration in the liquid phase.

### 3.4.1.3 Estimation of $(k_L a)_E$ from modeling

The equations (3.26) to (3.28) were solved simultaneously in the model. The procedure for the numerical solution, the computer program and the algorithm are given in Appendix G2. The stoichiometric ratio between the dye and ozone as mole basis ( $r_s$ ) was determined for *RBBR* and *AR-151* dyes from the simple mass balance in the gas-liquid reactor.  $r_s$  values were found as 0.1 mole dye/mole  $O_3$  for *RBBR* and 0.17 mole dye/mole  $O_3$  for *AR-151*. The reaction rate constant values were found as seen in Section 5.1.2 of this thesis, from the kinetic evaluation of semi-batch dye ozonation experiments conducted for *RBBR* and *AR-151*. The enhanced  $k_L a$  values were obtained from the numerical solution by fitting the liquid phase dye and ozone concentrations calculated from the model equations to the experimentally measured ones.

### 3.4.2 Catalytic ozonation

The reaction of ozone with dye molecules in a three phase catalytic system can be considered by the physical (mass transfer) resistances between gas, liquid phases and catalyst particles and the chemical resistances. The sketch showing the resistances involved in the ozonation of an organic molecule (dye) on the catalyst surface is shown in Figure 3.1.

By considering the overall steps and resistances in the modeling, the rate of absorption of  $O_3$  from gas phase to liquid interface and to the bulk of the liquid is shown in Equations (3.34) and (3.35):

$$\mu = k_G a (P_{O_3} - P_{O_3}^*) \quad (3.34)$$

$$\mu = k_L a (C_{O_3}^* - C_{O_3,L}) \quad (3.35)$$

Here,  $\mu$  is the rate of the ozone absorption;  $k_G$  and  $k_L$  are the mass transfer coefficients in the gas and liquid phases,  $P_{O_3}$  and  $P_{O_3}^*$  are the partial pressures of  $O_3$  in the gas phase and at the gas-liquid interface, respectively. The relation between the partial pressure of  $O_3$  and the concentration of  $O_3$  at the gas-liquid interface is found from the Henry's Law relation as stated in Equation (3.36) [196].

$$P_{O_3}^* = H_{O_3} C_{O_3}^* \quad (3.36)$$

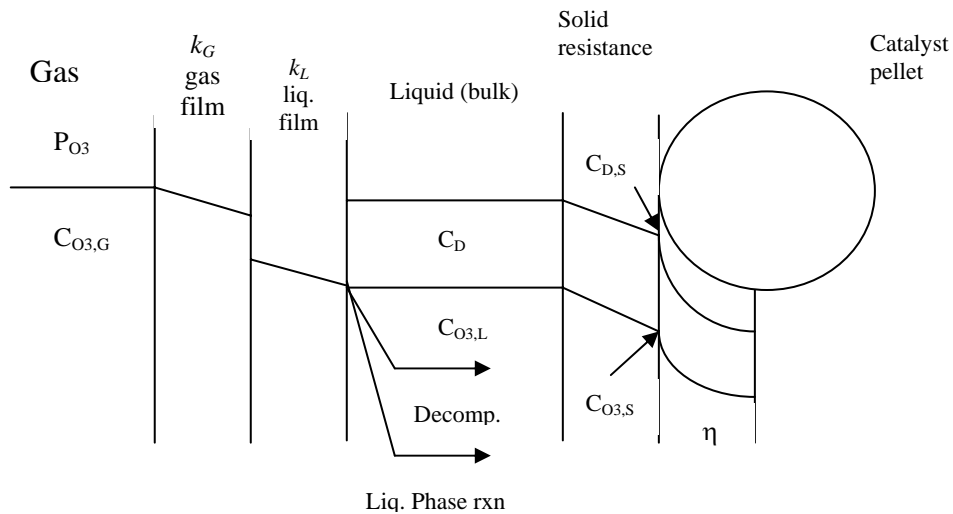


Figure 3.1. The resistances involved in the ozonation process in the three phase FBR.

In the bulk liquid phase, ozone reacts with organic molecules by a second order reaction with respect to both dissolved  $O_3$  concentration and organic concentration in the liquid phase as shown in Equation (3.37) [94,103,195]. Besides, at alkaline pH, ozone decomposes to radicals with Equation (3.38) [97,190]. Finally, the diffusion of

dissolved O<sub>3</sub> in the liquid phase onto the catalyst surface occurs [Equation (3.39)]. The total O<sub>3</sub> absorption rate is the addition of steps (3.37) to (3.39).

$$\mu_1 = kC_{O_3,L}C_D \quad (3.37)$$

$$\mu_2 = k_D C_{O_3,L} C_{-OH}^n \quad (3.38)$$

$$\mu_3 = k_s a_s m (C_{O_3,L} - C_{O_3,s}) \quad (3.39)$$

$$\mu = kC_{O_3,L}C_D + k_D C_{O_3,L} C_{-OH}^n + k_s a_s m (C_{O_3,L} - C_{O_3,s}) \quad (3.40)$$

In Equation (3.38)  $n$  is the order of hydroxyl ion concentration in the rate equation. The value of  $n$  mainly depends on the solution pH. In literature, different values of  $n$  were found; Sullivan and Roth [190] proposed  $n$  as 0.12 for the pH 0.5-10, whereas Stumm [97] used a value of 0.75 for  $n$  for pH 7.6-10.4. Here,  $k_s$  is the liquid-solid mass transfer coefficient,  $a_s$  is the external surface area of the catalyst particles and  $m$  is the solid loading per unit volume of the continuous reactor.

On the catalyst surface, a catalytic reaction between O<sub>3</sub> and dye molecules occurs. Since O<sub>3</sub> is the relatively slightly absorbed reactant from the gas to the liquid and then to the solid phase, it would be acceptable to consider the organics (the dyes) in excess concentration on the catalyst surface. Therefore, the reaction on the catalyst surface was assumed as a pseudo-first order reaction with respect to the O<sub>3</sub> concentration [Equation (3.41)].

$$\mu = k_R m C_{O_3,s} C_{D,s} = k'_R m C_{O_3,s} \quad (3.41)$$

Here,  $k_R$  is the reaction rate constant between the dye and ozone on the catalyst surface. On the catalyst surface, the diffusion rate of O<sub>3</sub> [Equation (3.39)] is equal to the surface reaction rate [Equation (3.41)]. Then,  $C_{O_3,s}$  is found as a function of  $C_{O_3,L}$  in Equation (3.43).

$$k'_R m C_{O_3,s} = k_s a_s m (C_{O_3,L} - C_{O_3,s}) \quad (3.42)$$

$$C_{O_3,s} = \frac{C_{O_3,L}}{1 + \frac{k'_R}{k_s a_s}} \quad (3.43)$$

$$\mu_3 = k_s a_s m \frac{C_{O_3,L}}{1 + \frac{k_s a_s}{k_R}} = \frac{C_{O_3,L}}{\frac{1}{k_s a_s m} + \frac{1}{k_R m}} \quad (3.44)$$

$$\mu = \left( kC_D + k_D C_{-OH}^n + \frac{1}{\frac{1}{k_s a_s m} + \frac{1}{k_R m}} \right) C_{O_3,L} \quad (3.45)$$

$$\mu = \frac{P_{O_3}}{\left[ \frac{1}{k_G a} + \frac{H_{O_3}}{k_L a} + \frac{H_{O_3}}{kC_D + k_D C_{-OH}^n + \frac{1}{\frac{1}{k_s a_s m} + \frac{1}{k_R m}}} \right]} \quad (3.46)$$

In the modeling of dye ozonation process with the catalyst, the equations were similar to those in the dye ozonation process without the catalyst. One additional term including the mass transfer of both the dye and ozone to the catalyst surface was written in the corresponding liquid phase equation for each reactant. Here, it was assumed that there was no diffusion of gaseous ozone onto the catalyst surface.

### 3.4.2.1 Model equations in FBR

*Mass balance for gaseous ozone*

$$\frac{Q_G}{A} \frac{dC_{O_3,G}}{dz} = -(k_L a)_E (C_{O_3}^* - C_{O_3,L}) \quad (3.47)$$

*Mass balance for liquid phase ozone*

$$\frac{Q_L}{A} \frac{dC_{O_3,L}}{dz} = -D_L \frac{d^2 C_{O_3,L}}{dz^2} + (k_L a)_E (C_{O_3}^* - C_{O_3,L}) - k \cdot C_D \cdot C_{O_3,L} - k_D C_{O_3,L} C_{-OH}^n - k_s \cdot a_s \cdot m \cdot (C_{O_3,L} - C_{O_3,s}) \quad (3.48)$$

Mass balance for the dye in the liquid phase

$$\frac{Q_L}{A} \frac{dC_D}{dz} = -D_L \frac{d^2 C_D}{dz^2} - r_s \cdot k \cdot C_D \cdot C_{O_3,L} - k_s \cdot a_s \cdot m \cdot (C_D - C_{D,s}) \quad (3.49)$$

Equations (3.48) and (3.49) include the terms, dye and ozone concentrations at the catalyst surface, namely  $C_{D,s}$  and  $C_{O_3,s}$ . Those equations were simplified by substituting Equation (3.44) into Equation (3.48). Also, the mass transfer of dye molecules from the liquid phase onto the catalyst is arranged by equating the mass transfer rate to the reaction rate on the catalyst surface [Equation (3.50)].

$$k_s a_s m (C_D - C_{D,s}) = r_s k'_R m C_{O_3,s} = r_s k'_R m \frac{C_{O_3,L}}{1 + \frac{k'_R}{k_s a_s}} = \frac{r_s C_{O_3,L}}{\frac{1}{k'_R m} + \frac{1}{k_s a_s m}} \quad (3.50)$$

$$\frac{Q_L}{A} \frac{dC_{O_3,L}}{dz} = -D_L \frac{d^2 C_{O_3,L}}{dz^2} + (k_L a)_E (C_{O_3}^* - C_{O_3,L}) - k \cdot C_D \cdot C_{O_3,L} - k_D C_{O_3,L} C_{-OH}^n - \frac{C_{O_3,L}}{\frac{1}{k'_R m} + \frac{1}{k_s a_s m}} \quad (3.51)$$

$$\frac{Q_L}{A} \frac{dC_D}{dz} = -D_L \frac{d^2 C_D}{dz^2} - r_s \cdot k \cdot C_D \cdot C_{O_3,L} - \frac{r_s C_{O_3,L}}{\frac{1}{k'_R m} + \frac{1}{k_s a_s m}} \quad (3.52)$$

Two different cases can be considered in the modeling:

(i) Rapid reaction on the catalyst surface

$$\frac{1}{k'_R m} \ll \frac{1}{k_s a_s m} \text{ and the term } \frac{C_{O_3,L}}{\frac{1}{k'_R m} + \frac{1}{k_s a_s m}} \text{ becomes almost equal to } k_s a_s m C_{O_3,L}.$$

(ii) Slow reaction on the catalyst surface

$$\frac{1}{k'_R m} \gg \frac{1}{k_s a_s m} \text{ and the term } \frac{C_{O_3,L}}{\frac{1}{k'_R m} + \frac{1}{k_s a_s m}} \text{ becomes } k'_R m C_{O_3,L}.$$

The boundary conditions of the model equations for catalytic dye ozonation are the same as those of the non-catalytic dye ozonation modeling.

### 3.4.2.2 Estimation of $(k_L a)_E$ from modeling

The equations (3.47), (3.51) and (3.52) were solved simultaneously in the model. The procedure for the numerical solution, the computer program and the algorithm are given in Appendix G3. The reaction rate constant values were found from the kinetic evaluation of semi-batch catalytic dye ozonation experiments conducted for *RBBR* and *AR-151* (Section 5.1.2). The equations were solved by considering fast reaction of the dye and ozone molecules on the catalyst. In literature, the reaction of ozone with the dye molecules was shown to be fast in the bulk liquid phase. [46, 103]. The enhanced  $k_L a$  values were found in the numerical solution to match the theoretically and experimentally determined dye and dissolved  $O_3$  concentrations in the liquid phase. For the determination of liquid-solid mass transfer coefficient ( $k_s$ ), the correlation proposed by Ohashi et al. [197] was used. This correlation was a good prediction of the liquid-solid mass transfer by calculating Sherwood number [Equation (3.53)]; then,  $k_s$  was found from Equation (3.54):

$$Sh = 2 + 0.52 \left( e^{1/3} d_{cat}^{4/3} \mu_L / \rho_L \right)^{0.59} Sc^{1/3} \quad (3.53)$$

$$Sh = \frac{k_s d_{cat}}{D_{O_3,D}} \quad (3.54)$$

$$Sc = \frac{\nu}{D_{O_3,D}} \quad (3.55)$$

where  $Sh$  is the Sherwood number,  $e$  is the energy dissipated per unit mass of liquid,  $Sc$  is the Schmidt number,  $\mu_L$  and  $\rho_L$  are the liquid viscosity and density, respectively,  $D_{O_3,D}$  is the diffusivity of  $O_3$  into dye solution, and  $\nu$  is the kinematic viscosity of the liquid. The energy dissipated was calculated from Equation (3.56) for three phase fluidized beds:

$$e = \frac{[(u_G + u_L)(\varepsilon_S \rho_S + \varepsilon_L \rho_L + \varepsilon_G \rho_G) - u_L \rho_L - u_G \rho_G]g}{\varepsilon_L \rho_L} \quad (3.56)$$

## CHAPTER 4

### MATERIALS AND METHODS

#### 4.1 Materials

*Acid Red-151 (AR-151)* and *Remazol Brilliant Blue R (RBBR)* are the dyes used in the sole ozonation and catalytic ozonation experiments. *AR-151* and *RBBR* dyes were obtained from Aldrich Chemical Company (Milwaukee, USA) and Acros Organics (New Jersey, USA), respectively and used without further purification. The other chemicals were used for the regulation of pH, for the determination of gas and liquid phase O<sub>3</sub> concentrations, for the preparation of the perfluorooctyl alumina (PFOA) catalyst and for the analysis in High Performance Liquid Chromatograph (HPLC). All the chemicals except used in HPLC analysis, were reagent grade and supplied from Aldrich Chemical Company or Acros Organics. The chemicals in HPLC analysis, HPLC grade chemicals were used. The water in the experiments was distilled and deionized water and for HPLC analysis, HPLC grade water was utilized. Alumina, in the form of  $\gamma$ -alumina, was used as the catalyst and the support for the PFOA catalyst.  $\gamma$ -alumina particles were received from Damla Kimya Limited Şti, Ankara; those particles were composed of different sizes so that they were sieved and the desired sized alumina particles were selected before using.

##### 4.1.1 Specifications of *AR-151* and *RBBR* dyes

*AR-151* is an azo dye containing two azo groups (-N=N- group) and one sulfonate group (-SO<sub>3</sub>Na). *RBBR* has no azo group, it is an anthraquinone dye with two sulfonate groups, one of which is carbonated (-SO<sub>2</sub>CH<sub>2</sub>CH<sub>2</sub>OSO<sub>3</sub>Na). The chemical structure of the dyes are represented in Figure 4.1. The maximum light absorption wavelengths of the dyes were 512 nm and 591 nm for *AR-151* and *RBBR*, respectively. Calibration curves describing the linear relationships between the dye concentration and absorbance at the maximum wavelength were obtained for these dyes and these curves are given in Appendix A.

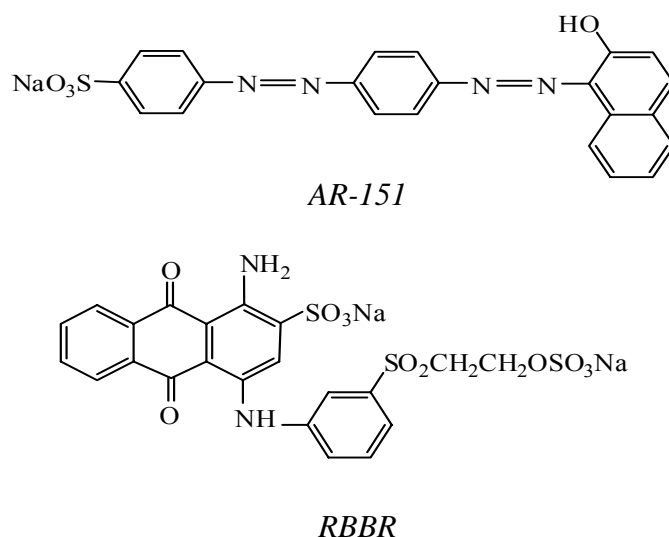


Figure 4.1. The chemical structures of the dyes used in the experiments

## 4.2 Apparatus

Throughout the study, two different types of reactors, namely a semi-batch reactor and a fluidized bed reactor were used. The kinetics of both *AR-151* and *RBBR* dyes in the presence and the absence of the catalysts were studied in the semi-batch reactor. Also, the efficiency of Alumina and PFOA catalyst in the dye ozonation process was investigated in the semi-batch experiments. Hydrodynamic studies and dye ozonation experiments at steady state were conducted in the fluidized bed reactor.

### 4.2.1 Semi-batch reactor

The experimental set-up used consists of 1 L rounded bottom glass reactor with several input/output ports for ozone gas inlet, and outlet, sampling, pH electrode and a mechanical stirrer [106]. The experimental set-up is shown in Figure 4.2. Ozone fed to the reactor is produced from dry air in the semi-batch experiments. Therefore, ozone gas inlet is attached to the Fischer type OZ-502 generator producing  $O_3$  from dry air. The gas flow rate is monitored by a flow meter on the generator and a rotameter is placed between the ozone generator and gas inlet of the reactor. After the flow meter, a three way valve is placed to measure  $O_3$  concentration in the inlet gas composing a mixture of  $O_3$  oxygen and nitrogen. For this purpose, before sending  $O_3$ /air mixture to the reactor, by changing the direction of flow in the three-way valve, the gas flow is sent to the gas

washing bottles which contain 2% potassium iodide (KI) solution. The temperature during the semi-batch experiments is kept at 25°C using a water bath. During the experiments, the reactor with its support part is placed into the water bath. The produced O<sub>3</sub>/air gas mixture diffuses into water through a stainless steel tube entering into the bottom of the reactor. A mixer with high speed at the bottom of the reactor, provides the uniform distribution of gas bubbles throughout the reactor. Gas washing bottles with 2% KI solution are placed to the outlet of the gas exiting from the reactor and they are used to determine the ozone concentration in the off-gas, by the KI method [198].

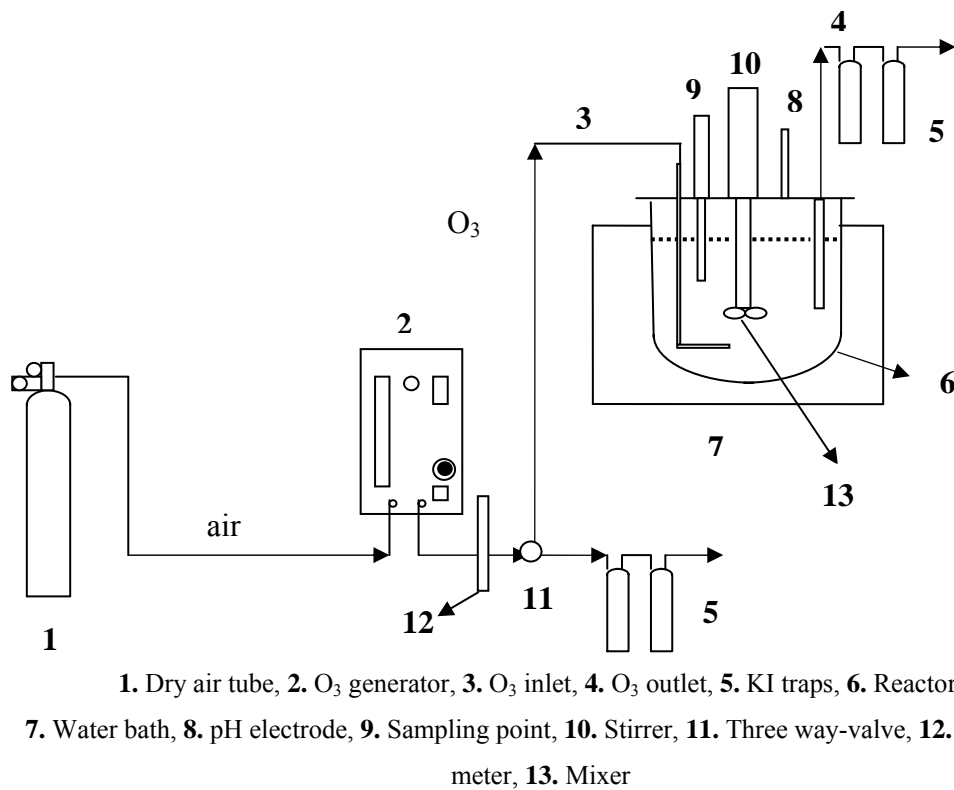


Figure 4.2. The semi-batch reactor

#### 4.2.2 Fluidized bed reactor

The fluidized bed reactor is a cylindrical plexiglass column with an inside diameter of 8 cm, wall thickness of 0.5 cm and a total height of 150 cm. All of the components of the reactor and experimental system are made of plexiglass, teflon or stainless steel to prevent corrosion by ozone. The liquid phase is fed to the column from just the bottom.

O<sub>3</sub> is produced from dry air or pure oxygen using Fischer OZ 502 or Ozomax 2VTTL types of ozone generators, respectively. A gas flow meter controls the flow rate of the gas. After the ozone generator, the gas flow is separated to two ways, one going to a gas flow meter controlling the flow rate of the gas to the reactor and the other going to a gas washing bottle collecting the excess gas. A ball valve is used to regulate the flow rate of the excess gas. After the flow meter, a three way valve is placed to determine the inlet gas phase O<sub>3</sub> concentration. As in the semi-batch system, the gas is sent to the KI traps by changing the direction of gas flow with the help of the valve.

O<sub>3</sub>/air or O<sub>3</sub>/oxygen mixture is the gas phase introduced to the reactor via a gas distributor 9 cm above the liquid entrance. Gas and liquid phases flow co-currently upward in the reactor. The gas distributor is composed of three glass discs. The configuration of the discs is shown in Figure 4.3. For the gas distributor, porous fritted discs with a diameter of 3 cm and a pore size of 40-50 μm are used. The overall height of the distributor with its tubes and discs is 4 cm. The gas flows into the discs separately from each other and the flow going to each disc is regulated by the valves placed before each disc. Inside the column, the fritted discs are placed in such a way that their distances from the sides of the column and from each other are equal forming an equilateral triangle. By this way and with the help of the valves, uniformity of gas flow is ensured in the column. In the catalytic ozonation experiments, the catalyst particles were filled into the column above a sieve positioned just above the gas distributor. The sieve is stainless steel with the openings of 0.5 mm and is placed 2 cm above the gas distributor.

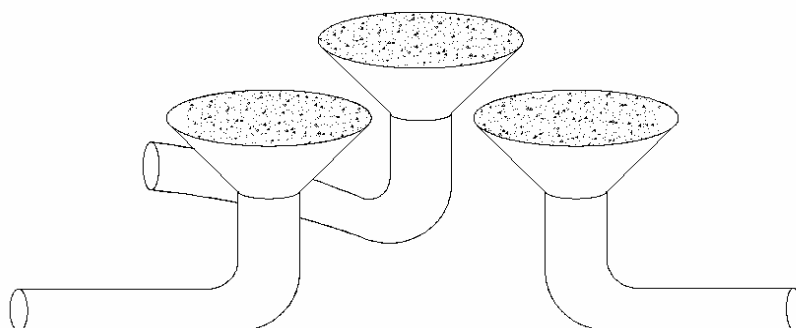


Figure 4.3. The configuration of the gas fritted discs.

The liquid storage tank has a capacity of 65 L. The liquid is pumped from the storage tank into the column by a Baldor type centrifugal pump with a power of 5 hP and pumping rate of 1725 rpm. At the exit of the pump, there is a by-pass valve to regulate the flow rate of the liquid. The pump working flow rate is in the range of 30-300 L/h. After the pump, the liquid flow is controlled by a liquid rotameter placed before the reactor. The liquid entering the reactor is distributed via a specially designed distributor for its uniform dispersion in the column. The liquid distributor is placed 3.5 cm above the liquid entrance. A schematic diagram of the liquid distributor is shown in Figure 4.4. It is a triangular pitch type perforated plate made of stainless steel. The distributor contains 613 evenly distributed holes with 1-mm diameter. The holes on the perforated plate are placed in configuration of 3 mm distance from center to center of the holes. The plate thickness is 0.8 mm.

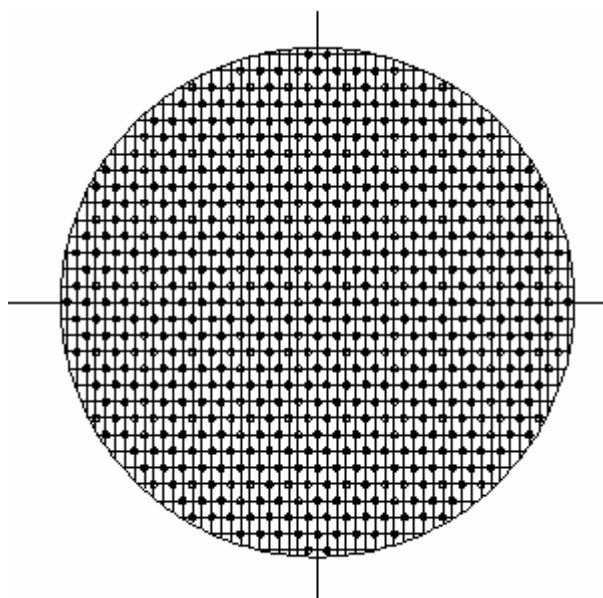


Figure 4.4. The configuration of the liquid distributor

Along the column height, there are some ports for manometer inlets, manometer outlets, liquid sampling, catalyst loading and liquid outlet. The pressure drops in the column are measured by two U-tube manometers along the column. The places of the manometer inlets and outlets are shown in Figures 4.5 and 4.6. These two manometers measure the

overall pressure drop along the column. U-tube manometers are filled with carbon tetrachloride ( $\text{CCl}_4$ ) as manometer liquid. The injection port placed 44 cm above the liquid entrance enables the loading of catalyst particles into the column.

There are eight sampling ports along the column. Samples are taken from the ports by the help of teflon stopcocks connected. Two of the ports are at the point where the gas distributor ends and they are situated on the opposite side of the column. The other two are positioned at 12 cm above the end of the gas distributor on the same side of the column as the other two. The other two sampling points lie 32 cm above the gas distributor and the last ones are at 88 cm above the liquid entrance. The configuration of the overall system is shown in Figure 4.5.

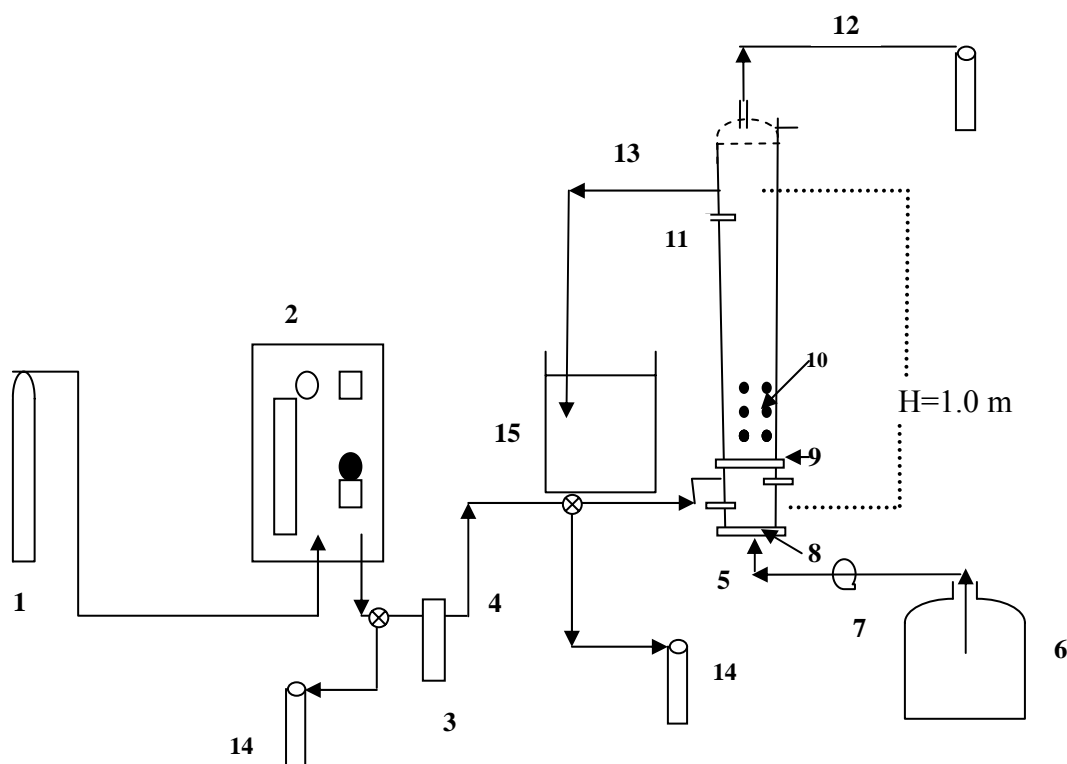


Figure 4.5. The schematic diagram of the overall fluidized bed system (un-scaled): 1- dry air tube, 2- ozone generator, 3- gas flowmeter, 4- ozone inlet, 5- liquid inlet, 6- liquid reservoir, 7- centrifugal pump, 8- liquid distributor, 9- gas distributor, 10- PFOA catalyst, 11- manometer taps, 12- ozone outlet, 13- liquid outlet, 14- KI traps, 15- liquid outlet tank.

At 100 cm above the liquid entrance, there is an outlet for the liquid stream. The liquid stream is sent from the outlet to a 50 L waste tank via a two way valve. The section between the liquid outlet and the top of the column is called “disengaging section”, in which only gas flows through the gas outlet. This section prevents the overflow of liquid stream into the gas outlet tubes. The gas stream flows from the top of the reactor through the teflon tubes connected to the washing bottles for the collection of unreacted ozone. The entrained particles are kept in the column by a screen placed just before the liquid outlet. The scaled drawing of the column with the other parts is given in Figure 4.6. Also, a photograph of the fluidized bed reactor can be seen in Figure 4.7.

### 4.3 Characterization of the catalysts

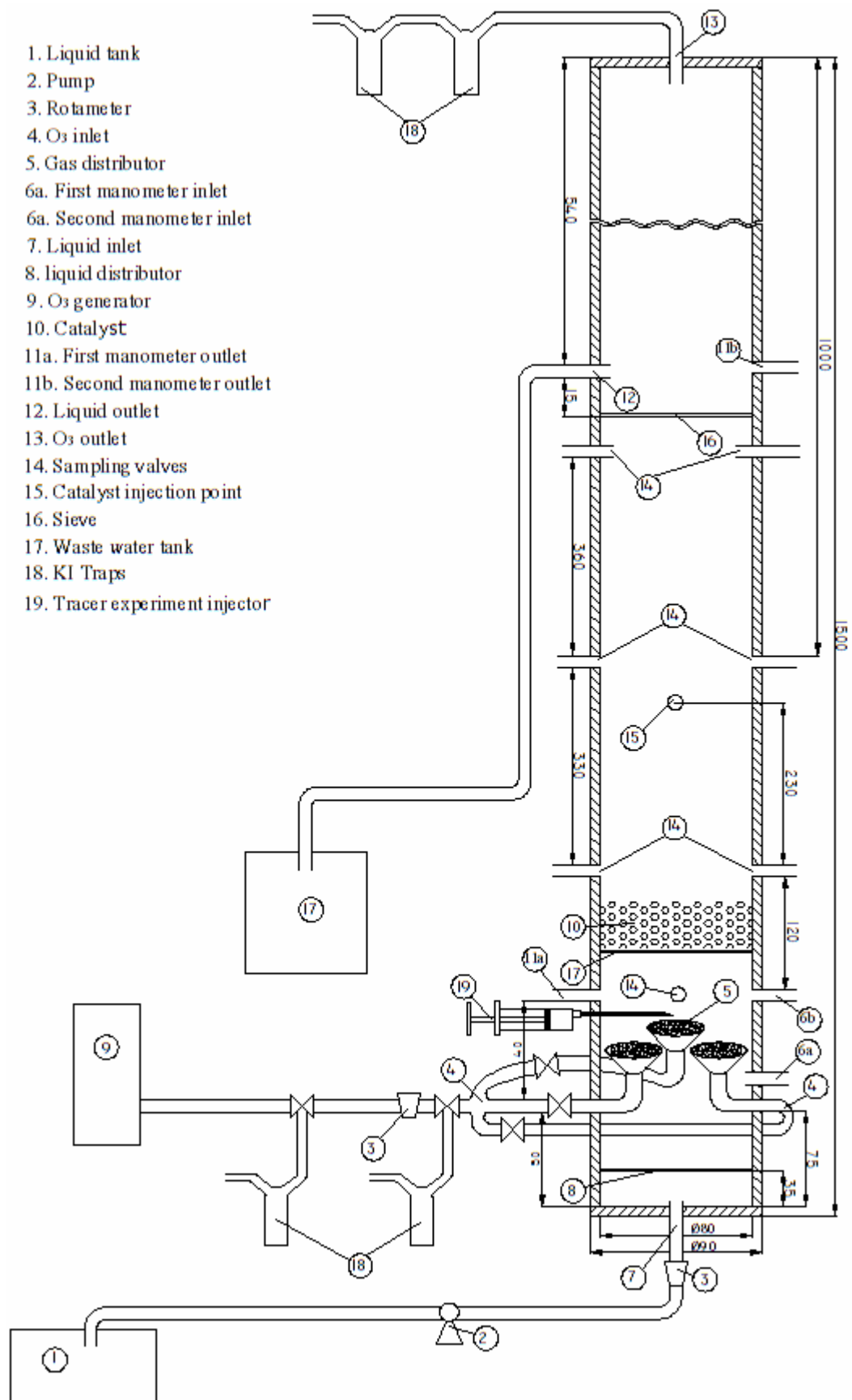
In the catalytic ozonation experiments, two different types of catalyst were used: one of them was alumina and the other one was PFOA. The PFOA catalyst was prepared from alumina.

#### 4.3.1 Specifications of alumina and perfluorooctyl alumina (PFOA)

The particles taken from Damla Kimya Ltd. Şti. are composed of activated gamma alumina ( $\gamma$ -Al<sub>2</sub>O<sub>3</sub>). Its main properties are shown in Table 4.1. The alumina was a mixture of different sized particles therefore the particles were sieved through wire mesh sieves of ASTM scales. After the particle size was investigated, the differential screen analysis was performed. Table 4.2 presents the results of the screen analysis. The particles of the size 1.6-2.4 mm (those remained on 8/10 mesh sieve) were collected and selected as the alumina catalyst and catalyst support in the preparation of perfluorooctyl alumina (PFOA).

Table 4.1. The main properties of activated alumina.

Content, %	Al <sub>2</sub> O <sub>3</sub> : 93.6 SiO <sub>2</sub> : 0.02 Fe <sub>2</sub> O <sub>3</sub> : 0.02 Na <sub>2</sub> O: 0.35
Loss on ignition, %	6
Crushing strength, kg	18.6
Abrasion loss, %	0.4



1. Liquid tank
2. Pump
3. Rotameter
4. O<sub>3</sub> inlet
5. Gas distributor
- 6a. First manometer inlet
- 6a. Second manometer inlet
7. Liquid inlet
8. liquid distributor
9. O<sub>3</sub> generator
10. Catalyst
- 11a. First manometer outlet
- 11b. Second manometer outlet
12. Liquid outlet
13. O<sub>3</sub> outlet
14. Sampling valves
15. Catalyst injection point
16. Sieve
17. Waste water tank
18. KI Traps
19. Tracer experiment injector

Figure 4.6. Schematics of the fluidized bed column (Scale 1:3, the column is scaled).



Figure 4.7. The photograph of the fluidized bed column.

Then, the density of alumina particles was determined by weighing a small amount of alumina and measuring its volume. After the preparation of PFOA particles, their density was calculated also. The average density of alumina and PFOA particles were found as 2570 kg/m<sup>3</sup> and 1250 kg/m<sup>3</sup>, respectively.

Table 4.2. Differential screen analysis of alumina particles.

Mesh	$\Delta\Phi_n$	$d_{cat}$ , mm	$d_{cat,ave}$ , mm
4/6	0.513	3.327	4.013
6/8	0.385	2.362	2.844
8/10	0.096	1.651	2.006
10/14	0.006	1.168	1.410

Alumina and PFOA catalysts were analyzed for the catalyst surface area and pore size distribution. The surface characterization analyses were made in the Central Laboratory of M.E.T.U. The surface areas of the catalysts were determined by physical adsorption of nitrogen on the solid surface using the BET method. The pore volume and pore size distribution were determined by the nitrogen adsorption/desorption method. The nitrogen desorption isotherm was used for the calculation of pores and average pore size. The characterization data are presented in Table 4.3. It was observed that alumina had the highest surface area, and the surface area decreased with the increasing amount of PFO acid in alumina. Since *AR-151* had an acidic character, the dye molecules could be adsorbed easily on the acidic alumina, whereas the adsorption on PFOA might be limited due to both its lower surface area and the hydrophobic surface characteristics.

Table 4.3. The characterization of alumina and PFOA.

Type of the catalyst	$A_{BET}$ , m <sup>2</sup> /g	$d_p$ , Å	$V_{T,p}$ , cc/g
Alumina	276.6	50.51	0.349
25% PFOA	209.6	50.27	0.263
50% PFOA	195.8	51.42	0.252
100% PFOA	140.8	49.53	0.174

The surface properties of alumina and PFOA catalysts before and after the dye ozonation process were characterized by the Surface Electron Microscopy (SEM) analysis realized in Metallurgy and Materials Engineering and and Fourier Transform Infrared (FT-IR) Spectroscopy analysis realized in Central Laboratory of M.E.T.U.

#### **4.3.2 Preparation of perfluorooctyl alumina (PFOA)**

Perfluorooctyl alumina (PFOA) catalyst was prepared according to the procedure given in the patent of Wiesermann et al. [199] and Kasprzyk-Hordern et al. [35]. As the product supplied from Damla Kimya, the particles were in different sizes in the mixture; therefore, firstly 2-mm alumina particles were obtained by sieving as explained before. Secondly, these alumina particles were calcined at 600°C in the calcination oven at least 6 hours to achieve  $\gamma$ -alumina type. Then, calcined alumina particles were used in the preparation of PFOA catalyst.

The PFOA catalyst was prepared with the impregnation of perfluorooctanoic acid on alumina particles. Perfluorooctanoic acid interacted with the hydroxyl groups on the alumina surface. For the preparation of PFOA called 100% in semi-batch experiments, first 6.48 g of perfluorooctanoic acid monohydrate (96% purity) was weighed and added to 100 mL of deionized water in a flask to make 0.15 M PFO acid solution. The solution was mixed with a magnetic stirrer at least half an hour to attain a homogeneous emulsion. Then, 10 grams of calcined alumina was weighed and added into the PFO acid solution. The PFO acid solution containing alumina was placed in a shaker whose temperature and shaking speed were previously regulated to 60°C and 400 rpm, respectively. The reaction between PFO acid and alumina required 4 hours at 60°C in the shaker. After the reaction was completed, the mixture was taken from the shaker and was cooled to the room temperature.

The filtration of the particles from the solution was an important process. First, the remained solution was separated from the particles by filtration in a vacuum filtration unit. Then, the particles were washed with 100 mL of 0.1 M NaHCO<sub>3</sub> solution at least 1 hour to remove the unreacted perfluorooctanoic acid molecules from the surface of the particles. The particles were filtered and washed with 200 mL of deionized water for 1 hour. Finally, the particles were dried at 60°C in an oven for 6 hours.

The other types of PFOA (25% (w/w) PFO on alumina and 50% (w/w) PFO on alumina) were also prepared by the reaction of different amounts of PFO acid with 10 g of alumina. For the preparation of 50% PFOA, 100 mL of 0.075M PFO acid was used with 10 g of alumina. Similarly, 25% PFOA was prepared by the reaction of 100 mL of 0.0375 M PFO acid with 10 g of alumina. Otherwise the amount of PFO acid to be reacted with alumina, all the procedure remained the same with that in the preparation of 100% PFOA.

#### **4.4 Experiments in semi batch reactor**

The efficiency of catalytic ozonation and the kinetics of the catalytic ozonation process were investigated in the semi-batch reactor continuously operating gas phase.

##### **4.4.1 Preparation of the dye solutions**

For an experimental run, a dye solution at the desired concentration was prepared by dissolving the required amount of the dye in 50 mL of deionized water for semi-batch experiments. To ensure complete dissolution of the dyes, the solution was mixed about half an hour on a magnetic stirrer at 40°C. The high temperature enabled the complete dissolution of the dyes in water, especially *AR-151* which was harder to dissolve. Then, the solution was cooled to the room temperature.

##### **4.4.2 Experimental procedure**

The reactor was operated in a semi-continuous mode by feeding ozone gas continuously into the reactor containing the dye solution at the desired initial concentration, at a chosen pH and at a temperature of 25°C. Buffer solutions of  $K_2HPO_4/KH_2PO_4/H_3PO_4$  were used for the adjustment of pH to 2.5 and 7 in the reaction medium. For pH = 13, sodium hydroxide (NaOH) was utilized. The pH values of the prepared solutions before and after ozonation were measured by using a WTW 330i pH-meter set. Before using, the pH-electrode was cleaned with 3 M KCl solution and the pH-meter was calibrated with the buffer solutions.

First, ozonation was applied to 950 mL of aqueous solution of which pH was regulated. For this purpose, the aqueous solution to be ozonated was prepared by adding 900 mL

of deionized water and 50 mL of buffer solution at the desired pH into the reactor. For the experiments at pH of 13, 4.5 g of NaOH was added into 950 mL deionized water to prepare the solution to be ozonated. The buffered solution in the reactor was ozonated for about 20 min to reach an equilibrium concentration of ozone at the operating conditions in the aqueous solution. The time to reach the equilibrium concentration of dissolved  $O_3$  was controlled by taking some aqueous samples from the reactor and analyzing them for dissolved  $O_3$  concentration. After 20 min of ozonation, 50 mL of dye solution of which preparation procedure being given in 4.4.1, was added into the reactor while continuously ozonating the contents of the reactor. For the analyses of COD, dye concentration and  $O_3$  concentration in the liquid phase, the samples at specific time intervals were withdrawn from the reactor into the sample bottles operated under vacuum in order to prevent the escape of  $O_3$  into the gas phase. One mL of 0.025 M sodium thiosulphate ( $Na_2S_2O_3$ ) solution was added into each sample bottle in order to remove any residual ozone in the sample for preventing the further reaction in the bottle. The reaction pH, types of catalysts, types of dyes, initial dye and ozone concentrations, and ozone dose were the independent variables in the experiments. The ranges of these variables are shown in Table 4.4. The gas flow rate, temperature, stirrer rate and catalyst dosage were kept constant at 150 L/h, 25°C, 300 rpm and 5 g, respectively.

Table 4.4. The variables in the semi-batch experiments.

Parameter	Value
$C_{D,i}$ , mg/L	100, 200, 400
$D_{O_3}$ , mmol/h	24.38, 35.42, 46.04
pH	2.5, 7.0, 13.0
Dye type	<i>AR-151</i> , <i>RBBR</i>
$Q_G$ , L/h	150
Stirrer rate rpm	300
Catalyst type	Alumina, (25%, 50%, 100%) PFOA
$COD_i$ , mg/L	<i>AR-151</i> : 200; <i>RBBR</i> : 232
$T$ , °C	25
$m_{cat}$ , g	5

The same procedure was followed also in the catalytic ozonation experiments. Only, before starting to ozonate the aqueous solution, the desired amount of catalyst was added into the reactor, which formed a heterogeneous phase in the system. The received samples from the reactor were kept waiting about an hour to ensure the settling of the turbid portion in the samples; thus, the accuracy in the results was guaranteed.

#### **4.5 Experiments in fluidized bed reactor (gas-liquid-solid)**

In the fluidized bed reactor, tracer experiments for the determination of liquid dispersion in the reactor, O<sub>3</sub> absorption experiments for the calculation of gas liquid mass transfer coefficient, experiments to specify the reactor hydrodynamics and dye ozonation experiments were conducted. The water used in all the experiments was distilled water. The dye solutions were prepared according to the procedure given before. However, the required amount of the dye was dissolved in 1 liter of distilled water instead of 50 mL deionized water. Again half an hour mixing at 40°C was needed to have a completely dissolved dye solution. Then, the prepared 1-liter solution was added to about 60-liter distilled water and was placed in 65-liter capacity storage tank.

In the fluidized bed experiments, ozone concentration in the gas phase was adjusted by the dose regulation button on the Fischer 502 ozone generator in which ozone was produced from dry air. For the experiments in which oxygen was the ozone producing gas, the gas phase ozone concentration was constant at the value of  $0.903 \pm 0.088$  mmol O<sub>3</sub>/L gas ( $43.30 \pm 4.22$  mg O<sub>3</sub>/L gas).

The experiments were conducted at the room temperature. The room temperature was  $18.6 \pm 1.2$ °C for the winter and  $24.8 \pm 1.4$ °C for the summer. Liquid samples were periodically taken from the column until the steady state was reached. Then, the experimental run at the steady state was continued by taking liquid samples along the height of the column.

##### **4.5.1 Tracer experiments**

The tracer experiments were conducted to determine the ideality of the flow distribution in the liquid phase. A tracer stimulus-response technique was used for studying the mixing characteristics of the reactor. The experiments were conducted at different gas

and liquid superficial velocities in the presence or absence of the particles. Tracer experiments in the presence of particles were conducted by the addition of 150 g PFOA into the column.

In general, the process model of the reactor is based on ideal plug flow. But, in small tubular reactors, a non-ideal pattern referred as “axial dispersion” is observed [29]. Tracer or “residence time distribution” experiments are conducted to find the axial dispersion level of the reactor. In the tracer experiments, a non-reactive tracer is injected into the reactor with a syringe at the inlet. The concentration of the tracer is changed according to a known function and the response of the function is found by measuring the tracer concentration at the outlet. The tracer can be given to the reactor as pulse or step input, by injecting a small volume of the tracer as a pulse or introducing it along the time, respectively. The dispersion in the liquid is a function of gas and liquid superficial velocities in the reactor.

In the tracer experiments, the gas phase was dry air whereas distilled water was the liquid phase. *RBBR* was selected as the tracer injected into the column since its concentration was followed easily by measuring its absorption at 591 nm in UV/visible spectrophotometer and it was an unreacted material with air. The injection was like a pulse input by the help of an injector. The injector was placed 8.5 cm above the liquid entrance. The tracer (*RBBR*) at a concentration of approximately 4 mg/L (corresponding to an amount of 76.3 mg tracer), was injected into the reactor and the distribution of the dye concentration was observed. From the sampling point at the top (sampling point 80 cm above the injector), samples were withdrawn at different time intervals and the samples were analyzed for *RBBR* concentration. In other words, the column height between the injection point and liquid outlet was 80 cm. For the tracer experiments, the variables were superficial gas and liquid velocities; gas velocity was varied between  $3.3 \times 10^{-3}$  m/s (corresponding to gas flow rate of 60 L/h) and  $11.1 \times 10^{-3}$  m/s ( $Q_G=200$  L/h), while the superficial liquid velocity was varied within the range of  $(1.7-19.4) \times 10^{-3}$  m/s, corresponding to liquid flow rates within the range of (30-350 L/h), respectively.

#### 4.5.2 Ozone absorption experiments

Gas-liquid volumetric mass transfer coefficient ( $k_{La}$ ) has an importance in ozonation reactions and its magnitude is strongly dependent on the reactor type, hydrodynamics, gas and liquid flow rates in the system and the presence of a chemical reaction. Therefore, the determination of  $k_{La}$  in the FBR at different flow conditions and in the presence and absence of the catalyst was needed. For this purpose, the absorption of ozone into the liquid phase was realized firstly in the absence of a chemical reaction; thus, the dye was not added in these experiments. Also, the decomposition reaction of  $O_3$  in the liquid phase was neglected by studying the absorption at the acidic pH of 2.5. Because the rate of ozone decomposition was known to be insignificant at acidic pH [39,44].

In the experiments, the FBR was operated by using distilled water at pH = 2.5 as the liquid phase and air/ $O_3$  or oxygen/ $O_3$  mixture as the gas phase. Ozone was produced from dry air or oxygen. About 60 L of distilled water was placed in the liquid storage tank. 1000 mL of 0.1 M  $H_2SO_4$  solution was added to regulate its pH to 2.5. After the preparation of the solution to be ozonated, ozonation started by operating the ozone generator regulated to required  $O_3$  dose and gas flow rate. The gas flow was sent to the gas washing bottles to measure the inlet  $O_3$  concentration in the gas before sending to the FBR. Then, the gas flow to the reactor was started by changing the three way valve direction. Meanwhile, the solution in the storage tank was pumped into the reactor. Afterwards, manometer taps were opened quickly to measure the pressure drop along the column. Samples were withdrawn from the sampling ports along the column and at different time intervals into 100-mL flask which containing a known volume of Indigo reagent solution to measure the residual (dissolved) ozone concentration. Ozone concentration in the outlet gas was determined by sending the off gas into gas washing bottles during the reaction [198].

The variables in the experiments are given in Table 4.5. Ozone concentrations in the gas at the inlet and outlet of the reactor, residual  $O_3$  concentrations in the liquid phase were determined. The experiments were conducted until the time of the steady state and steady state concentrations of ozone in the liquid phase were measured for different gas and liquid flow rates, bed heights and catalyst dosages. In the catalyzed experiments, the

required amount of the catalyst (alumina or PFOA) particles was filled into the reactor and the experiment was started. These experimental results were used to predict the liquid axial dispersion coefficients ( $D_L$ ) and gas-liquid mass transfer coefficients ( $k_L a$ ) from the modeling study according to the numerical method used which was given later in the thesis.

Table 4.5. Independent variables of the ozone absorption experiments in the FBR.

Experimental Parameters	Values
$Q_G, \text{L/h}$	45, 70, 100, 125, 150
$Q_L, \text{L/h}$	30, 80, 110, 150, 200, 250
$C_{O_3, G, in}, \text{mmol O}_3/\text{L gas}$	$0.306 \pm 0.017$
pH	$2.55 \pm 0.3$
Particles	Alumina, PFOA
$m_{cat}, \text{g}$	25, 35, 50, 75, 100, 125, 150, 175
$d_{cat}, \text{mm}$	2.0

#### 4.5.3 Hydrodynamic experiments in the reactor

The successful modeling and operation of a gas-liquid-solid fluidized bed system depend on the determination of reactor hydrodynamics at different operation conditions. Knowledge of minimum fluidization velocity enables the operation of the reactor at the fluidized conditions which brings its advantages increasing mass and heat transfer in the bed [200]. Therefore, the fluidization conditions were investigated at different gas and liquid flow rates in the presence of alumina or PFOA particles.

The minimum fluidization velocity is the superficial liquid velocity at which the particles begin to fluidize at the given superficial gas velocity [201]. The minimum liquid flow rate or velocity to fluidize the particles is found by observing the pressure drop increase along the column with the increase of liquid flow rate at a constant gas flow rate. When fluidized, the pressure drop across the bed no longer alters with increasing liquid flow rate. The liquid flow rate at which pressure drop starts to remain constant, corresponds to the minimum fluidization velocity at the studied gas flow rate [201].

The experiments to determine minimum fluidization velocity were carried out by using oxygen as the gas phase and distilled water as the liquid phase. The studied gas velocities were changed between  $1.66 \times 10^{-3}$  m/s ( $Q_G=30$  L/h) and  $8.30 \times 10^{-3}$  m/s ( $Q_G=150$  L/h) whereas the liquid velocity was changed between  $1.66 \times 10^{-3}$  m/s ( $Q_L=30$  L/h) and  $13.8 \times 10^{-3}$  m/s ( $Q_L=250$  L/h). Alumina or PFOA particles (25-125 g) were filled into the reactor. Gas flow was introduced to the reactor at a constant rate. The initial static bed height of the particles was 7.2 cm. Distilled water feed was started to the column with a constant flow rate and the pressure drop along the column was measured by the help of the U-tube manometers. Then, the liquid flow rate was gradually increased and the pressure drops were continuously measured. The minimum fluidization velocity was found by plotting pressure drop versus superficial liquid velocity at a given gas velocity. The liquid velocity at which the pressure drop began to not change any more with the increase of superficial liquid velocity corresponded to the minimum fluidization velocity.

In the column, the gas hold-up was evaluated with the height measurements from Equations (4.1) and (4.2).

$$A.h(1 - \varepsilon_G) = A.h_0 \quad (4.1)$$

$$\varepsilon_G = 1 - \frac{h_0}{h} \quad (4.2)$$

where,  $h$  is the height of the aerated liquid in the column and  $h_0$  is the original liquid height before the gas flow. For the gas-liquid system, the total of gas and liquid hold-up values is equal to one, as shown in Eqn. (4.3).

$$\varepsilon_G + \varepsilon_L = 1 \quad (4.3)$$

Similarly the hold-up values were found for the three phase system according to Equation (4.4). Now, the solid hold-up (loading) was found from the relationship given in Equation (4.5) between the catalyst loading amount ( $m_{cat}$ ), catalyst density ( $\rho_{cat}$ ), reactor cross-sectional area ( $A$ ) and expanded bed height ( $H_E$ ).

$$\varepsilon_G + \varepsilon_L + \varepsilon_S = 1 \quad (4.4)$$

$$\varepsilon_s = \frac{m_{cat}}{\rho_{cat} \cdot A \cdot H_E} \quad (4.5)$$

For the gas hold-up measurement, the reactor was filled with the distilled water in the absence of gas flow. Then, the liquid flow was stopped and the static (original) liquid height was measured. Afterwards, the gas was sent to the reactor at a constant flow rate; the aerated liquid height due to the gas flow was determined. For the reactor filled with the catalyst particles, the same procedure was applied; however in that case, 125 g of the particles were fed to the reactor and then, the liquid heights before and after the gas flow were measured. The solid hold-up was found from Equation (4.4) by measuring the expanded bed height during the experiment.

#### 4.5.4 Dye ozonation experiments

The fluidized bed experiments were conducted operating the column in co-currently continuous mode for gas and liquid flows entering at the bottom. Runs were performed with different values of catalyst dosage, particle size, gas and liquid flow rates and pH. In dye ozonation experiments, the same procedure used in the ozone absorption experiments was followed. Bubble and fluidized bed column experiments were carried out mainly at the acidic pH of 2.5 to eliminate the ozone decomposition reactions. Several experiments were done at pH 7.6 and 10.5 to understand the effects of pH on the ozonation and catalytic ozonation processes. The initial pH of the dye solution was adjusted by 0.1 M H<sub>2</sub>SO<sub>4</sub> solution to the pH of 2.5. For initial pH values of 7.6 and 10.5, 1 M NaOH and 0.1 M H<sub>2</sub>SO<sub>4</sub> solutions were used as needed to prevent the adverse effects of buffers on ozonation. Because it was known that phosphate buffer acted as a scavenger in ozonation process [39,41].

Similar to the ozonation experiments in the semi-batch reactor, the gas leaving the column was collected in a 600 mL washing bottle filled with 550 mL KI solution and the ozone concentration at the outlet gas was determined by the iodometric titration method [198].

The required amount of dye solution (65 L) was prepared as explained in the procedure of semi-batch experiments. The experiment was started by introducing the ozone gas mixture to the system. The gas flow rate and the ozone dosage were regulated. Before

feeding into the column, the ozone concentration in the inlet gas was determined by sending to the gas into a washing bottle containing 200 mL of KI solution. Then, the gas flow was started into the column by changing the direction of the gas from the washing bottle to the column. After a while, the liquid was from the column by operating the pump and its flow rate was regulated. The pressure taps were opened.

During operation, the samples were withdrawn from the sampling ports at different column heights and at different times until the steady state was reached in the column and the run at the steady state was started. The steady state was reached in 7.5 min after the beginning of the run and the complete run continued about 20 min. In one sampling point two samples were withdrawn: One sample was taken into 50 mL erlenmeyer containing 1-mL of 0.025 M sodium thiosulfate solution to quench the residual O<sub>3</sub> in the sample. This sample was analyzed for the TOC, the dye concentration, and the by-product concentrations. The other sample was added into a 100-mL volumetric flask in which Indigo reagent was placed and the dissolved O<sub>3</sub> concentration in the sample was measured. The pressure drop along the column was determined from the height difference of the manometer liquid.

For the catalytic ozonation experiments, the column was filled with the desired amount and size of alumina or PFOA particles. In these experiments, the expansion of the bed was recorded. In non-catalytic and catalytic experiments gas and liquid flow rates, gas phase O<sub>3</sub> concentration, inlet dye concentration, pH, catalyst type, catalyst dosage and catalyst size were the studied experimental variables. The experimental values are listed in Table 4.6.

## **4.6 Analytical methods**

Samples taken from the semi-batch or fluidized bed reactor were analyzed for dye concentration, dissolved ozone concentration, COD, TOC, ozonation by-products and for gaseous ozone concentration.

### **4.6.1 Determination of dye concentration**

Samples taken from the semi-batch or fluidized bed reactor were analyzed for the dye concentration. To find the dye concentration in a sample, calibration curves showing the

dye concentration versus the dye absorbance were obtained for *AR-151* and *RBBR* dyes at their maximum absorption wavelengths of 512 nm and 591 nm, respectively. The absorbance measurements of the dyes at different concentrations were accomplished in Hitachi U-3010 type UV-visible spectrophotometer. After measuring the absorbances of the dye samples taken from the reactor in the spectrophotometer, the concentrations corresponding to the measured absorbances were found from the calibration curves.

Table 4.6. Variables for non-catalytic and catalytic ozonation experiments in FBR.

Parameters	Values	
Ozone produced gas	Dry air, oxygen	
$Q_G$ , L/h	30, 70, 150	
$Q_L$ , L/h	30, 70, 150, 250	
$T$ , °C	25	
pH	2.5, 7.6, 10.5	
$C_{O_3,G,in}$ , mmol/L gas	0.336, 0.435, 0.525, 0.611, 0.986, 1.410	
Dye	<i>RBBR</i> , <i>AR-151</i>	
$C_{D,in} \times 10^2$ , mmol/L	for <i>RBBR</i>	4.8, 9.6, 14.4, 19.2
	for <i>AR-151</i>	6.6, 13.2, 19.8, 26.4
Catalyst	Alumina, PFOA	
$m_{cat}$ , g	0, 25, 75, 125	
$d_{cat}$ , mm	1.5, 2.0, 2.8	

#### 4.6.2 Determination of dissolved O<sub>3</sub> concentration

In acidic solution, ozone rapidly decolorizes indigo dye; the decrease in the absorbance of the dye is linear with increasing concentration of ozone. In this reaction, 1 mol indigo reacts with 1 mol of ozone. In the experiments of semi-batch or fluidized bed reactor, ozone concentration in the aqueous phase was determined by the Indigo method [198,202,203].

Indigo stock solution and indigo reagent used in the experiments were prepared according to the following procedure: 770 mg of potassium indigo trisulfonate with 0.5 mL H<sub>3</sub>PO<sub>4</sub> was dissolved in 1000 mL distilled water to obtain indigo stock solution.

Then, indigo reagent was prepared by mixing 100 mL of indigo stock solution, 10 g  $\text{NaH}_2\text{PO}_4$  and 7 mL  $\text{H}_3\text{PO}_4$  in a 1000 mL volumetric flask and by diluting to 1000 mL.

To each of a series of 100 mL volumetric flasks, 10 mL of indigo reagent was added. For the samples at high dissolved  $\text{O}_3$  concentrations, 20 or 30 mL of reagent was put. For blanks, one or more flasks were filled to the 100 mL-mark with distilled water. Samples of the ozone -containing water were transferred to the remaining test flask of the series. After adding the samples, a slightly blue color remained. Each of the test flasks was filled to the 100 mL-mark with water. After mixing, the residual absorbance of the ozone-containing samples and of the blank were measured at 600 nm in Hitachi spectrophotometer. The concentration of residual indigo was found from the indigo calibration curve, “indigo concentration versus absorbance” graph. The reacted indigo amount as mol basis, equivalent to residual ozone in the sample, was determined from the difference between the concentration of blank indigo and residual indigo.

#### **4.6.3 Chemical Oxygen Demand (COD) analysis**

Chemical Oxygen Demand (COD) analysis is applied widely for the wastewater characterization purposes. It determines the organic content in the sample by measuring the oxygen demand of the organics. The COD test uses a strong oxidant in an acid solution and heat to oxidize organic carbon to  $\text{CO}_2$  and  $\text{H}_2\text{O}$ . The most commonly used oxidant is potassium dichromate ( $\text{K}_2\text{Cr}_2\text{O}_7$ ). The oxidant is prepared in the sulfuric acid ( $\text{H}_2\text{SO}_4$ ) solution with a silver catalyst and a mercuric compound is used to reduce the interference with chloride ions.

In the present experiments COD analysis was performed according to the Standard Methods [198]. COD reagent was prepared by dissolving 6 g  $\text{K}_2\text{Cr}_2\text{O}_7$ , 6 g  $\text{Ag}_2\text{SO}_4$  and 3.6 g  $\text{HgSO}_4$  in 500 mL of 95-98% concentrated  $\text{H}_2\text{SO}_4$ . In the preparation, the compounds were added to  $\text{H}_2\text{SO}_4$  slowly to achieve the dissolution of them in the acid. Then, the solution was mixed at least 24-h on a magnetic stirrer for a complete dissolution.

The digestion procedure was as follows: 2 mL wastewater sample of which COD would be measured, was added into 3 mL of COD reagent in a 10 mL glass COD vial. A blank

was prepared by adding 2 mL of deionized water to the COD reagent (3 mL). Then, the vials were shaken at several times and placed in the WTW CR-3000 thermoreactor which was heated to 150°C before. The vials were heated in the thermoreactor at 150°C for 2 hours. The vials were removed from the reactor and they were cooled to the room temperature. The COD of the samples were determined with Hach DR-2010 portable spectrophotometer at a wavelength of 620 nm. COD of the blank was set to 0 mg/L COD; then, COD of the samples were measured directly in the unit of mg COD/L.

#### **4.6.4 Total Organic Carbon (TOC) analysis**

Total Organic Carbon (TOC) analysis was accomplished in Shimadzu V<sub>CPH</sub> type TOC analyzer. The TOC was found by measuring Total Carbon (TC) and Inorganic Carbon (IC) of the sample and then subtracting the IC value from the TC value. Before analyzing, the samples were filtrated through a 0.45 µm filter cartridges to eliminate from any residual in the samples. Additionally, high colored samples were diluted for the maintenance of the instrument.

#### **4.6.5 Determination of O<sub>3</sub> concentration in the gas phase**

The potassium iodide (KI) solution in the gas washing bottles reacts with the gaseous ozone absorbed into the KI solution and iodine (I<sub>2</sub>) is liberated. Then the titration of I<sub>2</sub> is realized by sodium thiosulfate and O<sub>3</sub> concentration in the gas phase is determined [198].

For the determination of O<sub>3</sub> concentration in the inlet and off gas, first KI solution (2%) was prepared by dissolving 20 g KI in 1000 mL distilled water which was freshly boiled and cooled. This solution was used for the low O<sub>3</sub> concentrations in the gas. For moderate and high O<sub>3</sub> concentrations, 60 g (6%) and 120 g (12%) of KI were dissolved in 1000 mL distilled water, respectively. 200 mL of prepared solution was placed in a washing bottle at the inlet of the gas and 550 mL of solution was put at the gas outlet. Then, the solution was ozonated; afterwards 10 mL and 27.5 mL of 0.5 N H<sub>2</sub>SO<sub>4</sub> solutions were added to the ozonated 200 and 550 mL of KI solutions, respectively. The subsequent solutions were titrated with 0.1 M sodium thiosulfate pentahydrate (Na<sub>2</sub>S<sub>2</sub>O<sub>3</sub>·5H<sub>2</sub>O) and the spent thiosulfate was recorded. For high O<sub>3</sub> concentrations instead of 0.1 M, 0.3 M thiosulfate solution was used.

#### 4.6.6 HPLC method for analysis of ozonation by-products

HPLC analysis was made to identify and measure carboxylic acids and aldehydes in the ozonated solutions. For the organic acids, the HPLC column used was Waters C18 Spherisorb 250 × 4.6 mm organic column. As the mobile phase 80% (v/v) 20 mM pH=2.5 KH<sub>2</sub>PO<sub>4</sub>/ H<sub>3</sub>PO<sub>4</sub> buffer and 20% 95/5 (v/v) acetonitrile/water mixture was used. The used detector was UV detector and the analysis was made at a wavelength of 200 nm. The flow rate of the mobile phase was 1 mL/min.

For aldehyde determination a method by Takeda et al. [204] was used. The direct determination of the aldehydes cannot be achieved in HPLC. Derivatization with some compounds was needed. In this respect, the derivatization of the aldehydes was applied by using 2,4-dinitrophenylhydrazine (DNPH) reagent and the derivatives were separated in HPLC by UV- absorption at 365 nm. Acetonitrile and methanol were the mobile phases of the system. First, the derivatization reagent was prepared. For this purpose, DNPH was recrystallized from acetonitrile and 20 mg of this recrystallized DNPH was dissolved in 15 mL solution mixture containing 12 M HCl, water and acetonitrile in the ratio of 2:5:1 (v/v/v). Then, 2 mL carbon tetrachloride was added into 15 mL-reagent solution. The solution was shaken 5 min and placed in a centrifuge (2000 rpm) to separate the phases. The solution was kept in the dark and used in two-weeks time [205].

The stock solutions were prepared by dissolving a certain amount of the aldehydes in an acetonitrile/water solvent (75/25 v/v). Then, 10 mL of sample was transferred into a 50 mL erlenmeyer containing 4 mL DNPH reagent, and was sealed tightly until the HPLC analysis. For the samples containing glyoxal, 1 mL DNPH reagent was sufficient. Then, the samples were shaken and waited for at least 1 h at room temperature before the HPLC analysis.

The separation of the aldehydes was achieved by using Symmetry C18 reverse-phase column. The detector was UV and operated at 365 nm. Two mobile phases were used: (A) HPLC grade water/methanol mixture (7/3 v/v) and (B) 90% acetonitrile in HPLC grade water. The program was gradient as follows: isocratic at 90% A for 6 min, 90% to 60% A in 24 min, 60% to 0% A in 10 min and isocratic at 100% B for 10 min (total 50 min/sample).

## CHAPTER 5

### RESULTS AND DISCUSSION

#### 5.1 Non-catalytic and catalytic ozonation experiments in semi-batch reactor

The ozonation of *AR-151* and *RBBR* separately was realized in the semi-batch reactor in the presence and absence of alumina or PFOA particles. The kinetics of ozonation and catalytic ozonation processes were investigated. The effect of the stirrer rate on the absorption of ozone into water was studied previously (Figure C.1 in Appendix C). According to the results of these experiments, the stirrer rate was regulated to 300 rpm (the optimum value) in the semi-batch experiments.

##### 5.1.1 Dye and COD removals in *AR-151* or *RBBR* aqueous dye solution

*AR-151* and *RBBR* solutions were ozonated at different conditions. The dye and COD removals were obtained and the most efficient conditions resulting in the highest dye and COD removal were determined.

###### 5.1.1.1 Ozonation Experiments

Ozonation experiments, without using catalysts, were carried out at different pH. At the acidic pH (pH 2.5), direct reaction of ozone with the dye molecule is dominant, since the concentration of  $HO^-$ , one of the most significant initiators of radical reactions, is low. At alkaline pH (pH=13),  $O_3$  molecules are decomposed into ions and radicals, therefore ozonation of dye molecules takes place mainly by radical reactions. Also, direct ozonation might be important with the undecomposed  $O_3$  as well. The contribution of direct and radical reactions at pH of 7 causes a complicated status since the concentrations of both the  $O_3$  and  $HO^-$  concentrations are lower [39, 110].

More than 90% dye removals were achieved in 30 min by the ozonation of *AR-151* or *RBBR* solution at the all studied pH values (Figure 5.1). The overall dye removal

efficiency after 30 min of reaction time, did not depend on solution pH significantly. The initial reaction rate of dyes showed differences from pH 2.5 to 13 as an indication of the contribution of direct or radical reaction mechanism. For *AR-151*, the initial rate was almost the same at pH 2.5 and 13, but a much lower initial rate was observed at pH 7. It was understood that both direct and radical reaction mechanisms were important in the ozonation of *AR-151*, giving high initial rates at pH 2.5. In *RBBR* ozonation, the highest initial dye removal rate occurred at alkaline pH showing that the radical reactions played a relatively more significant role in the oxidation mechanism.

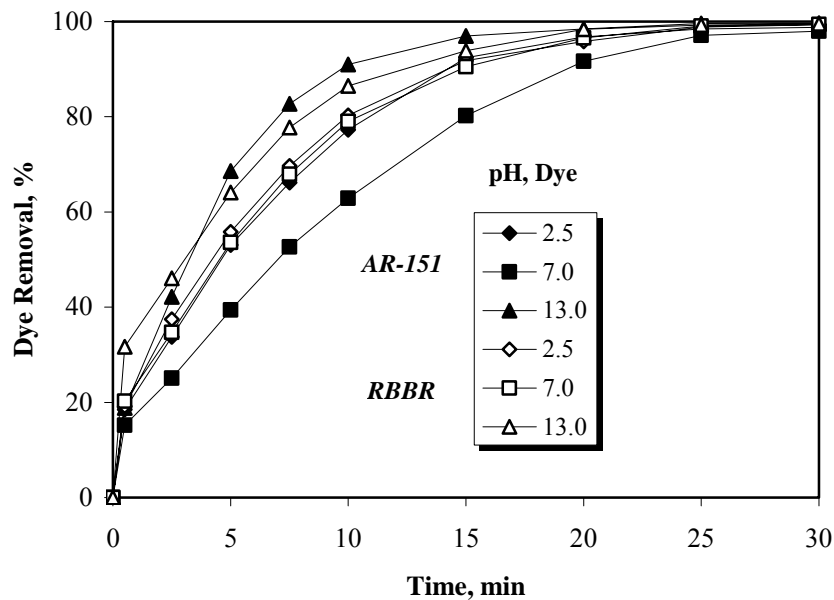


Figure 5.1. Dye removal values with ozonation at different pH values. Conditions:  $C_{D,i}=200$  mg/L,  $T=25^{\circ}\text{C}$ , stirrer rate =300 rpm,  $Q_G=150$  L/h,  $D_{O_2}=46.04$  mmol/h, reaction time =30 min. Bold shapes: *AR-151*; apparent: *RBBR*.

The effects of pH on COD removals in the ozonation of *AR-151* or *RBBR* are presented in Figure 5.2, where the highest COD removals were observed at pH 13 in concordance with the results of dye removal efficiencies (Figure 5.1). For *RBBR*, COD removal increased with the increasing pH. The increment was linear and it showed that the COD removal was mainly due to the radical reactions in the ozonation of *RBBR*. For *AR-151*, the COD removal showed a slight decrease at pH 7 compared to that at pH 2.5 for *AR-*

*151*, then increased again with the increasing pH. At pH of 7, both the dissolved O<sub>3</sub> and radical concentrations were low causing a decrease in COD removal.

#### **5.1.1.2 Catalytic ozonation experiments**

The catalytic ozonation experiments with *AR-151* or *RBBR* were conducted in the presence of Al<sub>2</sub>O<sub>3</sub>, 25%, 50%, and 100% PFOA; as a result the most efficient conditions were determined according to the dye and COD removal percentages. Ozonation of the aqueous solutions of each dye in the presence of alumina, or PFOA catalysts containing different amounts of PFO acid provided dye removal efficiencies up to 98-99%, depending on the catalyst type and solution pH (Table 5.1).

Thermogravimetric Analysis (TGA) was performed to understand the amount of carbon loading on the prepared PFOA types. The results of the TGA are given in Appendix I.2. According to the TGA, it can be said that the amount of carbon loaded on 100% PFOA was almost 35% higher than that loaded on 25% PFOA. The amount of hydrocarbon (perfluorooctanoic acid) affected the efficiency of the PFOA type.

In the ozonation with alumina, the adsorption of the dye molecules on the catalyst seemed to be an important mechanism. Since *AR-151* had an acidic character, its adsorption on the alumina surface became easier at pH = 2.5 and 7 which were the lower pH values than the pH<sub>PZC</sub> of alumina which was explained before in Section 2.4.1 (Table 2.4); similarly, the protonation of *RBBR* molecules at acidic pH made the adsorption of these molecules on the alumina surface easier [32,155,206]. The observation of red- or blue-dyed catalyst particles at the end of 30 min of the reaction at pH 2.5 and 7 was a strong sign of adsorption of *AR-151* or *RBBR*, respectively. Therefore, at a pH of 2.5, the dye removal occurred by direct ozonation and adsorption, in the ozonation with alumina. The intensity of the color decreased with the increase of PFO acid amount in the PFOA catalyst. It can be said that the effect of adsorption on dye removal in catalytic ozonation with PFOA was not very significant.

At pH 13, adsorption of the dye molecule on alumina was low; lower intensity of the blue or red color on the catalyst particles was observed. The adsorption of both *RBBR* and *AR-151* was easier at pH = 2.5 due to the protonation and acidic character of *RBBR*

and *AR-151*, respectively. At pH = 13, radical reactions played a significant role in the ozonation of the both dyes since the concentration of molecular ozone decreased by the decomposition reactions, and most of the dye molecules were degraded by the radicals. The decreasing effect of adsorption seemed to be compensated by the increasing contribution of radical reactions at pH 13; thus the overall dye removal efficiency became almost the same as that at pH 2.5 for both of the dyes with each catalyst type. Thomas et al. [206] showed that hydroxyl radicals were produced on the alumina surface at basic pH, enabling radical reactions to occur both in the liquid phase and also on the catalyst surface.

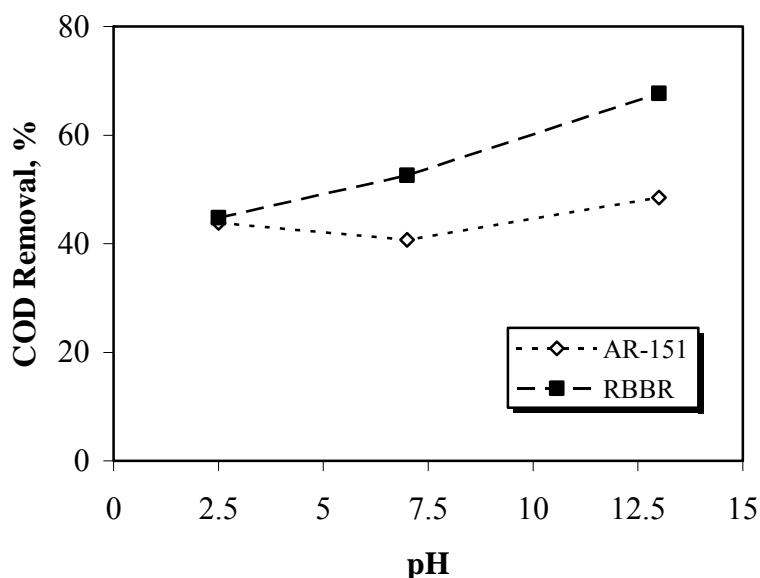


Figure 5.2. COD removal values obtained in ozonation of *AR-151* or *RBBR* at different pH values. Conditions:  $C_{D,i} = 200$  mg/L,  $T = 25^{\circ}\text{C}$ ; stirrer rate = 300 rpm;  $Q_G = 150$  L/h,  $D_{O_3} = 46.04$  mmol/h, reaction time = 30 min.

In the catalytic ozonation of *AR-151* with PFOA, the total dye removals in 30 min were found to be lower at pH 7 than those obtained at pH 2.5 and 13. However for *RBBR*, the dye removal at pH 7 was higher than those at pH 2.5 and pH 13. *RBBR* molecules were known to be more rigid and hydrophobic than *AR-151* due to its aromatic anthraquinone structure highly stabilized by resonance [208].

Table 5.1. Dye removal percentages for *AR-151* and *RBBR* for different pH values and catalyst types. Conditions:  $C_{D,i} = 200$  mg/L,  $T = 25^\circ\text{C}$ , stirrer rate = 300 rpm,  $Q_G = 150$  L/h,  $D_{O_3} = 46.04$  mmol/h, reaction time = 30 min.

Treatment	pH	Dye Removal, %	
		<i>AR-151</i>	<i>RBBR</i>
$O_3$ only	2.5	98.8	99.3
	7	98.0	99.4
	13	99.7	99.5
$O_3$ +alumina	2.5	97.4	97.5
	7	94.9	98.1
	13	95.5	98.3
$O_3$ + 25% PFOA	2.5	96.2	97.3
	7	91.3	99.6
	13	96.3	98.4
$O_3$ + 50% PFOA	2.5	96.1	97.6
	7	90.3	99.0
	13	97.9	97.7
$O_3$ + 100% PFOA	2.5	98.3	97.6
	7	94.8	99.4
	13	97.0	97.4

At pH 13, the total dye removal percentage was found to be less than those found with ozonation alone for all the catalysts used. The percent dye removal was increased by the change of the catalyst from alumina to 100% PFOA for *AR-151*. This indicated that the use of PFOA containing higher amounts of PFO acid would be more advantageous in the ozonation of *AR-151*. On the contrary, alumina and PFOA containing lower amounts of PFO acid were observed to give higher dye removal efficiencies for *RBBR* at pH 13. The results showed that ozone molecules oxidized *RBBR* with a higher efficiency than in the case of *AR-151* removal.

For the studied pH range, the COD reduction increased with the addition of each catalyst type compared to the ozonation alone as seen in Figure 5.3. For pH 2.5 and 7, the COD removal percentage increased with the increase of PFO acid amount in the catalyst, and the highest removal was observed at the condition where 100% PFOA was used. For *RBBR*, COD removal increased linearly with the PFO acid amount on alumina at pH 2.5 and 7. The most efficient PFOA type was found as 100% PFOA in removing COD from *AR-151* or *RBBR* solutions at pH values of 2.5 and 7.

Due to the adsorption of the dye molecules on alumina, there would be a competition for the surface active sites among the dye molecules and the ozonation by-products. For the alumina catalyst, the adsorption of *AR-151* or *RBBR* dye was more dominant than those of the by-products causing lower COD removals than those achieved by the PFOA types. This behavior explained the increase in COD removal with the increase of PFO acid amount. Some ozonation intermediates or by-products non-polar in nature were adsorbed onto the surface of 100% PFOA more easily than that of polar dye molecules. As a result, the degradation of those organics occurred on the catalyst surface in addition to their partial oxidation in the liquid bulk phase. The degradation of such organics in the bulk phase by molecular ozone was limited because most of the ozonation by-products were hardly degradable by ozone in the liquid phase [49].

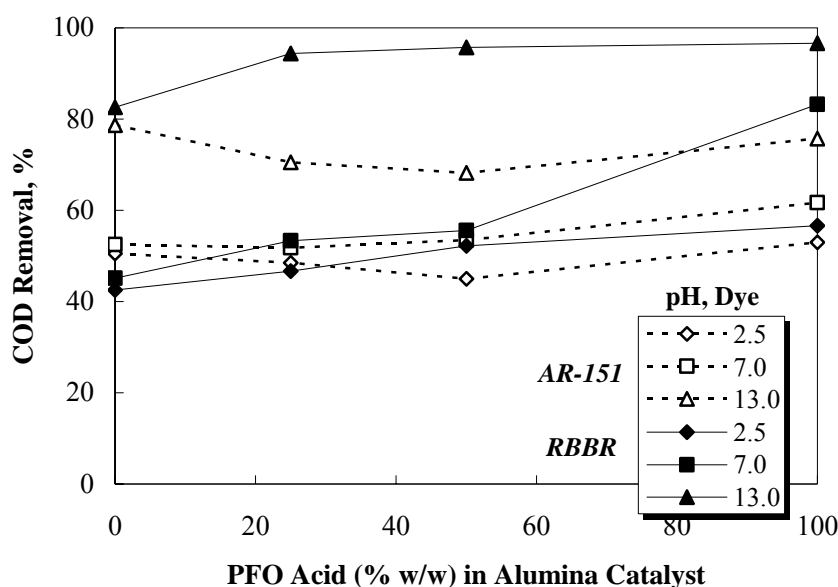


Figure 5.3. The change of COD removal from the dyes by catalytic ozonation. Conditions:  $C_{D,i} = 200$  mg/L,  $T = 25^\circ\text{C}$ ; stirrer rate = 300 rpm;  $Q_G = 150\text{L/h}$ ,  $D_{O_3} = 46.04$  mmol/h, reaction time = 30 min. Bold shapes: *AR-151*; apparent: *RBBR*.

Another important result was the increase of COD removal percentage with the increase of pH. Solution pH 7 was more effective than pH 2.5 for the removal of ozonation by-products in the *RBBR* or *AR-151* ozonation. The highest COD removal percentages were observed at pH 13 in accordance with the existence of more  $HO^\bullet$  radicals. At pH

13, no significant color change of the catalyst particles due to the adsorption of the *RBBR* or *AR-151* molecules, was observed for either alumina or any type of PFOA. This meant that the dye molecules were degraded in the aqueous phase only at that pH, but the ozonation by-products might possibly be degraded both in the aqueous phase and on the catalyst surface.

Higher COD reduction percentages were observed in the ozonation of *RBBR* solutions compared to those of *AR-151*. The limited effect of PFO acid amount on COD removal efficiency at pH 2.5 and 7 suggested that a relatively higher percentage of the reaction occurred in the aqueous phase rather than on the catalyst surface. At pH 13, the reduction of COD was more efficient especially in the case of *RBBR* than those at the lower pH values.

The effect of ozone dose ( $D_{O_3}$ ) on dye and COD removals in the catalytic ozonation (with 100% PFOA catalyst) was investigated while keeping the gas flow rate constant. The results showed that all the chosen ozone doses were sufficient to complete the removal of each dye with almost 100% efficiency so that it would be possible to observe the extent of by-product oxidation by measuring the total COD removals achieved in 30 min of ozonation. As seen in Figure. 5.4, the slowest dye removal cases are observed at the lowest ozone dose for both of the dyes. But, in 30 min of ozonation, the overall dye removal percentage is almost independent of the ozone dose. The dye removal rate increased with the ozone dose, except the initial ozonation rate of both *AR-151* and *RBBR*, which showed a low dependency on the ozone input.

COD reduction efficiency increased with the ozone dose, because of the higher amount of ozone being available for the degradation of ozonation by-products (Table 5.2). However, the increase of ozone dose from 24.38 mmol/h to 35.42 mmol/h showed a small improvement on the COD reduction for *AR-151*. During ozonation of dye molecules, double bonds and aromatic structure are broken first to yield smaller structured organics such as aldehydes. These organics also have a remarkable COD. Therefore in the second step, these aldehydes needing more ozone may be converted to carboxylic acids and may be partly transformed into gaseous products by further oxidation. Occurrence of relatively lower improvement on COD reduction, with the increase of ozone dose from 24.38 mmol/h to 35.42 mmol/h, may be due to the

oxidation of dye molecules to intermediates having different molecular weights. In the case of *RBBR* ozonation contrary to the case of *AR-151*, COD reductions were increased considerably with the increasing amount of dissolved  $O_3$  in the reactor.

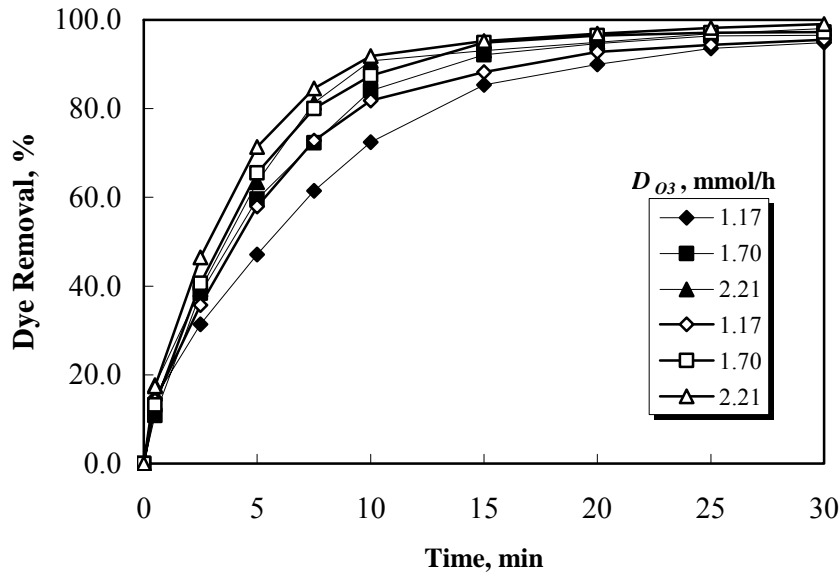


Figure 5.4. The effect of ozone dose on the dye removal. Conditions: catalyst = 100% PFOA,  $C_{D,i} = 100$  mg/L,  $T = 25^\circ\text{C}$ ; stirrer rate = 300 rpm;  $Q_G = 150$  L/h, reaction time = 30 min. Bold shapes: *AR-151*, pH 2.5; apparents: *RBBR*, pH 7.

Table 5.2. COD removals (%) of *AR-151* or *RBBR* by ozonation with 100% PFOA catalyst. Conditions:  $T=25^\circ\text{C}$ ; stirrer rate=300 rpm;  $Q_G=150$  L/h, reaction time=30 min.

Type of the dye	$D_{O_3}$ , mmol/h	$C_{D,i}$ , mg/L	COD Removal, %
<i>AR-151</i>	24.38	100	44.9
	35.42	100	48.3
		100	57.3
	46.04	200	53.0
		400	15.0
<i>RBBR</i>	24.38	100	32.1
	35.42	100	46.9
		100	65.6
	46.04	200	61.4
		400	35.2

Figure 5.5 shows the effect of initial dye concentration on percent dye removals for both of the dyes in the catalytic ozonation process. It was observed that the effect of initial dye concentration was considerable after the first minute of the reaction. In the ozonation of *RBBR*, the overall dye removal percentages after a reaction time of 30 min decreased slightly with the increasing initial dye concentration (Figure 5.5). The COD reduction, after 30 min of reaction time, decreased significantly when the initial dye concentration was increased. Because an increase in the initial dye concentration corresponded to an increase of by-product concentration in the solution. Then, the available ozone started to be consumed both for oxidation of intermediates and also for the continuing degradation of the original dye. Thus, this caused a decrease in the degradation rate of the dye in time, yielding a lower overall dye removal in 30 min of ozonation than that of the case with a lower initial dye concentration.

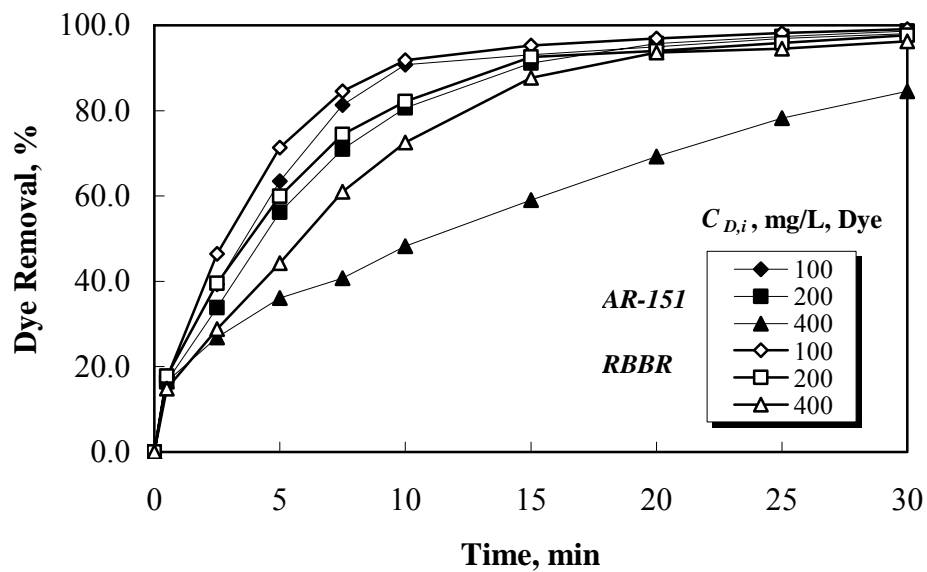


Figure 5.5. The effect of initial dye concentration on the dye removal. Conditions: catalyst =100% PFOA,  $D_{O_3}$  =46.04 mmol/h,  $T=25^\circ\text{C}$ , stirrer rate =300 rpm,  $Q_G$  =150L/h, reaction time =30 min. Bold shapes: *AR-151*, pH 2.5; apparent: *RBBR*, pH 7.

### 5.1.2 Kinetics of non-catalytic and catalytic ozonation-determination of reaction rate constants

The reaction kinetics of ozonation at pH 2.5, 7 and 13 were investigated for *AR-151* and *RBBR*, respectively.  $\ln(C_D/C_{D,i})$  versus  $t$  curves (Figures 5.6 and 5.7) were found to be

linear indicating a pseudo-first-order reaction at the equilibrium concentration of ozone in the aqueous phase at each pH (for the studied pH range) for both of the dyes. The values of pseudo-first-order and overall kinetic constants for the ozonation of *AR-151* and *RBBR* separately are summarized in Table 5.3. The overall kinetic constants ( $k$ ) were found to increase with the increase of pH from 2.5 to 13 for both of the dyes showing the effect of radical reactions on the dye ozonation kinetics.

The reaction kinetic was investigated for the catalytic ozonation process in the presence of alumina or the PFOA types prepared. Catalytic ozonation followed a pseudo-first-order reaction (Figures 5.8 and 5.9). But, the presence of the catalyst changed the pseudo-first order and overall reaction kinetic constants (Table 5.3). The effect of the catalysts on pseudo-first order and overall reaction kinetic constants depended on the pH; but as a general observation, the kinetic constants decreased by the addition of the catalyst into the system, especially at pH 13. A slightly higher kinetic constant of  $2.20 \text{ mM}^{-1} \text{ min}^{-1}$  was obtained in the catalytic ozonation of *RBBR* with 100% PFOA at pH 2.5. This might be attributed to the higher affinity of *RBBR* molecules, having relatively lower polarity due to their dipole moment of 3.3 Debye [209], to the organic phase saturated with molecular ozone on the surface of PFOA where the oxidation reaction took place. The higher kinetic constant in the removal of *RBBR* by sole ozonation at pH 13 showed that more powerful hydroxyl radicals degraded the dye molecules faster, while PFOA/O<sub>3</sub> system was based on molecular ozone reactions occurring at a slower rate; because ozone decomposition reactions were inhibited by PFOA [158].

At pH 2.5, the values of the pseudo-first order and overall kinetic constants were higher in the presence of 100% PFOA compared to the cases of using alumina and the other types of PFOA catalysts, showing that the most effective catalyst was 100% PFOA for *AR-151* and *RBBR* ozonations (Table 5.3).

The pseudo-first order and overall kinetic constants were found at different initial dye concentrations by keeping ozone concentration in the aqueous phase constant (Table 5.4). The pseudo-first order and overall kinetic constants were decreased with the increasing initial dye concentration. The reaction rates were affected by the change of  $C_{D,i}$  strongly in *AR-151* ozonation, whereas the decrease in the constants with the increase of  $C_{D,i}$  was smaller in the case of *RBBR*.

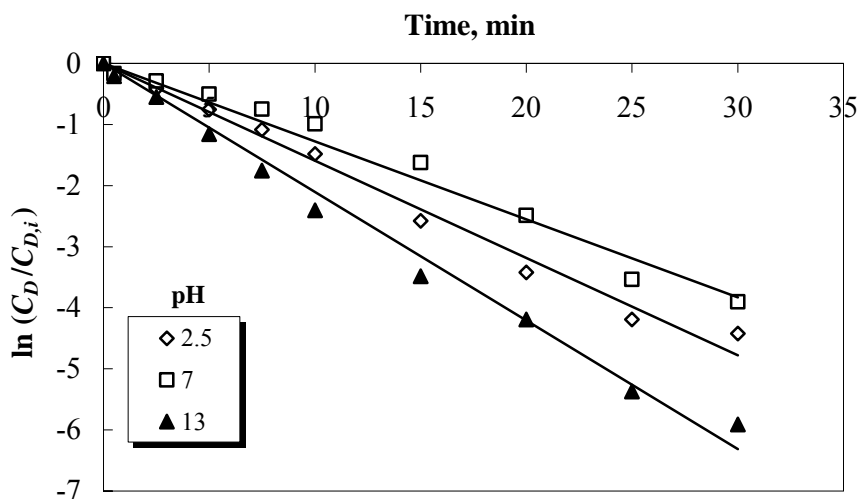


Figure 5.6. The pseudo-first order kinetic constants for *AR-151*. Conditions: ozonation only;  $C_{D,i} = 200$  mg/L,  $D_{O_3} = 46.04$  mmol/h,  $Q_G = 150$  L/h,  $T = 25^\circ\text{C}$ , stirrer rate = 300 rpm.

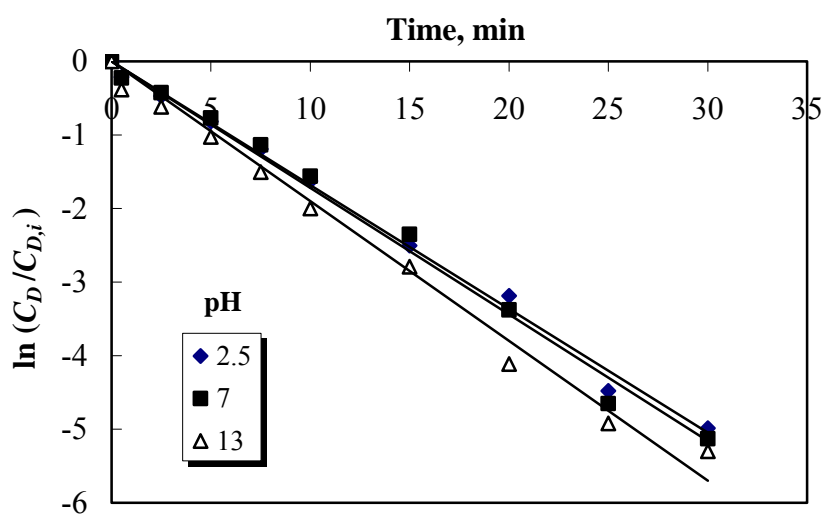


Figure 5.7. The pseudo-first order kinetic constants for *RBBR*. Conditions: ozonation only;  $C_{D,i} = 200$  mg/L,  $D_{O_3} = 46.04$  mmol/h,  $Q_G = 150$  L/h,  $T = 25^\circ\text{C}$ , stirrer rate = 300 rpm.

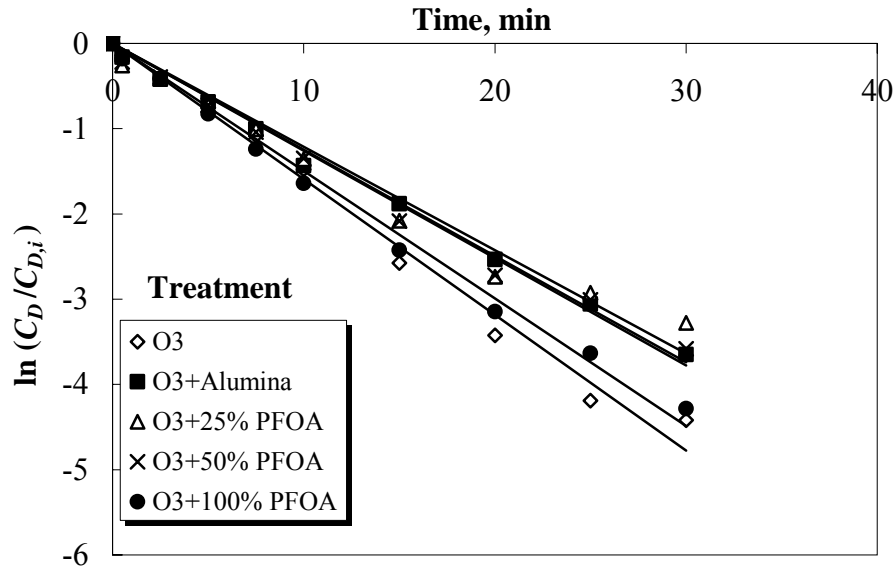


Figure 5.8. The pseudo-first order kinetic constants for *AR-151* at different treatment methods. Conditions:  $C_{D,i} = 200$  mg/L,  $D_{O_3} = 46.04$  mmol/h,  $m_{cat} = 5$  g,  $Q_G = 150$  L/h,  $T = 25^\circ\text{C}$ , stirrer rate = 300 rpm.

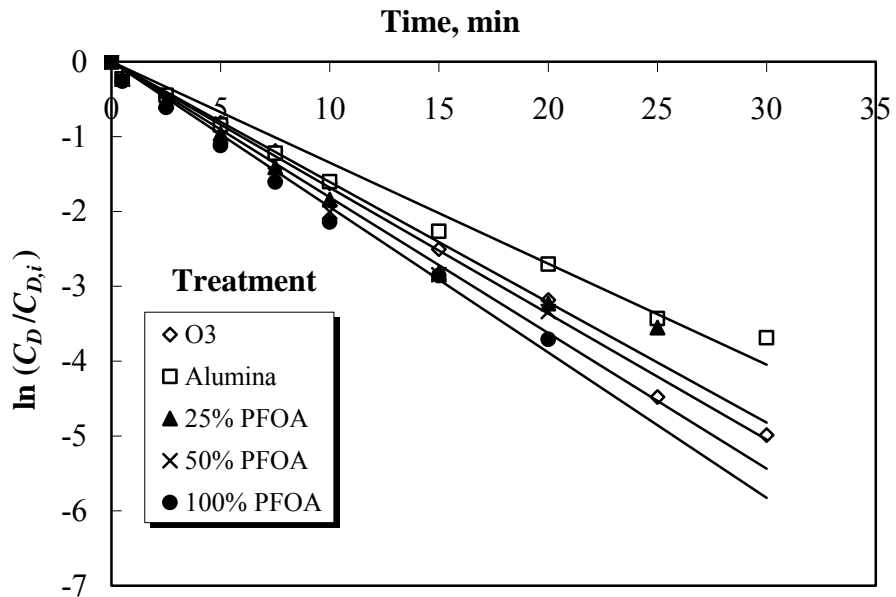


Figure 5.9. The pseudo-first order kinetic constants of *RBBR* at different treatment methods. Conditions:  $C_{D,i} = 200$  mg/L,  $D_{O_3} = 46.04$  mmol/h,  $m_{cat} = 5$  g,  $Q_G = 150$  L/h,  $T = 25^\circ\text{C}$ , stirrer rate = 300 rpm.

The pseudo-first-order rate constant  $k'$ , being equal to the multiplication of overall kinetic constant ( $k$ ) with the equilibrium concentration of ozone in the liquid phase ( $C_{O_3,e}$ ), increased with the increasing ozone dose, since the dissolved ozone concentration increased; but the overall kinetic constant,  $k$ , decreased. Therefore, the highest overall kinetic constant was found at the lowest  $D_{O_3}$  (24.38 mmol/h). Afterwards,  $k$  value did not change significantly by the slight increase in  $D_{O_3}$ .

Table 5.3. Pseudo-first order and overall kinetic constants for *AR-151* and *RBBR*, in cases of sole ozonation and catalytic ozonation. Conditions:  $C_{D,i} = 200$  mg/L,  $D_{O_3} = 46.04$  mmol/h,  $m_{cat} = 5$  g,  $Q_G = 150$  L/h,  $T = 25^\circ\text{C}$ , stirrer rate = 300 rpm.

Type of the dye	pH	Catalyst	$k', \text{min}^{-1}$	$k, \text{mM}^{-1} \text{min}^{-1}$
<i>AR-151</i>	2.5	-	0.159	1.81
		Alumina	0.125	1.42
		25% PFOA	0.121	1.38
		50% PFOA	0.126	1.43
	7	100% PFOA	0.150	1.70
		-	0.128	2.16
		Alumina	0.101	1.71
		25% PFOA	0.080	1.36
	13	50% PFOA	0.085	1.43
		100% PFOA	0.090	1.52
		-	0.210	5.99
		Alumina	0.136	3.86
	2.5	25% PFOA	0.128	3.64
		50% PFOA	0.130	3.72
100% PFOA		0.132	3.75	
-		0.168	1.91	
<i>RBBR</i>	2.5	Alumina	0.135	1.53
		25% PFOA	0.161	1.83
		50% PFOA	0.181	2.06
		100% PFOA	0.194	2.20
	7	-	0.172	2.91
		Alumina	0.135	2.28
		25% PFOA	0.194	3.28
		50% PFOA	0.158	2.67
	13	100% PFOA	0.168	2.84
		-	0.190	5.41
Alumina		0.132	3.77	
25% PFOA		0.152	4.32	
		50% PFOA	0.155	4.41
		100% PFOA	0.158	4.50

Table 5.4. Effect of ozone dose and initial dye concentration on kinetic constant in catalytic ozonation of *AR-151* or *RBBR*. Conditions:  $Q_G = 150$  L/h,  $T = 25^\circ\text{C}$ , stirrer rate = 300 rpm.

Dye	$D_{O_3}$ , mmol/h	$C_{D,i}$ , mg/L	$k'$ , $\text{min}^{-1}$	$k$ , $\text{mM}^{-1} \text{min}^{-1}$
<i>AR-151</i>	24.38	100	0.109	2.45
	35.42	100	0.140	1.88
		100	0.175	1.99
	46.04	200	0.150	1.70
		400	0.062	0.70
<i>RBBR</i>	24.38	100	0.134	4.96
	35.42	100	0.172	3.25
		100	0.197	3.33
	46.04	200	0.168	2.84
		400	0.135	2.27

## 5.2 Residence time distribution studies in fluidized bed reactor

The levels of liquid mixing in the absence and the presence of catalyst particles were investigated by the tracer technique [189] to determine the “residence time distribution (RTD) functions at different gas and liquid flow rates in a co-currently operated fluidized bed column.

### 5.2.1 Effects of gas and liquid flow rates on RTD distribution

The dispersion in the fluidized bed represents the ideal or non-ideal flow characteristics of the column. The large value of axial dispersion coefficient,  $D_L$  shows a completely mixed flow and plug flow occurs at small  $D_L$  values. The concentration profiles of ozone in the reactor will be affected by the non-ideal flow condition of the liquid phase. Therefore, the mixing level of the liquid phase needs to be determined for an appropriate modeling of the reactor.

The flow characteristics of the liquid phase was investigated by conducting tracer experiments. For this purpose, first, the reactor was operated without the catalyst particles as a bubble column to determine the degree of liquid mixing. Using the data of the tracer experiments, Péclet number ( $Pe_L$ ), axial dispersion coefficient ( $D_L$ ), and the approximate number of CSTRs ( $N_{CSTRs}$ ) in the column were determined at different gas

and liquid velocities. The representative residence time distribution curves at different liquid velocities are shown in Figure 5.10.

At the highest liquid velocity, the “residence time distribution” (RTD) curve was the narrowest one with the highest peak. The RTD curves were shifted to the right with the decreasing liquid velocity and the peak height was decreased. The RTD curves became narrower by the change of liquid velocity from  $u_L = 8.3 \times 10^{-3}$  m/s to  $19.4 \times 10^{-3}$  m/s. It seemed that liquid velocity had an important effect on the dispersion characteristics of the column. The pulse response of the tracer at  $u_L = 19.4 \times 10^{-3}$  m/s resembled to the pulse response of the tracer in a single CSTR. However, this trend was changed by the decrease of liquid velocity since the mixing was better at the higher liquid flow rates.

The results of the RTD experiments are given in Table 5.5. A higher gas or liquid velocity produced a higher  $D_L$ , indicating that the reactor was much closer to one CSTR condition. The calculated  $Pe_L$  enabled the determination of the  $N_{CSTRs}$  which represented the equivalent number of tanks in series to model the reactor. According to the results, it can be said that the number of CSTRs to model the bubble column decreased with the increasing  $u_G$  and  $u_L$ . This is because of the turbulence in the reactor which increased causing an increase in the degree of mixing within the column. As seen from Table 5.5, the column could be modeled as two CSTRs in series for all the studied gas and liquid velocities except at  $u_G = 3.3 \times 10^{-3}$  m/s for  $u_L = 8.3 \times 10^{-3}$  and  $11.1 \times 10^{-3}$  m/s. At that gas velocity, the modeling of the reactor became closer to three CSTRs in series since the calculated numbers of CSTRs were 3.1 and 2.8.

Similarly, Péclet number decreased with the increase of superficial liquid velocity. The effect of liquid velocity was seen more obviously at  $u_G = 3.3 \times 10^{-3}$  m/s. At the higher gas velocities, Péclet number was almost independent of the liquid velocity especially at  $u_G = 8.3 \times 10^{-3}$  m/s. As the liquid velocity increased, the holdup of liquid in the bed increased. This created more turbulence in the system increasing the mixing. From the calculated values, a correlation between  $D_L$  and  $u_L$  was obtained (Figure 5.11). The relationship between  $D_L$  and  $u_L$  was found to be linear for all the studied gas velocities.  $D_L$  was increased with the increase of  $u_L$ . The slope of “ $D_L$  vs.  $u_L$ ” linear curve increased with the increase of  $u_G$ .

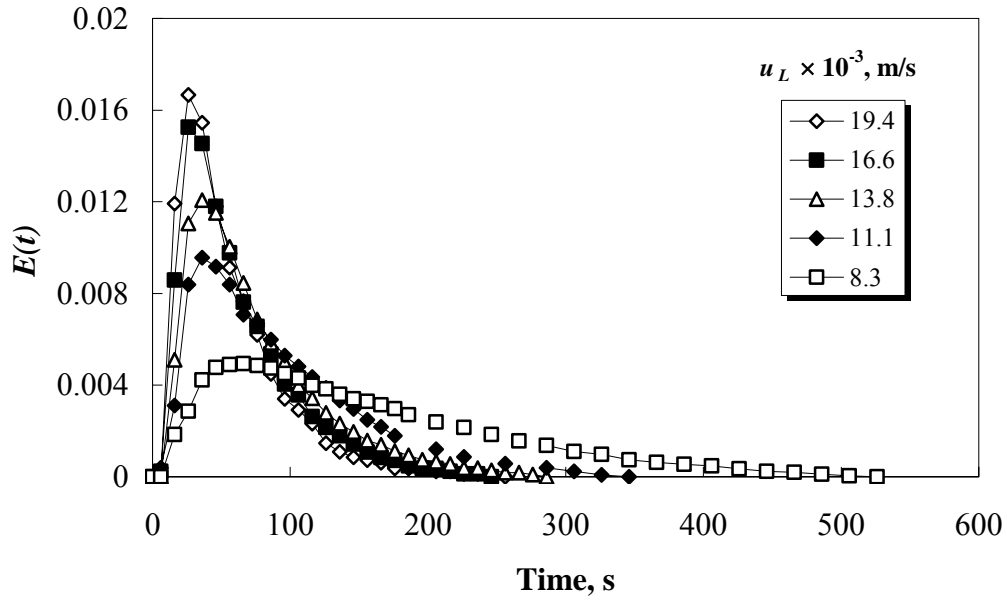


Figure 5. 10. The effect of superficial liquid velocity on the residence time distribution without the catalyst particles ( $u_G=5.5\times 10^{-3}$  m/s), Conditions: Tracer = *RBBR*, tracer concentration = 4 mg/L,  $T = 20.3^\circ\text{C}$ .

Table 5.5. Calculated results from the data. Conditions: Tracer = *RBBR*, tracer concentration = 4 mg/L,  $T = 20.3^\circ\text{C}$ .

$u_L \times 10^3$ , m/s ( $Q_L$ , L/h)	$u_G \times 10^3$ , m/s ( $Q_G$ , L/h)	$Q_G/Q_L$	$t_m$ , s	$\sigma^2/t_m^2$	$Pe_L$	$D_L \times 10^3$ , $\text{m}^2/\text{s}$	$N_{CSTRs}$
1.7 (30)	2.5 (45)	1.5	617.8	0.683	1.27	1.07	1.5
	3.9 (70)	2.3	687.4	0.747	0.94	1.45	1.3
	5.5 (100)	3.3	682.6	0.824	0.61	2.23	1.2
	7.0 (125)	4.2	550.0	0.871	0.43	3.16	1.1
	8.3 (150)	3.0	642.2	0.913	0.28	4.86	1.1
6.1 (110)	5.5 (100)	0.9	188.1	0.52	2.35	2.08	1.9
8.3 (150)	3.9 (70)	0.40	148.5	0.32	5.01	1.33	3.1
	5.5 (100)	0.66	146.2	0.500	2.56	2.59	2.0
	8.3 (150)	1.00	150.9	0.511	2.46	2.70	2.0
11.1 (200)	3.9 (70)	0.30	87.8	0.363	4.23	2.10	2.8
	5.5 (100)	0.50	93.3	0.450	3.06	2.90	2.2
	8.3 (150)	0.75	91.0	0.523	2.36	3.76	1.9
13.8 (250)	3.9 (70)	0.24	81.5	0.421	3.99	2.77	2.4
	5.5 (100)	0.40	73.3	0.440	3.17	3.48	2.3
	8.3 (150)	0.60	71.7	0.539	2.22	4.97	1.9
16.6 (300)	3.9 (70)	0.20	61.0	0.480	3.73	3.56	2.1
	5.5 (100)	0.33	61.7	0.441	3.17	4.19	2.3
	8.3 (150)	0.50	65.3	0.545	2.18	6.17	1.8
19.4 (350)	3.9 (70)	0.17	55.0	0.413	3.51	4.42	2.4
	5.5 (100)	0.28	55.9	0.485	2.70	5.75	2.1
	8.3 (150)	0.43	51.7	0.552	2.12	7.32	1.8

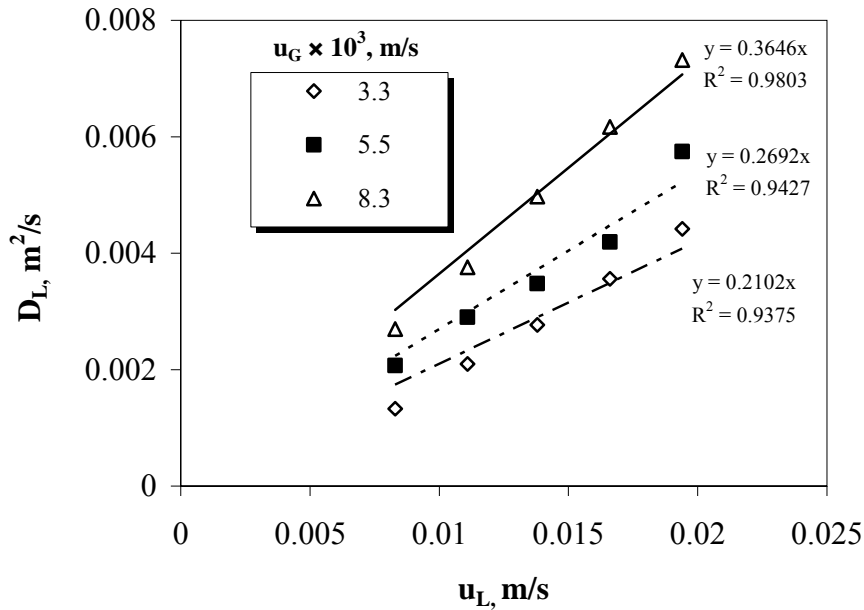


Figure 5.11. Effect of superficial liquid velocity on axial dispersion coefficient,  $D_L$  in the gas-liquid system. Conditions: Tracer = *RBBR*, tracer concentration = 4 mg/L,  $T = 20.3^\circ\text{C}$ .

### 5.2.2 Distribution behavior in the presence of the catalyst

The liquid phase mixing was investigated in the presence of catalyst particles in order to compare the gas-liquid and gas-liquid-solid systems in terms of  $D_L$  and  $Pe_L$ . The typical RTD curves at different liquid velocities are shown in Figure 5.12. By the increase of liquid velocity, the tracer tended to exit more quickly from the reactor exhibiting a better mixing compared to the lower liquid velocity conditions. At different gas and liquid velocities, the results of the RTD experiments were obtained (Table 5.6)

The value of  $D_L$  was found to be higher at the higher gas and liquid velocities because of the enhanced mixing with the flow. In addition, more turbulence was created in the reactor with the catalyst particles resulting better liquid mixing and this resulted in higher  $D_L$  values compared to those in the gas-liquid system. The calculated  $N_{CSTRs}$  was close to two especially at the low liquid velocities ( $u_L = 8.3 \times 10^{-3}$  to  $13.8 \times 10^{-3}$  m/s). At the higher velocities, the behaviour was closer to one CSTR. For the gas-liquid-solid reactor,  $N_{CSTRs}$  was around 1.4 and 2.0. This meant that at higher gas and liquid velocities, the reactor could be modeled as according to the one CSTR equation.

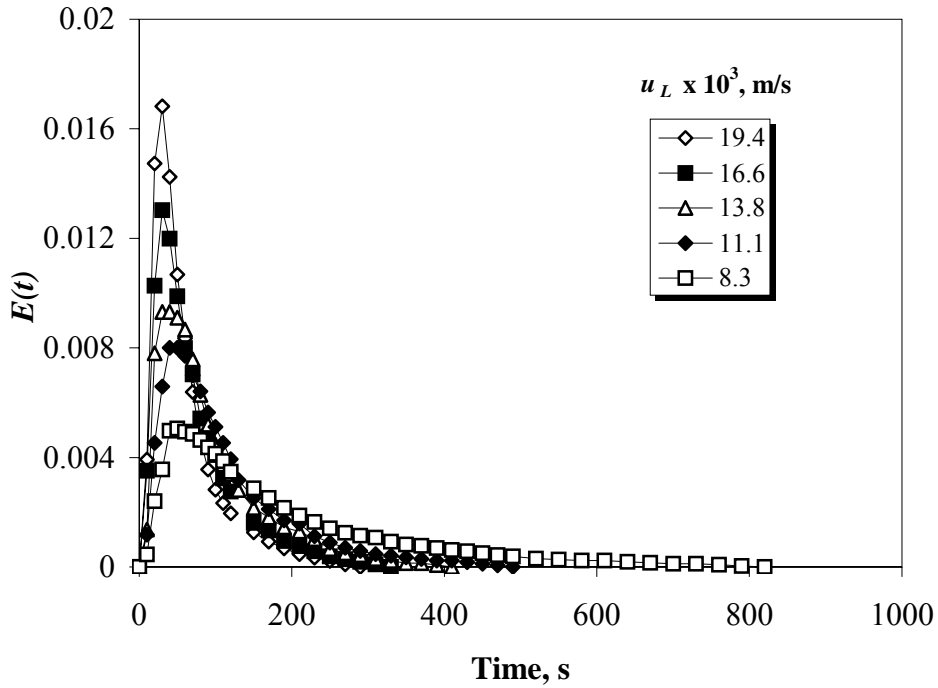


Figure 5.12. The effect of superficial liquid velocity on the residence time distribution with the catalyst particles ( $u_G=5.5\times 10^{-3}$  m/s). Conditions: Tracer = *RBBR*, tracer concentration = 4 mg/L,  $T = 20.3^\circ\text{C}$ .

Table 5.6. Calculated results from the residence time distribution data. Conditions: Tracer = *RBBR*, tracer concentration = 4 mg/L,  $T = 20.3^\circ\text{C}$ .

$u_L \times 10^3$ , m/s ( $Q_L$ , L/h)	$u_G \times 10^3$ , m/s ( $Q_G$ , L/h)	$Q_G/Q_L$	$t_m$ , s	$\sigma^2/t_m^2$	$Pe_L$	$D_L \times 10^3$ , m <sup>2</sup> /s	$N_{CSTRs}$
8.3 (150)	5.5 (100)	0.66	185.1	0.497	2.58	2.57	2.0
	8.3 (150)	1.00	196.2	0.553	2.11	3.15	1.8
	11.1 (200)	1.34	200.2	0.579	1.92	3.46	1.7
11.1 (200)	5.5 (100)	0.50	112.3	0.538	2.23	3.98	1.9
	8.3 (150)	0.75	116.6	0.570	1.98	4.48	1.8
	11.1 (200)	1.00	112.0	0.588	1.85	4.80	1.7
13.8 (250)	5.5 (100)	0.40	93.3	0.562	2.05	5.39	1.8
	8.3 (150)	0.60	91.5	0.610	1.71	6.46	1.6
	11.1 (200)	0.80	82.9	0.622	1.63	6.77	1.6
16.6 (300)	5.5 (100)	0.33	74.0	0.576	1.94	6.85	1.7
	8.3 (150)	0.50	67.4	0.629	1.59	8.35	1.6
	11.1 (200)	0.67	78.1	0.650	1.46	9.10	1.5
19.4 (350)	5.5 (100)	0.28	61.1	0.583	1.89	8.21	1.7
	8.3 (150)	0.43	63.2	0.674	1.32	11.76	1.4
	11.1 (200)	0.57	64.0	0.722	1.07	14.50	1.4

The relationship between the liquid velocity and the axial dispersion coefficient is shown in Figure 5.13. At the lowest gas velocity ( $u_G = 5.5 \times 10^{-3}$  m/s), axial dispersion coefficient changed linearly with the liquid velocity similar to the case of two phase system. However, at the higher liquid velocities, the relationship between  $D_L$  and  $u_L$  was exponential as seen in Figure 5.13, and the rapid increase of the dispersion coefficient with the liquid velocity showed that the presence of solids increased the mixing in the system and yielded efficient fluidization of catalyst particles.

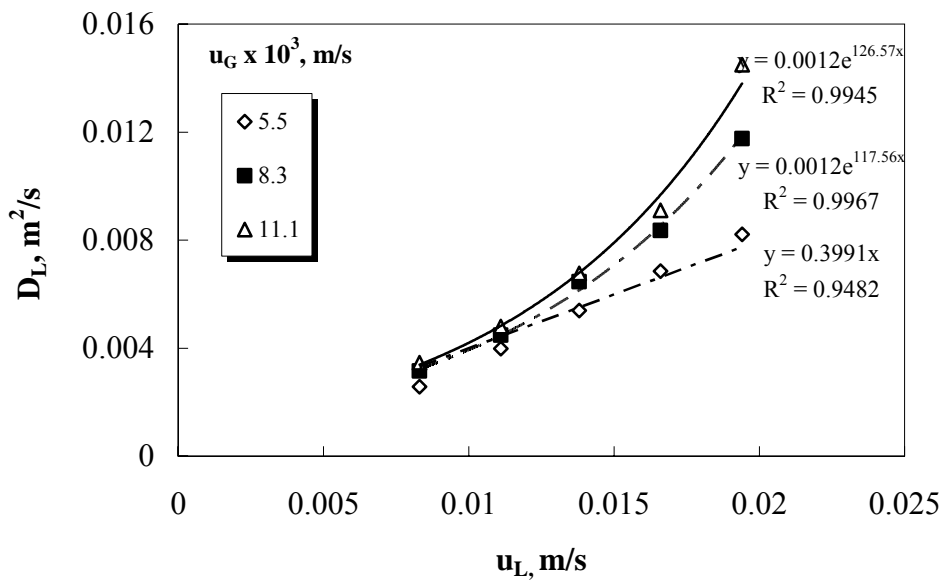


Figure 5.13. Effect of superficial liquid velocity on axial dispersion coefficient,  $D_L$  in the gas-liquid-solid system. Conditions: Tracer = *RBBR*, tracer concentration = 4 mg/L,  $T = 20.3^\circ\text{C}$ .

### 5.3 Reactor hydrodynamics

In the three phase reactor, solid particles are fluidized with the co-current flow of gas and liquid phases. The determination of main hydrodynamic properties of the reactor is important to realize the performance of the reactor at different operating conditions. Therefore, the hydrodynamic characteristics of the three phase (gas-liquid-solid) reactor

were studied to determine the minimum fluidization velocity ( $u_{L,min}$ ), the hold-up values of gas, liquid and solid phases and the behaviour of gas bubbles.

### 5.3.1 Minimum fluidization velocity in the column

The minimum fluidization velocity is the value superficial water velocity at which the particles begin to fluidize at a constant superficial air velocity. The  $u_{L,min}$  at different gas flow rates were determined in the column filled with catalyst particles. Because of the density difference between alumina and PFOA particles, the  $u_{L,min}$  values at different  $Q_G$  values were measured for both catalyst types separately. As seen in Figures 5.14 and 5.15, the  $u_{L,min}$  decreased as the gas velocity increased. Higher gas velocities enabled the fluidization of particles more giving additional force to fluidize them. The minimum fluidization velocities are given for PFOA catalyst in Table 5.7 at the studied gas flow rates. The pressure drop and minimum fluidization velocity for a given  $u_G$ , were increased in the case of alumina compared to those for PFOA. Higher liquid flow rates were needed to fluidize alumina.

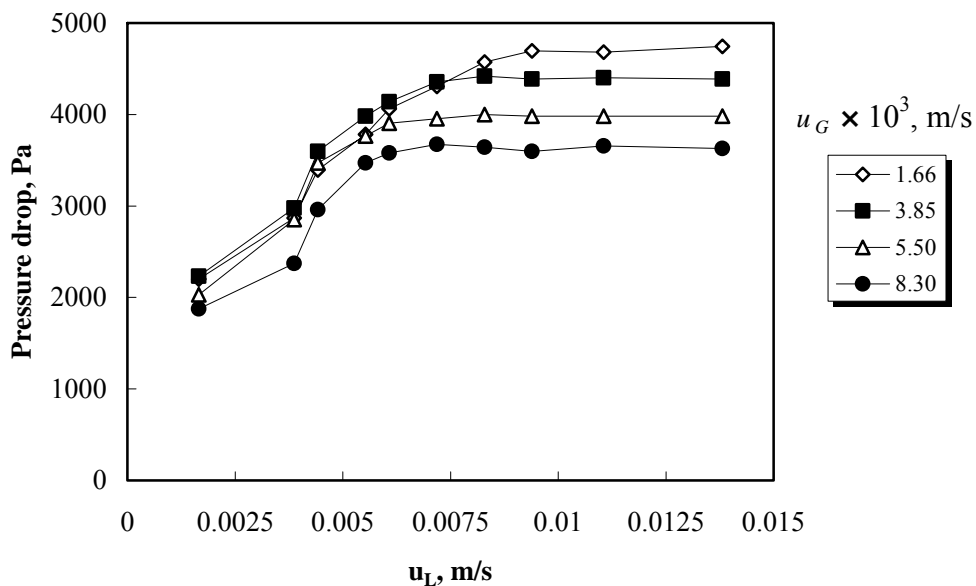


Figure 5.14. Pressure drop versus superficial liquid velocity data for different superficial gas velocities. Catalyst= PFOA,  $m_{cat} = 25$  g,  $d_{cat} = 2.0$  mm.

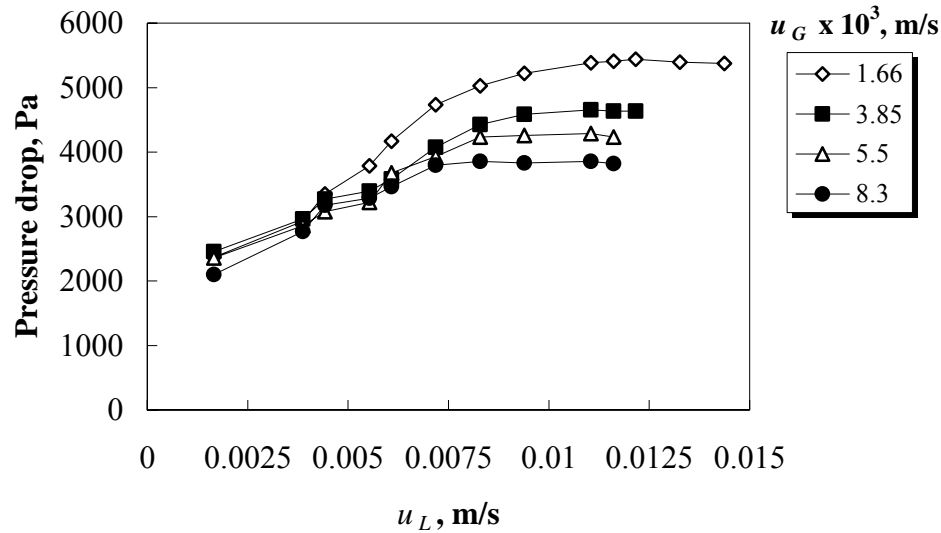


Figure 5.15. Pressure drop versus superficial liquid velocity data for different superficial gas velocities. Catalyst = alumina,  $m_{cat} = 25$  g,  $d_{cat} = 2.0$  mm.

As seen in Table 5.7, the  $u_{L,min}$  at  $Q_G = 150$  L/h was found at around  $6.1 \times 10^{-3}$  m/s ( $Q_L = 110$  L/h). At the same  $Q_G$ , the  $u_{L,min}$  for alumina was around  $7.2 \times 10^{-3}$  m/s ( $Q_L = 130$  L/h). At lower liquid velocities than the  $u_{L,min}$  at a constant  $Q_G$ , it was certain that the bed behaved like a packed bed. Contrarily, at higher liquid velocities, the reactor could be accepted as a fluidized bed reactor and the better fluidization occurred at the higher liquid velocities.

Table 5.7. Minimum fluidization velocities at the studied gas velocities. Catalyst=PFOA,  $m_{cat} = 25$  g,  $d_{cat} = 2.0$  mm.

$u_G \times 10^3$ , m/s ( $Q_G$ , L/h)	$u_{L,min} \times 10^3$ , m/s	$Q_{L,min}$ , L/h
1.66 (30)	9.39	170
3.85 (70)	7.46	135
5.50 (100)	6.90	125
8.83 (150)	6.08	110

Then, the effect of catalyst dosage was investigated on the minimum fluidization velocity. Figures 5.16 and 5.17 present the pressure drop curves at different catalyst dosages for PFOA and alumina, respectively. The effect of catalyst dosage on minimum

fluidization velocity was insignificant. For the studied particle dosages, the liquid velocity to fluidize the particles was the same. That result was also shown in the literature [201]. The forces applied to the particles during fluidization are gravitational force, buoyancy force and drag force. These forces and minimum fluidization velocity are not influenced by the catalyst dosage.

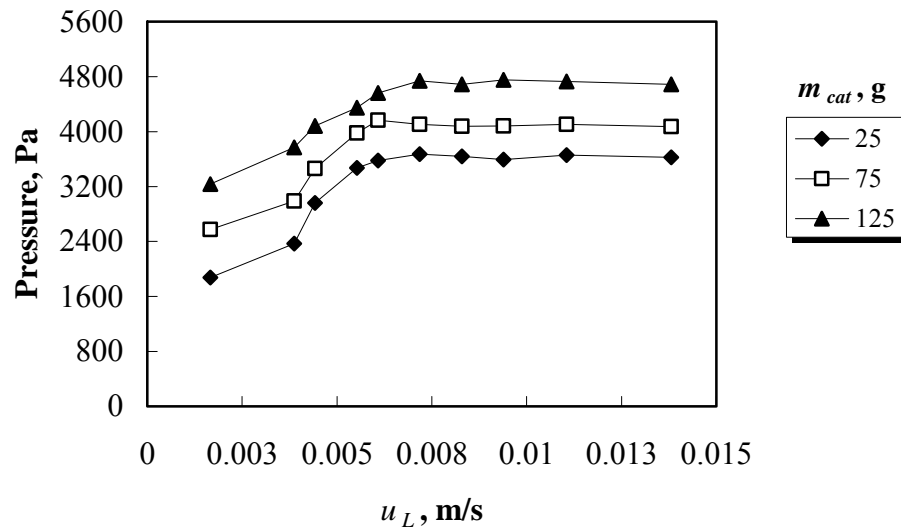


Figure 5.16. Pressure drop versus superficial water velocity data for different catalyst dosages.  $Q_G = 150$  L/h, catalyst = PFOA,  $d_{cat} = 2.0$  mm.

### 5.3.2 Determination of hold-up values for gas, liquid and solid phases

In the column, the gas hold-up was evaluated with the height measurement. The gas, liquid and solid phase hold-up values were obtained for different values of catalyst dosage, gas and liquid flow rates. Table 5.8 presents the hold-up values for the gas-liquid two-phase system. At a constant liquid flow rate, the gas hold-up increased with the increase of gas flow rate. It was observed that the bubble velocity and the number of bubbles per unit reactor volume increased with the increase of  $Q_G$  resulting in higher  $\varepsilon_G$ . Increasing  $Q_L$  decreased  $\varepsilon_G$  significantly. Jena et al. [201] and Safoniuk et al. [210] reported that the liquid flow rate had a minor effect on the change of  $\varepsilon_G$  in two or in three phase reactors. However, in this study the observed effect of  $Q_L$  on  $\varepsilon_G$  was significant.

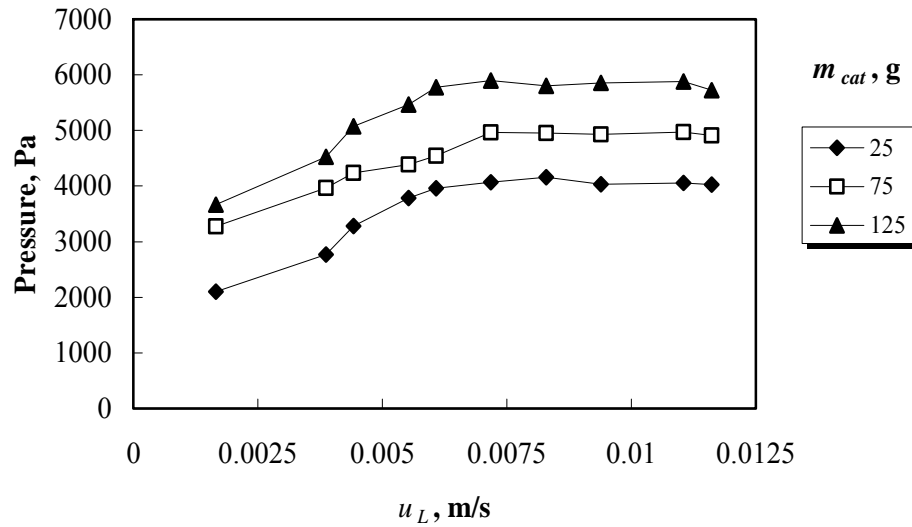


Figure 5.17. Pressure drop versus superficial liquid velocity data for different catalyst dosages.  $Q_G = 150$  L/h, catalyst = alumina,  $d_{cat} = 2.0$  mm.

Table 5.8. The calculated gas and liquid hold-up values for the experiments.  $A = 5.02 \times 10^{-3} \text{ m}^2$ ,  $\rho_{cat}$ : 1300 kg/m<sup>3</sup> for PFOA,  $\rho_{cat}$ : 2580 kg/m<sup>3</sup> for alumina.

$Q_G$ , L/h	$Q_L$ , L/h	$\varepsilon_G$	$\varepsilon_L$
70		0.036	0.964
100	30	0.057	0.943
150		0.073	0.927
70		0.020	0.980
100	150	0.035	0.965
150		0.049	0.951

The effect of catalyst dosage on the hold-up values was investigated in order to evaluate the importance of the particles on holdups. The results obtained at different gas flow rates showed that the solid phase hold-up increased with the increasing catalyst dosage (Table 5.9). However, gas and liquid hold-up values were decreased. That was due to the increase of turbulence with the higher amount of solids in the reactor. The increase of turbulence in the column probably caused the increase of interaction between gas, liquid and solid phases. In the three phase system, increasing  $Q_G$  positively affected the

gas hold-up. The effect of catalyst dosage on  $\varepsilon_G$  was more remarkable at the higher gas flow rates.

Table 5.9 The calculated gas, liquid and solid-phase hold-up values under different operating conditions.

Catalyst	$m_{cat}$ , g	$Q_G$ , L/h	$Q_L$ , L/h	$\varepsilon_G$	$\varepsilon_L$	$\varepsilon_S$
Alumina	25	30	200	0.012	0.887	0.101
	75			0.011	0.867	0.122
	125			0.011	0.862	0.127
PFOA	25			0.012	0.938	0.050
	75			0.011	0.929	0.060
	125			0.011	0.925	0.064
Alumina	25	70	150	0.019	0.880	0.101
	75			0.018	0.860	0.122
	125			0.018	0.855	0.127
PFOA	25			0.020	0.930	0.050
	75			0.017	0.923	0.060
	125			0.016	0.920	0.064
Alumina	25	100	150	0.027	0.872	0.101
	75			0.025	0.853	0.122
	125			0.024	0.849	0.127
PFOA	25			0.029	0.921	0.050
	75			0.027	0.913	0.060
	125			0.025	0.911	0.064
Alumina	25	150	150	0.045	0.851	0.104
	75			0.042	0.836	0.122
	125			0.042	0.832	0.126
PFOA	25			0.047	0.901	0.052
	75			0.045	0.894	0.061
	125			0.043	0.894	0.063

The performance of the two or three phase reactor depends on the flow conditions in the reactor. Zhang et al. [211] reported the flow regimes as schematics and graphs for gas-liquid and gas-liquid-solid systems. According to the graphs by Zhang et al. [211], the flow in the studied two or three phase reactor fitted to the “homogeneous bubbling regime”. At all the studied gas and liquid flow rates, it was observed that the gas phase uniformly flowed through the liquid phase with homogeneous bubbles. The bubble photographs were taken at different conditions during the experiments. These photographs are given in Appendix I.1. The calculations for the approximate bubble

sizes were performed using the definition of mean Sauter diameter [200]. According to the calculations of bubble diameter, it can be said that the size of the bubbles around the distributor was relatively smaller than those in the upper regions. Bubble size was enhanced while the gas flowed upward through the reactor. In the reactor, the coalescence of the bubbles around the distributor was not observed because of the high turbulence around the distributor. However, with the increase of the reactor height, the bubble size was increased due to the bubble coalescence.

The size of the bubbles was higher at the higher gas flow rates due to the increase of the bubble velocity whereas increasing the liquid flow rate decreased the bubble size enabling more turbulence in the column. Higher liquid flow rate ( $Q_L = 150$  L/h) resulted in more uniform bubbles compared to the slug flow of them at a lower  $Q_L$  ( $Q_L = 30$  L/h). At  $Q_L = 30$  L/h, the aggregates of the bubbles appeared especially on the top of the column.

The distribution of particles in the column was uniform while gas and liquid were flowing. At high gas and liquid velocities, a small amount of particles was carried to the top of the column (1 m), but most of them distributed homogeneously in the fluidized bed section.

The increase of gas flow rate increased the expansion of the bed. At the constant liquid flow rate of 150 L/h, the expanded bed height ( $H_E$ ) was 10.3-10.5 cm for  $Q_G=70$  L/h, whereas at a flow rate of  $Q_G=150$  L/h, 13.2-13.5 cm of  $H_E$  was observed. With the static bed height of 7.5 cm, the bed expansion ratios ( $H_E/H_S$ ) for  $Q_G=70$  and 150 L/h, were calculated as 1.39 and 1.79, respectively. This was a good operation range for a three phase fluidized bed compared with the expansion ratios reported in the literature [200,201].

#### **5.4 Ozone absorption experiments in the fluidized bed reactor**

The absorption of ozone in pure water includes the physical mass transfer process of ozone from gas to liquid phase. However during absorption, ozone may be decomposed into some radicals at especially alkaline pH, because of the instability of ozone [44,61]. At acidic pH, the contribution of ozone decomposition to the absorption process is

negligibly small. Therefore, the mass transfer of ozone is generally studied at acidic pH in order to prevent the decomposition of  $O_3$ .

The accurate design and modeling of ozone bubble columns and fluidized beds are based on the accurate determination of gas-liquid mass transfer coefficient,  $k_La$  at the operating conditions. In order to find  $k_La$ , ozone absorption experiments were conducted with and without the catalyst particles (alumina or PFOA). Each experiment required a start-up period of approximately 7.5 min to reach the steady-state concentration of dissolved  $O_3$  in the liquid phase ( $C_{O_3,L}$ ) but the reactor was operated until 20 min after the steady-state, as a total operation period.

#### **5.4.1 Ozonation experiments without particles at different gas and liquid flow rates**

The effect of gas or liquid flow rate on the absorption of ozone was investigated without alumina or PFOA particles in the reactor. Figure 5.18 represents the variation of  $C_{O_3,L}$  with the bed height ( $z$ ) and gas flow rate ( $Q_G$ ) in the column. Since the fluidized bed reactor was operated co-currently by feeding both the gas and liquid phases at the bottom, the steady-state ozone concentration in the liquid phase,  $C_{O_3,L}$ , increased with the increase of the bed height for all the studied conditions. Also, it was clear that steady-state  $C_{O_3,L}$  increased with the increasing gas flow rate (Figure 5.18).

As seen in Figure 5.18, the absorption rate of  $O_3$  up to 0.21 m of column height was high and then  $C_{O_3,L}$  increased almost linearly but with a slower rate by the increase of  $z$ . The concentration of  $O_3$  in the liquid phase increased significantly around the gas distributor. At the higher bed heights, the mass transfer rate of  $O_3$  from gas to liquid phase decreased because of the decreasing concentration driving force ( $\Delta C_{O_3,L}$ ).

The effect of liquid flow rate ( $Q_L$ ) on the  $C_{O_3,L}$  is shown in Figure 5.19. The higher liquid flow rate caused a lower  $C_{O_3,L}$  in the column. The applied gaseous amount of  $O_3$  per liter of liquid was decreased at the higher  $Q_L$ . Also, the contact time between the gas and liquid phases decreased by the increase of  $Q_L$ . Consequently, the time needed for  $O_3$  molecules to transfer from gas to liquid phase was less at the higher  $Q_L$  than that at the lower  $Q_L$  resulting in lower  $O_3$  absorption. The hydraulic retention time of the liquid ( $\tau_L$ ) was smaller at the higher  $Q_L$ , as seen in Table 5.10; as a result, a longer retention time of the liquid phase resulted in the increase of ozone transfer.

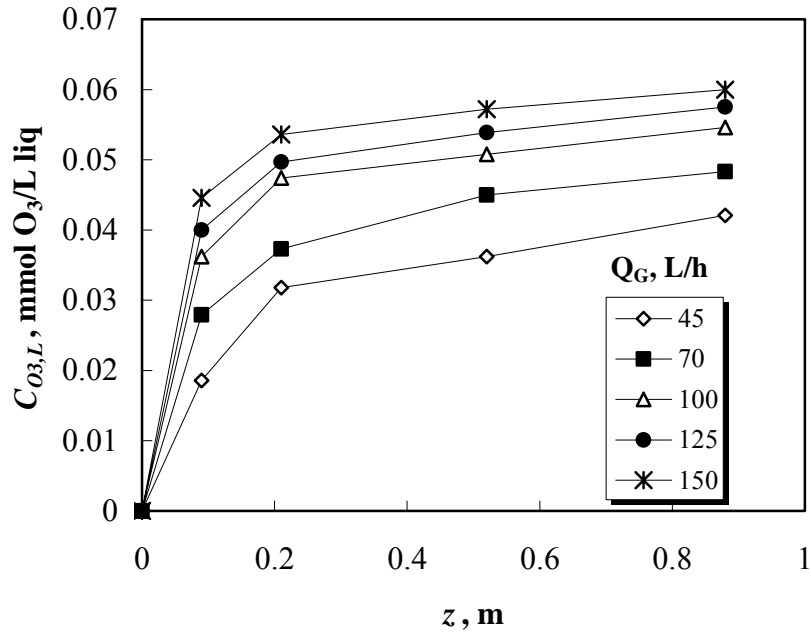


Figure 5.18. Steady-state  $C_{O_3,L}$  at different gas flow rates. Conditions:  $Q_L=30$  L/h,  $T = (22.0 \pm 0.9)^\circ\text{C}$ ,  $C_{O_3,G,in}=(0.306 \pm 0.017)$  mmol  $\text{O}_3/\text{L}$  gas, particles = none.

Table 5.10. Hydraulic retention time of liquid in the reactor at different  $Q_L$ . Effective reactor volume,  $V_{R,eff} = 5.02$  L.

$Q_L$ , L/h	$\tau_L$ , min
30	10.0
70	4.3
150	2.0
200	1.5
250	1.2
300	1.0
350	0.9

The liquid phase ozone concentrations measured in the experiments were used to determine  $D_L$  and  $k_L a$  values according to the model. At most conditions, the model predictions for  $C_{O_3,L}$  fitted well to those obtained experimentally for modified  $D_L$  and predicted  $k_L a$ . Figure 5.20 shows the comparison of experimental and theoretical liquid phase ozone concentrations at  $Q_G=150$  L/h and  $Q_L=30$  L/h. The model predicted gas phase ozone concentrations,  $C_{O_3,G,out}$ , as a function of column height. Since it was hard

to collect gaseous samples at different bed heights experimentally, only the predicted  $C_{O_3,G,out}$  values were compared with the experimental  $C_{O_3,G,out}$  values. The model and experimental  $C_{O_3,G,out}$  results were close to each other within an error margin between 1% and 22%, as shown in Table 5.11. As expected,  $C_{O_3,G,out}$  decreased by the increase of the column height.

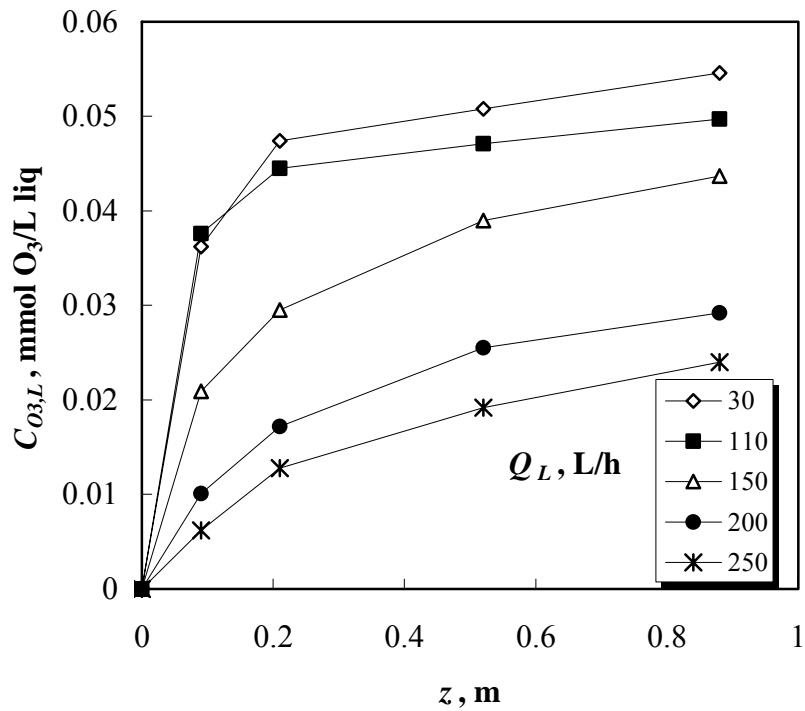


Figure 5.19.  $C_{O_3,L}$  at different liquid flow rates. Conditions:  $Q_G=100$  L/h,  $T=(22.0 \pm 0.9)^\circ\text{C}$ ,  $C_{O_3,G,in}=(0.306 \pm 0.017)$  mmol  $\text{O}_3/\text{L}$  gas, particles = none.

Generally the model predicted higher gas phase ozone concentrations than those of the experimentally obtained ones. In the model, ozone decomposition reaction term was neglected since the absorption experiments were conducted at acidic pH. The lower gas phase ozone concentrations might result from the minor amount of ozone decomposition.

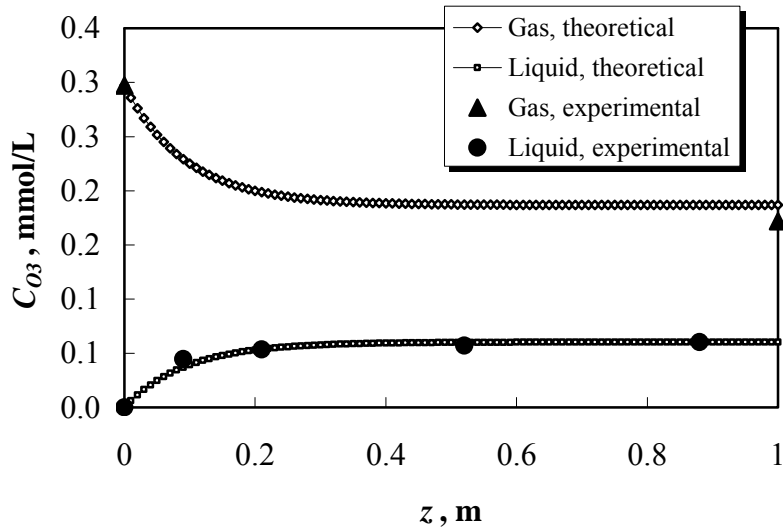


Figure 5.20. The comparison of theoretical and experimental steady state liquid phase ozone concentrations for the best fit of  $D_L$  and  $k_L a$  values. Conditions:  $Q_G = 150$  L/h,  $Q_L = 30$  L/h,  $T = 23^\circ\text{C}$ ,  $C_{O_3,G,in} = 0.298$  mmol  $\text{O}_3/\text{L}$  gas, catalyst = no,  $D_L = 1.2 \times 10^{-3}$   $\text{m}^2/\text{s}$ ,  $k_L a = 9.6 \times 10^{-2}$   $\text{s}^{-1}$ .

Table 5.11. Experimental and theoretical outlet gas  $\text{O}_3$  concentrations at different gas and liquid flow rates. Conditions:  $T = (22.0 \pm 0.9)^\circ\text{C}$ ,  $C_{O_3,G,in} = (0.306 \pm 0.017)$  mmol  $\text{O}_3/\text{L}$  gas, catalyst = none.

$Q_G$ , L/h	$Q_L$ , L/h	$C_{O_3,G,out}$ , mmol $\text{O}_3/\text{L}$ gas, theoretical	$C_{O_3,G,out}$ , mmol $\text{O}_3/\text{L}$ gas, experimental	Error, %
100	30	0.170	0.219	22.3
100	110	0.154	0.190	18.9
100	150	0.136	0.137	0.7
100	200	0.095	0.099	4.0
100	250	0.076	0.067	13.4
45	30	0.119	0.104	14.4
70	30	0.135	0.162	16.7
70	80	0.137	0.124	10.5
70	110	0.130	0.145	10.3
70	150	0.129	0.121	6.6
70	200	0.125	0.103	21.3
125	30	0.179	0.155	15.5
150	30	0.187	0.172	8.7
70	250	0.127	0.153	17.0

From the predicted  $k_La$  values, it can be revealed that ozone mass transfer was mainly dependent on the gas flow rate (Table 5.12). Increasing  $Q_G$  resulted in higher  $k_La$  values since smaller bubbles were produced at the higher  $Q_G$ , enhancing the surface area,  $a$ . In literature, the strong dependence of  $a$  on the gas velocity was reported [212,213]. However, the value of  $k_La$  was not affected by the liquid flow rate, considerably. The dependency of  $k_La$  on the gas velocity was investigated at  $Q_L=30$  L/h by drawing  $\ln(k_La)$  versus  $\ln(u_G)$  graph as shown in Figure 5.21. Equation (5.1), relating the  $k_La$  of the gas-liquid reactor and  $u_G$  was found. At  $Q_L=30$  L/h, the Reynolds number ( $Re_L = \frac{u_L d_{cat} \rho_L}{\mu_L}$ ) was 7266.

$$k_La = 0.544 \times (u_G)^{0.666} \quad (5.1)$$

Here,  $k_La$  is in the unit of  $\text{min}^{-1}$  and  $u_G$  is in the unit of  $\text{m h}^{-1}$ . The equation was compared with the equation found by Roustan et al. [212]. They found a similar relationship between  $k_La$  and  $u_G$  in the same units in a bubble column as shown in Equation (5.2).

$$k_La = 0.110 \times (u_G)^{0.615} \quad (5.2)$$

Table 5.12.  $D_L$  and  $k_La$  values predicted at different gas and liquid flow rates. Conditions:  $T = (22.0 \pm 0.9)^\circ\text{C}$ ,  $C_{O_3,G,in} = (0.306 \pm 0.017)$  mmol  $\text{O}_3/\text{L}$  gas, catalyst = none.

$Q_G$ , L/h	$Q_L$ , L/h	$Q_G/Q_L$	$D_L \times 10^3$ , $\text{m}^2/\text{s}$	$k_La \times 10^2$ , $\text{s}^{-1}$
100	30	3.33	1.3	6.4
100	110	0.91	1.8	5.0
100	150	0.67	2.0	4.9
100	200	0.50	6.1	5.0
100	250	0.40	9.2	4.9
45	30	1.50	3.1	4.2
70	30	2.33	3.6	4.8
70	80	0.88	4.0	3.7
70	110	0.64	4.5	3.3
70	150	0.47	5.2	2.6
70	200	0.35	5.9	2.1
125	30	4.17	1.5	7.3
150	30	5.00	1.2	9.6
70	250	0.28	6.5	1.4

Equation (5.2) was applicable for the turbulent flow of  $Re_L$  between 1912 and 2985. The difference between the constants of Equation (5.1) and (5.2) was probably due to the higher turbulence created in the studied column at  $Q_L=30$  L/h.

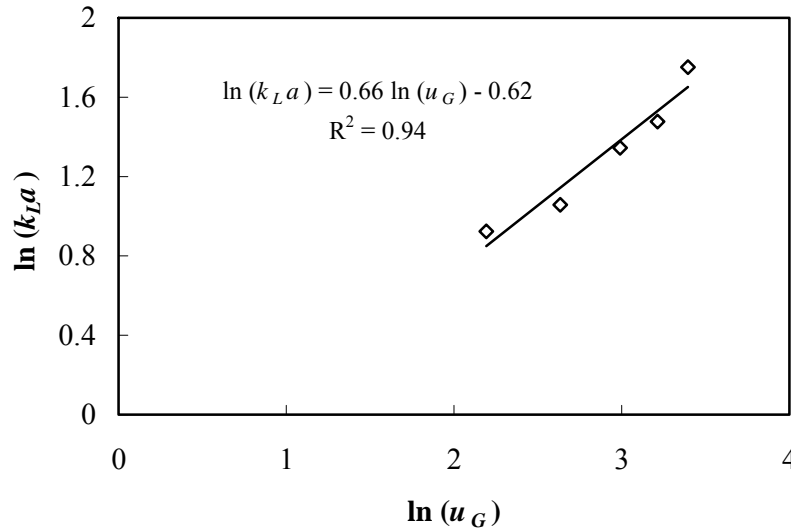


Figure 5.21. The relationship between  $k_{La}$  and  $u_G$  at  $Q_L=30$  L/h in the gas ( $O_3$ )-liquid (water) system.

#### 5.4.2 Ozonation experiments with particles at different catalyst dosages

Generally, the presence of the particles in a gas-liquid reactor enhances gas-liquid mass transfer [212]. Therefore, dissolved ozone concentrations are higher in the reactor. The effect of catalyst addition was investigated by conducting some experiments in the presence of alumina or PFOA particles at different catalyst dosages. Then,  $k_{La}$  values were found at every condition by comparing the model and experimental  $C_{O_3,L}$  results. Figure 5.22 shows the model-predicted gaseous ozone concentrations and the model-predicted and experimental liquid phase ozone concentrations for the condition  $Q_G=150$  L/h,  $Q_L=30$  L/h, catalyst =alumina and  $m_{cat}=25$  g.

Model-predicted and experimental  $C_{O_3,L}$  results fitted well to each other at most conditions for the determined  $k_{La}$  values. As seen in Table 5.13, although the increase of catalyst dosage resulted in a small increase of  $k_{La}$ , the presence of the particles in the

column affected the  $k_L a$  value insignificantly. The operating conditions of the fluidized bed affected the efficiency of the catalyst on  $k_L a$ . Most probably, at the studied conditions of  $Q_G=150$  L/h and  $Q_L=30$  L/h, the column was operated in the unfluidized condition; the enhancement of  $k_L a$  by the catalyst was not observed.

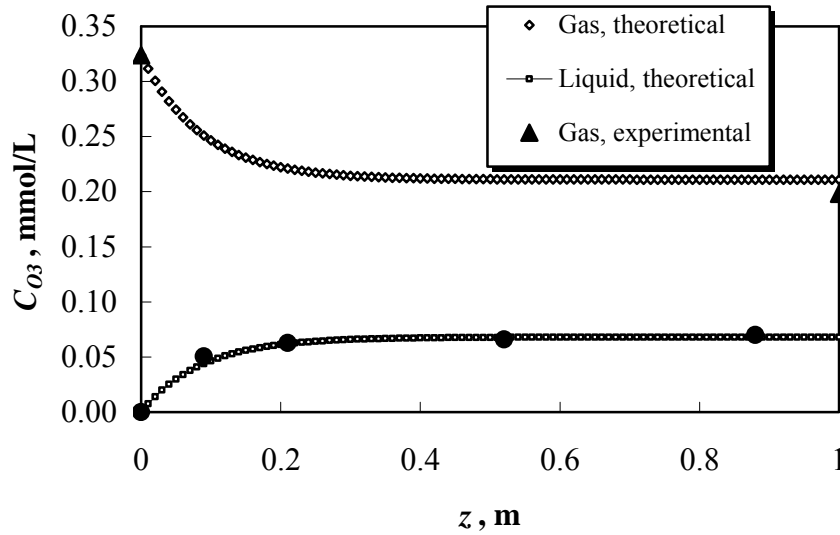


Fig. 5.22. The comparison of theoretical and experimental steady state liquid phase ozone concentrations for the best fit of  $D_L$  and  $k_L a$  values. Conditions:  $Q_G = 150$  L/h,  $Q_L = 30$  L/h,  $T = 23^\circ\text{C}$ ,  $C_{O_3,G,in} = 0.298$  mmol  $\text{O}_3/\text{L}$  gas, Catalyst=Alumina,  $m_{cat}=25$  g,  $D_L = 0.98 \times 10^{-3}$   $\text{m}^2/\text{s}$ ,  $k_L a = 9.8 \times 10^{-2}$   $\text{s}^{-1}$ .

Table 5.13.  $D_L$  and  $k_L a$  values for different catalyst loadings. Conditions:  $Q_G = 150$  L/h,  $Q_L = 30$  L/h,  $T = (22.0 \pm 0.9)^\circ\text{C}$ ,  $C_{O_3,G,in} = (0.306 \pm 0.017)$  mmol  $\text{O}_3/\text{L}$  gas, no dye in the medium, un-fluidized bed,  $u_{L,min} = 130$  L/h for alumina,  $u_{L,min} = 110$  L/h for PFOA.

Catalyst $m_{cat}, \text{g}$	Alumina		PFOA	
	$D_L \times 10^3, \text{m}^2/\text{s}$	$k_L a \times 10^2, \text{s}^{-1}$	$D_L \times 10^3, \text{m}^2/\text{s}$	$k_L a \times 10^2, \text{s}^{-1}$
0.0	1.20	9.6	1.20	9.6
25.0	0.98	9.8	1.20	9.8
35.0	0.99	9.8	1.00	10.0
50.0	0.99	9.85	1.20	9.98
75.0	1.02	10.2	1.27	11.0
100.0	1.03	9.9	1.32	10.7
125.0	1.13	9.9	1.35	10.5
150.0	1.21	9.83	1.15	9.96
175.0	1.25	9.78	1.25	9.84

Afterwards, the effect of catalyst dosage ( $m_{cat}$ ) on the ozone absorption was studied at the fluidized condition of  $Q_G=150$  L/h ( $u_G=8.33\times 10^{-3}$  m/s) and  $Q_L=150$  L/h ( $u_L=8.33\times 10^{-3}$  m/s). The calculated  $k_La$  values for each condition are given in Table 5.14. It was observed that the dissolved ozone concentration was increased by the increase of catalyst dosage at every column height for both alumina and PFOA (Figures 5.23 and 5.24).

Table 5.14.  $D_L$  and  $k_La$  values for different catalyst dosages. Conditions:  $Q_G = 150$  L/h,  $Q_L = 150$  L/h, pH = 2.5,  $T = (22.0 \pm 0.9)^\circ\text{C}$ ,  $C_{O_3,G,in} = (0.90 \pm 0.029)$  mmol  $\text{O}_3/\text{L}$  gas, no dye in the medium,  $d_{cat} = 2.0$  mm, fluidized bed,  $u_{L,min} = 130$  L/h for alumina,  $u_{L,min} = 110$  L/h for PFOA,  $H_E = 13.4$  cm,  $H_S = 7.5$  cm.

Catalyst $m_{cat}, \text{g}$	Alumina		PFOA	
	$D_L \times 10^3, \text{m}^2/\text{s}$	$k_La \times 10^2, \text{s}^{-1}$	$D_L \times 10^3, \text{m}^2/\text{s}$	$k_La \times 10^2, \text{s}^{-1}$
0.0	2.70	6.7	2.70	6.7
25.0	2.92	7.3	2.92	7.6
75.0	3.21	8.9	3.21	8.4
125.0	3.57	10.2	3.57	10.6

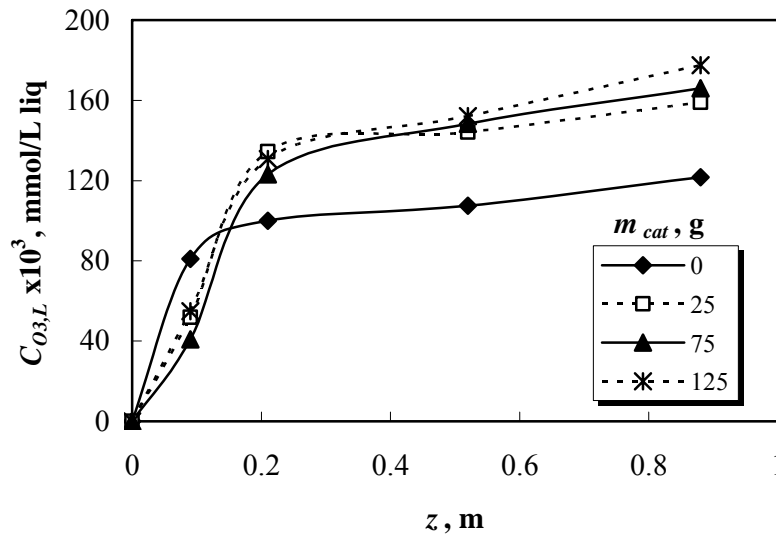


Figure 5.23. Dissolved ozone concentration curves for different catalyst dosages in the column.  $Q_G = 150$  L/h,  $Q_L = 150$  L/h, catalyst = alumina, pH = 2.5,  $T = (22.0 \pm 0.9)^\circ\text{C}$ ,  $C_{O_3,G,in} = (0.90 \pm 0.029)$  mmol  $\text{O}_3/\text{L}$  gas, no dye in the medium,  $d_{cat} = 2.0$  mm.

The effect of particles on  $k_{La}$  values was more significant at the fluidized condition of the column due to the increase in turbulence. In fluidized bed column,  $k_{La}$  increased with the increase of catalyst dosage for alumina and PFOA particles. At 125 g of particles, alumina and PFOA increased  $k_{La}$  1.52 and 1.58 times, respectively. Therefore, it can be concluded that the fluidization conditions had an important effect on the enhancement of  $k_{La}$  in the fluidized bed column.

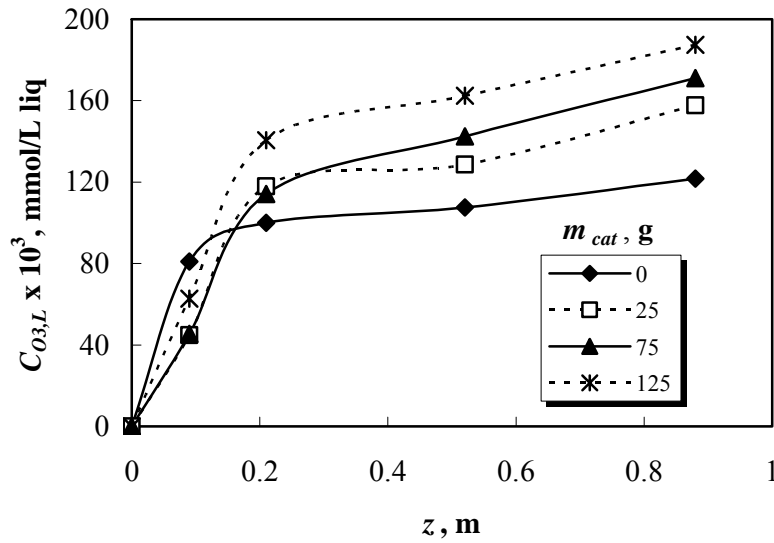


Figure 5.24. Dissolved ozone concentration curves for different catalyst dosages in the column.  $Q_G = 150$  L/h,  $Q_L = 150$  L/h, catalyst = PFOA, pH = 2.5,  $T = (22.0 \pm 0.9)^\circ\text{C}$ ,  $C_{O_3,G,in} = (0.90 \pm 0.029)$  mmol  $\text{O}_3/\text{L}$  gas, no dye in the medium,  $d_{cat} = 2.0$  mm.

## 5.5 Dye ozonation experiments in the fluidized bed reactor

The experiments performed for the ozonation of *RBBR* and *AR-151* solutions in the bed can be classified as ozonation experiments in the gas-liquid system and catalytic ozonation experiments with alumina or PFOA particles. In the sole ozonation experiments inlet dye concentration ( $C_{D,in}$ ), gas flow rate ( $Q_G$ ), liquid flow rate ( $Q_L$ ), inlet gas phase  $\text{O}_3$  concentration ( $C_{O_3,G,in}$ ) and  $Q_G/Q_L$  ratio were the main studied parameters. In catalytic ozonation experiments however, the effects of  $C_{D,in}$ ,  $Q_L$ ,  $C_{O_3,G,in}$ , catalyst dosage ( $m_{cat}$ ), catalyst particle size ( $d_{cat}$ ) and pH were investigated.

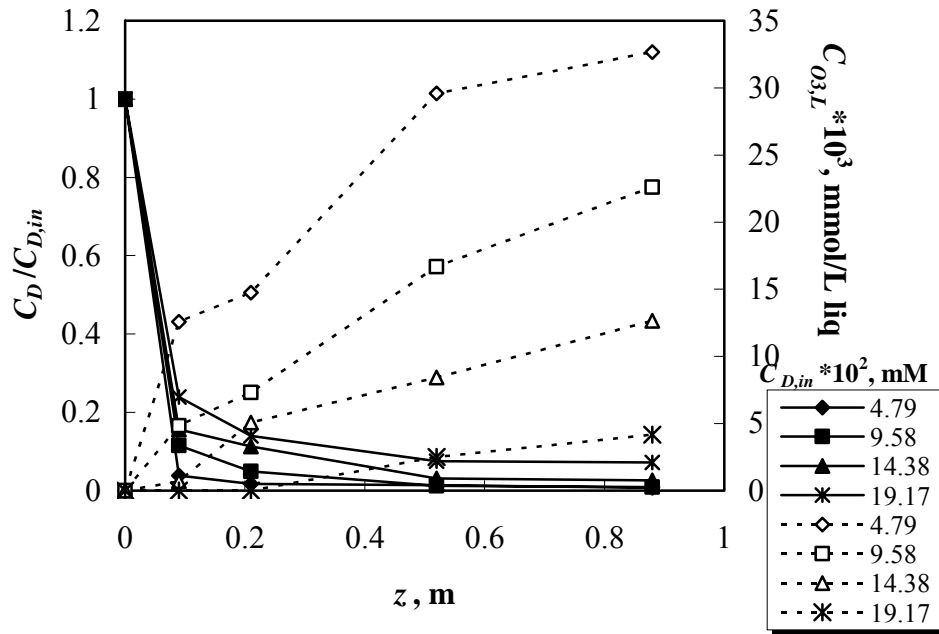
### 5.5.1 Ozonation experiments

Aqueous solutions of *AR-151* and *RBBR* dyes were ozonated to determine the dye, TOC removal values and ozone consumption during the continuous operation in the FBR.

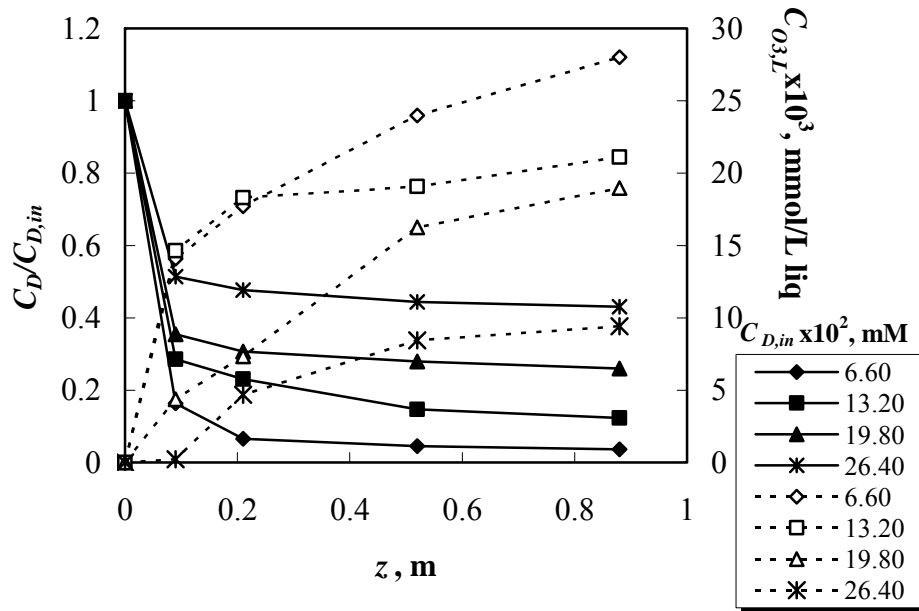
#### 5.5.1.1 Effects of gas and liquid flow rates and inlet dye concentration on ozonation efficiency of *AR-151* or *RBBR* dye without catalyst

Inlet dye concentration is an important parameter in order to evaluate the efficiency of ozonation process in terms of dye and TOC removals and ozone consumption per liter of liquid. Higher amount of dye consumes more ozone and certainly ozonation by-products are in higher amounts in the reaction medium. Therefore, the inlet dye concentration was selected as a predominant factor affecting the ozonation of the dyes.

The dye solutions at different inlet dye concentrations ( $C_{D,in}$ ) were ozonated in the fluidized column reactor operating without catalyst particles. The dye and  $O_3$  concentrations in the liquid phase were determined along the column at steady state. Dye concentration decreased with the increase of the column height for *RBBR* and *AR-151* dyes (Figures 5.25 and 5.26). Since both the dye solution and gaseous  $O_3$  were fed to the reactor at the bottom, ozone started to oxidize the dye molecules just at the top of the gas distributor and the degradation of the dye molecules continued with the increase of the column height. The rate of dye removal was significantly high at initial heights around the distributor (from reactor entrance to 0.21 m of the column) showing that the dye removal mainly occurred within the gas distributor. Then, the dye concentration decreased slowly. At the operating conditions of the gas-liquid reactor ( $Q_G = 150$  L/h and  $Q_L = 30$  L/h in Figure 5.25 or  $Q_G = 70$  L/h and  $Q_L = 30$  L/h in Figure 5.26), the reactor can be modeled as very close to one CSTR as represented in Table 5.5 indicating well mixing of the liquid within the reactor.

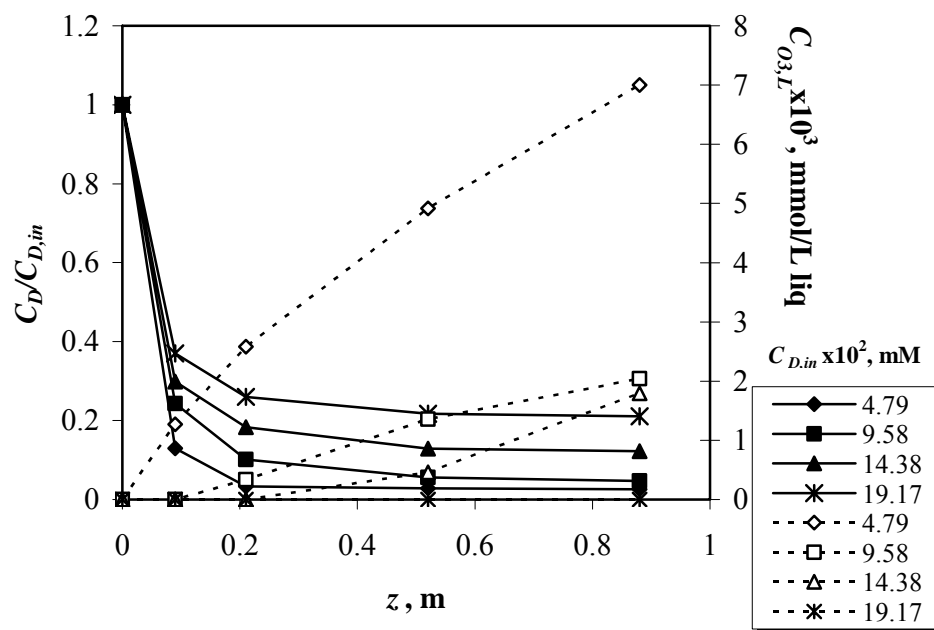


(a)

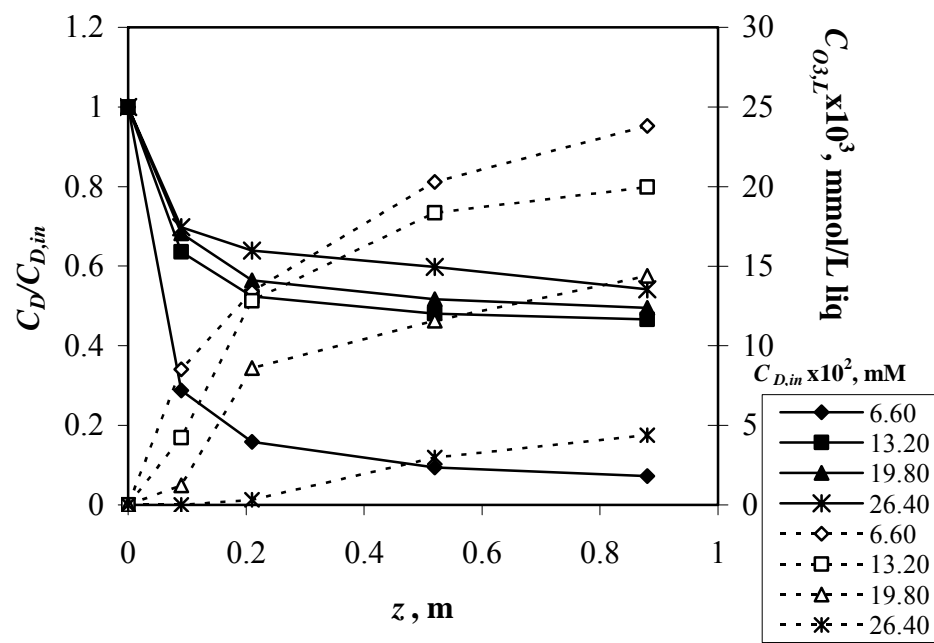


(b)

Figure 5. 25.  $C_D/C_{D,in}$  and  $C_{O_{3,L}}$  at different  $C_{D,in}$ . Conditions:  $Q_G = 150$  L/h,  $Q_L = 30$  L/h, pH = 2.54,  $T = 22.3^\circ\text{C}$ ,  $C_{O_{3,G,in}} = 0.306 \pm 0.017$  mmol  $\text{O}_3/\text{L}$  gas, no catalyst. Solid lines:  $C_D/C_{D,in}$ , dashed lines:  $C_{O_{3,L}}$ , (a): *RBBR*, (b): *AR-151*.



(a)



(b)

Figure 5. 26.  $C_D/C_{D,in}$  and  $C_{O_3,L}$  at different  $C_{D,in}$ . Conditions:  $Q_G = 70$  L/h,  $Q_L = 30$  L/h, pH = 2.54,  $T = 22.3^\circ\text{C}$ ,  $C_{O_3,G,in} = 0.306 \pm 0.017$  mmol  $\text{O}_3$ / L gas, no catalyst. Solid lines:  $C_D/C_{D,in}$ , dashed lines:  $C_{O_3,L}$ , (a): RBBR, (b): AR-151.

Ozone concentration in the liquid phase ( $C_{O_3,L}$ ) increased with the column height due to greater absorption of  $O_3$  molecules in liquid, while the reaction between the dye and  $O_3$  was taking place. The consumption of  $O_3$  in the liquid phase during the reaction resulted in the increase of the driving force for  $O_3$  mass transfer. Therefore, it can be revealed that the mass transfer of  $O_3$  was enhanced by the presence of the chemical reaction. However, the  $C_{O_3,L}$  values were much smaller in the dye ozonation experiments compared to those in the  $O_3$  absorption experiments because of the consumption of  $O_3$  in the reaction.

By the increase of  $C_{D,in}$ , the dye and TOC removals were decreased. The obtained percent dye removals for *AR-151* were much smaller than those of *RBBR*. It seemed that the change of  $C_{D,in}$  had a more significant effect on the ozonation of *AR-151* (Figure 5.25-b).

The gas flow rate could be an important parameter in ozonation of organics since applied  $O_3$  amount was increased with the gas flow rate keeping ozone dosage in the gas,  $C_{O_3,G,in}$  constant. Also, it was important for the reactor hydrodynamics by giving higher turbulence to the contents of the reactor. Hence, the effect of  $Q_G$  for constant  $C_{O_3,G,in}$  and constant  $Q_L$  was investigated for different  $C_{D,in}$  of *RBBR* and *AR-151*, separately. Figure 5.26 shows the dye removal and  $C_{O_3,L}$  at  $Q_G = 70$  L/h and  $Q_L = 30$  L/h. The dye concentrations in the column at these conditions (Figure 5.26) were remarkably higher than those obtained at the conditions of  $Q_G = 150$  L/h and  $Q_L = 30$  L/h (Figure 5.25) for especially *AR-151*. The  $C_{O_3,L}$  values at the lower  $Q_G$  decreased also. The drastic effect of  $Q_G$  on the dye removal was observed especially at high  $C_{D,in}$  ( $19.2 \times 10^{-2}$  mmol/L for *RBBR* and  $26.4 \times 10^{-2}$  mmol/L for *AR-151*) as seen in Figure 5.27.

It was shown that the change of  $Q_G$  was important on the TOC removal for both of the dyes since a dramatic decrease of the TOC removal percentage by decreasing  $Q_G$  was observed (Figure 5.27). In this case, it was better to define a parameter ‘‘Applied  $O_3$  dose’’ ( $Appl_{O_3}$ ) to represent the amount of  $O_3$  spent from the gas phase per liter of liquid. This parameter is calculated by Equation (5.3):

$$Appl_{O_3} = C_{O_3,G,in} \times \frac{Q_G}{Q_L} \quad (5.3)$$

where  $Appl_{O_3}$  is in mmol/L-liq,  $C_{O_3,G,in}$  is in mmol/L-gas, and  $Q_G$  and  $Q_L$  are in L-gas/h and L-liq/h, respectively.

At a lower  $Q_G$ , keeping  $Q_L$  constant, the applied  $O_3$  dose per liter of liquid was smaller as shown in Table 5.15. This meant that at a lower  $Q_G$ , the amount of  $O_3$  to oxidize the dye molecules was decreased. Additionally,  $k_{La}$ , which increased with  $Q_G$ , was smaller showing a lower rate of mass transfer. At  $Q_G=30$  L/h, the  $C_{O_3,L}$  was close to zero throughout the column showing that ozone was consumed immediately when absorbed into the liquid phase and ozone became the limited reactant. Therefore, the higher dye and TOC removal percentages could be achieved with the application of higher  $O_3$  doses in the gas. However, this implies a disadvantage for conventional ozonation of dye solutions from economical point of view.

At the lower  $Q_G$  ( $Q_G = 30$  L/h), the TOC removal percentages were much lower being between 2.3% and 17.9% for *RBBR* and between 6.7% and 22.4% for *AR-151*, although the dye removals were considerably higher. This demonstrated that the sole ozonation without the catalyst was not sufficient to achieve the desired high levels of TOC removal. As known from literature, the obtained TOC removal values were low since the ozonation by-products showed high resistance to oxidation by ozone and the process was not able to achieve complete mineralization to  $CO_2$  and  $H_2O$  [54,83].

Another important parameter in the ozonation of dyes was related to the amount of  $O_3$  that was consumed per liter of liquid. It is called “ $O_3$  consumption” ( $Cons_{O_3}$ ) and found from Equation (5.4):

$$Cons_{O_3} \text{ (mmol / L liq)} = (C_{O_3,G,in} - C_{O_3,G,out}) \times \frac{Q_G}{Q_L} \quad (5.4)$$

The increase of  $Cons_{O_3}$  by the increase of  $C_{D,in}$  and  $Q_G$  was clearly observed. When the  $C_{D,in}$  was increased, the concentrations of ozonation by-products also increased

resulting in higher O<sub>3</sub> consumptions. At the constant applied O<sub>3</sub> dose, O<sub>3</sub> consumption was an indication of O<sub>3</sub> usage efficiency. It meant the amount of needed ozone from the gas per liter of wastewater in a treatment process. In economical view, the increase of the  $Cons_{O_3}$  resulted in more O<sub>3</sub> usage. Therefore, at lower  $Q_G$ , even though the dye and TOC removals were lower, the consumption of less O<sub>3</sub> from the gas phase by lowering the gas flow rate could be advised in order to reduce the ozonation expenses.

Table 5.15. Ozone doses applied in the experiments.  $C_{O_3,G,in} = 0.306 \pm 0.017$  mmol O<sub>3</sub>/L gas.

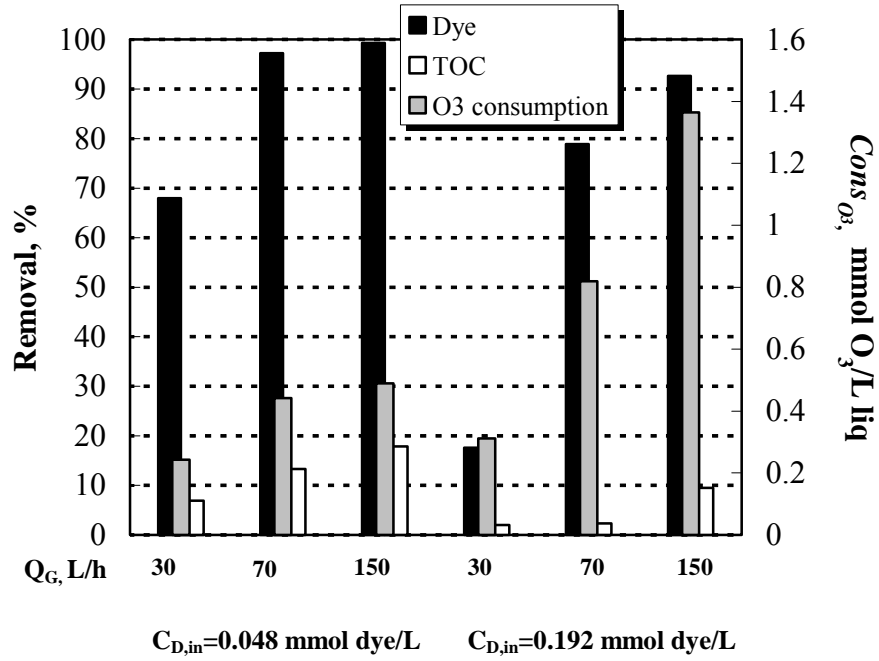
$Q_G$ , L/h	$Q_L$ , L/h	$Q_G/Q_L$	$Appl_{O_3}$ , mmol O <sub>3</sub> /L liq.
30	30	1.0	0.306
70	30	2.3	0.715
150	30	5.0	1.531
70	70	1.0	0.306
70	250	0.3	0.085

Some other parameters were evaluated to understand the actual efficiency of the ozonation process. A parameter called “O<sub>3</sub> consumption rate” ( $R_{cons,O_3}$ ) shows the percent ratio of O<sub>3</sub> consumed from the gas to the O<sub>3</sub> entering in the gas (Equation (5.5)). In addition, the utilization ratios of ozone for the dye removal ( $U_{O_3}$  (dye)) and TOC removal ( $U_{O_3}$  (TOC)) were found from Equations (5.6) and (5.7).

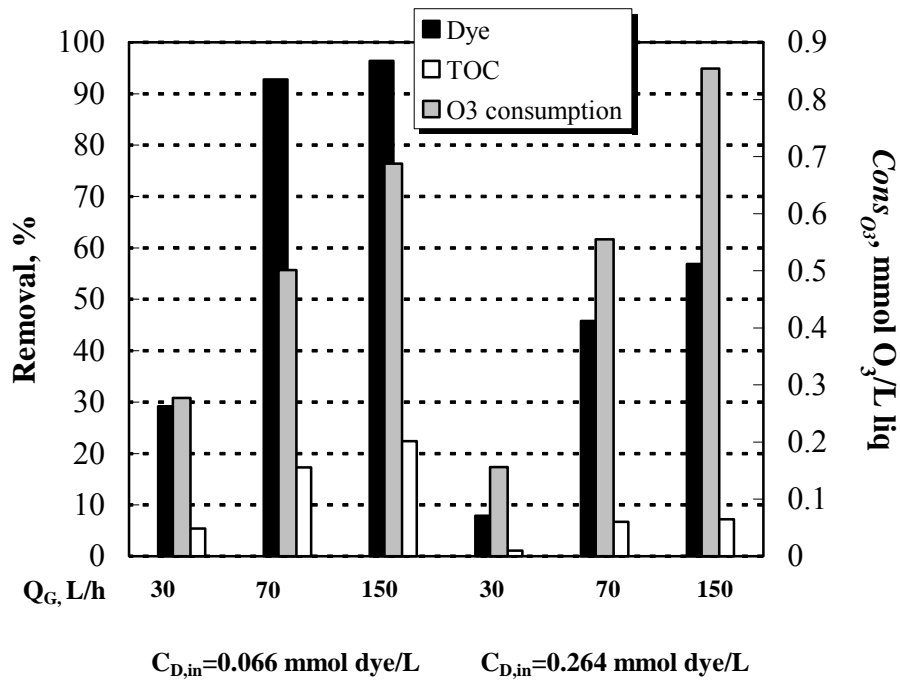
$$R_{cons,O_3} = \frac{(C_{O_3,G,in} - C_{O_3,G,out})}{C_{O_3,G,in}} \times 100 \quad (5.5)$$

$$U_{O_3} \text{ (dye)} = \frac{(C_{D,in} - C_{D,out}) \times Q_L}{(C_{O_3,G,in} - C_{O_3,G,out}) \times Q_G} \quad (5.6)$$

$$U_{O_3} \text{ (TOC)} = \frac{(TOC_{in} - TOC_{out}) \times Q_L}{(C_{O_3,G,in} - C_{O_3,G,out}) \times Q_G} \quad (5.7)$$



(a)



(b)

Figure 5.27. The effect  $Q_G$  on dye and TOC removals and  $O_3$  consumption at different  $C_{D,in}$ . Conditions:  $Q_L = 30$  L/h, pH = 2.51,  $T = 22.0^\circ\text{C}$ ,  $C_{O_3,G,in} = 0.306 \pm 0.017$  mmol  $O_3$ / L gas,  $z = 0.88$  m, particles= none, (a): RBBR, (b): AR-151.

As seen from Tables 5.16 to 5.18,  $R_{cons,O_3}$  was increased by the increase of  $C_{D,in}$  and by the decrease of  $Q_G$ . The highest efficiency in terms of consumption was achieved at the lower  $Q_G$  due to the increase of residence time of the gas in the reactor. Higher values of  $R_{cons,O_3}$  at the lower  $Q_G$  showed that  $O_3$  applied in the gas was consumed more efficiently for the degradation of the dye molecules and TOC. Similar results were obtained in the literature; Soares et al. [35] found that the highest  $O_3$  consumption rate was at the lowest applied  $O_3$  dose. However, it has to be highlighted that at a lower  $Q_G$ , the fluidization degree in the reactor decreased resulting in lower mass transfer rate of  $O_3$  to the liquid phase. Also, at  $Q_G = 30$  L/h, the  $Appl_{O_3}$  was very low resulting in smaller  $U_{O_3}$  values for both the dye and TOC, due to the limitation in the available dissolved  $O_3$  concentration in the reactor (Table 5.18). It is understood that at this condition process is controlled by the mass transfer of ozone.

Table 5. 16. Calculated  $R_{cons,O_3}$  and  $U_{O_3}$  for the dyes.  $Q_G=150$  L/h,  $Q_L=30$  L/h.  $Appl_{O_3} = 1.531$  mmol/L liq.

Dye	$C_{D,in} \times 10^2$ , mmol/L	$R_{cons,O_3}$ % from gas	$U_{O_3}$ (dye),mmol dye/mmol $O_3$	$U_{O_3}$ (TOC), mmol TOC/mmol $O_3$
<i>RBBR</i>	4.8	35.6	0.099	0.344
	9.6	57.0	0.097	0.290
	14.4	67.8	0.121	0.275
	19.2	87.3	0.121	0.264
<i>AR-151</i>	6.6	42.3	0.104	0.566
	13.2	48.8	0.115	0.552
	19.8	55.1	0.132	0.533
	26.4	55.7	0.125	0.503

The gas-liquid system utilized  $O_3$  more efficiently as mmol dye degraded per mmol  $O_3$  consumed when the inlet dye concentration was higher. That was probably due to the higher degradation rate of the dye with the higher  $C_{D,in}$  even though the consumed amount of ozone was also increased. The increase in the degradation of dye molecules was compensated with the increase in  $C_{D,in}$  causing a decrease in % dye removal. As  $C_{D,in}$  increased, the amount of TOC in the solution increased so that lower  $U_{O_3}$  (TOC)

values were achieved, this indicated that more O<sub>3</sub> was required to reach complete mineralization at the higher  $C_{D,in}$ .

Table 5.17. Calculated  $R_{cons,O_3}$  and  $U_{O_3}$  for the dyes.  $Q_G=70$  L/h,  $Q_L=30$  L/h.  $Appl_{O_3} = 0.715$  mmol/L liq.

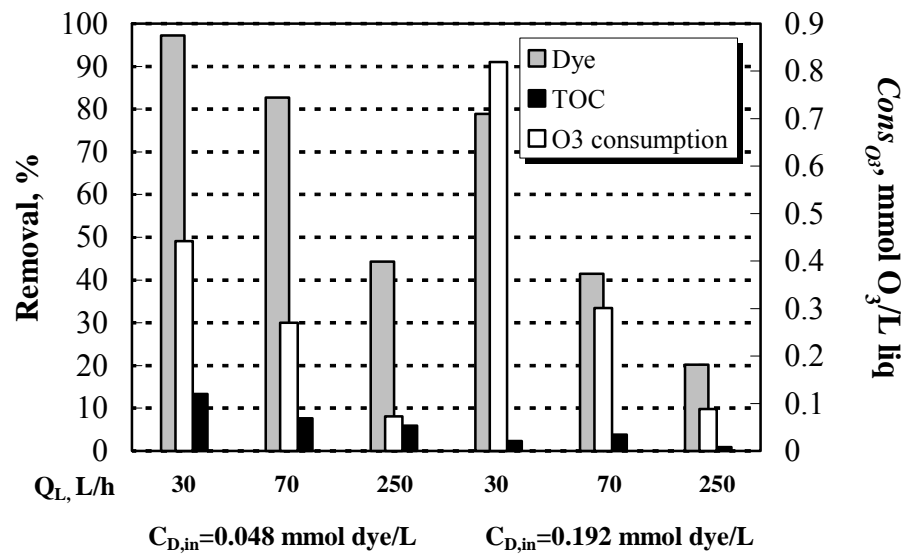
Dye	$C_{D,in} \times 10^2$ , mmol/L	$R_{cons,O_3}$ % from gas	$U_{O_3}$ (dye),mmol dye/mmol O <sub>3</sub>	$U_{O_3}$ (TOC), mmol TOC/mmol O <sub>3</sub>
<i>RBBR</i>	4.8	56.3	0.109	0.318
	9.6	81.9	0.140	0.353
	14.4	92.0	0.165	0.292
	19.2	99.3	0.181	0.118
<i>AR-151</i>	6.6	64.3	0.154	0.648
	13.2	62.7	0.138	0.585
	19.8	64.7	0.193	0.634
	26.4	68.5	0.220	0.689

Table 5.18. Calculated  $R_{cons,O_3}$  and  $U_{O_3}$  for the dyes.  $Q_G=30$  L/h,  $Q_L=30$  L/h.  $Appl_{O_3} = 0.314$  mmol/L liq.

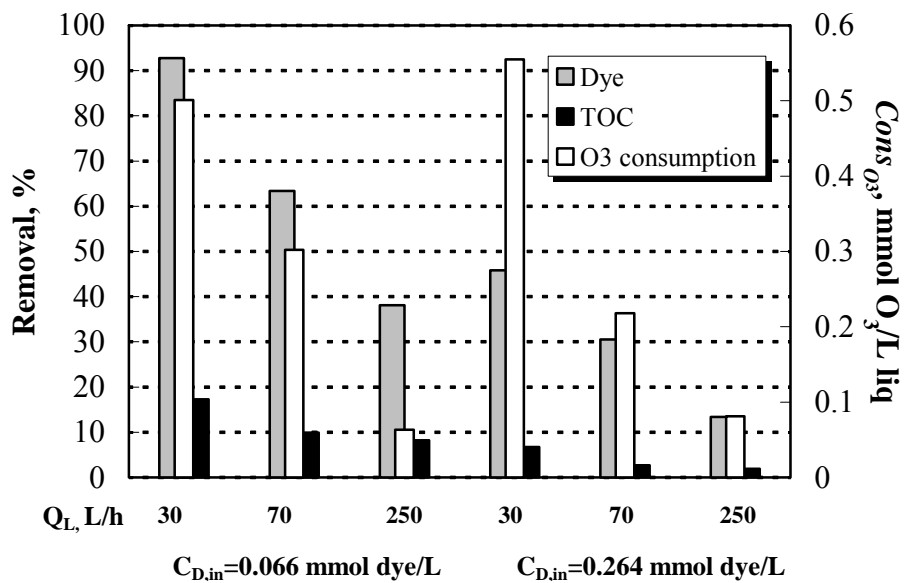
Dye	$C_{D,in} \times 10^2$ , mmol/L	$R_{cons,O_3}$ % from gas	$U_{O_3}$ (dye),mmol dye/mmol O <sub>3</sub>	$U_{O_3}$ (TOC), mmol TOC/mmol O <sub>3</sub>
<i>RBBR</i>	4.8	82.2	0.134	0.104
	19.2	99.4	0.107	0.065
<i>AR-151</i>	6.6	93.9	0.073	0.272
	26.4	94.7	0.068	0.201

The liquid flow rate was effective in the ozonation process in terms of contact time between the gas and liquid phases and the applied O<sub>3</sub> dose per liter of solution. Eventually, the experiments were performed to evaluate the change of  $Q_L$  for *RBBR* or *AR-151* degradation by ozone at  $Q_G=70$  L/h. The dye and TOC removal values were decreased significantly by the increase of  $Q_L$ . In fact, no remarkable TOC removal was observed at that condition. The increase of liquid flow rate caused lower residence time of liquid reducing the contact time between the dye solution and the gas phase. Therefore, the time for ozone to dissolve in the liquid phase and thus, the time for the ozonation reaction in the liquid phase was shortened. In addition, the applied ozone

dose was lowered by the increase of  $Q_L$  at the constant  $Q_G$  as seen in Table 5.15. Although it was advantageous to feed the ozonated solution with a higher flow rate, higher  $Q_L$  brought about the decrease in efficiency in terms of both dye and TOC removals. As seen in Figure 5.28, the consumed  $O_3$  amounts were reduced significantly showing that the process could not use the applied  $O_3$  with a higher percentage.



(a)



(b)

Figure 5.28. The effect of liquid flow rate on dye and TOC removals and  $O_3$  consumption. Conditions:  $Q_G = 70$  L/h, pH = 2.51, T = 22.0°C,  $C_{O_3,G,in} = 0.306 \pm 0.017$  mmol  $O_3$ /L gas,  $z = 0.88$  m, no catalyst, (a): RBBR, (b): AR-151.

The TOC removal percentages and consumed  $O_3$  values from the gas in the experiments are represented in Table 5.19. For the highest liquid flow rate ( $Q_L=250$  L/h), the TOC removal percentages were between 0.9% and 5.9% for *RBBR* and between 1.9% and 8.2% for *AR-151*. To get high dye and TOC removals it is advised to operate the reactor at the low liquid flow rates such as  $Q_L = 30$  L/h.

The utilization for the dye and TOC degradations was remarkably increased at the higher liquid flow rates comparing the results in Tables 5.17, 5.20 and 5.21. Because the decreases in the degraded amounts of both the dye and TOC was accompanied with the decreases in consumed amounts of  $O_3$ .

Table 5.19. % TOC removals and  $O_3$  consumption values at different gas and liquid flow rates. Conditions: pH = 2.51,  $T = 22.0^\circ\text{C}$ ,  $C_{O_3,G,in} = 0.306 \pm 0.017$  mmol  $O_3$ /L gas,  $z = 0.88$  m, particles= none.

Dye	$Q_G$ , L/h	$Q_L$ , L/h	$C_{D,in} \times 10^2$ , mmol/L	TOC Removal, %	$Cons_{O_3}$ , mmol/L liq
<i>RBBR</i>	150	30	4.8	17.9	0.493
			9.6	13.7	0.908
			14.4	9.8	1.080
			19.2	9.5	1.366
	70		4.8	13.3	0.442
			9.6	11.3	0.639
			14.4	7.2	0.736
			19.2	2.3	0.819
	250	4.8	5.9	0.073	
		9.6	3.1	0.082	
		14.4	1.7	0.083	
		19.2	0.9	0.088	
<i>AR-151</i>	150	30	6.6	22.4	0.681
			13.2	13.5	0.750
			19.8	9.8	0.804
			26.4	7.2	0.858
	70		6.6	17.3	0.502
			13.2	10.1	0.505
			19.8	7.4	0.531
			26.4	6.7	0.555
	250	6.6	8.2	0.063	
		13.2	5.3	0.075	
		19.8	4.1	0.078	
		26.4	1.9	0.081	

Table 5.20. Calculated  $R_{cons,O_3}$  and  $U_{O_3}$  for the dyes.  $Q_G=70$  L/h,  $Q_L=70$  L/h.  $Appl_{O_3} = 0.306$  mmol/L liq.

Dye	$C_{D,in} \times 10^2$ , mmol/L	$R_{cons,O_3}$ % from gas	$U_{O_3}$ (dye),mmol dye/mmol $O_3$	$U_{O_3}$ (TOC), mmol TOC/mmol $O_3$
<i>RBBR</i>	4.8	90.6	0.145	0.276
	19.2	95.9	0.271	0.527
<i>AR-151</i>	6.6	92.8	0.150	0.440
	26.4	96.3	0.253	0.494

Table 5.21. Calculated  $R_{cons,O_3}$  and  $U_{O_3}$  for the dyes.  $Q_G=70$  L/h,  $Q_L=250$  L/h.  $Appl_{O_3} = 0.085$  mmol/L liq.

Dye	$C_{D,in} \times 10^2$ , mmol/L	$R_{cons,O_3}$ % from gas	$U_{O_3}$ (dye),mmol dye/mmol $O_3$	$U_{O_3}$ (TOC), mmol TOC/mmol $O_3$
<i>RBBR</i>	4.8	92.7	0.301	0.835
	9.6	99.1	0.304	0.742
	14.4	99.7	0.363	0.571
	19.2	99.1	0.440	0.436
<i>AR-151</i>	6.6	69.6	0.444	2.044
	13.2	85.4	0.340	2.000
	19.8	87.2	0.403	1.815
	26.4	87.3	0.461	1.387

### 5.5.1.2 Effect of inlet ozone concentration on ozonation of *AR-151* or *RBBR* dye

With the increase of inlet ozone concentration ( $C_{O_3,G,in}$ ), the applied  $O_3$  dose per liter of liquid increased (Equation (5.3)).  $C_{O_3,G,in}$  exerted a positive effect on the dye conversion and by-product removal at the studied conditions.

The increase in  $C_{O_3,G,in}$  shows its effect by increasing the rate of mass transfer of  $O_3$ . The driving force for  $O_3$  was increased with the higher  $C_{O_3,G,in}$  giving an increase in  $C_{O_3,L}$  and the rate of dye oxidation consequently. The increases in dye and TOC removals were more significant in the case of high  $C_{D,in}$  (Table 5.22). However, as shown in Table 5.23, the dye removal was gradually increased by the increase in  $C_{O_3,G,in}$  at the lower inlet dye concentration since the amount of available  $O_3$  in the system was

sufficient to remove most of the dye molecules and the by-products from the solution. As a result, a remarkable increase in TOC removal was observed with  $C_{O_3,G,in}$ .

Table 5.22. The effect of inlet ozone concentration in the gas on dye removal, TOC removal and  $Cons_{O_3}$ .  $Q_G=70$  L/h,  $Q_L=30$  L/h,  $C_{D,in}=19.2 \times 10^{-2}$  mmol/L for *RBBR*,  $C_{D,in}=26.4 \times 10^{-2}$  mmol/L for *AR-151*, pH=2.5.

Dye	$C_{O_3,G,in}$ , mmol/L gas	Dye removal, %	TOC removal, %	$Cons_{O_3}$ , mmol/L liq
<i>RBBR</i>	0.317	78.9	2.3	0.819
	0.861*	98.9	9.6	1.273
<i>AR-151</i>	0.307	45.8	6.7	0.555
	0.913*	84.4	17.5	2.124

\* These experiments were conducted by producing ozone from pure oxygen.

Table 5.23. The effect of inlet ozone concentration in the gas on dye, TOC removal and  $O_3$  consumption.  $Q_G=70$  L/h,  $Q_L=30$  L/h,  $C_{D,in}=4.8 \times 10^{-2}$  mmol/L for *RBBR*,  $C_{D,in}=6.6 \times 10^{-2}$  mmol/L for *AR-151*, pH=2.5.

Dye	$C_{O_3,G,in}$ , mmol/L gas	Dye Removal, %	TOC Removal, %	$Cons_{O_3}$ , mmol/L liq
<i>RBBR</i>	0.336	97.4	13.3	0.442
	0.435	100.0	20.8	0.718
	0.525	100.0	24.8	0.861
	0.611	100.0	27.9	0.973
	0.986*	100.0	29.0	1.818
<i>AR-151</i>	0.334	91.5	17.3	0.501
	0.418	94.0	18.6	0.749
	0.497	97.2	20.4	0.813
	0.943*	99.2	24.8	1.870

\* These experiments were conducted by producing ozone from pure oxygen.

### 5.5.1.3 Effect of $Q_G/Q_L$ ratio in ozonation of *AR-151* and *RBBR* dyes

The increase of the gas and liquid flow rates in the same ratio in order to keep  $Q_G/Q_L$  ratio equal to 1, the dye and TOC removals were changed. At the highest gas and liquid flow rates (150 L/h), the dye and TOC removals were higher as well as  $O_3$  consumption (Figure 5.29 and 5.30). Applied  $O_3$  dose (or inlet  $O_3$  concentration in the gas) instead was constant. The increase of  $Q_G$  and  $Q_L$  at the same ratio, keeping  $Q_G/Q_L$  constant and

equal to 1, resulted in the decrease of the contact time between gas and liquid phases. Therefore, it would be expected that decreases of TOC and dye removals would occur by the increase in  $Q_G$  and  $Q_L$ . However, this did not happen due to the higher turbulence in the reactor at the higher gas and liquid flow rates; the mass transfer of ozone from gas phase to the liquid phase increased and more ozone was available to degrade more dye and TOC. As presented before, the mass transfer coefficient was mainly affected by the gas flow rate while liquid flow rate had a minor influence. In other words, the increase of the gas flow rate in the system affected the system performance more significantly than the change of the liquid flow rate in terms of  $O_3$  mass transfer to the liquid phase. The dissolved  $O_3$  concentrations were found to be higher at the higher  $Q_G$  and  $Q_L$  indicating the absorption of more  $O_3$  into the liquid phase.

The TOC removals and  $O_3$  consumptions are given in Table 5.24. Ozone consumption was increased with the increasing gas and liquid flow rates although  $O_3$  consumption rate remained almost constant and over 90% of the entering  $O_3$  in the gas was spent for the degradations of the dye and TOC (Tables 5.25 and 5.26). The ozone consumption rate was an important parameter for the economical consideration of the ozonation process. Here, in only ozonation process the ozone consumption rate was found be close to 100%, which meant higher costs from the economical point of view because of the inefficient use of gaseous ozone.

As shown in Tables 5.25 and 5.26, the utilization ratios for dye and TOC were increased by the increase of  $Q_G$  and  $Q_L$ . In other words, operation of the reactor at the higher gas and liquid flow rates, keeping  $Q_G/Q_L$  constant was advantageous. Although the applied  $O_3$  dose was the same at the studied flow rate conditions, dissolved  $O_3$  was utilized with higher efficiencies in dye and TOC removals at the higher  $Q_G$  and  $Q_L$ .

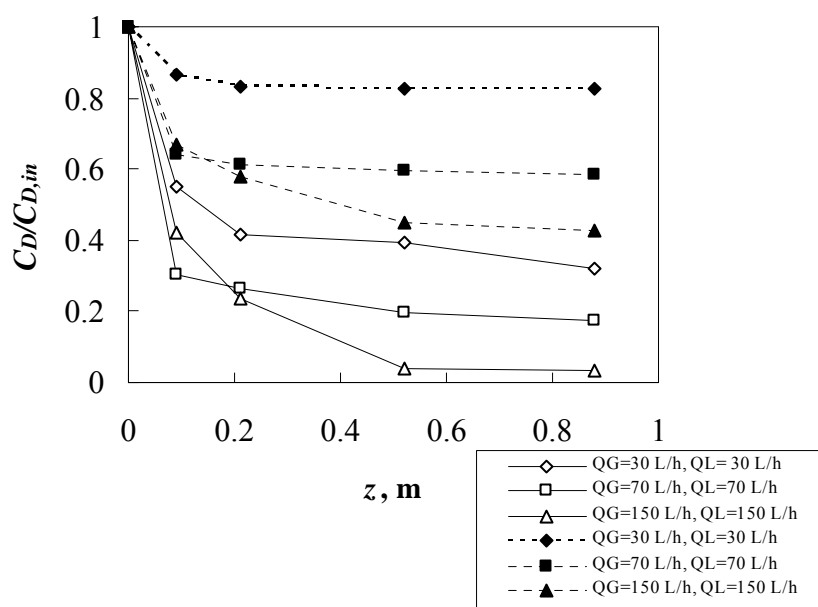


Figure 5.29.  $C_D/C_{D,in}$  ratio for different  $Q_G$  and  $Q_L$ . Conditions:  $Q_G/Q_L = 1.0$ , Dye = *RBBR*,  $\text{pH} = 2.54$ ,  $T = 22.3^\circ\text{C}$ ,  $C_{O_3,G,in} = 0.306 \pm 0.017$  mmol  $\text{O}_3/\text{L}$  gas, no catalyst. Solid lines: for  $C_{D,in} = 4.8 \times 10^{-2}$  mmol/L, dashed lines: for  $C_{D,in} = 19.2 \times 10^{-2}$  mmol/L.

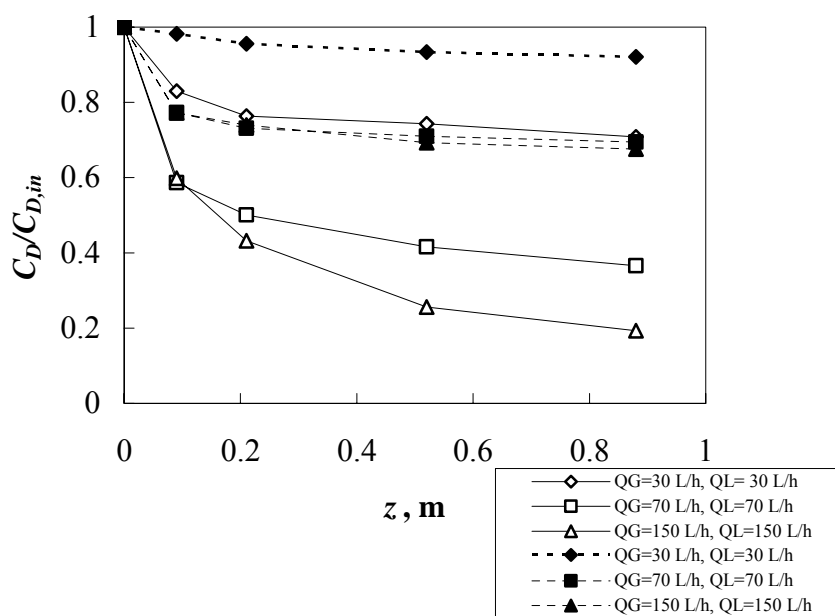


Figure 5.30.  $C_D/C_{D,in}$  ratio for different  $Q_G$  and  $Q_L$ . Conditions:  $Q_G/Q_L = 1.0$ , Dye = *AR-151*,  $\text{pH} = 2.54$ ,  $T = 22.3^\circ\text{C}$ ,  $C_{O_3,G,in} = 0.306 \pm 0.017$  mmol  $\text{O}_3/\text{L}$  gas, no catalyst. Solid lines: for  $C_{D,in} = 6.6 \times 10^{-2}$  mmol/L, dashed lines: for  $C_{D,in} = 26.4 \times 10^{-2}$  mmol/L.

Table 5.24. The effect of  $Q_G$  and  $Q_L$  on TOC removal and  $O_3$  consumption. Conditions:  $Q_G/Q_L = 1.0$ ,  $pH = 2.51$ ,  $T = 22.0^\circ C$ ,  $C_{O_3,G,in} = 0.306 \pm 0.017$  mmol  $O_3$ / L gas,  $z = 0.88$  m, particles= none.

Dye	$Q_G$ , L/h	$Q_L$ , L/h	$C_{D,in} \times 10^2$ , mmol/L	TOC removal, %	$Cons_{O_3}$ , mmol/L liq
<i>RBBR</i>	30	30	4.8	6.9	0.243
	70	70		7.6	0.270
	150	150		8.3	0.290
	30	30	19.2	2.0	0.312
	70	70		3.8	0.301
	150	150		4.4	0.375
<i>AR-151</i>	30	30	6.6	5.4	0.277
	70	70		9.9	0.302
	150	150		13.9	0.322
	30	30	26.4	1.1	0.297
	70	70		2.7	0.218
	150	150		3.8	0.232

Table 5.25. Calculated  $R_{cons,O_3}$  and  $U_{O_3}$  at different  $Q_G$  and  $Q_L$ . Conditions:  $Q_G/Q_L = 1.0$ , Dye = *RBBR*,  $pH = 2.54$ ,  $T = 22.3^\circ C$ ,  $C_{O_3,G,in} = 0.306 \pm 0.017$  mmol  $O_3$ /L gas, no catalyst,  $C_{D,in} = 4.8 \times 10^{-2}$  mmol/L.

$Q_G$ , L/h	$Q_L$ , L/h	$R_{cons,O_3}$ , %	$U_{O_3}$ (dye),mmol dye/mmol $O_3$	$U_{O_3}$ (TOC), mmol TOC/mmol $O_3$
30	30	82.2	1.74	0.026
70	70	90.6	1.89	0.069
150	150	90.8	2.10	0.075

Table 5.26. Calculated  $R_{cons,O_3}$  and  $U_{O_3}$  at different  $Q_G$  and  $Q_L$ . Conditions:  $Q_G/Q_L = 1.0$ , Dye = *AR-151*,  $pH = 2.54$ ,  $T = 22.3^\circ C$ ,  $C_{O_3,G,in} = 0.306 \pm 0.017$  mmol  $O_3$ / L gas, no catalyst,  $C_{D,in} = 6.6 \times 10^{-2}$  mmol/L.

$Q_G$ , L/h	$Q_L$ , L/h	$R_{cons,O_3}$ , %	$U_{O_3}$ (dye),mmol dye/mmol $O_3$	$U_{O_3}$ (TOC), mmol TOC/mmol $O_3$
30	30	93.9	0.683	0.068
70	70	92.8	1.42	0.11
150	150	94.6	1.85	0.13

#### 5.5.1.4 By-products of dye ozonation

According to the detailed HPLC analysis, it was possible to determine the main organic by-products of the ozonated dye solutions. First, the by-products were investigated for the non-catalytic ozonation. The inlet dye concentration, inlet gas ozone concentration, gas and liquid flow rates were the main parameters affecting the produced amounts of the by-products. The main by-products of *RBBR* and *AR-151* degradation were found to be oxalic acid (OA), acetic acid (AA) and glyoxalic acid (GA). The analysis made for the determination of aldehydes showed that the produced amount of aldehydes were considerably small and they were not detected in the solution mostly.

In the ozonation of *AR-151* and *RBBR* solutions, first the chromophore (color-giving) group of the dye was broken by ozone giving much smaller molecules of ozonation intermediates. The quick removal of the dye was an indication of that breakage. Then, these intermediates were degraded to more stable by-products such as carboxylic acids.

Figure 5.31 shows the concentration of the by-products as a function of axial direction ( $z$ ) and inlet dye concentration. The OA and GA concentrations were increased with the increasing  $z$  (height) of the reactor. This meant the continuous production of such carboxylic acids during the ozonation process. AA concentration was increased up to a point in the column and then a decrease was observed. Therefore, acetic acid was produced in the solution and then it was degraded by ozone resulting in the decrease of its concentration.

Higher inlet dye concentrations produced more ozonation by-products. The concentrations of all three species were increased by the increase of  $C_{D,in}$ . That was due to the oxidation of more dye molecules at the higher  $C_{D,in}$  resulting in the production of more ozonated products. In literature, oxalic acid was shown to be one of the main by-products of the dye ozonation [178,181]. Due to the symmetrical structure, the carbons on oxalic acid were stable. The degradation of oxalic acid by ozone was difficult; as a result, it was found as the main ozonation by-product of *RBBR* and *AR-151* degradation.

Acetic acid and glyoxalic acid were produced in the solution in high amounts. This showed that the oxidation by sole ozonation was insufficient to remove such organics

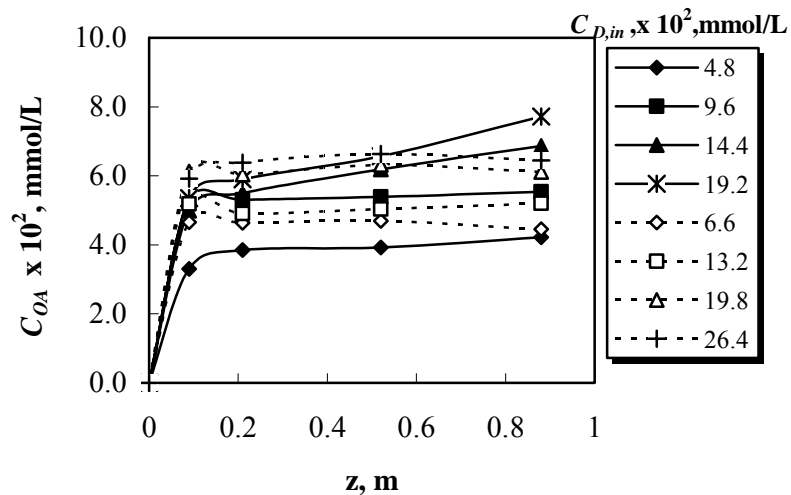
from the dye solutions. The products resulted in considerable amount of TOC; therefore, the TOC reductions by sole ozonation was low. The reduction of these organics did not lead to complete mineralization; in other words, the formation efficiency of CO<sub>2</sub> and H<sub>2</sub>O from the further oxidation of these organics was low.

The effect of gas flow rate on the by-product concentrations was studied. As seen in Figure 5.32, the concentrations of OA and GA were increased with the increasing  $Q_G$ . At a constant inlet O<sub>3</sub> concentration, the increase of  $Q_G$  meant the increase in applied O<sub>3</sub> to the solution. Therefore, the addition of more O<sub>3</sub> to the system caused more degradation of ozonation intermediates giving higher concentrations of OA and GA.

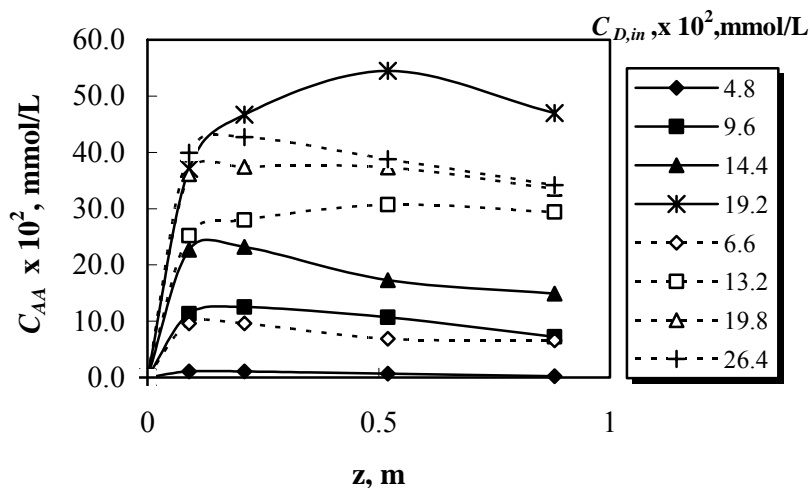
The concentration of AA decreased with the increasing  $Q_G$  (Figure 5.32b). That was due to the degradation of acetic acid in the solution by the additional ozone. Acetic acid in the presence of higher O<sub>3</sub> dose was converted into carbon dioxide and water lowering the TOC of the solution. Fontainer et al. [168] also showed that the mineralization required more ozone dose for a given organic solution.

According to Fontainer et al. [168], generation of carbon dioxide from ozonation of acetic acid proceeded through the formation of formaldehyde and formic acid. However, they stated that the oxidation of formaldehyde and formic acid was easy so that they were not observed in the medium as the final products. That was probably the main reason of for the un-detected formaldehyde and formic acid at the studied ozonation conditions of *AR-151* and *RBBR* dyes.

Similarly, the effect of  $Q_L$  was investigated for the formation of organic species as by-products. At the studied  $Q_L$  conditions, the observed glyoxalic concentration was very low that could not be detected. At the higher  $Q_L$  conditions, the applied O<sub>3</sub> doses per liter of liquid were small so that O<sub>3</sub> was not sufficient to produce glyoxalic acid. The OA concentrations were lowered by the increase of  $Q_L$  (Figure 5.33). Contrarily, AA concentrations were higher at the higher values of  $Q_L$  showing that AA was produced more at the lower ozone doses. From the results of the experiments at different  $Q_G$  and  $Q_L$ , it can be said that the degradation of AA in the solution was responsible for the removal of TOC (Figure 5.28, Table 5.19).



(a)



(b)

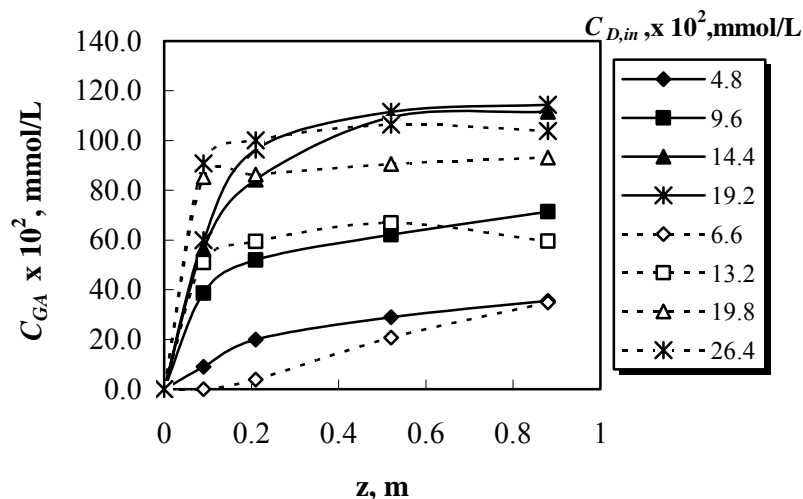


Figure 5.31. The by-products at different  $C_{D,in}$ . Conditions:  $Q_G = 150$  L/h,  $Q_L = 30$  L/h, pH = 2.54, T = 22.3°C,  $C_{O_3,G,in} = 0.306 \pm 0.017$  mmol O<sub>3</sub>/L gas, no catalyst. Solid lines: RBBR, dashed lines: AR-151, (a) OA, (b) AA, (c) GA.

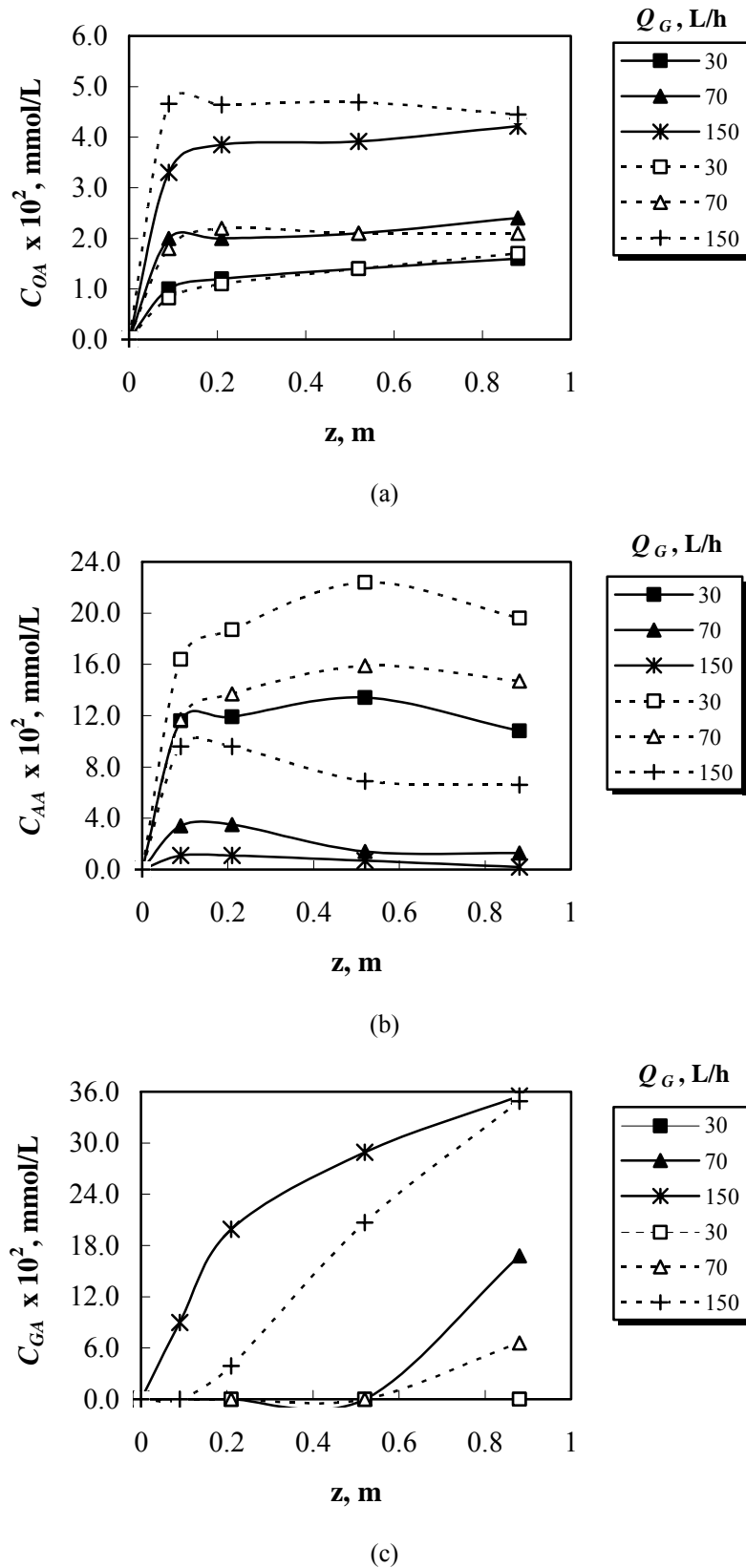
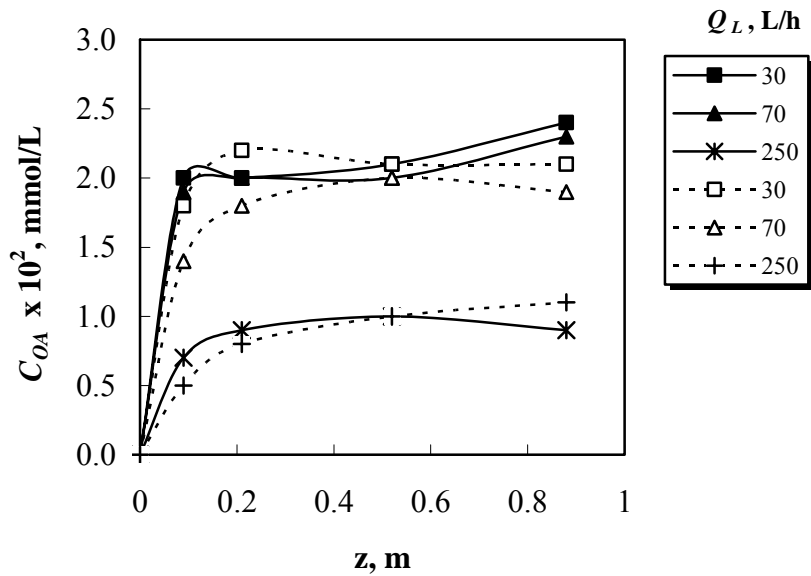
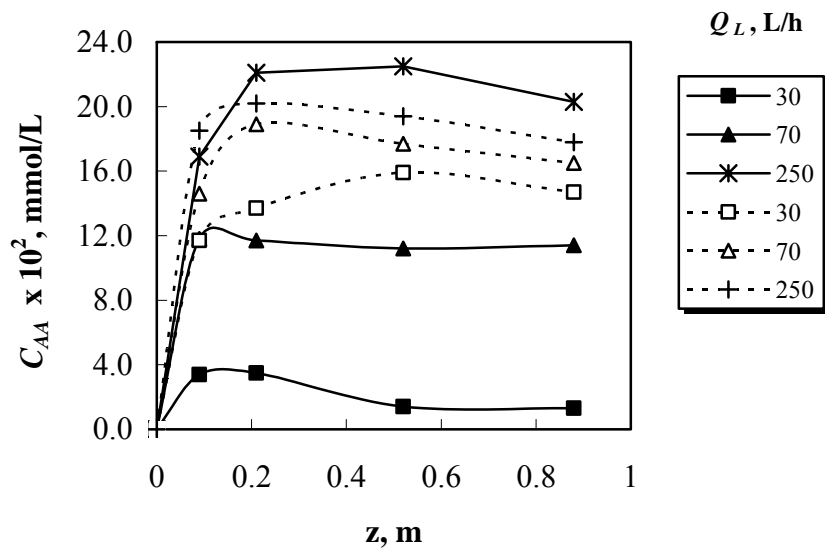


Figure 5.32. The by-products at different  $Q_G$ . Conditions:  $C_{D,in} = 4.8 \times 10^{-2}$  mmol/L for *RBBR*,  $C_{D,in} = 6.6 \times 10^{-2}$  mmol/L for *AR-151*,  $Q_L = 30$  L/h, pH = 2.54, T = 22.3°C,  $C_{O_3,G,in} = 0.306 \pm 0.017$  mmol  $O_3$ / L gas, no catalyst. Solid lines: *RBBR*, dashed lines: *AR-151*, (a) OA, (b) AA, (c) GA.



(a)



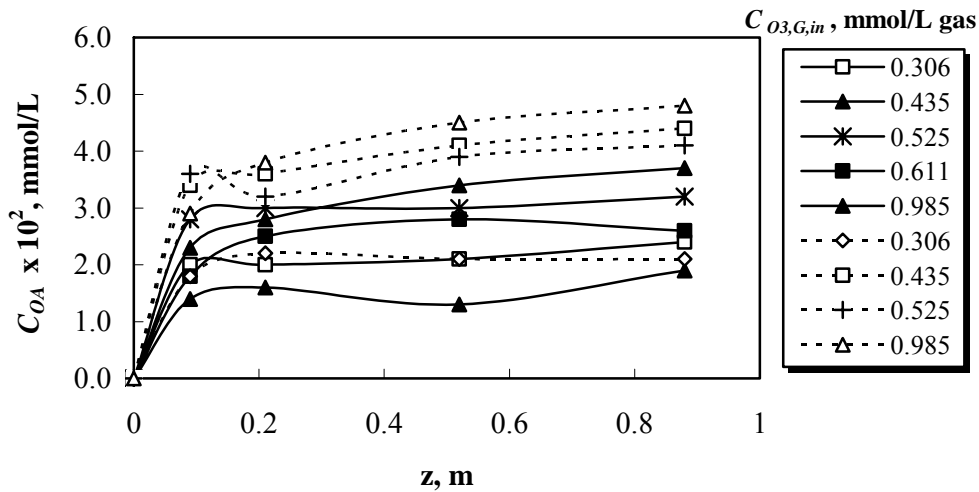
(b)

Figure 5.33. The by-products at different  $Q_L$ . Conditions:  $C_{D,in} = 4.8 \times 10^{-2}$  mmol/L for *RBBR*,  $C_{D,in} = 6.6 \times 10^{-2}$  mmol/L for *AR-151*,  $Q_G = 70$  L/h, pH = 2.54, T = 22.3°C,  $C_{O_3,G,in} = 0.306 \pm 0.017$  mmol  $O_3$ / L gas, no catalyst. Solid lines: *RBBR*, dashed lines: *AR-151*, (a) OA, (b) AA.

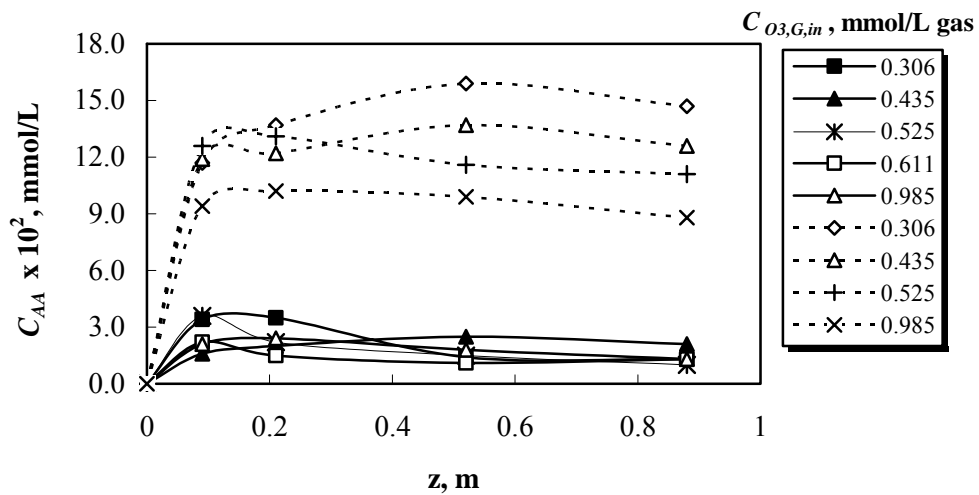
The ozone concentration in the inlet gas was an important process parameter such that more dye molecules were oxidized in the presence of higher  $O_3$  concentrations in the gas phase. As presented in Figure 5.34, it affected the by-product concentrations. Higher OA and GA concentrations were achieved with more  $O_3$ . At the lower  $O_3$  concentration, ozone provoked only the degradation of the dye molecules. The lower TOC removals indicated that the degradation of ozonation-by-products to  $CO_2$  and  $H_2O$  was low. The organics produced as a result of the oxidation were partially degraded to OA and GA so that their concentration in the liquid phase was low. At the higher  $O_3$  concentrations however, the organic intermediates were degraded by ozone to smaller organics such as oxalic and acetic acids as stated in the literature [171,178-180].

Finally, the by-products were investigated at different  $Q_G$  and  $Q_L$  values for  $Q_G/Q_L=1.0$ . By the increase of gas and liquid flow rates, keeping  $Q_G/Q_L$  constant, the concentration of by-products were changed. The increase of  $Q_G$  and  $Q_L$  resulted in higher turbulence in the reactor enhancing the dye and TOC removals as shown in Figures 5.29, 5.30 and Table 5.24. As a result, OA concentration increased by the increase of  $Q_G$  and  $Q_L$  and AA concentration decreased.

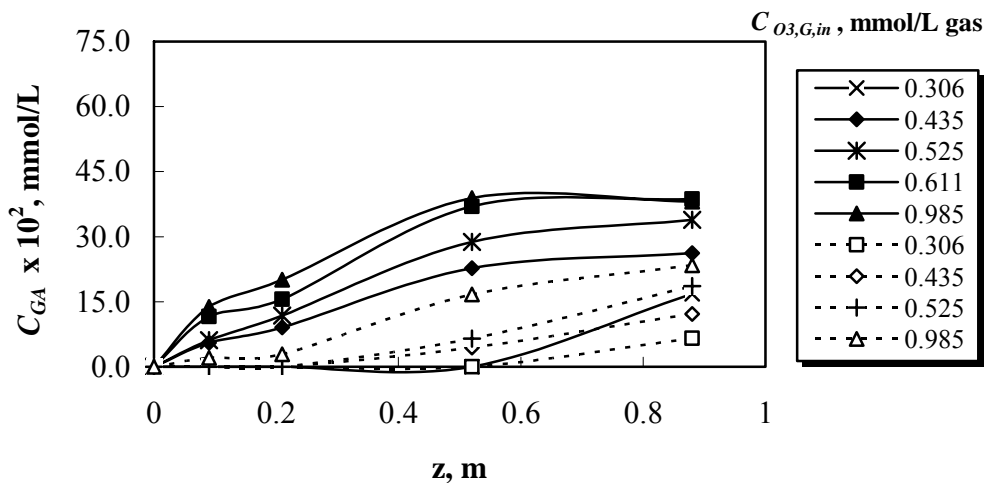
Most of the aliphatic compounds such as aldehydes, ketones and carboxylic acids react with molecular ozone slowly [49]. That was probably the reason of carboxylic acid accumulation in the solution by sole ozonation. Ozone concentration was sufficient to oxidize the aldehydes such as formaldehyde, acetaldehyde and glyoxal to the corresponding carboxylic acids and as a result, no aldehyde was found. Glaze et al. [129] and Miltner et al. [184] found that when the  $O_3$  dosage was high, aldehydes reacted with  $O_3$  to produce carboxylic acids.



(a)

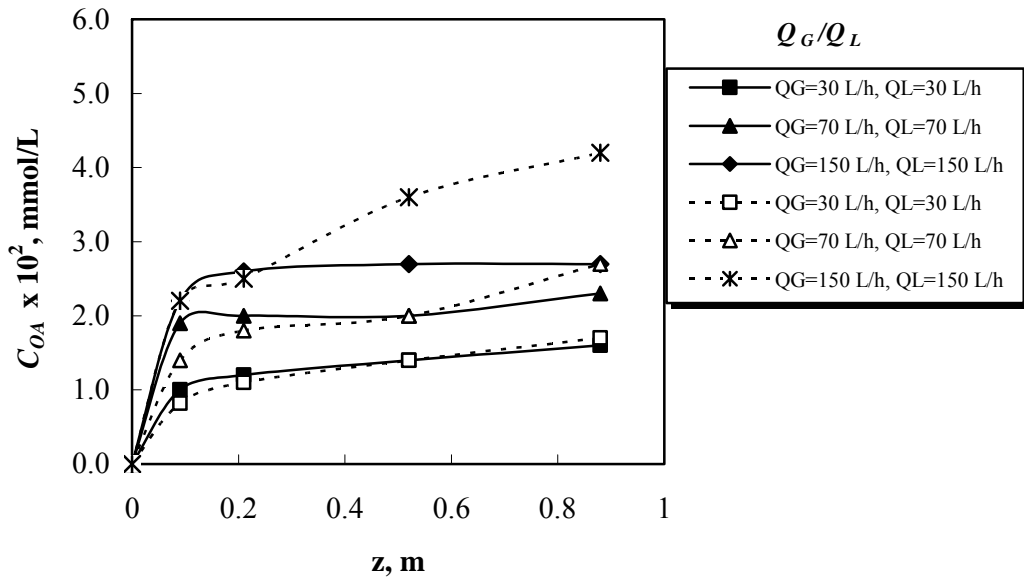


(b)

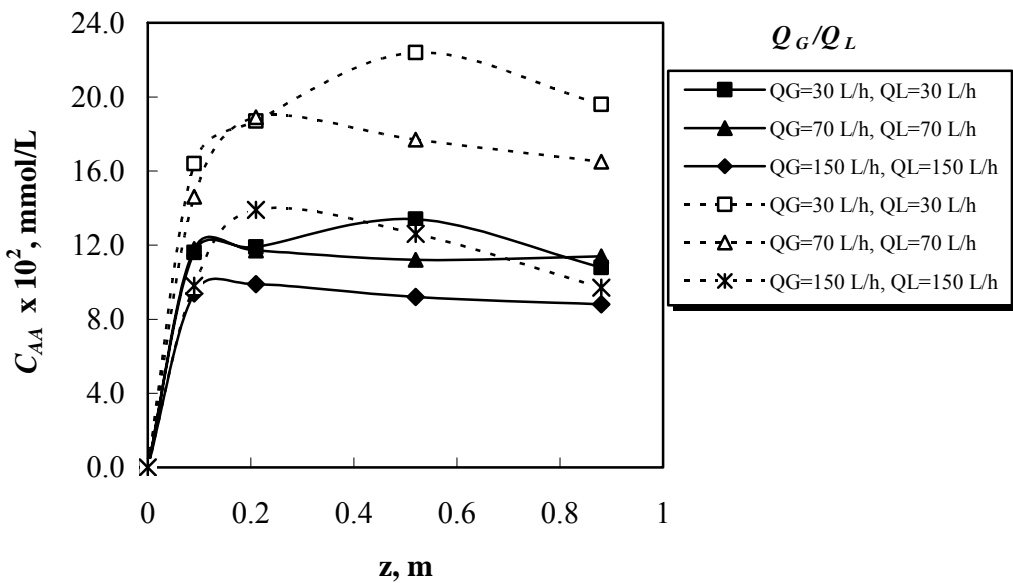


(c)

Figure 5.34. The by-products at different  $C_{O_3,G,in}$ . Conditions:  $C_{D,in} = 4.8 \times 10^{-2}$  mmol/L for *RBBR*,  $C_{D,in} = 6.6 \times 10^{-2}$  mmol/L for *AR-151*,  $Q_G = 70$  L/h,  $Q_L = 30$  L/h, pH = 2.54, T = 22.3°C, no catalyst. Solid lines: *RBBR*, dashed lines: *AR-151*, (a) OA, (b) AA, (c) GA.



(a)



(b)

Figure 5.35. The by-products at different  $Q_G$  and  $Q_L$ . Conditions:  $C_{D,in}=4.8 \times 10^{-2}$  mmol/L for *RBBR*,  $C_{D,in}=6.6 \times 10^{-2}$  mmol/L for *AR-151*,  $C_{O_3,G,in} = 0.306 \pm 0.017$  mmol  $O_3$ / L gas, pH = 2.54, T = 22.3°C, particles = none. Solid lines: *RBBR*, dashed lines: *AR-151*, (a) OA, (b) AA.

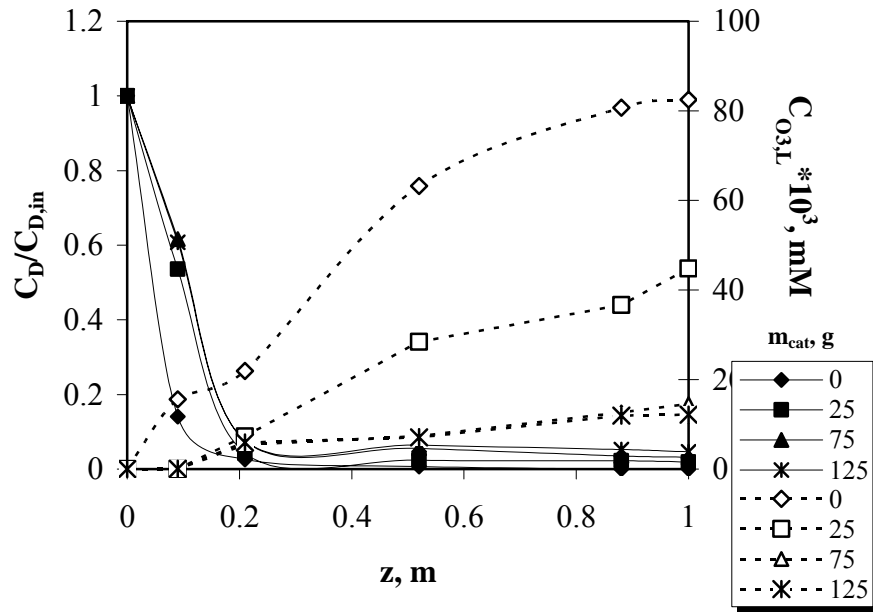
## 5.6 Dye ozonation in the presence of catalysts

The use of alumina and PFOA catalyst individually in the ozonation of *RBBR* and *AR-151* dyes separately was investigated in the fluidized bed reactor. The catalyst dosage was considered to be a significant parameter influencing the performance of the dye ozonation. Therefore, as a first step in the catalytic ozonation, each dye was ozonated using different alumina or PFOA dosages in the column.

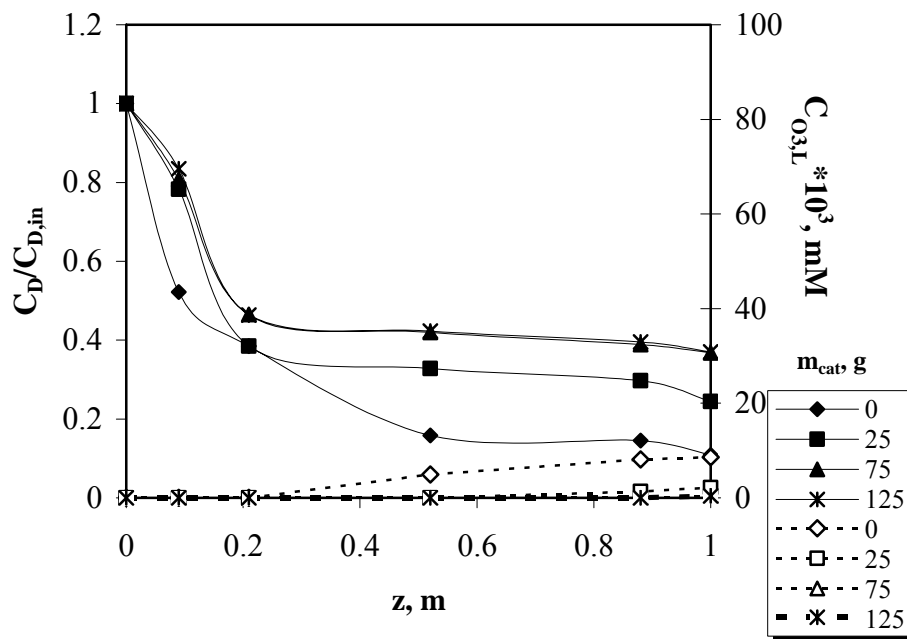
### 5.6.1 The effect of catalyst dosage on dye ozonation

The effect of catalyst dosage on the ozonation of *RBBR* and *AR-151* dyes is shown in Figures 5.36 to 5.39 for alumina and PFOA catalysts. To compare the effects of the catalyst at the low and high organic loading conditions, the dye solutions at a lower ( $C_{D,in}=4.8\times 10^{-2}$  mmol/L for *RBBR* and  $C_{D,in}=6.6\times 10^{-2}$  mmol/L for *AR-151*) and a higher inlet dye concentrations ( $C_{D,in}=19.2\times 10^{-2}$  mmol/L for *RBBR* and  $C_{D,in}=26.4\times 10^{-2}$  mmol/L for *AR-151*) were ozonated in the presence of the catalyst particles. Since the ozone concentration was sufficient to degrade most of the dye molecules in the reactor, the increase of catalyst dosage did not affect the dye removal significantly at the low inlet dye concentrations. However, at the high inlet dye concentration of each dye, the presence of the alumina or PFOA particles did not improve the dye removal. Even, the dye removal was decreased by the presence of the catalysts. Consequently, lower dye removals were obtained with the increase of alumina or PFOA dosage in the reactor at especially high inlet dye concentrations. As observed from Figures 5.36 to 5.39, ozonation of *RBBR* and *AR-151* dyes without the catalyst was more feasible to degrade the dye molecules in the solution.

The obtained dissolved ozone concentrations were lower in the presence of the catalysts and decreased by the increase of the catalyst dosage. Generally, at acidic pH, ozone molecules were stable and were not decomposed to oxidation radicals. However, several studies including the ozonation of some organics in the presence of alumina showed that even at acidic pH, alumina catalyst caused a decrease in dissolved ozone concentrations enabling the decomposition of ozone considerably [155,159]. The surface active groups on alumina were reported to react with dissolved  $O_3$  on the catalyst surface to produce  $O^\bullet$  radicals [152]. The catalyzing effect of alumina was due to the enhancement of oxidation by the produced radicals in the solution.

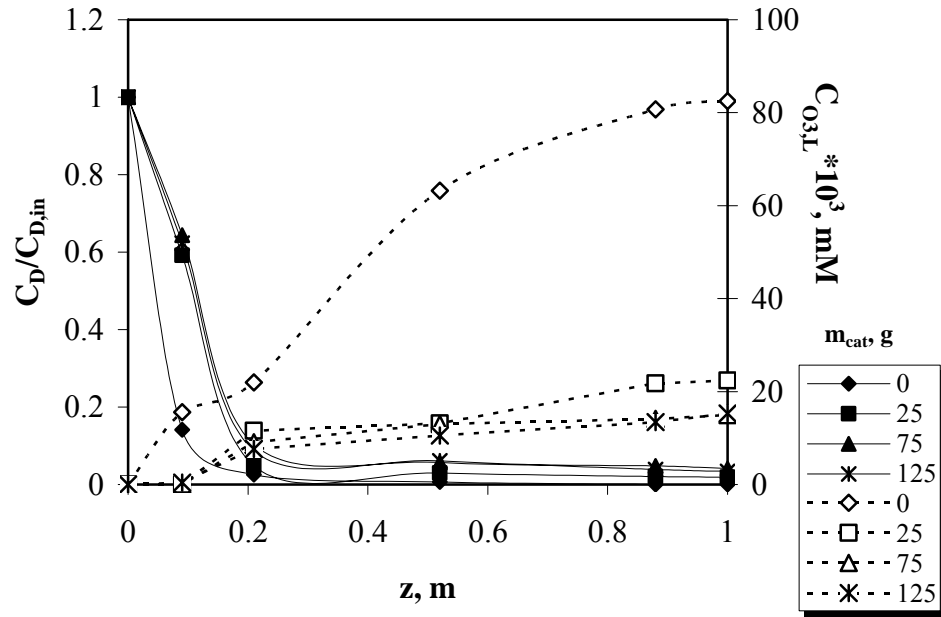


(a)

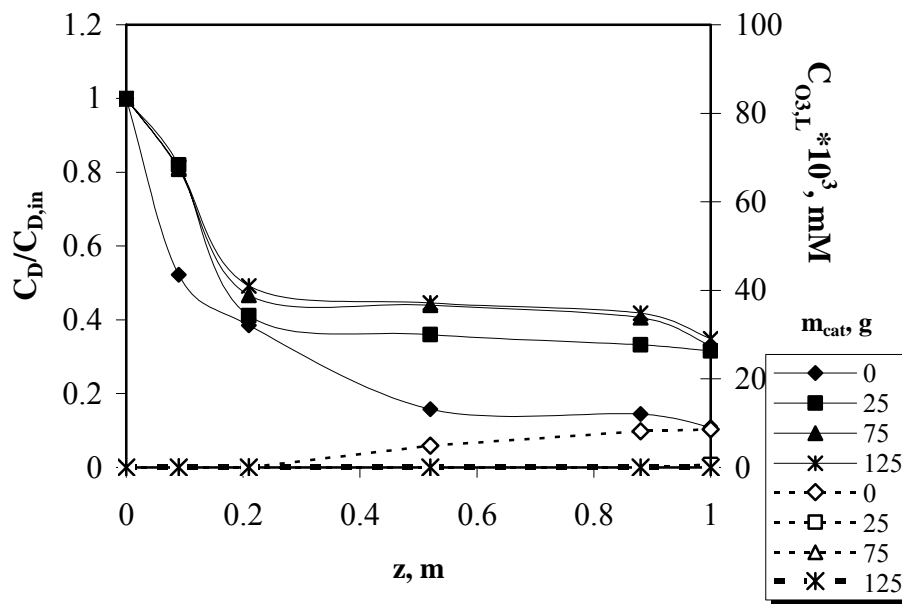


(b)

Figure 5.36. The effect of catalyst dosage on the dye removal and dissolved  $O_3$  concentration. Conditions:  $Q_G = 150$  L/h,  $Q_L = 150$  L/h, Dye = RBBR, pH=2.5,  $C_{O_3,G,in} = 0.92 \pm 0.09$  mmol/L gas, catalyst = Alumina,  $d_{cat} = 2.0$  mm, (a) for  $C_{D,in} = 4.8 \times 10^{-2}$  mmol/L, (b) for  $C_{D,in} = 19.2 \times 10^{-2}$  mmol/L,  $u_{L,min} = 130$  L/h,  $H_E = 12.6$  cm,  $H_S = 7.5$  cm.

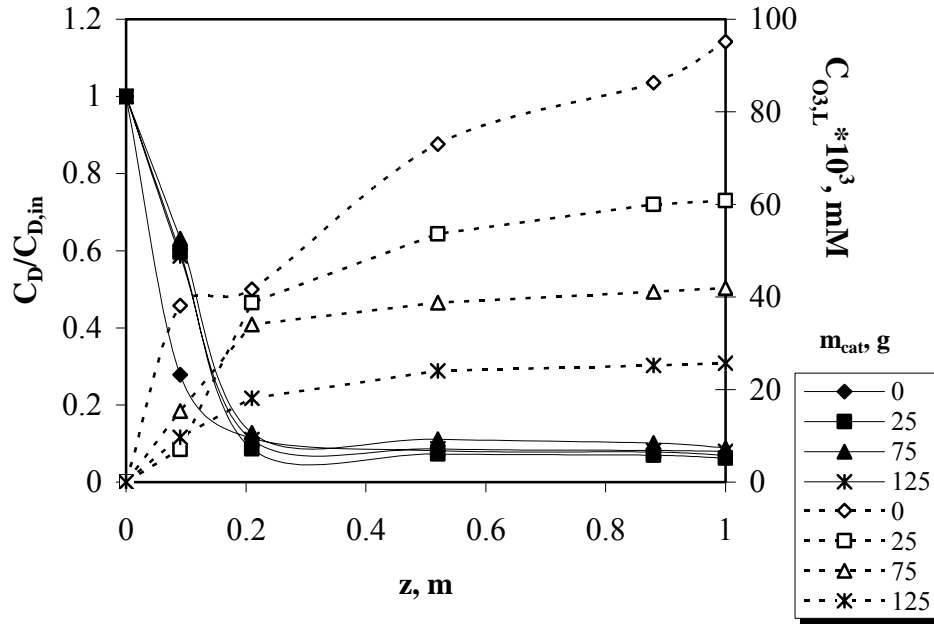


(a)

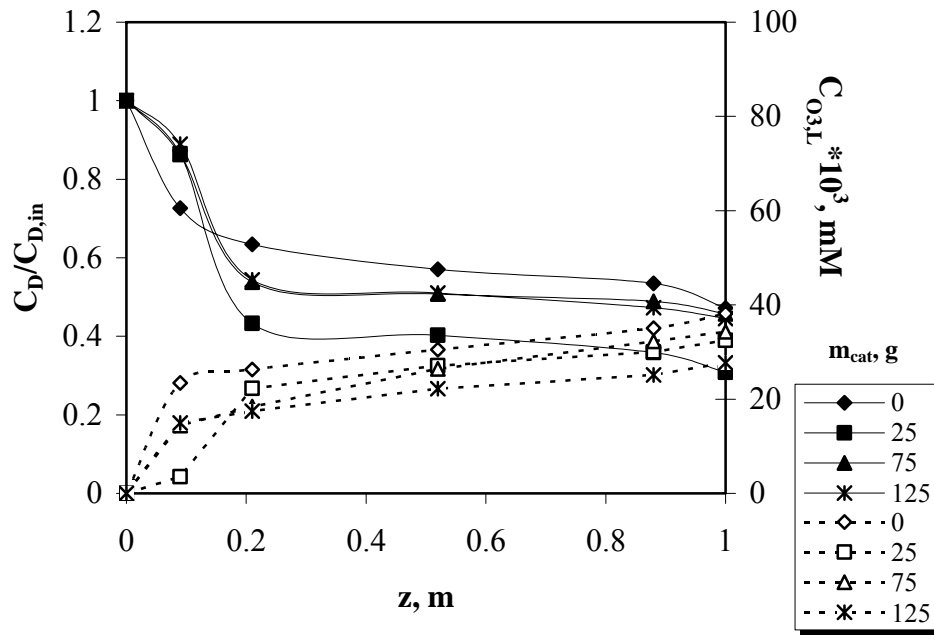


(b)

Figure 5.37. The effect of catalyst dosage on the dye removal and dissolved  $O_3$  concentration. Conditions:  $Q_G = 150 \text{ L/h}$ ,  $Q_L = 150 \text{ L/h}$ , Dye = *RBBR*,  $\text{pH} = 2.5$ ,  $C_{O_3,G,in} = 0.92 \pm 0.09 \text{ mmol/L}$  gas, catalyst = PFOA,  $d_{cat} = 2.0 \text{ mm}$ , (a) for  $C_{D,in} = 4.8 \times 10^{-2} \text{ mmol/L}$ , (b) for  $C_{D,in} = 19.2 \times 10^{-2} \text{ mmol/L}$ ,  $u_{L,min} = 110 \text{ L/h}$ ,  $H_E = 13.4 \text{ cm}$ ,  $H_S = 7.5 \text{ cm}$ .

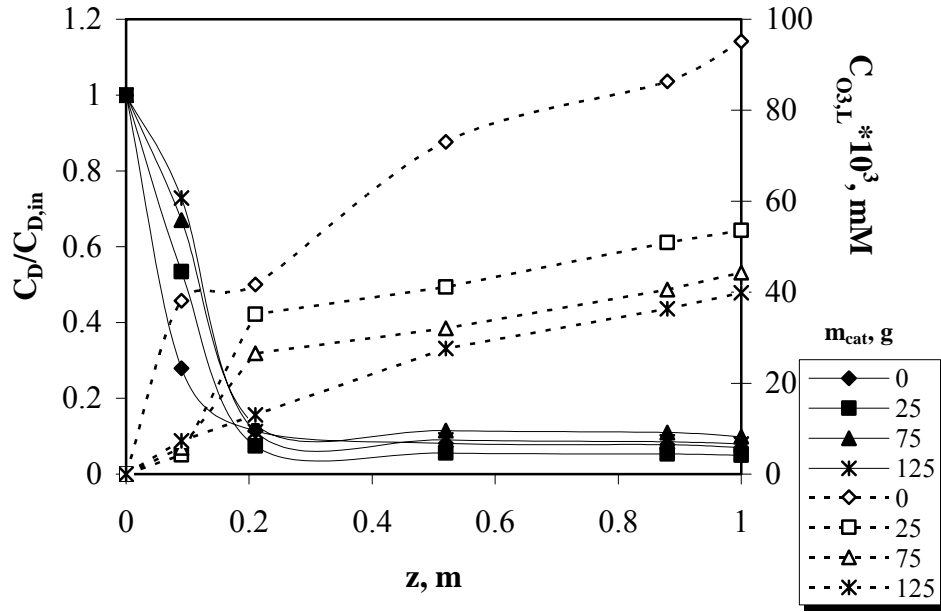


(a)

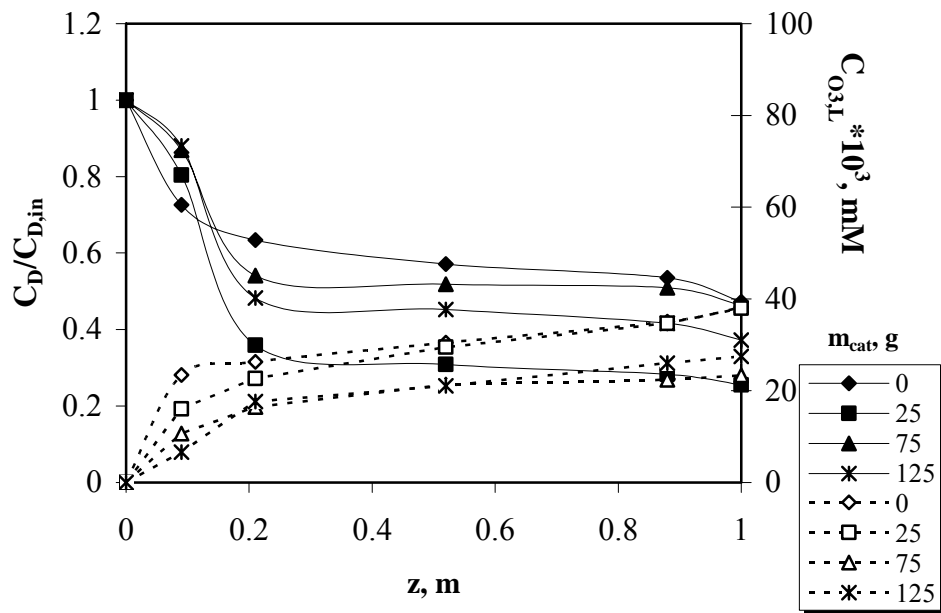


(b)

Figure 5.38. The effect of catalyst dosage on the dye removal and dissolved  $O_3$  concentration. Conditions:  $Q_G = 150$  L/h,  $Q_L = 150$  L/h, Dye = AR-151, pH= 2.5,  $C_{O_3,G,in} = 0.92 \pm 0.09$  mmol/L gas, catalyst = Alumina,  $d_{cat} = 2.0$  mm, (a) for  $C_{D,in} = 6.6 \times 10^{-2}$  mmol/L, (b) for  $C_{D,in} = 26.4 \times 10^{-2}$  mmol/L,  $u_{L,min} = 130$  L/h,  $H_E = 12.6$  cm,  $H_S = 7.5$  cm.



(a)



(b)

Figure 5.39. The effect of catalyst dosage on the dye removal and dissolved  $O_3$  concentration. Conditions:  $Q_G = 150$  L/h,  $Q_L = 150$  L/h, Dye = AR-151, pH= 2.5,  $C_{O_3,G,in} = 0.92 \pm 0.09$  mmol/L gas, catalyst = PFOA,  $d_{cat} = 2.0$  mm, (a) for  $C_{D,in} = 6.6 \times 10^{-2}$  mmol/L, (b) for  $C_{D,in} = 26.4 \times 10^{-2}$  mmol/L,  $u_{L,min} = 110$  L/h,  $H_E = 13.4$  cm,  $H_S = 7.5$  cm.

To understand the effect of alumina on ozone decomposition to radicals, several experiments were conducted in the semi-batch system by ozonating *AR-151* or *RBBR* dye solutions in the presence of alumina catalyst using a radical scavenger, namely carbonate ions. The removals of dye and TOC in the presence of the scavenger were compared with those obtained in the experiments without the scavenger. The compared results are shown in Figures 5.40 and 5.41 for *RBBR* and *AR-151*, respectively.

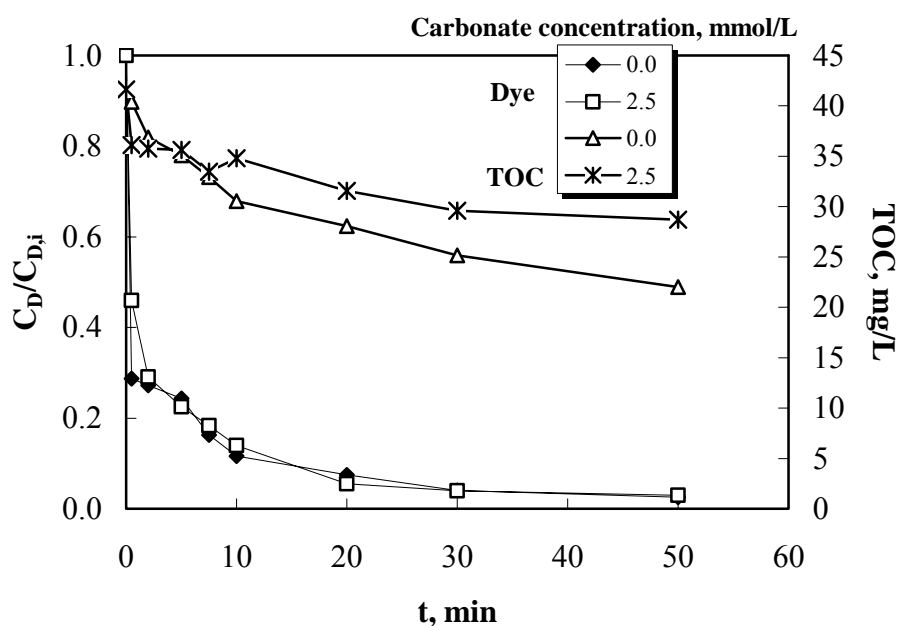


Figure 5.40 The comparison of dye and TOC removals in the presence or absence of a radical scavenger. Dye = *RBBR*,  $T = 25^{\circ}\text{C}$ , Scavenger = Carbonate,  $C_{D,i} = 0.16 \text{ mmol/L}$ , catalyst = Alumina,  $m_{cat} = 10 \text{ g}$ ,  $\text{pH} = 2.5$ , reactor = Semi-batch.

As seen from the results, the presence of a scavenger in the ozonation catalyzed by alumina affected the TOC removal significantly. With the scavenger, the TOC removal was decreased. This meant that alumina-catalyzed ozonation even at acidic pH resulted in the degradation of TOC by the radical reaction mechanism mainly. Otherwise, no influence of the radical scavenger would be observed at the acidic pH. However, the influence of the scavenger on the dye removal was small indicating that in the presence of alumina catalyst; the dye removal occurred mainly by the direct reaction of molecular ozone with the dye molecules. The results of such experiments showed that alumina

caused the decomposition of ozone in the system at acidic pH and TOC was significantly degraded by the radicals produced during ozone decomposition.

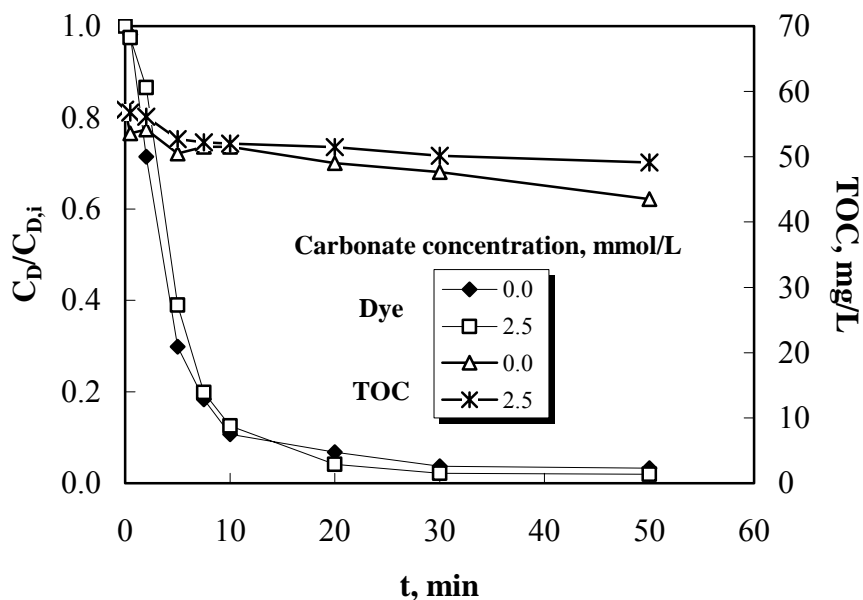
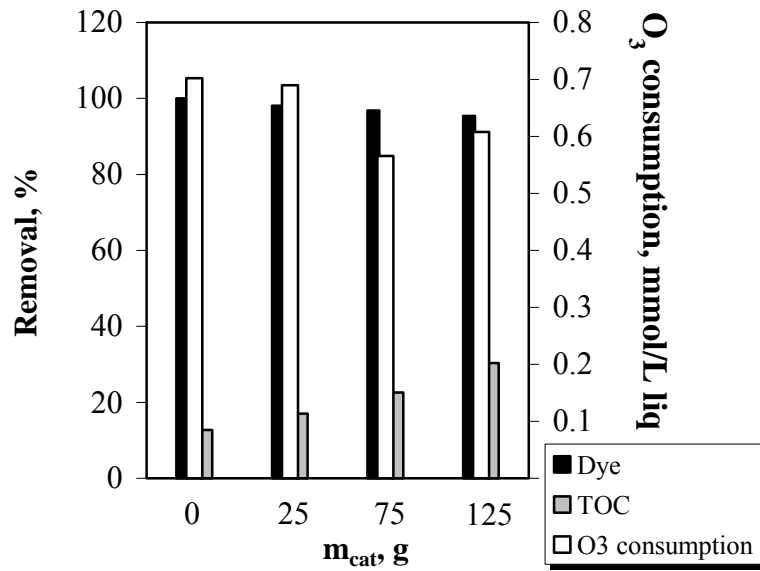
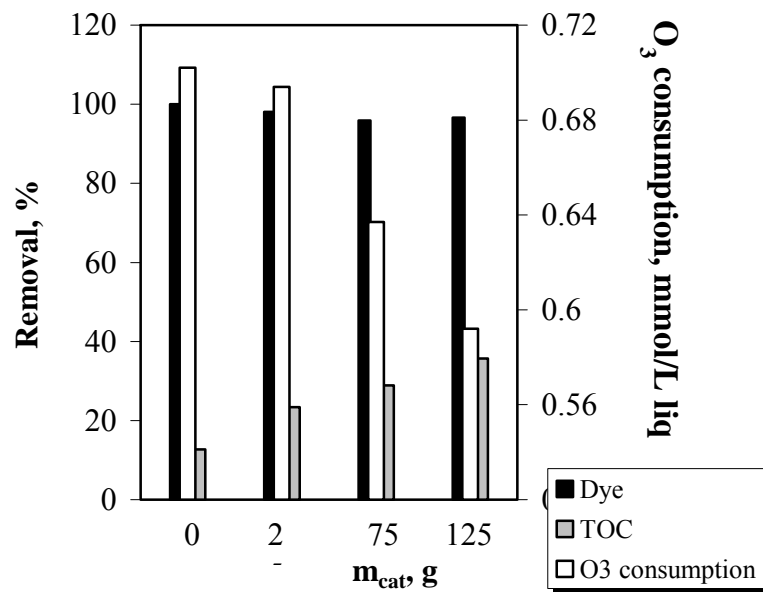


Figure 5.41. The comparison of dye and TOC removals in the presence or absence of a radical scavenger. Dye = AR-151, T = 25°C, Scavenger = carbonate,  $C_{D,i}$  = 0.22 mmol/L, catalyst = Alumina,  $m_{cat}$  = 10 g, pH = 2.5, reactor = Semi-batch.

The presence of alumina or PFOA was advantageous for TOC removal compared to the non-catalyzed ozonation. Both alumina and PFOA were effective in breaking up the organic pollutant molecules to small sized molecules and finally to carbon dioxide and water. As seen in Figures 5.42 and 5.43, the TOC removals were increased by the presence of alumina or PFOA catalyst. The increase of TOC reduction by alumina in ozonation was largely due to the generation of oxidative radicals. Since non-catalytic ozonation was not efficient in removing high percents of TOC from the solution as explained before, alumina could be offered as a good catalyst capable of reducing the TOC at a great extent in the catalytic ozonation. However, alumina was shown to be less effective than PFOA giving smaller TOC removals.

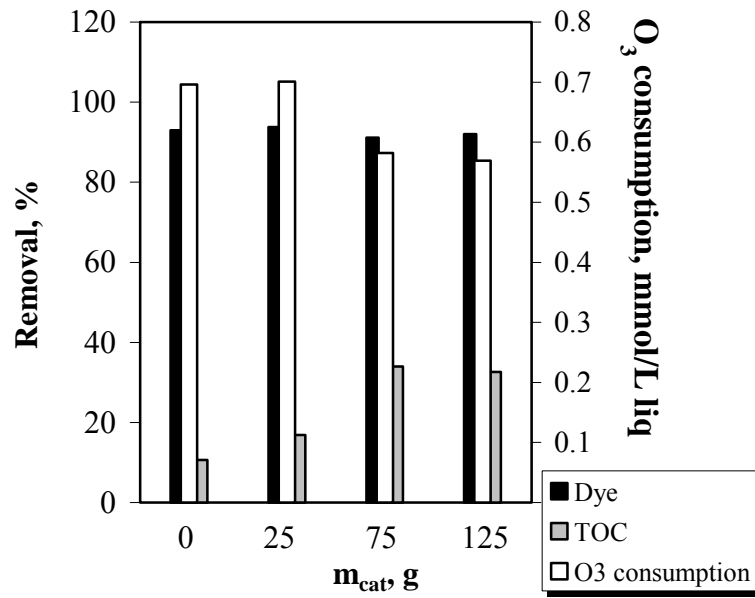


(a)

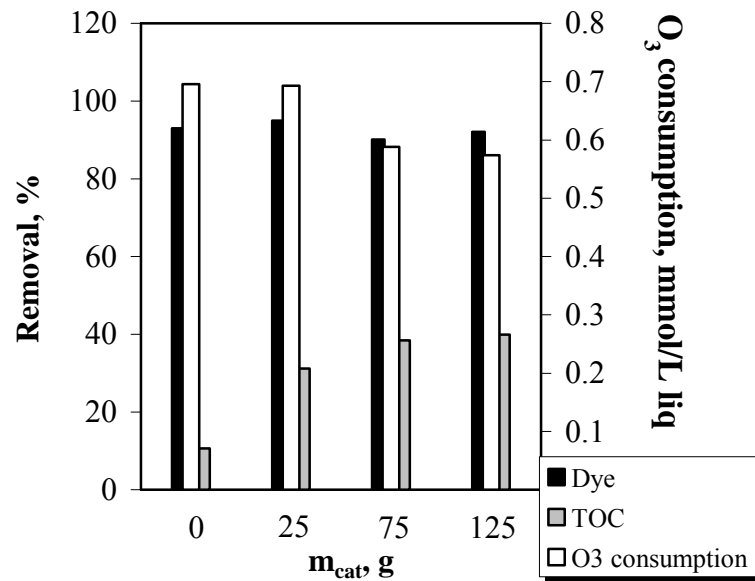


(b)

Figure 5.42. The effect of catalyst dosage on the dye removal, TOC removal and O<sub>3</sub> consumption. Conditions:  $Q_G = 150$  L/h,  $Q_L = 150$  L/h, Dye = *RBBR*,  $C_{D,in} = 4.8 \times 10^{-2}$  mmol/L, pH= 2.5,  $C_{O_3,G,in} = 0.92 \pm 0.09$  mmol/L gas,  $d_{cat} = 2.0$  mm, reactor = FBR,  $H_S = 7.5$  cm. (a) for catalyst = Alumina,  $u_{L,min} = 130$  L/h,  $H_E = 12.6$  cm, (b) for catalyst = *PFOA*,  $u_{L,min} = 110$  L/h,  $H_E = 13.4$  cm.



(a)



(b)

Figure 5.43. The effect of catalyst dosage on the dye removal, TOC removal and O<sub>3</sub> consumption. Conditions:  $Q_G = 150$  L/h,  $Q_L = 150$  L/h, Dye = AR-151,  $C_{D,in} = 6.6 \times 10^{-2}$  mmol/L, pH= 2.5,  $C_{O_3,G,in} = 0.92 \pm 0.09$  mmol/L gas,  $d_{cat} = 2.0$  mm, reactor =FBR,  $H_S = 7.5$  cm, (a) for catalyst = Alumina,  $u_{L,min} = 130$  L/h,  $H_E = 12.6$  cm, (b) for catalyst =PFOA,  $u_{L,min} = 110$  L/h,  $H_E = 13.4$  cm.

As it was apparent, the dosage of alumina and PFOA had an important influence on TOC removal. An increase in TOC removal was observed with the increasing alumina and PFOA dosage. The results clearly indicated that the catalysts improved the degradation of ozonation intermediates or by-products rather than the dye molecules since the dye removal was decreased with the increasing catalyst dosage for both of the dyes and both of the catalysts. The increase of TOC degradation by the increase in amount of alumina and PFOA was probably due to the increasing number of active sites on the catalyst surface to enhance the reaction.

With 125 g PFOA, the TOC reductions (%) were increased 2.8 times and 4.5 times in the ozonation of *RBBR* solutions with the initial dye concentration of  $4.8 \times 10^{-2}$  mmol/L and  $19.2 \times 10^{-2}$  mmol/L, respectively compared to those achieved in the ozonation alone. In the ozonation of *AR-151* solutions with the  $C_{D,in}$   $6.6 \times 10^{-2}$  mmol/L and  $26.4 \times 10^{-2}$  mmol/L, the increment ratios were 3.8 times and 5.6 times, respectively. PFOA/O<sub>3</sub> system was the most efficient system for the removal of TOC from the dye solution.

Similar to the alumina-catalyzed ozonation, the dissolved O<sub>3</sub> concentrations in the presence of PFOA were lower than those achieved in the sole ozonation. The PFOA catalyst enhanced the ozone solubility in the solution, therefore more ozone was available to be spent also for the degradation of ozonation by-products removing the TOC furthermore efficiently compared to the case of conventional ozonation. Thus, TOC removal was enhanced; as a result, the dissolved O<sub>3</sub> concentration in the liquid was decreased.

Consumed amount of O<sub>3</sub> from the gas phase was calculated per liter of liquid for the non-catalytic and catalytic ozonation. With the increase of the catalyst dosage, the O<sub>3</sub> consumption was decreased by using both catalysts, alumina and PFOA as seen in Figures 5.42, 5.43 and Table 5.27. Ozonation alone required a considerably higher ozone amount in the gas phase to achieve the same % dye and TOC removals. The use of catalysts resulted in lower O<sub>3</sub> amounts spent from the gas for the equal or greater dye and TOC removals. The dye solution to be ozonated required less ozone for the degradation of dye molecules and even for the TOC removal in the presence of the catalysts.

High ozone consumption from the gaseous ozone mixture with a low wastewater treatment efficiency means that ozone transfer efficiency to the liquid phase is low; as a result, some ozone is wasted from the gas phase without being used in the oxidation reactions. When a catalyst is used, firstly the ozone transfer efficiency into the wastewater is increased due to the better mixing in the reactor (turbulence created by the particles), secondly the decomposition of ozone into radicals, having oxidation potentials higher than that of ozone is enhanced, thirdly, the reaction becomes faster on the active sites of the catalyst surface.

Table 5.27. Dye and TOC removal percentages with inlet ozone consumptions at different catalyst dosages.  $Q_G = 150$  L/h,  $Q_L = 150$  L/h, pH= 2.5,  $C_{O_3,G,in} = 0.92 \pm 0.09$  mmol/L gas,  $d_{cat} = 2.0$  mm, reactor =FBR,  $H_S = 7.5$  cm, (a) for catalyst = Alumina,  $u_{L,min} = 130$  L/h,  $H_E = 12.6$  cm, (b) for catalyst =PFOA,  $u_{L,min} = 110$  L/h,  $H_E = 13.4$  cm.

Dye	Catalyst	$m_{cat,g}$	$C_{D,in} \times 10^2$ , mmol/L	Dye Removal, %	TOC Removal, %	$Cons_{O_3}$ mmol/L liq
RBBR	-	-	19.2	89.1	5.0	0.791
	Alumina	25		75.6	13.1	0.701
		75		63.2	17.8	0.581
		125		63.0	24.9	0.610
		25		68.4	9.8	0.691
	PFOA	75		67.0	15.7	0.662
		125		65.1	22.5	0.556
		-		-	52.8	5.6
AR-151	-	-	26.4	69.2	14.2	0.681
	Alumina	25		54.3	24.7	0.579
		75		55.5	25.8	0.554
		125		74.5	17.7	0.636
		25		53.7	23.4	0.583
	PFOA	75		62.7	28.9	0.588
		125				

In the presence of PFOA catalyst, even less ozone was wasted; the decrease in consumption of  $O_3$  from the gas, meaning the decrease in the consumed electric during the  $O_3$  production, will give an advantage to PFOA-catalyzed ozonation. Also, the increase of TOC removal while decreasing  $O_3$  wastage from the gas may be attributed to the enhancement of ozone utilization rate in the respect of TOC removal. To understand the positive effect exerted by alumina and PFOA,  $O_3$  consumption rates and utilization

ratios for the dyes were calculated. The results are shown in Table 5.28. The results suggested that the percent O<sub>3</sub> consumptions from the inlet gas for the attained dye and TOC removals were less in the presence of the catalysts.

Table 5. 28. O<sub>3</sub> consumption rates and utilization ratios at different catalyst dosages.  $Q_G = 150$  L/h,  $Q_L = 150$  L/h, pH= 2.5,  $C_{O_3,G,in} = 0.92 \pm 0.09$  mmol/L gas,  $d_{cat} = 2.0$  mm, reactor =FBR,  $H_S = 7.5$  cm, (a) for catalyst = Alumina,  $u_{L,min} = 130$  L/h,  $H_E = 12.6$  cm, (b) for catalyst =PFOA,  $u_{L,min} = 110$  L/h,  $H_E = 13.4$  cm.

Catalyst	$m_{cat}$ g	Dye	$C_{D,in} \times 10^2$ , mmol/L	$R_{cons,O_3}$ , %	$U_{O_3}$ (dye), mmol dye/mmol O <sub>3</sub>	$U_{O_3}$ (TOC), mmol TOC/mmol O <sub>3</sub>
-	-	<i>RBBR</i>	4.9	71.6	0.070	0.202
			18.1	80.1	0.204	0.238
		<i>AR151</i>	7.3	71.4	0.098	0.235
			25.4	72.1	0.195	0.443
Alumina	25	<i>RBBR</i>	4.8	71.1	0.069	0.266
			18.6	71.8	0.200	0.758
		<i>AR151</i>	6.8	71.3	0.091	0.346
			27.4	71.8	0.279	1.260
PFOA	25	<i>RBBR</i>	5.0	71.6	0.070	0.358
			18.6	71.8	0.184	0.578
		<i>AR151</i>	7.2	71.7	0.099	0.699
			31.2	70.9	0.365	1.862
Alumina	75	<i>RBBR</i>	5.0	62.0	0.085	0.458
			18.7	62.6	0.203	1.287
		<i>AR151</i>	5.9	62.2	0.093	0.746
			28.0	62.2	0.263	2.562
PFOA	75	<i>RBBR</i>	5.0	68.3	0.076	0.493
			18.7	62.7	0.215	1.073
		<i>AR151</i>	6.0	62.6	0.091	0.852
			28.2	62.6	0.259	2.317
Alumina	125	<i>RBBR</i>	5.1	65.1	0.079	0.555
			18.0	65.7	0.186	1.514
		<i>AR151</i>	6.4	62.1	0.104	0.725
			26.2	60.1	0.263	2.575
PFOA	125	<i>RBBR</i>	5.1	63.3	0.083	0.691
			18.3	62.2	0.215	1.709
		<i>AR151</i>	5.5	61.9	0.088	0.880
			25.5	62.5	0.272	2.791

The decrease of O<sub>3</sub> consumption rate by the presence of PFOA in ozonation showed that ozone that was transferred to the liquid phase with a higher efficiency in the presence of PFOA, was used in less amount but more efficiently than that in sole ozonation in a certain treatment time and for the same treatment efficiency obtained. Especially, at the higher doses of the catalysts, the consumption rate remained almost constant at around 62% indicating that the catalytic ozonation system consumed O<sub>3</sub> from the gas phase at almost the same percentage, but yielding higher TOC removal percentages with the increasing dosage of each catalyst.

The utilization ratios for TOC in the non-catalytic ozonation were low but increased with the increasing of inlet dye concentration. The presence of the catalyst increased the utilization for TOC considerably, and this ratio was increased by the increasing catalyst dosage. However, utilization for the dye in the catalytic ozonation was almost the same or slightly lower than that in the non-catalytic ozonation. The catalyst favored the utilization of O<sub>3</sub> for the TOC removal rather than for the dye removal.

The adsorption process of the dyes on alumina and PFOA was investigated to understand the importance of adsorption during ozonation. Figure 5.44 presents the effect of adsorption on the removal of *RBBR* and *AR-151* dyes. As observed, the adsorption of *RBBR* and *AR-151* dyes on alumina at acidic pH was important. Due to the hydrophobic nature of PFOA, the adsorption of the dye molecules on PFOA was limited. At the acidic pH, the dyes were in ionic form, being prevented from adsorption on PFOA.

Probably, due to the ionic character of the dye molecules at acidic pH, the dye degradation in PFOA/O<sub>3</sub> system was slowed down. Non-polar intermediates or by-products were preferentially adsorbed on the PFOA surface as the dye molecules continued to be ozonated in the bulk solution simultaneously [158,160]. The adsorption of non-polar organic species on the PFOA surface occurred filling the active sites. Therefore, the catalyst dosage was important enabling the increase of active sites. Ozone with a low polarity of 0.46 D (dipole moment) had an affinity to be adsorbed on the PFOA surface [32,35]. As a result, the reaction between O<sub>3</sub> and organic species occurred on the non-polar surface of PFOA.

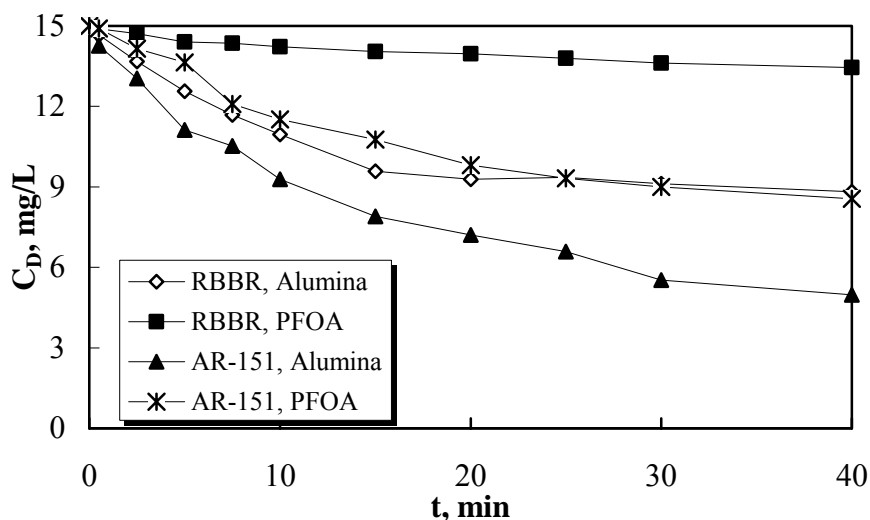


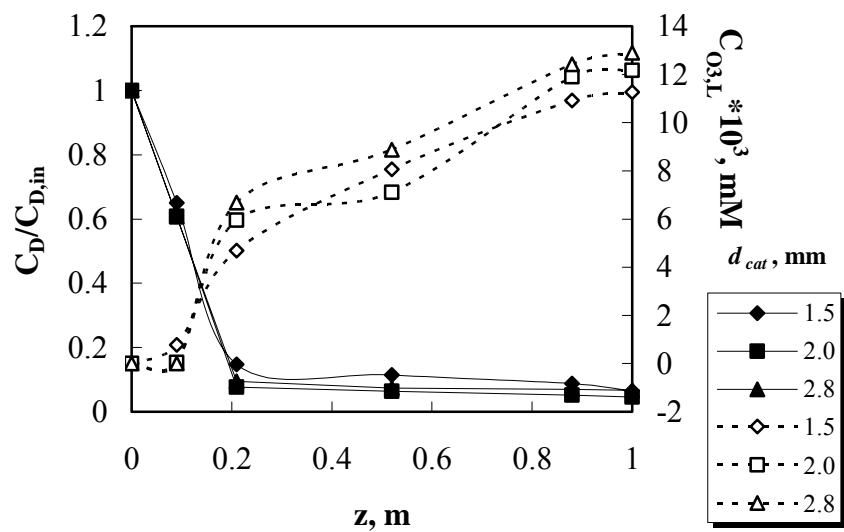
Figure 5.44. The adsorption of *RBBR* and *AR-151* dyes on alumina or PFOA. pH=3.6,  $C_{D,i}=15$  mg/L,  $T=25^{\circ}\text{C}$ ,  $m_{cat}=2$  g, reactor = Semi-batch.

The adsorption of the dye molecules on the alumina surface was more probable than those of ozonated by-products. At the acidic pH, the dye molecules were positively charged and the polar functional groups ( $-HO$  and  $-SO_3$  groups) of *AR-151* and *RBBR* resulted in the adsorption on the alumina surface.

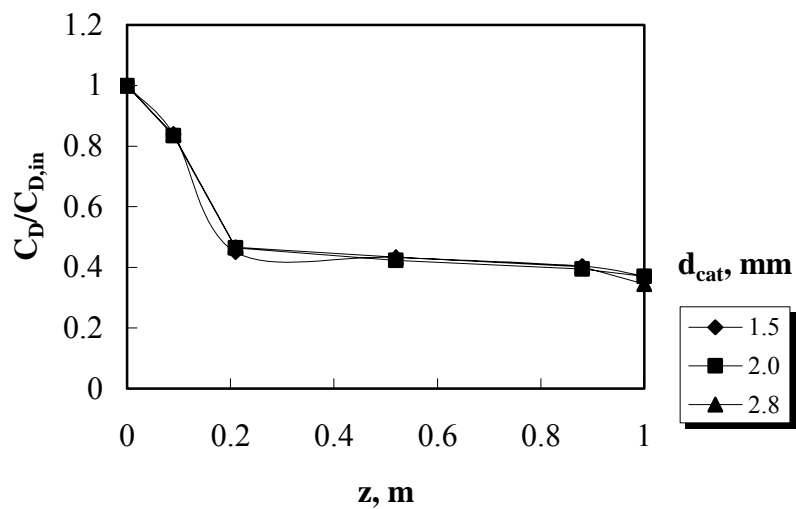
### 5.6.2 The effect of catalyst particle size on dye ozonation

The particle size of the catalyst may affect the rate of dye ozonation due to the change of internal mass transfer resistance in the catalyst pores. The internal mass transfer resistance becomes larger with the increasing particle size and the internal effectiveness factor ( $\eta$ ) showing the ratio of “actual overall rate of reaction in the pores” to “rate of reaction on the catalyst surface” is decreased [189]. Therefore, several experiments were conducted by changing the particle size in order to observe the effect of internal mass transfer.

The effect of catalyst particle size is presented in Figures 5.45 to 5.47. As deduced from these figures, particle size did not affect the dye removal rate significantly for both alumina and PFOA catalysts. Hence, the effect of internal mass transfer was almost negligible in the ozonation of dyes on the alumina or PFOA surface. The internal mass transfer did not limit the dye removal rate at the studied particle size conditions.



(a)



(b)

Figure 5.45. The effect of catalyst particle size on the dye removal. Conditions: Dye = *RBBR*,  $Q_G = 150$  L/h,  $Q_L = 150$  L/h, pH= 2.5,  $C_{O_3,G,in} = 0.92 \pm 0.09$  mmol/L gas, catalyst = alumina, (a)  $C_{D,in} = 4.8 \times 10^{-2}$  mmol/L, (b)  $C_{D,in} = 19.2 \times 10^{-2}$  mmol/L; solid lines with dark marks: for  $C_D/C_{D,in}$ ; dashed lines with light marks: for  $C_{O_3,L}$ .

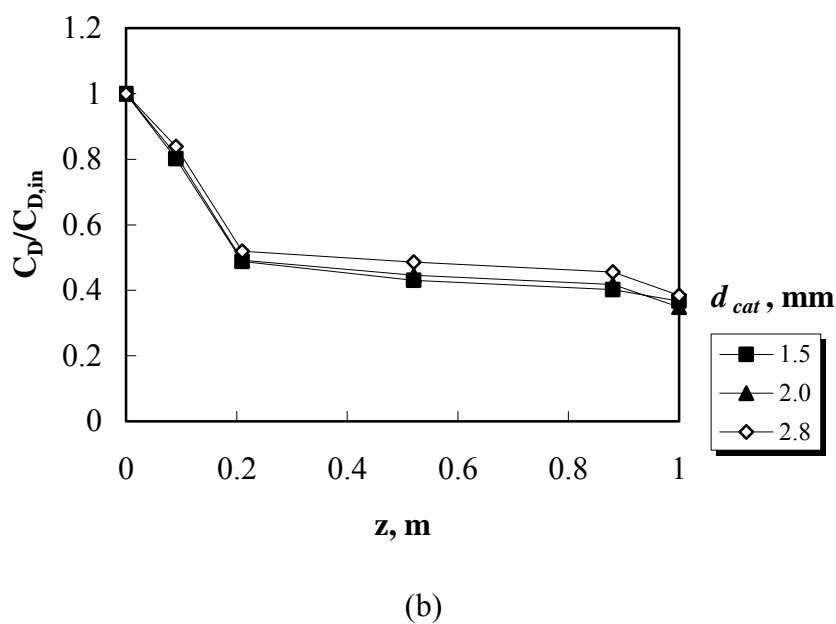
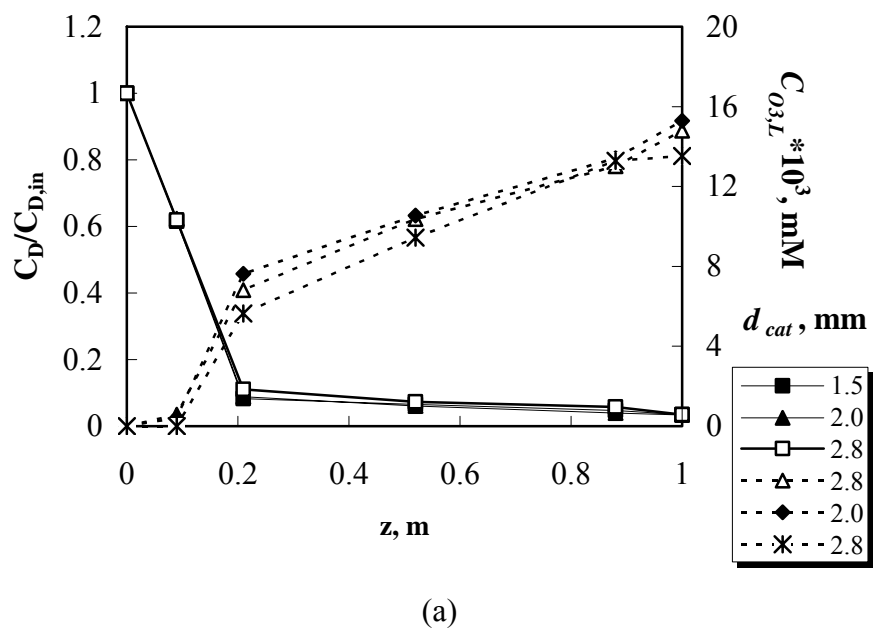
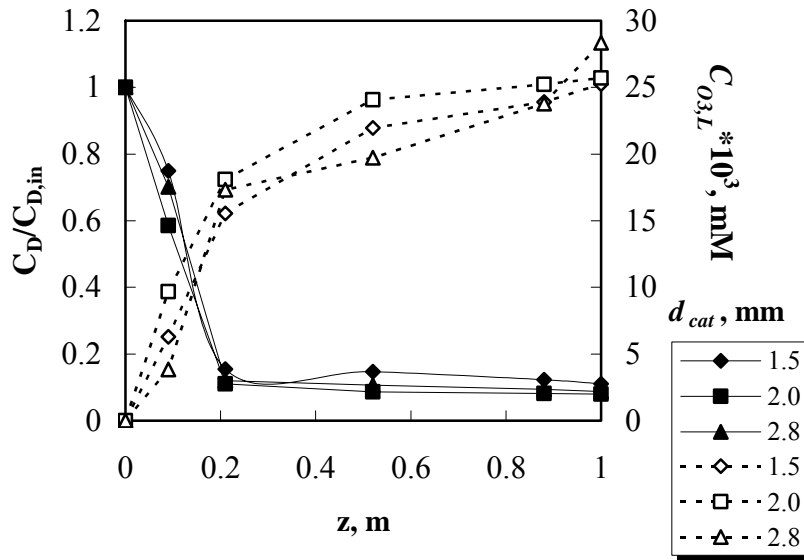
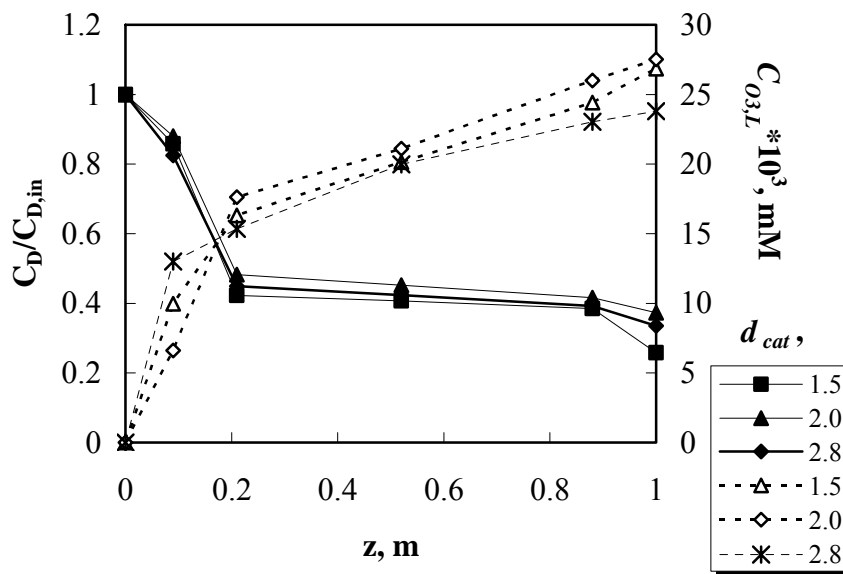


Figure 5.46. The effect of catalyst particle size on the dye removal. Conditions: Dye = *RBBR*,  $Q_G = 150$  L/h,  $Q_L = 150$  L/h, pH = 2.5,  $C_{O_3,G,in} = 0.92 \pm 0.09$  mmol/L gas, catalyst = PFOA, (a)  $C_{D,in} = 4.8 \times 10^{-2}$  mmol/L, (b)  $C_{D,in} = 19.2 \times 10^{-2}$  mmol/L; solid lines with dark marks: for  $C_D/C_{D,in}$ ; dashed lines with light marks: for  $C_{O_3,L}$ .



(a)



(b)

Figure 5.47. The effect of catalyst particle size on the dye removal. Conditions: Dye = AR-151,  $Q_G = 150$  L/h,  $Q_L = 150$  L/h, pH = 2.5,  $C_{O_3,G,in} = 0.92 \pm 0.09$  mmol/L gas,  $C_{D,in} = 6.6 \times 10^{-2}$  mmol/L; (a) catalyst = alumina, (b) catalyst=PFOA, solid lines with dark marks: for  $C_D/C_{D,in}$ ; dashed lines with light marks: for  $C_{O_3,L}$ .

TOC removal was slightly increased by the decrease of particle size (Table 5.29). The internal mass transfer resistance might be important in the case of further oxidation of the by-products on the catalyst surface. However, the slight change of the TOC enables to neglect the internal resistance compared to the effect of other resistances. Therefore, in the reaction modeling it would be acceptable to take the effectiveness factor as 1.0.

Table 5.29. Dye and TOC removal percentages with ozone consumption at different particle sizes.  $Q_G = 150$  L/h,  $Q_L = 150$  L/h, pH= 2.5,  $C_{O_3, Gi} = 0.92 \pm 0.09$  mmol/L gas,  $m_{cat} = 125$  g.

Dye	Catalyst	$d_{cat}$ , mm	$C_{D, in} \times 10^2$ , mmol/L	TOC removal, %	$Cons_{O_3}$ , mmol/L liq
RBBR	Alumina	1.5	4.8	31.7	0.553
		2.0		30.3	0.608
		2.8		29.2	0.596
	PFOA	1.5		35.9	0.588
		2.0		35.7	0.592
		2.8		33.2	0.575
	Alumina	1.5	19.2	26.4	0.645
		2.0		24.9	0.610
		2.8		24.5	0.620
	PFOA	1.5		24.8	0.591
		2.0		22.5	0.556
		2.8		29.0	0.603
AR-151	Alumina	1.5	6.6	32.9	0.614
		2.0		32.6	0.569
		2.8		29.5	0.542
	PFOA	1.5		40.6	0.569
		2.0		39.9	0.574
		2.8		37.8	0.608
	Alumina	1.5	26.4	26.7	0.623
		2.0		25.8	0.554
		2.8		28.7	0.613
	PFOA	1.5		30.5	0.597
		2.0		28.9	0.588
		2.8		31.1	0.575

### 5.6.3 Reproducibility of the experiments

The reproducibility of the experiments was examined by conducting several repeated experiments at the same conditions with or without the catalyst particles. As a representative example, Tables (5.30) and (5.31) show the dye removal, TOC removal and O<sub>3</sub> consumption results for *RBBR* and *AR-151* ozonation. The reliability of the data is ensured by the repeated experiments.

Table 5.30. Reproducibility of the experiments as dye removal, TOC removal and O<sub>3</sub> consumption. Dye = *RBBR*, pH=2.5,  $Q_G = 150$  L/h,  $Q_L = 150$  L/h,  $C_{D,in} = 6.6 \times 10^{-2}$  mmol/L,  $C_{O_3,Gi} = 0.92 \pm 0.02$  mmol O<sub>3</sub>/L gas,  $z = 0.88$  m, no catalyst.

Experiment date	Dye removal, %	TOC removal, %	$Cons_{O_3}$ , mmol/L liq
14.04.2008	100.0	12.7	0.702
21.06.2008	99.1	11.3	0.694
10.07.2008	98.6	14.5	0.699

Table 5.31. Reproducibility of the experiments as dye removal, TOC removal and O<sub>3</sub> consumption. Dye = *AR-151*, pH = 2.5,  $Q_G = 150$  L/h,  $Q_L = 150$  L/h,  $C_{D,in} = 26.4 \times 10^{-2}$  mmol/L,  $C_{O_3,Gi} = 0.92 \pm 0.02$  mmol O<sub>3</sub>/L gas,  $z = 0.88$  m, no catalyst.

Experiment date	Dye removal, %	TOC removal, %	$Cons_{O_3}$ , mmol/L liq
20.04.2008	52.8	5.6	0.710
28.06.2008	50.4	5.9	0.692
15.07.2008	55.3	5.6	0.707

In addition, the stability of the catalyst was investigated by conducting three consecutive runs by reusing the same particles of alumina or PFOA catalyst. After each use, the catalyst was washed by passing distilled water through the column. Table 5.32 presents the results of these repeated. Dye and TOC removal differences were below 5%. It reveals that the activity of the reused catalyst was not reduced during the repeated runs. However, the same catalysts were used at most twice consecutively in the other experiments to ensure reliability.

Table 5.32. Reproducibility of the FBR experiments as dye removal, TOC removal and O<sub>3</sub> consumption. pH = 2.5, Q<sub>G</sub> = 150 L/h, Q<sub>L</sub> = 150 L/h, C<sub>O<sub>3,G,in</sub></sub> = 0.92 ± 0.02 mmol O<sub>3</sub>/L gas, z = 0.88 m, m<sub>cat</sub> = 125 g, d<sub>cat</sub> = 2.0 mm.

Experiment date	Catalyst	Dye	C <sub>D,in</sub> × 10 <sup>2</sup> , mmol/L	Dye removal, %	TOC removal, %	Cons <sub>O<sub>3</sub></sub> , mmol/L liq
27.04.2008	PFOA (fresh)	<i>RBBR</i>	4.8	96.6	35.7	0.592
28.04.2008	PFOA (used once)		4.8	94.8	33.1	0.604
30.04.2008	PFOA (used twice)		19.2	62.7	20.6	0.584
02.05.2008	PFOA (fresh)		19.2	65.1	22.5	0.556
04.05.2008	PFOA (fresh)	<i>AR-151</i>	6.6	92.1	39.9	0.574
06.05.2008	PFOA (used once)		6.6	89.3	36.4	0.585
06.05.2008	PFOA (used twice)		26.4	58.4	26.2	0.602
11.05.2008	PFOA (fresh)		26.4	62.7	28.9	0.588

#### 5.6.4 Effect of Q<sub>L</sub> on catalytic ozonation

The effect Q<sub>L</sub> on the dye ozonation process without catalyst particles was explained in Section 5.3.1. In the *FBR*, the degree of mixing is an important factor for the dye and TOC degradations in the solutions. The increase in mass transfer coefficient in the presence of particles at the fluidized condition was impressive. However, as shown before, the increase of Q<sub>L</sub> caused a decrease in both the dye and TOC removals because of the lower O<sub>3</sub> doses applied and the shorter contact times between gas and liquid phases. Consequently, the study of Q<sub>L</sub> in catalytic ozonation was important to compare the reaction efficiency at the packed bed and fluidized bed conditions.

Tables 5.33 and 5.34 show the dye and TOC removals for low and high inlet dye concentrations of *RBBR* and *AR-151* at two different Q<sub>L</sub> values. The dye and TOC removals decreased with the increasing Q<sub>L</sub>. It seemed that the increase of Q<sub>L</sub>, consequently fluidization level, did not yield an improvement on the catalytic ozonation efficiencies of the dye and TOC removals. However, it would be better to compare the

process efficiency of catalytic ozonation with non-catalytic ozonation at the same  $Q_L$  conditions. That would provide a more beneficial observation for the enhancement of the process efficiency.

For this purpose, the ratios showing the increase in the TOC removals were calculated at the constant  $Q_L$  values. TOC removal increase was the ratio of “TOC removal obtained in catalytic ozonation” to “that in non-catalytic ozonation” at the same  $Q_L$ . The results are shown in Table 5.35. As seen, the increase of  $Q_L$  resulted in higher “TOC removal increase” in catalytic ozonation, and the TOC removal was enhanced more with the presence of PFOA particles at the higher  $Q_L$  ( $Q_L=230$  L/h).

Table 5.33. The effect of  $Q_L$  on dye and TOC removals. Conditions:  $Q_G=150$  L/h, pH = 2.5,  $C_{O_3,G,in} = 0.92\pm 0.09$  mmol/L gas,  $C_{D,in} = 4.8\times 10^{-2}$  mmol/L for *RBBR*,  $C_{D,in} = 6.6\times 10^{-2}$  mmol/L for *AR-151*,  $m_{cat} = 125$  g,  $d_{cat} = 2.0$  mm, reactor =FBR,  $H_S = 7.5$  cm, at  $Q_L=230$  L/h, (a) for catalyst = Alumina,  $u_{L,min} = 130$  L/h,  $H_E = 15.9$  cm, (b) for catalyst =PFOA,  $u_{L,min} = 110$  L/h,  $H_E = 17.2$  cm.

$Q_L$ , L/h	Dye	Catalyst	Dye removal, %	TOC removal, %
30	<i>RBBR</i>	-	100.0	30.9
		Alumina	98.6	45.7
		PFOA	99.8	48.7
230		-	88.0	8.3
		Alumina	58.0	27.6
		PFOA	70.1	32.4
30	<i>AR-151</i>	-	96.6	33.9
		Alumina	93.1	42.8
		PFOA	93.6	45.6
230		-	86.0	8.9
		Alumina	84.7	30.7
		PFOA	87.5	37.5

Table 5.34. The effect of  $Q_L$  on dye and TOC removals. Conditions:  $Q_G=150$  L/h, pH=2.5,  $C_{O_3,G,in} = 0.92\pm 0.09$  mmol/L gas,  $C_{D,in} = 19.2\times 10^{-2}$  mmol/L for *RBBR*,  $C_{D,in} = 26.4\times 10^{-2}$  mmol/L for *AR-151*,  $m_{cat}=125$  g,  $d_{cat}=2.0$  mm, reactor =FBR,  $H_S=7.5$  cm, at  $Q_L=230$  L/h, (a) for catalyst = Alumina,  $u_{L,min}=130$  L/h,  $H_E=15.9$  cm, (b) for catalyst =PFOA,  $u_{L,min}=110$  L/h,  $H_E=17.2$  cm.

$Q_L$ , L/h	Dye	Catalyst	Dye removal, %	TOC removal, %
30	<i>RBBR</i>	-	100.0	16.1
		Alumina	90.5	30.0
		PFOA	81.4	33.1
230		-	72.8	3.5
		Alumina	51.7	15.6
		PFOA	60.9	17.3
30	<i>AR-151</i>	-	89.8	21.3
		Alumina	92.0	32.6
		PFOA	79.0	35.5
230		-	25.8	4.2
		Alumina	36.7	19.3
		PFOA	29.3	22.4

Table 5.35. The effect of  $Q_L$  on “TOC removal increase” in catalytic ozonation. Conditions:  $Q_G = 150$  L/h, pH = 2.5,  $C_{O_3,G,in} = 0.92\pm 0.09$  mmol/L gas,  $m_{cat} = 125$  g,  $d_{cat} = 2.0$  mm, reactor =FBR,  $H_S=7.5$  cm, at  $Q_L=230$  L/h, (a) for catalyst = Alumina,  $u_{L,min}=130$  L/h,  $H_E=15.9$  cm, (b) for catalyst =PFOA,  $u_{L,min}=110$  L/h,  $H_E=17.2$  cm.

$Q_L$ , L/h	Dye	$C_{D,in}\times 10^2$ , mmol/L	Catalyst	TOC removal increase
30	<i>RBBR</i>	4.8	Alumina	1.48
			PFOA	1.58
		19.2	Alumina	1.86
			PFOA	2.06
230		4.8	Alumina	3.33
			PFOA	3.90
		19.2	Alumina	4.46
			PFOA	4.94
30	<i>AR-151</i>	6.6	Alumina	1.26
			PFOA	1.35
		26.4	Alumina	1.53
			PFOA	1.67
230		6.6	Alumina	3.45
			PFOA	4.21
		26.4	Alumina	4.60
			PFOA	5.33

### 5.6.5 Effect of pH on catalytic ozonation

The study of the effect of pH was important to find the possible contribution of radical reactions in the ozonation of dyes. Therefore, its effect was investigated by conducting ozonation experiments at pH=7 and 10 with and without the catalyst particles. The effect of pH on dye removal, TOC removal and O<sub>3</sub> consumption is presented graphically in Table 5.36 and Figures 5.48 and 5.49. For catalytic and non-catalytic ozonations, the highest dye removal was observed at pH=2.5 showing that the dye degradation was mainly due to the direct ozonation. The dye removal was observed to decrease with the increasing pH from 2.5 to 7 and then increased from pH 7 to 10. That was because the *AR-151* and *RBBR* dyes were preferentially degraded by molecular ozone and at neutral pH, O<sub>3</sub> concentration decreased due to the radical reactions and the concentration of radicals were not sufficiently high to degrade the dye molecules. However, TOC removal was increased with the increasing pH.

More ozone was consumed at the higher pH in the catalytic or non-catalytic ozonation processes. Especially, in alumina-catalyzed ozonation, the ozone consumption of the process was remarkably increased at pH=7 and 10. Probably, the increase of radical reactions of ozone in the presence of alumina caused this behaviour. The degradation of TOC was increased by the increase of pH. TOC removals in the ozonation of *RBBR* and *AR-151* solutions with PFOA were almost 1.5 times of those obtained in ozonation with PFOA at pH=2.5. Even with alumina catalyst, the enhancement of TOC removals with the increase of pH 2.5 to 10 was observed. At pH=10, due to the radical reactions in the bulk phase and even on the catalyst surface, the higher TOC removals were achieved in alumina-catalyzed ozonation.

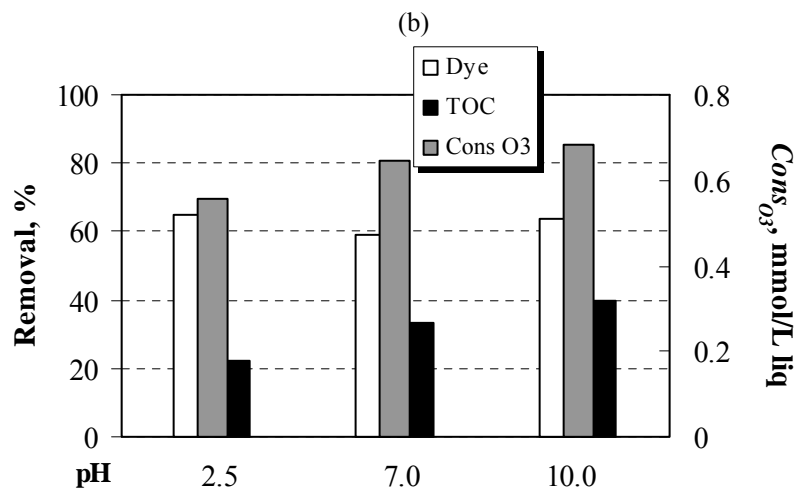
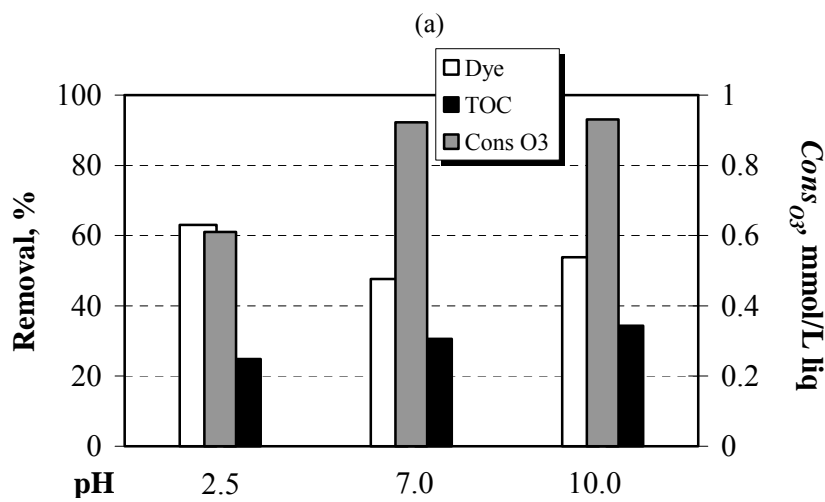
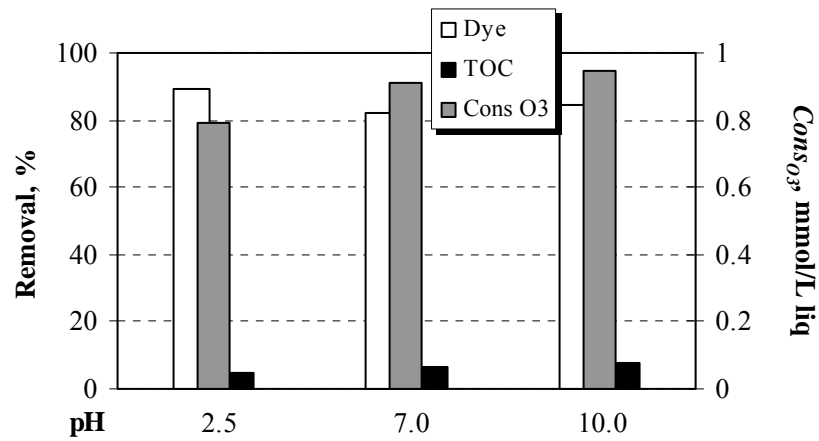
As stated before, at a pH higher than p<sub>H</sub>P<sub>ZC</sub> of alumina, alumina surface became negative by the increase of <sup>-</sup>OH ions. Therefore, at a pH of 10 (higher than p<sub>H</sub>P<sub>ZC</sub>), ozone was adsorbed on the alumina surface reacting with those <sup>-</sup>OH ions to produce hydroxyl radicals. These powerful radicals having oxidation potentials higher than that of ozone removed organics from the solution so that an effective amount of TOC was removed at pH=10 in the presence of alumina. The generation of hydroxyl radical has been shown as an important route in many catalytic ozonation reactions [155].

The dye removal at pH=10 was close to that found at pH=2.5 in the case of PFOA catalyzed ozonation. At pH=10, the stabilization of O<sub>3</sub> partially in the bulk solution with PFOA resulted in higher dye removal than that obtained in alumina catalyzed ozonation. The PFOA particles adsorbing non-polar O<sub>3</sub> molecules on the catalyst surface prevented their decomposition in the liquid bulk phase stabilizing them. TOC was enhanced at pH=10 compared to that at pH=2.5 because of the reaction with the stabilized O<sub>3</sub> and oxidative radicals produced at the very beginning of the operation.

Higher TOC removal at pH=10, was an indication of the effect of radical reactions; otherwise, the TOC removal obtained at pH=2.5 and 10 would be almost equal to each other and no enhancement of the degradation of TOC would occur. Therefore, it can be said that at pH=10, both the reaction of radicals in the bulk and the reaction of ozone on the PFOA surface, with the organics were important.

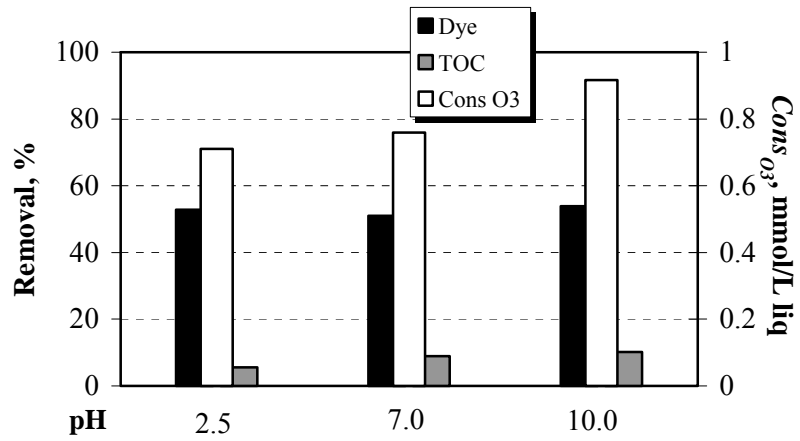
Table 5.36. The effect of pH on the  $R_{cons,O_3}$  and  $U_{O_3}$  for the dyes. Conditions:  $Q_G=150$  L/h,  $Q_L=150$  L/h,  $C_{O_3,G,in} = 0.92\pm 0.09$  mmol/L gas,  $C_{D,in} = 19.2\times 10^{-2}$  mmol/L for *RBBR*,  $C_{D,in} = 26.4\times 10^{-2}$  mmol/L for *AR-151*,  $m_{cat}=125$  g,  $d_{cat}=2.0$  mm, reactor =FBR,  $H_S=7.5$  cm, for catalyst = Alumina,  $u_{L,min}=130$  L/h,  $H_E=12.6$  cm, for catalyst =PFOA,  $u_{L,min}=110$  L/h,  $H_E=13.4$  cm.

pH	Catalyst	Dye	$R_{cons,O_3}$ , %	$U_{O_3}$ (dye), mmol dye/mmol O <sub>3</sub>	$U_{O_3}$ (TOC), mmol TOC/mmol O <sub>3</sub>
7.0	-	<i>RBBR</i>	92.7	0.165	0.279
		<i>AR151</i>	83.8	0.180	0.675
10.0		<i>RBBR</i>	96.1	0.167	0.339
		<i>AR151</i>	92.4	0.154	0.615
7.0	Alumina	<i>RBBR</i>	95.0	0.095	1.285
		<i>AR151</i>	91.5	0.134	1.848
10.0		<i>RBBR</i>	97.1	0.112	1.526
		<i>AR151</i>	96.3	0.138	2.008
7.0	PFOA	<i>RBBR</i>	66.7	0.180	2.118
		<i>AR151</i>	69.7	0.216	3.053
10.0		<i>RBBR</i>	69.1	0.172	2.327
		<i>AR151</i>	70.1	0.228	3.341

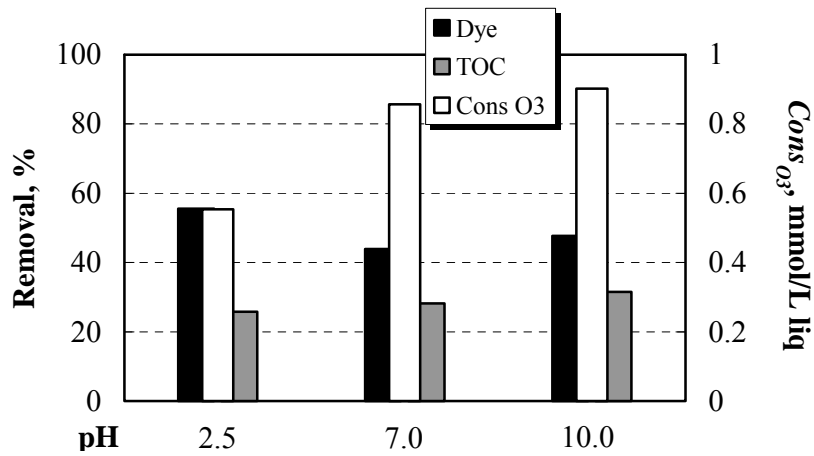


(c)

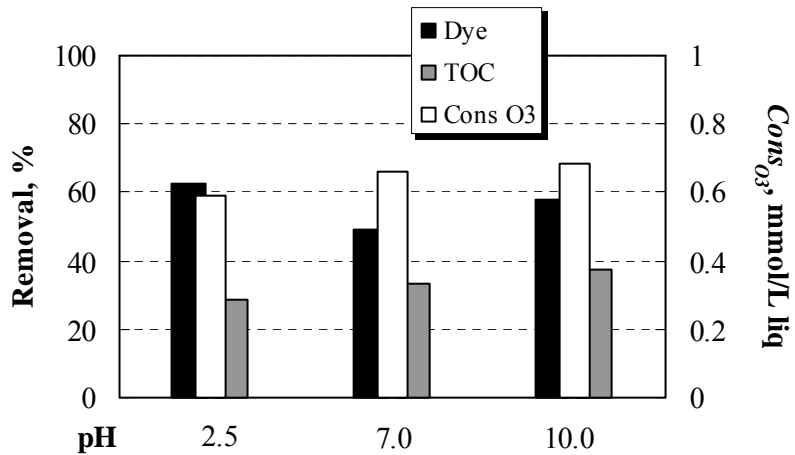
Figure 5.48. The effect of pH on dye removal, TOC removal and O<sub>3</sub> consumption. Conditions: Dye = RBBR,  $Q_G = 150$  L/h,  $Q_L = 150$  L/h,  $C_{O_3,G,in} = 0.92 \pm 0.09$  mmol/L gas,  $C_{D,in} = 19.2 \times 10^{-2}$  mmol/L,  $m_{cat} = 125$  g,  $d_{cat} = 2.0$  mm, (a) no cat., (b) alumina, (c) PFOA, reactor = FBR,  $H_S = 7.5$  cm, for catalyst = Alumina,  $u_{L,min} = 130$  L/h,  $H_E = 12.6$  cm, for catalyst = PFOA,  $u_{L,min} = 110$  L/h,  $H_E = 13.4$  cm.



(a)



(b)



(c)

Figure 5.49. The effect of pH on dye removal, TOC removal and O<sub>3</sub> consumption. Conditions: Dye =AR-151,  $Q_G=150$  L/h,  $Q_L=150$  L/h,  $C_{O_3,G,in}=0.92\pm 0.09$  mmol/L gas,  $C_{D,in}=26.4\times 10^{-2}$  mmol/L,  $m_{cat}=125$  g,  $d_{cat}=2.0$  mm, (a) no cat., (b) alumina, (c) PFOA. reactor =FBR,  $H_S=7.5$  cm, for catalyst = Alumina,  $u_{L,min}=130$  L/h,  $H_E=12.6$  cm, for catalyst =PFOA,  $u_{L,min}=110$  L/h,  $H_E=13.4$  cm.

The decrease of the dye removal in the presence of alumina or PFOA particles for especially RBBR dye can be explained by considering two possible reasons: First,  $O_3$  concentration in the liquid phase was limited so that  $O_3$  was spent for the degradation of ozonation by-products rather than the dye molecules in catalytic ozonation reducing the dye removal efficiency. Second,  $O_3$  was in sufficient amount but the dye oxidation reaction competed with the side reactions of ozone. Hence, several experiments were conducted at a higher inlet gas concentration of ozone ( $C_{O_3,G,in} = 1.42$  mmol/L gas) and in the presence of alumina or PFOA catalyst at different catalyst dosages to understand whether ozone was limited in the liquid. The inlet dye concentration was kept high ( $C_{D,in} = 22.4 \times 10^{-2}$  mmol/L for RBBR,  $C_{D,in} = 26.4 \times 10^{-2}$  mmol/L for AR-151) in order to observe the dye removal change clearly.

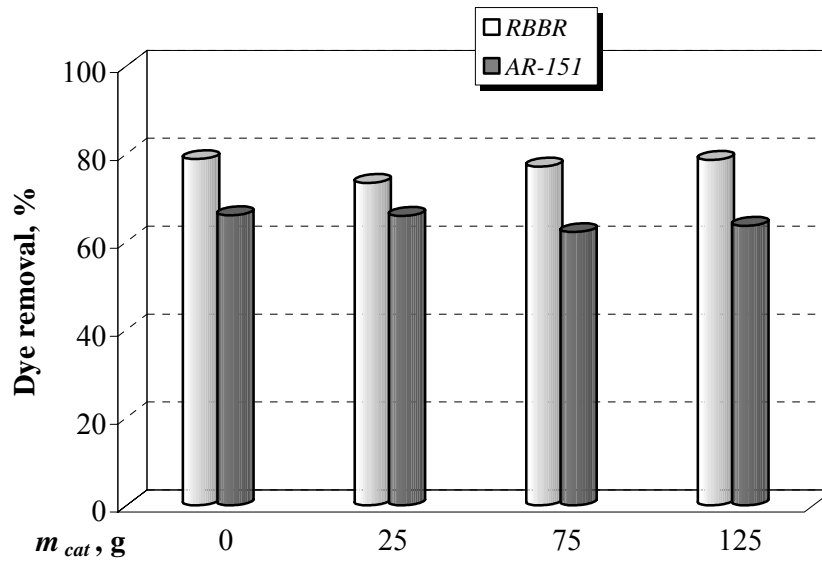
The results revealed that the dye removal was not affected significantly by the change of catalyst dosage; only a slight decrease was observed with the presence of alumina or PFOA (Figure 5.50). This indicated that the dye degradation by  $O_3$  mainly occurred in the bulk solution since the catalyst dosage did not affect the dye removal rate significantly. But, as stated before TOC removal was enhanced with the increase of the catalyst dosage (Table 5.37) and this proved the occurrence of reaction between the ozonation by-products and ozone on the catalyst surface [33-35].

The utilization ratio for the RBBR and AR-151 dyes was increased with the increasing catalyst dosage (Table 5.38). In other words, the catalyst resulted in lower amount of  $O_3$  to be needed to attain a specific dye conversion. That was probably due to the improvement of oxidative properties of ozone by adding solid catalyst to the system. The presence of alumina was shown to be responsible for the production of highly oxidative radicals, such as  $O^\bullet$  radicals at acidic pH and  $OH^\bullet$  radicals at alkaline pH [155,159,160]. These radicals were not selective to oxidize the organics; an efficient degradation of the organics was achieved by consuming  $O_3$  through only radical production. Also at acidic pH, some organics such as carboxylic acids containing dissociated groups were adsorbed on the positively charged alumina surface. The adsorption of carboxylic acids on alumina was shown to be very strong. Anions of organic acids were replaced by the surface hydroxyl groups of alumina. The removal of such organics by the adsorption on the alumina surface enhanced their degradation.

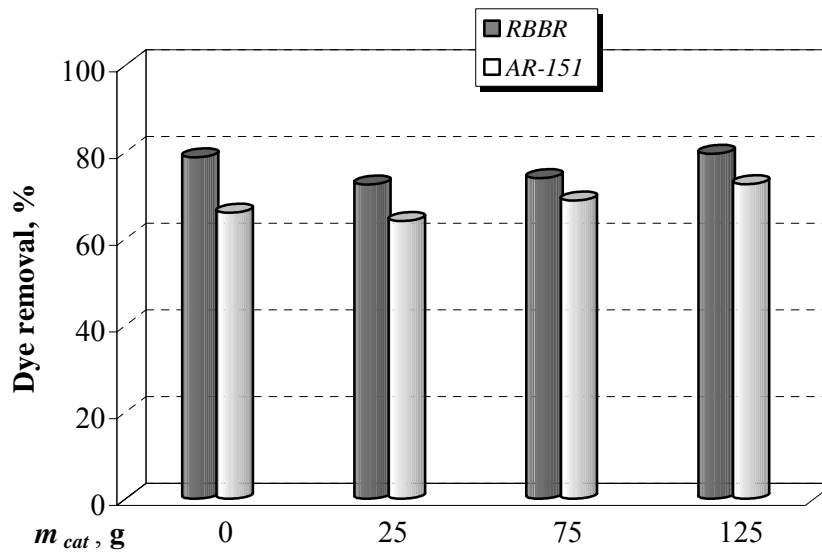
The lower O<sub>3</sub> consumption from the gas phase by the use of PFOA in ozonation was also shown in literature [155]. Kasprzyk-Hordern et al. [155] stated that PFOA catalyzed ozonation required 25 times lower ozone dosage than sole ozonation. The consumption of less O<sub>3</sub> was due to the use of O<sub>3</sub> with a greater efficiency in the presence of PFOA. The ozonation by-products were more resistant to oxidation by ozone only than the dye molecules so that the TOC removal was low in the non-catalytic ozonation. PFOA enhanced the reaction rate of by-products with ozone on the PFOA surface. Also, the non-polar catalytic phase increased the stability of O<sub>3</sub> in the aqueous solution preventing it from the decomposition [32,35]. Then, PFOA favoured the direct reaction of ozone with the organics in the bulk phase and on the catalyst surface.

Table 5.37. The effect of catalyst dosage on the TOC removal and  $Cons_{O_3}$ . Conditions:  $Q_G = 150$  L/h,  $Q_L = 150$  L/h, pH = 2.5,  $C_{O_3,G,in} = 1.42 \pm 0.13$  mmol/L gas,  $C_{D,in} = 22.4 \times 10^{-2}$  mmol/L for *RBBR*,  $C_{D,in} = 26.4 \times 10^{-2}$  mmol/L for *AR-151*, reactor =FBR,  $H_S = 7.5$  cm, for catalyst = Alumina,  $u_{L,min} = 130$  L/h,  $H_E = 12.6$  cm, for catalyst =PFOA,  $u_{L,min} = 110$  L/h,  $H_E = 13.4$  cm.

Catalyst	$m_{cat}$ , g	Dye	TOC Removal, %	$Cons_{O_3}$ mmol O <sub>3</sub> /L liq
-	-	<i>RBBR</i>	7.3	1.309
		<i>AR-151</i>	8.7	1.256
Alumina	25	<i>RBBR</i>	17.6	1.148
		<i>AR151</i>	16.3	1.021
	75	<i>RBBR</i>	21.3	0.993
		<i>AR151</i>	28.3	1.132
	125	<i>RBBR</i>	26.2	0.959
		<i>AR151</i>	32.6	1.062
PFOA	25	<i>RBBR</i>	16.1	1.181
		<i>AR151</i>	21.7	1.111
	75	<i>RBBR</i>	18.4	1.150
		<i>AR151</i>	33.2	1.100
	125	<i>RBBR</i>	23.0	1.021
		<i>AR151</i>	38.5	1.091



(a)



(b)

Figure 5.50. The effect of catalyst dosage on the dye removal. Conditions:  $Q_G=150$  L/h,  $Q_L=150$  L/h, pH=2.5,  $C_{O_3,G,in} = 1.42 \pm 0.13$  mmol/L gas,  $C_{D,in} = 22.4 \times 10^{-2}$  mmol/L for RBBR,  $C_{D,in} = 26.4 \times 10^{-2}$  mmol/L for AR-151, (a) alumina, (b) PFOA, reactor =FBR,  $H_S = 7.5$  cm, for catalyst = Alumina,  $u_{L,min} = 130$  L/h,  $H_E = 12.6$  cm, for catalyst =PFOA,  $u_{L,min} = 110$  L/h,  $H_E = 13.4$  cm.

Table 5.38. Calculated  $R_{cons,O_3}$  and  $U_{O_3}$  values for the dyes. Conditions:  $Q_G=150$  L/h,  $Q_L=150$  L/h, pH= 2.5,  $C_{O_3,G,in}=1.42\pm 0.13$  mmol/L gas,  $C_{D,in}=22.4\times 10^{-2}$  mmol/L for *RBBR*,  $C_{D,in}=26.4\times 10^{-2}$  mmol/L for *AR-151*, reactor =FBR,  $H_S=7.5$  cm, for catalyst = Alumina,  $u_{L,min}=130$  L/h,  $H_E=12.6$  cm, for catalyst =PFOA,  $u_{L,min}=110$  L/h,  $H_E=13.4$  cm.

Catalyst	$m_{cat}$ , g	Dye	$R_{cons,O_3}$ , %	$U_{O_3}$ (dye), mmol dye/mmol $O_3$	$U_{O_3}$ (TOC), mmol TOC/mmol $O_3$
-	-	<i>RBBR</i>	91.0	0.135	0.262
		<i>AR-151</i>	87.6	0.142	0.404
Alumina	25	<i>RBBR</i>	77.2	0.137	0.743
		<i>AR151</i>	73.6	0.136	0.973
	75	<i>RBBR</i>	69.8	0.170	0.992
		<i>AR151</i>	80.1	0.143	1.466
	125	<i>RBBR</i>	67.9	0.174	1.318
		<i>AR151</i>	76.2	0.174	1.903
PFOA	25	<i>RBBR</i>	85.4	0.130	0.644
		<i>AR151</i>	77.9	0.162	1.147
	75	<i>RBBR</i>	82.5	0.136	0.736
		<i>AR151</i>	77.6	0.186	1.888
	125	<i>RBBR</i>	75.9	0.169	1.090
		<i>AR151</i>	77.8	0.200	2.283

Kasprzyk-Hordern et al. [33-35] reported also that the effect of PFOA was small on the degradation of some organics which showed less resistivity toward oxidation by ozone. In this study also, in the presence of PFOA catalyst, the dye removal was lower but TOC removal was higher than those obtained in sole ozonation (Figures 5.42 and 5.43, Table 5.27). It can be concluded that the sole ozonation was beneficial for the degradation of organics which could be easily oxidized by ozone such as dye molecules while the PFOA catalyzed ozonation showed its efficiency on the resistant organics toward  $O_3$  such as most of the ozonation by-products. According to Kasprzk-Hordern et al. [33-35], PFOA was capable of adsorbing both ozone and resistant organics onto its surface and the oxidation of such organics occurred on the catalyst surface mainly. Since ozone was more stabilized on the PFOA surface, the oxidation efficiency of organics resistant to ozone was higher on the non-polar phase of PFOA. Also, the higher solubility of  $O_3$  in non-polar phase than in polar phase such as water resulted in more degradation of the resistant organics toward ozone.

### 5.6.6 Catalyst properties

The surface properties of alumina and PFOA catalysts before and after the dye ozonation process were characterized by the Surface Electron Microscopy (SEM) analysis realized in Metallurgy and Materials Engineering at M.E.T.U and and Fourier Transform Infrared (FT-IR) Spectroscopy analysis realized in the Central Laboratory of M.E.T.U.

The *FT-IR* spectra of the fresh calcined alumina and fresh PFOA are shown in Figures 5.51 and 5.52. On the surface of the fresh calcined alumina, there were peaks at 1379, 1394, 1505 and 1624  $\text{cm}^{-1}$ . The peak at 1637  $\text{cm}^{-1}$  could be attributed to the presence of moisture in the sample. The peaks at 1379, 1394 and 1505  $\text{cm}^{-1}$  might include several bands of OH stretching of surface groups [158, 214].

On the surface of PFOA prepared from calcined alumina, there were peaks at 1205, 1244  $\text{cm}^{-1}$  showing C-F stretching bonds, and peaks at 1313, 1358, 1398  $\text{cm}^{-1}$  coming from the calcined alumina [158]. Also, a peak at 1661  $\text{cm}^{-1}$  was observed and that band could represent C=O vibration on the PFOA [158]. Additionally, a peak at 1145  $\text{cm}^{-1}$  showed the C-C bond on the PFOA surface. Since, PFO acid contained C-F, C-C and C=O groups, those observed peaks represented the impregnation of PFO acid onto alumina surface.

The used catalysts were analyzed after the dye ozonation process. There was a peak at 2848  $\text{cm}^{-1}$  probably showing C-H stretching bond. This peak came from a surface adsorbed ozonation intermediate. A sharp peak at 1700-1800  $\text{cm}^{-1}$  might be due to the C=O vibrations on the alumina surface, resulting from a carboxylic acid produced on the alumina surface [158].

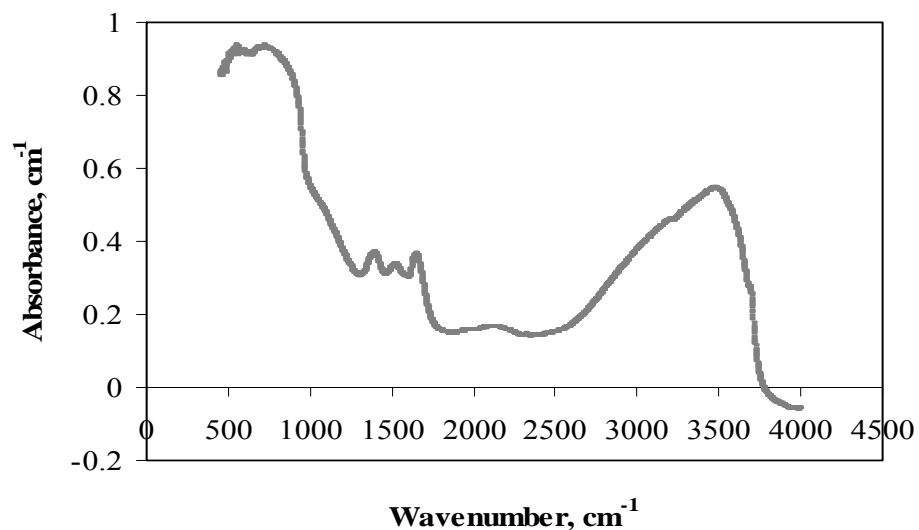


Figure 5.51 *FT-IR* spectra of fresh calcined alumina.

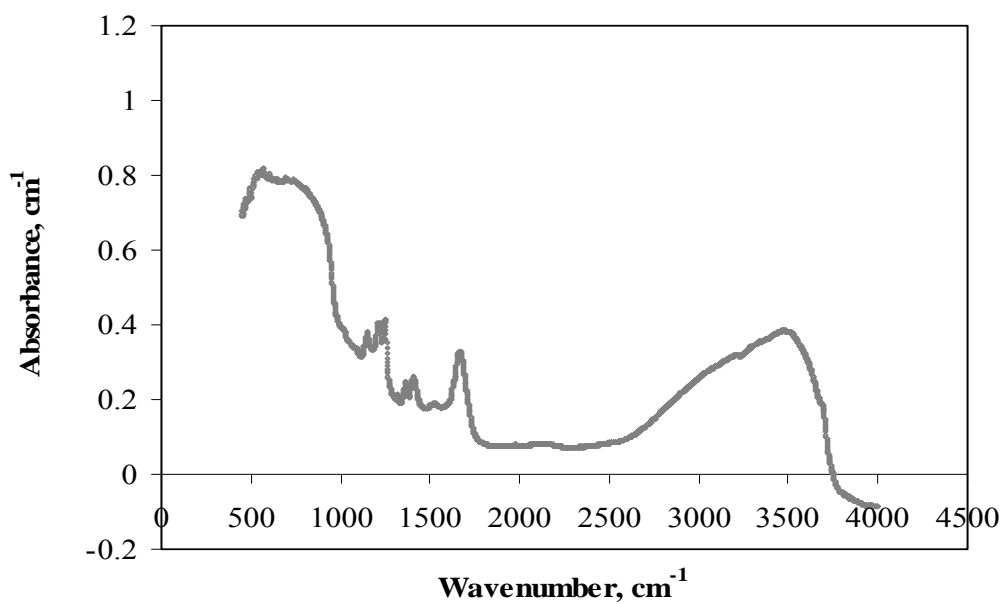


Figure 5.52 *FT-IR* spectra of fresh PFOA.

The FT-IR studies were realized for the used PFOA also. The spectra of used PFOA in *RBBR* ozonation is shown in Figure 5.53. The spectra contained peaks at 1143, 1151, 1367 cm<sup>-1</sup>, showing C-F stretching vibrations. In addition, the peak at 1637 cm<sup>-1</sup> was attributed to the C=O vibration coming both the PFO acid and the carboxylic acid by-

product of dye ozonation on the PFOA surface. New peak was appeared at  $2331\text{ cm}^{-1}$  after using the PFOA in the *RBBR* ozonation process. That peak represented OH stretching of organic intermediates produced during *RBBR* ozonation. The same peak was observed at  $2342\text{ cm}^{-1}$  in the ozonation of *AR-151* solution although the peak intensity was lower than that in PFOA used for *RBBR* ozonation (Figure 5.54). Therefore, on the PFOA surface, some by-products or intermediates containing OH stretching groups were produced. They were probably, carboxylic types of by-products. The C=O stretching peaks of those carboxylic groups were interfered with the peaks of PFO acid.

The spectrum of PFOA after ozonation experiments showed that during ozonation no change of the peaks representing the PFOA occurred (Figures 5.53 and 5.54). It can be concluded from the FT-IR studies, ozonation did not deactivate the PFOA catalyst. The existence of C-F bonds on the used PFOA indicated that ozone did not oxidize C-F bond.

#### **5.6.7 The effect of catalyst dosage on the concentrations of ozonation by-products**

The by-products of *AR-151* and *RBBR* ozonation were investigated in the presence of the catalysts at different catalyst dosages. Figures 5.55 and 5.56 show the change of oxalic acid (OA), acetic acid (AA), and formic acid (FA) concentrations with the catalyst dosage. Contrary to the sole ozonation results, glyoxalic acid (GA) was not produced during alumina- or PFOA-catalyzed ozonations. Instead, FA was produced during the catalytic ozonation process. As seen in Figures 5.55c and 5.56c, FA was observed at the higher catalyst dosages of 75 and 125 g, especially (15 and 25 g/L). The disappearance of glyoxalic acid from the solution and formation of formic acid revealed that probably some GA was oxidized to FA in the presence of the catalysts. Also, the reduction of GA concentration in parallel to the TOC degradation showed that some GA was mineralized to  $\text{CO}_2$  and  $\text{H}_2\text{O}$  in the process with the presence of the catalyst.

In the catalytic ozonation, especially with PFOA, the produced concentration of OA was observed higher than those found in the non-catalytic ozonation. The OA concentration increased with the increasing catalyst dosage for both of the catalysts. Therefore, the production of OA was enhanced by the presence of the catalysts. Since

OA was also found as a by-product in the sole ozonation of *RBBR* and *AR-151* dyes and its concentration changed with the catalyst dosage, the production of oxalic acid in the catalytic ozonation case occurred both in the bulk phase and on the catalyst surface.

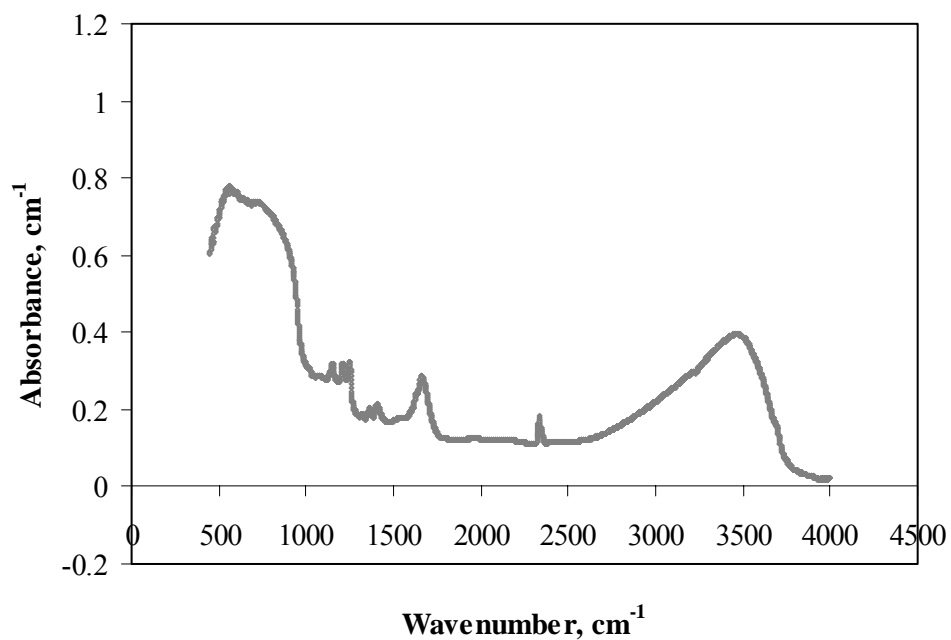


Figure 5.53 *FT-IR* spectra of PFOA used in *RBBR* ozonation in the FBR.

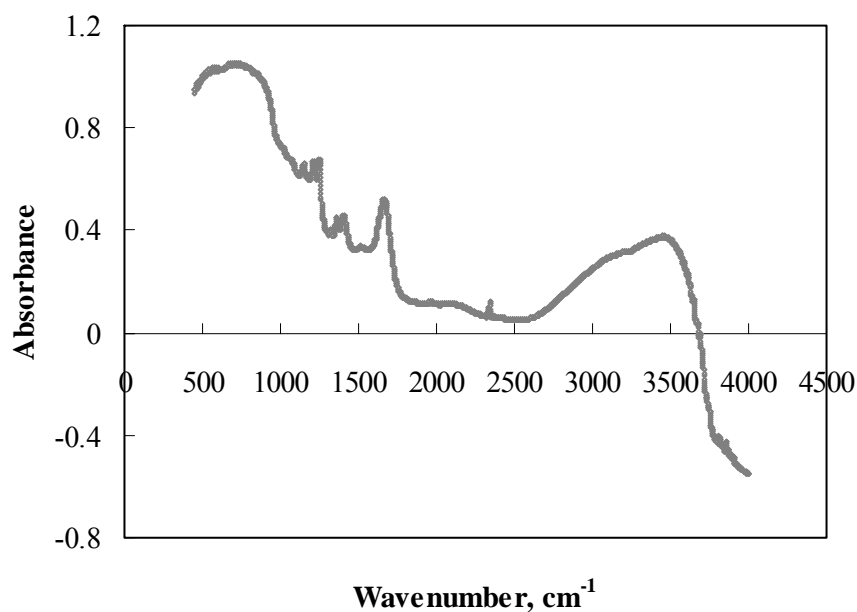
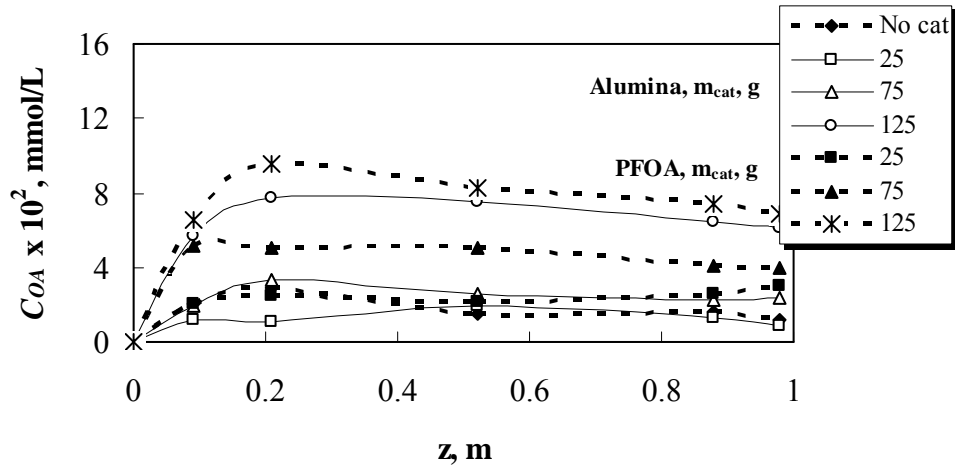
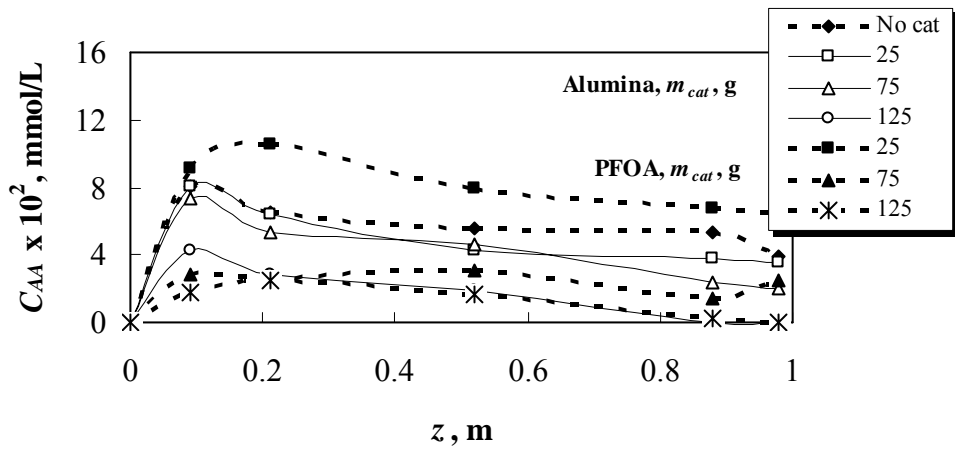


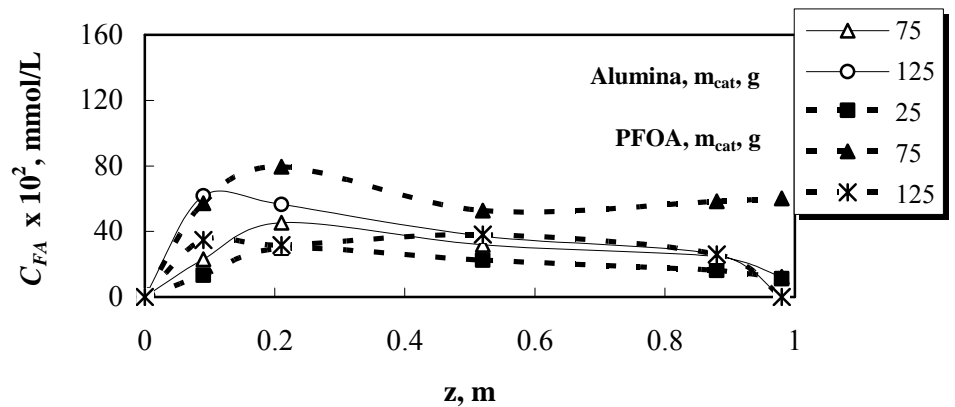
Figure 5.54 *FT-IR* spectra of PFOA used in *AR-151* ozonation in the FBR.



(a)



(b)

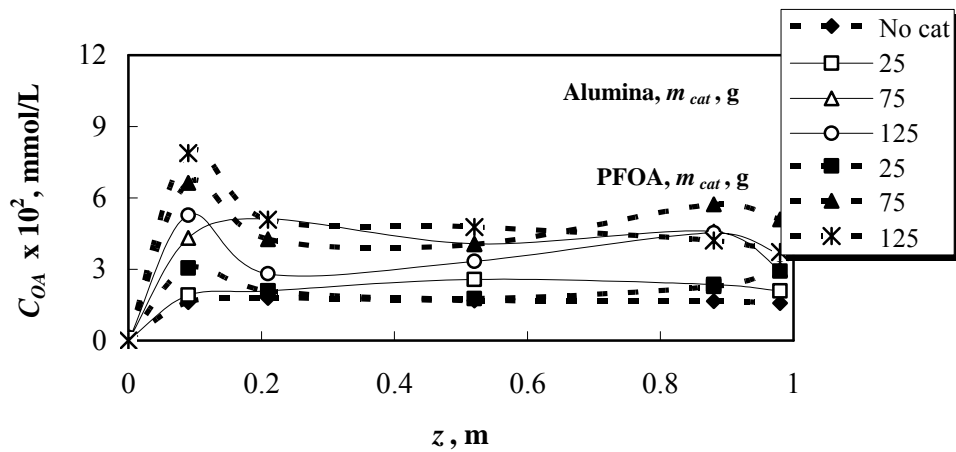


(c)

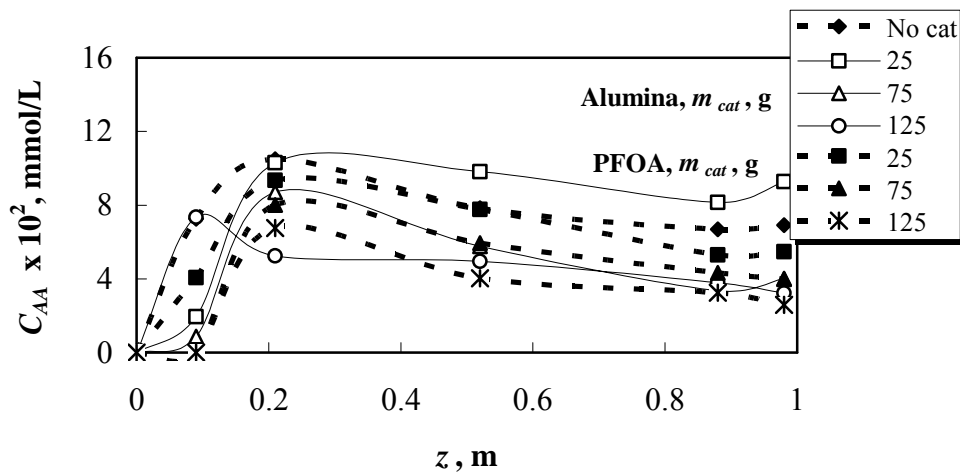
Figure 5.55. The by-products at different catalyst dosages. Conditions:  $Q_G = 150$  L/h,  $Q_L = 150$  L/h, pH = 2.54,  $T = 22.3^\circ\text{C}$ , dye = RBBR,  $C_{O_3,G,in} = 0.902 \pm 0.017$  mmol  $\text{O}_3/\text{L}$  gas,  $C_{D,in} = 4.8 \times 10^{-2}$  mmol/L, (a) OA, (b) AA, (c) FA, reactor = FBR,  $H_S = 7.5$  cm, for catalyst = Alumina,  $u_{L,min} = 130$  L/h,  $H_E = 12.6$  cm, for catalyst = PFOA,  $u_{L,min} = 110$  L/h,  $H_E = 13.4$  cm.

OA was produced in significant amounts in the presence of PFOA. This suggested in PFOA-catalyzed ozonation led to stable by-products such as OA. That was also shown in the literature. Kasprzyk-Hordern et al. [35] observed the increase of by-product concentration with PFOA catalyzed ozonation. However, they highlighted that OA, having two polar carboxylic groups, on the PFOA surface might cause the decrease of the hydrophobicity of PFOA. But, the high polarity of OA might also result in the desorption of it from the PFOA surface to the bulk liquid. The desorption of OA from the PFOA surface probably caused the increase of its concentration in the bulk. Then, a slight decrease of OA concentration was observed. Some OA molecules were oxidized by ozone during the catalytic ozonation process.

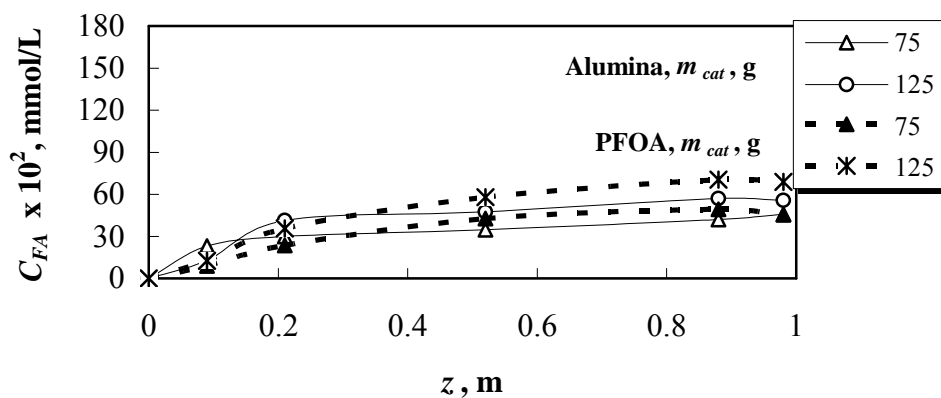
Acetic acid concentration increased at the initial heights of the column, where the dye and ozone molecules were encountered and then, tended to decrease. The formation rate of AA was higher than the elimination rate at the beginning but it reversed at the higher column heights since the elimination rate was increased due to the oxidation of AA by ozone and formation rate was lower due to the increased concentrations of AA. The oxidation of AA required the cleavage of C-C bond and that resulted in the degradation of AA molecule to CO<sub>2</sub> and H<sub>2</sub>O as stated Fontainer et al. [171]. As a result, the reduction in TOC was observed during this degradation. Besides, the production of CO<sub>2</sub> and H<sub>2</sub>O, Fontainer et al. [171] showed that AA might produce FA during its oxidation.



(a)



(b)



(c)

Figure 5.56. The by-products at different catalyst dosages. Conditions:  $Q_G = 150$  L/h,  $Q_L = 150$  L/h, pH = 2.54,  $T = 22.3^\circ\text{C}$ , dye = AR-151,  $C_{O_3,G,in} = 0.902 \pm 0.017$  mmol  $O_3$ /L gas,  $C_{D,in} = 6.6 \times 10^{-2}$  mmol/L, (a) OA, (b) AA, (c) FA, reactor = FBR,  $H_S = 7.5$  cm, for catalyst = Alumina,  $u_{L,min} = 130$  L/h,  $H_E = 12.6$  cm, for catalyst = PFOA,  $u_{L,min} = 110$  L/h,  $H_E = 13.4$  cm.

## 5.7. Modelling results of the dye ozonation experiments

The ozone absorption with simultaneously occurring chemical reaction between ozone and dye was modeled according to the modeling procedure explained in section 3.4 for the non-catalytic and catalytic ozonation processes. From the comparison of the predicted dye and ozone concentrations in the liquid phase with those obtained from the experiments, the enhanced volumetric mass transfer coefficient  $[(k_{La})_E]$ , enhancement factor ( $E$ ) and Hatta number ( $Ha$ ) were obtained.

### 5.7.1 Non-catalytic ozonation

The enhanced  $k_{La}$  values were found for the experiments at different inlet dye concentrations, gas and liquid flow rates. As shown previously, the change of  $Q_G$  and  $Q_L$  affected  $k_{La}$  values significantly in ozone absorption process. The mass transfer rate was higher at the higher  $Q_G$  and lower  $Q_L$  yielding the higher  $k_{La}$  values. These results showed the possible effect of mass transfer in the dye ozonation process at different operating conditions.

The calculated  $(k_{La})_E$  values are presented in Tables 5.39-5.41 at different conditions. The presence of the chemical reaction enabled higher  $k_{La}$  compared to ozone absorption only. Therefore, it can be said that mass transfer was enhanced by the presence of chemical reaction in the column. The enhancement was more remarkable with the increase of  $Q_L$  (comparing the  $E$  values in Tables 5.40 and 5.41). At the condition in which  $Q_L = 250$  L/h, ozonation of the *RBBR* molecules was limited compared to the experimental conditions at  $Q_L = 30$  L/h, and the dye molecules were in excess compared to ozone molecules. Due to the higher dye concentrations in the column, the effect of reaction kinetics was more dependent on the mass transfer.

Inlet dye concentration in gas-liquid operations played an important role in the enhancement of mass transfer [113]. Hatta number, a dimensionless parameter that compares the maximum possible reaction rate in the gas-liquid film to the maximum rate of physical absorption, represented the level of the enhancement. For a second order reaction like ozonation of organics, Hatta number ( $Ha$ ), was a function of the reactant concentration (dye concentration) and since the reactant concentration changed along the column height, Hatta number changed with  $z$  also. For this reason, the  $Ha$  values

were calculated for the average dye concentrations in the column. As shown,  $E$  and  $Ha$  were increased with the increase of inlet dye concentration as a result of the dependency of  $Ha$  to the inlet dye concentration (Equation 2.12). The rate of chemical reaction was increased by the increase of inlet dye concentration in the case of dye ozonation.  $Ha$  was calculated between 0.04-0.103 for *RBBR* and *AR-151* ozonation. This showed that especially at the higher inlet dye concentrations, the mass transfer of ozone from gas to liquid phase was enhanced by the chemical reaction.

Table 5.39. The determined enhanced  $k_{La}$  and  $E$  values at different conditions. No catalyst,  $Q_G = 150$  L/h,  $Q_L = 30$  L/h,  $Q_G/Q_L = 5.0$ .

Dye	$C_{O_3, G, in}$ , mmol/L gas	$C_{D, in} \times 10^2$ , mmol/L	$D_L \times 10^3$ , m <sup>2</sup> /s	$(k_{La})_E \times 10^2$ , s <sup>-1</sup>	$E$	$Ha$
-	0.306	0.0	1.2	9.6	-	-
<i>RBBR</i>	0.277	4.8	1.2	9.3	0.97	0.040
	0.319	9.6	1.2	9.8	1.02	0.057
	0.319	14.4	1.0	10.9	1.14	0.069
	0.313	19.2	0.9	12.6	1.31	0.080
	0.323	6.6	1.6	10.1	1.05	0.046
<i>AR-151</i>	0.306	13.2	1.4	13.6	1.43	0.065
	0.292	19.8	1.0	14.6	1.52	0.079
	0.308	26.4	1.0	15.2	1.58	0.092

It is known that if  $Ha < 0.02$ , the reaction is very slow and occurs in the bulk; if  $0.02 < Ha < 2$ , reaction is in intermediate level compared to mass transfer, can occur both in the bulk and in the film and if  $Ha > 2$ , the reaction is a fast reaction occurring in the film [113,114]. According to the calculated  $Ha$  values, the ozonation reaction in the column was carried both in the bulk and in the film. The reaction at those conditions was in the intermediate regime. Both of the kinetic and mass transfer resistances were found significant in the results modeling of the ozonation process. The comparison of the predicted and experimental results at several conditions is shown in Figures 5.57-5.60. The graphs at the other conditions are presented in Appendix H.

Table 5.40. The determined enhanced  $k_{La}$  and  $E$  values at different conditions. No catalyst,  $Q_G = 70$  L/h,  $Q_L = 30$  L/h,  $Q_G/Q_L = 2.3$ .

Dye	$C_{O_3, G, in}$ , mmol/L gas	$C_{D, in} \times 10^2$ , mmol/L	$D_L \times 10^3$ , m <sup>2</sup> /s	$(k_{La})_E \times 10^2$ , s <sup>-1</sup>	$E$	$Ha$
-	0.296	0.0	3.6	4.8	-	-
	0.336	4.8	3.5	5.1	1.06	0.038
<i>RBBR</i>	0.334	9.6	3.8	5.5	1.15	0.042
	0.343	14.4	3.6	5.8	1.21	0.055
	0.354	19.2	3.2	7.6	1.58	0.076
<i>AR-151</i>	0.334	8.3	3.0	5.4	1.13	0.044
	0.345	13.2	3.2	6.0	1.25	0.051
	0.351	19.8	3.7	6.4	1.33	0.062
	0.347	26.4	3.2	7.5	1.56	0.087

Table 5.41. The determined enhanced  $k_{La}$  and  $E$  values at different conditions. No catalyst,  $Q_G = 70$  L/h,  $Q_L = 250$  L/h,  $Q_G/Q_L = 0.28$ .

Dye	$C_{O_3, G, in}$ , mmol/L gas	$C_{D, in} \times 10^2$ , mmol/L	$D_L \times 10^3$ , m <sup>2</sup> /s	$(k_{La})_E \times 10^2$ , s <sup>-1</sup>	$E$	$Ha$
-	0.281	0.0	6.5	1.4	-	-
<i>RBBR</i>	0.332	4.8	6.5	1.5	1.07	0.058
	0.298	9.4	6.2	1.7	1.21	0.074
	0.317	14.4	5.8	2.3	1.64	0.088
	0.343	19.2	5.9	2.7	1.93	0.103
<i>AR-151</i>	0.324	6.6	7.2	1.3	0.93	0.041
	0.312	13.6	6.8	1.5	1.07	0.069
	0.318	19.8	6.9	1.9	1.36	0.085
	0.330	26.4	6.7	2.2	1.57	0.098

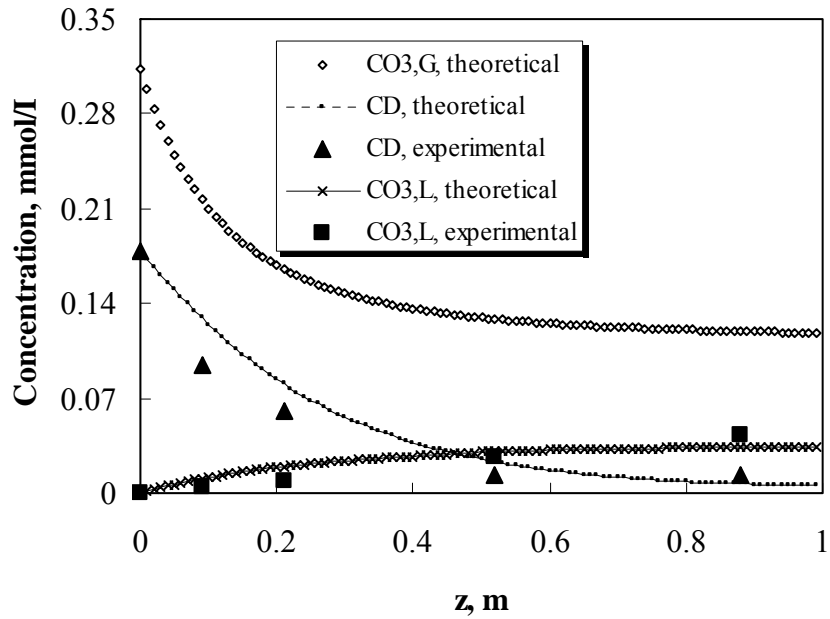


Figure 5.57 The comparison of theoretical and experimental steady state liquid phase ozone and dye concentrations for the best fit of  $D_L$  and  $k_L a$  values. Conditions:  $Q_G = 150$  L/h,  $Q_L = 30$  L/h, Dye = *RBBR*,  $C_{D,in} = 17.8 \times 10^{-2}$  mmol/L,  $T = 23^\circ\text{C}$ ,  $C_{O_3,G,in} = 0.313$  mmol  $\text{O}_3/\text{L}$  gas, no catalyst,  $D_L = 0.9 \times 10^{-3}$   $\text{m}^2/\text{s}$ ,  $k_L a = 12.6 \times 10^{-2}$   $\text{s}^{-1}$ .

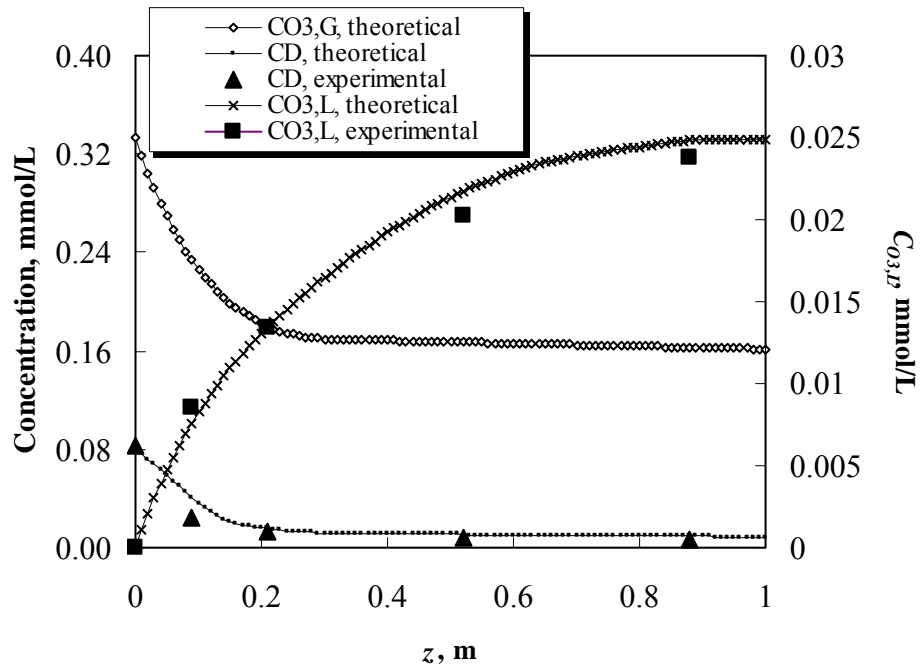


Figure 5.58 The comparison of theoretical and experimental steady state liquid phase ozone and dye concentrations for the best fit of  $D_L$  and  $k_L a$  values. Conditions:  $Q_G = 70$  L/h,  $Q_L = 30$  L/h, Dye = *AR-151*,  $C_{D,in} = 8.3 \times 10^{-2}$  mmol/L,  $T = 23^\circ\text{C}$ ,  $C_{O_3,G,in} = 0.334$  mmol  $\text{O}_3/\text{L}$  gas, no catalyst,  $D_L = 3.0 \times 10^{-3}$   $\text{m}^2/\text{s}$ ,  $k_L a = 5.4 \times 10^{-2}$   $\text{s}^{-1}$ .

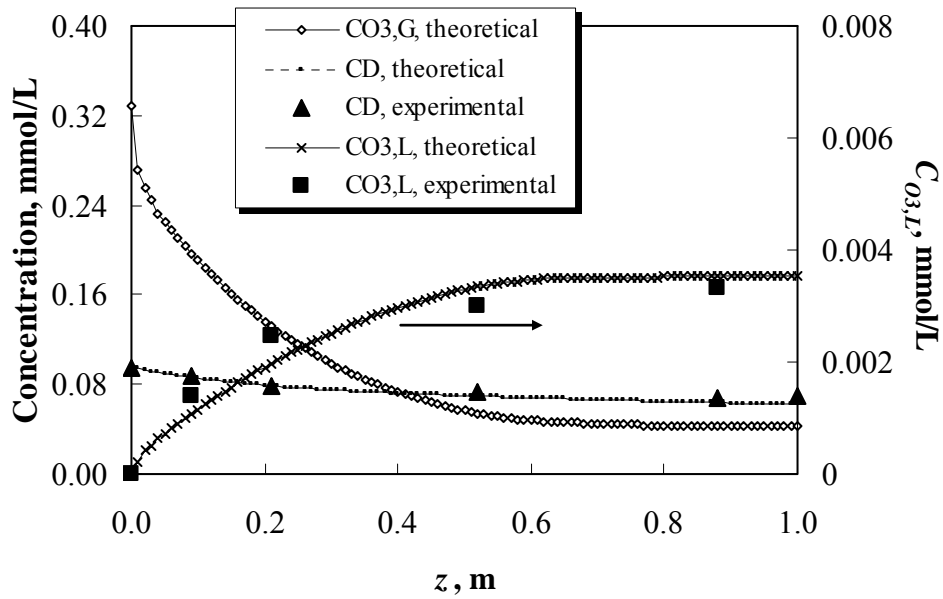


Figure 5.59 The comparison of theoretical and experimental steady state liquid phase ozone and dye concentrations for the best fit of  $D_L$  and  $k_L a$  values. Conditions:  $Q_G = 70$  L/h,  $Q_L = 250$  L/h, Dye = *RBBR*,  $C_{D,in} = 9.4 \times 10^{-2}$  mmol/L,  $T = 23^\circ\text{C}$ ,  $C_{O_3,G,in} = 0.332$  mmol  $\text{O}_3/\text{L}$  gas, catalyst = no,  $D_L = 6.2 \times 10^{-3}$   $\text{m}^2/\text{s}$ ,  $k_L a = 1.7 \times 10^{-2}$   $\text{s}^{-1}$ .

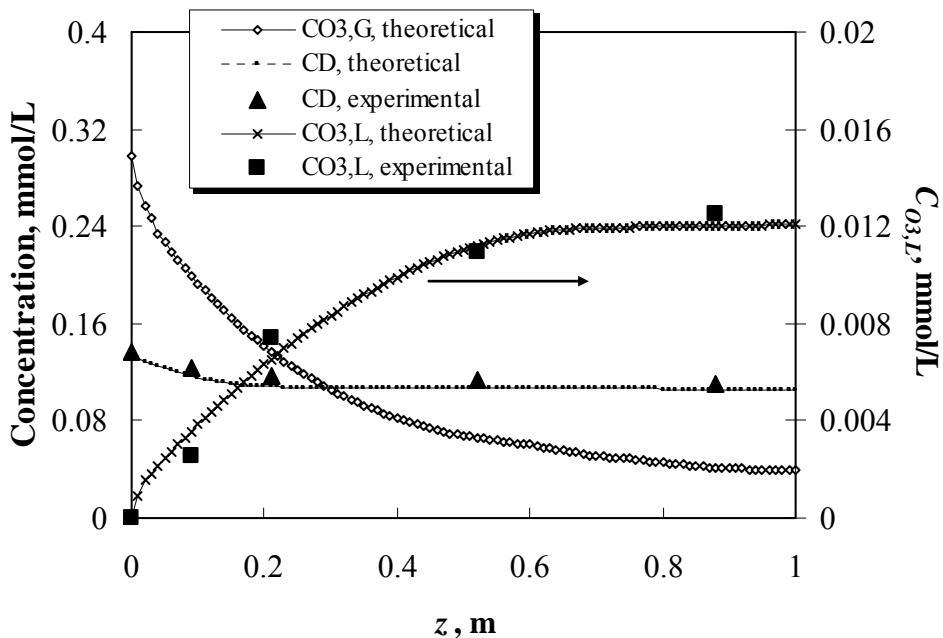


Figure 5.60 The comparison of theoretical and experimental steady state liquid phase ozone and dye concentrations for the best fit of  $D_L$  and  $k_L a$  values. Conditions:  $Q_G = 70$  L/h,  $Q_L = 250$  L/h, Dye = *AR-151*,  $C_{D,in} = 13.6 \times 10^{-2}$  mmol/L,  $T = 23^\circ\text{C}$ ,  $C_{O_3,G,in} = 0.298$  mmol  $\text{O}_3/\text{L}$  gas, no catalyst,  $D_L = 6.8 \times 10^{-3}$   $\text{m}^2/\text{s}$ ,  $k_L a = 1.5 \times 10^{-2}$   $\text{s}^{-1}$ .

### 5.7.2 Catalytic ozonation

The modeling equations were written for the catalytic dye ozonation in the presence of alumina or PFOA catalyst. For alumina catalyst, an additional ozone decomposition term was added to the mass balance equation for ozone in the liquid phase. This term was included also in the modeling of experiments at pH=7 and pH=10. The enhanced  $k_{LA}$  values were found for the experiments at different catalyst dosages and pH.

The calculated  $(k_{LA})_E$  values are presented in Tables 5.42 and 5.43 at different catalyst dosages for *AR-151* and *RBBR* dyes. In the experiments with the catalyst addition, it was found that the  $(k_{LA})_E$  was enhanced compared to non-catalytic conventional ozonation. In the conventional ozonation the calculated  $E$  values were 1.04 and 1.08 for the dye *RBBR* at  $C_{D,in} = 4.8 \times 10^{-2}$  mmol/L and  $19.2 \times 10^{-2}$  mmol/L, respectively. For *AR-151*, those values were obtained as 0.96 and 1.01 at  $C_{D,in} = 6.6 \times 10^{-2}$  mmol/L and  $26.4 \times 10^{-2}$  mmol/L, respectively. Those values were increased to 1.42 and 1.45 for *RBBR*; 1.45 and 1.53 for *AR-151* in the presence of 125 g PFOA catalyst. The enhancement factor was increased by the increase of the  $m_{cat}$  mainly due to the increase of  $(k_{LA})_E$  as presented before in Table 5.11.

Table 5.42. The determined enhanced  $k_{LA}$  and  $E$  values at different conditions. Dye= *RBBR*, pH = 2.5,  $Q_G = 150$  L/h,  $Q_L = 150$  L/h,  $Q_G/Q_L = 1.0$ ,  $D_L = 3.15 \times 10^{-3}$  m<sup>2</sup>/s,  $C_{O_3,G,in} = 0.969$  mmol/L gas,  $k_{LA} = 7.6 \times 10^{-2}$  s<sup>-1</sup>.

$C_{D,in} \times 10^2$ , mmol/L	Catalyst	$m_{cat}$ , g	$(k_{LA})_E \times 10^2$ , s <sup>-1</sup>	$E$
4.8	-	-	7.9	1.04
19.2			8.2	1.08
4.8	Alumina	25	8.4	1.11
19.2			8.7	1.14
4.8	Alumina	75	8.2	1.08
19.2			8.5	1.12
4.8	Alumina	125	9.1	1.20
19.2			9.9	1.30
4.8	PFOA	25	10.6	1.39
19.2			10.9	1.43
4.8	PFOA	75	10.2	1.34
19.2			10.7	1.41
4.8	PFOA	125	10.8	1.42
19.2			11.0	1.45

Table 5.43. The determined enhanced  $k_{La}$  and  $E$  values at different conditions. Dye= AR-151, pH = 2.5,  $Q_G$ = 150 L/h,  $Q_L$  = 150 L/h,  $Q_G/Q_L$  = 1.0,  $D_L$  =  $3.15 \times 10^{-3}$  m<sup>2</sup>/s,  $C_{O_3,G,in}$  = 0.969 mmol/L gas,  $k_{La}$  =  $7.6 \times 10^{-2}$  s<sup>-1</sup>.

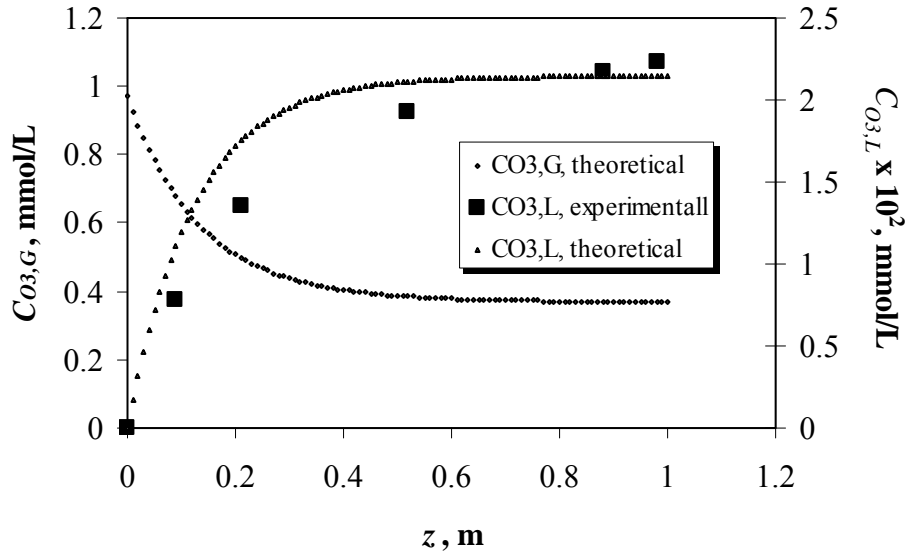
$C_{D,in} \times 10^2$ , mmol/L	Catalyst	$m_{cat}$ , g	$(k_{La})_E \times 10^2$ , s <sup>-1</sup>	$E$
6.6	-	-	7.3	0.96
26.4			7.7	1.01
6.6	Alumina	25	7.6	1.00
26.4			8.1	1.07
6.6	Alumina	75	8.4	1.11
26.4			8.9	1.17
6.6	Alumina	125	9.1	1.20
26.4			10.5	1.28
6.6	PFOA	25	9.3	1.22
26.4			10.2	1.34
6.6	PFOA	75	9.7	1.28
26.4			10.2	1.34
6.6	PFOA	125	11.0	1.45
26.4			11.6	1.53

The enhancement was more remarkable with the PFOA catalyst. Since PFOA had a lower density, the fluidization of the PFOA particles was easier than alumina particles and the mass transfer coefficient was enhanced by the presence of PFOA greatly. The effect of initial dye concentration had a slight effect on the enhancement factor, therefore it can be said that the effect of chemical reaction on the enhancement of the mass transfer rate was insignificant.

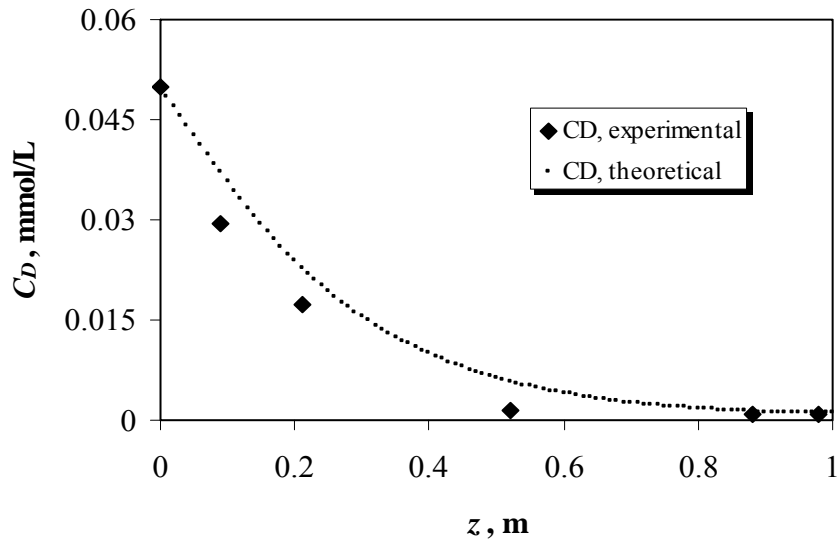
The increase of mass transfer rate due to the presence of the catalysts showed its effect on the TOC degradation significantly. More O<sub>3</sub> transferred to the bulk solution was consumed for the other organic pollutants such as ozonation by-products instead of the dye molecules. In other words, catalytic ozonation enhanced the degradation of ozonation intermediates by increasing the mass transfer rate of ozone.

The comparison of the predicted and experimental results at several conditions is shown in Figures 5.61-5.62. The experimental and modeling results of the dye and dissolved O<sub>3</sub> concentrations seemed to fit acceptably well. But, the dye and dissolved O<sub>3</sub> concentrations obtained from the model were slightly higher than those of experimental values. In the modeling, the dye concentration on the catalyst surface was accepted to be

equal to the dye concentration in the bulk solution since it was assumed that the dye concentration in the bulk was much higher than the dissolved  $O_3$  concentration. However, this fact did not happen at especially low concentrations of the dye.



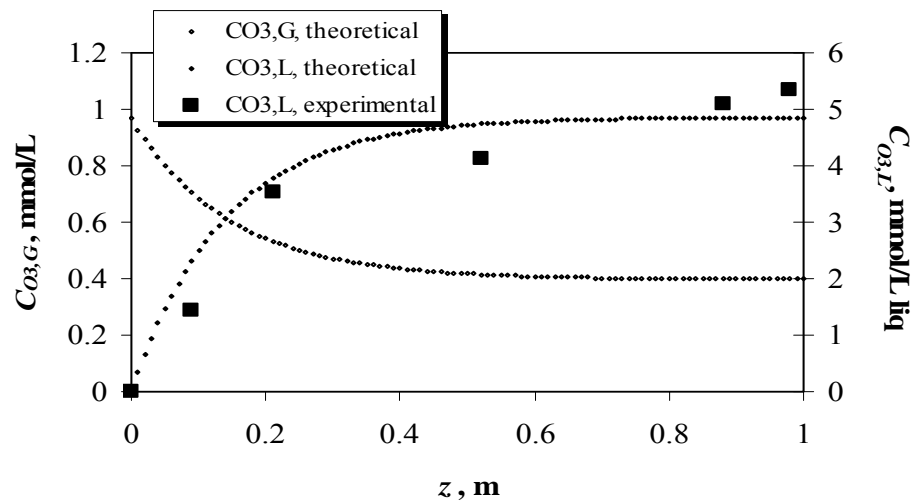
(a)



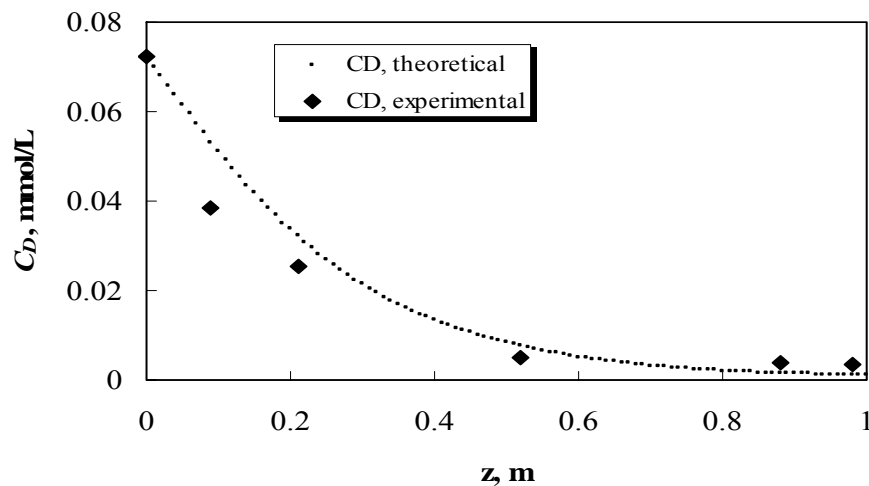
(b)

Figure 5.61. The comparison of predicted and experimental dye and  $O_3$  concentration values in dye ozonation. Conditions: Dye= *RBBR*,  $pH = 2.5$ ,  $Q_G = 150$  L/h,  $Q_L = 150$  L/h,  $Q_G/Q_L = 1.0$ ,  $D_L = 3.15 \times 10^{-3}$  m<sup>2</sup>/s,  $C_{O_3,G,in} = 0.969$  mmol/L gas,  $C_{D,in} = 5.0 \times 10^{-2}$  mmol/L, catalyst = PFOA,  $m_{cat} = 25$  g,  $(k_L a)_E = 10.6 \times 10^{-2}$  s<sup>-1</sup>. (a)  $C_D$ , (b)  $C_{O_3}$ .

The enhancement of  $k_L a$  was found for the catalytic ozonation experiments at pH 7 and 10. The results are presented in Table 5.44. The enhancement was much higher at pH=7 and 10 in the presence of alumina than that obtained at pH=2.5. That was probably due to the enhancement of ozone decomposition by the increase of pH even with alumina. The enhancement values with PFOA-ozonation were not affected by the pH change significantly. With PFOA, ozone decomposition was limited and ozone was stabilized partially even at pH = 7 and 10. Therefore, the effect of ozone decomposition was negligible.



(a)



(b)

Figure 5.62. The comparison of predicted and experimental dye and O<sub>3</sub> concentration values in dye ozonation. Conditions: Dye= AR-151, pH = 2.5,  $Q_G = 150$  L/h,  $Q_L = 150$  L/h,  $Q_G/Q_L = 1.0$ ,  $D_L = 3.15 \times 10^{-3}$  m<sup>2</sup>/s,  $C_{O_3,G,in} = 0.966$  mmol/L gas,  $C_{D,in} = 7.2 \times 10^{-2}$  mmol/L, catalyst = PFOA,  $m_{cat} = 25$  g,  $(k_L a)_E = 9.3 \times 10^{-2}$  s<sup>-1</sup>. (a) C<sub>D</sub>, (b) C<sub>O<sub>3</sub></sub>.

Table 5.44. The determined enhanced  $k_{La}$  and  $E$  values at different conditions.  $Q_G=150$  L/h,  $Q_L=150$  L/h,  $Q_G/Q_L=1.0$ ,  $D_L=3.15\times 10^{-3}$  m<sup>2</sup>/s,  $C_{O_3,G,in}=0.969$  mmol/L gas,  $m_{cat}=125$  g,  $k_{La}=7.6 \times 10^{-2}$  s<sup>-1</sup>.

Dye	pH	$C_{D,in} \times 10^2$ , mmol/L	Catalyst	$(k_{La})_E \times 10^2$ , s <sup>-1</sup>	$E$	
<i>RBBR</i>	7.0	19.2	-	7.7	1.01	
	10.0			8.5	1.12	
<i>AR-151</i>	7.0	26.4		7.1	0.93	
	10.0			8.1	1.07	
<i>RBBR</i>	7.0	19.2		Alumina	9.2	1.21
	10.0				10.5	1.38
<i>AR-151</i>	7.0	26.4	10.2		1.34	
	10.0		10.9		1.43	
<i>RBBR</i>	7.0	19.2	PFOA		10.0	1.32
	10.0				11.2	1.47
<i>AR-151</i>	7.0	26.4		11.1	1.46	
	10.0			11.0	1.45	

The values used in the modeling of catalytic ozonation reactions are given in Tables 5.45 and 5.46 for alumina and PFOA. The order of magnitude analysis were performed for the non-catalytic and catalytic ozonation reactions to find the importance of the mass transfer kinetic resistances. The results of the order of magnitude analysis are given in Appendix I.3. In the non-catalytic ozonation, the effect of the order of the mass transfer of ozone between the gas-liquid phase was the highest comparing the effects of other constituents. This showed that the transfer of ozone from gas to liquid phase occurred fast. The order of the magnitude of the chemical reaction affected the process almost (1/10) of the order of the gas-liquid mass transfer. The decrease of gas flow rate and increase of liquid flow rate resulted in the decrease of the effect of the gas-liquid mass transfer on the process. Meanwhile, the effect of chemical reaction gained importance.

In the catalytic ozonation, the order of the magnitude of liquid-solid mass transfer was calculated as much more higher than the orders of other resistances. This meant that the transfer of ozone from liquid to solid phase occurred very fast yielding no significant resistance. The other resistances were almost in the same order.

Table 5.45. The values used in the modeling of catalytic ozonation reactions. Conditions:  $Q_G = 150$  L/h,  $Q_L = 150$  L/h,  $T = (22.0 \pm 0.9)^\circ\text{C}$ ,  $C_{O_3,G,in} = 0.969$  mmol  $\text{O}_3/\text{L}$  gas, catalyst = Alumina,  $u_{L,min} = 130$  L/h,  $D_L = 3.15 \times 10^{-3}$   $\text{m}^2/\text{s}$ .

Dye	$C_{D,in} \times 10^2$ , mmol/L	$m_{cat}$ , g	$m$ , $\text{g}/\text{m}^3$	$k'_R \times 10^3$ , $\text{m}^3/(\text{g}\cdot\text{s})$	$k_s a_s \times 10^4$ , $\text{m}^3/(\text{g}\cdot\text{s})$	$(k_{LA})_E \times 10^2$ , $\text{s}^{-1}$
RBBR	4.8	25	5000	1.224	5.48	8.4
	19.2			4.896		8.7
	4.8	75	15000	1.224	6.17	8.2
	19.2			4.896		8.5
	4.8	125	25000	1.224	8.90	9.1
	19.2			4.896		9.9
AR-151	6.6	25	5000	1.564	5.48	7.6
	26.4			6.257		8.1
	6.6	75	15000	1.564	6.17	8.4
	26.4			6.257		8.9
	6.6	125	25000	1.564	8.90	9.1
	26.4			6.257		10.5

Table 5.46. The values used in the modeling of catalytic ozonation reactions. Conditions:  $Q_G = 150$  L/h,  $Q_L = 150$  L/h,  $T = (22.0 \pm 0.9)^\circ\text{C}$ ,  $C_{O_3,G,in} = 0.969$  mmol  $\text{O}_3/\text{L}$  gas, catalyst = PFOA,  $u_{L,min} = 110$  L/h,  $D_L = 3.15 \times 10^{-3}$   $\text{m}^2/\text{s}$ .

Dye	$C_{D,in} \times 10^2$ , mmol/L	$m_{cat}$ , g	$m$ , $\text{g}/\text{m}^3$	$k'_R \times 10^3$ , $\text{m}^3/(\text{g}\cdot\text{s})$	$k_s a_s \times 10^4$ , $\text{m}^3/(\text{g}\cdot\text{s})$	$(k_{LA})_E \times 10^2$ , $\text{s}^{-1}$
RBBR	4.8	25	5000	1.757	3.60	10.6
	19.2			7.027		10.9
	4.8	75	15000	1.757	4.70	10.2
	19.2			7.027		10.7
	4.8	125	25000	1.757	5.08	10.8
	19.2			7.027		11.0
AR-151	6.6	25	5000	1.868	3.60	9.3
	26.4			7.471		10.2
	6.6	75	15000	1.868	4.70	9.7
	26.4			7.471		10.2
	6.6	125	25000	1.868	5.08	11.0
	26.4			7.471		11.6

## CHAPTER 6

### CONCLUSIONS

In this study, ozonation and catalytic ozonation of Acid Red-151 (*AR-151*) and Remazol Brilliant Blue-R (*RBBR*) dyes were examined in a semi-batch and a fluidized bed reactors with or without alumina and perfluorooctylalumina (PFOA) catalysts. The effect of operating variables such as gas flow rate, liquid flow rate, inlet dye concentration, inlet ozone concentration, pH, catalyst dosage and catalyst particle size on the dye removals, chemical oxygen demand/total organic carbon (COD/TOC) removals, and ozone ( $O_3$ ) consumption per liter of wastewater were investigated. Models were developed for the ozone absorption and non-catalytic or catalytic dye ozonation processes.

Following conclusions were drawn according to the results obtained in the semi-batch studies:

1. Ozonation of the *RBBR* and *AR-151* aqueous solutions in the presence of alumina, or PFOA catalysts containing different amounts of perfluorooctanoic (PFO) acid resulted in dye removals up to 98-99%, depending on the pH and catalyst type. Catalytic ozonation with alumina or PFOA was a very effective method to remove both the dye and COD from the wastewaters containing textile dyes. Increasing the amount of PFO acid in PFOA catalyst enhanced its catalytic activity producing more alkyl chains on the alumina surface.
2. Ozone decomposition was enhanced by alumina at pH=13, yielding the highest COD removal for *AR-151* in the semi-batch reactor. For *RBBR*, the most effective catalyst was PFOA at pH=13 with respect to COD removal.
3. The non-catalytic and catalytic ozonations with alumina or PFOA followed a pseudo-first order reaction kinetics with respect to dye concentration. The pseudo-first order kinetic constants depended on the reaction pH and decreased generally by the addition of the catalysts into the ozonation system. The reaction rate constant was significantly affected by the increase of inlet dye concentration ( $C_{D,i}$ ) in *AR-151*

ozonation, whereas the rate constants decreased slightly with the increase of  $C_{D,i}$  in the ozonation of *RBBR* solutions.

4. At pH=13, the dye ozonation rate was lower in the presence of PFOA since ozone decomposition reactions were inhibited by PFOA
5. PFOA was found as a more effective catalyst for the ozonation of the *RBBR* dye due to the lower polarity of this dye than that of the *AR-151* dye.

The experiments in the FBR revealed the following conclusions:

1. The number of *CSTRs* to model the fluidized bed column in the absence and presence of the particles decreased with the increase of  $u_G$  and  $u_L$  due to the increasing turbulence in the column. The relationship between  $D_L$  and  $u_L$  was linear for all the studied gas velocities in non-catalytic process. In the catalyzed process, the relationship between  $D_L$  and  $u_L$  was exponential at the higher liquid velocities.
2. The column behaved almost as 2 or 3 *CSTRs* in series depending on the gas and liquid flow rates in the absence of the catalyst particles. The presence of the catalyst particles in the column resulted in higher axial dispersion coefficients showing a better mixing of the liquid phase. The column could be modeled with its behavior close to that of one-*CSTR* or two-*CSTRs* in series depending on  $Q_G$  and  $Q_L$ , in the presence of the particles.
3. Higher gas velocities enabled the fluidization of particles more giving additional force to fluidize them. The pressure drop and minimum fluidization velocity for a given  $u_G$ , were increased in the case of alumina compared to those for PFOA. Higher liquid flow rates were needed to fluidize alumina.
4. At lower liquid velocities than the  $u_{L,\min}$  at a constant  $Q_G$ , the bed behaved like a packed bed. Contrarily, at higher liquid velocities, the reactor could be accepted as fluidized and the better fluidization occurred at the higher liquid velocity. the  $u_{L,\min}$  at  $Q_G = 150$  L/h was found at around  $6.1 \times 10^{-3}$  m/s ( $Q_L = 110$  L/h). At the same  $Q_G$ , the  $u_{L,\min}$  for alumina was around  $7.2 \times 10^{-3}$  m/s ( $Q_L = 130$  L/h). At lower liquid velocities than the  $u_{L,\min}$  at a constant  $Q_G$ , it was certain that the bed behaved like a packed bed. Contrarily, at higher liquid velocities, the reactor could be accepted as fluidized and the better fluidization occurred at the higher liquid velocity.

5. Based on the developed model for ozone absorption process,  $k_{LA}$  values at different gas and liquid flow rates and catalyst dosages were obtained where  $k_{LA}$  values increased with the increasing  $Q_G$ .
6. The effect of catalyst dosage was dominant at the fluidized conditions of the column. At  $Q_L= 30$  L/h,  $k_{LA}$  did not change significantly by the change of catalyst dosage, whereas at a higher  $Q_L$  (150 L/h), for fluidized conditions,  $k_{LA}$  increased remarkably with the increasing dosage of alumina or PFOA. At the catalyst dosage of 125 g (alumina and PFOA) increased  $k_{LA}$  1.52 and 1.58 times, respectively compared to those obtained in non-catalytic ozonation.
7. The volumetric mass transfer coefficient was mainly dependent on the gas flow rate. Increasing  $Q_G$  resulted in higher  $k_{LA}$  values whereas an increase in  $Q_L$  decreased  $k_{LA}$  slightly.
8. Without the catalyst particles, the dye and TOC removals obtained in the FBR were affected by the change of  $Q_G$  and  $Q_L$ . Higher dye and TOC removals were achieved at the higher  $Q_G$  and lower  $Q_L$ . The applied  $O_3$  dose and gas-liquid phase contact time were the significant parameters to yield higher dye and TOC removals in the absence of the catalysts.
9. Dye and TOC removal percentages were high at low inlet dye concentrations. In addition, more  $O_3$  was consumed for higher  $C_{D,i}$ . At  $Q_G=150$  L/h,  $Q_L=30$  L/h, sole ozonation achieved 99.4% dye removal of *RBBR* and 96.5% of *AR-151* for the lowest  $C_{D,in}$ . At those conditions, TOC removals were obtained as 17.9% for *RBBR* and 22.4% for *AR-151*.
10. Conventional ozonation without using alumina or PFOA catalyst was not effective to get high levels of TOC removals. Both the dye and TOC removals were positively affected by the increase of inlet  $O_3$  concentration at the high inlet dye concentrations. The increase of inlet  $O_3$  concentration was advantageous in the enhancement of dye and TOC removal percentages. However,  $O_3$  consumption was increased in such cases requiring more  $O_3$  to be produced, which would not be economical.
11. The increase of catalyst dosage did not affect the dye removal significantly at the low and high inlet dye concentrations [ $C_{D,in} = (4.8-19.2)\times 10^{-2}$  mmol/L for *RBBR* and  $C_{D,in} = (6.6-26.4)\times 10^{-2}$  mmol/L for *AR-151*]. However, the alumina or PFOA catalyzed ozonation was more effective for the TOC removal compared to the non-catalyzed ozonation. The use of alumina or PFOA in ozonation resulted in

- degradation of large sized organic pollutant molecules to smaller sized molecules and finally to carbon dioxide and water.
12. The forces applied to the particles during fluidization are gravitational force, buoyancy force and drag force. These forces and minimum fluidization velocity were not influenced by the catalyst dosage.
  13. The increase of TOC removal by the increase in catalyst dosage suggested that adsorption process on the alumina or PFOA particles was important during catalytic ozonation.
  14. The presence of alumina decomposed ozone in the system at the acidic pH and the TOC was removed significantly by the degradation of organic molecules by the radicals produced due to the catalytic effect of alumina on the ozone decomposition.
  15. The addition of alumina or PFOA significantly reduced the consumed  $O_3$  amount per liter of solution. PFOA-catalyzed ozonation yielded much lower  $O_3$  consumptions than those achieved in alumina-catalyzed ozonation.
  16. The sole ozonation was beneficial for the degradation of organics which could be easily oxidized by ozone such as dye molecules while the PFOA catalyzed ozonation showed its efficiency on the resistant organics toward  $O_3$  such as most of the ozonation by-products.
  17. The effect of internal mass transfer was almost negligible in the ozonation of dyes on the surface of alumina or PFOA catalyst, since the catalyst particle size did not change the degradation rate of the dyes or TOC. Therefore, the effectiveness factor was taken as 1.0 considering the reaction on the catalyst surface only.
  18. The degradation of *AR-151* or *RBBR* dye by  $O_3$  mainly occurred in the bulk solution since the catalyst dosage did not affect the removal rate of the dye significantly.
  19. The oxidative properties of ozone were improved by adding solid catalyst to the system. Alumina resulted in the production of  $O^\bullet$  radicals in the solution at the acidic pH and  $OH^\bullet$  radicals at the alkaline pH during ozonation increasing the efficiency of the system, whereas PFOA enhanced the stability and solubility of  $O_3$  both in the non-polar alkyl phase and in the aqueous phase.
  20. The enhanced  $k_{La}$  values were found for the non-catalytic dye ozonation. The results showed that  $k_{La}$  values were enhanced by the chemical reaction between ozone and dye molecules. The reaction occurred in both the bulk solution and at the gas-liquid interface according to the calculated *Hatta* values.

21. The reaction occurred in both bulk solution and at the gas-liquid interface according to the calculated *Hatta* values.
22. By the addition of the catalyst into the system, the liquid hold-up changed significantly. From the flow characteristics observed in the column, it can be said that the gas phase was dispersed in the liquid. The liquid phase was the continuous phase.
23. The agreement between experimental and predicted results from this modeling study was found to be satisfactory.

## CHAPTER 7

### RECOMMENDATIONS

The primary objective of this study was to realize the catalytic ozonation of *AR-151* and *RBBR* solutions in the presence of alumina and PFOA catalysts and to obtain an efficient treatment process of dye ozonation in terms of higher dye removal, higher TOC removal and lower ozone consumption than conventional ozonation. The prepared dye solutions were synthetic solutions which did not represent the real textile wastewaters accurately. Since ozonation efficiency is strongly influenced by the wastewater content, in terms of future research, the next step would be the ozonation of real textile wastewaters in the presence of alumina or PFOA catalyst.

Another consideration as the future work would be the optimization of the process parameters in terms of higher mass transfer of ozone, higher dye and TOC removals and lower ozone consumptions from the applied gas. Lower liquid flow rate was beneficial to get higher dye and TOC removals but as shown, the fluidization degree of the FBR, decreased by lowering  $Q_L$ . In other words, the fluidized bed reactor in which catalytic ozonation would occur, must be constructed such that the fluidization of the particles would be realized at the lower  $Q_L$  values than those studied in this work. In this respect, the inside diameter so the cross-sectional area of the reactor must be lowered to obtain higher liquid velocities.

In the models developed for this study in the non-catalytic and catalytic ozonation processes, the consumption of dissolved ozone in the liquid phase for the oxidation of ozonation by-products was underestimated. In the models, only the change of dye concentration with respect to axial direction was considered. However, as in especially catalytic ozonation, the oxidation of some by-products occurred. In a more developed model, a mass balance for the main ozonation by-products would give a better comparison of the experimental and theoretical results.

## REFERENCES

- [1] Eremektar, G. Tekstil Endüstrisi Atıksularında İnert KOİ Örnek Uygulama. İ.T.Ü. 5. Endüstriyel Kirlenme Kontrolü Sempozyumu, 1996.
- [2] Samsunlu, A. Türkiye’de Tekstil Endüstrisi Kullanılmış Suların Arıtma Durumu. Tekstil Endüstrisinde Çevre Koruma Srmpozyumu, 3. Türk-Alman Çevre Teknolojileri İşbirliği, Ankara, 1996.
- [3] Vandevivere, P.C., Bianchi, R., Verstraete, W. Treatment and Reuse of Wastewater from the Textile Wet-Processing Industry: Review of Emerging Technologies. *J. Chem. Technol. Biotechnol.* 72, 289-302, 1998.
- [4] Moore, S.B., Ausley, L.W. Systems Thinking and Green Chemistry in the Textile Industry: Concepts, Technologies and Benefits *J. Cleaner Production*, 12, 585-601, 2004.
- [5] World Bank. Textiles, Pollution Prevention and Abatement Handbook. Environment Department Washington D.C. 1998.
- [6] Hao, O.J., Kim, H., Chiang, P. Decolorization of Wastewater. *Critical Reviews in Environmental Science and Technology*, 30(4), 449-505, 2000.
- [7] Üstün, G.E., Solmaz, S.K. Bir Organize Sanayi Bölgesi Atıksu Arıtma Tesisinden çıkan Atıksuların Tarımsal Amaçlı Sulama Suyu Olarak Yeniden Kullanılabilirliğinin Araştırılması. *Ekoloji*, 15(62), 55-61, 2007.
- [8] Gahr, F., Hermanutz, F., Oppermann, W. Ozonation-An Important Technique to Comply with New German Laws for Textile Wastewater Treatment. *Wat. Sci. Technol.* 30, 255-263, 1994.
- [9] Tzitzis, M., Vayenas, D.V., Lyberatos G. Pretreatment of Textile Industry Wastewaters with Ozone. *Wat. Sci. Technol.* 29, 151-160, 1994
- [10] Carliell, C.M., Barclay, S.J., Naidoo, N., Buckley, C.A., Mulholland, D.A., Senior, E. Microbial Decolorization of a Reactive Azo Dye Under Anaerobic Conditions. *Wat. SA.* 21, 61-69. 1995.

- [11] Platzek. T., Lang, C., Grohmann,G., Gi, U. S., Baltes, W. Formation of a carcinogenic aromatic amine from an azo dye by human skin bacteria in vitro. *Hum. Exp. Toxicol.*, 18. 522-559, 1999.
- [12] ETAD Information Notice, German ban of use of certain azo compounds in some consumer goods. *Text. Chem. Color* 28, 11–13, 1996.
- [13] Hsu, Y., Yen, C., Huang H. Multistage Treatment of High Strength Dye Wastewater by Coagulation and Ozonation, *J. Chem. Technol. Biotechnol.*, 71, 71-76, 1998.
- [14] Muthukumar, M., Selvakumar, N. Studies on the Effect of Inorganic Salts on Decolorization of Acid DyeEffluents by Ozonation. *Dyes and Pigments*, 62, 221-228, 2004.
- [15] Neamtu, M., Yediler, A., Siminiceanu, I., Macoveanu, M., Kettrup, A. Decolorization of Disperse Red-354 Azo Dye in Water be Several Oxidation Processes-A Comparative Study *Dyes and Pigments*, 60(1), 61-68, 2004.
- [16] Eren, H.A., Anış, P. Tekstil Boyama Atıksularının Ozonlama ile Renk Giderimi *Uludağ Üniversitesi Mühendislik-Mimarlık Fakültesi Dergisi*, 11(1), 83-, 2006.
- [17] Jiang, H., Bishop, P.L. (1994) “Aerobic Biodegradation of Azo Dyes in iofilms” *Wat.Sci.Technol.*, 29(10/11), 525-530.
- [18] Özdemir, O., Armağan, B., Turan, M., Çelik, M.S. Comparison of the Adsorption Characteristics of Azo Reactive Dyes on Mesoporous Minerals. *Dyes&Pigments*, 62, 49-60, 2004.
- [19] O’neill, C., Hawkwes, F.R., Hawkwes, D.L. Esteves, S., Wilcox, S.J. Anaerobic-Aerobic Biotreatment of Simulated Textile Effluent Containing Varied Ratios of Starch and Azo Dye. *Wat. Res.*, 34(8), 2355-2361, 2000a.
- [20] Sarasa, J., Roche, M.P., Ormad, M.P., Gimeno, H., Puig, A., Ovelleiro, J.L. (1998) “Treatment of Wastewater Resulting from Dyes Manufacturing with Ozone and Chemical Coagulation” *Wat. Res.*, 32(9), 2721-2727.
- [21] Kocaer, F.O., Alkan, U. Boyar Madde İçeren Tekstil Atıksularının Arıtım Alternatifleri. *Uludağ Üni. Müh Mimarlık Fak. Dergisi*, 7(1), 47-55, 2002.

- [22] Daneshvar, N., Oladegaragoze, A., Djafarzadeh, N. Decolorization of basic dye solutions by electrocoagulation: An investigation of the effect of operational parameters. *J. Hazard. Mater.*, 129, 116-122, 2006.
- [23] Lorimer, J.P., Mason, T.J., Plattes, M., Phull, S.S., Walton, D.J. Degradation of dye effluent. *Pure Appl. Chem.*, 73, 1957-1968, 2001.
- [24] Slokar, Y.M., Marechal, A.M.L. Methods of Decoloration of Textile Wastewaters. *Dyes&Pigments*, 37(4), 335-356, 1998.
- [25] Churchley, J.H. (1994) "Removal of Dyewaste Color from Sewage Effluent-The Use of a Full Scale Ozone Plant" *Wat.Sci.Technol.*, 30(3), 275-284.
- [26] Liakou, S., Zissi, U., Kornaros, M., Lyberatos, G. Combined Chemical and Biological Treatment of Azo Dye Containing Wastewaters. *Chem. Eng. Communications*, 190, 645-661, 2003.
- [27] Gökçen, F., Özbelge, T.A. Pre-ozonation of Aqueous Azo Dye (Acid Red-151) Followed by Activated Sludge Process. *J. Chem. Eng.* 123(3), 109-115, 2006.
- [28] Cooper, C., Burch R. An Investigation of Catalytic Ozonation for the Oxidation of Halocarbons in Drinking Water Preparation. *Wat. Res.*, 33(18),3695-3700, 1999.
- [29] Ernst, M., Lurot, F., Schrotter, J. Catalytic Ozonation of Refractory Organic Model Compounds in Aqueous Solution by Aluminum Oxide. *Applied Catalysis B: Environmental*, 47, 15-25, 2004.
- [30] Beltran, F.J., Rivas, J., Espinosa, R.M. A  $TiO_2/Al_2O_3$  catalyst to improve the ozonation of oxalic acid in water. *Applied Catalysis B: Environmental*, 47(2), 101-109, 2004.
- [31] Hassan M., Hawkyard, C.J. Ferral-catalyzed Ozonation of Aqueous Dyes in a Bubble-column Reactor. *Catal. Communications*, 3, 281-286, 2002.
- [32] Kasprzyk-Hordern, B., Ziolk, M., Nawrocki, J. Catalytic Ozonation and Methods of Enhancing Molecular Ozone Reactions in Water Treatment. *Applied Catalysis*, 43, 639-669, 2004.

- [33] Kasprzyk-Hordern B., Dabrowska, A., Swietlik, J., Nawrocki, J. Ozonation Enhancement with non-Polar Bonded Alumina Phases. *Ozone Sci. Eng.*, 26, 367-380, 2004.
- [34] Kasprzyk-Hordern, B., Dabrowska, A., Swietlik, J., Nawrocki, J. The Application of the Perfluorinated Bonded Alumina Phase for Natural Organic Matter Catalytic Ozonation. *J. Environ. Eng. Sci.*, 3, 41-50, 2004.
- [35] Kasprzyk-Hordern, B., Andrzejewski, P., Dabrowska, A., Czaczyk, K., Nawrocki, J. MTBE, DIPE, ETBE and TAME Degradation in Water Using Perfluorinated Phases as Catalysts for Ozonation Process. *Applied Catalysis B: Environmental*, 51, 51-66, 2004.
- [36] Rice, R.G. and Netzer, A. Handbook of Ozone Technology and Applications, Vol. 1, Ann Arbor Science, Michigan, 1982.
- [37] Soares, O.S., Orfao, J., Portela, D., Vieira, A., Pereira, F.R. Ozonation of textile effluents and dye solutions under continuous operation: Influence of operating parameters. *J. Hazard. Mater.* 137(3), 1664-1673, 2006.
- [38] Eriksson, M. Ms. Thesis. Ozone chemistry in aqueous solution-ozone decomposition and stabilization, Department of Chemistry, Royal Institute of Technology, Sweden, 2005.
- [39] Hoigné, J., and Bader, H. The Role of Hydroxyl Radical Reactions in Ozonation Process in Aqueous Solutions. *Wat. Res.*, Vol. 10, 377-385, 1976.
- [40] Staehelin, J., and Hoigné, J. Decomposition of Ozone in Water: Rate of Initiation by Hydroxide Ions and Hydrogen Peroxide, *Env. Sci. Technol.*, Vol. 16, 676, 1982.
- [41] Staehelin, J. and Hoigne, J. Decomposition of Ozone in Water in the Presence of Organic Solutes Acting as Promoters and Inhibitors of Radical Chain Reactions. *Env. Sci. Technol.*, 19(12), 1206-1213, 1985.
- [42] Carriere, J., Jones, P., Broadbent, A.D. Decolorization of textile dye solutions. *Ozone Sci. Eng.*, 15, 189-200, 1993.
- [43] Forni, L., Bahnemann, D., and Hart, E.J. Mechanism of the Hydroxide Ion Initiated Decomposition of Ozone in Aqueous Solution. *J. Phys. Chem.*, 86, 255-259, 1982.

- [44] Gurol, M.D. and Singer, P.C. Kinetics of Ozone Decomposition: A Dynamic Approach. *Env. Sci. Technol.*, 16(7), 377-383, 1982.
- [45] Yurteri, C., and Gürol, M.D. Ozone Consumption in Natural Waters: Effects of Background Organic Matter, pH and Carbonate Species. *Ozone Sci. Eng.*, 10, 272-282, 1988a.
- [46] Lopez-Lopez, A., Pic, J.S., Debellefontaine, H. Ozonation of azo dye in a semi-batch reactor: A determination of the molecular and radical contributions, *Chemosphere*, 66(11), 2120-2126, 2007.
- [47] Poznyak, T., Colindres, P., Chairez, I. Treatment of textile industry dyes by simple ozonation with water recirculation. *J. Mex. Chem. Soc.*, 51(2), 81-86, 2007
- [48] Hoigne, J. and Bader, H. Rate Constants of Reactions of Ozone with Organic and Inorganic Compounds in Water-I. *Wat. Res.*, 17, 173-183, 1983a.
- [49] Hoigne, J. and Bader, H. Rate Constants of Reactions of Ozone with Organic and Inorganic Compounds in Water-II *Wat. Res.*, 17, 185-194, 1983b.
- [50] Ledakowicz, S., Maciejewska, J., Perkowski, J., Biń, A. Ozonation of reactive blue 81 in the bubble column. *Water Sci. Technol.* 47, 47-52, 2001.
- [51] Bailey, P.S. Ozonation in Organic Chemistry, Academic P., Inc., New York, 1982.
- [52] Legube, M., and Vel Leitner, N. Catalytic Ozonation: a Promising Advanced Oxidation Technology for Water Treatment. *Catalysis Today*, 53, 61-72, 1999.
- [53] Oyama, S.T. Chemical and Catalytic Properties of Ozone. *Catalysis Today*, 42(3), 279-322, 2000.
- [54] Zhang, F., Yediler, A., Liang, X. Decomposition pathways and reaction intermediate formation of the purified, hydrolyzed azo reactive dye C.I. Reactive Red 120 during ozonation. *Chemosphere*, 67(4), 712-717, 2007.
- [55] Pryor, W.A., Gleicher, G.J., Church, D.F. Reaction of polycyclic aromatic hydrocarbons with ozone. Linear free-energy relationships and tests of likely rate-determining steps using simple molecular orbital correlations. *J. Org. Chem.* 48, 4198-4202, 1983.

- [56] Zerbinati, O., Ostacoli, G., Gastaldi, D., Zelano, V. Determination and identification by high performance liquid chromatography and spectrofluorimetry of twenty-three aromatic sulphonates in natural waters. *J. Chromatograph*, 640, 231-240, 1993.
- [57] Rivera-Utrilla, J., Sa´nchez-Polo, M., Mondaca, M.A., Zaror, C.A. Effect of ozone and ozone/activated carbon treatments on genotoxic activity of naphthalenesulphonic acids. *J. Chem. Technol. Biotechnol.* 77, 883–890, 2002.
- [58] Guiza, M., Ouderni, A., Ratel, A. Decomposition of dissolved ozone in the presence of activated carbon: an experimental study. *Ozone Sci Eng* 26, 299-307, 2004.
- [59] Alaton, İ.A., Balcioğlu, İ.A., Bahnemann, D.W. Advanced oxidation of a reactive dyebath effluent: Comparison of O<sub>3</sub>, H<sub>2</sub>O<sub>2</sub>/UV-C and TiO<sub>2</sub>/UV-A processes. *Wat. Res.*, 36(5), 1143-1154, 2002.
- [60] Buxton, G.V., Greenstock, C.L., Helman, W.P., Ross, A.B. Critical review of rate constants for reaction of hydrated electrons, hydrogen atoms and hydroxyl radicals ( $HO^{\bullet}/O^{\bullet}$ ) in aqueous solution. *J. Phys. Chem. Ref. Data* 17, 513-886, 1988.
- [61] Alder, M.G., and Hill, G.R. The Kinetics and Mechanism of Hydroxide Ion Catalyzed Ozone Decomposition in Aqueous Solution *J. Am. Chem. Soc.*, 72, 1884-1886, 1950.
- [62] Hernandez-Alonso, M., Coronado, J., Maira, A., Loddo, V., Augugliaro, V. Ozone enhanced activity of aqueous titanium dioxide suspensions for photocatalytic oxidation of free cyanide ions. *Appl. Cata. B: Environ.*, 19, 59-65, 2002.
- [63] Legube B., Guyon S. Dore M. Ozonation of aqueous solutions of nitrogen heterocyclic compounds: benzotriazoles, atrazine and amitrole. *Ozone Sci. Eng* 9(3), 233-246, 1987.
- [64] Chen, L. Effects of Factors and Interacted factors on the Optimal Decolorization Process of Methyl Orange by Ozone. *Wat. Res.*, 34(3), 974-982, 2000.
- [65] Ertaş, T.T., Gürol, M.D. Oxidation of diethylene glycol with ozone and modified fenton processes", *Chemosphere*, 47(3), 293-301, 2002.
- [66] Wu, J., Wang, T. Ozonation of aqueous azo dye in a semi-batch reactor *Wat. Res.*, 35(4), 1093-1099, 2001.

- [67] Reckhow, D. A. The ozonation of organic halide precursors: The effect of bicarbonate. *Wat. Res.*, 20, 987- 994, 1986.
- [68] Pi Y., Ernst, M., Schrotter, J. Effect of phosphate buffer upon CuO/Al<sub>2</sub>O<sub>3</sub> and Cu(II) catalyzed ozonation of oxalic acid solution. *Ozone Sci. Eng.*, 25, 393-397, 2003.
- [69] Wang, C., Yediler, A., Lienert, D., Wang, Z., Kettrup, M. Ozonation of an azo dye C.I. *Remazol Black 5* and toxicological assessment of its oxidation products. *Chemosphere*, 52(7), 1225-1232, 2003.
- [70] Chu, W., Ma, C. Quantitative prediction of direct and indirect dye ozonation kinetics. *Wat. Res.*, 34 (12), 3153-3160, 2000.
- [71] Beltran, F.J., Rivas, F.J., Espinoza, R.M. Catalytic ozonation of oxalic acid in an aqueous TiO<sub>2</sub> slurry reactor. *Applied Catalysis B: Environ.*, 39, 221-231, 2002.
- [72] Shu H., and Chang, M. Decolorization effects of six azo dyes by O<sub>3</sub>, UV/O<sub>3</sub> and UV/H<sub>2</sub>O<sub>2</sub> processes. *Dyes and Pigments*, 64, 297-303, 2005.
- [73] Liakou, S., Kornaros, M., Lyberatos, G. Pretreatment of azo dyes using ozone. *Wat. Sci. Technol.*, 36(2-3), 155-163, 1997.
- [74] Liakou, S., Pavlou, S., Lyberatos, G. Ozonation of azo dyes", *Wat. Sci. Tech.*, 35(4), 279-286, 1997.
- [75] Muthukumar, M., Selvakumar, N., Venkata, J. Effect of dye structure on decolouration of anionic dyes by using ozone. In Proceedings of the 15th Ozone World Congress of International Ozone Association, London, United Kingdom, 410-421, 2001.
- [76] Muthukumar, M., Sargunamani, D., Selvakumar, N. Statistical analysis of the effect of aromatic, azo and sulphonic acid groups on decolouration of acid dye effluents using advanced oxidation processes. *Dyes and Pigments*, 65, 151-158, 2005.
- [77] Walling, C. Fenton's reagent revisited, *Acc. Chem. Res.* 8, 125-131 1975.
- [78] Snider, E.H., Porter, J.J. Ozone treatment of dye waste", *J. WPCF*, 46(5), 886-894, 1974.

- [79] Kornmüller, A., Karcher, S., Jekel, M. Cucurbituril for water treatment. Part II: Ozonation and oxidative regeneration of cucurbituril. *Wat. Res.*, 35(14), 3317-3324, 2001.
- [80] Koyuncu, İ., Afşar, H. Decomposition of dyes in the textile wastewater with ozone. *J. Environ. Sci. Health*, A31(5), 1035-1041, 1996.
- [81] Konsowa, A.H. Decolorisation of wastewater containing direct dye by ozonation in a batch bubble column reactor, *Desalination*, 158, 233-240, 2003.
- [82] Adams, C.D., Gorg, S. Effect of pH and gas-phase ozone concentration on the decolorization of common textile dyes. *J. Environ. Eng.*, 293-298, 2002.
- [83] Neamtu, M., Siminiceanu, I., Yediler, A., Kettrup, A. Kinetics of decolorization and mineralization of reactive azo dyes in aqueous solution by the UV/H<sub>2</sub>O<sub>2</sub> oxidation. *Dyes and Pigments*, 53, 93-99, 2002.
- [84] Balcıoğlu, I.A., Arslan, İ. Partial oxidation of Reactive Dyestuffs and Synthetic Textile Dye-Bath by the O<sub>3</sub> and O<sub>3</sub>/H<sub>2</sub>O<sub>2</sub> Processes. *Wat. Sci. and Technol.*, 43(2), 221-228, 2001.
- [85] Sarayu, K., Swaminathan, K., Sandhya, S. Assessment of degradation of eight commercial reactive azo dyes individually and in mixture in aqueous solution by ozonation. *Dyes&Pigments*, 75, 362-368, 2007.
- [86] Garcia-Montano, J., Domenech, X., Garcia-Hortal, J.A., Torrades, F., Peral, J. The testing of several biological and chemical coupled treatments for Cibacron Red FN-R azo dye removal. *J. Hazard. Mater.*, 154, 484-490, 2008.
- [87] Hsu, Y.C., Chen, J.T., Yang, H.C. Decolorization of Dyes Using Ozone in a Gas-Induced Reactor. *AIChE.*, 47(1), 169-176, 2001.
- [88] Hsu, Y.C., Chen, J.T., Yang, H.C., Chen, J.H., Fang, C.F. Ozone Decolorization of Mixed-Dye Solutions in a Gas-Induced Reactor *Wat. Env. Res.*, 73(4), 494-503, 2001.
- [89] Sevimli, M.F., Sarıkaya, H.Z. Ozone treatment of textile effluents and dyes: Effect of applied ozone dose, pH and dye concentration. *J. Chem Technol. Biotechnol.*, 77, 842-850, 2002.

- [90] Arslan, I., Balcioğlu, I.A. Oxidative Treatment of Simulated Dyehouse Effluent by UV near UV-assisted Fenton's Reagent. *Chemosphere*, 39(15), 2767-2783, 1999.
- [91] Arslan, I., Balcioğlu, I.A. Effect of Common Reactive Dye Auxiliaries on the Ozonation Dyehouse Effluents Containing Vinylsulphone and Aminochlorotriazine Dyes. *Desalination*, 130, 61-71, 2000.
- [92] Peleg, M. The Chemistry of Ozone in the Treatment of Water. *Wat. Res.*, 10, 361-365, 1976.
- [93] Yurteri, C., Gürol, M.D. Evaluation of Kinetic Parameters for the Ozonation of Organic Micropollutants. *Wat. Sci. Technol.*, 21, 465-473, 1988B.
- [94] Özbelge, T.A., Erol, F. Effects of pH, Initiator, Scavenger and Surfactant on the Ozonation Mechanism of an Azo Dye (Acid Red-151) in a Batch Reactor. *in press*
- [95] Kabdaşlı, I., Ölmez, T., Tünay, O. Factors affecting colour removal from reactive dye bath by ozonation. *Wat. Sci. Technol.*, 45(12), 261-270, 2002.
- [96] Arslan, I., Balcioğlu, I.A. Degradation of Remazol Black B Dye and Its Simulated Dyebath Wastewater by Advanced Oxidation Processes in Heterogeneous and Homogeneous Media. *Color Technol.*, 117, 38-42, 2001.
- [97] Chu, W., Chan, K.H., Graham, N.J.D. Enhancement of ozone oxidation and its associated processes in the presence of surfactant: degradation of Atrazine. *Chemosphere*, 64, 931-936, 2006.
- [98] Namboodri, C.G., Perkins, W.S., Walsh, W.K. Decolorizing dyes with chlorine and ozone: Part I. *American Dyestuff Reporter*, 34, 18-22, 1994a.
- [99] Stumm, W. The Solubility of O<sub>3</sub> in Aqueous Solution. *Helv. Chem. Acta*, 37, 773-778, 1954.
- [100] Sotelo, J.L., Benitez, F.J., Beltran-Heredia, J. Ozone Decomposition in Water: Kinetic Study. *Ind. Eng. Chem. Res.*, 26, 39- 43, 1987.
- [101] Yang Y.M. Effects of ozone mass transfer on the formation and control of volatile organic compounds in drinking water. Master's Thesis. Taipei: Graduate Institute of Environmental Engineering, National Taiwan University, 1991.

- [102] Andreozzi, R., Marotta, R., Sanchirico, R. Manganese-Catalysed Ozonation of Glyoxalic Acid in Aqueous Solutions. *J. Chem. Tech. Biotechnol.*, 75, 59-65, 2000.
- [103] Saunders, F., Gould, J.P., Southerland, C.R. The Effect of Solute Competition on Ozonolysis of Industrial Dyes. *Wat. Res.*, 17(10), 1407-1419, 1983.
- [104] Masten S.J., and Hoigne, J. Comparison of Ozone and Hydroxyl Radical-Induced Oxidation of Hydrocarbons in Water. *Ozone Sci. Eng.*, 14, 197-214, 1992.
- [105] Trapido, M., Veressinina, Y., Hentunen, J.K., Hirvonen, A. Ozonation of Chlorophenols: Kinetics, By-Products and Toxicity. *Environ.Technol.* 18, 325-332, 1997.
- [106] Özbelge, T.A., Erol, F., Özbelge, H. Ö. A Kinetic Study on the Decolorization of Aqueous Solutions of *Acid Red-151* by Ozonation. *J. Env. Eng. Sci. Health: Part A.* A38(8), 1607-1623, 2003.
- [107] Shu, H.Y., Huang, C.R. Degradation of Commercial Azo Dyes in Water Using Ozonation and UV-Enhanced Ozonation Process. *Chemosphere*, 31, 3813-3825, 1995.
- [108] Baawain, M.S., El-Din, M.G., Smith, D.W. Artificial neural networks modeling of ozone bubble columns: Mass transfer coefficient, gas liquid hold-up and bubble size. *Ozone Sci. Eng.*, 29, 343-352, 2007.
- [109] Dankwerts, P. Gas-liquid reaction. Mc-Graw Hill, New York, 1970.
- [110] Sullivan, D.E., Roth, J.A. Kinetics of self-decomposition of ozone in aqueous solution. *AIChE Symp. Ser.*, 76, 142, 1980.
- [111] Reinik, J., Jacobsson, K., Kallas, J. 2,4-Xylidine degradation with ozonation: Mass transfer and reaction kinetics. *Ozone Sci. Eng.*, 26, 499-509, 2004.
- [112] Benbelkacem, H., Mathe, S., Debellefontaine, H. Ozonation of crotonic acid solutions: Comparison of two methods for the determination of the rate constant. *Ozone Sci. Eng.*, 26, 415-427, 2004.
- [113] Levenspiel, O. Chemical Reaction Engineering, Wiley, New York, 1999.

- [114] Beltran, F.J., Gomez-Serrano, V., Duran, A. Degradation kinetics of *p*-nitrophenol ozonation in water. *Wat. Res.*, 26(1), 9-17, 1992.
- [115] Astarita, G. Mass transfer with chemical reaction, Elsevier, New York, 1967.
- [116] Zhou, H., Smith, D.W. Ozone mass transfer in water and wastewater treatment: Experimental observations using a 2D-laser particle dynamics analyzer. *Wat. Res.*, 34, 909-921, 2000.
- [117] Rosal, R., Rodriguez, A., Zerhouni, M. Enhancement of gas-liquid mass transfer during the unsteady-state catalytic decomposition of ozone in water. *App. Catal. A: General*, 305, 160-175, 2006.
- [118] Mitani, M. M., Keller, A.A., Sandall, O.C., Rinker, R.G. Mass transfer of ozone using a microporous diffuser reactor system. *Ozone Sci. Eng.*, 27, 45-51, 2005.
- [119] Velasquez, M.T., Ramirez, I.M. Combined pretreatment of coagulation-ozonation for saline-stabilized Landfill Leachates. *Ozone Sci. Eng.*, 28, 309-316, 2006.
- [120] Zhou, H., Smith, D.W. Modeling of dissolved ozone concentration profiles in bubble columns. *J. Environ. Eng.*, 120(4), 821-841, 1995.
- [121] Lin, S.H., Lin, C.M. Treatment of Textile Waste Effluents by Ozonation and Chemical Coagulation. *Wat. Res.*, 27(2), 1743-1748, 1993.
- [122] Lin, S.H., Lai, C.L. Kinetic Characteristics of Textile Wastewater Ozonation in Fluidized and Fixed Activated Carbon Beds. *Wat. Res.*, 34 (3), 763-772, 2000.
- [123] Hsu, Y., Yen, C., Huang H. Multistage Treatment of High Strength Dye Wastewater by Coagulation and Ozonation. *J. Chem. Technol. Biotechnol.*, 71, 71-76, 1998.
- [124] Koch, M., Yediler, A., Lienert, D., Insel, G., Kettrup, A. Ozonation of Hydrolyzed Azo Dye Reactive Yellow 84 (CI). *Chemosphere*, 46(1), 109-113, 2002.
- [125] Gül, Ş., Serindağ, O., Boztepe, H. Effects of Ozonation on COD Elimination of Substituted Aromatic Compounds in Aqueous Solution. *Türk J. Chem.*, 23, 21-26, 1999.

- [126] Singer, P.C. Assessing ozonation research need in water treatment. *J. Am. Water Works Assoc.*, 78-88, 1990.
- [127] Szpyrkowicz, L., Juzzolino, C., Kaul, S.N. A Comparative Study on Oxidation of Disperse Dyes by Electrochemical Process, Ozone, Hypochlorite and Fenton Reagent. *Wat. Res.*, 35(9), 2129-2136, 2001.
- [128] Hoigne, J., Bader, H. Ozonation of Water : Selectivity and Rate of Oxidation of Solutes. *Ozone Sci. Eng.*, 1, 73-85, 1979.
- [129] Glaze, W.H. The Chemistry of Water Treatment Processes Involving Ozone, Hydrogen Peroxide and Ultraviolet Radiation. *Ozone Sci. Eng.*, 9(4), 335-343, 1987.
- [130] Karimi, A.A., Redman, J.A., Glaze, W.H., Stolarik, G.F. Evaluating an AOP for TCE and PCE removal. *J. AWWA*, 89(8), 41-53, 1997.
- [131] Sapach, R., Viraraghavan, T. An introduction to the use of hydrogen peroxide and ultraviolet radiation: An advanced oxidation process. *J. Environ. Health A: Environmental*, 32(8), 2355-2366, 1997
- [132] Bandara, J., Nadtochenko, V., Kiwi, J., Pulgarin, C. Dynamics of oxidant addition as a parameter in the modeling of dye mineralization (Orange-II) via Advanced Oxidation Technologies. *Water. Sci. Technol.*, 35, 87-93, 1997.
- [133] Bellamy, W.D., Hickman, G.T., Mueller, P.A., Ziemba, N. Treatment of VOC-contaminated groundwater by hydrogen peroxide and ozone oxidation. *J. WPCF.*, 63(2), 120-128, 1991.
- [134] Glaze, W.L., Kang, J.W. Advanced oxidation processes. Description of a kinetic model for the oxidation of hazardous materials in aqueous media with ozone and hydrogen peroxide in a semibatch reactor. *Chem. Res.*, 28(11), 1573-1580, 1989.
- [135] Peyton, G.R. Significance and treatment of volatile organic compounds in water supplies. *Oxidative Treatment Methods for Removal of Organic Compounds from Drinking Water Supplies*, Lewis Publisher, 313-362, 1990.
- [136] Oğuz, E., Keskinler, B. Removal of colour and COD from synthetic textile wastewaters using O<sub>3</sub>, PAC, H<sub>2</sub>O<sub>2</sub>, and HCO<sub>3</sub><sup>-</sup>. *J. Hazard. Mater.*, 151, 753-760, 2008.

- [137] Acar, E., Özbelge, T.A. Oxidation of Acid Red 151 aqueous solutions by the peroxone process and its kinetic evaluation. *Ozone Sci. Eng.*, 28(3), 155-164, 2006.
- [138] Rosenfelt, E.J., Linden, K.G., Canonica, S., Gunten, U. Comparison of the efficiency of  $HO^\bullet$  radical formation during ozonation and the advanced oxidation processes  $O_3/H_2O_2$  and UV/ $H_2O_2$ . *Wat. Res.*, 40, 3695-3704, 2006.
- [139] Skorska, M.B., Davis, W.T. A critical evaluation of the ozone/UV technology for the treatment of water contaminated with organic pollutants. *47th Purdue Industrial Waste Conference Proceedings*, 293-299, 1992.
- [140] Fazzini, L., Young, J.C. Use of ozone and ultraviolet oxidation to enhance the biological degradation of refractory organics in Landfill Leachate. *49th Purdue Industrial Waste Conference Proceedings*, 253-262, 1994.
- [141] Colonna, G.M., Caronna, T. Oxidative degradation of dyes by ultraviolet radiation in the presence of hydrogen peroxide. *Dyes&Pigments*, 211-220, 1999.
- [142] Contreras, S., Rodriguez, M., Chamarro, E., Esplugas, S. UV-and UV/Fe(III)-enhanced ozonation of nitrobenzene in aqueous solution. *J. Photochemistry&Photobiology A: Chemistry*, 142, 79-83, 2001.
- [143] Gomes de Moraes, S., Freire, R.S., Duran, N. Degradation and toxicity reduction of textile effluent by combined photocatalytic and ozonation processes. *Chemosphere*, 40, 369-373, 2000.
- [144] Sauleda, R., Brillas, E. Mineralization of aniline and 4-chlorophenol in acidic solution by ozonation catalyzed with  $Fe^{+2}$  and UVA light. *Appl. Catal. B: Environ.*, 29, 135-145, 2001.
- [145] Ledakowicz, S., Solecka, M., Zylla, R. Biodegradation, decolourisation and detoxification of textile wastewater enhanced by advanced oxidation processes. *J. Biotechnology*, 89, 175-184, 2001.
- [146] Sadik, W.A., Nashed, A.W. UV-induced decolourization of acid alizarine violet N by homogeneous advanced oxidation processes. *J. Chem Eng.*, 137, 525-528, 2008.
- [147] Shu, H.Y. Degradation of dyehouse effluent containing C.I. Direct Blue 199 by processes of ozonation, UV/ $H_2O_2$  and in sequence of ozonation with UV/ $H_2O_2$ . *J. Hazard. Mater.*, B133, 92-98, 2006.

- [148] Jans, U., Hoigne, J. Activated carbon and carbon black catalyzed transformation of aqueous ozone into OH-radicals. *Ozone Sci. Eng.*, 20, 67-90, 1998.
- [149] Ma J., Graham N.J.D. Manganese-catalysed ozonation for the destruction of atrazine-Effect of humic substances. *Wat. Res.*, 33(3), 785-793, 1999.
- [150] Gül, Ş., Özcan, Ö., Erbatur, O. Ozonation of C.I. reactive red 194 and C.I.reactive yellow 145 in aqueous solution in the presence of GAC. *Dyes&Pigments*, 1-6, 2006.
- [151] Wu, C.H., Kuo, C.Y., Chang, C.L. Decolorization of Azo Dyes using Catalytic Ozonation. *React. Kinet. Catal. Lett.* 91(1), 161-168, 2007.
- [152] Leitner, N.K., Fu, H. pH effects on catalytic ozonation of carboxylic acids with metal on metal oxides catalysts. *Topics in Catal.*, 33, 249-256, 2005.
- [153] Talapad, T., Neramittagapong, A., Neramittagapong, S. Degradation of Congo Red Dye by Ozonation. *Chiang Mai J.Sci.* 35(1), 63-68, 2008.
- [154] Delanoe, F., Acedo, B., Leitner, N.K., Legube, B. Relationship between the structure of Ru/CeO<sub>2</sub> catalysts and their activity in the catalytic ozonation of succinic acid aqueous solutions. *Appl. Catal. B: Environ.*, 29, 315-325, 2001.
- [155] Kasprzyk-Hordern, B. Chemistry of Alumina, Reactions in Aqueous Solution and its Application in Water Treatment. *Adv. Colloid Interf. Sci.*, 110, 19-48, 2004.
- [156] Bulanin, K.M., Lavalley, J.C, Lamotte, J., Mariey, L., Tsyganenko, N.M., Tsiganenko, A.A. Infrared study of ozone adsorption on CeOT. *J. Phys. Chem. B*, 102, 6809-6816, 1998.
- [157] Kasprzyk-Hordern, B., Nawrocki, J. Preliminary Results on Ozonation Enhancement by a Perfluorinated Bonded Alumina Phase. *Ozone Sci. Eng.*, 24(1), 63-68, 2002.
- [158] Kasprzyk, B., Nawrocki, J. The Feasibility of Using a Perfluorinated Bonded Alumina Phase in the Ozonation Process. *Ozone Sci. Eng.*, 25, 185-197, 2003.
- [159] Kasprzyk-Hordern B., Raczky-Stanislawiak, U. Swietlik, J., Nawrocki, J. Catalytic Ozonation of Natural Organic Matter on Alumina. *Applied Catalysis B: Environmental*, 62, 345-358, 2005.

- [160] Kasprzyk-Hordern, B., Andrzejewski, P., Nawrocki, J. Catalytic Ozonation of Gasoline Compounds in Model and Natural Water in the Presence of Perfluorinated Alumina Bonded Phase. *Ozone Sci. Eng.*, 27, 301-310, 2005.
- [161] Bandara, J., Mielczarski, J.A., Kiwi, J. I. Adsorption Mechanism of Chlorophenols on Iron Oxides, Titanium Oxide and Aluminum Oxide as Detected by Infrared Spectroscopy. *Applied Catalysis B: Environmental*, 34, 307-320, 2001.
- [162] Ni C.H., Chen J.N. Heterogeneous Catalytic Ozonation of 2-Chlorophenol Aqueous Solution with Alumina as a Catalyst. *Wat. Sci. Technol.*, 43, 213-220, 2001.
- [163] Einaga H., Futamura, S. Catalytic Oxidation of Benzene with Ozone over Alumina-Supported Manganese Oxides. *J. Cat.*, 227, 304-312, 2004.
- [164] Volk C., Roche, P., Joret, J., Paillard, H. Comparison of the Effect of Ozone, Ozone-Hydrogen Peroxide System and Catalytic Ozone on the Biodegradable Organic Matter of a Fulvic Acid Solution. *Wat. Res.*, 31(3), 650-656, 1997.
- [165] Hassan, M.M., Hawkyard, C.J. Decolourisation of dyes and dyehouse effluent in a bubble-column reactor by heterogeneous catalytic ozonation. *J. Chem. Technol&Biotechnol.* 81, 201-207, 2006.
- [166] Trapido, M., Veressinina, Y., Munter, R., Kallas, J. Catalytic Ozonation of m-Dinitrobenzene. *Ozone Sci. Eng.*, 27, 359-363, 2005.
- [167] Andreozzi, R., Caprio, V., Insola, A., Marotta, R., Tufano, V. The use of manganese dioxide as a heterogeneous catalyst for oxalic acid ozonation in aqueous solution. *Appl. Catal. A General*, 138, 75-81, 1996.
- [168] Paillard, H., Dore, M., Bourbigot, M. Prospect concerning applications of catalytic ozonation in drinking water treatment, *In Proc. 10th Ozone World Congr.*, 313-331, 1991.
- [169] Al Hayek, N., Legube, B., Dore, M. Fe<sup>+3</sup>/Al<sub>2</sub>O<sub>3</sub>-catalysed ozonation of phenol and its ozonation by-product. *Environ. Technol. Letters* 10, 415-425, 1989.
- [170] Ping, T.S., Hua, L.W., Quing, Z.J., Nan, C.C. Catalytic ozonation of sulfosalicylic acid, *Ozone Sci Eng*, 24, 117-122, 2002.

- [171] Fontainer, V., Farines, V., Albet, J., Baig, S., Molinier, J. Oxidation of Organic Pollutants of Water to Mineralization by Catalytic Ozonation. *Ozone Sci. Eng.*, 27, 115-128, 2005.
- [172] Balcıoğlu, I.A., Tarlan, E., Kıvılcımdan, C., Saçan, M.T. Merits of ozonation and catalytic ozonation pretreatment in the algal treatment of pulp and paper mill effluents. *J. Environ. Management*, 85, 918-926, 2007.
- [173] Udrea, I., Bradu, C. Ozonation of substituted phenols in aqueous solutions over CuO/Al<sub>2</sub>O<sub>3</sub> catalyst. *Ozone Sci. Eng.*, 25, 335-343, 2003.
- [174] Ma, J., Sui, M., Zhang, T., Guan, C. *Wat. Res.*, 39, 779, 2005.
- [175] Kissa, E. Fluorinated surfactants: synthesis, properties, applications. Marcel Dekker Inc., New York, 1994.
- [176] Abe, Fluorinated surfactants: synthesis, properties, applications. Marcel Dekker Inc., New York, 1994
- [177] Zhu, X., Z., Xu, X. The mechanism of Fe(III)-catalyzed ozonation of phenol. *J. Zhejiang Univ. SCI*, 5(12), 1543-1547, 2004.
- [178] Gutowska, A., Kaluzna-Czaplinska, J., Jozwiak, W.K. Degradation mechanism of Reactive Orange 113 dye by H<sub>2</sub>O<sub>2</sub>/Fe<sup>+2</sup> and ozone in aqueous solution. *Dyes&Pigments*, 74, 41-46, 2007.
- [179] Lopez, A., Ricco, G., Tiravanti, G. Biodegradability Enhancement of Refractory Pollutants by Ozonation: A Laboratory Invesitigation on an Azo-dyes Intermediate. *Wat. Sci. Technol.*, 38, 239-245, 1998.
- [180] Dabrowska,A.,Kasprzyk-Hordern, B. Aldehydes formation during water disinfection by ozonation and chlorination proc. *J. Glob. NEST*, 7(1), 61-71, 2005.
- [181] Can, Z.S., Gürol, M. Formaldehyde formation during ozonation of drinking water. *Ozone Sci. Eng.*, 25, 41-51, 2003.
- [182] Song, S., Ying, H., He, Z., Chen, J. Mechanism of decolorization and degradation of C.I. Direct Red 23 by ozonation combined with sonolysis. *Chemosphere*, 66, 1782-1788, 2007.

- [183] Mascolo, G., Lopez, A., James, H., Fielding, M. By-products formation during degradation of isoproturan in aqueous solution. I: Ozonation. *Wat. Res.*, 35(7), 1695-1704, 2001.
- [184] Miltner, R.J., Shukairy, H.M., Summers, R.S. Disinfection by-product formation and control by ozonation and biotreatment. *J. Am. Water Works Assoc.*, 84(11), 53-62, 1992.
- [185] Demirev, A., Nenov, V. Ozonation of Two Acidic Azo Dyes with Different Substituents. *Ozone Sci. Eng.*, 27, 475-485, 2005.
- [186] Qu, J., Li, H., Liu, H., He, H. Ozonation of alachlor catalyzed by Cu/Al<sub>2</sub>O<sub>3</sub> in water. *Catal. Today*, 90, 291-296, 2004.
- [187] Faria, P.C.C., Orfao, J.J.M., Pereira, M.F.R. Catalytic ozonation of sulfonated aromatic compounds in the presence of activated carbon. *Appl. Catal. B: Environ.*, in press, 2008.
- [188] Alvarez, P.M., Beltran, F.J., Pocostales, J.P., Masa, F.J. Preparation and structural characterization of Co/Al<sub>2</sub>O<sub>3</sub> catalysts for the ozonation of pyruvic acid. *Appl. Catal. B: Environ.*, 72, 322-330, 2007.
- [189] Fogler, H. S. "Elements of Chemical Reaction Engineering," 2<sup>nd</sup> Ed., Prentice-Hall International Editions, 1992.
- [190] Sullivan, D.E., Roth, J.A. *AIChE Symp. Ser.*, 76, 142, 1980.
- [191] Kuo, C.H. Mass Transfer in Ozone Absorption. *Environ. Prog.*, 1, 189-195, 1982.
- [192] Farines, V., Baig, S., Albet, J. Ozone Transfer from Gas to Water in a Co-current Upflow Packed Bed Reactor Containing Silica Gel. *J. Chem. Eng.*, 91, 67-73, 2003.
- [193] Beltran, F.J., Fernandez, L.A., Alvarez, P., Rodriguez, E. Comparison of Ozonation Kinetic Data from Film and Danckwerts Theories. *Ozone, Sci. Eng.*, 20, 403-420, 1998.
- [194] Lee, S.Y., Ruutel, P., Barratt, A., Tsui, Y.P. Impinging Zone Reactor and Its Mathematical Model for Ozonation of Wastewater. *Ozone Sci. Eng.* 21(5) 502-522, 1999.

- [195] Erol, F. A kinetic study on the decolorization of aqueous solutions of Acid Red-151 by ozonation, M. Sc., Chemical Engineering, M.E.T.U., 2002.
- [196] Perry, R.H., Green, D.W., Maloney, J.O. Chemical Engineers Handbook, 7th. Ed. New York, Mc-Graw-Hill Professional, 1997.
- [197] Ohashi, H., Kosaka, K., Hashimoto, K. *Proceedings of the 2<sup>nd</sup> Pacific Chemical Engineering Congress*, I, pp. 389, 1977.
- [198] Rand, M.C., Greenberg, A.E. and Taras, M.J. *Standard Methods for the Examination of Water and Wastewater*, 18th Ed. Washington D.C: American Public Health Association, 455-460, 1992.
- [199] Wieserman, L.F., Cross, K., Martin, E.S. 1991, US Patent 4.983,566, 1991.
- [200] Fan, L.S. Gas-Liquid-Solid Fluidization Engineering. Butterworths, Stoneham, 1989.
- [201] Jena, H.M., Sahoo, B.K., Roy, G.K., Meikap, B.C. Characterization of hydrodynamic properties of a gas-liquid-solid three-phase fluidized bed with regular shape spherical glass bead particles. *Chem Eng. J.* (in press), 2008.
- [202] Shechter, H. Spectrophotometric method for determination of ozone in aqueous solutions. *Wat. Res.*, 7, 729-739, 1973.
- [203] Bader, H., Hoigne, J. Determination of Ozone in Water by the Indigo Method. *Wat. Res.* 15: 449-455, 1981.
- [204] Takeda, K., Katoh, S., Nakatani, N., Sakugawa, H. Rapid and Highly Sensitive Determination of Low-Molecular-Weight Carbonyl Compounds in Drinking Water and Natural Water by Preconcentration HPLC with 2,4-Dinitrophenylhydrazine. *Anal. Sci*, 22, 1509-1514, 2006.
- [205] Kieber, R.J., Mopper, K. Determination of Picomolar Concentrations of Carbonyl Compounds in Natural Waters, Including Seawater, by Liquid Chromatography. *Environ. Sci. Technol.*, 24, 1477-1481, 1990.
- [206] Carlos, A.K., Wypych, F., Moraes, S., Duran, N., Nagata, N. Peralta-Zamora, P. Semiconductor-assisted Photocatalytic Degradation of Reactive Dyes in Aqueous Solution. *Chemosphere* 40:433-440, 2000.

- [207] Thomas, K., Hoggan, P.E., Marley, L., Lamote, J., Lavalley, J.C. Experimental and theoretical study of ozone adsorption on alumina. *Catal. Lett.*, 46, 77-82, 2005
- [208] Harris, R.G., Wells, J.D., Johnson, B.B. Selective adsorption of dyes and other organic molecules to kaolinite and oxide surfaces. *Colloid Surf. A.*, 180, 131-140, 2001.
- [209] Dapson, R.W. Dye-tissue interactions: mechanisms, quantification and bonding parameters for dyes used in biological staining, *Biotech., Histochem.*, 80(2), 49-72, 2005.
- [210] Safoniuk, M., Grace, J.R., Hackman, L., McKnight, C.A. Use of dimensional similitude for scale-up of hydrodynamics in three phase fluidized beds. *Chem. Eng. Sci.*, 54, 4961-4966, 1999.
- [211] Zhang, J.P., Grace, J.R., Epstein, N. Lim, K.S. Flow regime identification in gas-liquid flow and three-phase fluidized beds. *Chem. Eng. Sci.*, 52, 3979-3992, 1997.
- [212] Roustan, M., Want, R.Y., Wolbert, D. Modeling hydrodynamics and mass transfer parameters in a continuous ozone bubble column. *Ozone Sci., Eng.*, 18, 99-115, 1996.
- [213] Fan, L.S., Matsuura, A., Chern, S.H. Hydrodynamic characteristics of a gas-liquid-solid fluidized bed containing a binary mixture of particles. *A.I.C.H.E. J.*, 31, 1801-1810, 1985.
- [214] Einaga, H., Futamura, S. Catalytic oxidation of benzene with ozone over alumina-supported manganese oxides. *J. Catal.*, 227, 304-312, 2004.

## APPENDIX A

### CALIBRATION CURVES OF *AR-151* AND *RBBR* DYES

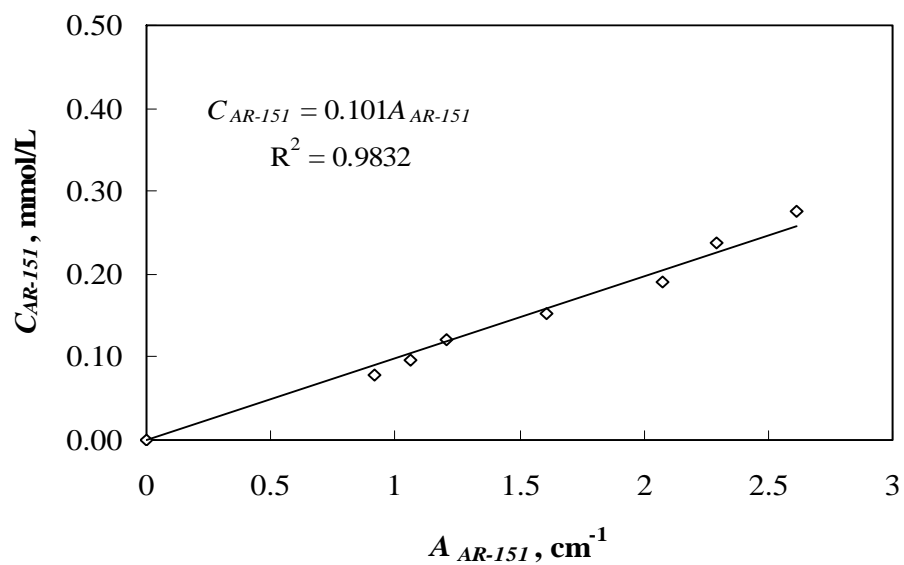


Figure A.1. The concentration versus absorbance values for *AR-151* at pH=2.5.

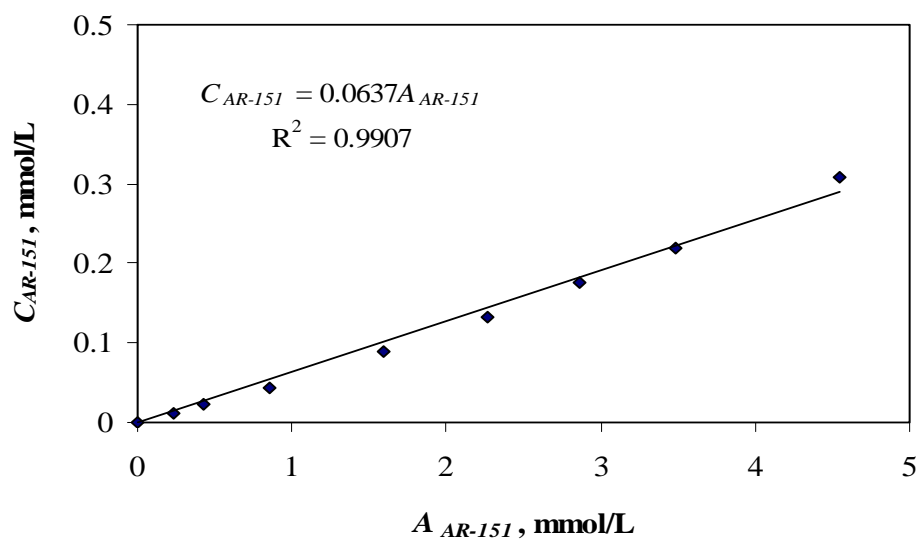


Figure A.2. The concentration versus absorbance values for *AR-151* at pH=7 and 10.

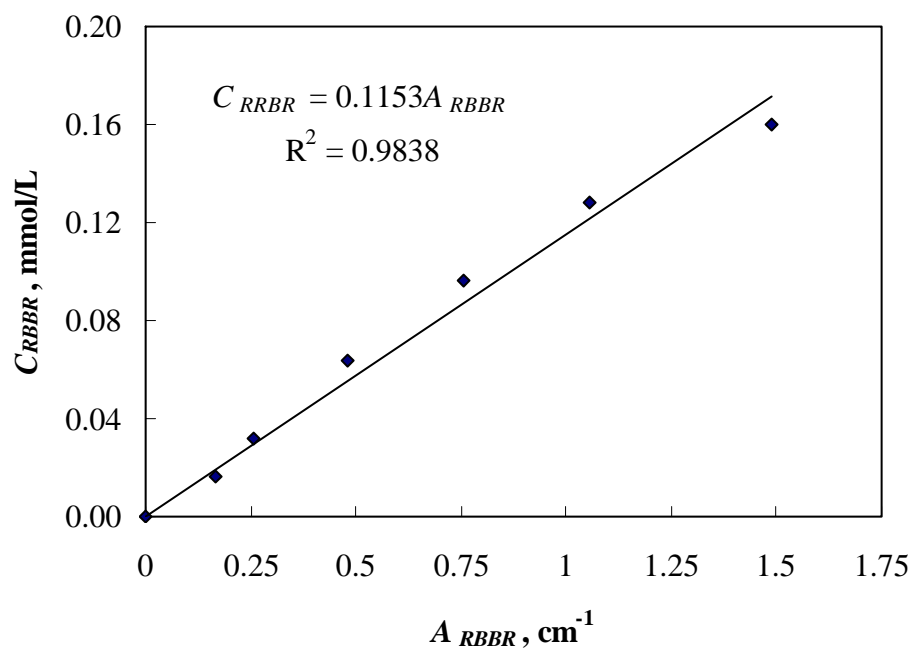


Figure A.3. The concentration versus absorbance values for RBBR at pH=2.5, 7 and 10.

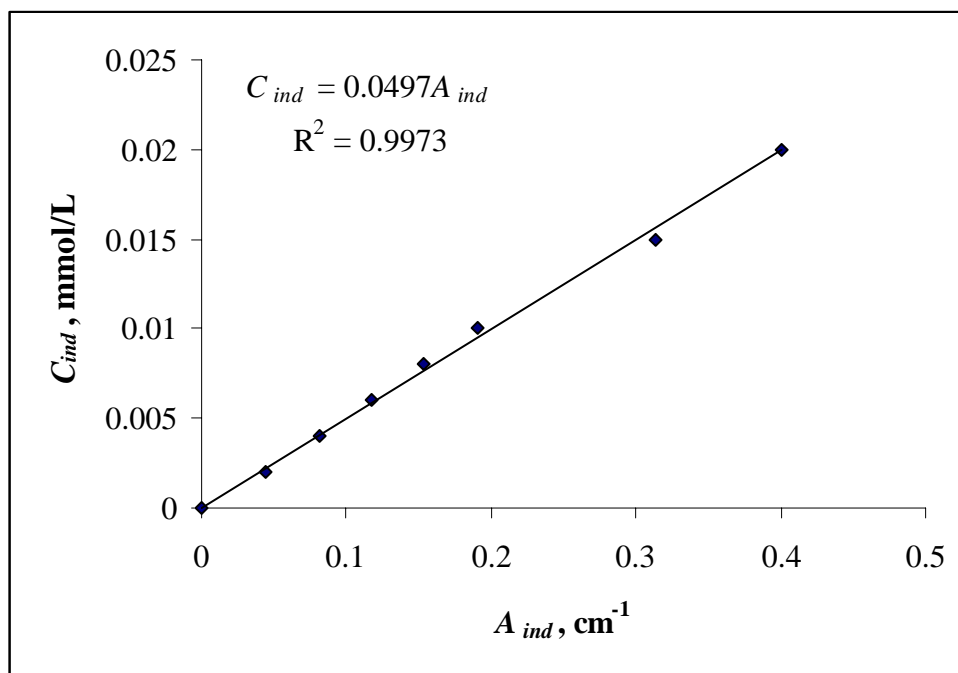


Figure A.4. The concentration versus absorbance values for indigo.

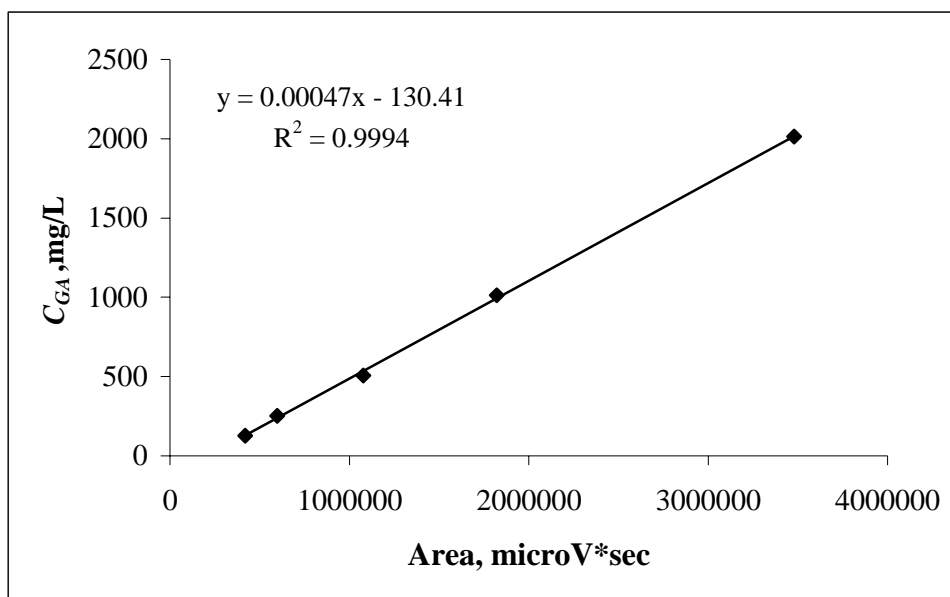


Figure A.5. The calibration curve of glyoxylic acid in HPLC.

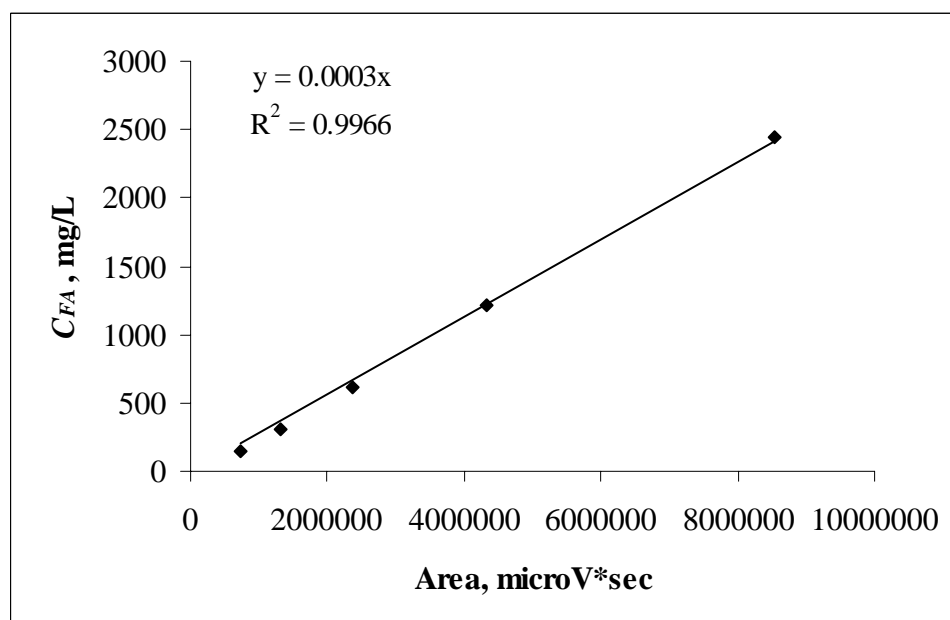


Figure A.6. The calibration curve of formic acid in HPLC.

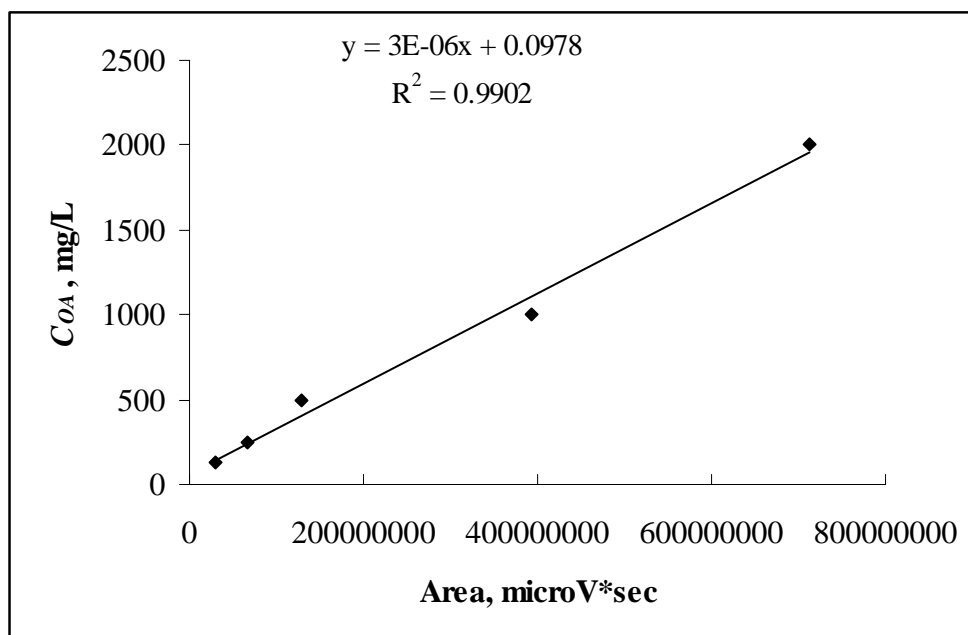


Figure A.7. The calibration curve of oxalic acid in HPLC.

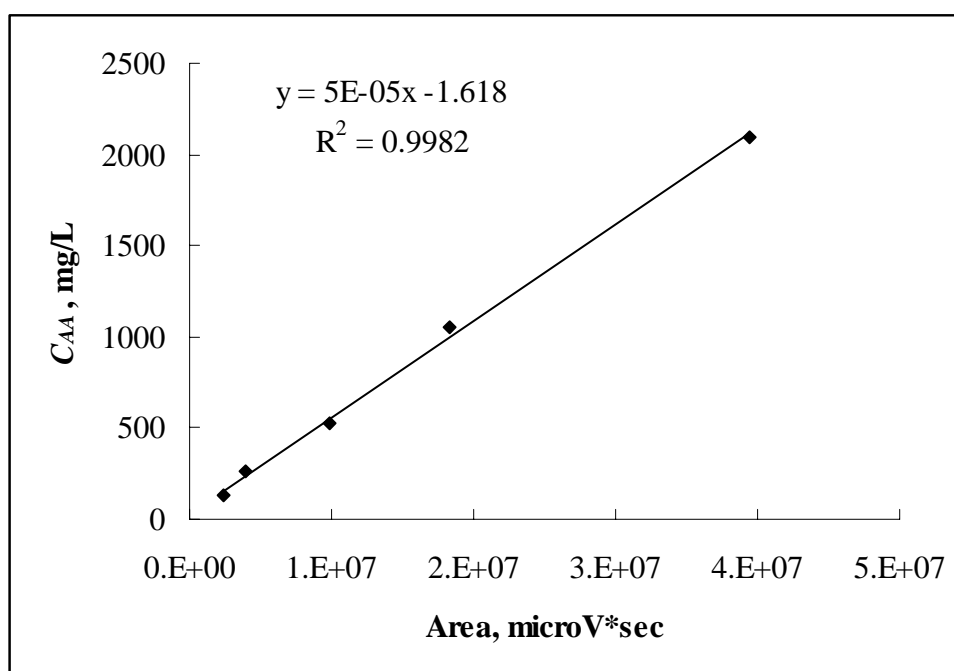


Figure A.8. The calibration curve of acetic acid in HPLC.

## APPENDIX B

### SAMPLE CALCULATIONS

#### B.1.The Calculation of Ozone Production

##### The determination of ozone concentration in the gas phase- KI Method

KI method can be used for the determination of ozone in air by adsorption of ozone in iodide solution. Ozone liberates iodine from 2% potassium iodide (KI) solution. After immediate acidification, the liberated iodine (Rxn. B1) is titrated with standard 0.1 M sodium thiosulfate ( $\text{Na}_2\text{S}_2\text{O}_3$ ) using starch indicator.



##### Calculation Procedure

Let's take the molarity of  $\text{Na}_2\text{S}_2\text{O}_3$  as M. The volume of thiosulfate solution spent for the determination of ozone is

$$\Delta V = V_{\text{thio}} - V_{\text{thio,blank}} \quad (\text{B3})$$

where  $V_{\text{thio,inlet}}$  is the titrant spent for the sample and  $V_{\text{thio,blank}}$  is the titrant for the blank.

The amount of  $\text{S}_2\text{O}_3^{-2}$  as mole:

$$n_{\text{S}_2\text{O}_3^{-2}} = M_{\text{thio}} [\text{mole/L}] \times (V_{\text{thio}} - V_{\text{thio,blank}}) [\text{mL}] \times \frac{1\text{L}}{1000\text{mL}} = (V_{\text{thio}} - V_{\text{thio,blank}}) \times M \times 10^{-3} \quad (\text{B4})$$

mole

Since 1 mole of ozone spends 2 moles of  $S_2O_3^{-2}$  in the reaction, the amount of ozone in the sample is,

$$n_{O_3,G} = \frac{1}{2} \times (V_{thio} - V_{thio,blank}) \times M_{thio} \times 10^{-3} \text{ mole ozone} \quad (B5)$$

The ozone dose is calculated for  $t$  (min) of ozonation:

$$D_{O_3} = \frac{n_{O_3,G}}{t} = \frac{(1/2) \times (V_{thio} - V_{thio,blank}) \times M_{thio} \times 10^{-3}}{t(\text{min})} \times \frac{60 \text{ min}}{1 \text{ h}} \quad (B6)$$

$$D_{O_3} = 0.03 \times (V_{thio} - V_{thio,blank}) \times M_{thio} \quad \text{mole } O_3/h \quad (B7)$$

Equation (B7) is multiplied by  $10^3$  to convert the unit of  $D_{O_3}$  from mole  $O_3/h$  to mmol  $O_3/h$ .

$$D_{O_3} = \frac{30 \times (V_{thio} - V_{thio,blank}) \times M_{thio}}{t(\text{min})} \text{ mmol } O_3/h \quad (B8)$$

Inlet ozone concentration (mmol  $O_3/L$  gas) in the gas can be calculated from ozone dose and volumetric gas flow rate:

$$C_{O_3,G} = \frac{D_{O_3}(\text{mmol } O_3/h)}{Q_G(\text{L gas/h})} \quad (B9)$$

Ozone concentration in the inlet gas can be calculated by determining the inlet ozone dose with Equation (B8).

$$C_{O_3,G,in} = \frac{D_{O_3,in}(\text{mmol } O_3/h)}{Q_G(\text{L gas/h})} \quad (B10)$$

Ozone concentration in the outlet gas can be calculated by determining the outlet ozone dose with Equation (B8).

$$C_{O_3,G,out} = \frac{D_{O_3,out} (mmol O_3/h)}{Q_G (L gas/h)} \quad (B11)$$

### B.1.1 Sample Calculation

For the ozonation experiment in the fluidized bed reactor at pH=2.5, Dye = *RBBR*,  $C_{D,in} = 4.8 \times 10^{-2}$  mmol/L *RBBR*,  $Q_G = 150$  L/h,  $Q_L = 30$  L/h, no catalyst, ozone concentrations in the inlet gas and outlet gas were calculated (Appendix F, run 1):

Inlet gas;

$$M_{thio} = 0.1 \text{ M}$$

$$V_{thio} = 27.8 \text{ mL}$$

$$V_{thio,blank} = 0.1 \text{ mL}$$

$$t = 2 \text{ min}$$

$$D_{O_3} = \frac{30 \times (V_{thio} - V_{thio,blank}) \times M_{thio}}{t(\text{min})} = \frac{30 \times (27.8 - 0.1) \times 0.1}{2} = 41.55 \text{ mmol O}_3/\text{h}$$

Ozone concentration in the inlet gas:

$$C_{O_3,G,in} = \frac{D_{O_3,in} (mmol O_3/h)}{Q_G (L gas/h)} = \frac{41.55 \text{ mmol/h}}{150 \text{ L gas/h}} = 0.277 \text{ mmol O}_3/\text{L gas}$$

Outlet gas;

$$M_{thio} = 0.1 \text{ M}$$

$$V_{thio} = 178.6 \text{ mL}$$

$$V_{thio,blank} = 0.1 \text{ mL}$$

$$t = 20 \text{ min}$$

$$D_{O_3} = \frac{30 \times (V_{thio} - V_{thio,blank}) \times M_{thio}}{t(\text{min})} = \frac{30 \times (178.6 - 0.1) \times 0.1}{20} = 26.78 \text{ mmol O}_3/\text{h}$$

Ozone concentration in the outlet gas:

$$C_{O_3,G,out} = \frac{D_{O_3,out} (mmol O_3/h)}{Q_G (L gas/h)} = \frac{26.78 mmol/h}{150 L gas/h} = 0.179 mmol O_3/L gas$$

## B.2 The calculation of dissolved O<sub>3</sub> concentration in the liquid phase

In order to determine the dissolved O<sub>3</sub> concentration in the liquid phase ( $C_{O_3,L}$ ), Indigo method is used as explained in Section 4.6.2. First, the calibration curve of indigo is obtained by measuring the absorbance of indigo reagent at different indigo concentrations.

$$C_{ind} = 4.97 \times 10^{-2} \times A_{ind} \quad (B12)$$

where  $C_{ind}$  is the indigo concentration as mmol/L and  $A_{ind}$  is the absorbance of the indigo in  $cm^{-1}$ .

Then, the concentration of the indigo blank is calculated:

$$C_b = 4.97 \times 10^{-2} \times A_b \quad (B13)$$

Here,  $C_b$  is the indigo blank concentration in mmol/L and  $A_b$  is the blank absorbance in  $cm^{-1}$ . Since both blank and samples are diluted to 100 mL (0.1 L), the number of moles of indigo and blank may be found:

$$n_{ind} = C_{ind} \times 0.1 = 4.97 \times 10^{-3} \times A_{ind} \quad (B14)$$

$$n_b = C_b \times 0.1 = 4.97 \times 10^{-3} \times A_b \quad (B15)$$

Here,  $n_{ind}$  is the mole of indigo in mmol and  $n_b$  is the mole of blank in mmol. The number of indigo reacted with ozone is calculated by substituting  $n_{ind}$  from  $n_b$ .

$$n_{ind,reacted} = 4.97 \times 10^{-3} \times (A_b - A_{ind}) \quad (B16)$$

Then, as stated by Hoigne and Bader [1981],  $C_{O_3,L}$  is calculated from the stoichiometric ratio of ozone reacting with indigo dye. One mole of  $O_3$  reacts with one mole of indigo.

$$n_{O_3} = n_{ind,reacted} = 4.97 \times 10^{-3} \times (A_b - A_{ind}) \quad (B17)$$

The concentration of ozone in the reactor is calculated after dividing the moles of  $O_3$  reacted by the sample volume taken. The sample volume is found from the difference of total indigo volume ( $V_T$ ) and blank indigo volume ( $V_b$ ):

$$C_{O_3,L} = \frac{n_{O_3}}{(V_T - V_b) \times 10^{-3}} = \frac{4.97 \times 10^{-3} \times (A_b - A_{ind})}{(V_T - V_b) \times 10^{-3}} \quad (B18)$$

$$C_{O_3,L} = \frac{4.97 \times (A_b - A_{ind})}{(V_T - V_b)} \quad (B19)$$

Here,  $C_{O_3,L}$  is in mmol/L and since  $V_T$  and  $V_b$  are in the units of mL so that a conversion factor of  $10^{-3}$  is added to the denominator of Equation (B18).

### B.2.1 Sample calculation

For the ozonation experiment in the fluidized bed reactor with pH=2.5, dye = *RBBR*,  $C_{D,in} = 4.8 \times 10^{-2}$  mmol/L,  $Q_G = 150$  L/h,  $Q_L = 30$  L/h, no catalyst,  $C_{O_3,L}$  was calculated for  $t = 10$  min,  $z = 0.09$  m (Appendix F, run 1, Table B2):

$$A_b = 0.174 \text{ cm}^{-1}$$

$$A_{ind} = 0.099 \text{ cm}^{-1}$$

$$V_T = 40.0 \text{ mL}$$

$$V_b = 10.0 \text{ mL}$$

$$C_{O_3,L} = \frac{4.97 \times (A_b - A_{ind})}{(V_T - V_b)} = \frac{4.97 \times (0.174 - 0.099)}{(40.0 - 10.0)} = 12.43 \times 10^{-3} \text{ mmol/L}$$

### B.3 The calculation of concentrations of *AR-151* and *RBBR* dyes

The concentration of *AR-151* or *RBBR* dye is calculated by using the dye calibration curve of each dye. For the concentration of *AR-151* in the experiments at pH=2.5, the Equation in Figure A1 is used:

$$C_D (AR-151) = 0.101 \times A_{AR-151} \quad (B20)$$

Here,  $C_D (AR-151)$  is the concentration of *AR-151* in mmol/L and  $A_{AR-151}$  is the absorbance of *AR-151* in  $\text{cm}^{-1}$ , at pH=2.5. For the concentration of *AR-151* in the experiments at pH=7 and 10, the Equation in Figure A2 is used:

$$C_D (AR-151) = 0.0637 \times A_{AR-151} \quad (B21)$$

For the concentration of *RBBR* in the experiments, the Equation in Figure A3 is used:

$$C_D (RBBR) = 0.1153 \times A_{RBBR} \quad (B22)$$

#### B.3.1 Sample calculation

\* For the ozonation experiment in the fluidized bed reactor with pH = 2.5, dye = *RBBR*,  $C_{D,in} = 4.8 \times 10^{-2}$  mmol/L,  $Q_G = 150$  L/h,  $Q_L = 30$  L/h, no catalyst,  $C_D (RBBR)$  was calculated for  $t = 10$  min,  $z = 0.09$  m (Appendix F, run 1, Table B1):

$$A_{RBBR} = 0.023 \text{ cm}^{-1}$$

$$C_D (RBBR) = 0.1153 \times A_{RBBR} = 0.1153 \times 0.023 = 0.27 \text{ mmol/L}$$

\* For the ozonation experiment in the fluidized bed reactor with pH=2.5, dye=*AR-151*,  $C_{D,in} = 7.3 \times 10^{-2}$  mmol/L,  $Q_G = 150$  L/h,  $Q_L = 30$  L/h,  $C_{O_3,G,in} = 0.322$  mmol/L gas, no catalyst,  $C_D (AR-151)$  was calculated for  $t = 10$  min,  $z = 0.09$  m (Appendix F, run 5, Table B):

$$C_D (AR-151) = 0.101 \times A_{AR-151} = 0.101 \times 0.122 = 1.23 \text{ mmol/L}$$

\* For the ozonation experiment in the fluidized bed reactor with pH=10.0, dye=AR-151,  $C_{D,in} = 27.0 \times 10^{-2}$  mmol/L,  $Q_G = 150$  L/h,  $Q_L = 150$  L/h,  $C_{O_3,G,in} = 0.950$  mmol/L gas, catalyst = PFOA,  $C_D (AR-151)$  was calculated for  $z = 0.52$  m (Appendix F, run 89, Table B):

$$C_D (AR-151) = 0.0637 \times A_{AR-151} = 0.0637 \times 2.419 = 15.41 \text{ mmol/L}$$

#### **B.4 Calculation of dye, TOC removals, O<sub>3</sub> consumption, O<sub>3</sub> consumption rate and utilization ratios**

The dye and TOC removals as the percentage are calculated from Equations (B23) and (B24).

$$\text{Dye removal (\%)} = \frac{C_{D,in} - C_{D,out}}{C_{D,in}} \times 100 \quad (\text{B23})$$

$$\text{TOC removal (\%)} = \frac{TOC_{in} - TOC_{out}}{TOC_{in}} \times 100 \quad (\text{B24})$$

Then, the consumption of ozone and consumption rate (%) are calculated from the inlet and outlet gaseous ozone concentrations found in Section B1. Also the applied ozone is calculated from inlet gaseous O<sub>3</sub> concentration.

$$\text{Cons}_{O_3} (\text{mmol} / \text{L liq}) = (C_{O_3,G,in} - C_{O_3,G,out}) \times \frac{Q_G}{Q_L} \quad (\text{B25})$$

$$R_{\text{cons},O_3} = \frac{(C_{O_3,G,in} - C_{O_3,G,out})}{C_{O_3,G,in}} \times 100 \quad (\text{B26})$$

$$\text{Applied } O_3 (\text{mmol} / \text{L liq}) = \frac{C_{O_3,G,in} \times Q_G}{Q_L} \quad (\text{B27})$$

The utilization ratios of dye and TOC concentrations to the consumed O<sub>3</sub> from inlet gas are calculated from Equations (B28) and (B29):

$$U_{O_3} (\text{dye}) = \frac{(C_{D,in} - C_{D,out}) \times Q_L}{(C_{O_3,G,in} - C_{O_3,G,out}) \times Q_G} \quad (\text{B28})$$

$$U_{O_3} (\text{TOC}) = \frac{(TOC_{in} - TOC_{out}) \times Q_L}{(C_{O_3,G,in} - C_{O_3,G,out}) \times Q_G} \quad (\text{B29})$$

#### B.4.1 Sample calculation

For the ozonation experiment in the fluidized bed reactor with pH = 2.5, dye = *RBBR*,  $C_{D,in} = 4.87 \times 10^{-2}$  mmol/L *RBBR*,  $Q_G = 150$  L/h,  $Q_L = 30$  L/h, no catalyst, the values were calculated for  $t = 20$  min,  $z = 0.88$  m (Appendix F, run 1):

$$C_{D,in} = 4.87 \times 10^{-2} \text{ mmol / L}$$

$$C_{D,out} = 0.03 \times 10^{-2} \text{ mmol / L}$$

$$TOC_{in} = 11.26 \text{ mg / L}$$

$$TOC_{out} = 9.24 \text{ mg / L}$$

$$C_{O_3,G,in} = 0.277 \text{ mmol / L gas}$$

$$C_{O_3,G,out} = 0.179 \text{ mmol / L gas}$$

$$\text{Dye removal (\%)} = \frac{C_{D,in} - C_{D,out}}{C_{D,in}} \times 100 = \frac{4.87 \times 10^{-2} - 0.03 \times 10^{-2}}{4.87 \times 10^{-2}} \times 100 = 99.4\%$$

$$\text{TOC removal (\%)} = \frac{TOC_{in} - TOC_{out}}{TOC_{in}} \times 100 = \frac{11.26 - 9.24}{11.26} \times 100 = 17.9\%$$

$$\text{Cons}_{O_3} = (C_{O_3,G,in} - C_{O_3,G,out}) \times \frac{Q_G}{Q_L} = (0.277 - 0.179) \times \frac{150}{30} = 0.490 \text{ mmol / L liq}$$

$$R_{cons,O_3} = \frac{(C_{O_3,G,in} - C_{O_3,G,out})}{C_{O_3,G,in}} \times 100 = \frac{(0.277 - 0.179)}{0.277} \times 100 = 35.6\%$$

$$Applied O_3 = \frac{C_{O_3,G,in} \times Q_G}{Q_L} = \frac{0.277 \times 150}{30} = 1.385 \text{ mmol / L liq}$$

$$U_{O_3} (dye) = \frac{(C_{D,in} - C_{D,out}) \times Q_L}{(C_{O_3,G,in} - C_{O_3,G,out}) \times Q_G} = \frac{(4.87 \times 10^{-2} - 0.03 \times 10^{-2}) \times 30}{(0.277 - 0.179) \times 150} = 0.099 \frac{\text{mmol dye}}{\text{mmol } O_3}$$

$$U_{O_3} (TOC) = \frac{(TOC_{in} - TOC_{out}) \times Q_L}{(C_{O_3,G,in} - C_{O_3,G,out}) \times Q_G} = \frac{\frac{(11.26 - 9.24)}{12} \times 30}{(0.277 - 0.179) \times 150} = 0.344 \frac{\text{mmol TOC}}{\text{mmol } O_3}$$

## B.5 Calculation of Henry's Law constant at different pH values

Henry's Law constant is calculated from the correlation of Sullivan [190]. Then, the equilibrium concentration of  $O_3$  is found from Equation (B31):

$$H_{O_3} = 3.84 \times 10^7 [OH^-]^{0.035} \exp\left(\frac{-2428}{T}\right) \quad (B30)$$

Here,  $H_{O_3}$  is the Henry's Law constant as Atm,  $OH^-$  is the hydroxyl ion concentration as mol/L, and  $T$  is the temperature in K.

$$C_{O_3,L}^* = \frac{\rho_w}{MW_w} \frac{RT}{H_{O_3}} C_{O_3,G} \quad (B31)$$

where  $\rho_w$  is the density of water as  $kg/m^3$ ,  $MW_w$  is the molecular weight of water as  $kg/kmol$ ,  $R$  is the gas constant as  $0.0821 \text{ atm}/(\text{mol.K})$ .

### B.5.1 Sample calculation

The Henry's Law constant and the equilibrium relationship is calculated for  $T = 20^\circ\text{C}$  and  $\text{pH} = 2.5$ .

$$[\text{OH}^-] = 10^{-11.5} \text{ mol/L}$$

$$T = 20^\circ\text{C} = 293 \text{ K}$$

$$\rho_w = 997 \text{ kg/m}^3$$

$$MW_w = 18 \text{ kg/kmol}$$

$$H_{O_3} = 3.84 \times 10^7 \times (10^{-11.5})^{0.035} \exp\left(\frac{-2428}{293}\right) = 3828.0 \text{ atm}$$

$$C_{O_3,L}^* = \frac{997 \left(\text{kg/m}^3\right)}{18 \left(\text{kg/kmol}\right)} \times \frac{0.0821 \left(\text{atm}\cdot\text{L}/(\text{mol}\cdot\text{K})\right) \times 293 \text{ K}}{3828.0 \text{ atm}} \times \frac{10^3 \text{ mol}}{1 \text{ kmol}} \times \frac{1 \text{ m}^3}{10^3 \text{ L}}$$

$$= 0.35 C_{O_3,G}$$

Henry's Law constants at pH=7 and 10 were calculated as 5501.3 atm and 7006.0 atm, respectively. The equilibrium constants in front of the symbol  $C_{O_3,G}$  were calculated as 0.244 and 0.191, for pH = 7 and 10, respectively.

## **B.6 Calculation of by-product concentration from their calibration curves**

In the HPLC, the peak areas of the by-products were obtained from the analysis. Then, the concentration of the by-products were calculated from their corresponding calibration curves as "Concentration vs. Peak area" calibration curves given in Appendix A.

### **B.6.1 Sample calculation**

The following peak area values of the by-products were obtained in the fluidized bed reactor with pH = 2.5, dye = *RBBR*,  $C_{D,in} = 4.87 \times 10^{-2}$  mmol/L *RBBR*,  $Q_G = 150$  L/h,  $Q_L = 30$  L/h, no catalyst, the values were calculated for  $t = 20$  min,  $z = 0.88$  m (Appendix F, run 1). At this run, no formic acid was observed in the HPLC analysis.

$$\text{Peak area (oxalic acid)} = 1232156 \mu\text{V}\cdot\text{s}$$

Peak area (acetic acid) = 34979  $\mu\text{V}\cdot\text{s}$

Peak area (glyoxylic acid) = 333417  $\mu\text{V}\cdot\text{s}$

$MW_{OA} = 90 \text{ mg/mmol}$

$MW_{GA} = 74 \text{ mg/mmol}$

$MW_{AA} = 60 \text{ mg/mmol}$

$$C_{OA} = 3 \times 10^{-6} \times \text{peak area (oxalic acid)} + 0.0978 \quad (\text{B32})$$

$$C_{OA} = 3 \times 10^{-6} \times 1232156 + 0.0978 = 3.794 \text{ mg OA/L} = 4.22 \times 10^{-2} \text{ mmol OA/L}$$

$$C_{GA} = 4.7 \times 10^{-4} \times \text{peak area (glyoxylic acid)} - 130.41 \quad (\text{B33})$$

$$C_{GA} = 4.7 \times 10^{-4} \times 333417 - 130.41 = 26.30 \text{ mg GA/L} = 35.5 \times 10^{-2} \text{ mmol GA/L}$$

$$C_{AA} = 5.0 \times 10^{-5} \times \text{peak area (acetic acid)} - 1.618 \quad (\text{B34})$$

$$C_{AA} = 5.0 \times 10^{-5} \times 34979 - 1.618 = 0.131 \text{ mg AA/L} = 0.218 \times 10^{-2} \text{ mmol AA/L}$$

## B.7 The determination of main parameters in tracer experiments

The area under  $C(t)$  versus  $t$  graph is determined by Trapezoidal rule, Simpson's one-third rule, Simpson's three-eighths rule, and general numerical integration rule [189].

Trapezoidal rule (two-point)

$$\int_{X_0}^{X_1} f(x) dx = \frac{h}{2} [f(X_0) + f(X_1)] \quad (\text{B35})$$

when  $h = X_1 - X_0$

Simpson's one-third rule (three-point):

$$\int_{X_0}^{X_2} f(x) dx = \frac{h}{3} [f(X_0) + 4f(X_1) + f(X_2)] \quad (\text{B36})$$

when  $h = \frac{X_2 - X_0}{2}$

Simpson's three-eighths rule (four-point):

$$\int_{X_0}^{X_3} f(x)dx = \frac{3}{8}h[f(X_0)+3f(X_1)+3f(X_2)+f(X_3)] \quad (\text{B37})$$

when  $h = \frac{X_3 - X_0}{3}$

General numerical integration rule: For N+1 points, where N is even,

$$\int_{X_0}^{X_N} f(x)dx = \frac{h}{3}[f(X_0)+4f(X_1)+2f(X_2)+4f(X_3)+2f(X_4)+\dots+4f(X_{N-1})+f(X_N)] \quad (\text{B38})$$

when  $h = \frac{X_N - X_0}{N}$

Table B.1. Data for tracer experiment of  $Q_G = 100$  L/h,  $Q_L = 200$  L/h, no catalyst.

Time, s	Abs, cm <sup>-1</sup>	C(t) mg/L	E(t)	tE(t), s	t-t <sub>m</sub>	(t-t <sub>m</sub> ) <sup>2</sup> E(t)
0	0	0.000	0	0.000	-93.28	0.00
6	0.005	0.493	0.00039	0.002	-87.28	2.96
16	0.040	3.943	0.00311	0.050	-77.28	18.56
26	0.108	10.646	0.00839	0.218	-67.28	37.99
36	0.123	12.125	0.00956	0.344	-57.28	31.36
46	0.118	11.632	0.00917	0.422	-47.28	20.50
56	0.108	10.646	0.00839	0.470	-37.28	11.66
66	0.091	8.971	0.00707	0.467	-27.28	5.26
76	0.086	8.478	0.00668	0.508	-17.28	2.00
86	0.077	7.590	0.00598	0.515	-7.28	0.32
96	0.068	6.703	0.00528	0.507	2.72	0.04
106	0.062	6.112	0.00482	0.511	12.72	0.78
116	0.056	5.520	0.00435	0.505	22.72	2.25
126	0.050	4.929	0.00389	0.490	32.72	4.16
136	0.043	4.239	0.00334	0.455	42.72	6.10
146	0.038	3.746	0.00295	0.431	52.72	8.21
156	0.032	3.154	0.00249	0.388	62.72	9.78
166	0.028	2.760	0.00218	0.361	72.72	11.51
176	0.023	2.267	0.00179	0.315	82.72	12.23
200	0.017	1.676	0.00132	0.264	106.72	15.05
220	0.012	1.183	0.00093	0.205	126.72	14.98
250	0.008	0.789	0.00062	0.155	156.72	15.27
270	0.006	0.591	0.00047	0.126	176.72	14.56
290	0.005	0.493	0.00039	0.113	196.72	15.04
310	0.003	0.296	0.00023	0.072	216.72	10.95
330	0.001	0.099	7.8E-05	0.026	236.72	4.36
350	0.000	0.000	0.000	0.000	256.72	0.00

For the data,

$$\int_0^{\infty} C(t)dt = 1268.36 \text{ mg.s/L}$$

Then,  $E(t)$  and  $tE(t)$  values are calculated.  $tE(t)$  values are drawn against time and the area under the curve is calculated by the numerical integration with the same methods given above. The area under the graph gives the mean residence time:

$$\int_0^{\infty} tE(t)dt = t_m = 93.3 \text{ s}$$

Mean residence time value is used to calculate the variance.  $(t-t_m)^2E(t)$  values are calculated; those values are drawn against  $t$  and the area under the curve is calculated to find the variance.

$$\int_0^{\infty} (t-t_m)^2 E(t)dt = \sigma^2 = 3917.4 \text{ s}^2$$

Péclet numbers at these conditions are found from the ratios,  $\frac{\sigma^2}{t_m^2}$ .

$$\frac{\sigma^2}{t_m^2} = \frac{3917.4}{(93.3)^2} = 0.450 = \frac{2}{Pe_L} - \frac{2}{Pe_L^2}(1 - e^{-Pe_L})$$

From the ratio, the Péclet number for these experimental conditions is calculated as 3.06. The axial liquid dispersion coefficient is found. Here,  $H_T$  is the column height from the injection point of the tracer to the point where tracer discharge.

$$u_L = \frac{Q_L}{\frac{\pi D_c^2}{4}} = 11.1 \times 10^{-3} \text{ m/s}$$

$$Pe_L = 3.06 = \frac{u_L H_T}{D_L} = \frac{11.1 \times 10^{-3} \times 0.8}{D_L}$$

$$D_L = 2.90 \times 10^{-3} \text{ m}^2/\text{s}$$

$$N_{CSTRs} = \frac{(t_m)^2}{\sigma^2} = 2.2$$

## APPENDIX C

### SEMI-BATCH EXPERIMENTS DATA

Table C.1. Initial COD values of the initial dye concentrations used for AR-151 and RBBR.

Dye	$C_{D,i}$ , mg/L	COD <sub>i</sub> , mg/L
AR-151	100	89
	200	200
	400	360
RBBR	100	96
	200	232
	400	460

Table C.2.  $C_D$  at different time. Conditions: Dye: AR-151,  $C_{D,i}=200$  mg/L,  $T=25^\circ\text{C}$ , stirrer rate=300 rpm,  $Q_G=150$  L/h, pH=2.5,  $D_{O_3}=2.21$  g/h.

Time, min	Absorbance, $\text{cm}^{-1}$	$C_D$ , mg/L	$\ln(C_D/C_{D,i})$
0	4.232	200.00	0.00
0.5	3.448	162.97	-0.20
2.5	2.804	132.53	-0.41
5.0	1.986	93.87	-0.76
7.5	1.433	67.70	-1.08
10	0.963	45.50	-1.48
15	0.322	15.22	-2.58
20	0.138	6.52	-3.42
25	0.064	3.03	-4.19
30	0.051	2.41	-4.42

Table C.3.  $C_D$  at different time. Conditions: Dye: AR-151,  $C_{D,i}=200$  mg/L,  $T=25^\circ\text{C}$ , stirrer rate=300 rpm,  $Q_G=150$  L/h, pH=7.0,  $D_{O_3}=2.21$  g/h.

Time, min	Absorbance, $\text{cm}^{-1}$	$C_D$ , mg/L	$\ln(C_D/C_{D,i})$
0	2.576	200.00	0.00
0.5	2.184	169.57	-0.17
2.5	1.929	149.77	-0.29
5.0	1.560	121.12	-0.50
7.5	1.220	94.72	-0.75
10	0.957	74.30	-0.99
15	0.509	39.52	-1.62
20	0.214	16.61	-2.49
25	0.074	5.75	-3.55
30	0.052	4.04	-3.90

Table C.4.  $C_D$  at different time. Conditions: Dye: AR-151,  $C_{D,i}=200$  mg/L,  $T=25^\circ\text{C}$ , stirrer rate=300 rpm,  $Q_G=150$  L/h, pH=13.0,  $D_{O_3}=2.21$  g/h.

Time, min	Absorbance, $\text{cm}^{-1}$	$C_D$ , mg/L	$\ln(C_D/C_{D,i})$
0	2.576	200.00	0.00
0.5	2.091	162.35	-0.21
2.5	1.489	115.61	-0.55
5.0	0.809	62.81	-1.16
7.5	0.446	34.63	-1.75
10	0.232	18.01	-2.41
15	0.078	6.06	-3.50
20	0.039	3.03	-4.19
25	0.011	0.85	-5.46
30	0.008	0.62	-5.77

Table C.5.  $C_D$  at different time. Conditions: Dye: AR-151,  $C_{D,i}=200$  mg/L,  $T=25^\circ\text{C}$ , stirrer rate=300 rpm,  $Q_G=150$  L/h, pH=2.5,  $D_{O_3}=2.21$  g/h, Catalyst=Alumina,  $m_{\text{cat}}=5$  g.

Time, min	Absorbance, $\text{cm}^{-1}$	$C_D$ , mg/L	$\ln(C_D/C_{D,i})$
0	4.232	200.00	0.00
0.5	3.596	169.95	-0.16
2.5	2.788	131.76	-0.42
5.0	2.131	100.70	-0.69
7.5	1.552	73.37	-1.00
10	1.009	47.67	-1.43
15	0.646	30.51	-1.88
20	0.335	15.84	-2.54
25	0.199	9.39	-3.06
30	0.110	5.20	-3.65

Table C.6.  $C_D$  at different time. Conditions: Dye: AR-151,  $C_{D,i}=200$  mg/L,  $T=25^\circ\text{C}$ , stirrer rate=300 rpm,  $Q_G=150$  L/h, pH=7.0,  $D_{O_3}=2.21$  g/h, Catalyst=Alumina,  $m_{\text{cat}}=5$  g.

Time, min	Absorbance, $\text{cm}^{-1}$	$C_D$ , mg/L	$\ln(C_D/C_{D,i})$
0	2.576	200.00	0.00
0.5	2.241	173.99	-0.14
2.5	1.929	149.77	-0.29
5.0	1.557	120.89	-0.50
7.5	1.256	97.52	-0.72
10	0.966	75.00	-0.98
15	0.541	42.00	-1.56
20	0.324	25.16	-2.07
25	0.197	15.30	-2.57
30	0.131	10.17	-2.98

Table C.7.  $C_D$  at different time. Conditions: Dye: AR-151,  $C_{D,i}=200$  mg/L,  $T=25^\circ\text{C}$ , stirrer rate=300 rpm,  $Q_G=150$  L/h, pH=13.0,  $D_{O_3}=2.21$  g/h, Catalyst=Alumina,  $m_{\text{cat}}=5$  g.

Time, min	Absorbance, $\text{cm}^{-1}$	$C_D$ , mg/L	$\ln(C_D/C_{D,i})$
0	2.576	200.00	0.00
0.5	2.092	162.42	-0.21
2.5	1.685	130.82	-0.42
5.0	1.182	91.77	-0.78
7.5	0.824	63.98	-1.14
10	0.621	48.21	-1.42
15	0.348	27.02	-2.00
20	0.168	13.04	-2.73
25	0.100	7.76	-3.25
30	0.041	3.18	-4.14

Table C.8.  $C_D$  at different time. Conditions: Dye: AR-151,  $C_{D,i}=200$  mg/L,  $T=25^\circ\text{C}$ , stirrer rate=300 rpm,  $Q_G=150$  L/h, pH=2.5,  $D_{O_3}=2.21$  g/h, Catalyst=25% PFOA,  $m_{\text{cat}}=5$  g.

Time, min	Absorbance, $\text{cm}^{-1}$	$C_D$ , mg/L	$\ln(C_D/C_{D,i})$
0	4.232	200.00	0.00
0.5	3.263	154.19	-0.26
2.5	2.791	131.91	-0.42
5.0	2.052	96.97	-0.72
7.5	1.544	72.98	-1.01
10	1.086	51.32	-1.36
15	0.529	25.00	-2.08
20	0.274	12.97	-2.74
25	0.227	10.71	-2.93
30	0.159	7.53	-3.28

Table C.9.  $C_D$  at different time. Conditions: Dye: AR-151,  $C_{D,i}=200$  mg/L,  $T=25^\circ\text{C}$ , stirrer rate=300 rpm,  $Q_G=150$  L/h, pH=7.0,  $D_{O_3}=2.21$  g/h, Catalyst=25% PFOA,  $m_{\text{cat}}=5$  g.

Time, min	Absorbance, $\text{cm}^{-1}$	$C_D$ , mg/L	$\ln(C_D/C_{D,i})$
0	2.576	200.00	0.00
0.5	2.139	166.07	-0.19
2.5	2.000	155.28	-0.25
5.0	1.687	130.98	-0.42
7.5	1.429	110.95	-0.59
10	1.189	92.31	-0.77
15	0.834	64.75	-1.13
20	0.531	41.23	-1.58
25	0.336	26.09	-2.04
30	0.223	17.31	-2.45

Table C.10.  $C_D$  at different time. Conditions: Dye: AR-151,  $C_{D,i}=200$  mg/L,  $T=25^\circ\text{C}$ , stirrer rate=300 rpm,  $Q_G=150$  L/h, pH=13.0,  $D_{O_3}=2.21$  g/h, Catalyst=25% PFOA,  $m_{\text{cat}}=5$  g.

Time, min	Absorbance, $\text{cm}^{-1}$	$C_D$ , mg/L	$\ln(C_D/C_{D,i})$
0	2.576	200.00	0.00
0.5	2.305	178.96	-0.11
2.5	1.674	129.97	-0.43
5.0	1.043	80.98	-0.90
7.5	0.663	51.48	-1.36
10	0.462	35.87	-1.72
15	0.196	15.22	-2.58
20	0.165	12.81	-2.75
25	0.136	10.56	-2.94
30	0.095	7.38	-3.30

Table C.11.  $C_D$  at different time. Conditions: Dye: AR-151,  $C_{D,i}=200$  mg/L,  $T=25^\circ\text{C}$ , stirrer rate=300 rpm,  $Q_G=150$  L/h, pH=2.5,  $D_{O_3}=2.21$  g/h, Catalyst=50% PFOA,  $m_{\text{cat}}=5$  g.

Time, min	Absorbance, $\text{cm}^{-1}$	$C_D$ , mg/L	$\ln(C_D/C_{D,i})$
0	4.232	200.00	0.00
0.5	3.401	160.71	-0.22
2.5	2.857	135.02	-0.39
5.0	2.052	96.97	-0.72
7.5	1.495	70.65	-1.04
10	1.099	51.94	-1.35
15	0.527	24.92	-2.08
20	0.279	13.20	-2.72
25	0.245	11.57	-2.85
30	0.166	7.84	-3.24

Table C.12.  $C_D$  at different time. Conditions: Dye: AR-151,  $C_{D,i}=200$  mg/L,  $T=25^\circ\text{C}$ , stirrer rate=300 rpm,  $Q_G=150$  L/h, pH=7.0,  $D_{O_3}=2.21$  g/h, Catalyst=50% PFOA,  $m_{\text{cat}}=5$  g.

Time, min	Absorbance, $\text{cm}^{-1}$	$C_D$ , mg/L	$\ln(C_D/C_{D,i})$
0	2.576	200.00	0.00
0.5	1.947	151.17	-0.28
2.5	1.731	134.39	-0.40
5.0	1.479	114.83	-0.55
7.5	1.226	95.19	-0.74
10	1.03	79.97	-0.92
15	0.686	53.26	-1.32
20	0.45	34.94	-1.74
25	0.28	21.74	-2.22
30	0.251	19.49	-2.33

Table C.13.  $C_D$  at different time. Conditions: Dye: AR-151,  $C_{D,i}=200$  mg/L,  $T=25^\circ\text{C}$ , stirrer rate=300 rpm,  $Q_G=150$  L/h, pH=13.0,  $D_{O_3}=2.21$  g/h, Catalyst=50% PFOA,  $m_{\text{cat}}=5$  g.

Time, min	Absorbance, $\text{cm}^{-1}$	$C_D$ , mg/L	$\ln(C_D/C_{D,i})$
0	2.576	200.00	0.00
0.5	2.322	180.28	-0.10
2.5	1.839	142.78	-0.34
5.0	1.283	99.61	-0.70
7.5	0.965	74.92	-0.98
10	0.814	63.20	-1.15
15	0.385	29.89	-1.90
20	0.154	11.96	-2.82
25	0.106	8.23	-3.19
30	0.054	4.19	-3.87

Table C.14.  $C_D$  at different time. Conditions: Dye: AR-151,  $C_{D,i}=200$  mg/L,  $T=25^\circ\text{C}$ , stirrer rate=300 rpm,  $Q_G=150$  L/h, pH=2.5,  $D_{O_3}=2.21$  g/h, Cat=100% PFOA,  $m_{\text{cat}}=5$  g.

Time, min	Absorbance, $\text{cm}^{-1}$	$C_D$ , mg/L	$\ln(C_D/C_{D,i})$
0	4.232	200.00	0.00
0.5	3.532	166.93	-0.18
2.5	2.799	132.30	-0.41
5.0	1.853	87.58	-0.83
7.5	1.227	58.00	-1.24
10	0.820	38.74	-1.64
15	0.296	13.98	-2.66
20	0.161	7.61	-3.27
25	0.112	5.28	-3.63
30	0.074	3.49	-4.05

Table C.15.  $C_D$  at different time. Conditions: Dye: AR-151,  $C_{D,i}=200$  mg/L,  $T=25^\circ\text{C}$ , stirrer rate=300 rpm,  $Q_G=150$  L/h, pH=7.0,  $D_{O_3}=2.21$  g/h, Cat=100% PFOA,  $m_{\text{cat}}=5$  g.

Time, min	Absorbance, $\text{cm}^{-1}$	$C_D$ , mg/L	$\ln(C_D/C_{D,i})$
0	2.576	200.00	0.00
0.5	2.221	172.44	-0.15
2.5	2.000	155.28	-0.25
5.0	1.684	130.75	-0.43
7.5	1.43	111.03	-0.59
10	1.208	93.79	-0.76
15	0.84	65.22	-1.12
20	0.465	36.10	-1.71
25	0.284	22.05	-2.21
30	0.133	10.33	-2.96

Table C.16.  $C_D$  at different time. Conditions: Dye: AR-151,  $C_{D,i}=200$  mg/L,  $T=25^\circ\text{C}$ , stirrer rate=300 rpm,  $Q_G=150$  L/h, pH=13.0,  $D_{O_3}=2.21$  g/h, Cat=100% PFOA,  $m_{\text{cat}}=5$  g.

Time, min	Absorbance, $\text{cm}^{-1}$	$C_D$ , mg/L	$\ln(C_D/C_{D,i})$
0	2.576	200.00	0.00
0.5	2.196	170.50	-0.16
2.5	1.768	137.27	-0.38
5.0	1.188	92.24	-0.77
7.5	0.813	63.12	-1.15
10	0.596	46.27	-1.46
15	0.356	27.64	-1.98
20	0.168	13.04	-2.73
25	0.097	7.53	-3.28
30	0.03	2.33	-

Table C.17.  $C_D$  at different time. Conditions: Dye: AR-151,  $C_{D,i}=100$  mg/L,  $T=25^\circ\text{C}$ , stirrer rate=300 rpm,  $Q_G=150$  L/h, pH=2.5,  $D_{O_3}=1.17$  g/h, Cat=100% PFOA,  $m_{\text{cat}}=5$  g.

Time, min	Absorbance, $\text{cm}^{-1}$	$C_D$ , mg/L	$\ln(C_D/C_{D,i})$
0	2.116	100.00	0.00
0.5	1.804	85.25	-0.16
2.5	1.452	68.63	-0.38
5.0	1.119	52.87	-0.64
7.5	0.815	38.51	-0.95
10	0.583	27.56	-1.29
15	0.310	14.67	-1.92
20	0.212	10.02	-2.30
25	0.136	6.44	-2.74
30	0.108	5.12	-2.97

Table C.18.  $C_D$  at different time. Conditions: Dye: AR-151,  $C_{D,i}=100$  mg/L,  $T=25^\circ\text{C}$ , stirrer rate=300 rpm,  $Q_G=150$  L/h, pH=2.5,  $D_{O_3}=1.70$  g/h, Cat=100% PFOA,  $m_{\text{cat}}=5$  g.

Time, min	Absorbance, $\text{cm}^{-1}$	$C_D$ , mg/L	$\ln(C_D/C_{D,i})$
0	2.116	100.00	0.00
0.5	1.718	81.21	-0.21
2.5	1.304	61.65	-0.48
5.0	0.854	40.37	-0.91
7.5	0.586	27.72	-1.28
10	0.337	15.92	-1.84
15	0.166	7.84	-2.55
20	0.113	5.36	-2.93
25	0.076	3.57	-3.33
30	0.074	3.49	-3.35

Table C.19.  $C_D$  at different time. Conditions: Dye: AR-151,  $C_{D,i}=100$  mg/L,  $T=25^\circ\text{C}$ , stirrer rate=300 rpm,  $Q_G=150$  L/h, pH=2.5,  $D_{O_3}=2.21$  g/h, Cat=100% PFOA,  $m_{\text{cat}}=5$  g.

Time, min	Absorbance, $\text{cm}^{-1}$	$C_D$ , mg/L	$\ln(C_D/C_{D,i})$
0	2.116	100.00	0.00
0.5	1.692	79.98	-0.22
2.5	1.285	60.71	-0.50
5.0	0.774	36.57	-1.01
7.5	0.396	18.71	-1.68
10	0.195	9.24	-2.38
15	0.146	6.91	-2.67
20	0.107	5.05	-2.99
25	0.066	3.11	-3.47
30	0.041	1.94	-3.94

Table C.20.  $C_D$  at different time. Conditions: Dye: AR-151,  $C_{D,i}=400$  mg/L,  $T=25^\circ\text{C}$ , stirrer rate=300 rpm,  $Q_G=150$  L/h, pH=2.5,  $D_{O_3}=2.21$  g/h, Cat=100% PFOA,  $m_{\text{cat}}=5$  g.

Time, min	Absorbance, $\text{cm}^{-1}$	$C_D$ , mg/L	$\ln(C_D/C_{D,i})$
0	8.464	400.00	0.00
0.5	7.069	334.10	-0.18
2.5	6.190	292.55	-0.31
5.0	5.408	255.59	-0.45
7.5	5.016	237.03	-0.52
10	4.383	207.14	-0.66
15	3.470	163.98	-0.89
20	2.606	123.14	-1.18
25	1.842	87.03	-1.53
30	1.306	61.72	-1.87

Table C.21.  $C_D$  at different time. Conditions: Dye: *RBBR*,  $C_{D,i}=200$  mg/L,  $T=25^\circ\text{C}$ , stirrer rate=300 rpm,  $Q_G=150$  L/h, pH=2.5,  $D_{O_3}=2.21$  g/h.

Time, min	Absorbance, $\text{cm}^{-1}$	$C_D$ , mg/L	$\ln(C_D/C_{D,i})$
0	2.200	200.00	0.00
0.5	1.779	161.73	-0.21
2.5	1.376	125.09	-0.47
5.0	0.972	88.36	-0.82
7.5	0.667	60.64	-1.19
10	0.433	39.36	-1.63
15	0.18	16.36	-2.50
20	0.091	8.27	-3.19
25	0.025	2.27	-4.48
30	0.015	1.36	-4.99

Table C.22.  $C_D$  at different time. Conditions: Dye: *RBBR*,  $C_{D,i}=200$  mg/L,  $T=25^\circ\text{C}$ , stirrer rate=300 rpm,  $Q_G=150$  L/h, pH=7.0,  $D_{O_3}=2.21$  g/h.

Time, min	Absorbance, $\text{cm}^{-1}$	$C_D$ , mg/L	$\ln(C_D/C_{D,i})$
0	2.200	200.00	0.00
0.5	1.755	159.55	-0.23
2.5	1.437	130.64	-0.43
5.0	1.021	92.82	-0.77
7.5	0.706	64.18	-1.14
10	0.462	42.00	-1.56
15	0.209	19.00	-2.35
20	0.075	6.82	-3.38
25	0.021	1.91	-4.65
30	0.013	1.18	-5.13

Table C.23.  $C_D$  at different time. Conditions: Dye: *RBBR*,  $C_{D,i}=200$  mg/L,  $T=25^\circ\text{C}$ , stirrer rate=300 rpm,  $Q_G=150$  L/h, pH=13.0,  $D_{O_3}=2.21$  g/h.

Time, min	Absorbance, $\text{cm}^{-1}$	$C_D$ , mg/L	$\ln(C_D/C_{D,i})$
0	2.200	200.00	0.00
0.5	1.503	136.64	-0.38
2.5	1.186	107.82	-0.62
5.0	0.790	71.82	-1.02
7.5	0.489	44.45	-1.50
10	0.298	27.09	-2.00
15	0.135	12.27	-2.79
20	0.036	3.27	-4.11
25	0.016	1.45	-4.92
30	0.011	1.00	-5.30

Table C.24.  $C_D$  at different time. Conditions: Dye: *RBBR*,  $C_{D,i}=200$  mg/L,  $T=25^\circ\text{C}$ , stirrer rate=300 rpm,  $Q_G=150$  L/h, pH=2.5,  $D_{O_3}=2.21$  g/h, Catalyst=Alumina,  $m_{\text{cat}}=5$  g.

Time, min	Absorbance, $\text{cm}^{-1}$	$C_D$ , mg/L	$\ln(C_D/C_{D,i})$
0	2.200	200.00	0.00
0.5	1.786	162.37	-0.21
2.5	1.402	127.46	-0.45
5.0	0.97	88.18	-0.82
7.5	0.682	62.00	-1.17
10	0.466	42.36	-1.55
15	0.247	22.45	-2.19
20	0.163	14.82	-2.60
25	0.083	7.55	-3.28
30	0.056	5.09	-3.67

Table C.25.  $C_D$  at different time. Conditions: Dye: *RBBR*,  $C_{D,i}=200$  mg/L,  $T=25^\circ\text{C}$ , stirrer rate=300 rpm,  $Q_G=150$  L/h, pH=7.0,  $D_{O_3}=2.21$  g/h, Catalyst=Alumina,  $m_{\text{cat}}=5$  g.

Time, min	Absorbance, $\text{cm}^{-1}$	$C_D$ , mg/L	$\ln(C_D/C_{D,i})$
0	2.200	200.00	0.00
0.5	1.964	178.55	-0.11
2.5	1.473	133.91	-0.40
5.0	1.043	94.82	-0.75
7.5	0.746	67.82	-1.08
10	0.529	48.09	-1.43
15	0.321	29.18	-1.92
20	0.185	16.82	-2.48
25	0.086	7.82	-3.24
30	0.042	3.82	-3.96

Table C.26.  $C_D$  at different time. Conditions: Dye: *RBBR*,  $C_{D,i}=200$  mg/L,  $T=25^\circ\text{C}$ , stirrer rate=300 rpm,  $Q_G=150$  L/h, pH=13.0,  $D_{O_3}=2.21$  g/h, Catalyst=Alumina,  $m_{\text{cat}}=5$  g.

Time, min	Absorbance, $\text{cm}^{-1}$	$C_D$ , mg/L	$\ln(C_D/C_{D,i})$
0	2.200	200.00	0.00
0.5	1.627	147.91	-0.30
2.5	1.224	111.27	-0.59
5.0	0.867	78.82	-0.93
7.5	0.618	56.18	-1.27
10	0.465	42.27	-1.55
15	0.272	24.73	-2.09
20	0.201	18.27	-2.39
25	0.101	9.18	-3.08
30	0.038	3.45	-4.06

Table C.27.  $C_D$  at different time. Conditions: Dye: *RBBR*,  $C_{D,i}=200$  mg/L,  $T=25^\circ\text{C}$ , stirrer rate=300 rpm,  $Q_G=150$  L/h, pH=2.5,  $D_{O_3}=2.21$  g/h, Catalyst=25% PFOA,  $m_{\text{cat}}=5$  g.

Time, min	Absorbance, $\text{cm}^{-1}$	$C_D$ , mg/L	$\ln(C_D/C_{D,i})$
0	2.200	200.00	0.00
0.5	1.750	159.09	-0.23
2.5	1.296	117.82	-0.53
5.0	0.842	76.55	-0.96
7.5	0.537	48.82	-1.41
10	0.349	31.73	-1.84
15	0.131	11.91	-2.82
20	0.087	7.91	-3.23
25	0.063	5.73	-3.55
30	0.060	5.45	-3.60

Table C.28.  $C_D$  at different time. Conditions: Dye: *RBBR*,  $C_{D,i}=200$  mg/L,  $T=25^\circ\text{C}$ , stirrer rate=300 rpm,  $Q_G=150$  L/h, pH=7.0,  $D_{O_3}=2.21$  g/h, Catalyst=25% PFOA,  $m_{\text{cat}}=5$  g.

Time, min	Absorbance, $\text{cm}^{-1}$	$C_D$ , mg/L	$\ln(C_D/C_{D,i})$
0	2.200	200.00	0.00
0.5	1.684	153.09	-0.27
2.5	1.242	112.91	-0.57
5.0	0.799	72.64	-1.01
7.5	0.489	44.45	-1.50
10	0.334	30.36	-1.89
15	0.126	11.45	-2.86
20	0.032	2.91	-4.23
25	0.015	1.36	-4.99
30	0.009	0.82	-5.50

Table C.29.  $C_D$  at different time. Conditions: Dye: *RBBR*,  $C_{D,i}=200$  mg/L,  $T=25^\circ\text{C}$ , stirrer rate=300 rpm,  $Q_G=150$  L/h, pH=13.0,  $D_{O_3}=2.21$  g/h, Cat=25% PFOA,  $m_{\text{cat}}=5$  g.

Time, min	Absorbance, $\text{cm}^{-1}$	$C_D$ , mg/L	$\ln(C_D/C_{D,i})$
0	2.200	200.00	0.00
0.5	1.594	144.91	-0.32
2.5	1.226	111.46	-0.58
5.0	0.828	75.27	-0.98
7.5	0.567	51.55	-1.36
10	0.410	37.27	-1.68
15	0.214	19.45	-2.33
20	0.070	6.36	-3.45
25	0.044	4.00	-3.91
30	0.036	3.27	-4.11

Table C.30.  $C_D$  at different time. Conditions: Dye: *RBBR*,  $C_{D,i}=200$  mg/L,  $T=25^\circ\text{C}$ , stirrer rate=300 rpm,  $Q_G=150$  L/h, pH=2.5,  $D_{O_3}=2.21$  g/h, Catalyst=50% PFOA,  $m_{\text{cat}}=5$  g.

Time, min	Absorbance, $\text{cm}^{-1}$	$C_D$ , mg/L	$\ln(C_D/C_{D,i})$
0	2.200	200.00	0.00
0.5	1.744	158.55	-0.23
2.5	1.285	116.82	-0.54
5.0	0.808	73.46	-1.00
7.5	0.486	44.18	-1.51
10	0.297	27.00	-2.00
15	0.128	11.64	-2.84
20	0.078	7.09	-3.34
25	0.049	4.45	-3.80
30	0.052	4.73	-3.74

Table C.31.  $C_D$  at different time. Conditions: Dye: *RBBR*,  $C_{D,i}=200$  mg/L,  $T=25^\circ\text{C}$ , stirrer rate=300 rpm,  $Q_G=150$  L/h, pH=7.0,  $D_{O_3}=2.21$  g/h, Catalyst=50% PFOA,  $m_{\text{cat}}=5$  g.

Time, min	Absorbance, $\text{cm}^{-1}$	$C_D$ , mg/L	$\ln(C_D/C_{D,i})$
0	2.200	200.00	0.00
0.5	1.736	157.82	-0.24
2.5	1.270	115.46	-0.55
5.0	0.792	72.00	-1.02
7.5	0.482	43.82	-1.52
10	0.311	28.27	-1.96
15	0.168	15.27	-2.57
20	0.122	11.09	-2.89
25	0.044	4.00	-3.91
30	0.022	2.00	-4.61

Table C.32.  $C_D$  at different time. Conditions: Dye: *RBBR*,  $C_{D,i}=200$  mg/L,  $T=25^\circ\text{C}$ , stirrer rate=300 rpm,  $Q_G=150$  L/h, pH=13.0,  $D_{O_3}=2.21$  g/h, Cat=50% PFOA,  $m_{\text{cat}}=5$  g.

Time, min	Absorbance, $\text{cm}^{-1}$	$C_D$ , mg/L	$\ln(C_D/C_{D,i})$
0	2.200	200.00	0.00
0.5	1.625	147.73	-0.30
2.5	1.241	112.82	-0.57
5.0	0.815	74.09	-0.99
7.5	0.551	50.09	-1.38
10	0.405	36.82	-1.69
15	0.184	16.73	-2.48
20	0.106	9.64	-3.03
25	0.058	5.27	-3.64
30	0.050	4.55	-3.78

Table C.33.  $C_D$  at different time. Conditions: Dye: *RBBR*,  $C_{D,i}=200$  mg/L,  $T=25^\circ\text{C}$ , stirrer rate=300 rpm,  $Q_G=150$  L/h, pH=2.5,  $D_{O_3}=2.21$  g/h, Cat=100% PFOA,  $m_{\text{cat}}=5$  g.

Time, min	Absorbance, $\text{cm}^{-1}$	$C_D$ , mg/L	$\ln(C_D/C_{D,i})$
0	2.200	200.00	0.00
0.5	1.692	153.82	-0.26
2.5	1.194	108.55	-0.61
5.0	0.717	65.18	-1.12
7.5	0.441	40.09	-1.61
10	0.259	23.55	-2.14
15	0.126	11.45	-2.86
20	0.093	8.45	-3.16
25	0.054	4.91	-3.71
30	0.053	4.82	-3.73

Table C.34.  $C_D$  at different time. Conditions: Dye: *RBBR*,  $C_{D,i}=200$  mg/L,  $T=25^\circ\text{C}$ , stirrer rate=300 rpm,  $Q_G=150$  L/h, pH=7.0,  $D_{O_3}=2.21$  g/h, Cat=100% PFOA,  $m_{\text{cat}}=5$  g.

Time, min	Absorbance, $\text{cm}^{-1}$	$C_D$ , mg/L	$\ln(C_D/C_{D,i})$
0	2.200	200.00	0.00
0.5	1.756	159.64	-0.23
2.5	1.312	119.27	-0.52
5.0	0.843	76.64	-0.96
7.5	0.524	47.64	-1.43
10	0.330	30.00	-1.90
15	0.130	11.82	-2.83
20	0.081	7.36	-3.30
25	0.046	4.18	-3.87
30	0.014	1.27	-5.06

Table C.35.  $C_D$  at different time. Conditions: Dye: *RBBR*,  $C_{D,i}=200$  mg/L,  $T=25^\circ\text{C}$ , stirrer rate=300 rpm,  $Q_G=150$  L/h, pH=13.0,  $D_{O_3}=2.21$  g/h, Cat=100% PFOA,  $m_{\text{cat}}=5$  g.

Time, min	Absorbance, $\text{cm}^{-1}$	$C_D$ , mg/L	$\ln(C_D/C_{D,i})$
0	2.200	200.00	0.00
0.5	1.630	148.18	-0.30
2.5	1.224	111.27	-0.59
5.0	0.809	73.55	-1.00
7.5	0.541	49.18	-1.40
10	0.374	34.00	-1.77
15	0.197	17.91	-2.41
20	0.124	11.27	-2.88
25	0.069	6.27	-3.46
30	0.057	5.18	-3.65

Table C.36.  $C_D$  at different time. Conditions: Dye: *RBBR*,  $C_{D,i}=100$  mg/L,  $T=25^\circ\text{C}$ , stirrer rate=300 rpm,  $Q_G=150$  L/h, pH=7.0,  $D_{O_3}=1.17$  g/h, Cat=100% PFOA,  $m_{\text{cat}}=5$  g.

Time, min	Absorbance, $\text{cm}^{-1}$	$C_D$ , mg/L	$\ln(C_D/C_{D,i})$
0	1.100	100.00	0.00
0.5	0.943	85.73	-0.15
2.5	0.707	64.27	-0.44
5.0	0.463	42.09	-0.87
7.5	0.299	27.18	-1.30
10	0.200	18.18	-1.70
15	0.129	11.73	-2.14
20	0.079	7.18	-2.63
25	0.062	5.64	-2.88
30	0.049	4.45	-3.11

Table C.37.  $C_D$  at different time. Conditions: Dye: *RBBR*,  $C_{D,i}=100$  mg/L,  $T=25^\circ\text{C}$ , stirrer rate=300 rpm,  $Q_G=150$  L/h, pH=7.0,  $D_{O_3}=1.70$  g/h, Cat=100% PFOA,  $m_{\text{cat}}=5$  g.

Time, min	Absorbance, $\text{cm}^{-1}$	$C_D$ , mg/L	$\ln(C_D/C_{D,i})$
0	1.100	100.00	0.00
0.5	0.955	86.82	-0.14
2.5	0.653	59.36	-0.52
5.0	0.379	34.45	-1.07
7.5	0.220	20.00	-1.61
10	0.138	12.55	-2.08
15	0.056	5.09	-2.98
20	0.039	3.55	-3.34
25	0.032	2.91	-3.54
30	0.030	2.73	-3.60

Table C.38.  $C_D$  at different time. Conditions: Dye: *RBBR*,  $C_{D,i}=100$  mg/L,  $T=25^\circ\text{C}$ , stirrer rate=300 rpm,  $Q_G=150$  L/h, pH=7.0,  $D_{O_3}=2.21$  g/h, Cat=100% PFOA,  $m_{\text{cat}}=5$  g.

Time, min	Absorbance, $\text{cm}^{-1}$	$C_D$ , mg/L	$\ln(C_D/C_{D,i})$
0	1.100	100.00	0.00
0.5	0.909	82.64	-0.19
2.5	0.589	53.55	-0.62
5.0	0.315	28.64	-1.25
7.5	0.170	15.45	-1.87
10	0.090	8.18	-2.50
15	0.052	4.73	-3.05
20	0.034	3.09	-3.48
25	0.020	1.82	-4.01
30	0.010	0.91	-4.70

Table C.39.  $C_D$  at different time. Conditions: Dye: *RBBR*,  $C_{D,i}=400$  mg/L,  $T=25^\circ\text{C}$ , stirrer rate=300 rpm,  $Q_G=150$  L/h, pH=7.0,  $D_{O_3}=2.21$  g/h, Cat=100% PFOA,  $m_{\text{cat}}=5$  g.

Time, min	Absorbance, $\text{cm}^{-1}$	$C_D$ , mg/L	$\ln(C_D/C_{D,i})$
0	4.400	400.00	0.00
0.5	3.746	340.54	-0.16
2.5	3.132	284.73	-0.34
5.0	2.452	222.91	-0.58
7.5	1.715	155.91	-0.94
10	1.207	109.73	-1.29
15	0.541	49.18	-2.10
20	0.282	25.64	-2.75
25	0.126	11.45	-3.55
30	0.093	8.45	-3.86

Table C.40. Measured and corrected COD values for *AR-151*.  $T = 25^\circ\text{C}$ , Stirrer rate = 300 rpm,  $Q_G = 150$  L/h, reaction time = 30 min.

pH	$D_{O_3}$ , g/h	$C_{D,i}$ , mg/L	Cat. Type	$\text{COD}_f$ , mg/L	
2.5	1.17	100	100% PFOA	49	
			100% PFOA	46	
	2.21	200	100	100% PFOA	38
			-	112	
			Alumina	99	
			25% PFOA	104	
			50% PFOA	110	
			100% PFOA	94	
400	100% PFOA	306			
7	2.21	200	-	119	
			Alumina	95	
			25% PFOA	96	
			50% PFOA	93	
			100% PFOA	77	
13	2210	200	-	107	
			Alumina	43	
			25% PFOA	59	
			50% PFOA	64	
			100% PFOA	49	

Table C.41. Measured and corrected COD values for *RBBR*.  $T = 25^{\circ}\text{C}$ , Stirrer rate = 300 rpm,  $Q_G = 150 \text{ L/h}$ , Reaction time = 30 min.

pH	$D_{O_3}$ , g/h	$C_{D,i}$ , mg/L	Cat. Type	$\text{COD}_i$ , mg/L
2.5	2.21	200	-	128
			Alumina	133
			25% PFOA	124
			50% PFOA	111
			100% PFOA	101
7	1.17	100	100% PFOA	65
	1.70	100	100% PFOA	51
	2.21	100	100% PFOA	33
			-	110
			Alumina	127
		200	25% PFOA	108
			50% PFOA	103
			100% PFOA	39
400			100% PFOA	298
13	2.21	200	-	75
			Alumina	40
			25% PFOA	13
			50% PFOA	10
			100% PFOA	8

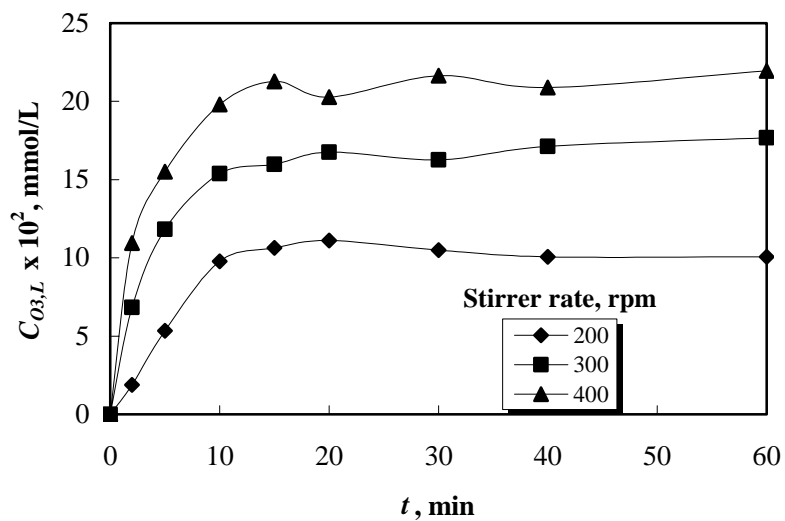


Figure C.1. The effect of stirrer rate on ozone absorption into water. Conditions:  $T=25^{\circ}\text{C}$ ,  $Q_G=150 \text{ L/h}$ ,  $D_{O_3}=46.04 \text{ mmol/h}$ , reaction time =60 min.

## APPENDIX D

### TRACER EXPERIMENTS DATA

Table D.1. Data for tracer experiment of  $Q_G=70$  L/h,  $Q_L=350$  L/h.

Time, s	Abs, $\text{cm}^{-1}$	C(t) mg/L	$E(t)$	$tE(t)$ , s	$t-t_m$	$(t-t_m)^2E(t)$
0	0.000	0.000	0.00000	0.0000	-55.045	0.000
8	0.005	0.493	0.00064	0.0052	-47.045	1.426
18	0.095	9.365	0.01224	0.2203	-37.045	16.795
28	0.133	13.111	0.01713	0.4797	-27.045	12.532
38	0.120	11.829	0.01546	0.5874	-17.045	4.491
48	0.098	9.661	0.01262	0.6060	-7.045	0.627
59	0.071	6.999	0.00915	0.5396	3.955	0.143
69	0.058	5.717	0.00747	0.5155	13.955	1.455
79	0.048	4.732	0.00618	0.4885	23.955	3.548
89	0.031	3.056	0.00399	0.3554	33.955	4.604
99	0.026	2.563	0.00335	0.3316	43.955	6.471
109	0.019	1.873	0.00245	0.2668	53.955	7.125
119	0.013	1.282	0.00167	0.1993	63.955	6.850
129	0.011	1.084	0.00142	0.1828	73.955	7.750
149	0.007	0.690	0.00090	0.1344	93.955	7.960
169	0.004	0.394	0.00052	0.0871	113.955	6.691
189	0.002	0.197	0.00026	0.0487	133.955	4.623
209	0.001	0.099	0.00013	0.0269	153.955	3.053
229	0.000	0.000	0.00000	0.0000	173.955	0.000

Table D.2. Data for tracer experiment of  $Q_G=100$  L/h,  $Q_L=350$  L/h.

Time, s	Abs, $\text{cm}^{-1}$	$C(t)$ mg/L	$E(t)$	$tE(t)$ , s	$t-t_m$	$(t-t_m)^2E(t)$
0	0	0.000	0.00000	0.0000	-55.852	0.000
6	0	0.000	0.00000	0.0000	-49.852	0.000
16	0.098	9.661	0.01192	0.1907	-39.852	18.931
26	0.137	13.505	0.01666	0.4332	-29.852	14.850
36	0.127	12.519	0.01545	0.5561	-19.852	6.088
46	0.097	9.562	0.01180	0.5427	-9.852	1.145
56	0.075	7.393	0.00912	0.5108	0.148	0.000
66	0.063	6.210	0.00766	0.5057	10.148	0.789
76	0.051	5.027	0.00620	0.4714	20.148	2.518
86	0.037	3.647	0.00450	0.3870	30.148	4.090
96	0.028	2.760	0.00341	0.3269	40.148	5.489
106	0.024	2.366	0.00292	0.3094	50.148	7.341
116	0.019	1.873	0.00231	0.2681	60.148	8.361
126	0.012	1.183	0.00146	0.1839	70.148	7.182
136	0.009	0.887	0.00109	0.1489	80.148	7.032
146	0.007	0.690	0.00085	0.1243	90.148	6.919
156	0.006	0.591	0.00073	0.1138	100.148	7.319
166	0.005	0.493	0.00061	0.1010	110.148	7.378
176	0.003	0.296	0.00036	0.0642	120.148	5.267
186	0.003	0.296	0.00036	0.0679	130.148	6.181
196	0.003	0.296	0.00036	0.0715	140.148	7.167
206	0.002	0.197	0.00024	0.0501	150.148	5.484
216	0.002	0.197	0.00024	0.0525	160.148	6.239
226	0.001	0.099	0.00012	0.0275	170.148	3.521
236	0.001	0.099	0.00012	0.0287	180.148	3.947
246	0.001	0.099	0.00012	0.0299	190.148	4.398
256	0.000	0.000	0.00000	0.0000	200.148	0.000

Table D.3. Data for tracer experiment of  $Q_G=150$  L/h,  $Q_L=350$  L/h.

Time, s	Abs, $\text{cm}^{-1}$	$C(t)$ mg/L	$E(t)$	$tE(t)$ , s	$t-t_m$	$(t-t_m)^2E(t)$
0	0	0.000	0.00000	0.0000	-51.710	0.000
8	0.028	2.760	0.00346	0.0277	-43.710	6.608
18	0.119	11.731	0.01470	0.2646	-33.710	16.703
28	0.135	13.308	0.01668	0.4669	-23.710	9.374
38	0.119	11.731	0.01470	0.5586	-13.710	2.763
48	0.092	9.069	0.01136	0.5455	-3.710	0.156
58	0.072	7.098	0.00889	0.5158	6.291	0.352
68	0.057	5.619	0.00704	0.4788	16.291	1.868
78	0.044	4.337	0.00543	0.4239	26.291	3.757
88	0.034	3.352	0.00420	0.3696	36.291	5.531
98	0.027	2.662	0.00334	0.3268	46.291	7.146
108	0.019	1.873	0.00235	0.2535	56.291	7.436
118	0.015	1.479	0.00185	0.2186	66.291	8.142
145	0.006	0.591	0.00074	0.1075	93.291	6.450
165	0.003	0.296	0.00037	0.0611	113.291	4.756
185	0.002	0.197	0.00025	0.0457	133.291	4.389
205	0.001	0.099	0.00012	0.0253	153.291	2.902
225	0	0.000	0.00000	0.0000	173.291	0.000

Table D.4. Data for tracer experiment of  $Q_G=70$  L/h,  $Q_L=300$  L/h.

Time, s	Abs, $\text{cm}^{-1}$	$C(t)$ mg/L	$E(t)$	$tE(t)$ , s	$t-t_m$	$(t-t_m)^2 E(t)$
0	0.000	0.000	0.00000	0.0000	-60.967	0.000
6	0.000	0.000	0.00000	0.0000	-54.967	0.000
16	0.054	5.323	0.00621	0.0994	-44.967	12.565
26	0.125	12.322	0.01438	0.3740	-34.967	17.588
36	0.137	13.505	0.01577	0.5675	-24.967	9.827
46	0.117	11.534	0.01346	0.6193	-14.967	3.016
56	0.099	9.759	0.01139	0.6380	-4.967	0.281
66	0.076	7.492	0.00875	0.5772	5.033	0.222
76	0.063	6.210	0.00725	0.5510	15.033	1.638
86	0.049	4.830	0.00564	0.4849	25.033	3.533
96	0.034	3.352	0.00391	0.3756	35.033	4.802
106	0.026	2.563	0.00299	0.3171	45.033	6.068
116	0.018	1.774	0.00207	0.2403	55.033	6.273
136	0.012	1.183	0.00138	0.1878	75.033	7.774
156	0.007	0.690	0.00081	0.1257	95.033	7.275
176	0.005	0.493	0.00058	0.1013	115.033	7.614
196	0.003	0.296	0.00035	0.0677	135.033	6.295
216	0.002	0.197	0.00023	0.0497	155.033	5.532
236	0.001	0.099	0.00012	0.0272	175.033	3.525
256	0.000	0.000	0.00000	0.0000	195.033	0.000

Table D.5. Data for tracer experiment of  $Q_G=100$  L/h,  $Q_L=300$  L/h.

Time, s	Abs, $\text{cm}^{-1}$	$C(t)$ mg/L	$E(t)$	$tE(t)$ , s	$t-t_m$	$(t-t_m)^2E(t)$
0	0	0.000	0.00000	0.0000	-61.731	0.000
6	0.002	0.197	0.00024	0.0014	-55.731	0.740
16	0.072	7.098	0.00858	0.1373	-45.731	17.941
26	0.128	12.618	0.01525	0.3965	-35.731	19.471
36	0.122	12.026	0.01454	0.5233	-25.731	9.624
46	0.099	9.759	0.01180	0.5426	-15.731	2.919
56	0.082	8.083	0.00977	0.5471	-5.731	0.321
66	0.064	6.309	0.00763	0.5033	4.270	0.139
76	0.055	5.422	0.00655	0.4980	14.270	1.334
86	0.045	4.436	0.00536	0.4611	24.270	3.158
96	0.034	3.352	0.00405	0.3889	34.270	4.758
106	0.03	2.957	0.00357	0.3789	44.270	7.005
116	0.022	2.169	0.00262	0.3041	54.270	7.720
126	0.018	1.774	0.00214	0.2702	64.270	8.859
136	0.015	1.479	0.00179	0.2431	74.270	9.858
146	0.012	1.183	0.00143	0.2088	84.270	10.154
156	0.009	0.887	0.00107	0.1673	94.270	9.530
166	0.007	0.690	0.00083	0.1385	104.270	9.068
176	0.006	0.591	0.00071	0.1258	114.270	9.335
186	0.004	0.394	0.00048	0.0886	124.270	7.360
196	0.003	0.296	0.00036	0.0701	134.270	6.444
206	0.003	0.296	0.00036	0.0736	144.270	7.440
216	0.002	0.197	0.00024	0.0515	154.270	5.671
226	0.001	0.099	0.00012	0.0269	164.270	3.215
236	0.001	0.099	0.00012	0.0281	174.270	3.619
246	0.000	0.000	0.00000	0.0000	184.270	0.000

Table D.6. Data for tracer experiment of  $Q_G=150$  L/h,  $Q_L=300$  L/h.

Time, s	Abs, $\text{cm}^{-1}$	$C(t)$ mg/L	$E(t)$	$tE(t)$ , s	$t-t_m$	$(t-t_m)^2 E(t)$
0	0	0.000	0.00000	0.0000	-65.312	0.000
6	0.007	0.690	0.00075	0.0045	-59.312	2.641
16	0.087	8.576	0.00933	0.1493	-49.312	22.689
26	0.136	13.406	0.01459	0.3792	-39.312	22.541
36	0.128	12.618	0.01373	0.4942	-29.312	11.795
46	0.106	10.449	0.01137	0.5229	-19.312	4.240
56	0.084	8.280	0.00901	0.5045	-9.312	0.781
66	0.071	6.999	0.00761	0.5026	0.688	0.004
76	0.057	5.619	0.00611	0.4646	10.688	0.698
86	0.046	4.535	0.00493	0.4243	20.688	2.112
96	0.038	3.746	0.00408	0.3912	30.688	3.838
106	0.031	3.056	0.00332	0.3524	40.688	5.504
116	0.025	2.464	0.00268	0.3110	50.688	6.889
136	0.016	1.577	0.00172	0.2334	70.688	8.574
156	0.011	1.084	0.00118	0.1840	90.688	9.703
176	0.008	0.789	0.00086	0.1510	110.688	10.512
196	0.006	0.591	0.00064	0.1261	130.688	10.990
216	0.004	0.394	0.00043	0.0927	150.688	9.741
236	0.003	0.296	0.00032	0.0759	170.688	9.374
256	0.002	0.197	0.00021	0.0549	190.688	7.800
276	0.001	0.099	0.00011	0.0296	210.688	4.761
296	0.000	0.000	0.00000	0.0000	230.688	0.000

Table D.7. Data for tracer experiment of  $Q_G=70$  L/h,  $Q_L=250$  L/h.

Time, s	Abs, $\text{cm}^{-1}$	$C(t)$ mg/L	$E(t)$	$tE(t)$ , s	$t-t_m$	$(t-t_m)^2E(t)$
0	0	0.000	0.00000	0.0000	-81.540	0.000
6	0.001	0.099	0.00009	0.0005	-75.540	0.506
16	0.051	5.027	0.00452	0.0724	-65.540	19.427
26	0.073	7.196	0.00647	0.1683	-55.540	19.969
36	0.106	10.449	0.00940	0.3384	-45.540	19.494
46	0.122	12.026	0.01082	0.4977	-35.540	13.665
56	0.116	11.435	0.01029	0.5761	-25.540	6.710
66	0.1	9.858	0.00887	0.5853	-15.540	2.141
76	0.095	9.365	0.00842	0.6403	-5.540	0.259
86	0.078	7.689	0.00692	0.5949	4.461	0.138
96	0.066	6.506	0.00585	0.5619	14.461	1.224
106	0.052	5.126	0.00461	0.4888	24.461	2.759
116	0.046	4.535	0.00408	0.4732	34.461	4.844
136	0.031	3.056	0.00275	0.3739	54.461	8.154
156	0.022	2.169	0.00195	0.3043	74.461	10.817
176	0.015	1.479	0.00133	0.2341	94.461	11.869
196	0.01	0.986	0.00089	0.1738	114.461	11.618
216	0.007	0.690	0.00062	0.1341	134.461	11.223
236	0.004	0.394	0.00035	0.0837	154.461	8.463
256	0.003	0.296	0.00027	0.0681	174.461	8.097
276	0.002	0.197	0.00018	0.0490	194.461	6.707
296	0.001	0.099	0.00009	0.0262	214.461	4.079

Table D.8. Data for tracer experiment of  $Q_G=100$  L/h,  $Q_L=250$  L/h.

Time, s	Abs, $\text{cm}^{-1}$	$C(t)$ mg/L	$E(t)$	$tE(t)$ , s	$t-t_m$	$(t-t_m)^2E(t)$
0	0	0.000	0.00000	0.0000	-73.386	0.000
6	0	0.000	0.00000	0.0000	-67.386	0.000
16	0.055	5.422	0.00511	0.0817	-57.386	16.822
26	0.119	11.731	0.01105	0.2873	-47.386	24.817
36	0.13	12.815	0.01207	0.4346	-37.386	16.876
46	0.124	12.224	0.01152	0.5297	-27.386	8.637
56	0.108	10.646	0.01003	0.5617	-17.386	3.032
66	0.091	8.971	0.00845	0.5578	-7.386	0.461
76	0.074	7.295	0.00687	0.5223	2.614	0.047
86	0.063	6.210	0.00585	0.5032	12.614	0.931
96	0.054	5.323	0.00502	0.4815	22.614	2.565
106	0.043	4.239	0.00399	0.4233	32.614	4.248
116	0.037	3.647	0.00344	0.3986	42.614	6.240
126	0.03	2.957	0.00279	0.3511	52.614	7.713
136	0.025	2.464	0.00232	0.3158	62.614	9.103
146	0.021	2.070	0.00195	0.2847	72.614	10.284
156	0.017	1.676	0.00158	0.2463	82.614	10.776
166	0.015	1.479	0.00139	0.2313	92.614	11.949
176	0.012	1.183	0.00111	0.1961	102.614	11.735
186	0.01	0.986	0.00093	0.1727	112.614	11.778
196	0.008	0.789	0.00074	0.1456	122.614	11.170
206	0.007	0.690	0.00065	0.1339	132.614	11.433
216	0.006	0.591	0.00056	0.1204	142.614	11.333
226	0.004	0.394	0.00037	0.0840	152.614	8.652
236	0.004	0.394	0.00037	0.0877	162.614	9.823
246	0.003	0.296	0.00028	0.0685	172.614	8.302
256	0.002	0.197	0.00019	0.0476	182.614	6.194
266	0.002	0.197	0.00019	0.0494	192.614	6.891
276	0.001	0.099	0.00009	0.0256	202.614	3.813
286	0.000	0.000	0.00000	0.0000	212.614	0.000

Table D.9. Data for tracer experiment of  $Q_G=150$  L/h,  $Q_L=250$  L/h.

Time, s	Abs, $\text{cm}^{-1}$	$C(t)$ mg/L	$E(t)$	$tE(t)$ , s	$t-t_m$	$(t-t_m)^2E(t)$
0	0	0.000	0.00000	0.0000	-71.707	0.000
10	0.022	2.169	0.00215	0.0215	-61.707	8.178
20	0.098	9.661	0.00957	0.1913	-51.707	25.578
30	0.127	12.519	0.01240	0.3719	-41.707	21.566
40	0.125	12.322	0.01220	0.4881	-31.707	12.268
50	0.109	10.745	0.01064	0.5320	-21.707	5.014
60	0.094	9.266	0.00918	0.5506	-11.707	1.258
70	0.081	7.985	0.00791	0.5535	-1.707	0.023
80	0.065	6.408	0.00635	0.5076	8.293	0.436
90	0.052	5.126	0.00508	0.4569	18.293	1.699
100	0.044	4.337	0.00430	0.4295	28.293	3.439
110	0.039	3.845	0.00381	0.4188	38.293	5.583
120	0.032	3.154	0.00312	0.3749	48.293	7.286
140	0.023	2.267	0.00225	0.3143	68.293	10.472
160	0.015	1.479	0.00146	0.2343	88.293	11.416
180	0.01	0.986	0.00098	0.1757	108.293	11.449
200	0.006	0.591	0.00059	0.1171	128.293	9.641
220	0.004	0.394	0.00039	0.0859	148.293	8.587
240	0.003	0.296	0.00029	0.0703	168.293	8.295
260	0.001	0.099	0.00010	0.0254	188.293	3.461
280	0.001	0.099	0.00010	0.0273	208.293	4.235
300	0.000	0.000	0.00000	0.0000	228.293	0.000

Table D.10. Data for tracer experiment of  $Q_G=70$  L/h,  $Q_L=200$  L/h.

Time, s	Abs, $\text{cm}^{-1}$	$C(t)$ mg/L	$E(t)$	$tE(t)$ , s	$t-t_m$	$(t-t_m)^2E(t)$
0	0	0.000	0.00000	0.0000	-87.760	0.000
6	0	0.000	0.00000	0.0000	-81.760	0.000
16	0.051	5.027	0.00391	0.0626	-71.760	20.157
26	0.103	10.153	0.00791	0.2055	-61.760	30.154
36	0.124	12.224	0.00952	0.3426	-51.760	25.498
46	0.125	12.322	0.00959	0.4413	-41.760	16.731
57	0.119	11.731	0.00913	0.5206	-30.760	8.642
67	0.107	10.548	0.00821	0.5502	-20.760	3.539
77	0.096	9.463	0.00737	0.5674	-10.760	0.853
87	0.082	8.083	0.00629	0.5476	-0.760	0.004
97	0.07	6.900	0.00537	0.5212	9.240	0.459
107	0.061	6.013	0.00468	0.5010	19.240	1.733
117	0.056	5.520	0.00430	0.5029	29.240	3.675
137	0.039	3.845	0.00299	0.4101	49.240	7.258
157	0.029	2.859	0.00223	0.3495	69.240	10.671
177	0.021	2.070	0.00161	0.2853	89.240	12.836
197	0.015	1.479	0.00115	0.2268	109.240	13.739
217	0.01	0.986	0.00077	0.1666	129.240	12.820
237	0.007	0.690	0.00054	0.1273	149.240	11.967
257	0.006	0.591	0.00046	0.1184	169.240	13.190
277	0.004	0.394	0.00031	0.0850	189.240	10.995
297	0.002	0.197	0.00015	0.0456	209.240	6.721
317	0.001	0.099	0.00008	0.0243	229.240	4.033
337	0.001	0.099	0.00008	0.0259	249.240	4.768
357	0.000	0.000	0.00000	0.0000	269.240	0.000

Table D.11. Data for tracer experiment of  $Q_G=100$  L/h,  $Q_L=200$  L/h.

Time, s	Abs, $\text{cm}^{-1}$	$C(t)$ mg/L	$E(t)$	$tE(t)$ , s	$t-t_m$	$(t-t_m)^2E(t)$
0	0	0.000	0.00000	0.0000	-93.277	0.000
6	0.005	0.493	0.00039	0.0023	-87.277	2.960
16	0.04	3.943	0.00311	0.0497	-77.277	18.565
26	0.108	10.646	0.00839	0.2182	-67.277	37.992
36	0.123	12.125	0.00956	0.3441	-57.277	31.362
46	0.118	11.632	0.00917	0.4219	-47.277	20.498
56	0.108	10.646	0.00839	0.4701	-37.277	11.664
66	0.091	8.971	0.00707	0.4668	-27.277	5.262
76	0.086	8.478	0.00668	0.5080	-17.277	1.995
86	0.077	7.590	0.00598	0.5147	-7.277	0.317
96	0.068	6.703	0.00528	0.5074	2.723	0.039
106	0.062	6.112	0.00482	0.5108	12.723	0.780
116	0.056	5.520	0.00435	0.5049	22.723	2.247
126	0.05	4.929	0.00389	0.4896	32.723	4.161
136	0.043	4.239	0.00334	0.4545	42.723	6.100
146	0.038	3.746	0.00295	0.4312	52.723	8.210
156	0.032	3.154	0.00249	0.3880	62.723	9.784
166	0.028	2.760	0.00218	0.3612	72.723	11.509
176	0.023	2.267	0.00179	0.3146	82.723	12.232
200	0.017	1.676	0.00132	0.2642	106.723	15.049
220	0.012	1.183	0.00093	0.2052	126.723	14.977
250	0.008	0.789	0.00062	0.1554	156.723	15.272
270	0.006	0.591	0.00047	0.1259	176.723	14.564
290	0.005	0.493	0.00039	0.1127	196.723	15.039
310	0.003	0.296	0.00023	0.0723	216.723	10.951
330	0.001	0.099	0.00008	0.0256	236.723	4.355
350	0.000	0.000	0.00000	0.0000	256.723	0.000

Table D.12. Data for tracer experiment of  $Q_G=150$  L/h,  $Q_L=200$  L/h.

Time, s	Abs, $\text{cm}^{-1}$	$C(t)$ mg/L	$E(t)$	$tE(t)$ , s	$t-t_m$	$(t-t_m)^2 E(t)$
0	0	0.000	0.00000	0.0000	-91.035	0.000
6	0.004	0.394	0.00029	0.0017	-85.035	2.062
16	0.066	6.506	0.00471	0.0753	-75.035	26.494
26	0.118	11.632	0.00841	0.2187	-65.035	35.584
36	0.131	12.914	0.00934	0.3362	-55.035	28.289
46	0.131	12.914	0.00934	0.4296	-45.035	18.943
56	0.123	12.125	0.00877	0.4911	-35.035	10.764
66	0.109	10.745	0.00777	0.5129	-25.035	4.871
76	0.098	9.661	0.00699	0.5310	-15.035	1.579
86	0.084	8.280	0.00599	0.5151	-5.035	0.152
96	0.071	6.999	0.00506	0.4860	4.965	0.125
106	0.062	6.112	0.00442	0.4686	14.965	0.990
116	0.055	5.422	0.00392	0.4549	24.965	2.444
126	0.048	4.732	0.00342	0.4312	34.965	4.184
146	0.035	3.450	0.00250	0.3643	54.965	7.539
166	0.027	2.662	0.00193	0.3196	74.965	10.818
186	0.02	1.972	0.00143	0.2652	94.965	12.860
206	0.015	1.479	0.00107	0.2203	114.965	14.135
226	0.012	1.183	0.00086	0.1934	134.965	15.585
246	0.008	0.789	0.00057	0.1403	154.965	13.697
266	0.006	0.591	0.00043	0.1138	174.965	13.096
286	0.005	0.493	0.00036	0.1020	194.965	13.551
306	0.004	0.394	0.00029	0.0873	214.965	13.179
326	0.002	0.197	0.00014	0.0465	234.965	7.873
346	0.002	0.197	0.00014	0.0493	254.965	9.270
366	0.001	0.099	0.00007	0.0261	274.965	5.391
386	0.001	0.099	0.00007	0.0275	294.965	6.203
406	0.000	0.000	0.00000	0.0000	314.965	0.000

Table D.13. Data for tracer experiment of  $Q_G=70$  L/h,  $Q_L=150$  L/h.

Time, s	Abs, $\text{cm}^{-1}$	$C(t)$ mg/L	$E(t)$	$tE(t)$ , s	$t-t_m$	$(t-t_m)^2E(t)$
0	0	0.000	0.00000	0.0000	-148.488	0.000
8	0.002	0.197	0.00010	0.0008	-140.488	1.880
18	0.047	4.633	0.00224	0.0403	-130.488	38.109
28	0.081	7.985	0.00386	0.1080	-120.488	55.997
38	0.116	11.435	0.00552	0.2099	-110.488	67.434
48	0.122	12.026	0.00581	0.2789	-100.488	58.665
58	0.123	12.125	0.00586	0.3397	-90.488	47.960
68	0.121	11.928	0.00576	0.3918	-80.488	37.328
78	0.115	11.336	0.00548	0.4272	-70.488	27.210
88	0.109	10.745	0.00519	0.4568	-60.488	18.991
98	0.101	9.956	0.00481	0.4713	-50.488	12.260
108	0.091	8.971	0.00433	0.4680	-40.488	7.104
118	0.087	8.576	0.00414	0.4889	-30.488	3.851
128	0.082	8.083	0.00390	0.4998	-20.488	1.639
148	0.067	6.605	0.00319	0.4722	-0.488	0.001
168	0.054	5.323	0.00257	0.4320	19.512	0.979
188	0.045	4.436	0.00214	0.4029	39.512	3.345
208	0.039	3.845	0.00186	0.3863	59.512	6.577
228	0.033	3.253	0.00157	0.3583	79.512	9.935
248	0.028	2.760	0.00133	0.3307	99.512	13.204
268	0.024	2.366	0.00114	0.3063	119.512	16.324
288	0.02	1.972	0.00095	0.2743	139.512	18.537
308	0.018	1.774	0.00086	0.2640	159.512	21.810
338	0.015	1.479	0.00071	0.2414	189.512	25.654
368	0.012	1.183	0.00057	0.2103	219.512	27.535
398	0.009	0.887	0.00043	0.1706	249.512	26.682
428	0.007	0.690	0.00033	0.1427	279.512	26.043
458	0.006	0.591	0.00029	0.1309	309.512	27.371
488	0.005	0.493	0.00024	0.1162	339.512	27.445
518	0.004	0.394	0.00019	0.0987	369.512	26.008
548	0.003	0.296	0.00014	0.0783	399.512	22.802
578	0.002	0.197	0.00010	0.0550	429.512	17.570
608	0.001	0.099	0.00005	0.0290	459.512	10.055
638	0.000	0.000	0.00000	0.0000	489.512	0.000

Table D.14. Data for tracer experiment of  $Q_G=150$  L/h,  $Q_L=150$  L/h.

Time, s	Abs, $\text{cm}^{-1}$	$C(t)$ mg/L	$E(t)$	$tE(t)$ , s	$t-t_m$	$(t-t_m)^2E(t)$
0	0	0.000	0.00000	0.0000	-150.898	0.000
10	0	0.000	0.00000	0.0000	-140.898	0.000
20	0.05	4.929	0.00216	0.0433	-130.898	37.061
30	0.09	8.872	0.00389	0.1168	-120.898	56.907
40	0.116	11.435	0.00502	0.2007	-110.898	61.714
50	0.124	12.224	0.00536	0.2682	-100.898	54.610
60	0.127	12.519	0.00549	0.3296	-90.898	45.394
70	0.126	12.421	0.00545	0.3815	-80.898	35.672
80	0.121	11.928	0.00523	0.4188	-70.898	26.311
90	0.116	11.435	0.00502	0.4516	-60.898	18.610
100	0.11	10.843	0.00476	0.4759	-50.898	12.328
110	0.103	10.153	0.00446	0.4901	-40.898	7.453
120	0.095	9.365	0.00411	0.4932	-30.898	3.923
130	0.091	8.971	0.00394	0.5118	-20.898	1.719
154	0.074	7.295	0.00320	0.4930	3.102	0.031
174	0.065	6.408	0.00281	0.4893	23.102	1.501
194	0.056	5.520	0.00242	0.4700	43.102	4.501
214	0.048	4.732	0.00208	0.4444	63.102	8.268
240	0.037	3.647	0.00160	0.3841	89.102	12.707
260	0.03	2.957	0.00130	0.3374	109.102	15.448
280	0.025	2.464	0.00108	0.3028	129.102	18.026
300	0.022	2.169	0.00095	0.2855	149.102	21.158
320	0.019	1.873	0.00082	0.2630	169.102	23.504
350	0.015	1.479	0.00065	0.2271	199.102	25.723
380	0.012	1.183	0.00052	0.1973	229.102	27.247
410	0.009	0.887	0.00039	0.1596	259.102	26.138
440	0.007	0.690	0.00030	0.1332	289.102	25.309
470	0.005	0.493	0.00022	0.1017	319.102	22.025
500	0.004	0.394	0.00017	0.0865	349.102	21.089
530	0.003	0.296	0.00013	0.0688	379.102	18.652
560	0.002	0.197	0.00009	0.0485	409.102	14.480
590	0.001	0.099	0.00004	0.0255	439.102	8.341
620	0.000	0.000	0.00000	0.0000	469.102	0.000

Table D.15. Data for tracer experiment of  $Q_G=200$  L/h,  $Q_L=350$  L/h. Cat=100% PFOA,  $m_{cat}=175$  g.

Time, s	Abs, $\text{cm}^{-1}$	$C(t)$ mg/L	$E(t)$	$tE(t)$ , s	$t-t_m$	$(t-t_m)^2E(t)$
0	0.000	0.000	0.00000	0.0000	-63.953	0.000
10	0.057	5.619	0.00630	0.0630	-53.953	18.333
20	0.134	13.209	0.01481	0.2961	-43.953	28.603
30	0.141	13.899	0.01558	0.4674	-33.953	17.960
40	0.119	11.731	0.01315	0.5259	-23.953	7.544
50	0.086	8.478	0.00950	0.4751	-13.953	1.850
60	0.065	6.408	0.00718	0.4309	-3.953	0.112
70	0.051	5.027	0.00564	0.3945	6.047	0.206
80	0.046	4.535	0.00508	0.4066	16.047	1.309
90	0.034	3.352	0.00376	0.3381	26.047	2.549
100	0.026	2.563	0.00287	0.2873	36.047	3.733
110	0.022	2.169	0.00243	0.2674	46.047	5.154
120	0.017	1.676	0.00188	0.2254	56.047	5.900
140	0.012	1.183	0.00133	0.1856	76.047	7.668
160	0.010	0.986	0.00110	0.1768	96.047	10.193
180	0.008	0.789	0.00088	0.1591	116.047	11.904
200	0.006	0.591	0.00066	0.1326	136.047	12.270
220	0.005	0.493	0.00055	0.1215	156.047	13.453
240	0.004	0.394	0.00044	0.1061	176.047	13.698
260	0.003	0.296	0.00033	0.0862	196.047	12.740
280	0.002	0.197	0.00022	0.0619	216.047	10.315
300	0.001	0.099	0.00011	0.0331	236.047	6.156
320	0.000	0.000	0.00000	0.0000	256.047	0.000

## APPENDIX E

### OZONE ABSORPTION EXPERIMENTS DATA

Table E.1. Liquid phase ozone concentration. Conditions:  $Q_G=150$  L/h,  $Q_L=30$  L/h,  $C_{O_3,G,in} = 0.298$  mmol/L,  $V_{blank}=10$  mL,  $A_{blank}=0.202$  cm<sup>-1</sup>,  $t=25$  min,  $V_{thio,in}=29.7$  mL,  $V_{thio,out}=214.7$  mL, catalyst=no.

$z$ , m	Time, min	$V_T$ , mL	$A_{ind}$ , cm <sup>-1</sup>	$C_{O_3,L}$ mmol/L
0.09	0			0.0000
	5	27.0	0.094	0.0433
	10	30.9	0.067	0.0416
	15	30.6	0.059	0.0442
	20	34.0	0.045	0.0408
	25	32.4	0.041	0.0446
0.21	0			0.0000
	5	30.3	0.049	0.0473
	10	31.0	0.031	0.0499
	15	32.2	0.012	0.0515
	20	32.7	0.007	0.0515
	25	25.3	0.077	0.0536
0.52	0			0.0000
	5	30.9	0.02	0.0528
	10	31.5	0.006	0.0546
	15	31.2	0.005	0.0556
	20	27.6	0.046	0.0553
	25	28.6	0.028	0.0572
0.88	0			0.0000
	5	28.5	0.042	0.0537
	10	27.9	0.038	0.0566
	15	27.8	0.03	0.0592
	20	27.5	0.037	0.0582
	25	27.4	0.032	0.0600

Table E.2. Liquid phase ozone concentration. Conditions:  $Q_G=100$  L/h,  $Q_L= 30$  L/h,  $C_{O_3,G,in} = 0.304$  mmol/L,  $V_{blank}=10$  mL,  $A_{blank}=0.197$  cm<sup>-1</sup>,  $t=20$  min,  $V_{thio,in}=20.3$  mL,  $V_{thio,out}=145.8$  mL. Catalyst=no.

$z, \text{ m}$	Time, min	$V_T, \text{ mL}$	$A_{ind}, \text{ cm}^{-1}$	$C_{O_3,L}$ mmol/L
0.08	0			0
	2.5	31.1	0.061	0.0320
	5	27	0.074	0.0360
	7.5	26.5	0.072	0.0377
	10	27.9	0.064	0.0369
	15	28.3	0.067	0.0353
	20	29.1	0.058	0.0362
0.21	0			
	2.5	26.2	0.06	0.0420
	5	30.4	0.005	0.0468
	7.5	29.9	0.02	0.0442
	10	28.6	0.019	0.0476
	15	32.3	0	0.0439
	20	23.1	0.072	0.0474
0.52	0			
	2.5	28.9	0.03	0.0439
	5	26.8	0.029	0.0497
	7.5	27	0.031	0.0485
	10	25.9	0.031	0.0519
	15	28.3	0.011	0.0505
	20	27.5	0.018	0.0508
0.88	0			
	2.5	28.1	0.018	0.0492
	5	23.4	0.047	0.0556
	7.5	26.9	0.011	0.0547
	10	25.4	0.027	0.0549
	15	25.4	0.031	0.0536
	20	26.3	0.018	0.0546

Table E.3. Steady state liquid phase ozone concentration. Conditions:  $Q_G=100$  L/h,  $Q_L=150$  L/h,  $C_{O_3,G,in} = 0.293$  mmol/L,  $V_{blank}=10$  mL,  $A_{blank}=0.141$  cm<sup>-1</sup>,  $t=20$  min,  $V_{thio,in}=19.5$  mL,  $V_{thio,out}=91.0$  mL, catalyst=no.

$z$ , m	$V_T$ , mL	$A_{ind}$ , cm <sup>-1</sup>	$C_{O_3,L}$ mmol/L
0.00	-	-	0.0000
0.09	26.9	0.070	0.0209
0.21	25.5	0.049	0.0295
0.52	25.8	0.017	0.0390
0.88	23.2	0.025	0.0437

Table E.4. Steady state liquid phase ozone concentration. Conditions:  $Q_G=100$  L/h,  $Q_L=200$  L/h,  $C_{O_3,G,in} = 0.302$  mmol/L,  $V_{blank}=10$  mL,  $A_{blank}=0.092$  cm<sup>-1</sup>,  $t=20$  min,  $V_{thio,in}=20.1$  mL,  $V_{thio,out}=65.9$  mL. Catalyst=no.

$z$ , m	$V_T$ , mL	$A_{ind}$ , cm <sup>-1</sup>	$C_{O_3,L}$ mmol/L
0.00	-	-	0.0000
0.09	33.6	0.044	0.0101
0.21	32.0	0.016	0.0172
0.52	26.0	0.010	0.0255
0.88	25.3	0.002	0.0292

Table E.5. Steady state liquid phase ozone concentration. Conditions:  $Q_G=70$  L/h,  $Q_L=30$  L/h,  $C_{O_3,G,in} = 0.297$  mmol/L,  $V_{blank}=10$  mL,  $A_{blank}=0.184$  cm<sup>-1</sup>,  $t=20$  min,  $V_{thio,in}=14.2$  mL,  $V_{thio,out}=91.1$  mL. Catalyst=no.

$z$ , m	$V_T$ , mL	$A_{ind}$ , cm <sup>-1</sup>	$C_{O_3,L}$ mmol/L
0.00	-	-	0.0000
0.09	23.0	0.051	0.0279
0.21	18.4	0.061	0.0373
0.52	23.7	0.000	0.0450
0.88	20.4	0.023	0.0483

Table E.6. Steady state liquid phase ozone concentration. Conditions:  $Q_G=100$  L/h,  $Q_L=110$  L/h,  $C_{O_3,G,in} = 0.294$  mmol/L,  $V_{blank}=10$  mL,  $A_{blank}=0.169$  cm<sup>-1</sup>,  $t=20$  min,  $V_{thio,in}=19.6$  mL,  $V_{thio,out}=126.8$  mL. No catalyst.

$z$ , m	$V_T$ , mL	$A_{ind}$ , cm <sup>-1</sup>	$C_{O_3,L}$ mmol/L
0.00	-	-	0.0000
0.09	31.0	0.010	0.0376
0.21	24.2	0.042	0.0445
0.52	19.5	0.079	0.0471
0.88	23.0	0.039	0.0497

Table E.7. Steady state liquid phase ozone concentration. Conditions:  $Q_G=100$  L/h,  $Q_L=250$  L/h,  $C_{O_3,G,in} = 0.291$  mmol/L,  $V_{blank}=10$  mL,  $A_{blank}=0.191$  cm<sup>-1</sup>,  $t=20$  min,  $V_{thio,in}=19.4$  mL,  $V_{thio,out}=44.6$  mL. Catalyst=no.

$z$ , m	$V_T$ , mL	$A_{ind}$ , cm <sup>-1</sup>	$C_{O_3,L}$ , mmol/L
0.00	-	-	0.0000
0.09	29.3	0.167	0.0062
0.21	28.7	0.143	0.0128
0.52	25.8	0.130	0.0192
0.88	21.4	0.136	0.0240

Table E.8. Steady state liquid phase ozone concentration. Conditions:  $Q_G=45$  L/h,  $Q_L=30$  L/h,  $C_{O_3,G,in} = 0.307$  mmol/L,  $V_{blank}=10$  mL,  $A_{blank}=0.137$  cm<sup>-1</sup>,  $t=17.5$  min,  $V_{thio,in}=9.2$  mL,  $V_{thio,out}=24.7$  mL. Catalyst=no.

$z$ , m	$V_T$ , mL	$A_{ind}$ , cm <sup>-1</sup>	$C_{O_3,L}$ , mmol/L
0.00	-	-	0.0000
0.09	24.9	0.081	0.0187
0.21	20.3	0.071	0.0318
0.52	21.2	0.055	0.0364
0.88	22.0	0.035	0.0422

Table E.9. Steady state liquid phase ozone concentration. Conditions:  $Q_G = 125$  L/h,  $Q_L = 30$  L/h,  $C_{O_3,G,in} = 0.305$  mmol/L,  $V_{blank} = 10$  mL,  $A_{blank} = 0.187$  cm<sup>-1</sup>,  $t = 20$  min,  $V_{thio,in} = 25.4$  mL,  $V_{thio,out} = 77.3$  mL. Catalyst = no.

$z$ , m	$V_T$ , mL	$A_{ind}$ , cm <sup>-1</sup>	$C_{O_3,L}$ , mmol/L
0.00	-	-	0.000
0.09	22.8	0.084	0.040
0.21	25.7	0.029	0.050
0.52	23.1	0.045	0.054
0.88	22.1	0.046	0.058

Table E.10. Steady state liquid phase ozone concentration. Conditions:  $Q_G = 150$  L/h,  $Q_L = 30$  L/h,  $C_{O_3,G,in} = 0.324$  mmol/L,  $V_{blank} = 10$  mL,  $A_{blank} = 0.213$  cm<sup>-1</sup>,  $t = 20$  min,  $V_{thio,in} = 32.4$  mL,  $V_{thio,out} = 291.9$  mL. Catalyst = alumina,  $m_{cat} = 25$  g.

$z$ , m	$V_T$ , mL	$A_{ind}$ , cm <sup>-1</sup>	$C_{O_3,L}$ , mmol/L
0.00	-	-	0.000
0.09	26.8	0.041	0.051
0.21	22.5	0.055	0.063
0.52	24.6	0.019	0.066
0.88	23.4	0.024	0.070

Table E.11. Steady state liquid phase ozone concentration. Conditions:  $Q_G = 150$  L/h,  $Q_L = 30$  L/h,  $C_{O_3,G,in} = 0.314$  mmol/L,  $V_{blank} = 10$  mL,  $A_{blank} = 0.218$  cm<sup>-1</sup>,  $t = 20$  min,  $V_{thio,in} = 32.4$  mL,  $V_{thio,out} = 200.2$  mL. Catalyst = alumina,  $m_{cat} = 35$  g.

$z$ , m	$V_T$ , mL	$A_{ind}$ , cm <sup>-1</sup>	$C_{O_3,L}$ , mmol/L
0.00	-	-	0.0000
0.09	24.5	0.082	0.0466
0.21	24.7	0.024	0.0656
0.52	25.2	0.012	0.0674
0.88	24.5	0.003	0.0737

Table E.12. Steady state liquid phase ozone concentration. Conditions:  $Q_G = 150$  L/h,  $Q_L = 30$  L/h,  $C_{O_3,G,in} = 0.314$  mmol/L,  $V_{blank} = 10$  mL,  $A_{blank} = 0.225$  cm<sup>-1</sup>,  $t = 19$  min,  $V_{thio,in} = 31.4$  mL,  $V_{thio,out} = 196.2$  mL. Catalyst = alumina,  $m_{cat} = 50$  g.

$z$ , m	$V_T$ , mL	$A_{ind}$ , cm <sup>-1</sup>	$C_{O_3,L}$ , mmol/L
0.00	-	-	0.0000
0.09	26.8	0.048	0.0524
0.21	23.5	0.040	0.0681
0.52	24.2	0.022	0.0711
0.88	22.2	0.037	0.0766

Table E.13. Steady state liquid phase ozone concentration. Conditions:  $Q_G = 150$  L/h,  $Q_L = 30$  L/h,  $C_{O_3,G,in} = 0.317$  mmol/L,  $V_{blank} = 10$  mL,  $A_{blank} = 0.219$  cm<sup>-1</sup>,  $t = 19$  min,  $V_{thio,in} = 31.7$  mL,  $V_{thio,out} = 196.2$  mL. Catalyst = alumina,  $m_{cat} = 75$  g.

$z$ , m	$V_T$ , mL	$A_{ind}$ , cm <sup>-1</sup>	$C_{O_3,L}$ , mmol/L
0.00	-	-	0.0000
0.09	27.5	0.038	0.0514
0.21	23.8	0.027	0.0691
0.52	21.5	0.045	0.0752
0.88	19.4	0.072	0.0777

Table E.14. Steady state liquid phase ozone concentration. Conditions:  $Q_G = 150$  L/h,  $Q_L = 30$  L/h,  $C_{O_3,G,in} = 0.317$  mmol/L,  $V_{blank} = 10$  mL,  $A_{blank} = 0.210$  cm<sup>-1</sup>,  $t = 19$  min,  $V_{thio,in} = 31.7$  mL,  $V_{thio,out} = 185.6$  mL. Catalyst = alumina,  $m_{cat} = 100$  g.

$z$ , m	$V_T$ , mL	$A_{ind}$ , cm <sup>-1</sup>	$C_{O_3,L}$ , mmol/L
0.00	-	-	0.0000
0.09	24.2	0.063	0.0515
0.21	21.0	0.062	0.0669
0.52	21.5	0.045	0.0713
0.88	20.0	0.055	0.0769

Table E15. Steady state liquid phase ozone concentration. Conditions:  $Q_G = 150$  L/h,  $Q_L = 30$  L/h,  $C_{O_3,G,in} = 0.339$  mmol/L,  $V_{blank} = 10$  mL,  $A_{blank} = 0.223$  cm<sup>-1</sup>,  $t = 19$  min,  $V_{thio,in} = 33.9$  mL,  $V_{thio,out} = 162.6$  mL. Catalyst = alumina,  $m_{cat} = 125$  g.

$z$ , m	$V_T$ , mL	$A_{ind}$ , cm <sup>-1</sup>	$C_{O_3,L}$ , mmol/L
0.00	-	-	0.0000
0.09	25.1	0.064	0.0523
0.21	22.6	0.045	0.0702
0.52	22.2	0.040	0.0745
0.88	20.3	0.058	0.0796

Table E.16. Steady state liquid phase ozone concentration. Conditions:  $Q_G = 150$  L/h,  $Q_L = 30$  L/h,  $C_{O_3,G,in} = 0.317$  mmol/L,  $V_{blank} = 10$  mL,  $A_{blank} = 0.222$  cm<sup>-1</sup>,  $t = 19$  min,  $V_{thio,in} = 34.8$  mL,  $V_{thio,out} = 153.0$  mL. Catalyst = alumina,  $m_{cat} = 150$  g.

$z$ , m	$V_T$ , mL	$A_{ind}$ , cm <sup>-1</sup>	$C_{O_3,L}$ , mmol/L
0.00	-	-	0.0000
0.09	26.6	0.044	0.0533
0.21	20.8	0.065	0.0722
0.52	22.5	0.031	0.0759
0.88	20.9	0.045	0.0807

Table E.17. Steady state liquid phase ozone concentration. Conditions:  $Q_G = 150$  L/h,  $Q_L = 30$  L/h,  $C_{O_3,G,in} = 0.336$  mmol/L,  $V_{blank} = 10$  mL,  $A_{blank} = 0.221$  cm<sup>-1</sup>,  $t = 19$  min,  $V_{thio,in} = 33.6$  mL,  $V_{thio,out} = 141.2$  mL. Catalyst = alumina,  $m_{cat} = 175$  g.

$z$ , m	$V_T$ , mL	$A_{ind}$ , cm <sup>-1</sup>	$C_{O_3,L}$ , mmol/L
0.00	-	-	0.0000
0.09	25.2	0.051	0.0556
0.21	22.2	0.045	0.0722
0.52	22.0	0.033	0.0779
0.88	20.7	0.046	0.0813

Table E.18. Steady state liquid phase ozone concentration. Conditions:  $Q_G = 150$  L/h,  $Q_L = 30$  L/h,  $C_{O_3,G,in} = 0.330$  mmol/L,  $V_{blank} = 10$  mL,  $A_{blank} = 0.218$  cm<sup>-1</sup>,  $t = 20$  min,  $V_{thio,in} = 33.0$  mL,  $V_{thio,out} = 272.3$  mL. Catalyst = PFOA,  $m_{cat} = 25$  g.

$z$ , m	$V_T$ , mL	$A_{ind}$ , cm <sup>-1</sup>	$C_{O_3,L}$ , mmol/L
0.00	-	-	0.0000
0.09	24.8	0.080	0.0460
0.21	25.2	0.048	0.0556
0.52	23.7	0.052	0.0602
0.88	20.5	0.086	0.0625

Table E.19. Steady state liquid phase ozone concentration. Conditions:  $Q_G = 150$  L/h,  $Q_L = 30$  L/h,  $C_{O_3,G,in} = 0.338$  mmol/L,  $V_{blank} = 10$  mL,  $A_{blank} = 0.230$  cm<sup>-1</sup>,  $t = 19$  min,  $V_{thio,in} = 33.8$  mL,  $V_{thio,out} = 243.8$  mL. Catalyst = PFOA,  $m_{cat} = 35$  g.

$z$ , m	$V_T$ , mL	$A_{ind}$ , cm <sup>-1</sup>	$C_{O_3,L}$ , mmol/L
0.00	-	-	0.0000
0.09	26.0	0.052	0.0553
0.21	23.8	0.041	0.0681
0.52	22.2	0.052	0.0725
0.88	20.1	0.070	0.0787

Table E.20. Steady state liquid phase ozone concentration. Conditions:  $Q_G = 150$  L/h,  $Q_L = 30$  L/h,  $C_{O_3,G,in} = 0.346$  mmol/L,  $V_{blank} = 10$  mL,  $A_{blank} = 0.227$  cm<sup>-1</sup>,  $t = 20$  min,  $V_{thio,in} = 34.6$  mL,  $V_{thio,out} = 221.5$  mL. Catalyst = PFOA,  $m_{cat} = 50$  g.

$z$ , m	$V_T$ , mL	$A_{ind}$ , cm <sup>-1</sup>	$C_{O_3,L}$ , mmol/L
0.00	-	-	0.0000
0.09	29.2	0.037	0.0492
0.21	23.2	0.039	0.0708
0.52	23.7	0.026	0.0729
0.88	20.8	0.054	0.0796

Table E.21. Steady state liquid phase ozone concentration. Conditions:  $Q_G = 150$  L/h,  $Q_L = 30$  L/h,  $C_{O_3,G,in} = 0.336$  mmol/L,  $V_{blank} = 10$  mL,  $A_{blank} = 0.232$  cm<sup>-1</sup>,  $t = 20$  min,  $V_{thio,in} = 33.6$  mL,  $V_{thio,out} = 210.8$  mL. Catalyst = PFOA,  $m_{cat} = 75$  g.

$z$ , m	$V_T$ , mL	$A_{ind}$ , cm <sup>-1</sup>	$C_{O_3,L}$ , mmol/L
0.00	-	-	0.0000
0.09	30.0	0.037	0.0485
0.21	25.8	0.026	0.0648
0.52	24.2	0.038	0.0679
0.88	22.7	0.037	0.0763

Table E.22. Steady state liquid phase ozone concentration. Conditions:  $Q_G = 150$  L/h,  $Q_L = 30$  L/h,  $C_{O_3,G,in} = 0.314$  mmol/L,  $V_{blank} = 10$  mL,  $A_{blank} = 0.255$  cm<sup>-1</sup>,  $t = 20$  min,  $V_{thio,in} = 31.4$  mL,  $V_{thio,out} = 208.8$  mL. Catalyst = PFOA,  $m_{cat} = 100$  g.

$z$ , m	$V_T$ , mL	$A_{ind}$ , cm <sup>-1</sup>	$C_{O_3,L}$ , mmol/L
0.00	-	-	0.0000
0.09	29.8	0.051	0.0512
0.21	25.0	0.055	0.0663
0.52	23.0	0.067	0.0719
0.88	22.0	0.064	0.0791

Table E.23. Steady state liquid phase ozone concentration. Conditions:  $Q_G = 150$  L/h,  $Q_L = 30$  L/h,  $C_{O_3,G,in} = 0.328$  mmol/L,  $V_{blank} = 10$  mL,  $A_{blank} = 0.235$  cm<sup>-1</sup>,  $t = 20$  min,  $V_{thio,in} = 32.8$  mL,  $V_{thio,out} = 203.5$  mL. Catalyst = PFOA,  $m_{cat} = 125$  g.

$z$ , m	$V_T$ , mL	$A_{ind}$ , cm <sup>-1</sup>	$C_{O_3,L}$ , mmol/L
0.00	-	-	0.0000
0.09	27.5	0.065	0.0483
0.21	25.4	0.026	0.0675
0.52	23.1	0.043	0.0729
0.88	20.9	0.057	0.0813

Table E.24. Steady state liquid phase ozone concentration. Conditions:  $Q_G = 150$  L/h,  $Q_L = 30$  L/h,  $C_{O_3,G,in} = 0.303$  mmol/L,  $V_{blank} = 10$  mL,  $A_{blank} = 0.234$  cm<sup>-1</sup>,  $t = 20$  min,  $V_{thio,in} = 30.3$  mL,  $V_{thio,out} = 198.7$  mL. Catalyst = PFOA,  $m_{cat} = 150$  g.

$z$ , m	$V_T$ , mL	$A_{ind}$ , cm <sup>-1</sup>	$C_{O_3,L}$ , mmol/L
0.00	-	-	0.0000
0.09	29.9	0.071	0.0407
0.21	25.0	0.049	0.0613
0.52	26.4	0.027	0.0627
0.88	22.8	0.051	0.0711

Table E.25. Steady state liquid phase ozone concentration. Conditions:  $Q_G = 150$  L/h,  $Q_L = 30$  L/h,  $C_{O_3,G,in} = 0.306$  mmol/L,  $V_{blank} = 10$  mL,  $A_{blank} = 0.231$  cm<sup>-1</sup>,  $t = 20$  min,  $V_{thio,in} = 30.6$  mL,  $V_{thio,out} = 212.0$  mL. Catalyst = PFOA,  $m_{cat} = 175$  g.

$z$ , m	$V_T$ , mL	$A_{ind}$ , cm <sup>-1</sup>	$C_{O_3,L}$ , mmol/L
0.00	-	-	0.0000
0.09	27.0	0.079	0.0444
0.21	25.1	0.030	0.0661
0.52	23.8	0.035	0.0706
0.88	22.5	0.045	0.0740

Table E.26. Steady state liquid phase ozone concentration. Conditions:  $Q_G = 70$  L/h,  $Q_L = 80$  L/h,  $C_{O_3,G,in} = 0.300$  mmol/L,  $V_{blank} = 10$  mL,  $A_{blank} = 0.236$  cm<sup>-1</sup>,  $t = 19$  min,  $V_{thio,in} = 14.0$  mL,  $V_{thio,out} = 104.6$  mL. Catalyst = no.

$z$ , m	$V_T$ , mL	$A_{ind}$ , cm <sup>-1</sup>	$C_{O_3,L}$ , mmol/L
0.00	-	-	0.0000
0.09	35.8	0.087	0.0288
0.21	29.2	0.103	0.0344
0.52	26.9	0.099	0.0403
0.88	24.1	0.105	0.0462

Table E.27. Steady state liquid phase ozone concentration. Conditions:  $Q_G = 70$  L/h,  $Q_L = 110$  L/h,  $C_{O_3,G,in} = 0.298$  mmol/L,  $V_{blank} = 10$  mL,  $A_{blank} = 0.238$  cm<sup>-1</sup>,  $t = 19$  min,  $V_{thio,in} = 13.9$  mL,  $V_{thio,out} = 100.1$  mL. Catalyst = no.

$z$ , m	$V_T$ , mL	$A_{ind}$ , cm <sup>-1</sup>	$C_{O_3,L}$ , mmol/L
0.00	-	-	0.0000
0.09	26.9	0.155	0.0243
0.21	27.1	0.128	0.0320
0.52	25.8	0.121	0.0368
0.88	23.6	0.129	0.0398

Table E.28. Steady state liquid phase ozone concentration. Conditions:  $Q_G = 70$  L/h,  $Q_L = 150$  L/h,  $C_{O_3,G,in} = 0.311$  mmol/L,  $V_{blank} = 10$  mL,  $A_{blank} = 0.244$  cm<sup>-1</sup>,  $t = 19$  min,  $V_{thio,in} = 14.5$  mL,  $V_{thio,out} = 89.5$  mL. Catalyst = no.

$z$ , m	$V_T$ , mL	$A_{ind}$ , cm <sup>-1</sup>	$C_{O_3,L}$ , mmol/L
0.00	-	-	0.0000
0.09	38.0	0.182	0.0110
0.21	29.9	0.154	0.0225
0.52	28.7	0.136	0.0287
0.88	25.2	0.148	0.0314

Table E.29. Steady state liquid phase ozone concentration. Conditions:  $Q_G = 70$  L/h,  $Q_L = 200$  L/h,  $C_{O_3,G,in} = 0.315$  mmol/L,  $V_{blank} = 10$  mL,  $A_{blank} = 0.231$  cm<sup>-1</sup>,  $t = 19$  min,  $V_{thio,in} = 14.7$  mL,  $V_{thio,out} = 80.0$  mL. Catalyst = no.

$z$ , m	$V_T$ , mL	$A_{ind}$ , cm <sup>-1</sup>	$C_{O_3,L}$ , mmol/L
0.00	-	-	0.0000
0.09	43.2	0.184	0.0070
0.21	32.2	0.167	0.0143
0.52	30.5	0.143	0.0213
0.88	25.4	0.150	0.0261

Table E.30. Steady state liquid phase ozone concentration. Conditions:  $Q_G = 70$  L/h,  $Q_L = 250$  L/h,  $C_{O_3,G,in} = 0.294$  mmol/L,  $V_{blank} = 10$  mL,  $A_{blank} = 0.222$  cm<sup>-1</sup>,  $t = 20$  min,  $V_{thio,in} = 29.4$  mL,  $V_{thio,out} = 193.6$  mL. Catalyst = no.

$z$ , m	$V_T$ , mL	$A_{ind}$ , cm <sup>-1</sup>	$C_{O_3,L}$ , mmol/L
0.00	-	-	0.0000
0.09	34.5	0.201	0.0043
0.21	36.7	0.172	0.0093
0.52	32.5	0.146	0.0168
0.88	33.2	0.127	0.0204

Table E.31. Steady state liquid phase ozone concentration. Conditions:  $Q_G = 150$  L/h,  $Q_L = 150$  L/h,  $C_{O_3,G,in} = 0.789$  mmol/L,  $V_{blank} = 30$  mL,  $A_{blank} = 0.568$  cm<sup>-1</sup>,  $t = 20$  min,  $V_{thio,in} = 24.9$  mL,  $V_{thio,out} = 94.0$  mL. Catalyst = no.  $M_{thio} = 0.3$  M.

$z$ , m	$V_T$ , mL	$A_{ind}$ , cm <sup>-1</sup>	$C_{O_3,L}$ , mmol/L
0.00	-	-	0.0000
0.09	47.7	0.279	0.0812
0.21	44.8	0.263	0.1024
0.52	44.2	0.260	0.1078
0.88	43.1	0.247	0.1218

Table E.32. Steady state liquid phase ozone concentration. Conditions:  $Q_G = 150$  L/h,  $Q_L = 150$  L/h,  $C_{O_3,G,in} = 0.862$  mmol/L,  $V_{blank} = 30$  mL,  $A_{blank} = 0.520$  cm<sup>-1</sup>,  $t = 20$  min,  $V_{thio,in} = 86.2$  mL,  $V_{thio,out} = 92.1$  mL. Catalyst = alumina,  $m_{cat} = 25$  g,  $d_{cat} = 2.0$  mm.  $M_{thio} = 0.3$  M for out.

$z$ , m	$V_T$ , mL	$A_{ind}$ , cm <sup>-1</sup>	$C_{O_3,L}$ , mmol/L
0.00	-	-	0.0000
0.09	60.2	0.205	0.0519
0.21	45.1	0.112	0.1344
0.52	44.3	0.105	0.1442
0.88	43.1	0.101	0.1590

Table E.33. Steady state liquid phase ozone concentration. Conditions:  $Q_G = 150$  L/h,  $Q_L = 150$  L/h,  $C_{O_3,G,in} = 0.904$  mmol/L,  $V_{blank} = 30$  mL,  $A_{blank} = 0.635$  cm<sup>-1</sup>,  $t = 20$  min,  $V_{thio,in} = 90.4$  mL,  $V_{thio,out} = 86.2$  mL. Catalyst = alumina, ,  $m_{cat} = 75$  g,  $d_{cat} = 2.0$  mm.  $M_{thio} = 0.3$  M for out.

$z$ , m	$V_T$ , mL	$A_{ind}$ , cm <sup>-1</sup>	$C_{O_3,L}$ , mmol/L
0.00	-	-	0.0000
0.09	69.1	0.314	0.0408
0.21	51.5	0.103	0.1230
0.52	49.8	0.045	0.1481
0.88	43.4	0.186	0.1665

Table E.34. Steady state liquid phase ozone concentration. Conditions:  $Q_G = 150$  L/h,  $Q_L = 150$  L/h,  $C_{O_3,G,in} = 0.928$  mmol/L,  $V_{blank} = 30$  mL,  $A_{blank} = 0.712$  cm<sup>-1</sup>,  $t = 20$  min,  $V_{thio,in} = 92.8$  mL,  $V_{thio,out} = 94.3$  mL. Catalyst = alumina, ,  $m_{cat} = 125$  g,  $d_{cat} = 2.0$  mm.  $M_{thio} = 0.3$  M for out.

$z$ , m	$V_T$ , mL	$A_{ind}$ , cm <sup>-1</sup>	$C_{O_3,L}$ , mmol/L
0.00	-	-	0.0000
0.09	58.6	0.396	0.0548
0.21	50.5	0.173	0.1307
0.52	52.2	0.031	0.1525
0.88	45.6	0.156	0.1771

Table E.35. Steady state liquid phase ozone concentration. Conditions:  $Q_G = 150$  L/h,  $Q_L = 150$  L/h,  $C_{O_3,G,in} = 0.953$  mmol/L,  $V_{blank} = 30$  mL,  $A_{blank} = 0.686$  cm<sup>-1</sup>,  $t = 20$  min,  $V_{thio,in} = 90.0$  mL,  $V_{thio,out} = 80.0$  mL. Catalyst = PFOA,  $m_{cat}=25$  g,  $d_{cat}=2.0$  mm,  $M_{thio} = 0.3$  M for out.

$z$ , m	$V_T$ , mL	$A_{ind}$ , cm <sup>-1</sup>	$C_{O_3,L}$ , mmol/L
0.00	-	-	0.0000
0.09	69.0	0.334	0.0449
0.21	52.0	0.164	0.1179
0.52	48.2	0.215	0.1285
0.88	47.3	0.137	0.1577

Table E.36. Steady state liquid phase ozone concentration. Conditions:  $Q_G = 150$  L/h,  $Q_L = 150$  L/h,  $C_{O_3,G,in} = 0.938$  mmol/L,  $V_{blank} = 30$  mL,  $A_{blank} = 0.629$  cm<sup>-1</sup>,  $t = 19$  min,  $V_{thio,in} = 93.8$  mL,  $V_{thio,out} = 33.0$  mL. Catalyst = PFOA,  $m_{cat} = 75$  g,  $d_{cat} = 2.0$  mm.  $M_{thio} = 0.3$  M for out.

$z, m$	$V_T, mL$	$A_{ind}, cm^{-1}$	$C_{O_3,L}, mmol/L$
0.00	-	-	0.0000
0.09	65.8	0.301	0.0454
0.21	48.0	0.215	0.1142
0.52	48.2	0.108	0.1423
0.88	44.5	0.129	0.1714

Table E.37. Steady state liquid phase ozone concentration. Conditions:  $Q_G = 150$  L/h,  $Q_L = 150$  L/h,  $C_{O_3,G,in} = 0.933$  mmol/L,  $V_{blank} = 30$  mL,  $A_{blank} = 0.666$  cm<sup>-1</sup>,  $t = 15$  min,  $V_{thio,in} = 93.3$  mL,  $V_{thio,out} = 84.6$  mL. Catalyst = PFOA,  $m_{cat} = 125$  g,  $d_{cat} = 2.0$  mm.  $M_{thio} = 0.3$  M for out.

$z, m$	$V_T, mL$	$A_{ind}, cm^{-1}$	$C_{O_3,L}, mmol/L$
0.00	-	-	0.0000
0.09	60.2	0.285	0.0627
0.21	52.0	0.043	0.1406
0.52	46.4	0.130	0.1625
0.88	45.9	0.067	0.1872

## APPENDIX F

### DYE OZONATION EXPERIMENTS DATA

#### Run 1

Conditions: pH=2.5,  $Q_G=150$  L/h,  $Q_L=30$  L/h,  $C_{O_3,G,in}=0.277$  mmol/L gas,  $C_{O_3,G,out}=0.179$  mmol/L gas,  $t=20$  min,  $V_{thio,inlet}=27.7$  mL,  $V_{thio,outlet}=178.5$  mL, Dye=RBBR,  $C_{D,in}=4.9 \times 10^{-2}$  mmol/L,  $TOC_{in}=11.26$  mg/L,  $A_b=0.174$  cm<sup>-1</sup>,  $V_b=10$  mL, no catalyst.

Table F.1. Dye concentration change.

$z, m$	$t, min$	$A_{RBBR}, cm^{-1}$	$C_D \times 10^2, mmol/L$
0.09	0	0.422	4.87
	2.5	0.096	1.11
	5.0	0.059	0.68
	7.5	0.028	0.32
	10	0.023	0.27
	15	0.021	0.24
	20	0.016	0.18
0.21	0	0.422	4.87
	2.5	0.047	0.54
	5	0.012	0.14
	7.5	0.005	0.06
	10	0.009	0.10
	15	0.007	0.08
	20	0.007	0.08
0.52	0	0.422	4.87
	2.5	0.021	0.24
	5	0.007	0.08
	7.5	0.002	0.02
	10	0.014	0.16
	15	0.003	0.03
	20	0.006	0.07
0.88	0	0.422	4.87
	2.5	0.031	0.36
	5	0.008	0.09
	7.5	0.003	0.03
	10	0.011	0.13
	15	0.003	0.03
	20	0.003	0.03

Table F.2. Dissolved O<sub>3</sub> concentration change.

<i>z</i> , m	<i>t</i> , min	<i>V<sub>T</sub></i> , mL	<i>A<sub>ind</sub></i> , cm <sup>-1</sup>	<i>C<sub>O<sub>3,L</sub></sub></i> × 10 <sup>3</sup> , mmol/L
0.09	0			0.00
	2.5	45.0	0.135	5.50
	5.0	38.0	0.104	12.50
	7.5	31.3	0.122	12.20
	10	40.0	0.099	12.43
	15	34.4	0.112	12.60
	20	31.5	0.119	12.60
0.21	0			0.00
	2.5	46.0	0.127	6.50
	5	40.2	0.085	14.60
	7.5	33.0	0.096	16.80
	10	45.6	0.065	15.30
	15	34.9	0.089	17.00
	20	39.5	0.086	14.70
0.52	0			0.00
	2.5	43.8	0.110	9.40
	5	37.6	0.076	17.70
	7.5	31.5	0.050	28.70
	10	30.8	0.042	31.60
	15	27.2	0.071	29.90
	20	34.2	0.030	29.60
0.88	0			0.00
	2.5	35	0.117	11.30
	5	30.1	0.084	22.30
	7.5	30	0.043	32.70
	10	24.2	0.077	34.00
	15	29	0.052	32.00
	20	27	0.061	33.10

Table F.3. TOC change.

<i>z</i> , m	TOC, mg/L
0.00	11.26
0.09	10.17
0.21	9.94
0.52	9.74
0.88	9.24

**Run 2**

Conditions: pH=2.5,  $Q_G=150$  L/h,  $Q_L=30$  L/h,  $C_{O_3,G,in}=0.319$  mmol/L gas,  $C_{O_3,G,out}=0.137$  mmol/L gas, t=20 min,  $V_{thio,inlet}=31.9$  mL,  $V_{thio,outlet}=137.2$  mL, Dye=RBBR,  $C_{D,in}=8.9 \times 10^{-2}$  mmol/L,  $TOC_{in}=23.04$  mg/L,  $A_{ind}=0.185$  cm<sup>-1</sup>, no catalyst.

Table F.4. Dye concentration change.

z, m	t, min	Abs, cm <sup>-1</sup>	$C_D \times 10^2$ , mmol/L
0.09	0	0.773	8.91
	2.5	0.232	2.68
	5.0	0.122	1.41
	7.5	0.114	1.31
	10	0.068	0.78
	15	0.076	0.88
	20	0.089	1.03
0.21	0	0.773	8.91
	2.5	0.17	1.96
	5	0.06	0.69
	7.5	0.049	0.57
	10	0.036	0.42
	15	0.025	0.29
	20	0.038	0.44
0.52	0	0.773	8.91
	2.5	0.096	1.11
	5	0.022	0.25
	7.5	0.009	0.10
	10	0.012	0.14
	15	0.008	0.09
	20	0.009	0.10
0.88	0	0.773	8.91
	2.5	0.087	1.00
	5	0.022	0.25
	7.5	0.008	0.09
	10	0.013	0.15
	15	0.011	0.13
	20	0.007	0.08

Table F.5. Dissolved O<sub>3</sub> concentration change.

<i>z</i> , m	<i>t</i> , min	<i>V<sub>T</sub></i> , mL	<i>A<sub>ind</sub></i> , cm <sup>-1</sup>	<i>C<sub>O<sub>3,L</sub></sub></i> × 10 <sup>3</sup> , mmol/L
0.09	0			0.00
	2.5	37	0.167	3.30
	5.0	25.2	0.175	3.10
	7.5	32.4	0.163	4.80
	10	41.5	0.152	5.20
	15	33.2	0.162	4.90
	20	37.5	0.158	4.90
0.21	0			0.00
	2.5	34	0.164	4.30
	5	39.9	0.147	6.30
	7.5	35	0.150	7.00
	10	44	0.135	7.30
	15	43.2	0.135	7.50
	20	49.1	0.129	7.10
0.52	0			0.00
	2.5	36.9	0.154	5.70
	5	33	0.141	9.40
	7.5	36	0.113	13.70
	10	38	0.086	17.70
	15	40	0.084	16.70
	20	38	0.095	15.90
0.88	0			0.00
	2.5	28	0.148	10.10
	5	30	0.138	11.70
	7.5	29.8	0.114	17.90
	10	30.8	0.090	22.70
	15	30.9	0.084	23.90
	20	30.9	0.090	22.60

Table F.6. TOC change.

<i>z</i> , m	TOC, mg/L
0.00	23.04
0.09	22.62
0.21	21.65
0.52	20.39
0.88	19.88

### Run 3

Conditions: pH=2.5,  $Q_G=150$  L/h,  $Q_L=30$  L/h,  $C_{O_3,G,in}=0.318$  mmol/L gas,  $C_{O_3,G,out}=0.103$  mmol/L gas,  $t=20$  min,  $V_{thio,inlet}=31.8$  mL,  $V_{thio,outlet}=128.1$  mL, Dye=RBBR,  $C_{D,in}=13.4 \times 10^{-2}$  mmol/L,  $TOC_{in}=36.28$  mg/L,  $A_{ind}=0.230$  cm<sup>-1</sup>, no catalyst.

Table F.7. Dye concentration change.

$z, m$	$t, min$	Abs, cm <sup>-1</sup>	$C_D \times 10^2, mmol/L$
0.09	0	1.163	13.41
	2.5	0.487	5.62
	5.0	0.254	2.93
	7.5	0.207	2.39
	10	0.208	2.40
	15	0.179	2.06
	20	0.181	2.09
	0.21	0	1.163
2.5		0.406	4.68
5		0.173	2.00
7.5		0.138	1.59
10		0.166	1.91
15		0.122	1.41
20		0.132	1.52
0.52		0	1.163
	2.5	0.309	3.56
	5	0.099	1.14
	7.5	0.045	0.52
	10	0.034	0.39
	15	0.035	0.40
	20	0.036	0.42
	0.88	0	1.163
2.5		0.298	3.44
5		0.09	1.04
7.5		0.043	0.50
10		0.024	0.28
15		0.032	0.37
20		0.03	0.35

Table F.8. Dissolved O<sub>3</sub> concentration change.

<i>z</i> , m	<i>t</i> , min	<i>V<sub>T</sub></i> , mL	<i>A<sub>ind</sub></i> , cm <sup>-1</sup>	<i>C<sub>O<sub>3,L</sub></sub></i> × 10 <sup>3</sup> , mmol/L
0.09	0			0.00
	2.5	33.2	0.232	0.00
	5.0	35	0.228	0.30
	7.5	34.1	0.227	0.60
	10	34	0.226	0.80
	15	36.1	0.227	0.60
	20	32.2	0.226	0.80
0.21	0			0.00
	2.5	35.3	0.221	1.70
	5	42.2	0.216	2.20
	7.5	43	0.199	4.70
	10	43	0.201	4.40
	15	44	0.197	4.90
	20	41.5	0.197	5.10
0.52	0			0.00
	2.5	37.2	0.210	3.60
	5	39	0.202	4.80
	7.5	31	0.201	6.90
	10	44	0.175	8.10
	15	33	0.191	8.40
	20	42.5	0.174	8.50
0.88	0			0.00
	2.5	29.1	0.209	5.40
	5	26.2	0.204	7.90
	7.5	32.1	0.180	11.20
	10	34	0.172	12.10
	15	32.2	0.173	12.80
	20	35	0.165	12.80

Table F.9. TOC change.

<i>z</i> , m	TOC, mg/L
0.00	36.28
0.09	34.84
0.21	33.03
0.52	32.91
0.88	32.72

**Run 4**

Conditions: pH=2.5,  $Q_G=150$  L/h,  $Q_L=30$  L/h,  $C_{O_3,G,in}=0.313$  mmol/L gas,  $C_{O_3,G,out}=0.040$  mmol/L gas,  $t=20$  min,  $V_{thio,inlet}=31.3$  mL,  $V_{thio,outlet}=39.8$  mL, Dye=RBBR,  $C_{D,in}=17.8 \times 10^{-2}$  mmol/L,  $TOC_{in}=45.54$  mg/L,  $A_{ind}=0.238$  cm<sup>-1</sup>, no catalyst.

Table F.10. Dye concentration change.

$z, m$	$t, min$	Abs, cm <sup>-1</sup>	$C_D \times 10^2, mmol/L$
0.09	0	1.545	17.82
	2.5	0.826	9.53
	5.0	0.585	6.75
	7.5	0.435	5.02
	10	0.37	4.27
	15	0.335	3.86
	20	0.389	4.49
	0.21	0	1.545
2.5		0.736	8.49
5		0.48	5.54
7.5		0.363	4.19
10		0.309	3.56
15		0.222	2.56
20		0.217	2.50
0.52		0	1.545
	2.5	0.694	8.00
	5	0.429	4.95
	7.5	0.235	2.71
	10	0.16	1.85
	15	0.117	1.35
	20	0.116	1.34
	0.88	0	1.545
2.5		0.699	8.06
5		0.415	4.79
7.5		0.228	2.63
10		0.162	1.87
15		0.111	1.28
20		0.114	1.31

Table F.11. Dissolved O<sub>3</sub> concentration change.

<i>z</i> , m	<i>t</i> , min	<i>V<sub>T</sub></i> , mL	<i>A<sub>ind</sub></i> , cm <sup>-1</sup>	<i>C<sub>O<sub>3,L</sub></sub></i> × 10 <sup>2</sup> , mmol/L
0.09	0			0.00
	2.5	31.2	0.238	0.00
	5.0	37.4	0.238	0.00
	7.5	33.7	0.238	0.00
	10	37.2	0.238	0.00
	15	39	0.238	0.00
	20	36.3	0.238	0.00
0.21	0			0.00
	2.5	35.9	0.238	0.00
	5	42.5	0.238	0.00
	7.5	41.7	0.238	0.00
	10	50	0.238	0.00
	15	47	0.238	0.00
	20	39	0.238	0.00
0.52	0			0.00
	2.5	37.3	0.238	0.00
	5	37	0.237	0.20
	7.5	39.1	0.231	1.20
	10	46	0.221	2.40
	15	48	0.217	2.70
	20	44.2	0.220	2.60
0.88	0			0.00
	2.5	29.1	0.238	0.00
	5	37.8	0.235	0.50
	7.5	37.7	0.228	1.90
	10	37.1	0.222	3.00
	15	37	0.215	4.20
	20	37	0.215	4.20

Table F.12. TOC change.

<i>z</i> , m	TOC, mg/L
0.00	45.54
0.09	44.37
0.21	43.30
0.52	42.37
0.88	41.21

**Run 5**

Conditions: pH=2.5,  $Q_G=150$  L/h,  $Q_L=30$  L/h,  $C_{O_3,G,in}=0.322$  mmol/L gas,  $C_{O_3,G,out}=0.186$  mmol/L gas,  $t=20$  min,  $V_{thio,inlet}=32.2$  mL,  $V_{thio,outlet}=185.8$  mL, Dye=AR-151,  $C_{D,in}=7.3 \times 10^{-2}$  mmol/L,  $TOC_{in}=20.70$  mg/L,  $A_{ind}=0.224$  cm<sup>-1</sup>, no catalyst.

Table F.13. Dye concentration change.

$z, m$	$t, min$	$A_{AR-151}, cm^{-1}$	$C_D \times 10^2, mmol/L$
0.09	0	0.727	7.34
	2.5	0.284	2.87
	5.0	0.146	1.47
	7.5	0.13	1.31
	10	0.122	1.23
	15	0.115	1.16
	20	0.119	1.20
0.21	0	0.727	7.34
	2.5	0.222	2.24
	5	0.09	0.91
	7.5	0.075	0.76
	10	0.059	0.60
	15	0.057	0.58
	20	0.047	0.47
0.52	0	0.727	7.34
	2.5	0.167	1.69
	5	0.066	0.67
	7.5	0.038	0.38
	10	0.033	0.33
	15	0.038	0.38
	20	0.033	0.33
0.88	0	0.727	7.34
	2.5	0.141	1.42
	5	0.063	0.64
	7.5	0.04	0.40
	10	0.029	0.29
	15	0.03	0.30
	20	0.026	0.26

Table F.14. Dissolved O<sub>3</sub> concentration change.

<i>z</i> , m	<i>t</i> , min	<i>V<sub>T</sub></i> , mL	<i>A<sub>ind</sub></i> , cm <sup>-1</sup>	<i>C<sub>O<sub>3,L</sub></sub></i> × 10 <sup>2</sup> , mmol/L
0.09	0			0.00
	2.5	35.3	0.149	14.70
	5.0	41.5	0.154	11.00
	7.5	32.5	0.171	11.70
	10	37.1	0.142	15.00
	15	40	0.139	14.10
	20	33.5	0.158	14.00
0.21	0			0.00
	2.5	42	0.140	13.00
	5	45	0.114	15.60
	7.5	40.3	0.116	17.70
	10	41	0.111	18.10
	15	43.5	0.104	17.80
	20	42	0.111	17.60
0.52	0			0.00
	2.5	36.8	0.147	14.30
	5	37	0.115	20.10
	7.5	34	0.115	22.60
	10	36	0.092	25.20
	15	35.5	0.101	24.00
	20	35	0.104	23.90
0.88	0			0.00
	2.5	31	0.164	14.20
	5	32.2	0.128	21.50
	7.5	34.3	0.106	24.10
	10	33.2	0.120	22.30
	15	31	0.128	22.70
	20	32.1	0.116	24.30

Table F.15. TOC change.

<i>z</i> , m	TOC, mg/L
0.00	20.70
0.09	18.32
0.21	17.21
0.52	16.61
0.88	16.07

**Run 6**

Conditions: pH=2.5,  $Q_G=150$  L/h,  $Q_L=30$  L/h,  $C_{O_3,G,in}=0.307$  mmol/L gas,  $C_{O_3,G,out}=0.157$  mmol/L gas,  $t=20$  min,  $V_{thio,inlet}=30.7$  mL,  $V_{thio,outlet}=157.0$  mL, Dye=AR-151,  $C_{D,in}=13.5 \times 10^{-2}$  mmol/L,  $TOC_{in}=36.82$  mg/L,  $A_{ind}=0.257$  cm<sup>-1</sup>, no catalyst.

Table F.16. Dye concentration change.

$z, m$	$t, min$	Abs, cm <sup>-1</sup>	$C_D \times 10^2, mmol/L$
0.09	0	1.338	13.51
	2.5	0.927	9.36
	5.0	0.707	7.14
	7.5	0.599	6.05
	10	0.506	5.11
	15	0.415	4.19
	20	0.382	3.86
	0.21	0	1.338
2.5		0.872	8.80
5		0.645	6.51
7.5		0.504	5.09
10		0.436	4.40
15		0.312	3.15
20		0.309	3.12
0.52		0	1.338
	2.5	0.809	8.17
	5	0.569	5.75
	7.5	0.39	3.94
	10	0.322	3.25
	15	0.251	2.53
	20	0.197	1.99
	0.88	0	1.338
2.5		0.799	8.07
5		0.569	5.75
7.5		0.382	3.86
10		0.311	3.14
15		0.228	2.30
20		0.165	1.67

Table F.17. Dissolved O<sub>3</sub> concentration change.

<i>z</i> , m	<i>t</i> , min	<i>V<sub>T</sub></i> , mL	<i>A<sub>ind</sub></i> , cm <sup>-1</sup>	<i>C<sub>O<sub>3,L</sub></sub></i> × 10 <sup>2</sup> , mmol/L
0.09	0			0.00
	2.5	36.3	0.179	1.10
	5.0	46.3	0.142	1.30
	7.5	46.5	0.138	1.35
	10	51.2	0.099	1.66
	15	52.5	0.107	1.52
	20	61.5	0.085	1.46
0.21	0			0.00
	2.5	49.2	0.130	1.36
	5	45.5	0.139	1.38
	7.5	41	0.136	1.62
	10	50.1	0.087	1.86
	15	49.1	0.093	1.83
	20	50.2	0.088	1.84
0.52	0			0.00
	2.5	42.8	0.155	1.24
	5	42.1	0.163	1.15
	7.5	42.1	0.128	1.69
	10	47.5	0.093	1.91
	15	46.1	0.088	2.05
	20	45	0.103	1.90
0.88	0			0.00
	2.5	32	0.177	1.36
	5	33	0.167	1.51
	7.5	34.2	0.151	1.77
	10	39.2	0.113	2.11
	15	37	0.122	2.12
	20	34	0.130	2.22

Table F.18. TOC change.

<i>z</i> , m	TOC, mg/L
0.00	36.82
0.09	33.92
0.21	32.77
0.52	32.21
0.88	31.85

**Run 7**

Conditions: pH=2.5,  $Q_G=150$  L/h,  $Q_L=30$  L/h,  $C_{O_3,G,in}=0.292$  mmol/L gas,  $C_{O_3,G,out}=0.131$  mmol/L gas,  $t=20$  min,  $V_{thio,inlet}=29.2$  mL,  $V_{thio,outlet}=131.9$  mL, Dye=AR-151,  $C_{D,in}=19.7 \times 10^{-2}$  mmol/L,  $TOC_{in}=52.48$  mg/L,  $A_{ind}=0.189$  cm<sup>-1</sup>, no catalyst.

Table F.19. Dye concentration change.

$z, m$	$t, min$	Abs, cm <sup>-1</sup>	$C_D \times 10^2, mmol/L$
0.09	0	1.95	19.72
	2.5	1.43	14.47
	5.0	1.17	11.81
	7.5	0.87	8.78
	10	0.75	7.57
	15	0.72	7.27
	20	0.69	6.97
	0.21	0	1.95
2.5		1.24	12.52
5		1.03	10.40
7.5		0.79	7.98
10		0.64	6.46
15		0.63	6.36
20		0.60	6.06
0.52		0	1.95
	2.5	1.26	12.76
	5	1.05	10.63
	7.5	0.76	7.67
	10	0.59	5.96
	15	0.58	5.86
	20	0.55	5.55
	0.88	0	1.95
2.5		1.26	12.70
5		0.91	9.19
7.5		0.70	7.07
10		0.58	5.86
15		0.52	5.25
20		0.51	5.12

Table F.20. Dissolved O<sub>3</sub> concentration change.

<i>z</i> , m	<i>t</i> , min	<i>V<sub>T</sub></i> , mL	<i>A<sub>ind</sub></i> , cm <sup>-1</sup>	<i>C<sub>O<sub>3,L</sub></sub></i> × 10 <sup>2</sup> , mmol/L
0.09	0			0.00
	2.5	49.80	0.181	0.10
	5.0	41.50	0.159	0.47
	7.5	51.00	0.142	0.57
	10	45.50	0.154	0.50
	15	38.00	0.169	0.35
	20	45.00	0.158	0.45
0.21	0			0.00
	2.5	43.20	0.149	0.60
	5	40.70	0.142	0.77
	7.5	46.20	0.139	0.69
	10	38.30	0.154	0.62
	15	37.50	0.160	0.52
	20	33.00	0.153	0.78
0.52	0			0.00
	2.5	36.80	0.127	1.14
	5	34.80	0.131	1.17
	7.5	35.00	0.130	1.17
	10	39.00	0.100	1.53
	15	28.30	0.128	1.66
	20	32.80	0.116	1.59
0.88	0			0.00
	2.5	31.20	0.158	0.74
	5	33.30	0.121	1.46
	7.5	33.80	0.146	0.90
	10	30.80	0.110	1.89
	15	27.20	0.122	1.94
	20	29.80	0.110	1.98

Table F.21. TOC change.

<i>z</i> , m	TOC, mg/L
0.00	52.48
0.09	50.65
0.21	49.62
0.52	48.79
0.88	47.33

**Run 8**

Conditions: pH=2.5,  $Q_G=150$  L/h,  $Q_L=30$  L/h,  $C_{O_3,G,in}=0.309$  mmol/L gas,  $C_{O_3,G,out}=0.137$  mmol/L gas,  $t=20$  min,  $V_{thio,inlet}=30.9$  mL,  $V_{thio,outlet}=137.2$  mL, Dye=AR-151,  $C_{D,in}=26.0 \times 10^{-2}$  mmol/L,  $TOC_{in}=71.90$  mg/L,  $A_{ind}=0.187$  cm<sup>-1</sup>, no catalyst.

Table F.22. Dye concentration change.

$z, m$	$t, min$	$A_{AR-151}, cm^{-1}$	$C_D \times 10^2, mmol/L$
0.09	0	2.579	26.04
	2.5	1.888	19.06
	5.0	1.544	15.59
	7.5	1.401	14.15
	10	1.371	13.84
	15	1.334	13.47
	20	1.325	13.38
0.21	0	1.953	19.72
	2.5	1.862	18.80
	5	1.548	15.63
	7.5	1.361	13.74
	10	1.254	12.66
	15	1.259	12.71
	20	1.229	12.41
0.52	0	1.953	19.72
	2.5	1.773	17.90
	5	1.315	13.28
	7.5	1.203	12.15
	10	1.155	11.66
	15	1.164	11.75
	20	1.144	11.55
0.88	0	1.953	19.72
	2.5	1.695	17.11
	5	1.355	13.68
	7.5	1.159	11.70
	10	1.143	11.54
	15	1.123	11.34
	20	1.112	11.23

Table F.23. Dissolved O<sub>3</sub> concentration change.

<i>z</i> , m	<i>t</i> , min	<i>V<sub>T</sub></i> , mL	<i>A<sub>ind</sub></i> , cm <sup>-1</sup>	<i>C<sub>O<sub>3,L</sub></sub></i> × 10 <sup>2</sup> , mmol/L
0.09	0			0.00
	2.5	39	0.187	0.00
	5.0	41.2	0.186	0.02
	7.5	42	0.185	0.03
	10	52.5	0.186	0.01
	15	48.1	0.185	0.03
	20	45.5	0.185	0.03
0.21	0			0.00
	2.5	36.5	0.167	0.38
	5	38.1	0.162	0.44
	7.5	35.8	0.160	0.52
	10	43.2	0.155	0.48
	15	33	0.164	0.50
	20	35.5	0.163	0.47
0.52	0			0.00
	2.5	28.3	0.163	0.65
	5	26.3	0.158	0.88
	7.5	31.3	0.151	0.84
	10	31.7	0.147	0.92
	15	34.1	0.146	0.85
	20	31.8	0.149	0.87
0.88	0			0.00
	2.5	29.5	0.156	0.79
	5	32	0.144	0.97
	7.5	32.5	0.141	1.02
	10	35	0.138	0.97
	15	36.2	0.138	0.93
	20	33.4	0.142	0.96

Table F.24. TOC change.

<i>z</i> , m	TOC, mg/L
0.00	71.90
0.09	69.35
0.21	68.52
0.52	68.04
0.88	66.72

**Run 9**

Conditions: pH=2.5,  $Q_G=70$  L/h,  $Q_L=30$  L/h,  $C_{O_3,G,in}=0.336$  mmol/L gas,  $C_{O_3,G,out}=0.147$  mmol/L gas,  $t=20$  min,  $V_{thio,inlet}=15.7$  mL,  $V_{thio,outlet}=68.6$  mL, Dye=RBBR,  $C_{D,in}=4.96 \times 10^{-2}$  mmol/L,  $TOC_{in}=12.67$  mg/L,  $A_{ind}=0.210$  cm<sup>-1</sup>, no catalyst.

Table F.25. Dye concentration change.

$z$ , m	$t$ , min	$A_{RBBR}$ , cm <sup>-1</sup>	$C_D \times 10^2$ , mmol/L
0.09	0	0.43	4.96
	5.0	0.093	1.07
	7.5	0.077	0.89
	10	0.07	0.81
	15	0.039	0.45
	20	0.056	0.65
0.21	0	0.43	4.96
	5	0.052	0.60
	7.5	0.038	0.44
	10	0.018	0.21
	15	0.008	0.09
	20	0.014	0.16
0.52	0	0.43	4.96
	5	0.037	0.43
	7.5	0.012	0.14
	10	0.012	0.14
	15	0.01	0.12
	20	0.007	0.08
0.88	0	0.43	4.96
	5	0.024	0.28
	7.5	0.013	0.15
	10	0.007	0.08
	15	0.011	0.13
	20	0.012	0.14

Table F.26. Dissolved O<sub>3</sub> concentration change.

<i>z</i> , m	<i>t</i> , min	<i>V<sub>T</sub></i> , mL	<i>A<sub>ind</sub></i> , cm <sup>-1</sup>	<i>C<sub>O<sub>3,L</sub></sub></i> × 10 <sup>2</sup> , mmol/L
0.09	0			0.00
	5.0	35	0.203	0.17
	7.5	34.2	0.203	0.17
	10	42.1	0.204	0.10
	15	48.1	0.200	0.16
	20	40	0.204	0.13
0.21	0			0.00
	5	35.2	0.198	0.28
	7.5	33	0.200	0.27
	10	49	0.196	0.22
	15	46.4	0.194	0.27
	20	53	0.192	0.26
0.52	0			0.00
	5	37.5	0.188	0.49
	7.5	29	0.193	0.53
	10	48	0.183	0.43
	15	43.2	0.181	0.53
	20	40	0.184	0.51
0.88	0			0.00
	5	31.1	0.199	0.31
	7.5	30.9	0.197	0.37
	10	35.2	0.181	0.70
	15	35.3	0.181	0.69
	20	38.7	0.176	0.70

Table F.27. TOC change.

<i>z</i> , m	TOC, mg/L
0.00	12.67
0.09	12.21
0.21	11.93
0.52	11.46
0.88	10.98

**Run 10**

Conditions: pH=2.5,  $Q_G=70$  L/h,  $Q_L=30$  L/h,  $C_{O_3,G,in}=0.334$  mmol/L gas,  $C_{O_3,G,out}=0.061$  mmol/L gas,  $t=20$  min,  $V_{thio,inlet}=15.6$  mL,  $V_{thio,outlet}=28.3$  mL, Dye=RBBR,  $C_{D,in}=9.40 \times 10^{-2}$  mmol/L,  $TOC_{in}=12.67$  mg/L,  $A_{ind}=0.203$  cm<sup>-1</sup>, no catalyst.

Table F.28. Dye concentration change.

$z$ , m	$t$ , min	$A_{RBBR}$ , cm <sup>-1</sup>	$C_D \times 10^2$ , mmol/L
0.09	0	0.815	9.40
	5.0	0.300	3.46
	7.5	0.266	3.07
	10	0.213	2.46
	15	0.196	2.26
	20	0.198	2.28
0.21	0	0.815	9.40
	5	0.238	2.74
	7.5	0.166	1.91
	10	0.126	1.45
	15	0.113	1.30
	20	0.082	0.95
0.52	0	0.815	9.40
	5	0.199	2.29
	7.5	0.11	1.27
	10	0.079	0.91
	15	0.074	0.85
	20	0.046	0.53
0.88	0	0.815	9.40
	5	0.186	2.14
	7.5	0.11	1.27
	10	0.069	0.80
	15	0.061	0.70
	20	0.038	0.44

Table F.29. Dissolved O<sub>3</sub> concentration change.

<i>z</i> , m	<i>t</i> , min	<i>V<sub>T</sub></i> , mL	<i>A<sub>ind</sub></i> , cm <sup>-1</sup>	<i>C<sub>O<sub>3,L</sub></sub></i> × 10 <sup>2</sup> , mmol/L
0.09	0			0.00
	5.0	36.3	0.203	0.00
	7.5	35.1	0.203	0.00
	10	39	0.203	0.00
	15	38.1	0.203	0.00
	20	39	0.203	0.00
0.21	0			0.00
	5	40.3	0.203	0.00
	7.5	40	0.201	0.03
	10	44.2	0.200	0.05
	15	48.2	0.201	0.03
	20	43.3	0.200	0.05
0.52	0			0.00
	5	32.5	0.203	0.00
	7.5	39.2	0.199	0.07
	10	34	0.197	0.15
	15	47.1	0.195	0.13
	20	45.1	0.195	0.13
0.88	0			0.00
	5	35.1	0.203	0.00
	7.5	29.2	0.197	0.17
	10	36.1	0.194	0.21
	15	39.3	0.193	0.21
	20	43	0.192	0.20

Table F.30. TOC change.

<i>z</i> , m	TOC, mg/L
0.00	24.02
0.09	23.58
0.21	22.94
0.52	22.25
0.88	21.31

**Run 11**

Conditions: pH=2.5,  $Q_G=70$  L/h,  $Q_L=30$  L/h,  $C_{O_3,G,in}=0.343$  mmol/L gas,  $C_{O_3,G,out}=0.027$  mmol/L gas,  $t=20$  min,  $V_{thio,inlet}=16.0$  mL,  $V_{thio,outlet}=12.7$  mL, Dye=RBBR,  $C_{D,in}=13.86 \times 10^{-2}$  mmol/L,  $M_{thio}=0.1$  M for out,  $TOC_{in}=35.78$  mg/L,  $V_{blank}=10$  mL,  $A_{ind}=0.258$  cm<sup>-1</sup>, no catalyst.

Table F.31. Dye concentration change.

$z, m$	$A_{RBBR}, cm^{-1}$	$C_D \times 10^2, mmol/L$
0	1.202	13.86
0.09	0.619	7.14
0.21	0.220	2.54
0.52	0.155	1.79
0.88	0.147	1.69

Table F.32. Dissolved O<sub>3</sub> concentration change.

$z, m$	$V_T, mL$	$A_{ind}, cm^{-1}$	$C_{O_3,L} \times 10^3, mmol/L$
0			0.00
0.09	37.2	0.258	0.00
0.21	44.8	0.251	0.98
0.52	40.4	0.249	1.54
0.88	33.0	0.249	1.92

Table F.33. TOC change.

$z, m$	TOC, mg/L
0.00	35.78
0.09	35.19
0.21	34.37
0.52	33.96
0.88	33.54
0.98	33.20

### Run 12

Conditions: pH=2.5,  $Q_G=70$  L/h,  $Q_L=30$  L/h,  $C_{O_3,G,in}=0.354$  mmol/L gas,  $C_{O_3,G,out}=0.003$  mmol/L gas,  $t=20$  min,  $V_{thio,inlet}=16.5$  mL,  $V_{thio,outlet}=1.2$  mL, Dye=RBBR,  $C_{D,in}=18.8 \times 10^{-2}$  mmol/L,  $M_{thio}=0.1$  M for out,  $TOC_{in}=50.33$  mg/L,  $V_{blank}=10$  mL,  $A_{ind}=0.259$  cm<sup>-1</sup>, no catalyst.

Table F.34. Dye concentration change.

$z, m$	$A_{RBBR}, cm^{-1}$	$C_D \times 10^2, mmol/L$
0	1.628	18.77
0.09	0.603	6.96
0.21	0.424	4.89
0.52	0.354	4.08
0.88	0.344	3.97

Table F.35. Dissolved O<sub>3</sub> concentration change.

$z, m$	$V_T, mL$	$A_{ind}, cm^{-1}$	$C_{O_3,L} \times 10^3, mmol/L$
0			0.00
0.09	45.2	0.259	0.00
0.21	46.3	0.239	2.70
0.52	44.0	0.236	3.40
0.88	38.5	0.235	4.20

Table F.36. TOC change.

$z, m$	TOC, mg/L
0.00	50.33
0.09	50.04
0.21	49.74
0.52	49.42
0.88	49.17

### Run 13

Conditions: pH=2.5,  $Q_G=70$  L/h,  $Q_L=30$  L/h,  $C_{O_3,G,in}=0.334$  mmol/L gas,  $C_{O_3,G,out}=0.119$  mmol/L gas,  $t=20$  min,  $V_{thio,inlet}=15.6$  mL,  $V_{thio,outlet}=55.7$  mL, Dye=AR-151,  $C_{D,in}=8.3 \times 10^{-2}$  mmol/L,  $M_{thio}=0.1$  M for out,  $TOC_{in}=22.56$  mg/L,  $V_{blank}=10$  mL,  $A_{ind}=0.235$  cm<sup>-1</sup>, catalyst=none.

Table F.37. Dye concentration change.

$z, \text{ m}$	$A_{AR-151}, \text{ cm}^{-1}$	$C_D \times 10^2, \text{ mmol/L}$
0	0.822	8.30
0.09	0.237	2.39
0.21	0.130	1.31
0.52	0.077	0.78
0.88	0.059	0.60

Table F.38. Dissolved  $\text{O}_3$  concentration change.

$z, \text{ m}$	$V_T, \text{ mL}$	$A_{ind}, \text{ cm}^{-1}$	$C_{\text{O}_3,L} \times 10^3, \text{ mmol/L}$
0			0.00
0.09	39.2	0.185	8.52
0.21	40.8	0.152	13.40
0.52	40.3	0.111	20.29
0.88	36.0	0.110	23.90

Table F.39. TOC change.

$z, \text{ m}$	TOC, mg/L
0.00	22.56
0.09	22.14
0.21	21.38
0.52	20.12
0.88	18.66

#### Run 14

Conditions:  $\text{pH}=2.5$ ,  $Q_G=70 \text{ L/h}$ ,  $Q_L=30 \text{ L/h}$ ,  $C_{\text{O}_3,G,in}=0.345 \text{ mmol/L}$  gas,  $C_{\text{O}_3,G,out}=0.129 \text{ mmol/L}$  gas,  $t=20 \text{ min}$ ,  $V_{\text{thio,inlet}}=16.1 \text{ mL}$ ,  $V_{\text{thio,outlet}}=60.1 \text{ mL}$ , Dye=AR-151,  $C_{D,in}=13.1 \times 10^{-2} \text{ mmol/L}$ ,  $M_{\text{thio}}=0.1 \text{ M}$  for out,  $\text{TOC}_{in}=35.02 \text{ mg/L}$ ,  $V_{\text{blank}}=10 \text{ mL}$ ,  $A_{ind}=0.238 \text{ cm}^{-1}$ , catalyst=none.

Table F.40. Dye concentration change.

$z, \text{ m}$	$A_{AR-151}, \text{ cm}^{-1}$	$C_D \times 10^2, \text{ mmol/L}$
0	1.293	13.06
0.09	0.822	8.31
0.21	0.678	6.84
0.52	0.622	6.28
0.88	0.603	6.09

Table F.41. Dissolved O<sub>3</sub> concentration change.

<i>z</i> , m	<i>V<sub>T</sub></i> , mL	<i>A<sub>ind</sub></i> , cm <sup>-1</sup>	<i>C<sub>O<sub>3,L</sub></sub></i> × 10 <sup>3</sup> , mmol/L
0			0.00
0.09	37.5	0.215	4.23
0.21	35.2	0.173	12.81
0.52	35.7	0.143	18.35
0.88	30.8	0.154	19.98

Table F.42. TOC change.

<i>z</i> , m	TOC, mg/L
0.00	35.02
0.09	34.45
0.21	33.85
0.52	33.04
0.88	31.48

### Run 15

Conditions: pH=2.5, *Q<sub>G</sub>*=70 L/h, *Q<sub>L</sub>*=30 L/h, *C<sub>O<sub>3,G,in</sub></sub>*=0.351 mmol/L gas, *C<sub>O<sub>3,G,out</sub></sub>* = 0.124 mmol/L gas, *t*=20 min, *V<sub>thio,inlet</sub>*=16.4 mL, *V<sub>thio,outlet</sub>*=57.8 mL, Dye=AR-151, *C<sub>D,in</sub>*=20.2×10<sup>-2</sup> mmol/L, *M<sub>thio</sub>*=0.1 M for out, *TOC<sub>in</sub>*=54.61 mg/L, *V<sub>blank</sub>*=10 mL, *A<sub>ind</sub>*=0.239 cm<sup>-1</sup>, catalyst=none.

Table F.43. Dye concentration change.

<i>z</i> , m	<i>A<sub>AR-151</sub></i> , cm <sup>-1</sup>	<i>C<sub>D</sub></i> × 10 <sup>2</sup> , mmol/L
0	2.004	20.23
0.09	1.367	13.80
0.21	1.130	11.41
0.52	1.036	10.46
0.88	0.991	10.01

Table F.44. Dissolved O<sub>3</sub> concentration change.

<i>z</i> , m	<i>V<sub>T</sub></i> , mL	<i>A<sub>ind</sub></i> , cm <sup>-1</sup>	<i>C<sub>O<sub>3,L</sub></sub></i> × 10 <sup>3</sup> , mmol/L
0			0.00
0.09	37.0	0.232	1.29
0.21	40.1	0.187	8.59
0.52	40.0	0.169	11.60
0.88	32.1	0.175	14.39

Table F.45. TOC change.

$z, \text{ m}$	TOC, mg/L
0.00	54.61
0.09	53.85
0.21	52.29
0.52	51.48
0.88	50.57

**Run 16**

Conditions: pH=2.5,  $Q_G=70 \text{ L/h}$ ,  $Q_L=30 \text{ L/h}$ ,  $C_{O_3,G,in}=0.347 \text{ mmol/L}$  gas,  $C_{O_3,G,out}=0.109 \text{ mmol/L}$  gas,  $t=20 \text{ min}$ ,  $V_{\text{thio,inlet}}=16.2 \text{ mL}$ ,  $V_{\text{thio,outlet}}=50.9 \text{ mL}$ , Dye=AR-151,  $C_{D,in}=26.6 \times 10^{-2} \text{ mmol/L}$ ,  $M_{\text{thio}}=0.1 \text{ M}$  for out,  $\text{TOC}_{in}=68.44 \text{ mg/L}$ ,  $V_{\text{blank}}=10 \text{ mL}$ ,  $A_{ind}=0.240 \text{ cm}^{-1}$ , catalyst=none.

Table F.46. Dye concentration change.

$z, \text{ m}$	$A_{AR-151}, \text{ cm}^{-1}$	$C_D \times 10^2, \text{ mmol/L}$
0	2.646	26.62
0.09	1.839	18.57
0.21	1.684	17.00
0.52	1.576	15.91
0.88	1.435	14.49

Table F.47. Dissolved  $O_3$  concentration change.

$z, \text{ m}$	$V_T, \text{ mL}$	$A_{ind}, \text{ cm}^{-1}$	$C_{O_3,L} \times 10^3, \text{ mmol/L}$
0			0.00
0.09	37.0	0.240	0.00
0.21	39.5	0.238	0.34
0.52	34.2	0.225	3.08
0.88	32.2	0.220	4.48

Table F.48. TOC change.

$z, \text{ m}$	TOC, mg/L
0.00	68.44
0.09	67.18
0.21	66.55
0.52	64.73
0.88	63.85

**Run 17**

Conditions: pH=2.5,  $Q_G=70$  L/h,  $Q_L=250$  L/h,  $C_{O_3,G,in}=0.281$  mmol/L gas,  $C_{O_3,G,out}=0.021$  mmol/L gas,  $t=20$  min,  $V_{thio,inlet}=13.1$  mL,  $V_{thio,outlet}=9.6$  mL, Dye=RBBR,  $C_{D,in}=5.0 \times 10^{-2}$  mmol/L,  $M_{thio}=0.1$  M for out,  $TOC_{in}=12.28$  mg/L,  $V_{blank}=10$  mL,  $A_{ind}=0.210$  cm<sup>-1</sup>, catalyst=none.

Table F.49. Dye concentration change.

$z, m$	$A_{RBBR}, cm^{-1}$	$C_D \times 10^2, mmol/L$
0	0.429	4.95
0.09	0.386	4.45
0.21	0.333	3.84
0.52	0.288	3.32
0.88	0.239	2.76

Table F.50. Dissolved O<sub>3</sub> concentration change.

$z, m$	$V_T, mL$	$A_{ind}, cm^{-1}$	$C_{O_3,L} \times 10^3, mmol/L$
0			0.00
0.09	30.6	0.209	0.24
0.21	32.9	0.205	1.09
0.52	33.8	0.196	2.92
0.88	31.8	0.189	4.79

Table F.51. TOC change.

$z, m$	TOC, mg/L
0.00	12.28
0.09	12.17
0.21	12.03
0.52	11.79
0.88	11.55

**Run 18**

Conditions: pH=2.5,  $Q_G=70$  L/h,  $Q_L=250$  L/h,  $C_{O_3,G,in}=0.296$  mmol/L gas,  $C_{O_3,G,out}=0.003$  mmol/L gas,  $t=20$  min,  $V_{thio,inlet}=13.8$  mL,  $V_{thio,outlet}=1.3$  mL, Dye=RBBR,  $C_{D,in}=9.4 \times 10^{-2}$  mmol/L,  $M_{thio}=0.1$  M for out,  $TOC_{in}=23.22$  mg/L,  $V_{blank}=10$  mL,  $A_{ind}=0.216$  cm<sup>-1</sup>, catalyst=none.

Table F.52. Dye concentration change.

$z, \text{ m}$	$A_{RBBR}, \text{ cm}^{-1}$	$C_D \times 10^2, \text{ mmol/L}$
0	0.818	9.43
0.09	0.753	8.68
0.21	0.688	7.93
0.52	0.631	7.28
0.88	0.602	6.84

Table F.53. Dissolved  $\text{O}_3$  concentration change.

$z, \text{ m}$	$V_T, \text{ mL}$	$A_{ind}, \text{ cm}^{-1}$	$C_{\text{O}_3,L} \times 10^3, \text{ mmol/L}$
0			0.00
0.09	37.7	0.208	1.40
0.21	33.8	0.204	2.48
0.52	32.7	0.202	3.01
0.88	33.5	0.200	3.33

Table F.54. TOC change.

$z, \text{ m}$	TOC, mg/L
0.00	23.22
0.09	23.06
0.21	22.95
0.52	22.59
0.88	22.49

### Run 19

Conditions:  $\text{pH}=2.5$ ,  $Q_G=70 \text{ L/h}$ ,  $Q_L=250 \text{ L/h}$ ,  $C_{\text{O}_3,G,in}=0.298 \text{ mmol/L gas}$ ,  $C_{\text{O}_3,G,out}=0.001 \text{ mmol/L gas}$ ,  $t=20 \text{ min}$ ,  $V_{\text{thio,inlet}}=13.9 \text{ mL}$ ,  $V_{\text{thio,outlet}}=0.4 \text{ mL}$ ,  $\text{Dye}=RBBR$ ,  $C_{D,in}=12.7 \times 10^{-2} \text{ mmol/L}$ ,  $M_{\text{thio}}=0.1 \text{ M for out}$ ,  $\text{TOC}_{in}=32.73 \text{ mg/L}$ ,  $V_{\text{blank}}=10 \text{ mL}$ ,  $A_{ind}=0.214 \text{ cm}^{-1}$ ,  $\text{catalyst}=\text{none}$ .

Table F.55. Dye concentration change.

$z, \text{ m}$	$A_{RBBR}, \text{ cm}^{-1}$	$C_D \times 10^2, \text{ mmol/L}$
0	1.103	12.72
0.09	0.978	11.28
0.21	0.913	10.53
0.52	0.869	10.02
0.88	0.841	9.70

Table F.56. Dissolved O<sub>3</sub> concentration change.

$z, \text{ m}$	$V_T, \text{ mL}$	$A_{ind}, \text{ cm}^{-1}$	$C_{O_3,L} \times 10^3, \text{ mmol/L}$
0			0.00
0.09	34.6	0.214	0.00
0.21	35.5	0.214	0.00
0.52	32.1	0.214	0.00
0.88	33.8	0.212	0.42

Table F.57. TOC change.

$z, \text{ m}$	TOC, mg/L
0.00	32.73
0.09	32.81
0.21	32.54
0.52	32.28
0.88	32.16

### Run 20

Conditions: pH=2.5,  $Q_G=70 \text{ L/h}$ ,  $Q_L=250 \text{ L/h}$ ,  $C_{O_3,G,in}=0.317 \text{ mmol/L gas}$ ,  $C_{O_3,G,out}=0.003 \text{ mmol/L gas}$ ,  $t=20 \text{ min}$ ,  $V_{thio,inlet}=14.8 \text{ mL}$ ,  $V_{thio,outlet}=1.4 \text{ mL}$ , Dye=RBBR,  $C_{D,in}=19.2 \times 10^{-2} \text{ mmol/L}$ ,  $M_{thio}=0.1 \text{ M for out}$ ,  $TOC_{in}=49.21 \text{ mg/L}$ ,  $V_{blank}=10 \text{ mL}$ ,  $A_{ind}=0.210 \text{ cm}^{-1}$ , catalyst=none.

Table F.58. Dye concentration change.

$z, \text{ m}$	$A_{RBBR}, \text{ cm}^{-1}$	$C_D \times 10^2, \text{ mmol/L}$
0	1.662	19.17
0.09	1.478	17.05
0.21	1.419	16.37
0.52	1.372	15.83
0.88	1.326	15.30

Table F.59. Dissolved O<sub>3</sub> concentration change.

$z, \text{ m}$	$V_T, \text{ mL}$	$A_{ind}, \text{ cm}^{-1}$	$C_{O_3,L} \times 10^3, \text{ mmol/L}$
0			0.00
0.09	32.9	0.210	0.00
0.21	38.7	0.210	0.00
0.52	31.6	0.210	0.00
0.88	39.6	0.209	0.17

Table F.60. TOC change.

z, m	TOC, mg/L
0.00	49.21
0.09	49.08
0.21	48.82
0.52	48.76
0.88	48.75

**Run 21**

Conditions: pH=2.5,  $Q_G=70$  L/h,  $Q_L=250$  L/h,  $C_{O_3,G,in}=0.324$  mmol/L gas,  $C_{O_3,G,out}=0.099$  mmol/L gas,  $t=20$  min,  $V_{thio,inlet}=15.1$  mL,  $V_{thio,outlet}=46.2$  mL, Dye=AR-151,  $C_{D,in}=7.4 \times 10^{-2}$  mmol/L,  $M_{thio}=0.1$  M for out,  $TOC_{in}=18.86$  mg/L,  $V_{blank}=10$  mL,  $A_{ind}=0.215$  cm<sup>-1</sup>, catalyst=none.

Table F.61. Dye concentration change.

z, m	$A_{AR-151}$ , cm <sup>-1</sup>	$C_D \times 10^2$ , mmol/L
0	0.730	7.37
0.09	0.569	5.75
0.21	0.505	5.10
0.52	0.478	4.83
0.88	0.452	4.56

Table F.62. Dissolved O<sub>3</sub> concentration change.

z, m	$V_T$ , mL	$A_{ind}$ , cm <sup>-1</sup>	$C_{O_3,L} \times 10^3$ , mmol/L
0			0.00
0.09	35.6	0.203	2.31
0.21	38.4	0.185	5.26
0.52	33.6	0.178	7.79
0.88	36.9	0.170	8.31

Table F.63. TOC change.

z, m	TOC, mg/L
0.00	18.86
0.09	18.65
0.21	18.21
0.52	17.84
0.88	17.31

**Run 22**

Conditions: pH=2.5,  $Q_G=70$  L/h,  $Q_L=250$  L/h,  $C_{O_3,G,in}=0.312$  mmol/L gas,  $C_{O_3,G,out}=0.045$  mmol/L gas,  $t=20$  min,  $V_{thio,inlet}=14.6$  mL,  $V_{thio,outlet}=21.0$  mL, Dye=AR-151,  $C_{D,in}=13.6 \times 10^{-2}$  mmol/L,  $M_{thio}=0.1$  M for out,  $TOC_{in}=33.78$  mg/L,  $V_{blank}=10$  mL,  $A_{ind}=0.218$  cm<sup>-1</sup>, catalyst=none.

Table F.64. Dye concentration change.

$z, m$	$A_{AR-151}, cm^{-1}$	$C_D \times 10^2, mmol/L$
0	1.347	13.60
0.09	1.216	12.28
0.21	1.164	11.75
0.52	1.130	11.41
0.88	1.095	11.06

Table F.65. Dissolved O<sub>3</sub> concentration change.

$z, m$	$V_T, mL$	$A_{ind}, cm^{-1}$	$C_{O_3,L} \times 10^3, mmol/L$
0			0.00
0.09	33.7	0.206	2.56
0.21	28.9	0.205	3.38
0.52	35.1	0.193	4.93
0.88	37.6	0.188	5.40

Table F.66. TOC change.

$z, m$	TOC, mg/L
0.00	33.78
0.09	33.27
0.21	32.79
0.52	32.31
0.88	31.99

**Run 23**

Conditions: pH=2.5,  $Q_G=70$  L/h,  $Q_L=250$  L/h,  $C_{O_3,G,in}=0.318$  mmol/L gas,  $C_{O_3,G,out}=0.041$  mmol/L gas,  $t=20$  min,  $V_{thio,inlet}=14.8$  mL,  $V_{thio,outlet}=19.1$  mL, Dye=AR-151,  $C_{D,in}=20.6 \times 10^{-2}$  mmol/L,  $M_{thio}=0.1$  M for out,  $TOC_{in}=54.37$  mg/L,  $V_{blank}=10$  mL,  $A_{ind}=0.211$  cm<sup>-1</sup>, catalyst=none.

Table F.67. Dye concentration change.

$z, \text{ m}$	$A_{AR-151}, \text{ cm}^{-1}$	$C_D \times 10^2, \text{ mmol/L}$
0	2.036	20.56
0.09	1.856	18.74
0.21	1.799	18.16
0.52	1.762	17.79
0.88	1.726	17.43

Table F.68. Dissolved  $\text{O}_3$  concentration change.

$z, \text{ m}$	$V_T, \text{ mL}$	$A_{ind}, \text{ cm}^{-1}$	$C_{\text{O}_3,L} \times 10^3, \text{ mmol/L}$
0			0.00
0.09	31.5	0.208	0.69
0.21	30.6	0.202	2.17
0.52	37.8	0.194	3.04
0.88	33.0	0.195	3.46

Table F.69. TOC change.

$z, \text{ m}$	TOC, mg/L
0.00	54.37
0.09	53.80
0.21	53.13
0.52	52.85
0.88	52.68

### Run 24

Conditions:  $\text{pH}=2.5$ ,  $Q_G=70 \text{ L/h}$ ,  $Q_L=250 \text{ L/h}$ ,  $C_{\text{O}_3,G,in}=0.330 \text{ mmol/L gas}$ ,  $C_{\text{O}_3,G,out} = 0.042 \text{ mmol/L gas}$ ,  $t=20 \text{ min}$ ,  $V_{\text{thio,inlet}}=15.4 \text{ mL}$ ,  $V_{\text{thio,outlet}}=19.6 \text{ mL}$ , Dye=AR-151,  $C_{D,in}=27.7 \times 10^{-2} \text{ mmol/L}$ ,  $M_{\text{thio}}=0.1 \text{ M}$  for out,  $\text{TOC}_{in}=70.28 \text{ mg/L}$ ,  $V_{\text{blank}}=10 \text{ mL}$ ,  $A_{ind}=0.214 \text{ cm}^{-1}$ , catalyst=none.

Table F.70. Dye concentration change.

$z, \text{ m}$	$A_{AR-151}, \text{ cm}^{-1}$	$C_D \times 10^2, \text{ mmol/L}$
0	2.740	27.67
0.09	2.518	25.42
0.21	2.444	24.68
0.52	2.392	24.15
0.88	2.373	23.96

Table F.71. Dissolved O<sub>3</sub> concentration change.

<i>z</i> , m	<i>V<sub>T</sub></i> , mL	<i>A<sub>ind</sub></i> , cm <sup>-1</sup>	<i>C<sub>O<sub>3,L</sub></sub></i> × 10 <sup>3</sup> , mmol/L
0			0.00
0.09	29.6	0.214	0.00
0.21	34.8	0.213	0.25
0.52	40.4	0.208	0.98
0.88	39.5	0.203	1.35

Table F.72. TOC change.

<i>z</i> , m	TOC, mg/L
0.00	70.28
0.09	70.07
0.21	69.55
0.52	69.11
0.88	68.94

### Run 25

Conditions: pH=2.5, *Q<sub>G</sub>*=30 L/h, *Q<sub>L</sub>*=30 L/h, *C<sub>O<sub>3,G,in</sub></sub>*=0.295 mmol/L gas, *C<sub>O<sub>3,G,out</sub></sub>* = 0.002 mmol/L gas, *t*=20 min, *V<sub>thio,inlet</sub>*=5.9 mL, *V<sub>thio,outlet</sub>*=0.4 mL, Dye=*RBBR*, *C<sub>D,in</sub>*=4.80×10<sup>-2</sup> mmol/L, *M<sub>thio</sub>*=0.1 M for out, *TOC<sub>in</sub>*=14.05 mg/L, *V<sub>blank</sub>*=10 mL, *A<sub>ind</sub>*=0.254 cm<sup>-1</sup>, no catalyst.

Table F.73. Dye concentration change.

<i>z</i> , m	<i>A<sub>RBBR</sub></i> , cm <sup>-1</sup>	<i>C<sub>D</sub></i> × 10 <sup>2</sup> , mmol/L
0	0.413	4.76
0.09	0.231	2.66
0.21	0.172	1.98
0.52	0.162	1.86
0.88	0.132	1.52

Table F.74. Dissolved O<sub>3</sub> concentration change.

<i>z</i> , m	<i>V<sub>T</sub></i> , mL	<i>A<sub>ind</sub></i> , cm <sup>-1</sup>	<i>C<sub>O<sub>3,L</sub></sub></i> × 10 <sup>3</sup> , mmol/L
0			0.00
0.09	42.5	0.254	0.00
0.21	43.6	0.254	0.00
0.52	41.0	0.257	0.00
0.88	34.1	0.253	0.21

Table F.75. TOC change.

z, m	TOC, mg/L
0.00	14.05
0.09	14.01
0.21	13.85
0.52	13.26
0.88	13.08

**Run 26**

Conditions: pH=2.5,  $Q_G=30$  L/h,  $Q_L=30$  L/h,  $C_{O_3,G,in}=0.315$  mmol/L gas,  $C_{O_3,G,out}=0.003$  mmol/L gas, t=20 min,  $V_{thio,inlet}=6.3$  mL,  $V_{thio,outlet}=0.6$  mL, Dye=RBBR,  $C_{D,in}=18.6 \times 10^{-2}$  mmol/L,  $M_{thio}=0.1$  M for out,  $TOC_{in}=46.74$  mg/L,  $V_{blank}=10$  mL,  $A_{ind}=0.181$  cm<sup>-1</sup>, no catalyst.

Table F.76. Dye concentration change.

z, m	$A_{RBBR}$ , cm <sup>-1</sup>	$C_D \times 10^2$ , mmol/L
0	1.610	18.57
0.09	1.390	16.03
0.21	1.338	15.43
0.52	1.331	15.36
0.88	1.326	15.30

Table F.77. TOC change.

z, m	TOC, mg/L
0.00	46.74
0.09	46.69
0.21	46.24
0.52	46.12
0.88	45.82

**Run 27**

Conditions: pH=2.5,  $Q_G=70$  L/h,  $Q_L=70$  L/h,  $C_{O_3,G,in}=0.298$  mmol/L gas,  $C_{O_3,G,out}=0.028$  mmol/L gas, t=20 min,  $V_{thio,inlet}=13.9$  mL,  $V_{thio,outlet}=13.1$  mL, Dye=RBBR,  $C_{D,in}=4.70 \times 10^{-2}$  mmol/L,  $M_{thio}=0.1$  M for out,  $TOC_{in}=12.33$  mg/L,  $V_{blank}=10$  mL,  $A_{ind}=0.250$  cm<sup>-1</sup>, no catalyst.

Table F.78. Dye concentration change.

$z, \text{ m}$	$A_{RBBR}, \text{ cm}^{-1}$	$C_D \times 10^2, \text{ mmol/L}$
0	0.411	4.74
0.09	0.124	1.43
0.21	0.108	1.25
0.52	0.080	0.92
0.88	0.071	0.82

Table F.79. Dissolved  $\text{O}_3$  concentration change.

$z, \text{ m}$	$V_T, \text{ mL}$	$A_{ind}, \text{ cm}^{-1}$	$C_{\text{O}_3,L} \times 10^3, \text{ mmol/L}$
0			0.00
0.09	44.3	0.250	0.00
0.21	43.9	0.250	0.00
0.52	45.8	0.239	1.53
0.88	33.0	0.241	1.94

Table F.80. TOC change.

$z, \text{ m}$	TOC, mg/L
0.00	12.33
0.09	9.96
0.21	9.73
0.52	9.66
0.88	9.40

### Run 28

Conditions:  $\text{pH}=2.5$ ,  $Q_G=70 \text{ L/h}$ ,  $Q_L=70 \text{ L/h}$ ,  $C_{\text{O}_3,G,in}=0.302 \text{ mmol/L gas}$ ,  $C_{\text{O}_3,G,out}=0.001 \text{ mmol/L gas}$ ,  $t=20 \text{ min}$ ,  $V_{\text{thio,inlet}}=14.1 \text{ mL}$ ,  $V_{\text{thio,outlet}}=0.4 \text{ mL}$ ,  $\text{Dye}=RBBR$ ,  $C_{D,in}=18.1 \times 10^{-2} \text{ mmol/L}$ ,  $M_{\text{thio}}=0.1 \text{ M for out}$ ,  $\text{TOC}_{in}=46.51 \text{ mg/L}$ ,  $V_{\text{blank}}=8 \text{ mL}$ ,  $A_{ind}=0.122 \text{ cm}^{-1}$ , no catalyst.

Table F.81. Dye concentration change.

$z, \text{ m}$	$A_{RBBR}, \text{ cm}^{-1}$	$C_D \times 10^2, \text{ mmol/L}$
0	1.572	18.13
0.09	1.010	11.66
0.21	0.964	11.11
0.52	0.939	10.82
0.88	0.920	10.61

Table F.82. TOC change.

$z$ , m	TOC, mg/L
0.00	46.51
0.09	46.06
0.21	45.63
0.52	45.40
0.88	44.73

**Run 29**

Conditions: pH=2.5,  $Q_G=150$  L/h,  $Q_L=150$  L/h,  $C_{O_3,G,in}=0.361$  mmol/L gas,  $C_{O_3,G,out}=0.071$  mmol/L gas,  $t=20$  min,  $V_{thio,inlet}=36.1$  mL,  $V_{thio,outlet}=71.0$  mL, Dye=*RBBR*,  $C_{D,in}=4.8 \times 10^{-2}$  mmol/L,  $M_{thio}=0.1$  M for out,  $TOC_{in}=12.99$  mg/L,  $V_{blank}=10$  mL,  $A_{ind}=0.209$  cm<sup>-1</sup>, no catalyst.

Table F.83. Dye concentration change.

$z$ , m	$A_{RBBR}$ , cm <sup>-1</sup>	$C_D \times 10^2$ , mmol/L
0	0.420	4.84
0.09	0.178	2.05
0.21	0.100	1.15
0.52	0.017	0.19
0.88	0.015	0.17

Table F.84. Dissolved O<sub>3</sub> concentration change.

$z$ , m	$V_T$ , mL	$A_{ind}$ , cm <sup>-1</sup>	$C_{O_3,L} \times 10^3$ , mmol/L
0			0.00
0.09	45.8	0.204	0.64
0.21	43.1	0.197	1.85
0.52	35.3	0.180	5.73
0.88	37.2	0.176	6.03

Table F.85. TOC change.

$z$ , m	TOC, mg/L
0.00	12.99
0.09	12.58
0.21	12.41
0.52	12.33
0.88	11.92

**Run 30**

Conditions: pH=2.5,  $Q_G=150$  L/h,  $Q_L=150$  L/h,  $C_{O_3,G,in}=0.345$  mmol/L gas,  $C_{O_3,G,out}=0.005$  mmol/L gas,  $t=20$  min,  $V_{thio,inlet}=38.0$  mL,  $V_{thio,outlet}=5.3$  mL, Dye=RBBR,  $C_{D,in}=18.7 \times 10^{-2}$  mmol/L,  $M_{thio}=0.1$  M for out,  $TOC_{in}=48.20$  mg/L,  $V_{blank}=8$  mL,  $A_{ind}=0.122$  cm<sup>-1</sup>, no catalyst.

Table F.86. Dye concentration change.

$z, m$	$A_{RBBR}, cm^{-1}$	$C_D \times 10^2, mmol/L$
0	1.621	18.69
0.09	1.082	12.48
0.21	0.939	10.82
0.52	0.724	8.35
0.88	0.692	7.98

Table F.87. TOC change.

$z, m$	TOC, mg/L
0.00	48.20
0.09	46.88
0.21	46.65
0.52	46.86
0.88	46.09

**Run 31**

Conditions: pH=2.5,  $Q_G=30$  L/h,  $Q_L=30$  L/h,  $C_{O_3,G,in}=0.295$  mmol/L gas,  $C_{O_3,G,out}=0.018$  mmol/L gas,  $t=20$  min,  $V_{thio,inlet}=5.9$  mL,  $V_{thio,outlet}=3.6$  mL, Dye=AR-151,  $C_{D,in}=6.9 \times 10^{-2}$  mmol/L,  $M_{thio}=0.1$  M for out,  $TOC_{in}=16.72$  mg/L,  $V_{blank}=7$  mL,  $A_{ind}=0.151$  cm<sup>-1</sup>, no catalyst.

Table F.88. Dye concentration change.

$z, m$	$A_{AR-151}, cm^{-1}$	$C_D \times 10^2, mmol/L$
0	0.678	6.85
0.09	0.563	5.69
0.21	0.518	5.23
0.52	0.504	5.09
0.88	0.480	4.85

Table F.89. Dissolved O<sub>3</sub> concentration change.

<i>z</i> , m	<i>V<sub>T</sub></i> , mL	<i>A<sub>ind</sub></i> , cm <sup>-1</sup>	<i>C<sub>O<sub>3,L</sub></sub></i> × 10 <sup>3</sup> , mmol/L
0			0.00
0.09	38.2	0.149	0.32
0.21	31.6	0.142	1.82
0.52	29.8	0.140	2.40
0.88	20.6	0.139	4.39

Table F.90. TOC change.

<i>z</i> , m	TOC, mg/L
0.00	16.72
0.09	16.47
0.21	16.02
0.52	15.87
0.88	15.81

### Run 32

Conditions: pH=2.5, *Q<sub>G</sub>*=30 L/h, *Q<sub>L</sub>*=30 L/h, *C<sub>O<sub>3,G,in</sub></sub>*=0.323 mmol/L gas, *C<sub>O<sub>3,G,out</sub></sub>* = 0.026 mmol/L gas, *t*=20 min, *V<sub>thio,inlet</sub>*=6.5 mL, *V<sub>thio,outlet</sub>*=5.2 mL, Dye=AR-151, *C<sub>D,in</sub>*=26.7×10<sup>-2</sup> mmol/L, *M<sub>thio</sub>*=0.1 M for out, TOC<sub>in</sub>=68.53 mg/L, *V<sub>blank</sub>*=10 mL, *A<sub>ind</sub>*=0.173 cm<sup>-1</sup>, no catalyst.

Table F.91. Dye concentration change.

<i>z</i> , m	<i>A<sub>AR-151</sub></i> , cm <sup>-1</sup>	<i>C<sub>D</sub></i> × 10 <sup>2</sup> , mmol/L
0	2.647	26.72
0.09	2.599	26.24
0.21	2.529	25.54
0.52	2.472	24.96
0.88	2.437	24.61

Table F.92. TOC change.

<i>z</i> , m	TOC, mg/L
0.00	68.53
0.09	68.31
0.21	68.05
0.52	67.83
0.88	67.78

**Run 33**

Conditions: pH=2.5,  $Q_G=70$  L/h,  $Q_L=70$  L/h,  $C_{O_3,G,in}=0.326$  mmol/L gas,  $C_{O_3,G,out}=0.023$  mmol/L gas,  $t=20$  min,  $V_{thio,inlet}=15.2$  mL,  $V_{thio,outlet}=10.9$  mL, Dye=AR-151,  $C_{D,in}=7.2 \times 10^{-2}$  mmol/L,  $M_{thio}=0.1$  M for out,  $TOC_{in}=15.88$  mg/L,  $V_{blank}=8$  mL,  $A_{ind}=0.174$  cm<sup>-1</sup>, no catalyst.

Table F.93. Dye concentration change.

$z, m$	$A_{AR-151}, cm^{-1}$	$C_D \times 10^2, mmol/L$
0	0.711	7.18
0.09	0.417	4.21
0.21	0.356	3.60
0.52	0.296	2.99
0.88	0.260	2.63

Table F.94. Dissolved O<sub>3</sub> concentration change.

$z, m$	$V_T, mL$	$A_{ind}, cm^{-1}$	$C_{O_3,L} \times 10^3, mmol/L$
0			0.00
0.09	38.5	0.138	5.86
0.21	31.1	0.143	6.70
0.52	32.7	0.131	8.65
0.88	30.5	0.122	11.49

Table F.95. TOC change.

$z, m$	TOC, mg/L
0.00	15.88
0.09	15.41
0.21	14.63
0.52	14.37
0.88	14.31

**Run 34**

Conditions: pH=2.5,  $Q_G=70$  L/h,  $Q_L=70$  L/h,  $C_{O_3,G,in}=0.304$  mmol/L gas,  $C_{O_3,G,out}=0.086$  mmol/L gas,  $t=20$  min,  $V_{thio,inlet}=14.2$  mL,  $V_{thio,outlet}=40.1$  mL, Dye=AR-151,  $C_{D,in}=28.1 \times 10^{-2}$  mmol/L,  $M_{thio}=0.1$  M for out,  $TOC_{in}=72.56$  mg/L,  $V_{blank}=10$  mL,  $A_{ind}=0.103$  cm<sup>-1</sup>, no catalyst.

Table F.96. Dye concentration change.

$z, \text{ m}$	$A_{AR-151}, \text{ cm}^{-1}$	$C_D \times 10^2, \text{ mmol/L}$
0	2.784	28.11
0.09	2.152	21.73
0.21	2.035	20.55
0.52	1.977	19.96
0.88	1.935	19.54

Table F.97. Dissolved  $\text{O}_3$  concentration change.

$z, \text{ m}$	$V_T, \text{ mL}$	$A_{ind}, \text{ cm}^{-1}$	$C_{\text{O}_3,L} \times 10^3, \text{ mmol/L}$
0			0.00
0.09	33.6	0.103	0.00
0.21	36.8	0.103	0.00
0.52	32.1	0.103	0.00
0.88	35.6	0.102	0.10

Table F.98. TOC change.

$z, \text{ m}$	TOC, mg/L
0.00	72.56
0.09	72.13
0.21	71.68
0.52	71.05
0.88	70.60

### Run 35

Conditions:  $\text{pH}=2.5$ ,  $Q_G=150 \text{ L/h}$ ,  $Q_L=150 \text{ L/h}$ ,  $C_{\text{O}_3,G,in}=0.340 \text{ mmol/L gas}$ ,  $C_{\text{O}_3,G,out}=0.018 \text{ mmol/L gas}$ ,  $t=20 \text{ min}$ ,  $V_{\text{thio,inlet}}=34.0 \text{ mL}$ ,  $V_{\text{thio,outlet}}=18.3 \text{ mL}$ ,  $\text{Dye}=AR-151$ ,  $C_{D,in}=7.8 \times 10^{-2} \text{ mmol/L}$ ,  $M_{\text{thio}}=0.1 \text{ M for out}$ ,  $\text{TOC}_{in}=15.88 \text{ mg/L}$ ,  $V_{\text{blank}}=8 \text{ mL}$ ,  $A_{ind}=0.221 \text{ cm}^{-1}$ , no catalyst.

Table F.99. Dye concentration change.

$z, \text{ m}$	$A_{AR-151}, \text{ cm}^{-1}$	$C_D \times 10^2, \text{ mmol/L}$
0	0.771	7.78
0.09	0.462	4.66
0.21	0.333	3.36
0.52	0.197	1.99
0.88	0.149	1.50

Table F.100. Dissolved O<sub>3</sub> concentration change.

<i>z</i> , m	<i>V<sub>T</sub></i> , mL	<i>A<sub>ind</sub></i> , cm <sup>-1</sup>	<i>C<sub>O<sub>3,L</sub></sub></i> × 10 <sup>3</sup> , mmol/L
0			0.00
0.09	44.0	0.159	9.06
0.21	37.9	0.142	14.07
0.52	37.0	0.122	18.22
0.88	34.2	0.121	20.54

Table F.101. TOC change.

<i>z</i> , m	TOC, mg/L
0.00	15.65
0.09	15.08
0.21	14.21
0.52	13.89
0.88	13.67

### Run 36

Conditions: pH=2.5, *Q<sub>G</sub>*=150 L/h, *Q<sub>L</sub>*=150 L/h, *C<sub>O<sub>3,G,in</sub></sub>*=0.338 mmol/L gas, *C<sub>O<sub>3,G,out</sub></sub>* = 0.106 mmol/L gas, *t*=20 min, *V<sub>thio,inlet</sub>*=33.8 mL, *V<sub>thio,outlet</sub>*=106.4 mL, Dye=AR-151, *C<sub>D,in</sub>*=27.5×10<sup>-2</sup> mmol/L, *M<sub>thio</sub>*=0.1 M for out, *TOC<sub>in</sub>*=70.79 mg/L, *V<sub>blank</sub>*=10 mL, *A<sub>ind</sub>*=0.095 cm<sup>-1</sup>, no catalyst.

Table F.102. Dye concentration change.

<i>z</i> , m	<i>A<sub>AR-151</sub></i> , cm <sup>-1</sup>	<i>C<sub>D</sub></i> × 10 <sup>2</sup> , mmol/L
0	2.723	27.49
0.09	2.102	21.22
0.21	2.014	20.34
0.52	1.887	19.05
0.88	1.840	18.58

Table F.103. Dissolved O<sub>3</sub> concentration change.

<i>z</i> , m	<i>V<sub>T</sub></i> , mL	<i>A<sub>ind</sub></i> , cm <sup>-1</sup>	<i>C<sub>O<sub>3,L</sub></sub></i> × 10 <sup>3</sup> , mmol/L
0			0.00
0.09	30.2	0.094	2.85
0.21	24.7	0.072	7.62
0.52	25.9	0.043	16.38
0.88	22.9	0.050	17.35

Table F.104. TOC change.

z, m	TOC, mg/L
0.00	70.79
0.09	70.48
0.21	69.58
0.52	68.92
0.88	68.10

**Run 37**

Conditions: pH=2.5,  $Q_G=150$  L/h,  $Q_L=150$  L/h,  $C_{O_3,G,in}=0.981$  mmol/L gas,  $C_{O_3,G,out}=0.279$  mmol/L gas,  $t=20$  min,  $V_{thio,inlet}=32.7$  mL,  $V_{thio,outlet}=93.1$  mL, Dye=RBBR,  $C_{D,in}=4.90 \times 10^{-2}$  mmol/L,  $M_{thio}=0.3$  M for out,  $TOC_{in}=13.34$  mg/L,  $V_{blank}=20$  mL,  $A_{ind}=0.374$  cm<sup>-1</sup>, no catalyst.

Table F.105. Dye concentration change.

z, m	$A_{RBBR}$ , cm <sup>-1</sup>	$C_D \times 10^2$ , mmol/L
0	0.425	4.90
0.09	0.060	0.69
0.21	0.011	0.13
0.52	0.003	0.03
0.88	0.000	0.00
0.98	0.000	0.00

Table F.106. Dissolved O<sub>3</sub> concentration change.

z, m	$V_T$ , mL	$A_{ind}$ , cm <sup>-1</sup>	$C_{O_3,L} \times 10^3$ , mmol/L
0			0.00
0.09	48.1	0.286	15.6
0.21	43.3	0.271	21.9
0.52	39.3	0.129	63.2
0.88	36.2	0.111	80.7
0.98	40.1	0.041	82.5

Table F.107. TOC change.

z, m	TOC, mg/L
0.00	13.34
0.09	12.47
0.21	12.08
0.52	11.88
0.88	11.81
0.98	11.64

**Run 38**

Conditions: pH=2.5,  $Q_G=150$  L/h,  $Q_L=150$  L/h,  $C_{O_3,G,in}=0.987$  mmol/L gas,  $C_{O_3,G,out}=0.196$  mmol/L gas,  $t=20$  min,  $V_{thio,inlet}=32.9$  mL,  $V_{thio,outlet}=65.3$  mL, Dye=RBBR,  $C_{D,in}=18.1 \times 10^{-2}$  mmol/L,  $M_{thio}=0.3$  M for out,  $TOC_{in}=45.26$  mg/L,  $V_{blank}=20$  mL,  $A_{ind}=0.438$  cm<sup>-1</sup>, no catalyst.

Table F.108. Dye concentration change.

$z, m$	Abs, cm <sup>-1</sup>	$C_D \times 10^2, mmol/L$
0	1.566	18.1
0.09	0.818	9.4
0.21	0.603	7.0
0.52	0.248	2.9
0.88	0.227	2.6
0.98	0.170	2.0

Table F.109. Dissolved O<sub>3</sub> concentration change.

$z, m$	$V_T, mL$	$A_{ind}, cm^{-1}$	$C_{O_3,L} \times 10^3, mmol/L$
0			0.00
0.09	46.0	0.438	0.00
0.21	44.5	0.438	0.00
0.52	41.6	0.417	4.92
0.88	41.6	0.403	8.15
0.98	45.1	0.430	8.79

Table F.110. TOC change.

$z, m$	TOC, mg/L
0.00	45.26
0.09	45.05
0.21	44.90
0.52	43.95
0.88	43.34
0.98	43.00

**Run 39**

Conditions: pH=2.5,  $Q_G=150$  L/h,  $Q_L=150$  L/h,  $C_{O_3,G,in}=0.975$  mmol/L gas,  $C_{O_3,G,out}=0.279$  mmol/L gas,  $t=20$  min,  $V_{thio,inlet}=32.5$  mL,  $V_{thio,outlet}=92.9$  mL, Dye=AR-151,  $C_{D,in}=7.34 \times 10^{-2}$  mmol/L,  $M_{thio}=0.3$  M for out,  $TOC_{in}=45.26$  mg/L,  $V_{blank}=20$  mL,  $A_{ind}=0.437$  cm<sup>-1</sup>, no catalyst.

Table F.111. Dye concentration change.

$z, \text{ m}$	Abs, $\text{cm}^{-1}$	$C_D \times 10^2, \text{ mmol/L}$
0	0.727	7.34
0.09	0.203	2.05
0.21	0.083	0.84
0.52	0.059	0.59
0.88	0.057	0.57
0.98	0.052	0.52

Table F.112. Dissolved  $\text{O}_3$  concentration change.

$z, \text{ m}$	$V_T, \text{ mL}$	$A_{ind}, \text{ cm}^{-1}$	$C_{\text{O}_3, L} \times 10^3, \text{ mmol/L}$
0			0.00
0.09	41.5	0.272	38.15
0.21	47.9	0.203	41.69
0.52	43.0	0.099	73.04
0.88	37.5	0.133	86.33
0.98	34.0	0.169	95.15

Table F.113. TOC change.

$z, \text{ m}$	TOC, $\text{mg/L}$
0.00	18.45
0.09	17.68
0.21	17.01
0.52	16.82
0.88	16.61
0.98	16.49

### Run 40

Conditions:  $\text{pH}=2.5$ ,  $Q_G=150 \text{ L/h}$ ,  $Q_L=150 \text{ L/h}$ ,  $C_{\text{O}_3, G, in}=0.952 \text{ mmol/L gas}$ ,  $C_{\text{O}_3, G, out}=0.266 \text{ mmol/L gas}$ ,  $t=20 \text{ min}$ ,  $V_{\text{thio, inlet}}=32.8 \text{ mL}$ ,  $V_{\text{thio, outlet}}=91.5 \text{ mL}$ , Dye=AR-151,  $C_{D, in}=25.4 \times 10^{-2} \text{ mmol/L}$ ,  $M_{\text{thio}}=0.3 \text{ M}$  for out,  $\text{TOC}_{in}=45.26 \text{ mg/L}$ ,  $V_{\text{blank}}=20 \text{ mL}$ ,  $A_{ind}=0.437 \text{ cm}^{-1}$ , no catalyst.

Table F.114. Dye concentration change.

$z$ , m	Abs, $\text{cm}^{-1}$	$C_D \times 10^2$ , mmol/L
0	2.516	25.4
0.09	1.826	18.4
0.21	1.595	16.1
0.52	1.437	14.5
0.88	1.345	13.6
0.98	1.187	12.0

Table F.115. Dissolved  $\text{O}_3$  concentration change.

$z$ , m	$V_T$ , mL	$A_{ind}$ , $\text{cm}^{-1}$	$C_{\text{O}_3,L} \times 10^3$ , mmol/L
0			0.00
0.09	41.9	0.329	23.42
0.21	44.3	0.303	26.29
0.52	38.0	0.321	30.52
0.88	36.1	0.318	35.04
0.98	55.0	0.163	38.19

Table F.116. TOC change.

$z$ , m	TOC, mg/L
0.00	64.82
0.09	64.04
0.21	62.05
0.52	61.79
0.88	61.23
0.98	61.17

**Run 41**

Conditions:  $\text{pH}=2.5$ ,  $Q_G=150$  L/h,  $Q_L=150$  L/h,  $C_{\text{O}_3,G,in}=0.970$  mmol/L gas,  $C_{\text{O}_3,G,out}=0.280$  mmol/L gas,  $t=20$  min,  $V_{\text{thio,inlet}}=97.0$  mL,  $V_{\text{thio,outlet}}=93.2$  mL, Dye=*RBBR*,  $C_{D,in}=4.8 \times 10^{-2}$  mmol/L,  $M_{\text{thio}}=0.3$  M for out,  $\text{TOC}_{in}=12.93$  mg/L,  $V_{\text{blank}}=20$  mL,  $A_{ind}=0.463$   $\text{cm}^{-1}$ , catalyst=Alumina,  $m_{cat}=25$  g,  $d_{cat}=2.0$  mm.

Table F.117. Dye concentration change.

$z$ , m	Abs, $\text{cm}^{-1}$	$C_D \times 10^2$ , mmol/L
0	0.418	4.82
0.09	0.224	2.60
0.21	0.018	0.21
0.52	0.010	0.11
0.88	0.009	0.10
0.98	0.008	0.09

Table F.118. Dissolved O<sub>3</sub> concentration change.

<i>z</i> , m	<i>V<sub>T</sub></i> , mL	<i>A<sub>ind</sub></i> , cm <sup>-1</sup>	<i>C<sub>O<sub>3,L</sub></sub></i> × 10 <sup>3</sup> , mmol/L
0			0.00
0.09	48.7	0.463	0.00
0.21	44.0	0.428	7.20
0.52	46.2	0.313	28.44
0.88	46.0	0.271	36.65
0.98	53.2	0.164	44.79

Table F.119. TOC change.

<i>z</i> , m	TOC, mg/L
0.00	12.93
0.09	12.85
0.21	11.52
0.52	11.46
0.88	11.14
0.98	10.73

### Run 42

Conditions: pH=2.5, *Q<sub>G</sub>*=150 L/h, *Q<sub>L</sub>*=150 L/h, *C<sub>O<sub>3,G,in</sub></sub>*=0.977 mmol/L gas, *C<sub>O<sub>3,G,out</sub></sub>* = 0.276 mmol/L gas, *t*=20 min, *V<sub>thio,inlet</sub>*=97.7 mL, *V<sub>thio,outlet</sub>*=92.0 mL, Dye=*RBBR*, *C<sub>D,in</sub>*=18.6×10<sup>-2</sup> mmol/L, *M<sub>thio</sub>*=0.3 M for out, *TOC<sub>in</sub>*=48.80 mg/L, *V<sub>blank</sub>*=20 mL, *A<sub>ind</sub>*=0.492 cm<sup>-1</sup>, catalyst=Alumina, *m<sub>cat</sub>*=25 g, *d<sub>cat</sub>*=2.0 mm.

Table F.120. Dye concentration change.

<i>z</i> , m	Abs, cm <sup>-1</sup>	<i>C<sub>D</sub></i> × 10 <sup>2</sup> , mmol/L
0	1.611	18.58
0.09	1.262	14.55
0.21	0.621	7.16
0.52	0.529	6.10
0.88	0.479	5.52
0.98	0.393	4.53

Table F.121. Dissolved O<sub>3</sub> concentration change.

<i>z</i> , m	<i>V<sub>T</sub></i> , mL	<i>A<sub>ind</sub></i> , cm <sup>-1</sup>	<i>C<sub>O<sub>3,L</sub></sub></i> × 10 <sup>3</sup> , mmol/L
0			0.00
0.09	46.5	0.492	0.00
0.21	43.1	0.492	0.00
0.52	43.1	0.492	0.00
0.88	45.9	0.485	1.38
0.98	50.2	0.480	2.15

Table F.122. TOC change.

z, m	TOC, mg/L
0.00	48.80
0.09	45.36
0.21	44.94
0.52	44.10
0.88	43.04
0.98	42.42

### Run 43

Conditions: pH=2.5,  $Q_G=150$  L/h,  $Q_L=150$  L/h,  $C_{O_3,G,in}=0.983$  mmol/L gas,  $C_{O_3,G,out}=0.282$  mmol/L gas,  $t=20$  min,  $V_{thio,inlet}=98.3$  mL,  $V_{thio,outlet}=93.9$  mL, Dye=AR-151,  $C_{D,in}=6.8 \times 10^{-2}$  mmol/L,  $M_{thio}=0.3$  M for out,  $TOC_{in}=17.25$  mg/L,  $V_{blank}=20$  mL,  $A_{ind}=0.466$  cm<sup>-1</sup>, catalyst=Alumina,  $m_{cat}=25$  g,  $d_{cat}=2.0$  mm.

Table F.123. Dye concentration change.

z, m	Abs, cm <sup>-1</sup>	$C_D \times 10^2$ , mmol/L
0	0.675	6.81
0.09	0.402	4.06
0.21	0.058	0.59
0.52	0.049	0.50
0.88	0.047	0.47
0.98	0.042	0.42

Table F.124. Dissolved O<sub>3</sub> concentration change.

z, m	$V_T$ , mL	$A_{ind}$ , cm <sup>-1</sup>	$C_{O_3,L} \times 10^3$ , mmol/L
0			0.00
0.09	49.5	0.424	7.08
0.21	46.9	0.256	38.79
0.52	44.0	0.207	53.63
0.88	41.7	0.204	60.00
0.98	39.2	0.231	60.83

Table F.125. TOC change.

z, m	TOC, mg/L
0.00	17.25
0.09	16.83
0.21	15.02
0.52	14.67
0.88	14.63
0.98	14.34

**Run 44**

Conditions: pH=2.5,  $Q_G=150$  L/h,  $Q_L=150$  L/h,  $C_{O_3,G,in}=0.948$  mmol/L gas,  $C_{O_3,G,out}=0.267$  mmol/L gas,  $t=20$  min,  $V_{thio,inlet}=94.8$  mL,  $V_{thio,outlet}=89.0$  mL, Dye=AR-151,  $C_{D,in}=27.4 \times 10^{-2}$  mmol/L,  $M_{thio}=0.3$  M for out,  $TOC_{in}=71.60$  mg/L,  $V_{blank}=20$  mL,  $A_{ind}=0.472$  cm<sup>-1</sup>, catalyst=Alumina,  $m_{cat}=25$  g,  $d_{cat}=2.0$  mm.

Table F.126. Dye concentration change.

$z$ , m	Abs, cm <sup>-1</sup>	$C_D \times 10^2$ , mmol/L
0	2.718	27.44
0.09	2.350	23.73
0.21	1.176	11.87
0.52	1.094	11.22
0.88	0.975	9.84
0.98	0.838	8.46

Table F.127. Dissolved O<sub>3</sub> concentration change.

$z$ , m	$V_T$ , mL	$A_{ind}$ , cm <sup>-1</sup>	$C_{O_3,L} \times 10^3$ , mmol/L
0			0.00
0.09	47.0	0.453	3.54
0.21	47.2	0.350	22.31
0.52	39.3	0.367	27.13
0.88	37.7	0.365	30.04
0.98	44.2	0.314	32.50

Table F.128. TOC change.

$z$ , m	TOC, mg/L
0.00	71.60
0.09	68.94
0.21	65.35
0.52	63.28
0.88	62.57
0.98	61.40

**Run 45**

Conditions: pH=2.5,  $Q_G=150$  L/h,  $Q_L=150$  L/h,  $C_{O_3,G,in}=0.969$  mmol/L gas,  $C_{O_3,G,out}=0.275$  mmol/L gas,  $t=20$  min,  $V_{thio,inlet}=96.9$  mL,  $V_{thio,outlet}=91.6$  mL, Dye=RBBR,  $C_{D,in}=5.0 \times 10^{-2}$  mmol/L,  $M_{thio}=0.3$  M for out,  $TOC_{in}=12.72$  mg/L,  $V_{blank}=20$  mL,  $A_{ind}=0.474$  cm<sup>-1</sup>, catalyst=PFOA,  $m_{cat}=25$  g,  $d_{cat}=2.0$  mm.

Table F.129. Dye concentration change.

$z, \text{ m}$	Abs, $\text{cm}^{-1}$	$C_D \times 10^2, \text{ mmol/L}$
0	0.429	4.95
0.09	0.254	2.93
0.21	0.021	0.24
0.52	0.013	0.15
0.88	0.009	0.10
0.98	0.008	0.09

Table F.130. Dissolved  $\text{O}_3$  concentration change.

$z, \text{ m}$	$V_T, \text{ mL}$	$A_{ind}, \text{ cm}^{-1}$	$C_{\text{O}_3, L} \times 10^3, \text{ mmol/L}$
0			0.00
0.09	53.2	0.474	0.00
0.21	48.8	0.407	11.54
0.52	50.0	0.395	13.17
0.88	43.2	0.372	21.75
0.98	48.2	0.347	22.35

Table F.131. TOC change.

$z, \text{ m}$	TOC, $\text{mg/L}$
0.00	12.72
0.09	11.51
0.21	10.84
0.52	10.26
0.88	9.93
0.98	9.74

### Run 46

Conditions:  $\text{pH}=2.5$ ,  $Q_G=150 \text{ L/h}$ ,  $Q_L=150 \text{ L/h}$ ,  $C_{\text{O}_3, G, in}=0.963 \text{ mmol/L gas}$ ,  $C_{\text{O}_3, G, out}=0.272 \text{ mmol/L gas}$ ,  $t=20 \text{ min}$ ,  $V_{\text{thio, inlet}}=96.3 \text{ mL}$ ,  $V_{\text{thio, outlet}}=90.7 \text{ mL}$ , Dye=*RBBR*,  $C_{D, in}=18.6 \times 10^{-2} \text{ mmol/L}$ ,  $M_{\text{thio}}=0.3 \text{ M}$  for out,  $\text{TOC}_{in}=48.87 \text{ mg/L}$ ,  $V_{\text{blank}}=20 \text{ mL}$ ,  $A_{ind}=0.470 \text{ cm}^{-1}$ , catalyst=*PFOA*,  $m_{cat}=25 \text{ g}$ ,  $d_{cat}=2.0 \text{ mm}$ .

Table F.132. Dye concentration change.

$z$ , m	Abs, $\text{cm}^{-1}$	$C_D \times 10^2$ , mmol/L
0	1.613	18.60
0.09	1.322	15.24
0.21	0.663	7.65
0.52	0.581	6.70
0.88	0.536	6.18
0.98	0.510	5.88

Table F.133. Dissolved  $\text{O}_3$  concentration change.

$z$ , m	$V_T$ , mL	$A_{ind}$ , $\text{cm}^{-1}$	$C_{\text{O}_3,L} \times 10^3$ , mmol/L
0			0.00
0.09	48.6	0.470	0.00
0.21	43.0	0.470	0.00
0.52	46.5	0.470	0.00
0.88	41.2	0.470	0.00
0.98	51.2	0.469	0.67

Table F.134. TOC change.

$z$ , m	TOC, mg/L
0.00	48.87
0.09	47.93
0.21	46.71
0.52	45.00
0.88	44.50
0.98	44.08

#### Run 47

Conditions:  $\text{pH}=2.5$ ,  $Q_G=150$  L/h,  $Q_L=150$  L/h,  $C_{\text{O}_3,G,in}=0.966$  mmol/L gas,  $C_{\text{O}_3,G,out} = 0.273$  mmol/L gas,  $t=20$  min,  $V_{\text{thio,inlet}}=96.6$  mL,  $V_{\text{thio,outlet}}=91.1$  mL, Dye=AR-151,  $C_{D,in}=7.2 \times 10^{-2}$  mmol/L,  $M_{\text{thio}}=0.3$  M for out,  $\text{TOC}_{in}=18.63$  mg/L,  $V_{\text{blank}}=20$  mL,  $A_{ind}=0.467$   $\text{cm}^{-1}$ , catalyst=PFOA,  $m_{cat}=25$  g,  $d_{cat}=2.0$  mm.

Table F.135. Dye concentration change.

$z$ , m	Abs, $\text{cm}^{-1}$	$C_D \times 10^2$ , mmol/L
0	0.716	7.22
0.09	0.382	3.86
0.21	0.053	0.54
0.52	0.049	0.50
0.88	0.038	0.38
0.98	0.036	0.36

Table F.136. Dissolved O<sub>3</sub> concentration change.

$z, \text{ m}$	$V_T, \text{ mL}$	$A_{ind}, \text{ cm}^{-1}$	$C_{O_3,L} \times 10^3, \text{ mmol/L}$
0			0.00
0.09	51.8	0.440	4.23
0.21	45.0	0.290	35.19
0.52	46.1	0.251	41.13
0.88	40.0	0.262	50.94
0.98	49.2	0.152	53.58

Table F.137. TOC change.

$z, \text{ m}$	TOC, mg/L
0.00	18.63
0.09	18.09
0.21	17.61
0.52	15.89
0.88	14.67
0.98	12.82

**Run 48**

Conditions: pH=2.5,  $Q_G=150 \text{ L/h}$ ,  $Q_L=150 \text{ L/h}$ ,  $C_{O_3,G,in}=0.897 \text{ mmol/L gas}$ ,  $C_{O_3,G,out}=0.261 \text{ mmol/L gas}$ ,  $t=20 \text{ min}$ ,  $V_{thio,inlet}=89.7 \text{ mL}$ ,  $V_{thio,outlet}=86.9 \text{ mL}$ , Dye=AR-151,  $C_{D,in}=31.2 \times 10^{-2} \text{ mmol/L}$ ,  $M_{thio}=0.3 \text{ M for out}$ ,  $TOC_{in}=80.31 \text{ mg/L}$ ,  $V_{blank}=20 \text{ mL}$ ,  $A_{ind}=0.438 \text{ cm}^{-1}$ , catalyst=PFOA,  $m_{cat}=25 \text{ g}$ ,  $d_{cat}=2.0 \text{ mm}$ .

Table F.138. Dye concentration change.

$z, \text{ m}$	Abs, $\text{cm}^{-1}$	$C_D \times 10^2, \text{ mmol/L}$
0	3.090	31.20
0.09	2.485	25.09
0.21	1.110	11.21
0.52	0.954	9.63
0.88	0.875	8.83
0.98	0.788	7.96

Table F.139. Dissolved O<sub>3</sub> concentration change.

$z, \text{ m}$	$V_T, \text{ mL}$	$A_{ind}, \text{ cm}^{-1}$	$C_{O_3,L} \times 10^3, \text{ mmol/L}$
0			0.00
0.09	47.2	0.350	16.06
0.21	42.3	0.336	22.71
0.52	45.2	0.288	29.54
0.88	37.2	0.318	34.67
0.98	60.2	0.131	37.94

Table F.140. TOC change.

z, m	TOC, mg/L
0.00	80.31
0.09	76.53
0.21	73.92
0.52	70.25
0.88	68.42
0.98	66.10

**Run 49**

Conditions: pH=2.5,  $Q_G=150$  L/h,  $Q_L=150$  L/h,  $C_{O_3,G,in}=0.913$  mmol/L gas,  $C_{O_3,G,out}=0.347$  mmol/L gas, t=20 min,  $V_{thio,inlet}=91.3$  mL,  $V_{thio,outlet}=83.9$  mL, Dye=RBBR,  $C_{D,in}=5.0 \times 10^{-2}$  mmol/L,  $M_{thio}=0.3$  M for out,  $TOC_{in}=13.74$  mg/L,  $V_{blank}=20$  mL,  $A_{ind}=0.426$  cm<sup>-1</sup>, catalyst=Alumina,  $m_{cat}=75$  g,  $d_{cat}=2.0$  mm.

Table F.141. Dye concentration change.

z, m	Abs, cm <sup>-1</sup>	$C_D \times 10^2$ , mmol/L
0	0.432	4.98
0.09	0.266	3.07
0.21	0.033	0.38
0.52	0.024	0.28
0.88	0.015	0.17
0.98	0.014	0.16

Table F.142. Dissolved O<sub>3</sub> concentration change.

z, m	$V_T$ , mL	$A_{ind}$ , cm <sup>-1</sup>	$C_{O_3,L} \times 10^3$ , mmol/L
0			0.00
0.09	47.0	0.426	0.00
0.21	45.0	0.399	5.40
0.52	46.3	0.387	7.35
0.88	45.0	0.362	12.67
0.98	61.2	0.306	14.50

Table F.143. TOC change.

z, m	TOC, mg/L
0.00	13.74
0.09	12.46
0.21	12.05
0.52	11.28
0.88	10.84
0.98	10.63

**Run 50**

Conditions: pH=2.5,  $Q_G=150$  L/h,  $Q_L=150$  L/h,  $C_{O_3,G,in}=0.928$  mmol/L gas,  $C_{O_3,G,out}=0.347$  mmol/L gas,  $t=20$  min,  $V_{thio,inlet}=92.8$  mL,  $V_{thio,outlet}=86.8$  mL, Dye=RBBR,  $C_{D,in}=18.7 \times 10^{-2}$  mmol/L,  $M_{thio}=0.3$  M for out,  $TOC_{in}=50.37$  mg/L,  $V_{blank}=20$  mL,  $A_{ind}=0.421$  cm<sup>-1</sup>, catalyst=Alumina,  $m_{cat}=75$  g,  $d_{cat}=2.0$  mm.

Table F.144. Dye concentration change.

$z, m$	Abs, cm <sup>-1</sup>	$C_D \times 10^2, mmol/L$
0	1.618	18.66
0.09	1.307	15.07
0.21	0.752	8.67
0.52	0.679	7.83
0.88	0.629	7.25
0.98	0.595	6.87

Table F.145. Dissolved O<sub>3</sub> concentration change.

$z, m$	$V_T, mL$	$A_{ind}, cm^{-1}$	$C_{O_3,L} \times 10^3, mmol/L$
0			0.00
0.09	44.4	0.421	0.00
0.21	41.3	0.421	0.00
0.52	45.1	0.421	0.00
0.88	42.3	0.421	0.00
0.98	56.2	0.418	0.40

Table F.146. TOC change.

$z, m$	TOC, mg/L
0.00	50.37
0.09	47.83
0.21	44.48
0.52	42.09
0.88	41.72
0.98	41.40

**Run 51**

Conditions: pH=2.5,  $Q_G=150$  L/h,  $Q_L=150$  L/h,  $C_{O_3,G,in}=0.935$  mmol/L gas,  $C_{O_3,G,out}=0.353$  mmol/L gas,  $t=20$  min,  $V_{thio,inlet}=93.5$  mL,  $V_{thio,outlet}=88.2$  mL, Dye=AR-151,  $C_{D,in}=5.9 \times 10^{-2}$  mmol/L,  $M_{thio}=0.3$  M for out,  $TOC_{in}=15.34$  mg/L,  $V_{blank}=20$  mL,  $A_{ind}=0.467$  cm<sup>-1</sup>, catalyst=Alumina,  $m_{cat}=75$  g,  $d_{cat}=2.0$  mm.

Table F.147. Dye concentration change.

$z$ , m	Abs, $\text{cm}^{-1}$	$C_D \times 10^2$ , mmol/L
0	0.586	5.92
0.09	0.370	3.74
0.21	0.075	0.76
0.52	0.065	0.66
0.88	0.059	0.59
0.98	0.052	0.53

Table F.148. Dissolved  $\text{O}_3$  concentration change.

$z$ , m	$V_T$ , mL	$A_{ind}$ , $\text{cm}^{-1}$	$C_{\text{O}_3,L} \times 10^3$ , mmol/L
0			0.00
0.09	47.6	0.382	15.31
0.21	49.0	0.268	34.10
0.52	48.2	0.247	38.77
0.88	42.1	0.284	41.15
0.98	51.5	0.201	41.98

Table F.149. TOC change.

$z$ , m	TOC, mg/L
0.00	15.34
0.09	12.69
0.21	11.35
0.52	10.85
0.88	10.37
0.98	10.13

**Run 52**

Conditions:  $\text{pH}=2.5$ ,  $Q_G=150$  L/h,  $Q_L=150$  L/h,  $C_{\text{O}_3,G,in}=0.931$  mmol/L gas,  $C_{\text{O}_3,G,out}=0.352$  mmol/L gas,  $t=20$  min,  $V_{\text{thio,inlet}}=93.1$  mL,  $V_{\text{thio,outlet}}=88.0$  mL, Dye=AR-151,  $C_{D,in}=28.0 \times 10^{-2}$  mmol/L,  $M_{\text{thio}}=0.3$  M for out,  $\text{TOC}_{in}=72.18$  mg/L,  $V_{\text{blank}}=20$  mL,  $A_{ind}=0.432$   $\text{cm}^{-1}$ , catalyst=Alumina,  $m_{cat}=75$  g,  $d_{cat}=2.0$  mm.

Table F.150. Dye concentration change.

$z$ , m	Abs, $\text{cm}^{-1}$	$C_D \times 10^2$ , mmol/L
0	2.775	28.02
0.09	2.395	24.18
0.21	1.494	15.08
0.52	1.425	14.39
0.88	1.356	13.38
0.98	1.268	12.80

Table F.151. Dissolved O<sub>3</sub> concentration change.

$z, \text{ m}$	$V_T, \text{ mL}$	$A_{ind}, \text{ cm}^{-1}$	$C_{O_3,L} \times 10^3, \text{ mmol/L}$
0			0.00
0.09	44.6	0.361	14.40
0.21	47.8	0.329	18.40
0.52	45.0	0.299	26.42
0.88	38.2	0.314	32.25
0.98	42.80	0.275	34.29

Table F.153. TOC change.

$z, \text{ m}$	TOC, mg/L
0.00	72.18
0.09	65.73
0.21	61.55
0.52	58.62
0.88	56.29
0.98	54.38

**Run 53**

Conditions: pH=2.5,  $Q_G=150 \text{ L/h}$ ,  $Q_L=150 \text{ L/h}$ ,  $C_{O_3,G,in}=0.933 \text{ mmol/L gas}$ ,  $C_{O_3,G,out}=0.296 \text{ mmol/L gas}$ ,  $t=20 \text{ min}$ ,  $V_{thio,inlet}=31.1 \text{ mL}$ ,  $V_{thio,outlet}=74.0 \text{ mL}$ , Dye=RBBR,  $C_{D,in}=5.0 \times 10^{-2} \text{ mmol/L}$ ,  $M_{thio}=0.3 \text{ M for out}$ ,  $TOC_{in}=13.05 \text{ mg/L}$ ,  $V_{blank}=20 \text{ mL}$ ,  $A_{ind}=0.430 \text{ cm}^{-1}$ , catalyst=PFOA,  $m_{cat}=75 \text{ g}$ ,  $d_{cat}=2.0 \text{ mm}$ .

Table F.154. Dye concentration change.

$z, \text{ m}$	Abs, $\text{cm}^{-1}$	$C_D \times 10^2, \text{ mmol/L}$
0	0.435	5.02
0.09	0.280	3.23
0.21	0.045	0.52
0.52	0.025	0.29
0.88	0.021	0.24
0.98	0.018	0.21

Table F.155. Dissolved O<sub>3</sub> concentration change.

$z, \text{ m}$	$V_T, \text{ mL}$	$A_{ind}, \text{ cm}^{-1}$	$C_{O_3,L} \times 10^3, \text{ mmol/L}$
0			0.00
0.09	49.5	0.430	0.00
0.21	53.5	0.369	9.10
0.52	47.2	0.359	13.04
0.88	41.6	0.369	14.10
0.98	51.5	0.335	14.98

Table F.156. TOC change.

z, m	TOC, mg/L
0.00	13.05
0.09	11.95
0.21	11.26
0.52	10.37
0.88	9.83
0.98	9.28

### Run 54

Conditions: pH=2.5,  $Q_G=150$  L/h,  $Q_L=150$  L/h,  $C_{O_3,G,in}=0.930$  mmol/L gas,  $C_{O_3,G,out} = 0.347$  mmol/L gas,  $t=20$  min,  $V_{thio,inlet}=93.2$  mL,  $V_{thio,outlet}=86.7$  mL, Dye=*RBBR*,  $C_{D,in}=18.7 \times 10^{-2}$  mmol/L,  $M_{thio}=0.3$  M for out,  $TOC_{in}=47.81$  mg/L,  $V_{blank}=10$  mL,  $A_{ind}=0.225$  cm<sup>-1</sup>, catalyst=PFOA,  $m_{cat}=75$  g,  $d_{cat}=2.0$  mm.

Table F.157. Dye concentration change.

z, m	Abs, cm <sup>-1</sup>	$C_D \times 10^2$ , mmol/L
0	1.621	18.69
0.09	1.312	15.13
0.21	0.757	8.73
0.52	0.714	8.23
0.88	0.658	7.59
0.98	0.534	6.16

Table F.158. Dissolved O<sub>3</sub> concentration change.

z, m	$V_T$ , mL	$A_{ind}$ , cm <sup>-1</sup>	$C_{O_3,L} \times 10^3$ , mmol/L
0			0.00
0.09	33.5	0.225	0.00
0.21	35.3	0.225	0.00
0.52	38.0	0.225	0.00
0.88	32.1	0.225	0.00
0.98	41.1	0.222	0.42

Table F.159. TOC change.

z, m	TOC, mg/L
0.00	47.81
0.09	44.26
0.21	42.18
0.52	41.74
0.88	41.03
0.98	40.30

**Run 55**

Conditions: pH=2.5,  $Q_G=150$  L/h,  $Q_L=150$  L/h,  $C_{O_3,G,in}=0.940$  mmol/L gas,  $C_{O_3,G,out}=0.352$  mmol/L gas,  $t=20$  min,  $V_{thio,inlet}=94.0$  mL,  $V_{thio,outlet}=88.0$  mL, Dye=AR-151,  $C_{D,in}=6.0 \times 10^{-2}$  mmol/L,  $M_{thio}=0.3$  M for out,  $TOC_{in}=15.65$  mg/L,  $V_b=20$  mL,  $A_b=0.435$  cm<sup>-1</sup>, catalyst=PFOA,  $m_{cat}=75$  g,  $d_{cat}=2.0$  mm.

Table F.160. Dye concentration change.

$z, m$	Abs, cm <sup>-1</sup>	$C_D \times 10^2, mmol/L$
0	0.591	5.97
0.09	0.396	4.00
0.21	0.077	0.78
0.52	0.068	0.69
0.88	0.065	0.66
0.98	0.059	0.59

Table F.161. Dissolved O<sub>3</sub> concentration change.

$z, m$	$V_T, mL$	$A_{ind}, cm^{-1}$	$C_{O_3,L} \times 10^3, mmol/L$
0			0.00
0.09	48.3	0.402	5.79
0.21	45.8	0.297	26.58
0.52	45.4	0.271	32.08
0.88	40.2	0.270	40.60
0.98	45.7	0.206	44.29

Table F.162. TOC change.

$z, m$	TOC, mg/L
0.00	15.65
0.09	12.38
0.21	11.57
0.52	10.32
0.88	9.95
0.98	9.64

**Run 56**

Conditions: pH=2.5,  $Q_G=150$  L/h,  $Q_L=150$  L/h,  $C_{O_3,G,in}=0.931$  mmol/L gas,  $C_{O_3,G,out}=0.348$  mmol/L gas,  $t=20$  min,  $V_{thio,inlet}=93.1$  mL,  $V_{thio,outlet}=86.9$  mL, Dye=AR-151,  $C_{D,in}=28.2 \times 10^{-2}$  mmol/L,  $M_{thio}=0.3$  M for out,  $TOC_{in}=69.29$  mg/L,  $V_{blank}=10$  mL,  $A_{ind}=0.235$  cm<sup>-1</sup>, catalyst=PFOA,  $m_{cat}=75$  g,  $d_{cat}=2.0$  mm.

Table F.163. Dye concentration change.

z, m	Abs, cm <sup>-1</sup>	C <sub>D</sub> × 10 <sup>2</sup> , mmol/L
0	2.792	28.19
0.09	2.427	24.50
0.21	1.510	15.25
0.52	1.446	14.60
0.88	1.422	14.36
0.98	1.294	13.07

Table F.164. Dissolved O<sub>3</sub> concentration change.

z, m	V <sub>T</sub> , mL	A <sub>ind</sub> , cm <sup>-1</sup>	C <sub>O<sub>3,L</sub></sub> × 10 <sup>3</sup> , mmol/L
0			0.00
0.09	30.3	0.191	10.67
0.21	29.3	0.171	16.46
0.52	32.3	0.139	21.33
0.88	28.5	0.152	22.38
0.98	31.5	0.134	23.40

Table F.165. TOC change.

z, m	TOC, mg/L
0.00	69.29
0.09	64.82
0.21	60.58
0.52	57.26
0.88	55.14
0.98	53.08

**Run 57**

Conditions: pH=2.5, Q<sub>G</sub>=150 L/h, Q<sub>L</sub>=150 L/h, C<sub>O<sub>3,G,in</sub></sub>=0.934 mmol/L gas, C<sub>O<sub>3,G,out</sub></sub>=0.326 mmol/L gas, t=15 min, V<sub>thio,inlet</sub>=93.4 mL, V<sub>thio,outlet</sub>=81.4 mL, Dye=RBBR, C<sub>D,in</sub>=5.1×10<sup>-2</sup> mmol/L, M<sub>thio</sub>=0.3 M for out, TOC<sub>in</sub>=13.35 mg/L, V<sub>blank</sub>=20 mL, A<sub>ind</sub>=0.461 cm<sup>-1</sup>, catalyst=Alumina, m<sub>cat</sub>=125 g, d<sub>cat</sub>=2.0 mm.

Table F.166. Dye concentration change.

z, m	Abs, cm <sup>-1</sup>	C <sub>D</sub> × 10 <sup>2</sup> , mmol/L
0	0.439	5.06
0.09	0.267	3.08
0.21	0.034	0.39
0.52	0.028	0.32
0.88	0.023	0.27
0.98	0.020	0.23

Table F.167. Dissolved O<sub>3</sub> concentration change.

z, m	V <sub>T</sub> , mL	A <sub>ind</sub> , cm <sup>-1</sup>	C <sub>O<sub>3,L</sub></sub> × 10 <sup>3</sup> , mmol/L
0			0.00
0.09	53.5	0.461	0.04
0.21	52.1	0.423	5.96
0.52	48.1	0.346	7.21
0.88	46.2	0.398	11.90
0.98	49.3	0.389	12.17

Table F.168. TOC change.

z, m	TOC, mg/L
0.00	13.35
0.09	12.06
0.21	11.36
0.52	10.75
0.88	10.04
0.98	9.30

### Run 58

Conditions: pH=2.5, Q<sub>G</sub>=150 L/h, Q<sub>L</sub>=150 L/h, C<sub>O<sub>3,G,in</sub></sub>=0.928 mmol/L gas, C<sub>O<sub>3,G,out</sub></sub>=0.318 mmol/L gas, t=15 min, V<sub>thio,inlet</sub>=92.8 mL, V<sub>thio,outlet</sub>=79.4 mL, Dye=RBBR, C<sub>D,in</sub>=18.0×10<sup>-2</sup> mmol/L, M<sub>thio</sub>=0.3 M for out, TOC<sub>in</sub>=44.50 mg/L, V<sub>blank</sub>=10 mL, A<sub>ind</sub>=0.216 cm<sup>-1</sup>, catalyst=Alumina, m<sub>cat</sub>=125 g, d<sub>cat</sub>=2.0 mm.

Table F.169. Dye concentration change.

z, m	Abs, cm <sup>-1</sup>	C <sub>D</sub> × 10 <sup>2</sup> , mmol/L
0	1.561	18.00
0.09	1.304	15.04
0.21	0.727	8.35
0.52	0.660	7.61
0.88	0.616	7.10
0.98	0.578	6.66

Table F.170. Dissolved O<sub>3</sub> concentration change.

z, m	V <sub>T</sub> , mL	A <sub>ind</sub> , cm <sup>-1</sup>	C <sub>O<sub>3,L</sub></sub> × 10 <sup>3</sup> , mmol/L
0			0.00
0.09	40.5	0.216	0.00
0.21	38.3	0.216	0.00
0.52	37.2	0.216	0.00
0.88	35.1	0.216	0.00
0.98	36.2	0.214	0.40

Table F.171. TOC change.

z, m	TOC, mg/L
0.00	44.50
0.09	40.35
0.21	38.59
0.52	35.62
0.88	35.04
0.98	33.42

**Run 59**

Conditions: pH=2.5,  $Q_G=150$  L/h,  $Q_L=150$  L/h,  $C_{O_3,G,in}=0.917$  mmol/L gas,  $C_{O_3,G,out}=0.348$  mmol/L gas,  $t=15$  min,  $V_{thio,inlet}=91.7$  mL,  $V_{thio,outlet}=86.9$  mL, Dye=AR-151,  $C_{D,in}=6.4 \times 10^{-2}$  mmol/L,  $M_{thio}=0.3$  M for out,  $TOC_{in}=15.18$  mg/L,  $V_{blank}=20$  mL,  $A_{ind}=0.472$  cm<sup>-1</sup>, catalyst=Alumina,  $m_{cat}=125$  g,  $d_{cat}=2.0$  mm.

Table F.173. Dye concentration change.

z, m	Abs, cm <sup>-1</sup>	$C_D \times 10^2$ , mmol/L
0	0.637	6.43
0.09	0.373	3.77
0.21	0.070	0.71
0.52	0.055	0.56
0.88	0.052	0.52
0.98	0.051	0.51

Table F.174. Dissolved O<sub>3</sub> concentration change.

z, m	$V_T$ , mL	$A_{ind}$ , cm <sup>-1</sup>	$C_{O_3,L} \times 10^3$ , mmol/L
0			0.00
0.09	48.3	0.417	9.67
0.21	48.8	0.367	18.10
0.52	45.0	0.355	24.06
0.88	43.2	0.354	25.23
0.98	42.0	0.352	25.71

Table F.175. TOC change.

z, m	TOC, mg/L
0.00	15.18
0.09	13.89
0.21	12.54
0.52	12.05
0.88	11.17
0.98	10.23

**Run 60**

Conditions: pH=2.5,  $Q_G=150$  L/h,  $Q_L=150$  L/h,  $C_{O_3,G,in}=0.922$  mmol/L gas,  $C_{O_3,G,out}=0.368$  mmol/L gas,  $t=15$  min,  $V_{thio,inlet}=92.2$  mL,  $V_{thio,outlet}=92.0$  mL, Dye=AR-151,  $C_{D,in}=26.2 \times 10^{-2}$  mmol/L,  $M_{thio}=0.3$  M for out,  $TOC_{in}=66.36$  mg/L,  $V_{blank}=10$  mL,  $A_{ind}=0.237$  cm<sup>-1</sup>, catalyst=Alumina,  $m_{cat}=125$  g,  $d_{cat}=2.0$  mm.

Table F.176. Dye concentration change.

$z$ , m	Abs, cm <sup>-1</sup>	$C_D \times 10^2$ , mmol/L
0	2.598	26.23
0.09	2.309	23.31
0.21	1.414	14.28
0.52	1.325	13.38
0.88	1.229	12.41
0.98	1.156	11.67

Table F.177. Dissolved O<sub>3</sub> concentration change.

$z$ , m	$V_T$ , mL	$A_{ind}$ , cm <sup>-1</sup>	$C_{O_3,L} \times 10^3$ , mmol/L
0			0.00
0.09	36.5	0.157	14.96
0.21	34.7	0.150	17.48
0.52	32.0	0.139	22.21
0.88	27.3	0.157	25.10
0.98	28.6	0.133	27.71

Table F.178. TOC change.

$z$ , m	TOC, mg/L
0.00	66.36
0.09	60.58
0.21	55.73
0.52	52.84
0.88	51.47
0.98	49.24

**Run 61**

Conditions: pH=2.5,  $Q_G=150$  L/h,  $Q_L=150$  L/h,  $C_{O_3,G,in}=0.935$  mmol/L gas,  $C_{O_3,G,out}=0.343$  mmol/L gas,  $t=15$  min,  $V_{thio,inlet}=93.5$  mL,  $V_{thio,outlet}=85.7$  mL, Dye=RBBR,  $C_{D,in}=5.1 \times 10^{-2}$  mmol/L,  $M_{thio}=0.3$  M for out,  $TOC_{in}=13.75$  mg/L,  $V_{blank}=20$  mL,  $A_{ind}=0.459$  cm<sup>-1</sup>, catalyst=PFOA,  $m_{cat}=125$  g,  $d_{cat}=2.0$  mm.

Table F.179. Dye concentration change.

$z, \text{ m}$	Abs, $\text{cm}^{-1}$	$C_D \times 10^2, \text{ mmol/L}$
0	0.441	5.09
0.09	0.275	3.17
0.21	0.039	0.45
0.52	0.027	0.31
0.88	0.017	0.20
0.98	0.015	0.17

Table F.180. Dissolved  $\text{O}_3$  concentration change.

$z, \text{ m}$	$V_T, \text{ mL}$	$A_{ind}, \text{ cm}^{-1}$	$C_{\text{O}_3,L} \times 10^3, \text{ mmol/L}$
0			0.00
0.09	52.0	0.456	0.42
0.21	50.7	0.412	7.63
0.52	50.2	0.395	10.54
0.88	45.1	0.391	13.42
0.98	46.1	0.379	15.29

Table F.181. TOC change.

$z, \text{ m}$	TOC, $\text{mg/L}$
0.00	13.75
0.09	11.06
0.21	10.58
0.52	9.23
0.88	9.00
0.98	8.84

### Run 63

Conditions:  $\text{pH}=2.5$ ,  $Q_G=150 \text{ L/h}$ ,  $Q_L=150 \text{ L/h}$ ,  $C_{\text{O}_3,G,in}=0.894 \text{ mmol/L gas}$ ,  $C_{\text{O}_3,G,out}=0.338 \text{ mmol/L gas}$ ,  $t=15 \text{ min}$ ,  $V_{\text{thio,inlet}}=89.4 \text{ mL}$ ,  $V_{\text{thio,outlet}}=84.5 \text{ mL}$ , Dye=*RBBR*,  $C_{D,in}=18.3 \times 10^{-2} \text{ mmol/L}$ ,  $M_{\text{thio}}=0.3 \text{ M}$  for out,  $\text{TOC}_{in}=50.68 \text{ mg/L}$ ,  $V_{\text{blank}}=10 \text{ mL}$ ,  $A_{ind}=0.249 \text{ cm}^{-1}$ , catalyst=PFOA,  $m_{cat}=125 \text{ g}$ ,  $d_{cat}=2.0 \text{ mm}$ .

Table F.182. Dye concentration change.

$z, \text{ m}$	Abs, $\text{cm}^{-1}$	$C_D \times 10^2, \text{ mmol/L}$
0	1.589	18.32
0.09	1.292	14.90
0.21	0.782	9.02
0.52	0.708	8.16
0.88	0.665	7.67
0.98	0.554	6.39

Table F.183. Dissolved O<sub>3</sub> concentration change.

<i>z</i> , m	<i>V<sub>T</sub></i> , mL	<i>A<sub>ind</sub></i> , cm <sup>-1</sup>	<i>C<sub>O<sub>3,L</sub></sub></i> × 10 <sup>3</sup> , mmol/L
0			0.00
0.09	35.8	0.249	0.00
0.21	39.5	0.249	0.00
0.52	34.8	0.249	0.00
0.88	34.5	0.249	0.00
0.98	42.4	0.233	2.44

Table F.184. TOC change.

<i>z</i> , m	TOC, mg/L
0.00	50.68
0.09	46.92
0.21	44.81
0.52	43.90
0.88	41.72
0.98	39.28

### Run 64

Conditions: pH=2.5, *Q<sub>G</sub>*=150 L/h, *Q<sub>L</sub>*=150 L/h, *C<sub>O<sub>3,G,in</sub></sub>*=0.927 mmol/L gas, *C<sub>O<sub>3,G,out</sub></sub>*=0.353 mmol/L gas, *t*=15 min, *V<sub>thio,inlet</sub>*=92.7 mL, *V<sub>thio,outlet</sub>*=88.3 mL, Dye=AR-151, *C<sub>D,in</sub>*=5.5×10<sup>-2</sup> mmol/L, *M<sub>thio</sub>*=0.3 M for out, TOC<sub>in</sub>=15.18 mg/L, *V<sub>blank</sub>*=20 mL, *A<sub>ind</sub>*=0.445 cm<sup>-1</sup>, catalyst=PFOA, *m<sub>cat</sub>*=125 g, *d<sub>cat</sub>*=2.0 mm.

Table F.185. Dye concentration change.

<i>z</i> , m	Abs, cm <sup>-1</sup>	<i>C<sub>D</sub></i> × 10 <sup>2</sup> , mmol/L
0	0.544	5.49
0.09	0.396	4.00
0.21	0.061	0.62
0.52	0.049	0.50
0.88	0.046	0.46
0.98	0.043	0.43

Table F.186. Dissolved O<sub>3</sub> concentration change.

<i>z</i> , m	<i>V<sub>T</sub></i> , mL	<i>A<sub>ind</sub></i> , cm <sup>-1</sup>	<i>C<sub>O<sub>3,L</sub></sub></i> × 10 <sup>3</sup> , mmol/L
0			0.00
0.09	52.5	0.392	7.33
0.21	49.0	0.369	13.02
0.52	45.0	0.326	27.63
0.88	46.8	0.249	36.35
0.98	47.3	0.226	39.85

Table F.187. TOC change.

z, m	TOC, mg/L
0.00	15.18
0.09	13.72
0.21	12.81
0.52	11.66
0.88	10.28
0.98	9.12

**Run 65**

Conditions: pH=2.5,  $Q_G=150$  L/h,  $Q_L=150$  L/h,  $C_{O_3,G,in}=0.941$  mmol/L gas,  $C_{O_3,G,out}=0.354$  mmol/L gas,  $t=15$  min,  $V_{thio,inlet}=94.1$  mL,  $V_{thio,outlet}=88.4$  mL, Dye=AR-151,  $C_{D,in}=25.5 \times 10^{-2}$  mmol/L,  $M_{thio}=0.3$  M for out,  $TOC_{in}=68.13$  mg/L,  $V_{blank}=10$  mL,  $A_{ind}=0.238$  cm<sup>-1</sup>, catalyst=PFOA,  $m_{cat}=125$  g,  $d_{cat}=2.0$  mm.

Table F.188. Dye concentration change.

z, m	Abs, cm <sup>-1</sup>	$C_D \times 10^2$ , mmol/L
0	2.523	25.47
0.09	2.221	22.43
0.21	1.217	12.29
0.52	1.141	11.52
0.88	1.049	10.59
0.98	0.941	9.50

Table F.189. Dissolved O<sub>3</sub> concentration change.

z, m	$V_T$ , mL	$A_{ind}$ , cm <sup>-1</sup>	$C_{O_3,L} \times 10^3$ , mmol/L
0			0.00
0.09	36.6	0.203	6.63
0.21	36.5	0.144	17.63
0.52	36.8	0.124	21.10
0.88	32.3	0.121	26.00
0.98	36.6	0.091	27.52

Table F.190. TOC change.

z, m	TOC, mg/L
0.00	68.13
0.09	60.73
0.21	55.79
0.52	52.94
0.88	51.63
0.98	48.44

**Run 66**

Conditions: pH=2.5,  $Q_G=150$  L/h,  $Q_L=30$  L/h,  $C_{O_3,G,in}=0.940$  mmol/L gas,  $C_{O_3,G,out}=0.355$  mmol/L gas, t=15 min,  $V_{thio,inlet}=94.0$  mL,  $V_{thio,outlet}=88.7$  mL, Dye=RBBR,  $C_{D,in}=5.2 \times 10^{-2}$  mmol/L,  $M_{thio}=0.3$  M for out,  $TOC_{in}=13.75$  mg/L,  $V_{blank}=20$  mL,  $A_{ind}=0.461$  cm<sup>-1</sup>, catalyst=no.

Table F.191. Dye concentration change.

z, m	Abs, cm <sup>-1</sup>	$C_D \times 10^2$ , mmol/L
0	0.424	5.24
0.09	0.005	0.75
0.21	0.001	0.15
0.52	0.000	0.00
0.88	0.000	0.00
0.98	0.000	0.00

Table F.192. Dissolved O<sub>3</sub> concentration change.

z, m	$V_T$ , mL	$A_{ind}$ , cm <sup>-1</sup>	$C_{O_3,L} \times 10^3$ , mmol/L
0			0.00
0.09	48.8	0.131	56.98
0.21	36.1	0.167	90.75
0.52	36.3	0.020	134.46
0.88	34.0	0.043	148.40
0.98	33.9	0.023	156.52

Table F.193. TOC change.

z, m	TOC, mg/L
0.00	13.75
0.09	10.20
0.21	9.75
0.52	9.41
0.88	9.33
0.98	9.22

**Run 67**

Conditions: pH=2.5,  $Q_G=150$  L/h,  $Q_L=30$  L/h,  $C_{O_3,G,in}=0.953$  mmol/L gas,  $C_{O_3,G,out}=0.340$  mmol/L gas, t=15 min,  $V_{thio,inlet}=95.3$  mL,  $V_{thio,outlet}=85.0$  mL, Dye=RBBR,  $C_{D,in}=17.9 \times 10^{-2}$  mmol/L,  $M_{thio}=0.3$  M for out,  $TOC_{in}=50.94$  mg/L,  $V_{blank}=20$  mL,  $A_{ind}=0.464$  cm<sup>-1</sup>, catalyst=no.

Table F.194. Dye concentration change.

$z$ , m	Abs, $\text{cm}^{-1}$	$C_D \times 10^2$ , mmol/L
0	1.553	17.91
0.09	0.153	1.76
0.21	0.072	0.83
0.52	0.003	0.04
0.88	0.000	0.00
0.98	0.000	0.00

Table F.195. Dissolved  $\text{O}_3$  concentration change.

$z$ , m	$V_T$ , mL	$A_{ind}$ , $\text{cm}^{-1}$	$C_{\text{O}_3,L} \times 10^3$ , mmol/L
0			0.00
0.09	56.0	0.422	5.85
0.21	51.0	0.405	9.42
0.52	48.2	0.295	29.72
0.88	45.1	0.203	51.68
0.98	52.4	0.108	54.60

Table F.196. TOC change.

$z$ , m	TOC, mg/L
0.00	50.94
0.09	48.62
0.21	45.72
0.52	44.81
0.88	43.58
0.98	42.74

**Run 68**

Conditions:  $\text{pH}=2.5$ ,  $Q_G=150$  L/h,  $Q_L=30$  L/h,  $C_{\text{O}_3,G,in}=0.917$  mmol/L gas,  $C_{\text{O}_3,G,out}=0.340$  mmol/L gas,  $t=15$  min,  $V_{\text{thio,inlet}}=91.7$  mL,  $V_{\text{thio,outlet}}=85.1$  mL, Dye=AR-151,  $C_{D,in}=8.1 \times 10^{-2}$  mmol/L,  $M_{\text{thio}}=0.3$  M for out,  $\text{TOC}_{in}=17.98$  mg/L,  $V_{\text{blank}}=20$  mL,  $A_{ind}=0.471$   $\text{cm}^{-1}$ , catalyst=no.

Table F.197. Dye concentration change.

$z$ , m	Abs, $\text{cm}^{-1}$	$C_D \times 10^2$ , mmol/L
0	0.800	8.07
0.09	0.059	0.596
0.21	0.042	0.424
0.52	0.029	0.293
0.88	0.028	0.283
0.98	0.027	0.273

Table F.198. Dissolved O<sub>3</sub> concentration change.

<i>z</i> , m	<i>V<sub>T</sub></i> , mL	<i>A<sub>ind</sub></i> , cm <sup>-1</sup>	<i>C<sub>O<sub>3,L</sub></sub></i> × 10 <sup>3</sup> , mmol/L
0			0.00
0.09	44.2	0.215	53.02
0.21	40.8	0.197	65.48
0.52	39.3	0.117	92.44
0.88	38.0	0.121	96.65
0.98	41.2	0.034	102.44

Table F.199. TOC change.

<i>z</i> , m	TOC, mg/L
0.00	17.98
0.09	15.63
0.21	14.51
0.52	12.84
0.88	12.02
0.98	11.88

### Run 69

Conditions: pH=2.5, *Q<sub>G</sub>*=150 L/h, *Q<sub>L</sub>*=30 L/h, *C<sub>O<sub>3,G,in</sub></sub>*=0.954 mmol/L gas, *C<sub>O<sub>3,G,out</sub></sub>* = 0.315 mmol/L gas, *t*=14.33 min, *V<sub>thio,inlet</sub>*=95.3 mL, *V<sub>thio,outlet</sub>*=75.3 mL, Dye=AR-151, *C<sub>D,in</sub>*=24.7×10<sup>-2</sup> mmol/L, *M<sub>thio</sub>*=0.3 M for out, *TOC<sub>in</sub>*=69.53 mg/L, *V<sub>blank</sub>*=20 mL, *A<sub>ind</sub>*=0.468 cm<sup>-1</sup>, catalyst=no.

Table F.200. Dye concentration change.

<i>z</i> , m	Abs, cm <sup>-1</sup>	<i>C<sub>D</sub></i> × 10 <sup>2</sup> , mmol/L
0	2.446	24.70
0.09	0.647	6.53
0.21	0.380	3.84
0.52	0.273	2.76
0.88	0.250	2.52
0.98	0.225	2.27

Table F.201. Dissolved O<sub>3</sub> concentration change.

<i>z</i> , m	<i>V<sub>T</sub></i> , mL	<i>A<sub>ind</sub></i> , cm <sup>-1</sup>	<i>C<sub>O<sub>3,L</sub></sub></i> × 10 <sup>3</sup> , mmol/L
0			0.00
0.09	52.0	0.321	22.83
0.21	51.8	0.250	34.06
0.52	53.0	0.196	40.96
0.88	44.0	0.252	44.73
0.98	50.5	0.162	49.85

Table F.202. TOC change.

z, m	TOC, mg/L
0.00	69.53
0.09	65.85
0.21	62.38
0.52	59.04
0.88	56.84
0.98	54.72

**Run 70**

Conditions: pH=2.5,  $Q_G=150$  L/h,  $Q_L=30$  L/h,  $C_{O_3,G,in}=0.973$  mmol/L gas,  $C_{O_3,G,out} = 0.344$  mmol/L gas,  $t=14.33$  min,  $V_{thio,inlet}=97.3$  mL,  $V_{thio,outlet}=91.7$  mL, Dye=*RBBR*,  $C_{D,in}=5.3 \times 10^{-2}$  mmol/L,  $M_{thio}=0.3$  M for out,  $TOC_{in}=15.82$  mg/L,  $V_{blank}=20$  mL,  $A_{ind}=0.404$  cm<sup>-1</sup>, catalyst=alumina,  $m_{cat}=125$  g,  $d_{cat}=2.0$  mm.

Table F.202. Dye concentration change.

z, m	Abs, cm <sup>-1</sup>	$C_D \times 10^2$ , mmol/L
0	0.459	5.29
0.09	0.138	1.59
0.21	0.043	0.50
0.52	0.041	0.47
0.88	0.025	0.29
0.98	0.007	0.07

Table F.203. Dissolved O<sub>3</sub> concentration change.

z, m	$V_T$ , mL	$A_{ind}$ , cm <sup>-1</sup>	$C_{O_3,L} \times 10^3$ , mmol/L
0			0.00
0.09	52.9	0.381	3.52
0.21	47.3	0.069	61.0
0.52	43.5	0.065	71.69
0.88	39.8	0.108	74.21
0.98	43.4	0.038	77.65

Table F.204. TOC change.

z, m	TOC, mg/L
0.00	15.82
0.09	12.36
0.21	10.19
0.52	9.01
0.88	8.81
0.98	8.60

### Run 71

Conditions: pH=2.5,  $Q_G=150$  L/h,  $Q_L=30$  L/h,  $C_{O_3,G,in}=0.967$  mmol/L gas,  $C_{O_3,G,out}=0.346$  mmol/L gas,  $t=16$  min,  $V_{thio,inlet}=96.7$  mL,  $V_{thio,outlet}=92.2$  mL, Dye=RBBR,  $C_{D,in}=18.2 \times 10^{-2}$  mmol/L,  $M_{thio}=0.3$  M for out,  $TOC_{in}=47.46$  mg/L,  $V_{blank}=20$  mL,  $A_{ind}=0.462$  cm<sup>-1</sup>, catalyst=alumina,  $m_{cat}=125$  g,  $d_{cat}=2.0$  mm.

Table F.205. Dye concentration change.

$z, m$	Abs, cm <sup>-1</sup>	$C_D \times 10^2, \text{mmol/L}$
0	1.581	18.23
0.09	0.960	11.07
0.21	0.179	2.06
0.52	0.168	1.94
0.88	0.156	1.80
0.98	0.150	1.73

Table F.206. Dissolved O<sub>3</sub> concentration change.

$z, m$	$V_T, \text{mL}$	$A_{ind}, \text{cm}^{-1}$	$C_{O_3,L} \times 10^3, \text{mmol/L}$
0			0.00
0.09	50.2	0.462	0.00
0.21	51.0	0.462	0.00
0.52	53.5	0.430	4.75
0.88	49.5	0.418	7.42
0.98	58.8	0.399	8.13

Table F.207. TOC change.

$z, m$	TOC, mg/L
0.00	47.46
0.09	43.26
0.21	40.72
0.52	37.61
0.88	34.85
0.98	33.22

### Run 72

Conditions: pH=2.5,  $Q_G=150$  L/h,  $Q_L=30$  L/h,  $C_{O_3,G,in}=0.902$  mmol/L gas,  $C_{O_3,G,out}=0.359$  mmol/L gas,  $t=15.5$  min,  $V_{thio,inlet}=90.2$  mL,  $V_{thio,outlet}=92.7$  mL, Dye=AR-151,  $C_{D,in}=7.6 \times 10^{-2}$  mmol/L,  $M_{thio}=0.3$  M for out,  $TOC_{in}=19.55$  mg/L,  $V_{blank}=20$  mL,  $A_{ind}=0.467$  cm<sup>-1</sup>, catalyst=alumina,  $m_{cat}=125$  g,  $d_{cat}=2.0$  mm.

Table F.208. Dye concentration change.

$z$ , m	Abs, $\text{cm}^{-1}$	$C_D \times 10^2$ , mmol/L
0	0.749	7.56
0.09	0.208	2.10
0.21	0.059	0.59
0.52	0.053	0.53
0.88	0.048	0.48
0.98	0.045	0.45

Table F.209. Dissolved  $\text{O}_3$  concentration change.

$z$ , m	$V_T$ , mL	$A_{ind}$ , $\text{cm}^{-1}$	$C_{\text{O}_3,L} \times 10^3$ , mmol/L
0			0.00
0.09	56.5	0.390	10.48
0.21	50.0	0.289	29.48
0.52	56.1	0.212	35.10
0.88	51.2	0.222	39.02
0.98	59.1	0.150	40.29

Table F.210. TOC change.

$z$ , m	TOC, mg/L
0.00	19.55
0.09	16.83
0.21	14.72
0.52	13.37
0.88	12.28
0.98	11.18

**Run 73**

Conditions:  $\text{pH}=2.5$ ,  $Q_G=150$  L/h,  $Q_L=30$  L/h,  $C_{\text{O}_3,G,in}=0.945$  mmol/L gas,  $C_{\text{O}_3,G,out}=0.353$  mmol/L gas,  $t=15.5$  min,  $V_{\text{thio,inlet}}=96.9$  mL,  $V_{\text{thio,outlet}}=91.3$  mL, Dye=AR-151,  $C_{D,in}=23.8 \times 10^{-2}$  mmol/L,  $M_{\text{thio}}=0.3$  M for out,  $\text{TOC}_{in}=62.52$  mg/L,  $V_{\text{blank}}=20$  mL,  $A_{ind}=0.463$   $\text{cm}^{-1}$ , catalyst=alumina,  $m_{cat}=125$  g,  $d_{cat}=2.0$  mm.

Table F.211. Dye concentration change.

$z$ , m	Abs, $\text{cm}^{-1}$	$C_D \times 10^2$ , mmol/L
0	2.356	23.79
0.09	2.003	20.22
0.21	0.775	7.83
0.52	0.712	7.20
0.88	0.674	6.81
0.98	0.656	6.61

Table F.212. Dissolved O<sub>3</sub> concentration change.

<i>z</i> , m	<i>V<sub>T</sub></i> , mL	<i>A<sub>ind</sub></i> , cm <sup>-1</sup>	<i>C<sub>O<sub>3,L</sub></sub></i> × 10 <sup>3</sup> , mmol/L
0			0.00
0.09	45.7	0.393	13.58
0.21	50.0	0.314	24.69
0.52	50.2	0.282	29.79
0.88	48.8	0.284	30.90
0.98	51.0	0.266	31.58

Table F.213. TOC change.

<i>z</i> , m	TOC, mg/L
0.00	62.52
0.09	59.83
0.21	55.72
0.52	50.73
0.88	47.36
0.98	43.01

#### Run 74

Conditions: pH=2.5, *Q<sub>G</sub>*=150 L/h, *Q<sub>L</sub>*=30 L/h, *C<sub>O<sub>3,G,in</sub></sub>*=0.969 mmol/L gas, *C<sub>O<sub>3,G,out</sub></sub>* = 0.345 mmol/L gas, *t*=15.5 min, *V<sub>thio,inlet</sub>*=96.9 mL, *V<sub>thio,outlet</sub>*=91.9 mL, Dye=*RBBR*, *C<sub>D,in</sub>*=5.1×10<sup>-2</sup> mmol/L, *M<sub>thio</sub>*=0.3 M for out, TOC<sub>in</sub>=15.79 mg/L, *V<sub>blank</sub>*=20 mL, *A<sub>ind</sub>*=0.452 cm<sup>-1</sup>, catalyst=PFOA, *m<sub>cat</sub>*=125 g, *d<sub>cat</sub>*=2.0 mm.

Table F.214. Dye concentration change.

<i>z</i> , m	Abs, cm <sup>-1</sup>	<i>C<sub>D</sub></i> × 10 <sup>2</sup> , mmol/L
0	0.446	5.14
0.09	0.119	1.37
0.21	0.018	0.21
0.52	0.008	0.09
0.88	0.006	0.07
0.98	0.001	0.01

Table F.215. Dissolved O<sub>3</sub> concentration change.

<i>z</i> , m	<i>V<sub>T</sub></i> , mL	<i>A<sub>ind</sub></i> , cm <sup>-1</sup>	<i>C<sub>O<sub>3,L</sub></sub></i> × 10 <sup>3</sup> , mmol/L
0			0.00
0.09	48.2	0.441	2.02
0.21	50.0	0.305	24.42
0.52	52.0	0.285	25.52
0.88	47.0	0.278	32.02
0.98	49.0	0.252	34.21

Table F.252. Dye concentration change.

z, m	Abs, cm <sup>-1</sup>	$C_D \times 10^2$ , mmol/L
0	1.660	19.14
0.09	1.505	17.35
0.21	1.286	14.83
0.52	0.899	10.37
0.88	0.828	9.55
0.98	0.801	9.24

Table F.253. TOC change.

z, m	TOC, mg/L
0.00	49.33
0.09	47.64
0.21	45.82
0.52	44.90
0.88	43.85
0.98	41.63

**Run 89**

Conditions: pH=2.5,  $Q_G=150$  L/h,  $Q_L=230$  L/h,  $C_{O_3,G,in}=0.989$  mmol/L gas,  $C_{O_3,G,out}=0.242$  mmol/L gas,  $t=10.0$  min,  $V_{thio,inlet}=98.9$  mL,  $V_{thio,outlet}=$  mL, Dye=*RBBR*,  $C_{D,in}=18.3 \times 10^{-2}$  mmol/L,  $M_{thio}=0.3$  M for out,  $TOC_{in}=49.07$  mg/L,  $V_{blank}=10$  mL,  $A_{ind}=0.208$  cm<sup>-1</sup>, catalyst=PFOA,  $m_{cat}=125$  g,  $d_{cat}=2.0$  mm.

Table F.254. Dye concentration change.

z, m	Abs, cm <sup>-1</sup>	$C_D \times 10^2$ , mmol/L
0	1.583	18.26
0.09	1.381	15.92
0.21	1.105	12.74
0.52	0.877	10.11
0.88	0.748	8.63
0.98	0.619	7.14

Table F.255. TOC change.

z, m	TOC, mg/L
0.00	49.07
0.09	46.33
0.21	45.71
0.52	43.74
0.88	41.86
0.98	40.58

**Run 90**

Conditions: pH=2.5,  $Q_G=150$  L/h,  $Q_L=150$  L/h,  $C_{O_3,G,in}=1.439$  mmol/L gas,  $C_{O_3,G,out}=0.130$  mmol/L gas,  $t=$  min,  $V_{thio,inlet}=143.9$  mL,  $V_{thio,outlet}=21.7$  mL, Dye=RBBR,  $C_{D,in}=22.4 \times 10^{-2}$  mmol/L,  $M_{thio}=0.3$  M for out,  $TOC_{in}=56.37$  mg/L,  $V_{blank}=10$  mL,  $A_{ind}=0.210$  cm<sup>-1</sup>, catalyst=no.

Table F.256. Dye concentration change.

$z, m$	Abs, cm <sup>-1</sup>	$C_D \times 10^2, \text{mmol/L}$
0	1.942	22.40
0.09	1.107	12.77
0.21	0.875	10.09
0.52	0.549	6.33
0.88	0.455	5.25
0.98	0.413	4.76

Table F.257. Dissolved O<sub>3</sub> concentration change.

$z, m$	$V_T, \text{mL}$	$A_{ind}, \text{cm}^{-1}$	$C_{O_3,L} \times 10^3, \text{mmol/L}$
0			0.00
0.09	47.2	0.210	0.00
0.21	48.9	0.207	0.41
0.52	52.0	0.179	3.61
0.88	45.0	0.178	4.56
0.98	63.8	0.144	6.12

Table F.258. TOC change.

$z, m$	TOC, mg/L
0.00	56.37
0.09	55.88
0.21	54.24
0.52	53.67
0.88	53.01
0.98	52.25

**Run 91**

Conditions: pH=2.5,  $Q_G=150$  L/h,  $Q_L=150$  L/h,  $C_{O_3,G,in}=1.433$  mmol/L gas,  $C_{O_3,G,out}=0.177$  mmol/L gas,  $t=10$  min,  $V_{thio,inlet}=143.3$  mL,  $V_{thio,outlet}=29.5$  mL, Dye=AR-151,  $C_{D,in}=27.0 \times 10^{-2}$  mmol/L,  $M_{thio}=0.3$  M for out,  $TOC_{in}=70.03$  mg/L,  $V_{blank}=10$  mL,  $A_{ind}=0.196$  cm<sup>-1</sup>, catalyst=no.

Table F.259. Dye concentration change.

$z, \text{ m}$	Abs, $\text{cm}^{-1}$	$C_D \times 10^2, \text{ mmol/L}$
0	2.678	27.04
0.09	1.591	16.06
0.21	1.310	13.22
0.52	1.161	11.73
0.88	1.079	10.90
0.98	0.910	9.19

Table F.260. Dissolved  $\text{O}_3$  concentration change.

$z, \text{ m}$	$V_T, \text{ mL}$	$A_{ind}, \text{ cm}^{-1}$	$C_{O_3,L} \times 10^3, \text{ mmol/L}$
0			0.00
0.09	37.4	0.172	4.33
0.21	37.0	0.162	6.28
0.52	38.1	0.152	7.71
0.88	33.0	0.155	8.78
0.98	42.5	0.127	10.59

Table F.261. TOC change.

$z, \text{ m}$	TOC, $\text{mg/L}$
0.00	70.03
0.09	68.84
0.21	65.91
0.52	65.13
0.88	64.29
0.98	63.94

**Run 92**

Conditions:  $\text{pH}=2.5$ ,  $Q_G=150 \text{ L/h}$ ,  $Q_L=150 \text{ L/h}$ ,  $C_{O_3,G,in}=1.487 \text{ mmol/L gas}$ ,  $C_{O_3,G,out}=0.339 \text{ mmol/L gas}$ ,  $t=10 \text{ min}$ ,  $V_{\text{thio,inlet}}=148.7 \text{ mL}$ ,  $V_{\text{thio,outlet}}=56.5 \text{ mL}$ , Dye=*RBBR*,  $C_{D,in}=21.4 \times 10^{-2} \text{ mmol/L}$ ,  $M_{\text{thio}}=0.3 \text{ M}$  for out,  $\text{TOC}_{in}=58.21 \text{ mg/L}$ ,  $V_{\text{blank}}=10 \text{ mL}$ ,  $A_{ind}=0.202 \text{ cm}^{-1}$ , catalyst=alumina,  $m_{cat}=25 \text{ g}$ ,  $d_{cat}=2.0 \text{ mm}$ .

Table F.262. Dye concentration change.

$z, \text{ m}$	Abs, $\text{cm}^{-1}$	$C_D \times 10^2, \text{ mmol/L}$
0	1.857	21.41
0.09	0.833	9.60
0.21	0.644	7.43
0.52	0.595	6.86
0.88	0.535	6.17
0.98	0.494	5.70

Table F.263. Dissolved O<sub>3</sub> concentration change.

$z, \text{ m}$	$V_T, \text{ mL}$	$A_{ind}, \text{ cm}^{-1}$	$C_{O_3,L} \times 10^3, \text{ mmol/L}$
0			0.00
0.09	46.4	0.202	0.00
0.21	45.0	0.164	6.56
0.52	42.7	0.147	9.56
0.88	40.0	0.135	12.46
0.98	57.2	0.067	15.04

Table F.264. TOC change.

$z, \text{ m}$	TOC, mg/L
0.00	58.21
0.09	55.38
0.21	52.29
0.52	48.75
0.88	48.11
0.98	47.97

**Run 93**

Conditions: pH=2.5,  $Q_G=150 \text{ L/h}$ ,  $Q_L=150 \text{ L/h}$ ,  $C_{O_3,G,in}=1.388 \text{ mmol/L}$  gas,  $C_{O_3,G,out}=0.367 \text{ mmol/L}$  gas,  $t=9.17 \text{ min}$ ,  $V_{thio,inlet}=138.8 \text{ mL}$ ,  $V_{thio,outlet}=56.0 \text{ mL}$ , Dye=AR-151,  $C_{D,in}=29.0 \times 10^{-2} \text{ mmol/L}$ ,  $M_{thio}=0.3 \text{ M}$  for out,  $TOC_{in}=58.21 \text{ mg/L}$ ,  $V_{blank}=10 \text{ mL}$ ,  $A_{ind}=0.196 \text{ cm}^{-1}$ , catalyst=alumina,  $m_{cat}=25 \text{ g}$ ,  $d_{cat}=2.0 \text{ mm}$ .

Table F.265. Dye concentration change.

$z, \text{ m}$	Abs, $\text{cm}^{-1}$	$C_D \times 10^2, \text{ mmol/L}$
0	2.871	28.99
0.09	1.572	15.87
0.21	1.072	10.82
0.52	1.041	10.51
0.88	0.989	9.99
0.98	0.980	9.90

Table F.266. Dissolved O<sub>3</sub> concentration change.

$z, \text{ m}$	$V_T, \text{ mL}$	$A_{ind}, \text{ cm}^{-1}$	$C_{O_3,L} \times 10^3, \text{ mmol/L}$
0			0.00
0.09	43.5	0.196	0.00
0.21	40.5	0.195	1.35
0.52	43.3	0.182	3.10
0.88	34.0	0.181	4.50
0.98	43.2	0.136	10.02

Table F.267. TOC change.

z, m	TOC, mg/L
0.00	73.15
0.09	69.44
0.21	67.81
0.52	64.28
0.88	62.53
0.98	61.23

**Run 94**

Conditions: pH=2.5,  $Q_G=150$  L/h,  $Q_L=150$  L/h,  $C_{O_3,G,in}=1.423$  mmol/L gas,  $C_{O_3,G,out}=0.430$  mmol/L gas,  $t=9.5$  min,  $V_{thio,inlet}=142.3$  mL,  $V_{thio,outlet}=43.5$  mL, Dye=RBBR,  $C_{D,in}=21.8 \times 10^{-2}$  mmol/L,  $M_{thio}=0.3$  M for out,  $TOC_{in}=55.47$  mg/L,  $V_{blank}=10$  mL,  $A_{ind}=0.197$  cm<sup>-1</sup>, catalyst=alumina,  $m_{cat}=75$  g,  $d_{cat}=2.0$  mm.

Table F.268. Dye concentration change.

z, m	Abs, cm <sup>-1</sup>	$C_D \times 10^2$ , mmol/L
0	1.893	21.83
0.09	1.490	17.18
0.21	0.835	9.63
0.52	0.695	8.01
0.88	0.566	6.53
0.98	0.433	4.99

Table F.269. Dissolved O<sub>3</sub> concentration change.

z, m	$V_T$ , mL	$A_{ind}$ , cm <sup>-1</sup>	$C_{O_3,L} \times 10^3$ , mmol/L
0			0.00
0.09	49.7	0.197	0.00
0.21	49.0	0.195	0.27
0.52	48.5	0.181	2.12
0.88	45.0	0.172	3.56
0.98	56.5	0.160	3.96

Table F.270. TOC change.

z, m	TOC, mg/L
0.00	55.47
0.09	50.87
0.21	46.35
0.52	44.20
0.88	43.99
0.98	43.65

## APPENDIX G

### COMPUTER PROGRAMS

#### G.1 Ozone absorption experiments

The ozone absorption process is described by the transfer of O<sub>3</sub> from gas phase to liquid phase in a co-currently operated column. Gaseous ozone (x) transfers to the liquid phase (y) at steady state in addition to the axially dispersed liquid phase. The equations describing the process are:

$$\frac{Q_G}{A} \frac{dx}{dz} = -(k_L a)(bx - y) \quad (\text{G.1})$$

$$\frac{Q_L}{A} \frac{dy}{dz} = D_L \frac{d^2 y}{dz^2} + (k_L a)(bx - y) \quad (\text{G.2})$$

The boundary conditions for the species are:

$$\text{at } z = 0, \quad x = x_0 \text{ and } y = 0;$$

$$\text{at } z = H, \quad \frac{dy}{dz} = 0$$

where  $x_0$  is the inlet condition of gaseous ozone at  $z=0$ .

##### G.1.1 Solution of Equation (G.1)

$$\frac{dx}{dz} = A_1(bx - y) \quad (\text{G.3})$$

where  $A_1 = \frac{-(k_L a)A}{Q_G}$

Then, discretization is applied to Equation (G.3)

$$\frac{x_{i+1} - x_i}{\Delta z} = A_1.(bx_i - y_i) \quad (\text{G.4})$$

$$x_{i+1} = x_i + A_1.\Delta z.(bx_i - y_i) \quad (\text{G.5})$$

$$x_{i+1} = (1 + A_1.\Delta z.b).x_i - A_1.\Delta z.y_i \quad (\text{G.6})$$

For  $i = 1$       $x_i = x_0$       $y_i = 0.0$

### G.1.2 Solution of Equation (G.2)

$$-D_L \frac{d^2 y}{dz^2} + \frac{Q_L}{A} \frac{dy}{dz} - (k_L a).(bx - y) = 0 \quad (\text{G.7})$$

$$-D_L \frac{d^2 y}{dz^2} + \frac{Q_L}{A} \frac{dy}{dz} + (k_L a).y - (k_L a).b.x = 0 \quad (\text{G.8})$$

$$\frac{d^2 y}{dz^2} + B \frac{dy}{dz} + Cy = Dx \quad (\text{G.9})$$

where  $B = -\frac{Q_L}{A.D_L}$ ,  $C = -\frac{(k_L a)}{D_L}$  and  $D = -\frac{(k_L a)b}{D_L}$

The discretization for the first and second derivatives of y is applied.

$$\frac{y_{i+1} - 2y_i + y_{i-1}}{(\Delta z)^2} + B \frac{y_{i+1} - y_{i-1}}{2\Delta z} + Cy_i = Dx_i \quad (\text{G.10})$$

$$Ey_{i-1} + Fy_i + Gy_{i+1} = Dx_i \quad (\text{G.11})$$

where  $E = \frac{1}{(\Delta z)^2} - \frac{B}{2\Delta z}$ ,  $F = C - \frac{2}{(\Delta z)^2}$ , and  $G = \frac{1}{(\Delta z)^2} + \frac{B}{2\Delta z}$

At the boundary where  $i=N$ ,

$$\frac{y_{N+1} - y_{N-1}}{\Delta z} = 0 \quad (\text{G.12})$$

$$\frac{y_{N-1} - 2y_N + y_{N+1}}{(\Delta z)^2} + B \frac{y_{N+1} - y_{N-1}}{2\Delta z} + Cy_N = Dx_N \quad (\text{G.13})$$

$$\frac{y_{N-1} - 2y_N + y_{N+1}}{(\Delta z)^2} + Cy_N = Dx_N \quad (\text{G.14})$$

$$Hy_{N-1} + Fy_N = Dx_N \quad (\text{G.15})$$

where  $H = \frac{2}{(\Delta z)^2}$ , and  $F = C - \frac{2}{(\Delta z)^2}$

### G.1.3 Fortran program

```

PROGRAM MAIN_1
  IMPLICIT NONE
  INTEGER N, I, ITER
  PARAMETER ( N = 101 )
  DOUBLE PRECISION X, Y, DZ, A1, B, C, D, AA, BB, CC, DD, P, Q, E,
1      F, G, H, Z, XNOLD, TOL
  DIMENSION X(N), Y(N), AA(N), BB(N), CC(N), DD(N), P(N), Q(N)
C
  DATA A1, B, C, D, X(1) / -12.015D0, -1.442D0, -86.609D0, -29.014D0,
1      14.54D0 /
C
C
C... INITIALIZATION:
C
  OPEN (6, FILE='RESULT7.DAT')
  DZ = 1.0D0 / (N - 1)
  E = 1.0D0 / DZ**2 - B / (2.0*DZ)
  F = C - 2.0 / DZ**2
  G = 1.0 / DZ**2 + B / (2.0*DZ)
  H = 2.0 / DZ**2
  TOL = 1.0D-6
C
  DO 10 I = 1, N
    Y(I) = 0.0D0
10 CONTINUE
  XNOLD = 0.0D0
C... LEFT BC:
C

```

```

        CC(1) = 0.0D0
        AA(1) = 1.0D0
        BB(1) = 0.0D0
        DD(1) = 0.0D0
C
C... INTERNAL GRIDS:
C
    DO 20 I = 2, N-1
        CC(I) = -E
        AA(I) = F
        BB(I) = -G
20 CONTINUE
C
C... RIGHT BC:
C
        CC(N) = -H
        AA(N) = F
        BB(N) = 0.0D0
C
C... ITERATION SECTION:
C
    DO 60 ITER = 1, 100
    DO 30 I = 2, N
        X(I) = (1.0D0 + A1*0.35*DZ) * X(I-1) - A1*DZ*Y(I-1)
30 CONTINUE
C
    DO 40 I = 2, N
        DD(I) = D*X(I)
40 CONTINUE
C
    CALL TDMA (Y, AA, BB, CC, DD, N, P, Q)
C
    IF (DABS(XNOLD - X(N)) .LT. TOL) GOTO 70
        XNOLD = X(N)
60 CONTINUE
C
70 WRITE(6,*) ' ITER = ',ITER
    WRITE(6,*) DABS(XNOLD - X(N))
C
    Z = 0.0D0
    DO 50 I = 1, N
        WRITE(6,*) Z, X(I), Y(I)
        Z = Z + DZ
50 CONTINUE
C
    STOP
    END

```

## Subroutine Program

```
=====
SUBROUTINE TDMA ( PHI, A, B, C, D, N, P, Q )
C  =====
C
C THIS SUBROUTINE SOLVES A SYSTEM OF N LINEAR SIMULTANEOUS
C EQUATIONS
C HAVING A TRIDIAGONAL COEFFICIENT MATRIX.
C
C AHMET N. ERASLAN
C IOWA STATE UNIVERSITY
C AMES, IOWA 50011
C
C ARGUMENT LIST :
C -----
C N      : NUMBER OF SIMULTANEOUS EQUATIONS.
C
C PHI    : SOLUTION VECTOR
C
C A,B,C,D : COEFFICIENT VECTORS OF LENGTH N
C
C P,Q    : DUMMY VECTORS USED IN RECURRENCE RELATIONS
C
C INTEGER I, K, M, N, NL
C DOUBLE PRECISION A, B, C, D, DENOM, P, PHI, Q
C DIMENSION A(N), B(N), C(N), D(N), P(N), PHI(1), Q(N)
C
C EVALUATE P(1) & Q(1) :
C
C P(1) = B(1) / A(1)
C Q(1) = D(1) / A(1)
C
C USE RECURRENCE RELATIONS TO FIND P(I), Q(I), I = 2,3,...,N :
C
C DO 10 I = 2 , N
C   DENOM = 1.0 / (A(I) - C(I) * P(I-1))
C   P(I) = B(I) * DENOM
10  Q(I) = ( D(I) + C(I) * Q(I-1) ) * DENOM
C   PHI(N) = Q(N)
C
C BACK SUBSTITUTE P(I), Q(I), I = N-1,N-2,...,1 TO FIND PHI(N-1),
C PHI(N-2),...,PHI(1) :
C
C NL = N - 1
C DO 20 K = 1 , NL
C   M = N - K
20  PHI(M) = P(M) * PHI(M+1) + Q(M)
C   RETURN
C   END
```

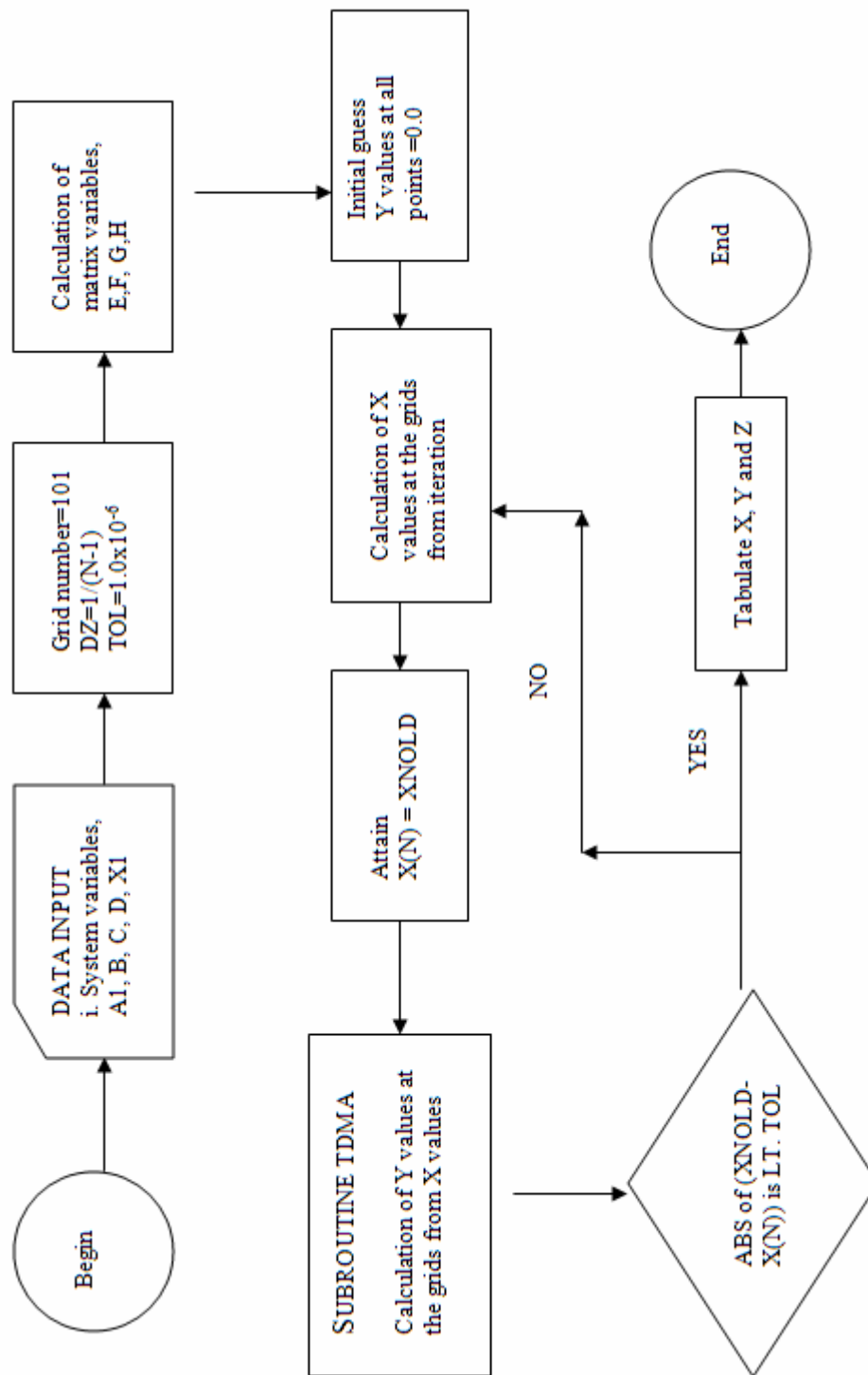


Figure G.1. The flowchart of the computer program for absorption of ozone.

## G.2 Dye ozonation experiments

The reaction of ozone with an organic molecule (dye) is described in a co-currently operated three phase reactor. First, gaseous ozone (x) is transferred to the liquid phase (y) by convection and axial dispersion. Then, in the liquid phase it reacts with the organic (p) according to the first order reaction with respect to both the dye and ozone concentrations. The equations describing the process at the steady state are:

$$\frac{Q_G}{A} \frac{dx}{dz} = -(k_L a)(bx - y) \quad (\text{G.16})$$

$$\frac{Q_L}{A} \frac{dy}{dz} = D_L \frac{d^2 y}{dz^2} + (k_L a)(bx - y) - k \cdot p \cdot y - k_D \cdot C_{OH}^n \cdot y \quad (\text{G.17})$$

$$\frac{Q_L}{A} \frac{dp}{dz} = D_L \frac{d^2 p}{dz^2} - r_s \cdot k \cdot p \cdot y \quad (\text{G.18})$$

The boundary conditions for the species are:

$$\begin{aligned} \text{at } z = 0, & \quad x = x_0, \quad y = 0, \quad p = p_0; \\ \text{at } z = H, & \quad \frac{dy}{dz} = 0, \quad \frac{dp}{dz} = 0 \end{aligned}$$

The solution of Equation (G.16) is the same applied in Section (G1.1.1).

### G.2.1 Solution of Equation (G.17)

$$D_L \frac{d^2 y}{dz^2} - \frac{Q_L}{A} \frac{dy}{dz} + (k_L a)(bx - y) - k \cdot p \cdot y - k_D \cdot C_{OH}^n \cdot y = 0 \quad (\text{G.19})$$

$$D_L \frac{d^2 y}{dz^2} - \frac{Q_L}{A} \frac{dy}{dz} - [(k_L a) + k \cdot p - k_D C_{OH}^n] y + (k_L a) \cdot b \cdot x = 0 \quad (\text{G.20})$$

$$\frac{d^2 y}{dz^2} + B \frac{dy}{dz} + \overline{Cl}(y) \cdot y = Dx \quad (\text{G.21})$$

where  $B = -\frac{Q_L}{S \cdot D_L}$ ,  $\overline{Cl}(y) = R + W \cdot p$  for  $R = \frac{-(k_L a) - k_D C_{OH}^n}{D_L}$  and

$$W = \frac{-k}{D_L}, D = -\frac{(k_L a)b}{D_L}$$

$$\frac{y_{i+1} - 2y_i + y_{i-1}}{(\Delta z)^2} + B \frac{y_{i+1} - y_{i-1}}{2\Delta z} + \overline{C1}(y) \cdot y_i = Dx_i \quad (G.22)$$

$$Ey_{i-1} + \overline{F1}(y) \cdot y_i + Gy_{i+1} = Dx_i \quad (G.23)$$

where  $E = \frac{1}{(\Delta z)^2} - \frac{B}{2\Delta z}$ ,  $\overline{F1}(y) = \overline{C1}(y) - \frac{2}{(\Delta z)^2}$  and  $G = \frac{1}{(\Delta z)^2} + \frac{B}{2\Delta z}$

At the boundary where  $i=N$ ,

$$\frac{y_{N+1} - y_{N-1}}{\Delta z} = 0 \quad (G.24)$$

$$\frac{y_{N-1} - 2y_N + y_{N+1}}{(\Delta z)^2} + B \frac{y_{N+1} - y_{N-1}}{2\Delta z} + \overline{C1}(y_N) \cdot y_N = Dx_N \quad (G.25)$$

$$\frac{y_{N-1} - 2y_N + y_{N+1}}{(\Delta z)^2} + \overline{C1}(y_N) \cdot y_N = Dx_N \quad (G.26)$$

$$Hy_{N-1} + \overline{F1}_N \cdot y_N = Dx_N \quad (G.27)$$

where  $H = \frac{2}{(\Delta z)^2}$  and  $\overline{F1}_N = \overline{C1}(y_N) - \frac{2}{(\Delta z)^2}$

### G.2.2 Solution of Equation (G.18)

$$\frac{Q_L}{S} \frac{dp}{dz} = D_L \frac{d^2 p}{dz^2} - r_s \cdot k \cdot p \cdot y \quad (G.28)$$

$$D_L \frac{d^2 p}{dz^2} - \frac{Q_L}{S} \frac{dp}{dz} - r_s \cdot k \cdot p \cdot y = 0 \quad (G.29)$$

$$\frac{d^2 p}{dz^2} + B \frac{dp}{dz} + \overline{C2}(y) \cdot p = 0 \quad (G.30)$$

where  $B = \frac{-Q_L}{S.D_L}$ ,  $\overline{C2}(y) = V.y$  for  $V = \frac{-r_s.k}{D_L}$

$$\frac{p_{i+1} - 2p_i + p_{i-1}}{(\Delta z)^2} + B \frac{p_{i+1} - p_{i-1}}{2\Delta z} + \overline{C1}(y).p_i = 0 \quad (G.31)$$

$$Ep_{i-1} + \overline{F2}(y).p_i + Gp_{i+1} = 0 \quad (G.32)$$

for  $E = \frac{1}{(\Delta z)^2} - \frac{B}{2\Delta z}$ ,  $\overline{F2}(y) = \overline{C2}(y) - \frac{2}{(\Delta z)^2}$  and  $G = \frac{1}{(\Delta z)^2} + \frac{B}{2\Delta z}$

At the boundary where  $i=N$ ,

$$\frac{p_{N+1} - p_{N-1}}{\Delta z} = 0 \quad (G.33)$$

$$\frac{p_{N-1} - 2p_N + p_{N+1}}{(\Delta z)^2} + B \frac{p_{N+1} - p_{N-1}}{2\Delta z} + \overline{C2}(y_N).p_N = 0 \quad (G.34)$$

$$\frac{2(p_{N-1} - p_N)}{(\Delta z)^2} + \overline{C12}(y_N).p_N = 0 \quad (G.35)$$

$$Hp_{N-1} + \overline{F2}_N.y_N = 0 \quad (G.36)$$

for  $H = \frac{2}{(\Delta z)^2}$ , and  $\overline{F2}_N = \overline{C2}(y_N) - \frac{2}{(\Delta z)^2}$

### G.2.3 Fortran program

```

PROGRAM MAIN_1
  IMPLICIT NONE
  INTEGER N, I, ITER
  PARAMETER ( N = 101 )
  DOUBLE PRECISION X, Y, DZ, A1, B, D, AA, BB, CC, DD, PDUMMY, Q, E,
  1      F, G, H, Z, XNOLD, TOL, R, W, V, C, P, PIN
  DIMENSION X(N), Y(N), AA(N), BB(N), CC(N), DD(N), PDUMMY(N), Q(N),
  1      P(N)
  DATA A1, B, D, X(1) / -11.219D0, -2.632D0, -10.333D0, 0.966D0 /
  DATA R, W / -29.524D0, -52.254D0 /

```

```

DATA V, PIN / -261.270D0, 0.0722D0 /
C
C... INITIALIZATION:
C
OPEN (6, FILE='RESULT.DAT')
DZ = 1.0D0 / (N - 1)
E = 1.0D0 / DZ**2 - B / (2.0*DZ)
G = 1.0 / DZ**2 + B / (2.0*DZ)
H = 2.0 / DZ**2
TOL = 1.0D-7
C
Z = 0.0D0
DO 10 I = 1, N
P(I) = -0.99*PIN*Z + PIN
Y(I) = 0.0D0
Z = Z + DZ
10 CONTINUE
XNOLD = 0.0D0
C
C... LEFT BC:
C
CC(1) = 0.0D0
AA(1) = 1.0D0
BB(1) = 0.0D0
C
C... INTERNAL GRIDS:
C
DO 20 I = 2, N-1
CC(I) = -E
BB(I) = -G
20 CONTINUE
C
C... RIGHT BC:
C
CC(N) = -H
BB(N) = 0.0D0
C
C... ITERATION SECTION:
C
DO 60 ITER = 1, 100
DO 30 I = 2, N
X(I) = (1.0D0 + A1*0.35*DZ) * X(I-1) - A1*DZ*Y(I-1)
30 CONTINUE
C
DD(1) = 0.0D0
DO 40 I = 2, N
C = R + W*P(I)
AA(I) = C - 2.0/DZ**2
DD(I) = D*X(I)
40 CONTINUE

```

```

CALL TDMA (Y, AA, BB, CC, DD, N, PDUMMY, Q)
C
DD(1) = PIN
DO 41 I = 2, N
  C = V*Y(I)
  AA(I) = C - 2.0/DZ**2
  DD(I) = 0.0D0
41 CONTINUE
C
CALL TDMA (P, AA, BB, CC, DD, N, PDUMMY, Q)
C
IF (DABS(XNOLD - X(N)) .LT. TOL) GOTO 70
  XNOLD = X(N)
60 CONTINUE
70 CONTINUE
C
  WRITE(6,*) ' ITER = ',ITER
  WRITE(6,*) DABS(XNOLD - X(N))
C
Z = 0.0D0
DO 50 I = 1, N
  WRITE(6,100) Z, X(I), Y(I), P(I)
  Z = Z + DZ
50 CONTINUE
C
STOP
100 FORMAT(4(2X,F16.6))
END

```

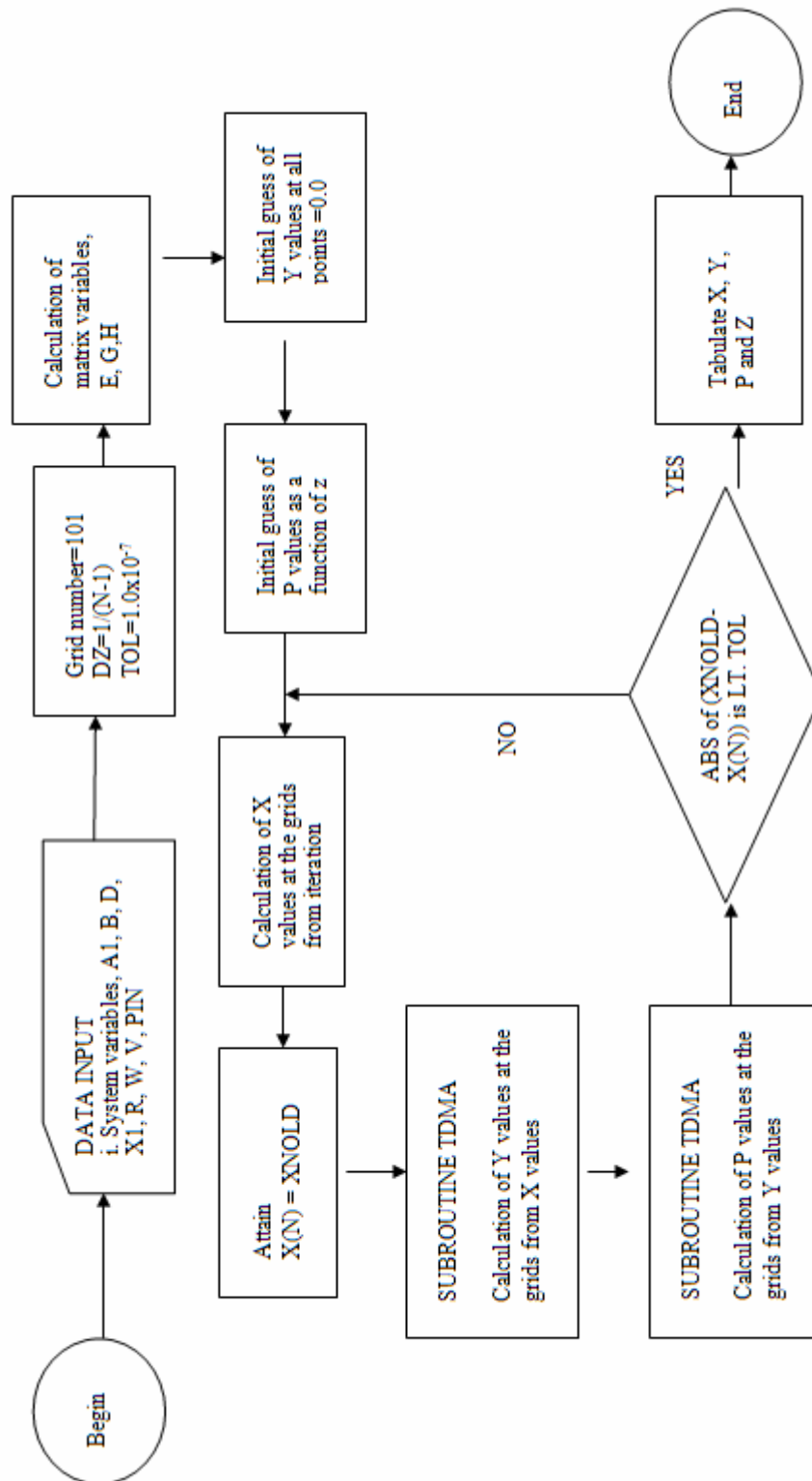


Figure G.2. The flowchart of the computer program for dye ozonation.

### G.3 Catalytic dye ozonation experiments

In the liquid phase, in addition to the terms of mass transfer from gas to liquid phase, axial dispersion, chemical reaction and ozone decomposition, the term of mass transfer from liquid to solid phase was added to the equations [Eqns. (3.50) and (3.51)]. The equations describing the process at the steady state are:

$$\frac{Q_G}{A} \frac{dx}{dz} = -(k_L a)(bx - y) \quad (\text{G.37})$$

$$\frac{Q_L}{A} \frac{dy}{dz} = D_L \frac{d^2 y}{dz^2} + (k_L a)(bx - y) - k_p \cdot y - k_D \cdot C_{OH}^n y - M1 \cdot y \quad (\text{G.38})$$

$$\frac{Q_L}{A} \frac{dp}{dz} = D_L \frac{d^2 p}{dz^2} - r_s \cdot k_p \cdot y - r_s \cdot M1 \cdot y \quad (\text{G.39})$$

where  $M1 = \frac{1}{\frac{1}{k_R' m} + \frac{1}{k_s a_s m}}$ .

The boundary conditions for the species are:

$$\text{at } z = 0, \quad x = x_0, \quad y = 0, \quad p = p_0;$$

$$\text{at } z = H, \quad \frac{dy}{dz} = 0, \quad \frac{dp}{dz} = 0$$

The solution of Equation (G.37) is the same applied in Section (G1.1.1).

#### G.3.1 Solution of Equation (G.38)

$$D_L \frac{d^2 y}{dz^2} - \frac{Q_L}{A} \frac{dy}{dz} + (k_L a)(bx - y) - k_p \cdot y - k_D \cdot C_{OH}^n y - M1 \cdot y = 0 \quad (\text{G.40})$$

$$D_L \frac{d^2 y}{dz^2} - \frac{Q_L}{A} \frac{dy}{dz} - [(k_L a) + k_p - k_D C_{OH}^n - M1]y + (k_L a)bx = 0 \quad (\text{G.41})$$

$$\frac{d^2 y}{dz^2} + B \frac{dy}{dz} + \overline{CC}(y) \cdot y = Dx \quad (\text{G.42})$$

where  $B = -\frac{Q_L}{S.D_L}$ ,  $\overline{C3}(y) = R1 + W.p$  for  $R1 = \frac{-(k_L a) - k_D C_{OH}^n - M1}{D_L}$  and

$$W = \frac{-k}{D_L}, D = -\frac{(k_L a)b}{D_L}$$

$$\frac{y_{i+1} - 2y_i + y_{i-1}}{(\Delta z)^2} + B \frac{y_{i+1} - y_{i-1}}{2\Delta z} + \overline{C3}(y).y_i = Dx_i \quad (G.43)$$

$$Ey_{i-1} + \overline{F3}(y).y_i + Gy_{i+1} = Dx_i \quad (G.44)$$

where  $E = \frac{1}{(\Delta z)^2} - \frac{B}{2\Delta z}$ ,  $\overline{F3}(y) = \overline{C3}(y) - \frac{2}{(\Delta z)^2}$  and  $G = \frac{1}{(\Delta z)^2} + \frac{B}{2\Delta z}$

At the boundary where  $i=N$ ,

$$\frac{y_{N+1} - y_{N-1}}{\Delta z} = 0 \quad (G.45)$$

$$\frac{y_{N-1} - 2y_N + y_{N+1}}{(\Delta z)^2} + B \frac{y_{N+1} - y_{N-1}}{2\Delta z} + \overline{C3}(y_N).y_N = Dx_N \quad (G.46)$$

$$\frac{y_{N-1} - 2y_N + y_{N+1}}{(\Delta z)^2} + \overline{C3}(y_N).y_N = Dx_N \quad (G.47)$$

$$Hy_{N-1} + \overline{F3}_N.y_N = Dx_N \quad (G.48)$$

where  $H = \frac{2}{(\Delta z)^2}$  and  $\overline{F3}_N = \overline{C3}(y_N) - \frac{2}{(\Delta z)^2}$

### G.3.2 Solution of Equation (G.39)

$$\frac{Q_L}{A} \frac{dp}{dz} = D_L \frac{d^2 p}{dz^2} - r_s.k.p.y - r_s.M1.y \quad (G.49)$$

$$D_L \frac{d^2 p}{dz^2} - \frac{Q_L}{S} \frac{dp}{dz} - r_s \cdot k \cdot p \cdot y - r_s \cdot M1 \cdot y = 0 \quad (G.50)$$

$$\frac{d^2 p}{dz^2} + B \frac{dp}{dz} + \overline{C2}(y) \cdot p - r_s \cdot M1 \cdot y = 0 \quad (G.51)$$

where  $B = \frac{-Q_L}{S \cdot D_L}$ ,  $\overline{C2}(y) = V \cdot y$  for  $V = \frac{-r_s \cdot k}{D_L}$

$$\frac{p_{i+1} - 2p_i + p_{i-1}}{(\Delta z)^2} + B \frac{p_{i+1} - p_{i-1}}{2\Delta z} + \overline{C2}(y) \cdot p_i - r_s \cdot M1 \cdot y_i = 0 \quad (G.52)$$

$$E p_{i-1} + \overline{F2}(y) \cdot p_i + G p_{i+1} = r_s \cdot M1 \cdot y_i \quad (G.53)$$

for  $E = \frac{1}{(\Delta z)^2} - \frac{B}{2\Delta z}$ ,  $\overline{F2}(y) = \overline{C2}(y) - \frac{2}{(\Delta z)^2}$  and  $G = \frac{1}{(\Delta z)^2} + \frac{B}{2\Delta z}$

At the boundary where  $i=N$ ,

$$\frac{p_{N+1} - p_{N-1}}{\Delta z} = 0 \quad (G.54)$$

$$\frac{p_{N-1} - 2p_N + p_{N+1}}{(\Delta z)^2} + B \frac{p_{N+1} - p_{N-1}}{2\Delta z} + \overline{C2}(y_N) \cdot p_N = r_s \cdot M1 \cdot y_N \quad (G.55)$$

$$\frac{2(p_{N-1} - p_N)}{(\Delta z)^2} + \overline{C2}(y_N) \cdot p_N = r_s \cdot M1 \cdot y_N \quad (G.56)$$

$$H p_{N-1} + \overline{F2}_N \cdot y_N = r_s \cdot M1 \cdot y_N \quad (G.57)$$

for  $H = \frac{2}{(\Delta z)^2}$ , and  $\overline{F2}_N = \overline{C2}(y_N) - \frac{2}{(\Delta z)^2}$

### G.3.3 Fortran program

```
PROGRAM MAIN_1
  IMPLICIT NONE
  INTEGER N, I, ITER
  PARAMETER ( N = 101 )
```

```

DOUBLE PRECISION X, Y, DZ, A1, B, D, AA, BB, CC, DD, PDUMMY, Q, E,
1      F, G, H, Z, XNOLD, TOL, R1, W, V, C, P, PIN, M1
DIMENSION X(N), Y(N), AA(N), BB(N), CC(N), DD(N), PDUMMY(N), Q(N),
1      P(N)
      DATA A1, B, D, X(1) / -11.219D0, -2.632D0, -10.333D0, 0.966D0 /
      DATA R1, W, RS / -29.524D0, -52.254D0, 0.1D0 /
      DATA V, PIN, M1 / -261.270D0, 0.0722D0, 0.0678D0 /
C
C... INITIALIZATION:
C
      OPEN (6, FILE='RESULT.DAT')
      DZ = 1.0D0 / (N - 1)
      E = 1.0D0 / DZ**2 - B / (2.0*DZ)
      G = 1.0 / DZ**2 + B / (2.0*DZ)
      H = 2.0 / DZ**2
      TOL = 1.0D-7
C
      Z = 0.0D0
      DO 10 I = 1, N
      P(I) = -0.99*PIN*Z + PIN
      Y(I) = 0.0D0
      Z = Z + DZ
10 CONTINUE
      XNOLD = 0.0D0
C
C... LEFT BC:
C
      CC(1) = 0.0D0
      AA(1) = 1.0D0
      BB(1) = 0.0D0
C
C... INTERNAL GRIDS:
C
      DO 20 I = 2, N-1
      CC(I) = -E
      BB(I) = -G
20 CONTINUE
C
C... RIGHT BC:
C
      CC(N) = -H
      BB(N) = 0.0D0
C
C... ITERATION SECTION:
C
      DO 60 ITER = 1, 100
      DO 30 I = 2, N
      X(I) = (1.0D0 + A1*0.35*DZ) * X(I-1) - A1*DZ*Y(I-1)
30 CONTINUE
C

```

```

DD(1) = 0.0D0
DO 40 I = 2, N
    C = R1 + W*P(I)
    AA(I) = C - 2.0/DZ**2
    DD(I) = D*X(I)
40 CONTINUE
CALL TDMA (Y, AA, BB, CC, DD, N, PDUMMY, Q)
C
DD(1) = PIN
DO 41 I = 2, N
    C = V*Y(I)
    AA(I) = C - 2.0/DZ**2
    DD(I) = RS*M1*Y(I)
41 CONTINUE
C
CALL TDMA (P, AA, BB, CC, DD, N, PDUMMY, Q)
C
IF (DABS(XNOLD - X(N)) .LT. TOL) GOTO 70
    XNOLD = X(N)
60 CONTINUE
70 CONTINUE
C
    WRITE(6,*) ' ITER = ',ITER
    WRITE(6,*) DABS(XNOLD - X(N))
C
Z = 0.0D0
DO 50 I = 1, N
    WRITE(6,100) Z, X(I), Y(I), P(I)
    Z = Z + DZ
50 CONTINUE
C
STOP
101 FORMAT(4(2X,F16.6))
END

```

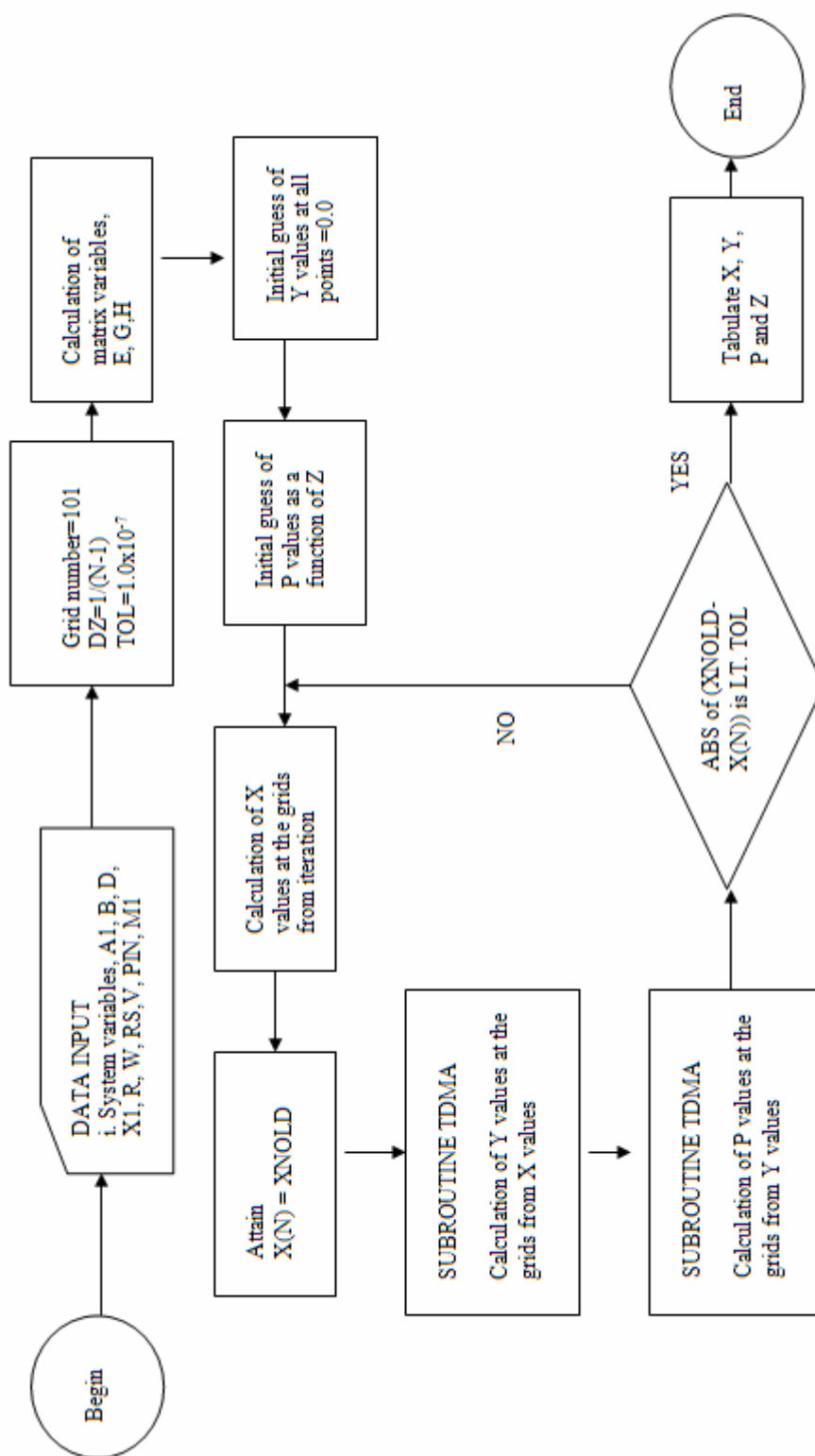


Figure G.3. The flowchart of the computer program for catalytic dye ozonation.

## APPENDIX H

### MODELING GRAPHS

#### H.1 Ozone absorption graphs

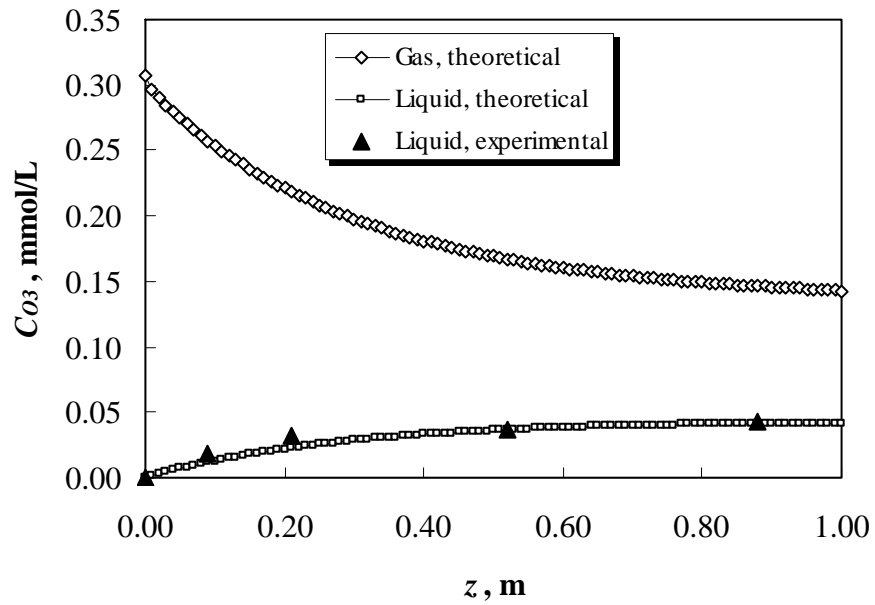


Figure H.1. The comparison of theoretical and experimental steady state liquid phase ozone concentrations for the best fit of  $D_L$  and  $k_L a$  values. Conditions:  $Q_G = 45$  L/h,  $Q_L = 30$  L/h,  $T = 23^\circ\text{C}$ ,  $C_{O_3,G,in} = 0.307$  mmol  $\text{O}_3/\text{L}$  gas, catalyst = no,  $D_L = 3.1 \times 10^{-3}$   $\text{m}^2/\text{s}$ ,  $k_L a = 4.2 \times 10^{-2}$   $\text{s}^{-1}$ .

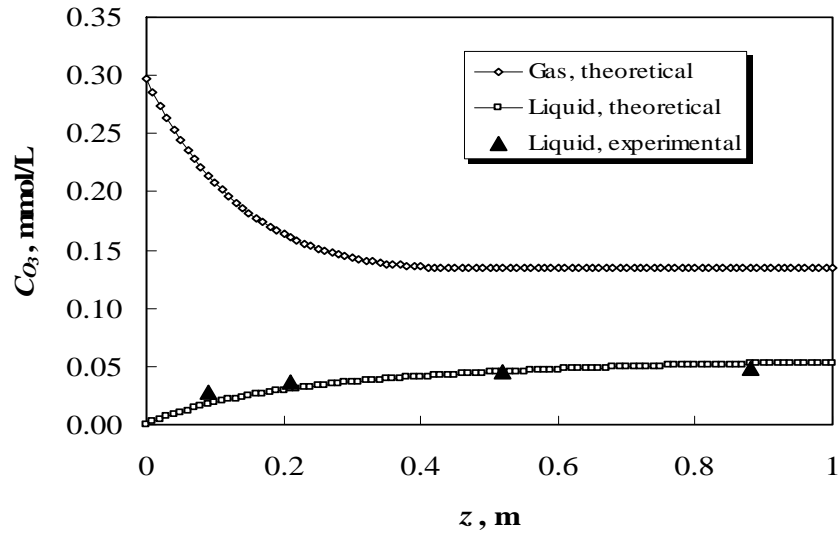


Figure H.2. The comparison of theoretical and experimental steady state liquid phase ozone concentrations for the best fit of  $D_L$  and  $k_L a$  values. Conditions:  $Q_G = 70$  L/h,  $Q_L = 30$  L/h,  $T = 23^\circ\text{C}$ ,  $C_{O_3,G,in} = 0.297$  mmol  $\text{O}_3/\text{L}$  gas, catalyst = no,  $D_L = 3.6 \times 10^{-3}$   $\text{m}^2/\text{s}$ ,  $k_L a = 4.8 \times 10^{-2}$   $\text{s}^{-1}$ .

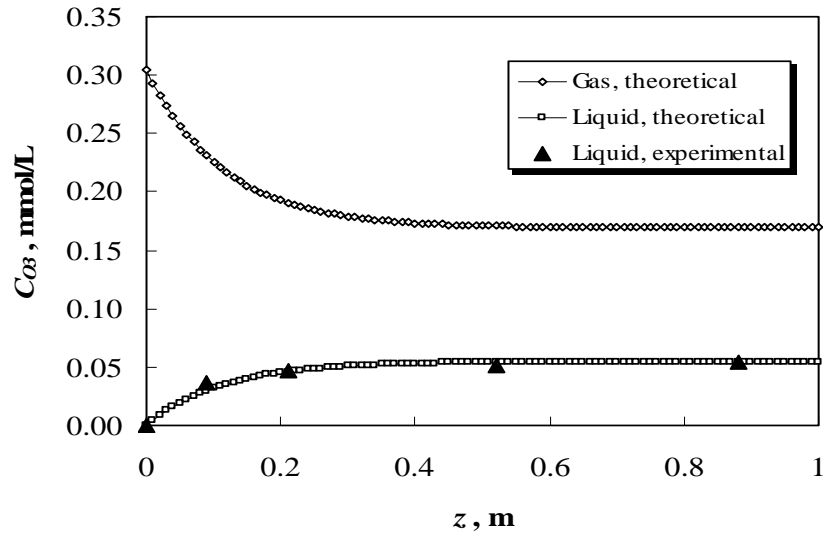


Figure H.3. The comparison of theoretical and experimental steady state liquid phase ozone concentrations for the best fit of  $D_L$  and  $k_L a$  values. Conditions:  $Q_G = 100$  L/h,  $Q_L = 30$  L/h,  $T = 23^\circ\text{C}$ ,  $C_{O_3,G,in} = 0.304$  mmol  $\text{O}_3/\text{L}$  gas, catalyst = no,  $D_L = 1.3 \times 10^{-3}$   $\text{m}^2/\text{s}$ ,  $k_L a = 6.4 \times 10^{-2}$   $\text{s}^{-1}$ .

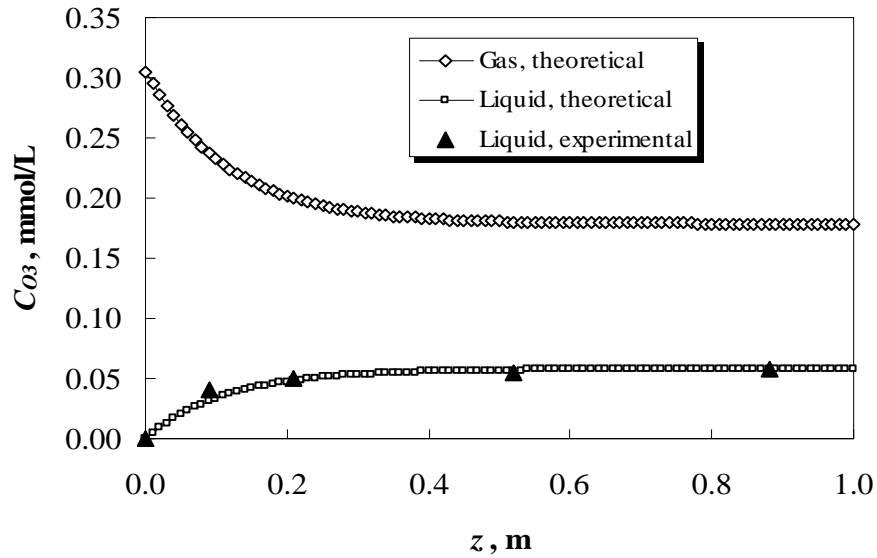


Figure H.4. The comparison of theoretical and experimental steady state liquid phase ozone concentrations for the best fit of  $D_L$  and  $k_L a$  values. Conditions:  $Q_G = 125$  L/h,  $Q_L = 30$  L/h,  $T = 23^\circ\text{C}$ ,  $C_{O_3,G,in} = 0.305$  mmol  $\text{O}_3/\text{L}$  gas, catalyst = no,  $D_L = 1.5 \times 10^{-3}$   $\text{m}^2/\text{s}$ ,  $k_L a = 7.3 \times 10^{-2}$   $\text{s}^{-1}$ .

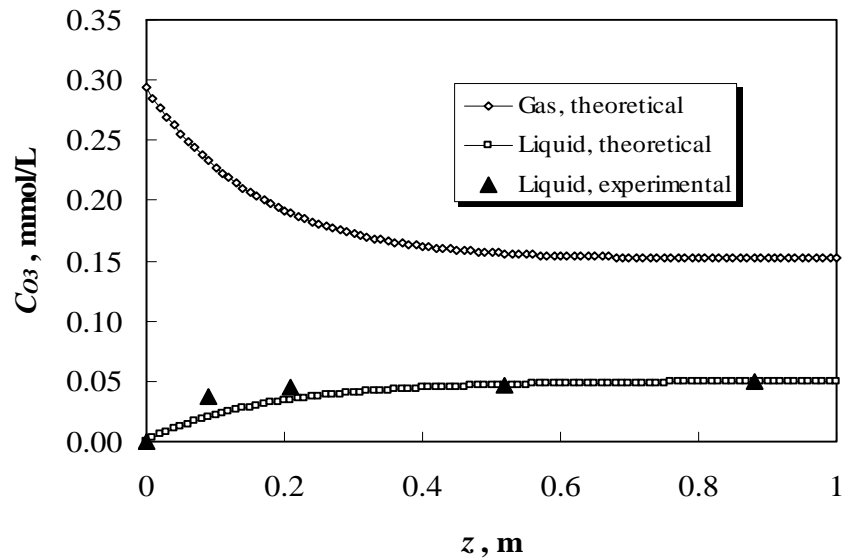


Figure H.5. The comparison of theoretical and experimental steady state liquid phase ozone concentrations for the best fit of  $D_L$  and  $k_L a$  values. Conditions:  $Q_G = 100$  L/h,  $Q_L = 110$  L/h,  $T = 23^\circ\text{C}$ ,  $C_{O_3,G,in} = 0.294$  mmol  $\text{O}_3/\text{L}$  gas, catalyst = no,  $D_L = 1.8 \times 10^{-3}$   $\text{m}^2/\text{s}$ ,  $k_L a = 5.0 \times 10^{-2}$   $\text{s}^{-1}$ .

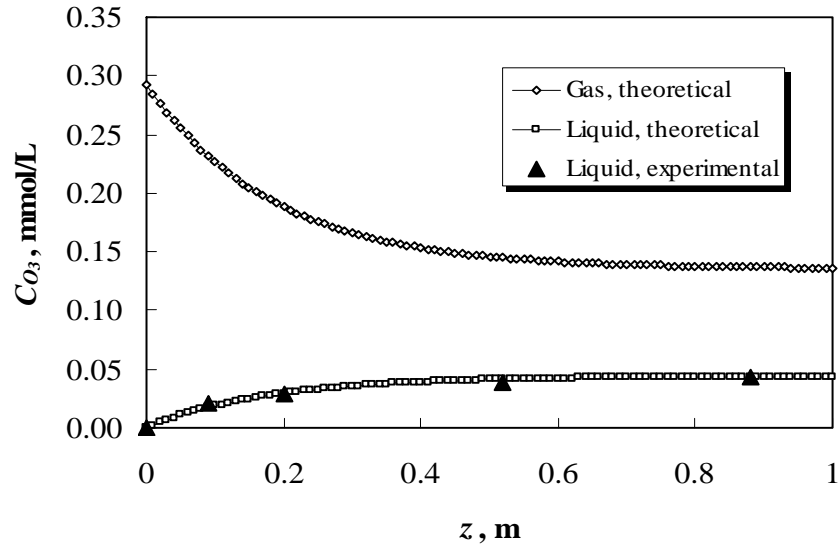


Figure H.6. The comparison of theoretical and experimental steady state liquid phase ozone concentrations for the best fit of  $D_L$  and  $k_L a$  values. Conditions:  $Q_G = 100$  L/h,  $Q_L = 150$  L/h,  $T = 23^\circ\text{C}$ ,  $C_{O_3,G,in} = 0.293$  mmol  $\text{O}_3/\text{L}$  gas, catalyst = no,  $D_L = 2.0 \times 10^{-3}$   $\text{m}^2/\text{s}$ ,  $k_L a = 4.9 \times 10^{-2}$   $\text{s}^{-1}$ .

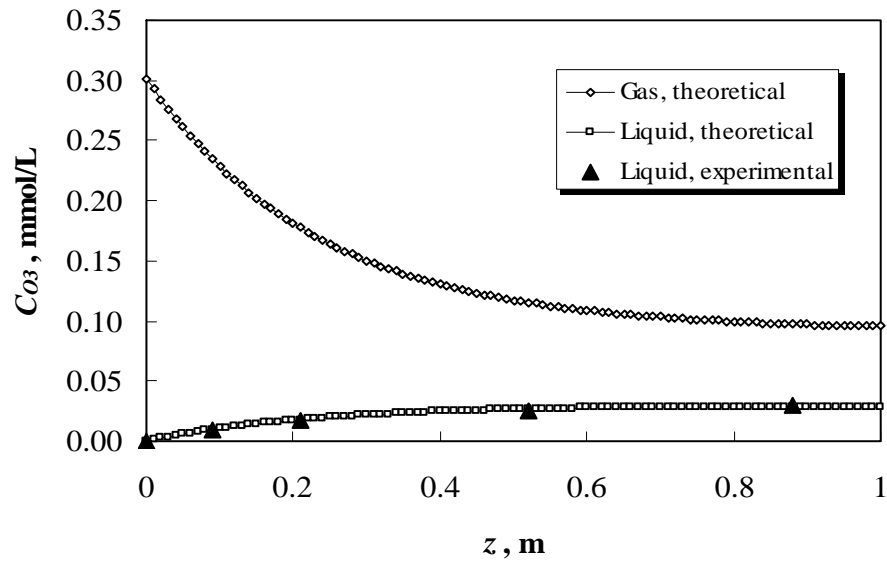


Figure H.7. The comparison of theoretical and experimental steady state liquid phase ozone concentrations for the best fit of  $D_L$  and  $k_L a$  values. Conditions:  $Q_G = 100$  L/h,  $Q_L = 200$  L/h,  $T = 23^\circ\text{C}$ ,  $C_{O_3,G,in} = 0.293$  mmol  $\text{O}_3/\text{L}$  gas, catalyst = no,  $D_L = 6.1 \times 10^{-3}$   $\text{m}^2/\text{s}$ ,  $k_L a = 5.0 \times 10^{-2}$   $\text{s}^{-1}$ .

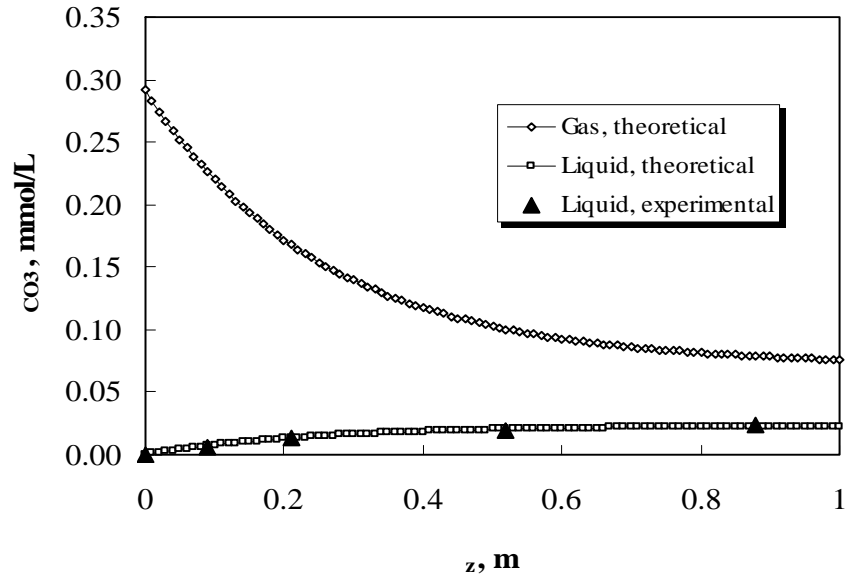


Figure H.8. The comparison of theoretical and experimental steady state liquid phase ozone concentrations for the best fit of  $D_L$  and  $k_L a$  values. Conditions:  $Q_G = 100$  L/h,  $Q_L = 250$  L/h,  $T = 23^\circ\text{C}$ ,  $C_{O_3,G,in} = 0.291$  mmol  $\text{O}_3/\text{L}$  gas, catalyst = no,  $D_L = 9.2 \times 10^{-3}$   $\text{m}^2/\text{s}$ ,  $k_L a = 4.9 \times 10^{-2}$   $\text{s}^{-1}$ .

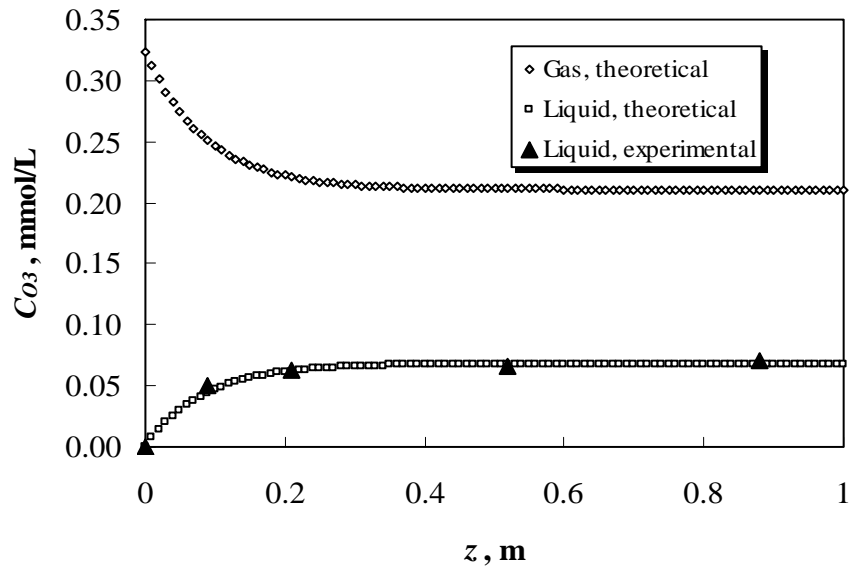


Figure H.9. The comparison of theoretical and experimental steady state liquid phase ozone concentrations for the best fit of  $D_L$  and  $k_L a$  values. Conditions:  $Q_G = 150$  L/h,  $Q_L = 30$  L/h,  $T = 23^\circ\text{C}$ ,  $C_{O_3,G,in} = 0.324$  mmol  $\text{O}_3/\text{L}$  gas, catalyst = alumina,  $m_{cat} = 25$  g,  $D_L = 0.98 \times 10^{-3}$   $\text{m}^2/\text{s}$ ,  $k_L a = 9.8 \times 10^{-2}$   $\text{s}^{-1}$ .

## H.2 Dye ozonation graphs

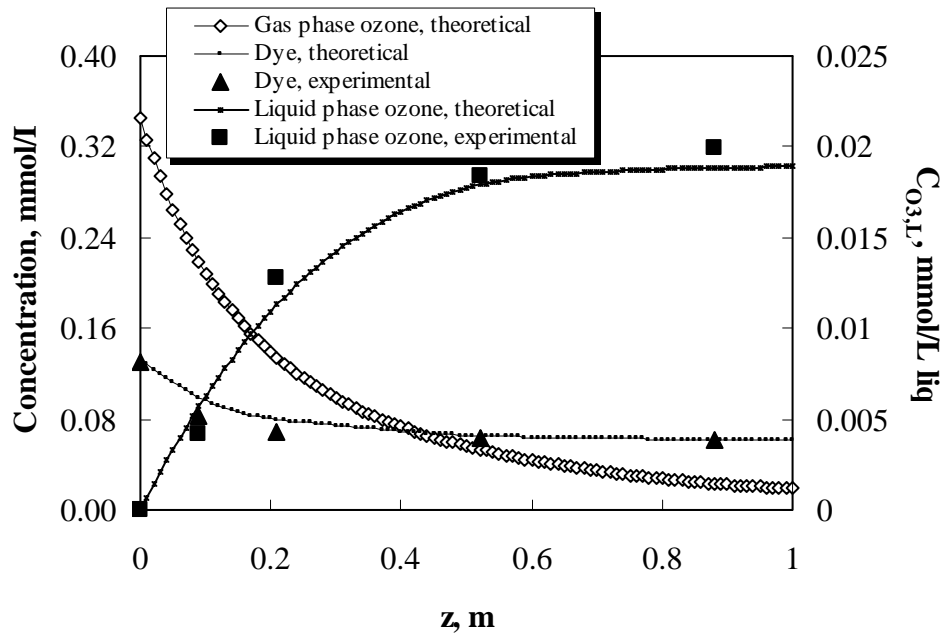


Figure H.10. The comparison of theoretical and experimental steady state liquid phase ozone and dye concentrations for the best fit of  $D_L$  and  $k_L a$  values. Conditions:  $Q_G = 70$  L/h,  $Q_L = 30$  L/h, Dye = AR-151,  $C_{D,in} = 13.1 \times 10^{-2}$  mmol/L,  $T = 23^\circ\text{C}$ ,  $C_{O_3,G,in} = 0.345$  mmol  $\text{O}_3/\text{L}$  gas, no catalyst,  $D_L = 3.2 \times 10^{-3}$   $\text{m}^2/\text{s}$ ,  $k_L a = 6.0 \times 10^{-2}$   $\text{s}^{-1}$ .

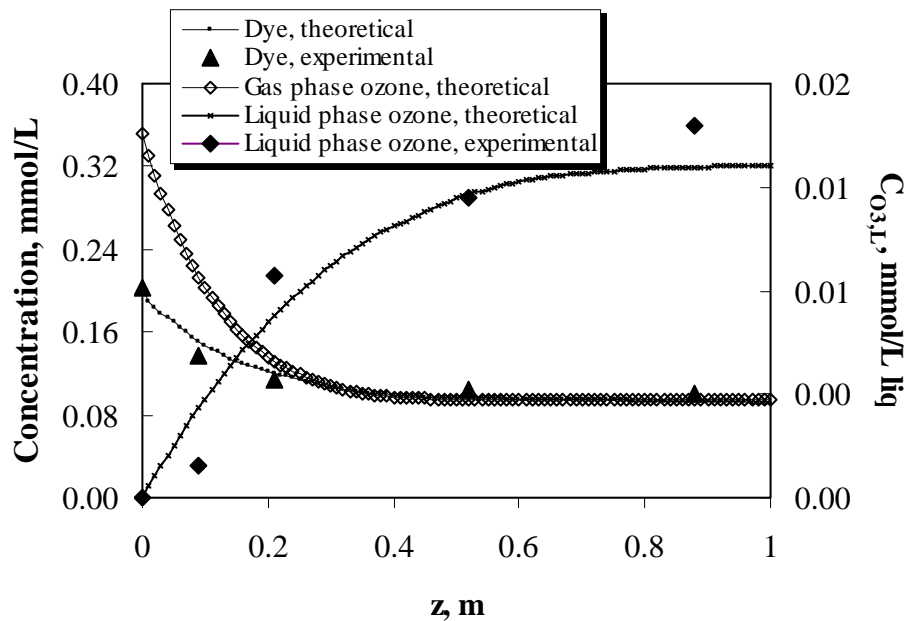


Figure H.11. The comparison of theoretical and experimental steady state liquid phase ozone and dye concentrations for the best fit of  $D_L$  and  $k_L a$  values. Conditions:  $Q_G = 70$  L/h,  $Q_L = 30$  L/h, Dye = AR-151,  $C_{D,in} = 20.2 \times 10^{-2}$  mmol/L,  $T = 23^\circ\text{C}$ ,  $C_{O_3,G,in} = 0.351$  mmol  $\text{O}_3/\text{L}$  gas, no catalyst,  $D_L = 3.7 \times 10^{-3}$   $\text{m}^2/\text{s}$ ,  $k_L a = 6.4 \times 10^{-2}$   $\text{s}^{-1}$ .

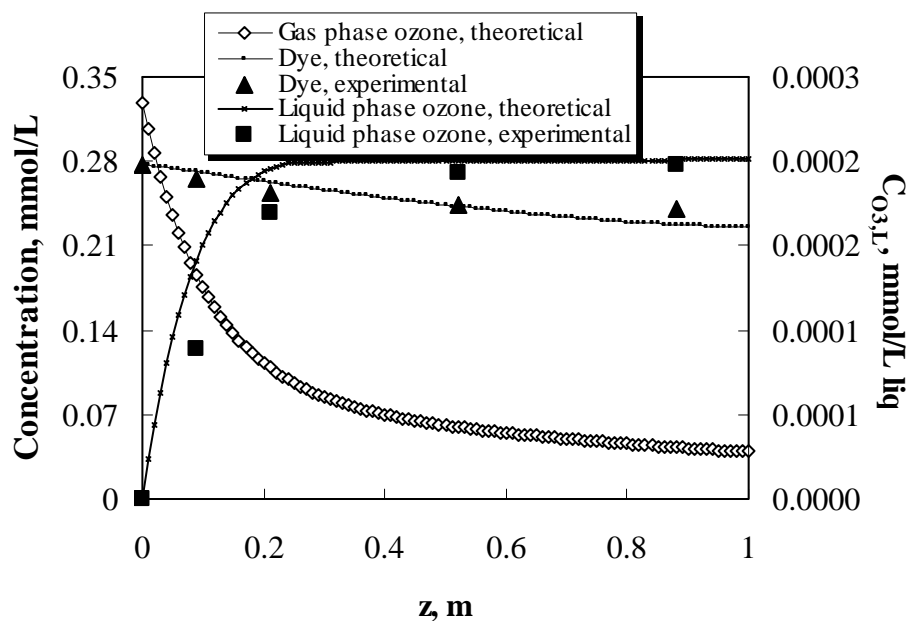


Figure H.12. The comparison of theoretical and experimental steady state liquid phase ozone and dye concentrations for the best fit of  $D_L$  and  $k_L a$  values. Conditions:  $Q_G = 70$  L/h,  $Q_L = 250$  L/h, Dye = AR-151,  $C_{D,in} = 27.7 \times 10^{-2}$  mmol/L,  $T = 23^\circ\text{C}$ ,  $C_{O_3,G,in} = 0.329$  mmol  $\text{O}_3/\text{L}$  gas, no catalyst,  $D_L = 6.7 \times 10^{-3}$   $\text{m}^2/\text{s}$ ,  $k_L a = 2.2 \times 10^{-2}$   $\text{s}^{-1}$ .

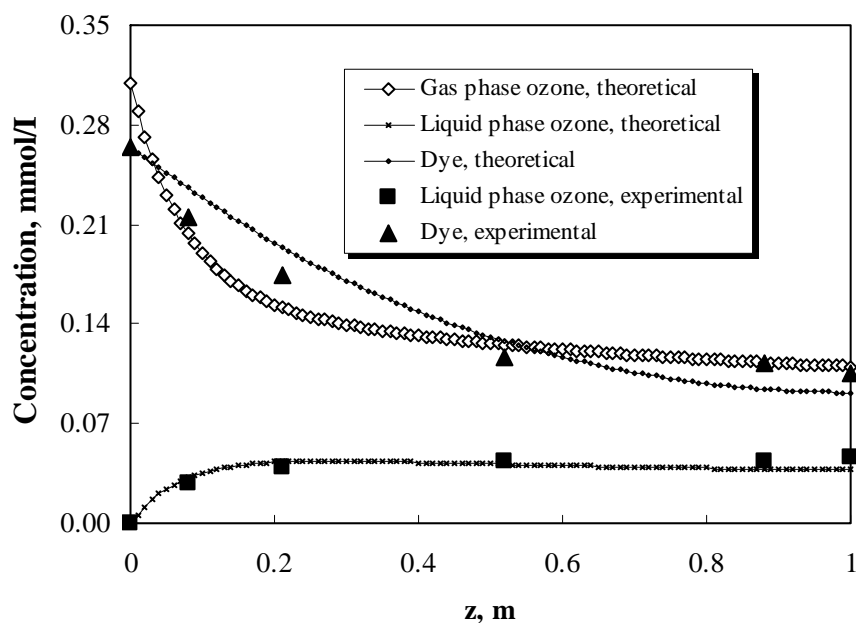


Figure H.13. The comparison of theoretical and experimental steady state liquid phase ozone and dye concentrations for the best fit of  $D_L$  and  $k_L a$  values. Conditions:  $Q_G = 150$  L/h,  $Q_L = 30$  L/h, Dye = AR-151,  $C_{D,in} = 26.4 \times 10^{-2}$  mmol/L,  $T = 23^\circ\text{C}$ ,  $C_{O_3,G,in} = 0.308$  mmol  $\text{O}_3/\text{L}$  gas, no catalyst,  $D_L = 1.0 \times 10^{-3}$   $\text{m}^2/\text{s}$ ,  $k_L a = 15.2 \times 10^{-2}$   $\text{s}^{-1}$ .

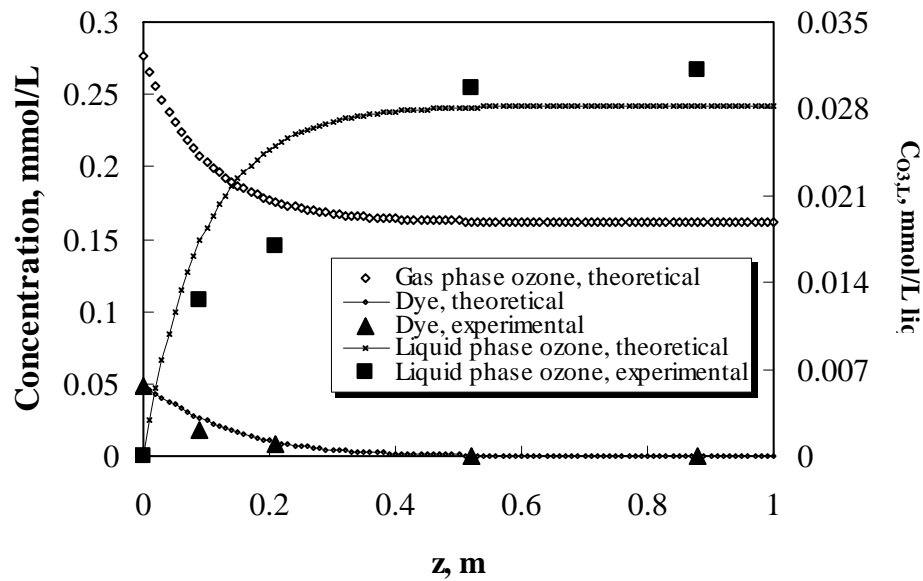


Figure H.14. The comparison of theoretical and experimental steady state liquid phase ozone and dye concentrations for the best fit of  $D_L$  and  $k_L a$  values. Conditions:  $Q_G = 150$  L/h,  $Q_L = 30$  L/h, Dye = *RBBR*,  $C_{D,in} = 4.9 \times 10^{-2}$  mmol/L,  $T = 23^\circ\text{C}$ ,  $C_{O_3,G,in} = 0.277$  mmol  $\text{O}_3$ /L gas, no catalyst,  $D_L = 1.2 \times 10^{-3}$   $\text{m}^2/\text{s}$ ,  $k_L a = 9.6 \times 10^{-2}$   $\text{s}^{-1}$ .

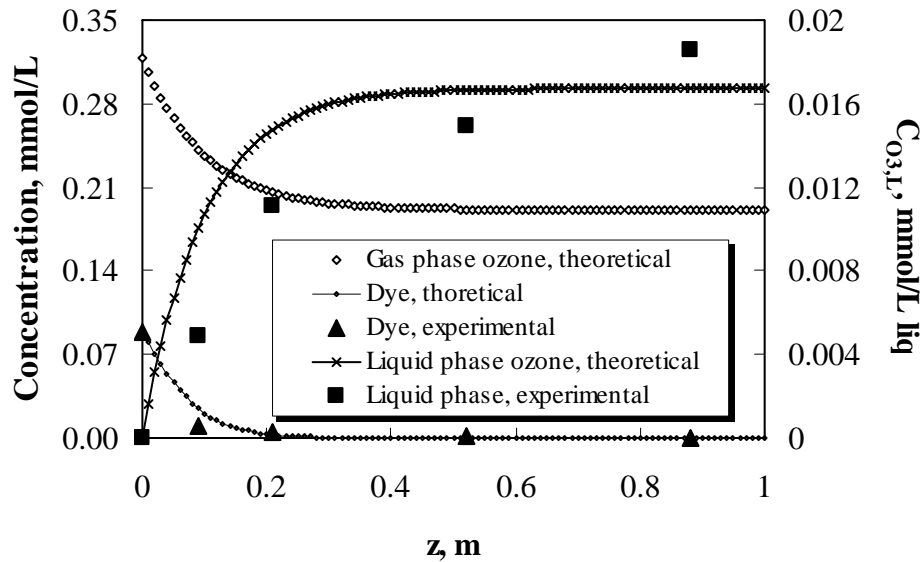


Figure H.15. The comparison of theoretical and experimental steady state liquid phase ozone and dye concentrations for the best fit of  $D_L$  and  $k_L a$  values. Conditions:  $Q_G = 150$  L/h,  $Q_L = 30$  L/h, Dye = *RBBR*,  $C_{D,in} = 8.9 \times 10^{-2}$  mmol/L,  $T = 23^\circ\text{C}$ ,  $C_{O_3,G,in} = 0.319$  mmol  $\text{O}_3$ /L gas, no catalyst,  $D_L = 1.2 \times 10^{-3}$   $\text{m}^2/\text{s}$ ,  $k_L a = 9.8 \times 10^{-2}$   $\text{s}^{-1}$ .

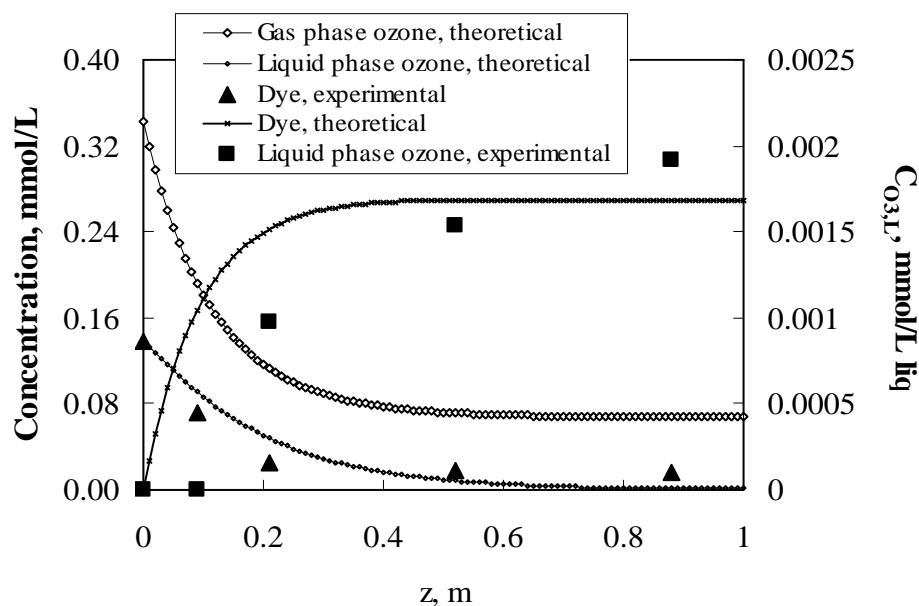


Figure H.16. The comparison of theoretical and experimental steady state liquid phase ozone and dye concentrations for the best fit of  $D_L$  and  $k_L a$  values. Conditions:  $Q_G = 70$  L/h,  $Q_L = 30$  L/h, Dye = *RBBR*,  $C_{D,in} = 13.9 \times 10^{-2}$  mmol/L,  $T = 23^\circ\text{C}$ ,  $C_{O_3,G,in} = 0.343$  mmol  $\text{O}_3/\text{L}$  gas, no catalyst,  $D_L = 3.6 \times 10^{-3}$   $\text{m}^2/\text{s}$ ,  $k_L a = 5.8 \times 10^{-2}$   $\text{s}^{-1}$ .

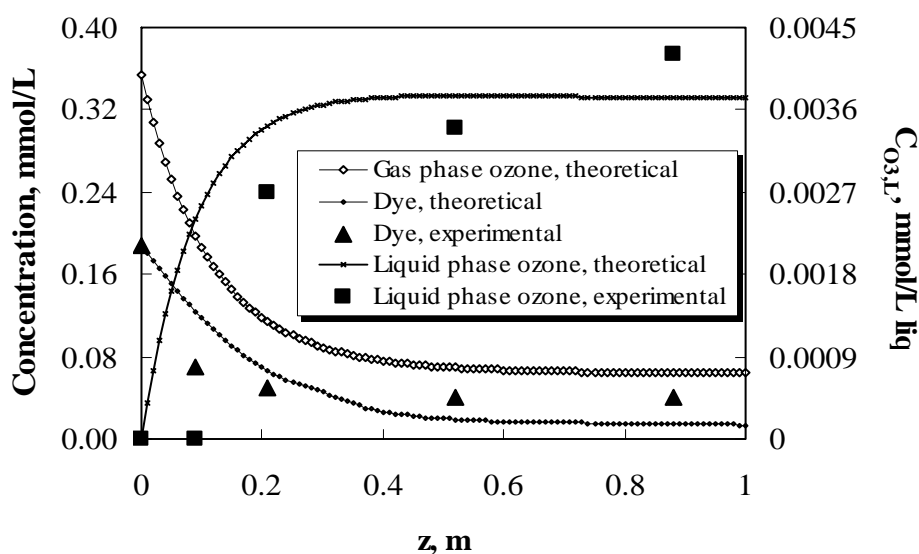


Figure H.17. The comparison of theoretical and experimental steady state liquid phase ozone and dye concentrations for the best fit of  $D_L$  and  $k_L a$  values. Conditions:  $Q_G = 70$  L/h,  $Q_L = 30$  L/h, Dye = *RBBR*,  $C_{D,in} = 18.8 \times 10^{-2}$  mmol/L,  $T = 23^\circ\text{C}$ ,  $C_{O_3,G,in} = 0.354$  mmol  $\text{O}_3/\text{L}$  gas, no catalyst,  $D_L = 3.2 \times 10^{-3}$   $\text{m}^2/\text{s}$ ,  $k_L a = 7.6 \times 10^{-2}$   $\text{s}^{-1}$ .

## APPENDIX I

### BUBBLE AND CATALYST PROPERTIES

#### I.1 Bubble size graphs



Figure I.1. The bubble behaviour in FBR at  $Q_G = 70$  L/h,  $Q_L = 150$  L/h, around the gas distributor. Mean size bubble diameter = 1.74 mm.



Figure I.2. The bubble behaviour in FBR at  $Q_G = 70$  L/h,  $Q_L = 150$  L/h, in the middle of the column. Mean size bubble diameter = 2.19 mm.



Figure I.3. The bubble behaviour in FBR at  $Q_G = 70$  L/h,  $Q_L = 150$  L/h, on the top of the column. Mean size bubble diameter = 2.73 mm.

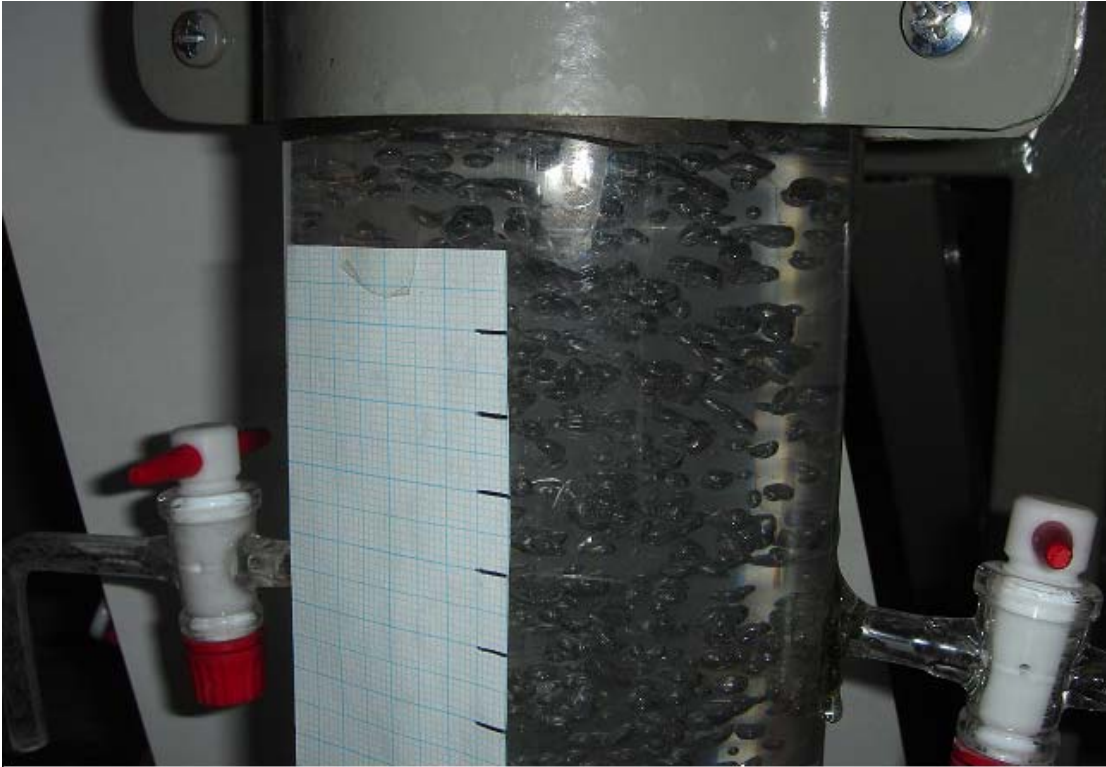


Figure I.4. The bubble behaviour in FBR at  $Q_G = 150$  L/h,  $Q_L = 150$  L/h, around the gas distributor. Mean size bubble diameter = 2.16 mm.



Figure I.5. The bubble behaviour in FBR at  $Q_G = 150$  L/h,  $Q_L = 150$  L/h, in the middle of the column. Mean size bubble diameter = 2.63 mm.



Figure I.6. The bubble behaviour in FBR at  $Q_G = 150$  L/h,  $Q_L = 150$  L/h, on the top of the column. Mean size bubble diameter = 2.79 mm.



Figure I.7. The bubble behaviour in FBR at  $Q_G = 150$  L/h,  $Q_L = 250$  L/h, around the gas distributor. Mean size bubble diameter = 1.85 mm.



Figure I.8. The bubble behaviour in FBR at  $Q_G = 150$  L/h,  $Q_L = 250$  L/h, in the middle of the column. Mean size bubble diameter = 2.31 mm.



Figure I.9. The bubble behaviour in FBR at  $Q_G = 150$  L/h,  $Q_L = 250$  L/h, on the top of the column. Mean size bubble diameter = 2.47 mm.

## I.2 Thermogravimetric Analysis (TGA) graphs

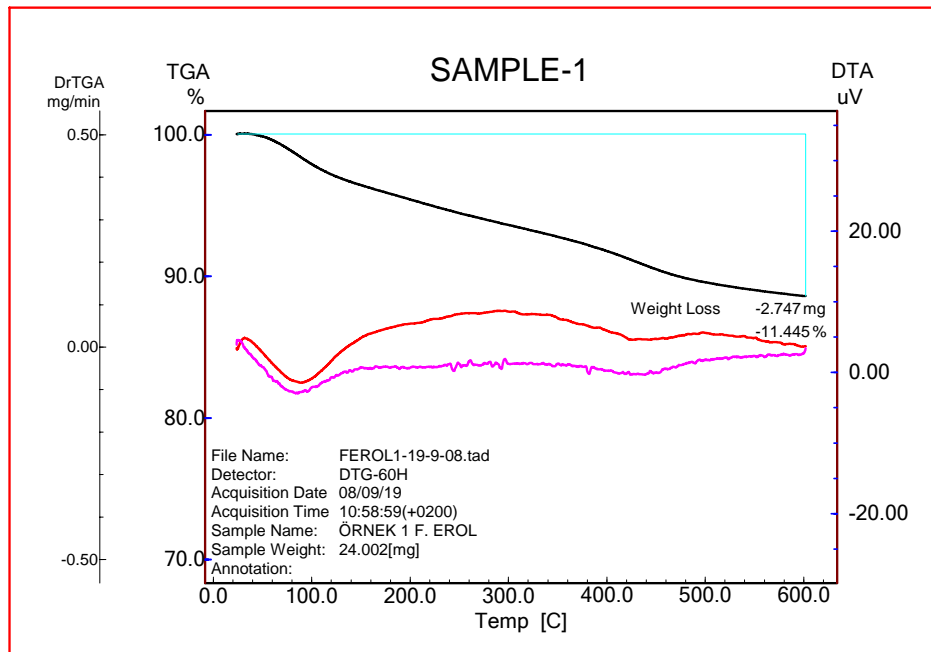


Figure I.10. TGA of alumina.

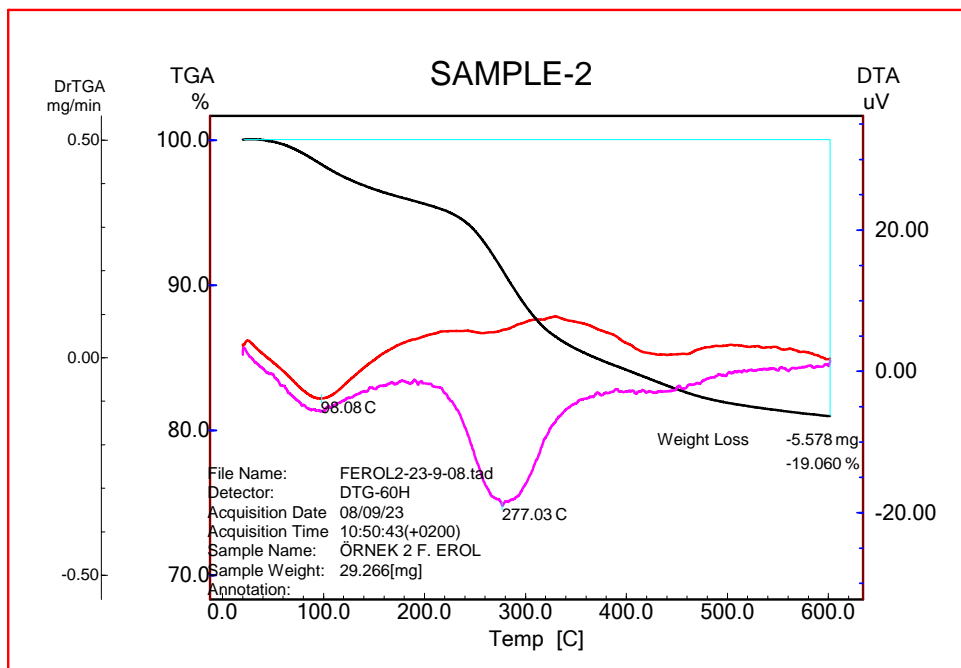


Figure I.11. TGA of 25% PFOA.

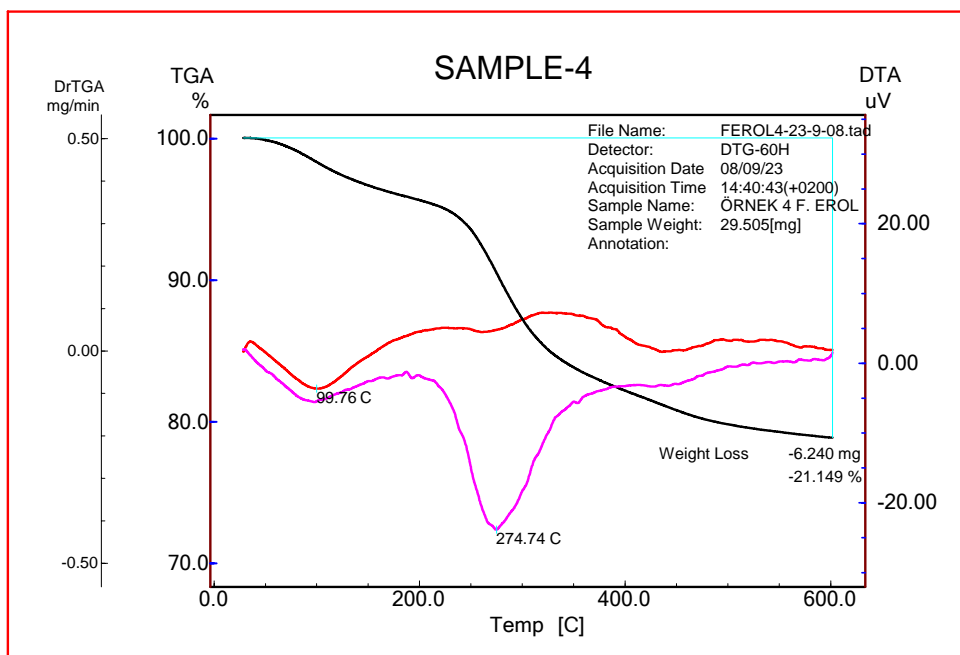


Figure I.12. TGA of 50% PFOA.

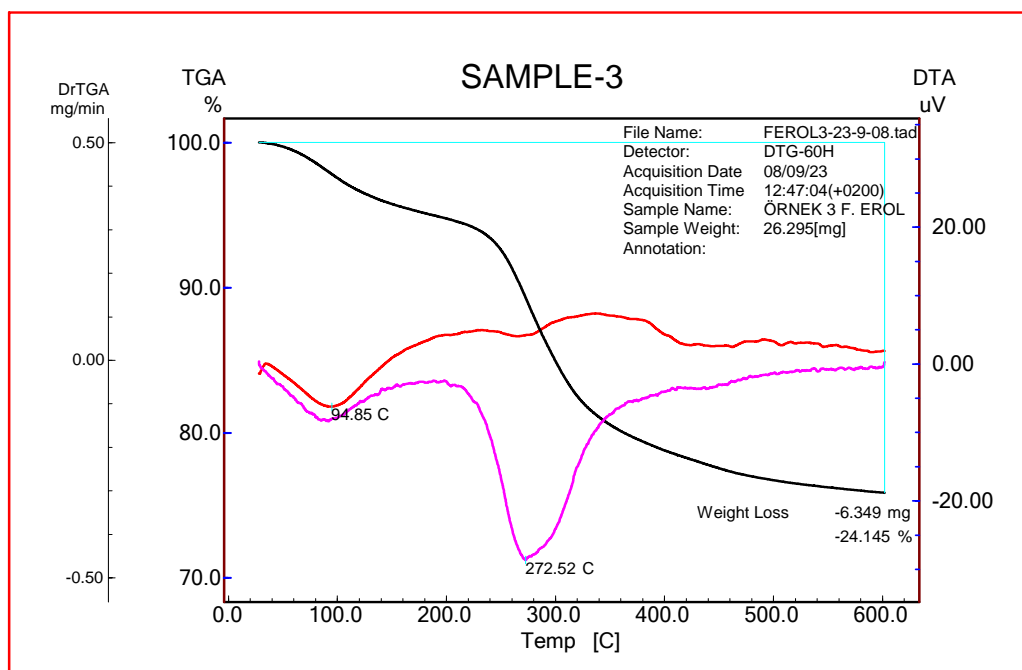


Figure I.13. TGA of 100% PFOA.

### I.3 Order of magnitude analysis

Table I.1. The “Order of magnitude” analysis in dye ozonation. Catalyst: none,  $Q_G = 150$  L/h,  $Q_L = 30$  L/h.

Dye	$C_{D,in} \times 10^2$ , mmol/L	Order of liq. conv. mass transfer $\times 10^4$ , mmol/(L.s)	Order of gas-liq. mass transfer $\times 10^4$ , mmol/(L.s)	Order of liq. diff. mass transfer $\times 10^4$ , mmol/(L.s)	Order of reaction kinetics $\times 10^4$ , mmol/(L.s)
<i>RBBR</i>	4.8	4.59	90.2	3.32	4.24
	9.6	5.29	109.4	3.83	9.77
	14.4	5.29	121.7	3.19	14.65
	19.2	5.19	138.0	2.82	19.17
<i>AR-151</i>	6.6	5.36	114.2	5.17	6.44
	13.2	5.08	145.7	4.28	12.20
	19.8	4.84	149.2	2.92	17.46
	26.4	5.11	163.9	3.08	24.56

Table I.2. The “Order of magnitude” analysis in dye ozonation. Catalyst: none,  $Q_G = 70$  L/h,  $Q_L = 30$  L/h.

Dye	$C_{D,in} \times 10^2$ , mmol/L	Order of liq. conv. mass transfer $\times 10^4$ , mmol/(L.s)	Order of gas-liq. mass transfer $\times 10^4$ , mmol/(L.s)	Order of liq. diff. mass transfer $\times 10^4$ , mmol/(L.s)	Order of reaction kinetics $\times 10^4$ , mmol/(L.s)
<i>RBBR</i>	4.8	5.57	60.0	11.8	5.14
	9.6	5.54	64.3	12.7	10.2
	14.4	5.69	69.6	12.3	15.8
	19.2	5.87	94.1	11.3	21.7
<i>AR-151</i>	6.6	5.54	63.1	10.0	6.7
	13.2	5.72	72.4	11.0	13.8
	19.8	5.82	78.6	13.0	21.0
	26.4	5.76	91.1	11.1	27.8

Table I.3. The “Order of magnitude” analysis in dye ozonation. Catalyst: none,  $Q_G = 70$  L/h,  $Q_L = 250$  L/h.

Dye	$C_{D,in} \times 10^2$ , mmol/L	Order of liq. conv. mass transfer $\times 10^4$ , mmol/(L.s)	Order of gas-liq. mass transfer $\times 10^4$ , mmol/(L.s)	Order of liq. diff. mass transfer $\times 10^4$ , mmol/(L.s)	Order of reaction kinetics $\times 10^4$ , mmol/(L.s)
<i>RBBR</i>	4.8	45.9	17.4	21.6	5.1
	9.6	41.2	17.7	18.5	9.1
	14.4	43.8	25.5	18.4	14.6
	19.2	47.4	32.4	20.2	21.0
<i>AR-151</i>	6.6	44.8	14.7	23.3	6.5
	13.2	43.1	16.4	21.2	12.4
	19.8	44.0	21.2	21.9	19.0
	26.4	45.6	25.4	22.1	26.3

Table I.4. The “Order of magnitude” analysis in dye ozonation. Catalyst: alumina,  $Q_G = 150$  L/h,  $Q_L = 150$  L/h.

Dye	$C_{D,in} \times 10^2$ , mmol/L	$m_{cat}$ , g	Order of liq. conv. mass transfer $\times 10^4$ , mmol/(L.s)	Order of gas-liq. mass transfer $\times 10^4$ , mmol/(L.s)	Order of liq. diff. mass transfer $\times 10^4$ , mmol/(L.s)	Order of reaction kinetics $\times 10^4$ , mmol/(L.s)	Order of liq-solid mass transfer $\times 10^4$ , mmol/(L.s)
RBBR	4.8	25	8.04	28.49	3.05	1.48	1833.20
	19.2		8.04	29.51	3.05	5.93	2386.50
	4.8	75	8.04	27.81	3.05	1.48	5961.32
	19.2		8.04	28.83	3.05	5.93	7962.32
	4.8	125	8.04	30.86	3.05	1.48	12398.35
	19.2		8.04	33.58	3.05	5.93	18062.93
AR-151	6.6	25	8.04	25.78	3.05	1.93	1965.34
	26.4		8.04	27.47	3.05	7.73	2439.88
	6.6	75	8.04	28.49	3.05	1.93	6429.91
	26.4		8.04	30.18	3.05	7.73	8160.92
	6.6	125	8.04	30.86	3.05	1.93	13638.66
	26.4		8.04	35.61	3.05	7.73	18681.72

Table I.5. The “Order of magnitude” analysis in dye ozonation. Catalyst: PFOA,  $Q_G = 150$  L/h,  $Q_L = 150$  L/h.

Dye	$C_{D,in} \times 10^2$ , mmol/L	$m_{cat}$ , g	Order of liq. conv. mass transfer $\times 10^4$ , mmol/(L.s)	Order of gas-liq. mass transfer $\times 10^4$ , mmol/(L.s)	Order of liq. diff. mass transfer $\times 10^4$ , mmol/(L.s)	Order of reaction kinetics $\times 10^4$ , mmol/(L.s)	Order of liq-solid mass transfer $\times 10^4$ , mmol/(L.s)
RBBR	4.8	25	8.04	35.95	3.05	1.48	1449.06
	19.2		8.04	36.97	3.05	5.93	1661.16
	4.8	75	8.04	34.59	3.05	1.48	5392.03
	19.2		8.04	36.29	3.05	5.93	6406.66
	4.8	125	8.04	36.63	3.05	1.48	9550.17
	19.2		8.04	37.31	3.05	5.93	11482.71
AR-151	6.6	25	8.04	31.54	3.05	1.93	1463.87
	26.4		8.04	34.59	3.05	7.73	1665.99
	6.6	75	8.04	32.90	3.05	1.93	5460.55
	26.4		8.04	34.59	3.05	7.73	6430.63
	6.6	125	8.04	37.31	3.05	1.93	9679.25
	26.4		8.04	39.34	3.05	7.73	11528.93

# CURRICULUM VITAE

## PERSONAL INFORMATION

Surname, Name: Erol, Funda

Nationality: Turkish (TC)

Date and Place of Birth: 30 August 1977, Ankara

Marital status: Single

Phone: +90 312 210 4367

Fax: +90 312 210 2600

e-mail: [wwwferol@metu.edu.tr](mailto:wwwferol@metu.edu.tr)

## EDUCATION

<b>Degree</b>	<b>Institution</b>	<b>Year of Graduation</b>
PhD	METU Chemical Engineering	2008
MS	METU Chemical Engineering	2002
BS	METU Chemical Engineering	1999
High School	Bursa Fen Lisesi, Bursa	1994

## WORK EXPERIENCE

<b>Year</b>	<b>Place</b>	<b>Enrollment</b>
2001-2006	METU Department of Chemical Engineering	Teaching Assistant
1999-2001	METU Department of Chemical Engineering	Research Assistant
1998 July	AKKİM	Intern Engineering Student

## FOREIGN LANGUAGES

Advanced English, Fluent Italian

## PUBLICATIONS

1. Özbelge, T.A., Erol, F., Özbelge, H. Ö. A Kinetic Study on the Decolorization of Aqueous Solutions of *Acid Red-151* by Ozonation. *J. Env. Eng. Sci. Health: Part A*. A38(8), 1607-1623, 2003.
2. Erol, F. Özbelge, T.A. Catalytic ozonation with non-polar bonded alumina phases for treatment of aqueous dye solutions in a semi-batch reactor. *J. Chem. Eng.*, 139, 272-283, 2008.
3. Özbelge, T.A., Erol, F. Effects of pH, Initiator, Scavenger and Surfactant on the Ozonation Mechanism of an Azo Dye (*Acid Red-151*) in a Batch Reactor. *Chem Eng. Comm.*, 196, 1-17, 2008.
4. Erol, F., Özbelge, H.Ö., Özbelge, T.A. Modeling of catalytic ozonation process in a three phase reactor. *in press*.
5. Özbelge, T.A., Özbelge, H.Ö. and F. Erol “A Kinetic Study on the Decolorization of Aqueous Solutions of Acid-Red 151 by Ozonation” presented as a poster in Eastern Meditterreanean Chemical Engineering Conference EMCC (intl.), May 20-24, 2001, METU, Ankara, Turkey, Book of Abstracts, CC 8.2, 165-166.
6. Tülay A. Özbelge, Funda Erol and H. Önder Özbelge “ A Kinetic Study on the Decolorization of Aqueous Solutions of Acid Red – 151 by Ozonation”, Intl. Conference on the Environmental Problems of the Mediterranean Region (EPMR-2002), 12-15 April 2002, Near East University, Nicosia, TRNC, Book of Abstracts, 63.
7. Funda Erol, H. Önder Özbelge and Tülay A. Özbelge, “ Treatment of Azo Dye Solutions and Textile Wastewater by Ozonation” presented in the thematic session of ‘Chemical and Catalytic Processes’; EMCC-3 (Third Eastern Mediterranean Chemical Engineering Conference) 13-15 May 2003, Thessaloniki, Greece.
8. Funda Erol and Tülay A. Özbelge “Asit Kırmızı-151 ve Remazol Mavisi boyaalarının katalitik ozonlama ile akışkan yataklı reaktörde arıtılması” presented as a poster in 8. National Chemical Engineering Conference UKMK 8, August 26-29, 2008, University of İnönü, Malatya, Turkey, Book of Abstracts.